

Atti
-21-

ATTI

1. *Il controllo terminologico delle risorse elettroniche in rete: tavola rotonda, Firenze 27 gennaio 2000*, a cura di Paola Capitani, 2001
2. *Commemorazione di Michele Della Corte*, a cura di Laura Della Corte, 2001
3. *Disturbi del comportamento alimentare: dagli stili di vita alla patologia*, a cura di Corrado D'Agostini, 2002
4. *Proceedings of the third International Workshop of the IFIP WG5.7 Special interest group on Advanced techniques in production planning & control : 24-25 February 2000, Florence, Italy*, edited by Marco Garetti, MarioTucci, 2002
5. *DC-2002: Metadata for E-Communities: Supporting Diversity And Convergence 2002: Proceedings of the International Conference on Dublin Core and Metadata for e-Communities, 2002, October 13-17, 2002, Florence, Italy*, organized by Associazione Italiana Biblioteche [et al.], 2002
6. *Scholarly Communication and Academic Presses: Proceedings of the International Conference, 22 March 2001, University of Firenze, Italy*, edited by Anna Maria Tammaro, 2002
7. *Recenti acquisizioni nei disturbi del comportamento alimentare*, a cura di Alessandro Casini, Calogero Surrenti, 2003
8. *Proceedings of Physmod 2003 International Workshop on Physical Modelling of Flow and Dispersion Phenomena*, edited by Giampaolo Manfreda e Daniele Contini, 2003
9. *Public Administration, Competitiveness and Sustainable Development*, edited by Gregorio Arena, Mario P. Chiti, 2003
10. *Authority control: definizioni ed esperienze internazionali: atti del convegno internazionale, Firenze, 10-12 febbraio 2003*, a cura di Mauro Guerrini e Barbara B. Tillet; con la collaborazione di Lucia Sardo, 2003
11. *Le tesi di laurea nelle biblioteche di architettura*, a cura di Serena Sangiorgi, 2003
12. *Models and analysis of vocal emissions for biomedical applications: 3rd international workshop: december 10-12, 2003 : Firenze, Italy*, a cura di Claudia Manfredi, 2004
13. *Statistical Modelling. Proceedings of the 19th International Workshop on Statistical Modelling: Florence (Italy) 4-8 july, 2004*, edited by Annibale Biggeri, Emanuele Dreassi, Corrado Lagazio, Marco Marchi, 2004
14. *Studi per l'insegnamento delle lingue europee : atti della prima e seconda giornata di studio (Firenze, 2002-2003)*, a cura di Maria Carlota Nicolás Martínez, Scott Staton, 2004.
15. *L'Archivio E-prints dell'Università di Firenze: prospettive locali e nazionali. Atti del convegno (Firenze, 10 febbraio 2004)*, a cura di Patrizia Cotoneschi, 2004
16. *TRIZ Future Conference 2004. Florence, 3-5 November 2004*, edited by Gaetano Cascini, 2004
17. *Mobbing e modernità : la violenza morale sul lavoro osservata da diverse angolature per coglierne il senso, definirne i confini. Punti di vista a confronto. Atti del Convegno Firenze, 20 aprile 2004*, a cura di Aldo Mancuso, 2004
18. *Lo spazio sociale europeo. Atti del convegno internazionale di studi Fiesole (Firenze), 10-11 ottobre 2003*, a cura di Laura Leonardi, Antonio Varsori, 2005
19. *AIMETA 2005 Atti del XVII Congresso dell'Associazione Italiana di Meccanica Teorica e Applicata, Firenze, 11-15 settembre 2005*, a cura di Claudio Borri, Luca Facchini, Giorgio Federici, Mario Primicerio, 2005
20. *Giornata CEFTrain - CEFTrain Day. Conference Proceedings and Partner Contributions. Firenze, Italy, 7 may 2005*, edited by Elizabeth Guerin, 2005

**MODELS AND ANALYSIS
OF VOCAL EMISSIONS
FOR BIOMEDICAL APPLICATIONS**

4th INTERNATIONAL WORKSHOP

October 29-31, 2005

Firenze, Italy

Edited by

Claudia Manfredi

Firenze University Press

2005

Models and analysis of vocal emissions for biomedical applications :
4th international workshop: october 29-31, 2005 : Firenze, Italy /
edited by Claudia Manfredi. – Firenze : Firenze university press,
2005.

(Atti, 21)

<http://digital.casalini.it/8884533201>

Stampa a richiesta disponibile su <http://epress.unifi.it>

ISBN 88-8453-320-1 (online)

ISBN 88-8453-319-8 (print)

612.78 (ed. 20)

Voce - Patologia medica

Responsibility for the contents rests entirely with the authors. The editors and the organising committee of the MAVEBA 2003 accept no responsibility for any errors, omissions, or views expressed in this publication.

No part of this publication can be reproduced, stored in a retrieval system, or transmitted in any form or by any means without the permission of the editors. Permission is not required to copy abstracts of papers, on condition that a full reference of the source is given.

Cover: designed by CdC, Firenze, Italy.

© 2005 Firenze University Press

Università degli Studi di Firenze

Firenze University Press

Borgo Albizi, 28, 50122 Firenze, Italy

<http://epress.unifi.it/>

Printed in Italy



MAVEBA 2005

INTERNATIONAL PROGRAM COMMITTEE

S. Aguilera (ES)	A. Barney (UK)	D. Berckmans (BE)	P. Brusaglioni (I)
S. Cano Ortiz (CU)	R. Carlson (SE)	M. Clements (USA)	J. Doorn (AR)
U. Eysholdt (D)	O. Fujimura (JP)	H. Herzel (D)	D. Howard (UK)
A. Izvorski (PL)	M. Kob (D)	A. Krot (BY)	U. Laine (FI)
C. Larson (USA)	F. Locchi (I)	J. Lucero (BR)	C. Manfredi (I)
C. Marchesi (I)	W. Mende (D)	V. Misun (CZ)	C. Moore (UK)
X. Pelorson (F)	P. Perrier (F)	R. Ritchings (UK)	S. Ruffo (I)
O. Schindler (I)	A. Schuck (BR)	R. Shiavi (USA)	H. Shutte (NL)
J. Sundberg (SE)	J. Svec (CZ)	R. Tadeusiewicz (PL)	I. Titze (USA)
U. Uergens (D)	G. Valli (I)	K. Wermke (D)	W. Ziegler (D)

LOCAL ORGANISING COMMITTEE

C. Manfredi, Dept. of Electronics and Telecommunications, Faculty of Engineering - Conference Chair
L. Bocchi, Dept. of Electronics and Telecommunications, Faculty of Engineering
P. Brusaglioni, Dept. of Physics, Faculty of Maths, Physics and Natural Sciences - Conference Chair
F. Locchi, Dept. of Clinical Physiology, Faculty of Medicine.
C. Marchesi, Dept. of Systems and Computer Science, Faculty of Engineering.
S. Ruffo, Dept. of Energetics, Faculty of Engineering.
G. Valli, Dept. of Electronics and Telecommunications, Faculty of Engineering

SPONSORS

Ente CRF – Ente Cassa di Risparmio di Firenze



ISCA - International Speech and Communication Association



AIIMB - Associazione Italiana Ingegneria Medica e Biologica



INFN – Istituto Nazionale per la Fisica della Materia



CONTENTS

Foreward.....	XI
---------------	----

Special session on Voice pathology classification

C. Berry, T. Ritchings, “ <i>A comparative study of intelligent voice quality assessment using impedance and acoustic signals</i> ”	3-6
C. J. Moore , K. Manickam, N. Slevin, “ <i>Voicing recovery in males following radiotherapy for larynx cancer</i> ”	7-10
N. Sáenz-Lechón, J.I. Godino-Llorente, V. Osma-Ruiz, P. Gómez-Vilda, S. Aguilera-Navarro, “ <i>A methodology to evaluate pathological voice detection systems</i> ”	11-14
N. Sáenz-Lechón, J.I. Godino-Llorente, V. Osma-Ruiz, P. Gómez-Vilda, S. Aguilera-Navarro, “ <i>Effects of MP3 encoding on voice pathology detection: results with MFCC parameters</i> ”	15-18
J. Schoentgen, “ <i>Towards a classification of phonatory features of disordered voices</i> ”	19-22
W. Sheta, T. Ritchings, C. Berry, “ <i>Intelligent voice quality assessment post-treatment using genetic programming</i> ”	23-26

Voice recovering / enhancement

H. Kuwabara, “ <i>A method for changing speech quality and its application to pathological voices</i> ”	29-32
R. Pietruch, A. Grzanka, W. Konopka, M. Michalska, “ <i>Methods for formant extraction in speech of patients after total laryngectomy</i> ”	33-36
C. Manfredi, C. Marino, F. Dori, E. Iadanza, “ <i>Optimised GSVD for dysphonic voice quality enhancement</i> ”	37-40

Special session on Physical and mechanical models and devices

T. Vampola, J. Horacek, J. Vesely, J. Vokral, “ <i>Modelling of influence of velopharyngeal insufficiency on phonation of vowel /a/</i> ”	43-46
R. Zaccarelli, C. Elemans, W.T. Fitch, H. Herzel, “ <i>Two-mass models of the bird Syrinx</i> ”	47-50
N. Ruty, J. Cisonni, X. Pelorson, P. Perrier, P. Badin, A. Van Hirtum, “ <i>A physical model for articulatory speech synthesis. theoretical and numerical principles</i> ”	51-54
F. Avanzini, S. Maratea, C. Drioli, “ <i>Physiological control of low-dimensional glottal models with applications to voice source parameter matching</i> ”	55-58

P. Gómez, C. Lázaro, R. Fernández, A. Nieto, J.I. Godino, R. Martínez, F. Díaz, A. Álvarez, K. Murphy, V. Nieto, V. Rodellar, F.J. Fernández-Camacho, “ <i>Using biomechanical parameter estimates in voice pathology detection</i> ”	59-62
R. Orr, B. Cranen, “ <i>The effect of the flow mask on phonation</i> ”	63-66
Ch. Jeannin, P. Perrier, Y. Payan, A. Dittmar, B. Grosgeat, “ <i>A non-invasive device to measure mechanical interaction between tongue, palate and teeth during speech production</i> ”	67-70

Poster session

P. Alku, J. Horacek, M. Airas, A.M. Laukkanen, “ <i>Assessment of glottal inverse filtering by using aeroelastic modelling of phonation and fe modelling of vocal tract</i> ”	73-76
L. Bocchi, S. Bianchi, C. Manfredi, N. Migali, G. Cantarella, “ <i>Quantitative analysis of videokymographic images and audio signals in dysphonia</i> ”	(Paper not available)
P. Brusciagioni, “ <i>A note on jitter estimation</i> ”	(Paper not available)
M. Guarino, A. Costa, S. Patelli, M. Silva, D. Berckmans, “ <i>Cough analysis and classification by labelling sound in swine respiratory disease</i> ”	77-80
J. Hanquinet, F. Grenez, J. Schoentgen, “ <i>Wave-morphing in the framework of a glottal pulse model</i> ”	81-83
T. Kitamura, P. Mokhtari, H. Takemoto, “ <i>Changes of vocal tract shape and area function by F0 shift</i> ”	85-88
M. Kob, J. Stoffers, Ch. Neuschaefer-Rube, “ <i>Comparison of LPC analysis and impedance vocal tract measurements</i> ”	89-91
C. Manfredi, B. Maraschi, A. Berlusconi, G. Cantarella, “ <i>Objective pre- and post-surgical voice analysis</i> ”	(Paper not available)
V. Misun, “ <i>Source voice characteristics of the artificial vocal folds</i> ”	93-96
T. Orzechowski, A. Izvorski, I. Gatkowska, M. Rudzinska, “ <i>Automatic classification of voice disorders in course of neurodegenerative disease</i> ”	97-100
M. Sovilj, T. Adamovic, M. Subotic, N. Stevovic, “ <i>Newborn’s cry from risk and normal pregnancies</i> ”	101-104
K. Manickam, H. Li, “ <i>Complexity analysis of normal and deaf infant cry acoustic waves</i> ”	105-108

Special session on Methods for voice measurements

A. Fourcin, “ <i>Clinical voice measurement using EGG/LX signals</i> ”	111-114
R. Shrivastav, “ <i>From vocal quality measurement to perception</i> ”	115-118

J.G. Svec, F. Sram, M. Fric, Q. Qiu, H.K. Schutte, “ <i>What can be seen in videokymographic images?</i> ”	119
S. Bianchi, L. Bocchi, C. Manfredi, G. Cantarella, N. Migali, “ <i>Objective vocal fold vibration assessment from videokymographic images</i> ”	121-124
S. Mantha, L. Mongeau, T. Siegmund, “ <i>Dynamic digital image correlation of a dynamic physical model of the vocal folds</i> ”	125-128
S. Ciecwiwa, D. Deliyiski, T. Zielinski, “ <i>Fast FFT-based motion compensation for laryngeal high-speed videoendoscopy</i> ”	129-132
H.S. Shaw, D.D. Deliyiski, “ <i>Vertical motion during modal and pressed phonation: magnitude and symmetry</i> ”	133-136
H.S. Shaw, D.D. Deliyiski, “ <i>Mucosal wave magnitude: presence, extent, and symmetry in normophonic speakers</i> ”	137-140
S.T. Takano, K.K. Kinoshita, K.H. Honda, “ <i>Measurement of cricothyroid articulation using high-resolution MRI and 3D pattern matching</i> ”	141-144

Voice modelling and analysis

H.J. Fell, J. MacAuslan, “ <i>Vocalisation analysis tools</i> ”	147-150
P. Svancara, J. Horacek, “ <i>Numerical modelling of effect of tonsillectomy on production of Czech vowels /a/ and /i/</i> ”	151-154
A. Kacha, F. Grenez, J. Schoentgen, “ <i>Generalized variogram analysis of vocal dysperiodicities in connected speech</i> ”	155-158
T. Wurzbacher, R. Schwarz, H. Toy, U. Eysholdt, J. Lohscheller, “ <i>Modelling of non-stationary phonation for classification of vocal folds vibrations</i> ”	159-162
F.M. Martinez, J.C. Goddard, A.M. Martinez, “ <i>Analysis of Spanish synthesized speech signals using spectral and basis pursuit representations</i> ”	163-166
F.R. Drepper, “ <i>Voiced excitation as entrained primary response of a reconstructed glottal master oscillator</i> ”	167-170
J.J. Turunen, T. Lipping, J.T. Tantt, “ <i>Speech analysis using Higuchi fractal dimension</i> ”	171-174

Special session on Neurological dysfunctions

R. Shiavi, “ <i>Quantitative and experimental approaches for investigating neurological/psychological dysfunction</i> ”	(Paper not available)
L. Cnockaert, J. Shoentgen, P. Auzou, C. Ozsancak, F. Grenez, “ <i>Effect of Parkinson’s disease on vocal tremor</i> ”	177-180

K.S. Subari, D.M. Wilkes, R. Shiavi, S. Silverman, M. Silverman, “*Evaluation of speaker normalization for suicidality assessment*” 181-184

Infant cry – Singing voice

K. Wermke, W. Mende, A. Kempf, C. Manfredi, P. Brusaglioni, A. Stellzig-Eisenhauer, “*Interaction patterns between melodies and resonance frequencies in infants’ pre-speech utterances*” 187-190

R. Nicollas, J. Giordano, L. Francius, J. Vicente, Y. Burtschell, M. Medale, B. Nazarian, M. Roth, M. Ouaknine, A. Giovanni, “*Aerodynamical model of human newborn larynx: an approach of the first cry*” 191-193

S. Adachi, J. Yu, “*High-pitched voice simulation using a two-dimensional vocal fold model*” 195-198

J. Sundberg, “*Effect of vocal loudness variation on the voice source*” 199

N. Amir, O. Amir, O. Michaeli, “*Assessing vibrato quality of singing students*” 201-203

Non-human sounds

M. Gamba, C. Giacoma, “*Vocal production mechanism in ruffed lemurs: a prosimian model for the basis of primate phonation*” 207-210

J.-M. Aerts, P. Jans, D. Halloy, P. Gustin, D. Berckmans, “*Labelling of cough data from pigs for on-line disease monitoring by sound analysis*” 211-214

Author Index..... 215-216



MAVEBA 2005

FOREWARD

Welcome to the 4th International Workshop on Models and Analysis of Vocal Emissions for Biomedical Applications, MAVeBA 2005, 29-31 October 2005, Firenze, Italy.

In the light of previous editions, held in 1999, 2001, and 2003 respectively, all in Firenze, the Workshop aims at investigating into main aspects of voice modelling and analysis, ranging from fundamental research to all kinds of biomedical applications and related established and advanced technologies. It offers the participants an interdisciplinary platform for presenting and discussing new knowledge both in the field of models and analysis of speech signals and in that of emerging imaging techniques.

Contacts between specialists active in research and industrial developments could take advantage from the Workshop structure, comprising both Special Sessions devoted to a set of relevant topics, and standard Sessions, covering a wide area of voice analysis research, for biomedical applications.

Four Special Sessions were organised and co-ordinated by specialists in the field, collecting contributions about new and emerging techniques. Each Session is introduced by a review paper, presenting the state-of-the-art in the field, pointing out present knowledge, limitations and future directions. The selected topics are:

1. Voice pathology classification
2. Physical and mechanical models and devices
3. Methods for voice measurements
4. Neurological dysfunctions

As for regular Sessions, the relevant topics are: voice recovering, enhancement of voice quality during rehabilitation and after surgery, voice modelling and analysis of vocal emissions, newborn and infant cry analysis, singing voice. A short Session is also devoted to non-human sounds, and their possible relationships to humans.

All the papers collected in this book of Proceedings are of high scientific level, as they were reviewed by at least two anonymous referees, and cover the most relevant fields of research in voice signals and images analysis. We would like to thank the members of the organising committee and all the reviewers, who gave freely of their time to assess the highly disparate work of the workshop, helping in improving the quality of the papers.

We have also benefited from the efforts of the administrative staff within our University: office for Research and International Relations, Logistic office, and the staff of the Faculty of Engineering and of the Department of Electronics and Telecommunications, that devoted a lot of time and efforts to make this workshop a successful one. Special thanks to our University Orchestra and Chorus, and to the members of “Capriccio Armonico” dancing group for their generous participation.

Finally, our gratitude goes to the supporters and sponsors, who contribute much to the success of the MAVeBA workshop.

Dott. Claudia Manfredi
Conference Chair

Prof. Piero Bruscazioni
Conference Chair

Special session on
Voice pathology classification

A COMPARATIVE STUDY OF INTELLIGENT VOICE QUALITY ASSESSMENT USING IMPEDANCE AND ACOUSTIC SIGNALS

Carl Berry & Tim Ritchings

School of Computing, Science and Engineering,
University of Salford, UK
c.berry2@salford.ac.uk

Abstract: Objective assessment techniques for classifying voice quality for patients recovering from treatment for cancer of the larynx should lead to more effective recovery than the present approach, which is very subjective and depends heavily on the experience of the individual Speech and Language Therapist (SALT). This work follows an earlier study where an Artificial Neural Network (ANN) was trained on parameters derived from electrolaryngograph electrical impedance (EGG) signals recorded while a patient was phonating /i/ as steadily as possible, and gave an indication of voice quality inline with the standard UK Speech and Language Therapist (SALT) seven point scale. The applicability of this approach to voice quality assessment of acoustic signals is described, and the results are found to compare very well with those derived from the impedance signals. It was also noted that for both the impedance and the acoustic signals, the ANNs were able to classify the very good (recovered) and the very poor (abnormal) voices well, but performed quite badly with the mid-range classifications, raising questions about the accuracy of these classifications.

Keywords: Voice quality, classification, Artificial Neural Network, acoustic, impedance.

I. INTRODUCTION

In the UK, voice quality assessment for patients recovering from treatment for cancer of the larynx is undertaken by Speech and Language Therapists (SALT), who use a standard 7-point classification scale ranging from Lx0-Lx6, with Lx0 being a near normal (recovered) voice while Lx6 represents an abnormal, very poor quality voice. The approach taken to reach a classification is very subjective and depends to a large extent on the experience of the SALT.

This work is concerned with a series of investigations aimed at producing an intelligent computer-based system which can provide objective classifications of voice quality in patients recovering from cancer of the larynx patients in line with the UK standard 7-point classification scale.

Previous work [1,2] has demonstrated that accurate classifications could be obtained from a Multi Layer Perceptron (MLP) Artificial Neural Network (ANN) which was trained on a combination short-term and long-term parameters derived from electrolaryngograph electrical impedance (EGG) signals while a patient was phonating /i/ as steadily as possible. Although, acoustic signals were recorded at the same time as the impedance signals, they were not analysed as they appeared much noisier than the EGG signals. However, classification of voice quality from the acoustic signals is advantageous, if possible, as highly specialised and expensive equipment (the electrolaryngograph) will not be necessary, and this raises the possibility of screening in a GP's practice, rather than in the secondary care centres.

A preliminary assessment of the acoustic signals is described here, and the resulting classifications that have been achieved with the ANN approach are compared with those obtained for the impedance signals.

II. TREATMENT OF VOICE SIGNALS

A. Collection of Voice Signals

The patient's voice data was collected by the Christie Hospital and the South Manchester hospital using an electrolaryngograph PCLX system [3]. The equipment simultaneously records the electrical impedance signal via pads placed at specific positions on the patient's neck at the same time as the acoustic voice signal using a microphone. In these studies, the patient was attempts to steadily phonate the /i/ sound. This process means that two datasets are collected, one showing the EGG and a second showing acoustic variation, allowing for a direct comparison between the two sets. In the work only the male voices were used as the number of female voices in the dataset was too small to give an accurate assessment, a feature of the dataset is that most cancer of the larynx patients are male. Voice quality was subjectively classified by a SALT for each patient using their 7-point scale. The number of patients in each of the 7 categories is shown in Table 1.

Lx0	Lx1	Lx2	Lx3	Lx4	Lx5	Lx5
22	36	25	33	26	25	11

Table 1. Patients in each SALT category

B. Signal Pre-processing

In order to be able to extract the short and long term parameters used in the classification process, a number of pre-processing stages were applied to the impedance and acoustic datasets. Initially the signals were stationarised to remove drift, split into 50 ms frames (Hanning windows overlapping by 25 ms) and then converted to the autocorrelation form of the signal to remove some of the noise components. Once these processes were complete, the frames were examined to check if they contained silence or sound. This involved comparing the frames with a sample of silence frame recorded under the same conditions, and used zero point crossing and short term amplitudes as checks. Once the silence frames have been removed, the remaining frames were separated into voiced and unvoiced frames; voiced frames containing vocal phonation while unvoiced

containing no recognisable speech. This was achieved using the cepstrum based approach as described in [4]. The Fundamental Harmonic Normalisation (FHN) as described in [5] was then calculated from Power Spectrum Density (PSD) and then this structure (typical examples are shown in Fig 2) was modelled by fitting a Gaussian Mixture Model (GMM) in order to reduce the number of parameters needed to describe the signal.

C. Parameter Extraction

A total of 22 short and long term parameters are extracted for use with classification, as detailed in [1,2]. The short term parameters consist of 15 parameters relating to the mean, standard deviation and peak of the gaussians used to describe the fundamental frequency and first four harmonics in the frame (if they can be detected); the value of the fundamental frequency in each frame (F_0), the noise threshold value (N_0), the FHN Noise Energy

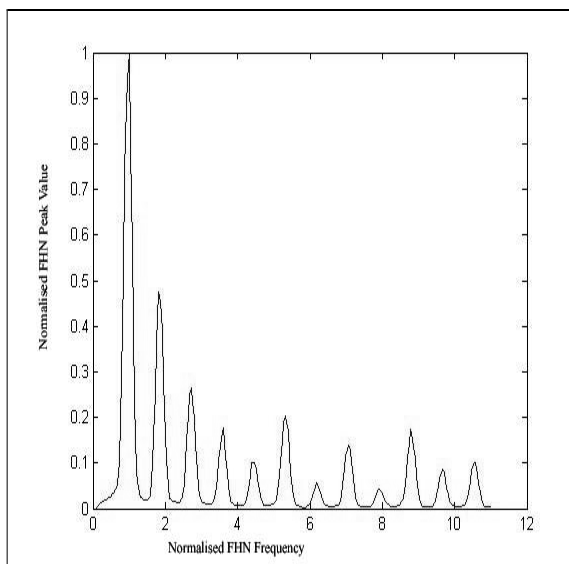


Figure 2a FHN plot of good quality impedance signal

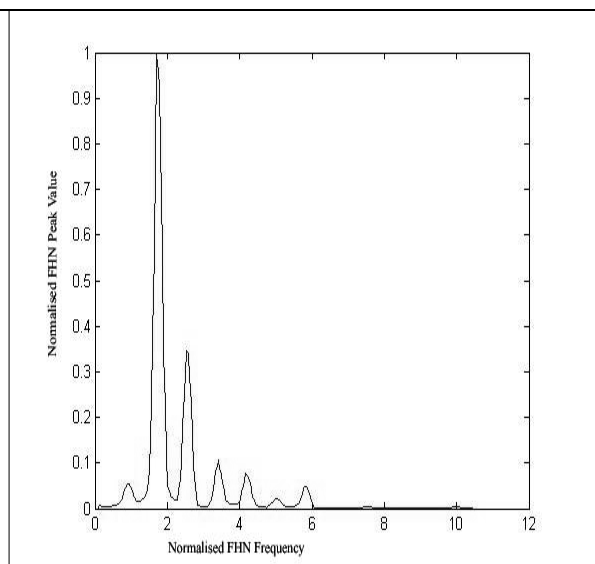


Figure 2b FHN plot of good quality acoustic signal

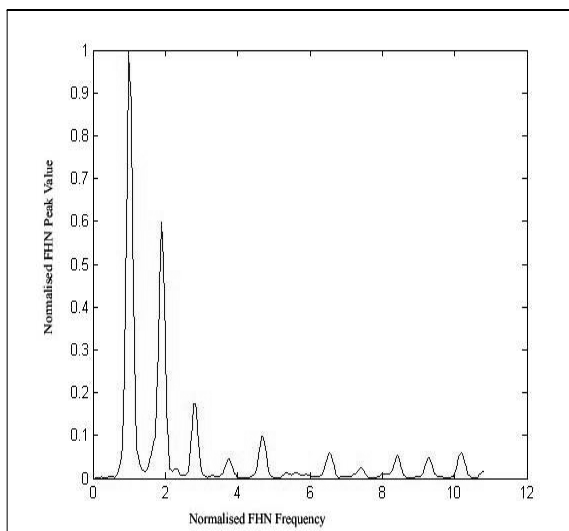


Figure 2c FHN plot of poor quality impedance signal

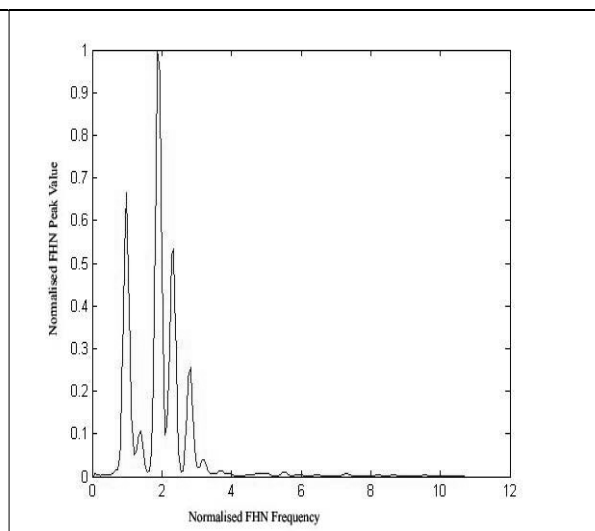


Figure 2d FHN plot of poor quality acoustic signal

(FHNNE) and the Residual Harmonic Energy (RHE). The 3 long-term parameters were extracted from the speaker's whole voiced speech. These included the mean fundamental frequency across all frames (MF_0), a measure of jitter of the fundamental frequency between frames (J_0) and the ratio of voiced to unvoiced frames.

D. The classification technique

Once the parameters have been extracted, a 3 layer feed-forward ANN with a sigmoidal activation function in the hidden layer, and using backpropagation of errors, is used for classification purposes. The ANN had 22 inputs, one for each of the short-term and long-term parameters derived from the voice signals, and 7 outputs, corresponding to the SALT categories. The "leave one out" cross validation strategy was used as it generally regarded as one of the most accurate methods and by leaving out a single patient's voice sample we can ensure to avoid inter versus intra speaker effects [2].

3. COMPARISON OF IMPEDANCE AND ACOUSTIC SIGNALS

A. Observed differences between the signal types.

When the FHN spectra of the impedance and acoustic signals were examined visually, a number of differences can be observed. Figs. 2a and 2b show the spectra derived for a good quality pathological voice (Lx0) for the impedance and acoustic signals respectively. A clear difference is that for the impedance signal, the largest peak belongs to the fundamental frequency, whilst in the acoustic signal it is the 1st harmonic. This is normal and corresponds to the pattern that would be expected from a human voice. However, even in this good quality voice the acoustic signal only shows six harmonics, as compared to eleven for the impedance signal. It should also be noted that the peak of the fundamental frequency is very small in the acoustic signal, making it difficult to detect with the techniques used for the impedance signals.

This figure also shows typical FHN impedance (Fig 2c) and acoustic (Fig 2d) spectra for a poor quality

voice (Lx5). Again, the impedance signal shows many more harmonic structures. This reduction of harmonics also has an impact on the number of parameters that are available for use with the classification algorithms, and in the case of fig 2b, for example, it would only be possible to extract short term parameters for the fundamental frequency and the first 2 harmonics meaning that the model would be missing 6 short term parameters relating to the 4th and 5th harmonics. In some cases the situation is even worse, and in the extremely bad voices or very poor frames, it is not unusual to find the fundamental frequency and a single harmonic as the only recognisable structures.

Finally, it may be seen from Fig 2d that the acoustic signal suffers from far more noise between the harmonics than the impedance signal, making it much more difficult to fit the Gaussian Mixture Models. This also causes the centres of the harmonic structures to be shifted away from their correct positions in the FHN.

B. Classification differences between the signal types.

Classifications were made for both the impedance and acoustic signals, using the same parameters and training and verification procedures. In the cases where harmonics were not found, these parameters were set to zero. The resulting classifications are shown in Table 2.

As the acoustic signals are generally noisier than the impedance signals, with a poorer quality output, leading to typically fewer parameters, it was expected that the acoustic classifications would be less accurate than those obtained for the impedance signals. Surprisingly, this turns out to not be the case, and it can be seen in the Table that there is very little difference between the final classifications achieved for the two types of voice signal.

It should also be noted that for both types of signal, the ANNs give the best classifications for the worst voices (Lx5-6), obtained good results for the best quality voices (Lx0-1), but had difficulty correctly classifying the mid-range of voices (Lx2-4).

As results from other approaches to voice quality classification have found differences between the computer-based classifications and the SALT assessments in the upper middle categories [5], it was decided to repeat the training and classification of both the

Class	Impedance signal predicted class %							Acoustic signal predicted class %							
	0	1	2	3	4	5	6	0	1	2	3	4	5	6	
Lx0	50	17	13	8	12	0	0	Lx0	45	27	18	9	0	0	0
Lx1	25	48	15	5	7	0	0	Lx1	8	47	8	19	8	8	0
Lx2	2	12	12	27	30	8	10	Lx2	4	20	16	40	12	8	0
Lx3	5	7	10	28	40	8	2	Lx3	3	21	21	21	15	15	3
Lx4	13	5	8	27	37	7	3	Lx4	8	15	8	30	35	4	0
Lx5	0	0	8	13	20	43	15	Lx5	0	12	4	24	4	32	24
Lx6	0	0	0	15	20	30	35	Lx6	0	0	0	0	9	36	55
Impedance Results : Overall accuracy = 36.2%							Acoustic Results : Overall accuracy = 35.7%								

Table 2. Percentage of correctly classified voices on SALT 7-point scale for impedance and acoustic data.

impedance and acoustic using only three nodes in the ANN output layer, corresponding to “good” (Lx0-1), “medium” (Lx2-4) and “bad” (Lx5-6) classifications of voice quality. The results that were obtained are presented in Table 3.

	Impedance %	Acoustic %
Good (Lx0-1)	64	63
Medium (Lx2-4)	26	32
Bad (Lx5-6)	83	91

Table 3. Percentage of correctly classified voices on 3-point scale for impedance and acoustic signals

Again, it should be noted that similar classifications were obtained for the impedance and acoustic signals, and that the ANNs give the best classifications for the “bad” voices.

V. CONCLUSIONS.

A comparative study of voice quality assessment of patients recovering from cancer of the larynx has been made using impedance and acoustic signals. Following earlier work, a collection of short-term and long-term parameters were extracted from each type of signal and input to a ANN, which was successfully trained to match the SALT’s assessment of the patient’s voice quality using their 7-point scale.

The impedance signal taken gained from the electrolaryngograph is a much cleaner signal than it’s equivalent acoustic version, and generally showed more harmonics and contains less noise in the signal. The acoustic signal was more difficult to work with, having fewer harmonics, and the pre-processing stages had to be carried out far more carefully and occasionally produced extra errors that didn’t occur with the impedance signal, such as badly fitting Gaussian Mixture Models. However the extra parameters that can be routinely derived from the impedance did not appear to lead to more accurate classifications. This was particularly encouraging as it may allow further research to be carried out using microphones instead of the more expensive and specialised electrolaryngograph.

It was also noted that for both the impedance and the acoustic signals, the ANNs were able to classify the very good (recovered) and the very poor (abnormal) voices well, but performed quite badly with the mid-range classifications. This observation was reproduced when the signals were re-classified

into a 3-point scale of “good”, “medium” and “bad” voices.

The reason for the poor classifications in the mid-range categories of the 7-point scale and the “medium” category” in the 3-point scale is not yet clear. One possibility is that the SALT are more comfortable with classifying the extreme cases of abnormal and recovered voices, and are less consistent, or possibly less able, to distinguish the intermediate (recovering) voices. If this is the case, then the accuracy and usefulness of the 7-point scale for voice quality assessment would need to be examined.

Alternatively, these problems may be associated with the makeup of frames within a recovering voice, where it might be expected that some frames will be effectively normal, while other are still abnormal. The ANN training process would try and classify all these frames as being characteristic of one of the mid-range categories, as that is the SALT’s overall classification of the patient’s voice. This possibility is currently under investigation, and it may be necessary to classify individual frames within the voice signal, and then investigate ways of combine the results to achieve closer agreement with the SALT classifications in the mid-range categories.

REFERENCES

- [1] Ritchings RT, McGillion M, Moore CJ “Pathological voice quality assessment using artificial neural networks.” *Medical Engineering and Physics* 24 (2002) , pp561-564, PII S1350-4533(02)00064-4.
- [2] Godino-Llorente, JI, Ritchings, RT, Berry C “The Effects of Inter and Intra Speaker Variability on Pathological Voice Quality Assessment” *3rd International Workshop on Models and Analysis of Vocal Emissions for Biomedical Applications*, Firenze, Italy 2003.
- [3] Fourcin, A.J., Abberton E., Miller, D, Howell D. Laryngograph : “Speech pattern element tools for therapy, training and assessment.” *European Journal of Disorders of Communication* 30(2), 1996, pp.101-115
- [4] Rabiner, L. and Juang, B.H. Fundamentals of speech recognition. New Jersey Prentice Hall, 1993.
- [5] Moore C.J., Manickam K., Slavin N. “Voicing recovery in males following radiotherapy for larynx cancer.” *4th International Workshop on Models and Analysis of Vocal Emissions for Biomedical Applications*, Firenze, Italy 2005.

VOICING RECOVERY IN MALES FOLLOWING RADIOTHERAPY FOR LARYNX CANCER

C J Moore¹, K Manickam¹, and N Slevin²

¹North Western Medical Physics, HQ at Christie Hospital NHS Trust, Manchester, UK

²Clinical Department of Oncology, Christie Hospital NHS Trust, Manchester UK

Abstract: Larynx cancer patients receive radiotherapy as a non-invasive alternative to surgery and cure rates are high. Inevitably this impacts vocal fold functionality. Hence, voice recovery as a pre-requisite for resuming normal life is of special interest. Voicing recovery following radiotherapy is studied in this paper.

Complexity analysis, using approximate entropy to concisely quantify the collective spectral pattern derived from the electro-glottogram, has revealed a double banded male normal voicing reference standard. Forty-eight male larynx cancer patients have been studied by applying this technique in parallel with an unrestricted perceptual analysis before and one year after radiotherapy.

Two thirds of radiotherapy patients had improved voice quality one year after treatment. Approximate entropy increased to reach normal population reference levels. These patients were predominantly in the less aberrant perceptual categories. However, a quarter of patients showed reduced approximate entropy and were predominantly in the most aberrant perceptual categories.

Complexity analysis has the potential to be a reliable, single parameter measure of voicing quality for use in monitoring radiotherapy patient recovery.

Speech and Language Therapists (SALTs) working at the Christie Hospital have been engaged to assess the impact of radiotherapy one year after treatment. A patient's normal voice, prior to the appearance of cancer, is rarely recorded. Hence, SALT subjective assessment reflects experience and the audibility of aberrant voicing. Inevitably this is complicated by differences in clinical technique and opinion [7]. Assessment at the Christie, requires patients to phonate vowels and provide a sample of connected speech. An electro-glottogram (EGG) and acoustic digital recording form the core record of such an examination [8]. The VPAS scheme guides assessment with voice quality eventually binned into a multi-category scale, which, at its most challenging, ranges from 0 (normal) to 6 (severely aberrant). Throughout assessment a SALT knows the phase of treatment reached by the patient, which, along with full knowledge of the stage of the cancer itself and examinations such as endoscopy, inevitably heightens expectations and introduces bias.

Mathematical analysis of the entire range of spectral features in voicing is rarely deployed in the routine cancer clinic. Most disconcertingly there is no definition of what constitutes normal voicing and therefore no scientific or physical reference standard. As a result, it has not been possible to explain how cancer patients subjected to intense vocal fold irradiation during radiotherapy can recover vocal fold functionality to a level that could be considered to be "normal".

This paper shows that vocal fold vibration as evidenced through the EGG impedance time series of vowel phonation can be deployed to differentiate the healthy normal population, quantify cancer patient voicing and to track the pattern of cancer patient recovery following radiotherapy. The approach reported is based on the regularity statistic 'approximate entropy' (ApEn) [9] applied for the first time to detect collective changes across the entire EGG spectral pattern.

I. INTRODUCTION

United Kingdom cancer statistics for 2001 show that the larynx is the site for nearly a third of all 7820 new head and neck cancers and that well over 4 times as many men than women suffered from the disease [1]. Hence, it is as prevalent as cervix cancer in women, though it attracts far less public attention. The five year survival of larynx cancer patients following treatment is good, at approximately two-thirds. Hence, quality of life in terms of voice preservation is important for a large number of individuals wishing to resume normal life.

Radiotherapy arguably has fewer side effects than surgery, which is self evidently more invasive. However, the measure of recovery of voice quality after radiotherapy has not been concisely and objectively quantified. Irradiation effects may leave the targeted tissues intact but they do impact the tissue mechanics and perturb vocal fold functionality for months after treatment [2], which in turn directly influence voice quality [3-6]

II. THEORY

Vowel phonation is predominantly driven by vocal fold vibration. Vocal folds function is impaired by physical damage arising from malignant disease and associated therapy. Fold vibration is accompanied by impedance variations across the thyroid area. These trans-larynx impedance changes can be detected during phonation using a laryngograph. Successive measurements form a time series that usually has a

distinctive waveform structure that is known as the EGG [1,2]. This correlates well with vocal fold vibration and is virtually free from tract resonance. The EGG has not found widespread use amongst SALTs, at least in the UK. Sustained vowel phonation produces a more or less regular EGG waveform, which is ideally suited to characterisation in the frequency domain via the changes seen in the corresponding power spectral pattern [10,11].

To generate an EGG spectrum, the EGG time series are segmented into short frames, stationarised by finite differencing, variance reduced with a suitable function such as the Hanning window, autocorrelated and then fast Fourier transformed. This produces a sequence of frame power spectral density estimate (fPSD) [3]. However, the dynamic effects of fundamental frequency variation from frame to frame need to be removed in order to maximally reveal spectral shape. Therefore, the fPSD are individually normalised relative to the frequency and power of the frame fundamental (F_0) itself. This fundamental harmonic normalisation approach produces what the authors call the FHN-PSD for each frame in which all features are on a common normalised harmonic scale rather than frequency scale [12]. The frame FHN-PSD can then be averaged to reinforce any shared spectral pattern ready for characterisation. A normal individual would be expected to have vocal folds that vibrate most regularly, producing rich harmonic patterns within an envelope showing lengthy decay. If these patterns have common characteristics, and the literature is full of examples, then a suitable form of regularity statistic sensitive to the collective pattern will resolve this into a useful normal population reference standard.

In a single value ApEn quantifies the repeatability of the pattern sampled from a time series itself. No assumptions need to be made about the shape or functional basis of the patterns being sought. Given N data points $\{u(i)\}=u(1),u(2),\dots,u(N)$ and commencing with the i^{th} point, vector sequences $\bar{x}(1)$ to $\bar{x}(N-m+1)$ are formed from m values $\bar{x}(i)=\{u(i),\dots,u(i+m-1)\}$. The Pincus ApEn [9] is interpreted heuristically as a measure of the average logarithmic likelihood, over all sequences $\bar{x}(1)$ to $\bar{x}(N-m+1)$, such that any sequence in the data series $\{u(i)\}$, which is within a tolerance r of the given sequence $\bar{x}(i)$ of length m , remains within the same tolerance when the length of both sequences is increased by one data point. Tolerance r is proportional to the measured series standard deviation σ , i.e. $r = k \sigma$ where k is a constant. It is necessary to determine k empirically so that the widest range of complexity values is achieved. ApEn had been used to study complexity changes in cardiac ECG time series, which show the presence or absence of vital, highly individual feedback mechanisms placing demands on the heart.

ApEn was primarily developed for use in time series analysis and was not used for characterising changes in the spectral pattern, being reserved for comparing fluctuations in a small number of pre-selected peaks. In the realms of speech analysis Moore et al reported the development of a vowel phonation reference standard in for normal males using the ApEn of the truncated FHN-PSD spectral pattern considered collectively [13].

Cancer patients with malignant lesions, possibly infiltrating the vocal folds, would be expected to have abnormal voicing characteristics. However, patients present with cancer in different stages of development and their treatment planned accordingly. Consequently, their vowel FHN-PSDs and corresponding ApEn values might reasonably be expected to vary from nearly normal to completely aberrant. Moore et al [13] have shown that this is indeed the case. Clinical opinion [2] suggests that the most obvious side effects of curative radiotherapy are likely to resolve, leaving stabilised voicing, after one year. In this paper pre-therapy and one year post-therapy ApEn complexities, derived from vowel phonation, are compared. The aim is to identify recovery patterns in male larynx cancer patients, relative to the ApEn reference standard already established for normal males.

III. METHODOLOGY

Eighty-nine male volunteers provided the reference standard for this study. Each subject was connected to an electro-laryngograph and asked to phonate sustained vowel /i/ for up to 4 seconds. The output impedance signal was digitised at a sampling rate of at 20kHz. The digital EGG data files, excluding 4 compromised files, were subjected to ApEn complexity analysis using software written in IDL from Research Systems International (UK). This software first stationarised the time series to remove background noise and mains contamination. The resultant time series were then split into consecutive data frames, each 1000 samples long. The auto-covariance of each frame was computed and the maximum used to determine F_0 . A multiplicative Hanning window was applied to each frame to reduce the variance at high lags before estimating the PSD by fast Fourier transformation. Each frame PSD was then normalised using the FHN approach described by Moore et al [12]. This left the harmonics as integer multiples of the frame F_0 with all other spectral components at non-integer multiples. The frame FHN-PSD were then averaged for each subject. Since, spectral shape variation in and around the normalised F_0 peak is minimal, by design, the averaged FHN PSD was removed below the maximum of the first true harmonic peak, H_2 , and above the maximum of the seventh harmonic peak, H_8 . The logarithm of the truncated FHN PSD was then taken in order to minimise any trend in the spectral pattern. ApEn values were then calculated as described by Moore et al. [13]

Forty-eight male larynx cancer patients attending the Christie Hospital for radiotherapy, volunteered and were consented for approved study. EGG data was collected prior to and one year after radiotherapy and ApEn analysed as described for the normal voicing volunteers. On both occasions each patient was also perceptually assessed by an experienced SALT. No restriction was imposed on the data used for the perceptual assessment, which included acoustic data and access to patient hospital records. Guided by VPAS, the SALT categorised patient voice quality onto a seven point scale ranging from normal (category-0, CAT0) to completely aberrant (category-7, CAT7).

IV. RESULTS

Fig. 1 shows the ApEn complexity distribution for the healthy male normals reported by Moore et al. The bimodal nature of these data was tested by Gaussian mixtures model fitting using maximum likelihood [28]. They concluded ($p < 0.001$) that two normal groups G1 and G2 existed, characterised by complexity values 0.340 (± 0.035) and 0.183 (± 0.057) with relative weights 62% and 38% respectively. Members of G1 exhibited strong EGG FHN-PSD features whilst those in G2 were weak, especially in the higher frequency harmonics.

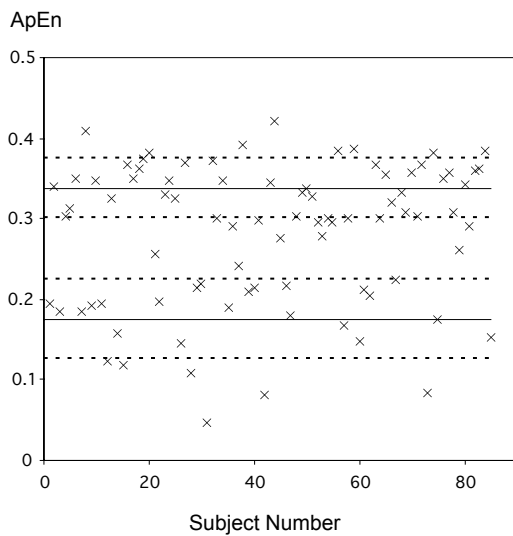


Fig. 1

ApEn (crosses) for normal males. G1 (upper) and G2 (lower) population means are full horizontal lines. Standard deviations are dashed lines above and below.

Fig. 2 and Fig. 3 show the ApEn complexity results for larynx cancer patients measured before and, health permitting, one year after radiotherapy, arranged by pre-treatment SALT perceptual category, CATn ($n=1,2,\dots,7$). Post treatment categorisation is indicated by single digit

numbers placed side-on and above the CAT indication. Dashed boxes indicate the G1 and G2 standard deviation boundaries as a complexity reference standard for normal voicing. Patients showing increased ApEn after treatment appear in Fig. 2 whilst patients showing reduced ApEn appear in Fig. 3. ApEn values before treatment are indicated using circular symbols, whilst triangular symbols indicate those one year post treatment.

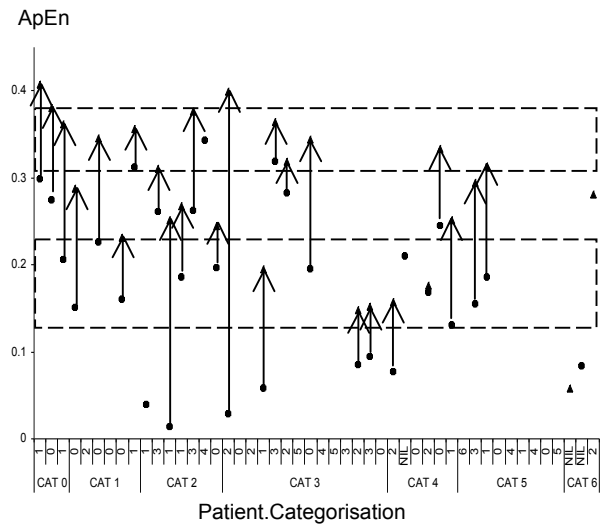


Fig. 2

Patients with increased ApEn 1 year after treatment.

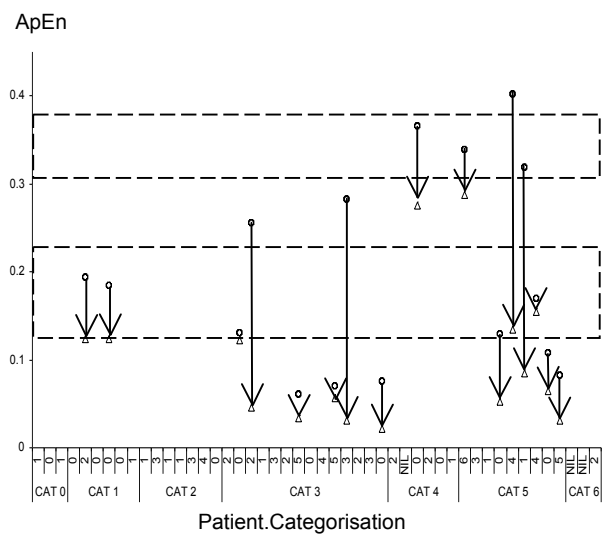


Fig. 3

Patients with decreased ApEn 1 year after treatment.

V. DISCUSSION

Of the 48 cancer cases considered, ApEn analysis indicated that one year after radiotherapy two-thirds would develop improved vocal fold functionality and

the G1 and G2 reference standards). Only one quarter of cases would be below normal voicing bounds and distinctly pathological.

Fig. 2 demonstrates that patients assigned a less aberrant pre-treatment category by SALT perceptual analysis have improved ApEn post treatment. This takes the individual into a normal voicing pattern, with spectral features enhanced at least to the lower level of normality seen in the G2 male population. Those individuals already in the G2 normal band prior to treatment predominantly improve after one year to become members of the ideal G1 population characterised by well developed harmonics in the vowel FHN-PSD.

Fig. 3 shows the converse is true for patients assigned by SALT perceptual analysis to the most aberrant pre-treatment categories. Whilst a handful show almost no change, many deteriorate and actually fall below the normal band defined by the G2 male population.

In 28 cases, the direction of complexity analysis changes agreed with SALTs perceptual assessment. Out of nine cases where the SALT indicated a large improvement, only four showed a corresponding improvement in complexity and five showed a reduction in complexity. The ApEn spectral evidence for these cases prompted SALT re-assessment of three individuals and a reduced categorisation more in line with that suggested by ApEn analysis.

What must not be forgotten, as mentioned in the introduction, is that the direction of change in SALT categorisation is undoubtedly biased since the SALTs must be aware of the patients' details including their treatment stage and pre-treatment categorisation. They expect an improvement in patients' voice quality one-year after radiotherapy. It is plausible that, in the context of SALT dealings with cancer patients, the perceptual definition of normal voicing equates to the lower ApEn, G2 reference standard. This would explain how SALTs could describe post-cancer, post-irradiation individuals as entirely normal in CAT0. These factors could be pursued further if unlabelled recordings were used for normal volunteers and patients taken pre and post treatment.

Most of the differences between SALT perception and ApEn complexity analysis occur in CAT 4-5. The authors believe that where patients present before radiotherapy with poor voicing then it is simply easier to perceptually detect, and as a result overrate, voice improvements. Furthermore, it should be remembered that the utility of perceptual categorisation depends on reliability. In this study there is some evidence, though not conclusive, that perceptual categorisation onto a 7 point scale has a standard deviation of at least 1 bin, i.e. a variation of up to 2 bins, is highly likely.

VI. CONCLUSION

Spectral ApEn complexity analysis of trans-larynx impedance measurements has allowed the recovery pattern of vocal fold functionality and voicing in male radiotherapy cancer cases to be examined. Using a single objective parameter to quantify the collective spectral pattern of vowel phonation, the majority of radiotherapy patients are seen to recover to levels of normality seen in the general, healthy population. Many patients recover to the normal G2 band with its characteristically weak harmonic structures. This probably reflects residual damage that SALTs find entirely acceptable.

REFERENCES

- [1] Cancer-Stats Incidence, *CRUK*, March 2005.
- [2] Benninger, S, Gillen J, Thieme P, et al, 'Factors associated with recurrence & voice quality following radiation therapy for T1 & T2 glottic carcinomas.' *Laryngoscope*, vol. 104(3), pp. 294-8, 1994.
- [3] Hoyt D, Lettinga J, Leopold K & Fisher S, 'The Effect of Head & Neck Radiation Therapy on Voice Quality', *Laryngoscope*, vol.102, pp. 477-480, 1992.
- [4] Moore C, Slevin N, Winstanley S, et al, 'Computerised Quantification & 3D-Visualisation of Voice Quality Changes following Radiotherapy for Carcinoma of the Larynx', *Brit Comp Soc Procs- Current Perspectives Healthcare Computing*, pp. 137-145, 1999.
- [5] Spector J G, Sessions D G, Chao K C et al, 'Stage I (T1, M0, N0) Squamous Cell Carcinoma of the Laryngeal Glottis: Therapeutic Results & Voice preservation', *Head and Neck*, pp. 707-717, 1999.
- [6] Verdonck-De Leeuw I & Koopmans-Van Beinum F, 'The effect of radiotherapy on various acoustical, clinical and perceptual pitch measures', *Procs ICPHS Stockholm4*, pp. 610-613. 1995.
- [7] Baken R & Orlikoff, 'Voice measurement: Is More Better?', *Logopedics Phoniatrics Vocology*, vol. 22:4, pp. 147-151, 1997.
- [8] Fourcin A, 'Electrolaryngographic Assessment of Vocal Fold Function', *Jnl Phonetics*, vol. 14, pp. 435-442, 1986.
- [9] Pincus S M, 'Approximate Entropy as a Measure of System Complexity'. *Proc. Natl. Acad. Sci. USA*, vol. 15; 88 (6), pp. 2297-2301, 1991
- [10] Priestley M, *Spectral Analysis & Time Series*, Academic Press. 1981
- [11] Rabiner L & Schafer R, *Digital Processing of Speech Signals*, Prentice Hall, USA, 1978.
- [12] Moore C, Slevin N & Winstanley S, 'Characterising Vowel Phonation By Fundamental Spectral Normalisation of Lx-Waveforms', *Procs Intl Workshop Models & Analysis of Vocal Emissions for Biomedical Appls*, Florence, Italy, pp. 1-6, 1999.
- [13] Moore C, Manickam K, Willard T et al, 'Spectral Pattern Complexity Analysis & The Quantification of Speech Normality in Healthy & Radiotherapy Patient Groups', *Med Eng Phys*, vol. 26, pp, 191-301, 2004.

A METHODOLOGY TO EVALUATE PATHOLOGICAL VOICE DETECTION SYSTEMS

Nicolás Sáenz-Lechón¹, Juan I. Godino-Llorente², Víctor Osma-Ruiz², Pedro Gómez-Vilda³,
Santiago Aguilera-Navarro¹

¹ Dept. Tecnología Fotónica, E.T.S.I. Telecomunicación, Universidad Politécnica de Madrid,
Ciudad Universitaria, 28040 Madrid (Spain)

² Dept. Ingeniería de Circuitos y Sistemas, Universidad Politécnica de Madrid, Spain.

³ Dept. Arquitectura y Tecnología de Sistemas Informáticos, Universidad Politécnica de Madrid, Spain.

Abstract: This paper describes some methodological issues to be considered when designing systems for automatic detection of voice pathology, in order to allow comparisons with previous or future experiments.

The proposed methodology is built around Kay Elemetrics voice disorders database, which is the only one commercially available. Discussion about key points on this database is included.

Any experiment should have a cross-validation strategy, and results should supply, along with the final confusion matrix, confidence intervals for all measures. Detector performance curves such as DET plots are also considered.

An example of the methodology is provided, with an experiment based on short-term parameters and Multi-layer Perceptrons.

Keywords: Voice pathology detection, pathological voice databases, cross-validation, Multi-Layer Perceptrons.

I. INTRODUCTION

In the last decade there has been a lot of work done on automatic detection and classification of voice pathologies, by means of acoustic analysis, parametric and non parametric feature extraction, automatic pattern recognition or statistical methods. A lot of research groups in speech technology have addressed in some moment these problems. However, there is a lack of uniformity in these approaches that makes very difficult to estate valid conclusions throughout the proposed methods.

As it is impossible to compare results when the experiments are performed with a private database, we have decided to concentrate on works with Kay Elemetrics database [1], which is rather extended. But even when this database was employed in the state of the art, there were many differences in the way the files were chosen and handled. Also, the experiments were carried out with such different criteria, that comparisons were fruitless. We aim to develop a method that allows comparing results from different classifiers and features.

Detection of voice pathology is much related to a speaker verification task, where a candidate sample is compared against two different models (target and impostors vs. normal and pathological). The system must provide a hard decision and a confidence score about to which model belongs the sample. So

we have adopted some methodological issues that are usual in speaker verification [2].

The paper is organized as follows: Section II covers the Kay Elemetrics database and discusses some of its particularities. Section III contains an overview of previous work on pathological voice detection using this database. Sections IV and V present the proposed methodology and describe a simple experiment of detection based upon it. Finally, Section VI presents discussion and conclusions.

II. KAY'S DATABASE OVERVIEW

Kay Elemetrics database [1] was delivered in 1994. It was recorded by the MEEI Voice and Speech Lab. and in Kay Elemetrics. It contains recordings of sustained phonation of vowel /a/ (53 normal and 657 pathological) and continuous speech, (53 normal and 661 pathological). For this description we will focus on the former ones.

The database also includes clinical and personal details of the subjects and acoustic analysis data for the recordings, extracted with the *Multi-Dimensional Voice Program* (MDVP). The recordings were performed in matching acoustic conditions, using *Kay Computerized Speech Lab* (CSL). Every subject was asked to produce a sustained phonation of vowel /a/ at a comfortable pitch at loudness for at least 3 seconds. The process was repeated three times for each subject, and a speech pathologist chose the best sample for the database.

Although the database is the most widespread and available of all the voice quality databases, it has some key points that should be carefully taken into account when used for research purposes:

- Not all the pathological patients have a corresponding recording nor diagnose, and there are some patients with more than one recording, from different visits to the clinic. Fig. 1 shows detailed information about the pathological subset of recordings of vowel /a/.
- The files have different sampling frequencies. Normal and a small percentage of pathological files have 50 kHz, whereas most of the pathological ones have 25 kHz. All files should be down-sampled to 25 kHz before further processing.

- Normal and pathological recordings were made at different locations, assumedly under the same acoustic conditions, but there's no guarantee that this fact has no influence in an automatic detection system.
- Normal subjects were not clinically evaluated, although according to [3], none of them had "complaints or history of voice disorders".
- The files are already edited to include only the stable part of them. Several studies [4] consider that onset and offset parts of the phonation contain more acoustic information than stable parts.
- Normal and pathological files have different lengths, maybe due to the fact that is difficult for some pathological subjects to phonate for a long time. When training automatic models, one has to assure that the length is not used as a parameter for discriminating between classes.
- There is only one phonation per patient. Sometimes is useful to dispose of several samples of the same vowel to model intra-speaker variability or samples of different vowels [5].
- There are a heterogeneous number of pathologies in the database, probably because they were included as they were captured in the clinical practice.
- There are a lot of files labelled with several diagnoses, pertaining sometimes to different categories (e.g. physical and neuromuscular). According to [6], the only mutually exclusive possible categorization is at the highest level (i.e. "normal" and "pathological").
- There are a scarce number of normal recordings, compared to the number of pathological ones. This is a problem for training supervised pattern recognition systems, which work best with large amounts of data and well balanced between the different classes.
- There is no perceptual evaluation of the recordings, which would be very useful for research purposes. For this matter, there should be a similar number of recordings of each perceptual rank.
- There are no video recordings (stroboscopy, endoscopy). The importance of this kind of material is highlighted in [7].
- There are no electroglottographic data with the voice registers. EGG signals have demonstrated to be an important complement for acoustic analysis and detection of pathology [8;9].

	# Visits	# Patients
Pathological data	720	617
With audio recording	657	566
Without diagnosis	306	253
Diagnosis "normal"	6	6
Remainder files	345	307

Fig. 1: Pathological recordings of vowel /a/ in Kay database.

III. PATHOLOGICAL VOICE DETECTION

This section presents an overview of previous works in the literature using Kay Elemetrics database. The objective here is

to concentrate on the way they handle the database and how they design and evaluate the results of the experiments.

In [10], Qi and Hillman employed 48 voices from Kay to test an algorithm to compute a harmonics to noise ratio (HNR) in the spectral domain. They employed some of the original files, not publicly available, before being edited.

In 1998, Cheol-Woo *et al.* [11] proposed two novelty measures, based on the wavelet transform, and compared their discriminative power against some MDVP features.

In her paper of 1998, Wester [12] compared linear regression techniques and hidden Markov models to detect voice pathologies. She employed 36 normal and 607 pathological voices from the running speech files. Some HNR-based features were extracted by acoustic analysis every 10 ms. 80% of the data were used to train the system and the rest were for testing. The word "sunlight" was segmented from each file, and perceptually evaluated by two expert listeners. Results were favourable to HMMs yielding best results of nearly 65% of correct classification rate.

Parsa and Jamieson, in 2000 [3] broached the detection task based on 6 different noise measurements. They employed 53 normal and 173 pathological voices, enumerated in an appendix. All files were down-sampled at 25 kHz, were chosen to have a diagnosis and the age distributions of both groups were similar. They only used the first second in each file. Discrimination results were obtained comparing the histograms of the two classes and ROC curves were employed to compare them. They yield a best accuracy of 98.7%.

Hadjitodorov and Mitev in 2002 [13] describe a system or acoustic analysis of voice, which also allows the automatic detection of pathology, using jitter, shimmer and noise measures. Classification is achieved by means of Linear Discriminant Analysis (LDA) and Nearest Neighbours clustering. They employed 106 normal ("two phonations by each non pathological speaker") and 638 pathological files. The total accuracy of the system was 92.7%.

Dibazar and Narayanan [14] presented some of the best results in pathology detection with this database. They used all the files in the database, along with MDVP parameters, and short-term MFCCs and F0. They classified the voices with HMMs, to achieve a best accuracy of 98.3%, though they don't give many methodological details due to the great amount of experiments broached.

Maguire *et al.*, 2003 [15] propose a pathology detector, based on sustained phonation, combining long-term acoustic, spectral and *cepstral* parameters. They used 58 normal and 573 pathological voices. The classifier was LDA with a 10 folds cross-validation strategy. They achieved 87.16% accuracy with a subset of the MDVP parameters.

Godino *et al.* have several papers using Kay's database. In [16] they employed 53 normal files and 82 pathological files, the latter chosen randomly among the whole database. All files were down-sampled to 25 kHz. The files were short-term parameterised using MFCCs and their derivatives, and the detector system was based on neural networks (MLP and LVQ). The training test was composed with 70% of the files from each class. Results were presented with confusion matrices, providing confidence intervals for the measurements.

Moran *et al.* [6] presented a telephone system for detecting voice pathologies, with the same data and classifying scheme as

[15]. They used 36 short-term parameters based on jitter, shimmer and noise measures. The system yielded 89.1% accuracy for the original data and 74.15% for simulated telephone data.

Marinaki *et al.* [17] implemented a system to distinguish between 21 normal voices and 42 voices with two different pathologies (vocal fold paralysis and edema). Patients had also others pathologies. They use short-term LPC parameters, Principal Components and LDA to classify the voices. Results yielded nearly 85% of accuracy and were presented through ROC curves.

Although all these works represent novel contributions to pathological voice detection or voice quality assessment, using the same database also, their achievements and conclusions are not easily comparable, due to a lack of uniformity when computing and presenting the results.

IV. METHODOLOGY

Having in mind all of the considerations presented in the previous sections, we aimed to develop a fixed methodology for designing experiments to detect pathological voices from normal ones. This method should allow comparisons between different experiments, in order to outline the benefits of each approach.

The first thing to fix is the database. We decided to use Kay Elemetrics', due to its availability. We have considered only a subset of all the possible files, 53 normal and 173 pathological voices, according to [3]. Features sex and age are uniformly distributed between the two classes.

Files are arranged in two sets, one for training and one for testing and validating the results. We have chosen a 70%-30% split for these sets. Feature extraction from the files is accomplished after these sets are built.

Once the system is trained, the test set is employed to estimate the performance of the detector. The final results are presented through confusion matrices (Fig. 2), where we define the next measures: *True positive* (TP) is the ratio between pathological files correctly classified and the total number of pathological voices. *False negative* (FN) is the ratio between pathological files wrongly classified and the total number of pathological files. *True negative* (TN) is the ratio between normal files correctly classified and the total number of normal files. *False positive* (FP) is the ratio between normal files wrongly classified and the total number of normal files. The final accuracy of the system is the sum of TP and TN.

		Actual diagnosis	
		Pathological	Normal
Detector's decision	Pathological	TP	FP
	Normal	FN	TN

Fig. 2: Typical aspect of a confusion matrix. TP, FP, FN and TN stand for True Positive, False Positive, False Negative and True Negative respectively. See text for definitions.

We have adopted a cross-validation scheme, namely the *bootstrap* method [18; chapter 9] to assess the generalization of the model. Each experiment is repeated N times, with a different test set, randomly chosen from the whole set of files. The final

results are averaged across these repetitions, and confidence intervals are computed using the standard deviation of the measures.

When we use short-term parameters, such as MFCCs, accuracies for both frames and files are presented.

During the system testing, a score representing the likelihood of the input vector for belonging to the desired class (i.e. pathological voice) is produced. These scores are compared to a threshold value in order to compute the confusion matrix. If we move this threshold we obtain a set of possible operating points for the system, which can be represented through a *Detector Error Tradeoff* (DET) plot [19], widely used in speaker verification. In this plot, the false positives are plotted against the false negatives, for different threshold values (Fig. 3). Another choice is to represent the false positives in terms of the true positives in a *Receiver Operating Characteristic* (ROC) [20].

V. AN EXAMPLE DETECTOR

The goal of the following experiment is not to improve the results of previous works in the state of the art, but to illustrate the proposed methodology with a brief example. We have designed an automatic system based on 18 short-term MFCCs parameters, following [16], using 20 ms windows with 50% overlapping. The detector is a basic MLP with a hidden layer of 12 neurons. Learning is carried out by backpropagation algorithm with momentum [21, chapter 6]. The input layer has as many inputs as MFCC parameters and the output layer has two neurons.

We repeat the experiment 10 times, combining the files detailed in [3] in the training and test sets randomly. Fig. 3 shows the mean and standard deviation values of the confusion matrix.

		Actual diagnosis	
		Pathological	Normal
Detector's decision	Pathological	91.36±5.34	16.72±5.02
	Normal	8.64±5.34	83.28±5.02

Fig. 3: Results of the classification (in %) given in a frame basis (mean ± std dev).

The total accuracy of the system is 87.49%±2.80. The accuracy on file basis (percentage of recordings correctly classified) is 88.97%±4.12. The DET plot on Fig. 4 shows the overall performance of the detector, the chosen point of operation (marked with a star) and the point of minimum error rate (small circle). The DET is drawn from the scores obtained with the 10 test sets.

VI. CONCLUSIONS

The only way to improve and to profit from others works is to have objective means to measure the efficiency of different approaches. We have described a set of requirements that a detector of voice pathologies should meet to allow comparisons between systems.

As far as we know, there were no previous works in the literature addressing these issues. We intend to continue the research in pathological voice detection and classification using the presented methodology.

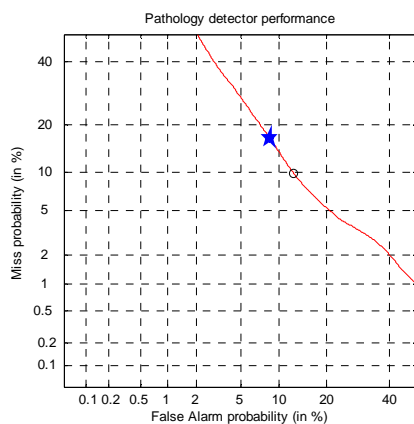


Fig. 4: DET plot for the designed detector.

VII. ACKNOWLEDGEMENTS

This work was supported under the grants: TIC-2003-08956-C02-00 and TIC-2002-0273 from the *Ministry of Science and Technology* and AP2001-1278 from the *Ministry of Education* of Spain.

REFERENCES

- [1] Massachusetts Eye and Ear Infirmary, *Voice Disorders Database, Version.1.03* [CD-ROM], Lincoln Park, NJ: Kay Elemetrics Corp, 1994.
- [2] Campbell, J. P., "Speaker recognition: a tutorial," *IEEE Proceedings*, vol. 85, no. 9, pp. 1437-1462, Sept.1997.
- [3] Parsa, V. and Jamieson, D. G., "Identification of pathological voices using glottal noise measures," *Journal of Speech, Language and Hearing Research*, vol. 43, no. 2, pp. 469-485, Apr.2000.
- [4] de Krom, G., "Consistency and reliability of voice quality ratings for different types of speech fragments," *Journal of Speech and Hearing Research*, vol. 37, no. 5, pp. 985-1000, Oct.1994.
- [5] Horii, Y., "Jitter and shimmer in sustained vocal fry phonation," *Folia Phoniatica*, vol. 37, pp. 81-86, 1985.
- [6] Reilly, R. B., Moran, R., and Lacy, P. D., "Voice pathology assessment based on a dialogue system and speech analysis," in *Proceedings of the American Association of Artificial Intelligence Fall Symposium on Dialogue Systems for Health Communication*, Washington DC, USA, Nov.2004.
- [7] Fröhlich, M., Michaelis, D., and Kruse, E., "Image sequences as necessary supplement to a pathological voice database," in *Proceedings of Voicedata '98*, Utrecht, Netherlands, pp. 64-69, Jan.1998.
- [8] Ritchings, R. T., McGillion, M. A., and Moore, C. J., "Pathological voice quality assessment using artificial neural networks," *Medical Engineering & Physics*, vol. 24, no. 8, pp. 561-564, 2002.
- [9] Childers, D. G. and Sung-Bae, K., "Detection of laryngeal function using speech and electroglottographic data," *IEEE Transactions on Biomedical Engineering*, vol. 39, no. 1, pp. 19-25, Jan.1992.
- [10] Qi, Y. and Hillman, R. E., "Temporal and spectral estimations of harmonics-to-noise ratio in human voice signals," *Journal of the Acoustical Society of America*, vol. 102, no. 1, pp. 537-543, 1997.
- [11] Cheol-Woo, J. and Dae-Hyun, K., "Analysis of disordered speech signal using wavelet transform," in *Proceedings of ICSLP '98*, Sydney, Australia, 1998.
- [12] Wester, M., "Automatic classification of voice quality: comparing regression models and hidden Markov models," in *Proceedings of Voicedata '98*, Utrecht, Netherlands, pp. 92-97, Jan.1998.
- [13] Hadjitodorov, S. and Mitev, P., "A computer system for acoustic analysis of pathological voices and laryngeal disease screening," *Medical Engineering & Physics*, vol. 24, no. 6, pp. 419-429, July2002.
- [14] Dibazar, A. A., Narayanan, S., and Berger, T. W., "Feature analysis for automatic detection of pathological speech," in *Proceedings of the Second Joint EMBS/BMES Conference*, vol. 1, Houston, TX, USA, pp. 182-183, Nov.2002.
- [15] Maguire, C., deChazal, P., Reilly, R. B., and Lacy, P. D., "Identification of voice pathology using automated speech analysis," in *Proceedings of MAVEB A 2003*, Florence, Italy, pp. 259-262, Dec.2003.
- [16] Godino-Llorente, J. I. and Gómez-Vilda, P., "Automatic detection of voice impairments by means of short-term cepstral parameters and neural network based detectors," *IEEE Transactions on Biomedical Engineering*, vol. 51, no. 2, pp. 380-384, Feb.2004.
- [17] Marinaki, M., Kotropoulos, C., Pitas, I., and Maglaveras, N., "Automatic detection of vocal fold paralysis and edema," in *Proceedings of ICSLP '04*, Jeju Island, South Korea, Nov.2004.
- [18] Duda, R. O., Hart, P. E., and Stork, D. G., *Pattern classification*, 2 ed., Wiley Interscience, 2000.
- [19] Martin, A. F., Doddington, G. R., Kamm, T., Ordowski, M., and Przybocki, M. A., "The DET curve in assessment of detection task performance," in *Proceedings of Eurospeech '97*, vol. IV, Rhodes, Crete, pp. 1895-1898, 1997.
- [20] Hanley, J. A. and McNeil, B. J., "The meaning and use of the area under a receiver operating characteristic (ROC) curve," *Radiology*, vol. 143, no. 1, pp. 29-36, Apr.1982.
- [21] Haykin, S., *Neural networks*, New York: Macmillan, 1994.

EFFECTS OF MP3 ENCODING ON VOICE PATHOLOGY DETECTION: RESULTS WITH MFCC PARAMETERS

Nicolás Sáenz-Lechón¹, Juan I. Godino-Llorente², Víctor Osma-Ruiz², Pedro Gómez-Vilda³,
Santiago Aguilera-Navarro¹

¹ Dept. Tecnología Fotónica, E.T.S.I. Telecomunicación, Universidad Politécnica de Madrid,
Ciudad Universitaria, 28040 Madrid (Spain)

² Dept. Ingeniería de Circuitos y Sistemas, Universidad Politécnica de Madrid, Spain.

³ Dept. Arquitectura y Tecnología de Sistemas Informáticos, Universidad Politécnica de Madrid, Spain.

Abstract: This paper presents a performance comparison for a voice pathology detection system dealing with different types of audio data. Several files of sustained phonation of vowel /a/, from Kay Elemetrics database, were encoded with MP3 algorithm with various bit rates (160, 48 and 24 kbps). A multilayer perceptron classifier is then used to automatically detect the normal from the pathologica files. Results are compared with those obtained for the original database, using confusion matrices and DET plots.

There are no significant differences between the designed detectors

Keywords: Voice pathology detection, Multi-Layer Perceptrons, MPEG Audio layer 3 (MP3).

I. INTRODUCTION

There are several studies in the literature dealing with automatic detection of voice pathologies, based on speech databases gathered in matching acoustic conditions, which yielded high accuracy rates [1-3]. Recently, there has been some work done on voice pathology detection under non-ideal conditions, such as [4], where they evaluate the performance of a detector when the voices are transmitted over conventional telephone lines.

In this work, we were interested in studying how MP3 encoding of speech signals affects the capability of a system to detect voice pathologies. MP3 is an interesting format because of its capability for the transmission of speech samples over the Internet or through low speed data channels (like GSM).

The paper is organized as follows: Section II describes the MP3 audio encoding process, Section III presents the database and the speech corpora used in this work. Sections IV to VII describe the detection system. Finally, Section VIII shows the results and Section IX presents some conclusions and discussion.

II. TYPES OF DIGITAL AUDIO CODING

PCM (*Pulse Code Modulation*) [5] is a common method for storing and transmitting uncompressed digital audio. Since it is a generic format, it can be read by most audio applications. PCM is a straight representation of the binary digits (1s and 0s) of sample values.

WAV is the default format for digital audio on Windows PCs. WAV files are usually coded in PCM format, which means they are uncompressed and take up a lot of space (WAV files can also be coded in other formats, including MP3).

MPEG is a working group established under the joint direction of the *International Standards Organisation / International Electrotechnical Commission* (ISO/IEC) to create standards for digital video and audiophonic compression [6]. More precisely, MPEG defines the syntax of audio and video format needing low data rates, as well as operations to be undertaken by decoders. MPEG Audio is based on perceptual encoding techniques, which take advantage of the characteristics of human hearing and remove sounds that most people can't hear. The file extension for the audio layer (layer 3) of a MPEG file is MP3 [7;8]. This layer uses perceptual audio coding and psychoacoustic compression to remove redundant or irrelevant sound signals (Fig. 1). It uses a hybrid filter bank which consists of a polyphase filter and a *Modified Discrete Cosine Transform* (MDCT), to increase the resolution of the frequency at certain bands.

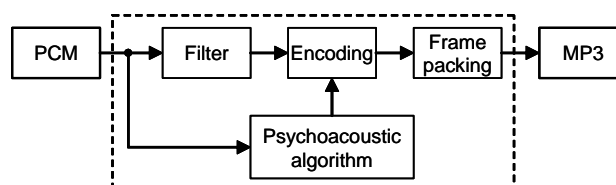


Fig. 1: Basic scheme of the MP3 encoding process.

The encoder first divides the signal into multiple sub-bands, so the encoded signal can be better optimized to the response of the human ear. Sounds below the threshold of hearing at each band can be removed by the encoder. Furthermore, the ear is most sensitive to frequencies between 2 kHz and 4 kHz, so less information can be removed from this range without affecting the quality of the sound. Moreover, quiet sounds are “masked” by louder sounds that are close to them in frequency and time. Since you can’t hear these sounds, they can be removed from the signal without affecting the perceived quality. MPEG encoders rely on the resolution used in the uncompressed audio file to set the range of resolution that will be used for the encoded file. The resolution of the encoded file is varied according to the complexity of the signal to achieve compression.

III. DATABASE

Kay Elemetrics database [9] was employed for this work, due mainly to its availability. It was recorded by the *Massachusetts Eye and Ear Infirmary Voice and Speech Lab.* and contains recordings of sustained phonation of vowel /a/ (53 normal and 657 pathological). We have considered only a subset of all the possible files, 53 normal and 173 pathological voices, according to [10]. This decision was adopted in order to avoid recordings without a diagnosis and because the selected files form a compact set: features sex and age are uniformly distributed between the two classes. The files were down-sampled to 25 kHz when necessary.

Based on these files, we have established four different corpora of voices for the experiments (Fig. 2). The first one comprises the original files, recorded in the standard WAV format. The three other sets were created through MP3 encoding of the former files, with different bit rates (160 kbps, 48 kbps and 24 kbps). For subsequent processing, the files were decoded back to WAV format.

#	Original (wav)	Mp3 encoding	Decoding (wav)
1	25 kHz; 16 bits	—	—
2	25 kHz; 16 bits	24 kHz; 160 kbps	24 kHz; 16 bits
3	25 kHz; 16 bits	24 kHz; 48 kbps	24 kHz; 16 bits
4	25 kHz; 16 bits	24 kHz; 24 kbps	24 kHz; 16 bits

Fig. 2: Summary of the four speech corpora used in this work.

IV. FEATURE EXTRACTION

It is well known that the acoustic signal contains information about the vocal tract and the excitation source. The idea for this research was to use a short-term non-parametric approach to model the effects of pathologies on both the excitation (vocal folds) and the

vocal tract. The feature extraction procedure (Fig. 3) is described in the next paragraphs.

The speech recordings are divided into 20 ms frames, applying a Hamming window to smooth the extremes. Windows are overlapped every 10 ms. At this point, the frames corresponding to silence or unvoiced fragments of speech are detected and marked for subsequent removal.

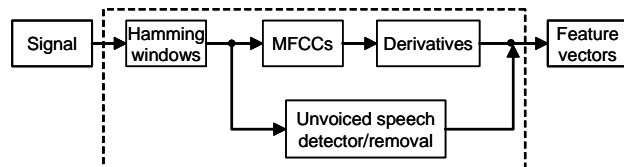


Fig. 3: Overview of the feature extraction procedure.

Afterwards, several mel cepstral coefficients are estimated from each frame using a non-parametric FFT-based approach. MFCC parameters [11;12] are obtained calculating the discrete cosine transform (DCT) over the logarithm of the energy in several frequency bands, disposed in the “mel scale”. The number of bands is $M = \text{round}(4 \cdot \ln(\text{sampling frequency}))$.

Each band in the frequency domain is bandwidth dependant of the central frequency of the filter. The higher the frequency, the wider is the bandwidth. Such method is based on the human perception system, establishing a logarithmic relationship between the real frequency scale (Hz) and the perceptual frequency scale (mels) (Eq. 1).

$$F_{mel} = 2595 \cdot \log_{10} \left(1 + \frac{F_{Hz}}{700} \right) \quad (1)$$

A better representation of the dynamic behaviour of speech can be obtained by including the first temporal derivatives of the parameters among neighbour frames [12]. The first derivative (delta) provides information about the dynamics of the time-variation in MFCC parameters. Their calculation is achieved by means of anti-symmetric moving-average Finite Impulse Response (FIR) filters to avoid phase distortion of the temporal sequence.

The number of MFCCs parameters considered in this work ranges from 12 to 32 in order to find the optimal dimensionality for our purposes.

After the calculation of features, vectors corresponding to silence or unvoiced sounds are removed. The total number of vectors obtained from the files is nearly 32,000 (15,000 normal; 17,000 pathological).

V. THE ANN DETECTOR

Artificial neural networks (ANN) have been widely used in pattern recognition and voice pathology detection. A feedforward multilayer perceptron (MLP) with a single hidden layer has been chosen for this purpose. The

learning algorithm used is *backpropagation with momentum* [13, chapter 6].

The input layer has as many inputs as MFCCs parameters. The output layer has two neurons that map their outputs to a value in the range [0, 1] by means of a sigmoid function (Eq. 2).

$$f(x) = \frac{1}{1 + e^{-x}} \quad (2)$$

The network is trained by successive iterations of the algorithm, reducing the mean squared error over the training set. Generalization of the learning is assessed with the test set.

VI. EVALUATION PROCEDURE

Files are arranged in two sets, one for training and one for testing and validating the results. We have chosen a 70%-30% split for these sets. Feature extraction from the files is accomplished after these sets are built. The vectors of the training set are normalised in the range [0, 1]. The same transformation is then applied to the test set.

Once the system is trained, the test set is employed to estimate the performance of the detector. The final results are presented through confusion matrices (Fig. 4), where we define the next measures: True positive (TP) is the ratio between normal files correctly classified and the total number of normal voices. False negative (FN) is the ratio between wrongly classified normal files and the total number of normal files. True negative (TN) is the ratio between pathological files correctly classified and the total number of pathological files. False positive (FP) is the ratio between pathological files wrongly classified and the total number of pathological files. The final accuracy or correct classification rate (CCR) of the system is the average of TP and TN.

		Actual diagnosis	
		Normal	Pathological
Detector's decision	Normal	TP	FP
	Pathological	FN	TN

Fig. 4: Typical confusion matrix. TP, FP, FN and TN stand for True Positive, False Positive, False Negative and True Negative respectively. See text for definitions.

We have employed a cross-validation scheme, namely the *bootstrap* method [14; chapter 9] to assess the generalization of the model. Each experiment is repeated 10 times, with a different test set, randomly chosen from the whole set of files. The final results are averaged across these repetitions, and confidence intervals are computed using the standard deviation of the measures. Accuracy for both frames and files is presented.

During the system testing, a score representing the likelihood of the input vector for belonging to the desired class (i.e. pathological voice) is produced. These scores are compared to a threshold value in order to compute the confusion matrix. If we move this threshold we obtain a set of possible operating points for the system, which can be represented through a Detector Error Tradeoff (DET) plot [15], widely used in speaker verification. In this plot, the false positives are plotted against the false negatives, for different threshold values (Fig. 7).

VII. RESULTS

For each one of the speech corpora, several experiments were performed in order to achieve the best possible combination of input features (different number of MFCC parameters, with and without derivatives) and neural network parameters (different number of nodes in the hidden, learning rates, etc.).

Fig. 5 presents a summary of best results for the different corpora (wav and mp3, with different bit rates) given in a frame basis. Fig. 6 shows the corresponding results on a file basis.

Corpus	Features	Confusion matrix	
1	16 MFCC + delta 20 neurons	83.34±4.32	9.30±3.37
		16.66±4.32	90.70±3.37
		CCR: 87.38±1.81	
2	16 MFCC + delta 10 neurons	85.01±7.81	12.12±4.26
		14.99±7.81	87.88±4.26
		CCR: 86.51±3.67	
3	20 MFCC + delta 14 neurons	83.28±7.71	10.54±2.91
		16.72±7.71	89.46±2.91
		CCR: 86.53±4.30	
4	28 MFCC + delta 16 neurons	79.24±8.96	±3.99
		20.76±8.96	89.50±3.99
		CCR: 84.67±4.87	

Fig. 5: Results of the classification (in %) given in a frame basis (mean ± std dev) for the different corpora.

Corpus	Features	CCR
1	16 MFCC + delta; 20 neurons	87.79±2.86
2	16 MFCC + delta; 10 neurons	87.5±4.06
3	20 MFCC + delta; 14 neurons	87.94±4.21
4	28 MFCC + delta; 16 neurons	86.76±4.80

Fig. 6: Results of the best correct classification rate (in %) given in a file basis (mean ± std dev) for the different corpora.

Fig. 7 shows four DET plots that represent the averaged individual systems described in Figs. 5 and 6. The curves are drawn from the scores obtained with the 10 test sets of each experiment.

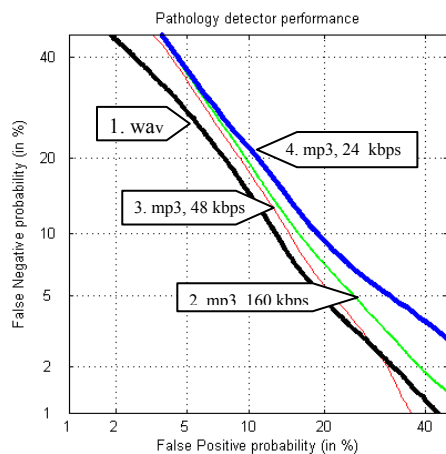


Fig. 7: DET plots comparing the performance of the averaged systems.

VII. CONCLUSIONS

As it can be seen from Fig. 7, the performance of the original WAV files seems to be better than the mp3. But if we considered the confidence intervals, as reflected in Fig. 5 by the standard deviations, we must conclude that there are no significant differences between such systems.

MP3 coding transforms the energy in bands in a similar way than MFCCs. The part of the signal that is lost due to the compression seems to be not significant for pathology detection. Performance with MP3 may be somewhat inferior to that with the original WAV files, but MP3 needs less storage space.

More experiments have to be carried out to confirm this conclusion. We have to test also the performance of this detector with maximum MP3 compression (bit rate of 8 kbps).

VII. ACKNOWLEDGEMENTS

This work was supported under the grants: TIC-2003-08956-C02-00 and TIC-2002-0273 from the Ministry of Science and Technology and AP2001-1278 from the Ministry of Education of Spain.

REFERENCES

[1] Gavidia-Ceballos, L. and Hansen, J. H. L., "Direct speech feature estimation using an iterative EM algorithm for vocal fold pathology detection," *IEEE Transactions on Biomedical Engineering*, vol. 43, no. 4, pp. 373-383, Apr.1996.

[2] Godino-Llorente, J. I. and Gómez-Vilda, P., "Automatic detection of voice impairments by means of short-term cepstral parameters and neural network based

detectors," *IEEE Transactions on Biomedical Engineering*, vol. 51, no. 2, pp. 380-384, Feb.2004.

[3] Ritchings, R. T., McGillion, M. A., and Moore, C. J., "Pathological voice quality assessment using artificial neural networks," *Medical Engineering & Physics*, vol. 24, no. 8, pp. 561-564, 2002.

[4] Reilly, R. B., Moran, R., and Lacy, P. D., "Voice pathology assessment based on a dialogue system and speech analysis," in *Proceedings of the American Association of Artificial Intelligence Fall Symposium on Dialogue Systems for Health Communication*, Washington DC, USA, Nov.2004.

[5] ITU G.711 (11/88). Pulse code modulation (PCM) of voice frequencies. 1988.

[6] "Audio & multimedia MPEG audio layer 3," *Fraunhofer Institute for Digital Media Technology*, available at <http://www.iis.fraunhofer.de/amm/techinf/layer3/index.html>, 2005.

[7] ISO/IEC 11172-3. ISO-MPEG Audio Layer-3. Information technology - Coding of moving pictures and associated audio for digital storage media at up to about 1,5 Mbit/s. Part 3: Audio. 1993.

[8] ISO/IEC 13818-3. Generic coding of moving pictures and associated audio information. Part 3: Audio. 1998.

[9] Massachusetts Eye and Ear Infirmary, *Voice Disorders Database, Version.1.03* [CD-ROM], Lincoln Park, NJ: Kay Elemetrics Corp, 1994.

[10] Parsa, V. and Jamieson, D. G., "Identification of pathological voices using glottal noise measures," *Journal of Speech, Language and Hearing Research*, vol. 43, no. 2, pp. 469-485, Apr.2000.

[11] Davis, S. B. and Mermelstein, P., "Comparison of parametric representations for monosyllabic word recognition in continuously spoken sentences," *IEEE Transactions on Acoustics, Speech and Signal Processing*, vol. 28, no. 4, pp. 357-366, Aug.1980.

[12] Rabiner, L. R. and Juang, B. H., *Fundamentals of speech recognition*, Englewood Cliffs, NJ: Prentice Hall, 1993.

[13] Haykin, S., *Neural networks*, New York: Macmillan, 1994.

[14] Duda, R. O., Hart, P. E., and Stork, D. G., *Pattern classification*, 2 ed., Wiley Interscience, 2000.

[15] Martin, A. F., Doddington, G. R., Kamm, T., Ordowski, M., and Przybocki, M. A., "The DET curve in assessment of detection task performance," in *Proceedings of Eurospeech '97*, vol. IV, Rhodes, Crete, pp. 1895-1898, 1997.

TOWARDS A CLASSIFICATION OF PHONATORY FEATURES OF DISORDERED VOICES

J. Schoentgen

National Fund for Scientific Research, Belgium

Department "Signals and Waves", Faculty of Applied Sciences, Université Libre de Bruxelles, Brussels
jschoent@ulb.ac.be

The purpose of the presentation is to give an overview of phonatory features of disordered voices and propose a classificatory framework. Generally speaking, phonatory features are numerical cues that summarize properties of speech signals or other voice-related signals that are obtained non-invasively, and which are clinically relevant. The object of a classificatory framework is to ease the planning of future experiments and the exploitation of the existing literature, which is diverse with regard to pathologies studied, speaker tasks, speaker performance, speech material, vocal symptoms, sensors and sought for relations with other levels of description.

I. INTRODUCTION

The purpose of the presentation is to give an overview of phonatory features of disordered voices and propose a classificatory framework. Generally speaking, phonatory features are numerical cues or measurements that are clinically relevant and that summarize properties of speech signals or other signals that are obtained non-invasively, and which report on a speaker's voice. Typically, the acquisition of phonatory features involves the (non-invasive) recording of signals that are relevant to laryngeal function, the signal processing that discards irrelevant signal properties and the summary of the clinically-relevant properties by means of a handful of numbers.

The purpose of the extraction of phonatory features in a clinical framework is the documentation of the voice of patients, their longitudinal follow-up during treatment (e.g. before and after surgery) as well as comparisons with normophonic speakers.

The goal of the presentation is not to discuss a classification of the mathematical forms of clinical cues per se. This would be an ineffectual exercise because most of the extant features are heuristically defined and their mathematical or statistical properties have been explored superficially only. The goal is rather to classify phonatory cues in relation to the use they have been put to.

Indeed, the scientific as well as clinical literature devoted to phonatory features of voice disorders is abundant. However, its diversity is impressive with regard to the pathologies or handicaps that have been studied, the vocal symptoms that have been described, the vocal tasks speakers have been asked to carry out and the linguistic, paralinguistic and extralinguistic performances that have been examined, the sensors that have been used and the speech material that has been recorded, as well as the correlations that have been examined.

As a consequence, it is difficult to distil general rules or compare results obtained in different frameworks. The purpose of a classification is therefore to ease the planning of future experiments and the exploitation of the existing literature.

II. CLASSIFICATORY FRAMEWORK

The following is a proposal of a grid that may be used to classify different feature-based approaches to the assessment of voice disorders.

Etiology

The types of pathologies or handicaps the effects on voice of which have been investigated are wide and varied. Typically, one distinguishes voice problems that are the consequences of organic alterations of the vocal folds from those that are dysfunctional, i.e. voice disorders that are not the consequence of observable structural changes of the vocal folds [1]. Voice problems caused by motor disorders are a third category. An example of the latter is the voice of Parkinson speakers. A separate category are substitution voices, the purpose of which is to enable speech communication by speakers who have lost the capacity of producing voice by means of the vibration of the true vocal folds.

Whether voice disorders that have different causes must be described by different sets of phonatory features is not clear at present. Generally speaking, speech and voice problems owing to motor disorders are kept separate from voice disorders that are the consequence of laryngeal pathologies [6]. A possible exception is vocal fold paralysis.

Speech material

One major distinction between approaches to voice assessment rests on the speech material. Indeed, the speech material that is analyzed may be connected speech or sustained speech sounds. Sustained speech sounds may again be subdivided according to whether onsets and offsets are included in the analysis frame or not. Connected speech is often presented as ideal; analyses of stationary speech fragments are the rule, however [5]. The reason is that many signal processing schemes are based on assumptions of local stationarity and local periodicity. These assumptions may not be valid in the case of hoarse speakers emitting connected speech [2].

Speaker tasks

Tasks refer to what is requested from a speaker during vocal assessment. Tasks that subjects are the most frequently asked to carry out are speaking, which includes sustaining speech sounds, singing (when appropriate), vocal loading, as well as profiling.

Vocal loading consists in recording the phonatory features of a speaker, followed by reading out loud a text for some time (e.g. 45 minutes) and recording the same features again. The purpose is to track vocal alterations that are the consequence of burdening the larynx [7].

Finally, profiling is the discovery of the limits of phonatory performance, e.g. loudest possible voice, softest possible voice, highest possible pitch, lowest possible pitch, maximum phonation time, etc [9].

Speaker performance

Speaker performance refers to the actual capacity that is examined. Phonatory performance may be subdivided into registers, phonation types, voicing, prosody and vocal quality.

Known speech registers are creak, modal voice and falsetto. Examples of phonation types are breathy voice, soft voice, modal voice, loud voice, pressed voice and so forth [3].

Voicing is the capacity of the speaker to voice and un-voice speech sounds. Prosody refers to the capacity to control intonation, accentuation, and rhythm, as well as speech rate. Voice quality, finally, designates vocal timbre, e.g. hoarseness, roughness, vocal tremor or quaver, and so forth.

Instrumentation

Instrumentation refers to the equipment that is used to obtain signals non-invasively that report on the phonatory performance of speakers. The microphone signal is the most often used; it evolves proportionally to acoustic pressure and therefore proportionally to the speech signal that is recorded by the ear of a listener. Other signals that can be obtained non-invasively are the electroglottogram and photoglottogram. The former is reported to evolve proportionally to the vocal fold contact surface and the latter to the glottal area. One other sensor that is used frequently is the flow mask that enables recording airflow rate, as well as, occasionally, intra-oral pressure.

Signals

One major distinction is the one between features that describe the phonatory source signal and those that describe the speech signal. The phonatory signal is the acoustic signal that is generated at the glottis via the vibration of the vocal fold and pulsatile airflow. The speech signal is emitted at the mouth consequent to the propagation of the acoustic wave through the vocal tract. Observing the glottal source signal directly is difficult. Often, it is replaced by auxiliary signals such as the photoglottographic or electroglottographic signals that report on glottal properties directly.

Transform domains

At present, a systematic classification of clinical signal processing schemes is not possible because most schemes involve a heuristic processing stage that may differ from task to task and from study to study.

A possible processing-related categorization is based on the type of signal transform that is involved. Examples are Fourier, Hilbert or Wavelet transforms. When no signal transformation is carried out, the corresponding phonatory features are temporal; otherwise they acquire properties that are typical of the corresponding transform domains [8].

Vocal symptoms

One core distinction between phonatory features is the one that pertains to vocal symptoms. Vocal symptoms are the speech properties that are believed to be clinically relevant, that report on the state of the glottis and that the signal processing is aimed at. Typically one distinguishes between signal dysperiodicity,

signal morphology, and supra-segmental as well as coordinative features.

Coordinative features refer to the onset and offset of voicing in relation to supra-glottal events. Examples of relevant supra-glottal events are obstruent check and release or resonant onset and offset. The most often studied coordinative cue is vocal onset time, which is the signed time interval between the release of an obstruent and the onset of voicing, on which hinges the distinction between voiced and unvoiced obstruents. This language-typical interval, which may be short, requires a fine control of glottal adduction and abduction with regard to supra-glottal articulation. Voice onset time is therefore frequently studied in relation to motor speech disorders or substitution voices, which are suspected to impede fine control of voicing [10].

Supra-segmental features pertain to intonation, accentuation, rhythm, speech rate as well as average phonatory frequency, the variability of the phonatory frequency, and average loudness, i.e. sound pressure level. In a clinical framework, speech rate, the average and spread of phonatory frequency, as well as sound pressure level are the most popular.

Morphological features refer in practice to the shape attributes of the glottal source signal. Examples are the open quotient, closing quotient, speed quotient, the amplitude of the volume velocity as well as the amplitude of the negative peak of the differentiated volume velocity [3]. An example of a spectral morphological feature is the spectral balance, which quantifies harmonic richness. Morphological features have been mainly used to characterize phonation types.

Morphological, supra-segmental as well as coordinative features are not confined to clinical applications. These features have been widely studied by phoneticians, linguists, psychologists and engineers because they report on speech and voice production as well as perception in general.

Features that are typically clinical are those that describe irregularities of the movement of the vocal folds. Generally speaking, one distinguishes between non-modal vibratory regimes that cause diplophonia, biphonation and random cycles, and external perturbations (i.e. modulation noise), turbulence noise and breathiness (i.e. additive noise), unsolicited vibrations of the false vocal folds or ary-epiglottal folds, as well as uncontrolled transients, such as voice breaks, register breaks, octave jumps and so forth.

External perturbations give rise to vocal jitter and shimmy, as well as vocal frequency and amplitude tremor. The main contribution to shimmy and amplitude tremor of the speech

cycles is the modulation distortion by the vocal tract of phonatory jitter and phonatory frequency tremor. Other causes are the transfer of acoustic energy from cycle to cycle, as well as tremor of the speech articulators. Phonatory shimmy or phonatory amplitude tremor contribute only feebly to speech shimmy or speech amplitude tremor [4].

Correlation

More often than not, clinicians attempt to correlate observed acoustic features with data recorded at other levels of description. Data, correlations with which are sought for, are typically diagnostic, glottal, aerodynamic or perceptual, with a preference for the latter.

III. KNOWN PROBLEMS

Known problems with extant phonatory features are the following.

Signal processing

The most popular acoustic features are those that quantify the degree of irregularity of the vocal cycles. Typical examples are the period perturbation quotient, amplitude perturbation quotient, jitter in %, harmonics-to-noise ratio and so forth. More often than not, the signal processing involves methods that are based on assumptions of local stationarity and local periodicity that enable heuristics to detect and isolate vocal cycles or spectral harmonics. These heuristics may fail in the case of severely hoarse voices. As a consequence, insertion or omission errors are frequent in the case of highly irregular signals. These errors bias the values of the calculated features. As a consequence, phonatory features that describe vocal perturbations are thought to be reliable only when extracted from sustained speech sounds uttered by feebly or moderately hoarse speakers.

Another issue is measurement precision. Indeed, perturbations of cycle length may be small, e.g. less than one percent for speech cycle lengths, less than ten percent for speech cycle amplitudes. As a consequence, signal processing request precautions with regard to measurement precision. Otherwise, measurements may be biased by quantization noise, for instance.

Labelling

Labelling refers to the custom of giving phonatory features names that allude to vocal symptoms rather than to the measurements that are actually performed. For instance, features

that summarize the dysperiodicity of glottal cycle lengths are often referred to as vocal jitter, although cycle length dysperiodicity may also be influenced by average phonatory frequency, additive noise, frequency tremor, non-modal dynamic regimes of the vocal folds and non-flat intonation, for instance.

Redundancy

The number of phonatory features that have been proposed in the literature is large. Software that is sold for clinical assessment of voice typically comprises tens of numerical cues that can be computed for a single sustained sound. Studies have shown that sub-sets of phonatory features are correlated with each other. Sub-sets of correlated features are roughly coextensive with the groups of vocal symptoms that are discussed above [5].

Interpretation

Even very simple measurements are influenced by multiple factors. Examples are given above for the perturbations of the speech cycle lengths, as well as for the perturbations of the speech cycle amplitudes, which are generated via modulation distortion. These observations suggest that phonatory features are difficult to interpret because they are determined by multiple causes that may be interdependent.

Stationary fragments of sustained speech sounds

One of the more frequently heard complaints is that many acoustic cues can only be obtained reliably for stationary fragments of sustained speech sounds. The reasons have been discussed in the section on signal processing. A consequence is that, at present, the effects of voice disorders on connected or natural speech are less well understood. Problems that are non-resolved are not only issues in signal processing, but also the choice of the phonatory features, the choice of speech material, as well as the perceptual assessment of connected speech fragments that are short or phonetically complex.

IV. SUMMARY

The following Table summarizes some of the factors that distinguish different approaches to voice assessment.

Etiology	organic, dysfunctional, and motor disorders, substitution voices
Transforms	Fourier, Hilbert, and Wavelet transforms (if applicable)
Signals	glottal source, speech signal

Material	connected speech, sustained speech sounds, stationary fragments of sustained speech sounds
Symptoms	dysperiodic, morphologic, supra-segmental, coordinative
Tasks	speaking, singing, loading, profiling
Performance	registers, phonation types, voicing, prosody, voice quality
Sensors	microphone, electroglottograph, photoglottograph, flow mask

REFERENCES

The synthetic description of feature-based vocal assessment that is given here rests on a large number of articles, which cannot be listed because of lack of space. References that are cited below are only pointers to further reading.

[1] Boone D., McFarlane S. (1996) *The voice and voice therapy*, Prentice Hall, NJ.

[2] Bettens F., Grenez F., Schoentgen J. (2005) Estimation of vocal dysperiodicities in disordered connected speech by means of distant-sample bidirectional linear predictive analysis, *J. Acoust. Soc. Am.*, 117, 1, 328-337.

[3] Alku P., Vilkman E. (1996) A comparison of glottal voice source quantification parameters in breathy, normal and pressed phonation of female and male speakers, *Folia Phoniatica et Logopaedica*, 48, 240-254.

[4] Schoentgen J. (2003) Spectral models of additive and modulation noise in speech and phonatory excitation signals, *J. Acoust. Soc. Am.*, 113, 1, 553-562.

[5] Dejonckere Ph., Remacle M., Fresnel-Elbaz E., Woisard V., Crevier-Buchman L., Millet B. (1996) Differential perceptual evaluation of pathological voice quality: reliability and correlations with acoustic measurement, *Rev. Laryngol. Otol. Rhinol.*, 117, 3, 219-224.

[6] Till J., Yorkston K., Beukelman D. (1994) *Motor speech disorders – Advances in assessment and treatment*, Brookes Publ., Baltimore.

[7] Vilkman E., Lauri E., Alku P., Sala E., Sihvo M. (1999) Effects of prolonged oral reading on F0, SPL, sub-glottal pressure and amplitude characteristics, *J. Voice*, 13, 2, 303-315.

[8] Baken R., Daniloff R. (1991) *Readings in clinical spectrography of speech*, Singular Publ., San Diego.

[9] Heylen L., Wuyts F., Mertens F., De Bodt M., Van de Heyning P. (2002) Normative voice range profiles of male and female professional voice users, *J. Voice*, 16, 1, 1-7.

[10] Ziegler W., Deger K. (1998) *Clinical Phonetics and Linguistics*, Whurr Publ., London, 435-449.

INTELLIGENT VOICE QUALITY ASSESSMENT POST-TREATMENT USING GENETIC PROGRAMMING

Walaa Sheta¹, Tim Ritchings² & Carl Berry²

¹Mubarak City for Scientific Research,
Burg El-Arab, Egypt
wsheta@mcit.gov.eg

²School of Computing, Science and Engineering,
University of Salford, UK

Abstract: Objective techniques for assessing and classifying voice quality for patients recovering from treatment for cancer of the larynx have largely focussed on their use of Artificial Neural Networks (ANN). The results of a preliminary study are reported, where a Genetic Programming (GP) has been trained to classify recovered (normal) and abnormal voices in acoustic data, and produced much more accurate results than an ANN. In addition, the GP is able to provide impact factors for the various voice parameters, and suggests that only 6 of the 22 short-term and long-term parameters used in the current ANN studies are contributing significantly to the classifications.

Keywords: Voice quality, classification, Artificial Neural Network, Genetic Algorithms, acoustic signals.

I. INTRODUCTION

The use of intelligent computer-based techniques to support decision making in clinical applications, have been investigated over the years for a wide variety of clinical data. Although Genetic Programming (GP) has not been used extensively for medical applications to date, the early results for cancer diagnosis [1,2] were found to be better than with an Artificial Neural Network (ANN). In another study [3], a grammar-based GP variant was used for knowledge extraction from medical databases, where the rules for the diagnosis were derived from an algorithm that uncovers relationships among data attributes. The outcomes of different types of classifiers, including ANNs and genetic programs have also been reported [4].

This study is part of a larger project which is concerned with developing objective techniques for voice quality assessment in patients recovering from cancer of the larynx. The earlier investigations have concentrated on the use of Artificial Neural Networks (ANN) to firstly distinguish recovered (normal) and abnormal voices [5] on the basis of a collection of short-term and long-term parameters derived from the

patient's voice signals, and more recently, classify voices on the 7-point scale for voice quality used by Speech and Language Therapists (SALT) in the UK [6]. Similar classifications have now been obtained for both electrical impedance (EGG) and acoustic data, with the best results for voices in the extremes categories on this scale (normal and abnormal), while those for the mid-categories have been poor [7].

A preliminary assessment of use of Genetic Programming to classify normal (recovered) and abnormal acoustic signals is described here. The resulting classifications are compared with those obtained from an ANN for the same signal parameters and training regimes..

II. TREATMENT OF VOICE SIGNALS

A. Collection of Voice Signals

The patient's voice data was collected by the Christie Hospital and the South Manchester hospital using an electrolaryngograph PCLX system [8]. The equipment simultaneously records the electrical impedance signal via pads placed at specific positions on the patient's neck at the same time as the acoustic voice signal using a microphone. In these studies, the patient was attempts to steadily phonate the /i/ sound. Although two datasets are collected, only the acoustic data have been used to date in this study. In the work only the male voices were used as the number of female voices in the dataset was too small to give an accurate assessment, a feature of the dataset is that most cancer of the larynx patients are male.

Voice quality was subjectively classified by a SALT for each patient using their standard 7-point classification scale ranging from Lx0-Lx6, with Lx0 being a near normal (recovered) voice while Lx6 represents an abnormal, very poor quality voice. The approach taken to reach a classification is very subjective and depends to a large extent on the experience of the SALT. In this study the Lx0 and Lx1 voices were combined and considered as the normals, while Lx5 and Lx6 voices were combined to give the abnormal, The number of patients in these two categories is shown in Table 1.

Normal (Lx0,Lx1)	Abnormal (Lx5,Lx6)
58	36

Table 1. Patient numbers used in this study

B. Signal Pre-processing

In order to be able to extract the short and long term parameters used in the classification process, a number of pre-processing stages were applied to the voice signals. Initially the signals were stationarised to remove drift, split into 50 ms frames (Hanning windows overlapping by 25 ms) and then converted to the autocorrelation form of the signal to remove some of the noise components. Once these processes were complete, the frames were examined to check if they contained silence or sound. This involved comparing the frames with a sample of silence frame recorded under the same conditions, and used zero point crossing and short term amplitudes as checks. Once the silence frames have been removed, the remaining frames were separated into voiced and unvoiced frames; voiced frames containing vocal phonation while unvoiced containing no recognisable speech. This was achieved using the cepstrum based approach as described in [9]. The Fundamental Harmonic Normalisation (FHN) as described in [10] was then calculated from Power Spectrum Density (PSD) and then this structure was modelled by fitting a Gaussian Mixture Model (GMM) in order to reduce the number of parameters needed to describe the signal.

C. Parameter Extraction

A total of 22 short-term and long-term parameters are extracted for use with classification, as detailed in [5,6]. The short term parameters consist of 15 parameters relating to the mean, standard deviation and peak of the gaussians used to describe the fundamental frequency and first four harmonics in the frame (if they can be detected) ($M_{0.4}$, $SD_{0.4}$, $P_{0.4}$); the value of the fundamental frequency in each frame (F_0), the noise threshold value (N_0), the FHN Noise Energy (FHNNE) and the Residual Harmonic Energy (RHE). The 3 long-term parameters were extracted from the speaker's whole voiced speech. These included the mean fundamental frequency across all frames (MF_0), a measure of jitter of the fundamental frequency between frames (J_0) and the ratio of voiced to unvoiced frames (VS).

D. The GP classification technique

Linear Genetic Programming was used to classify the normal and abnormal voices. An experiment with 7

runs was performed using this technique, the runs only differing in their choice of a random seed. The common parameter settings used in the experiment are given in Table 2.

Parameter	Value
Population size	512
Max no of tournaments	150000
Mutation frequency	30
Crossover frequency	30
Max program size	256
Instruction set	+ - * / sin() log()

Table 2. Parameter settings for the GP

All 22 short-term and long-term parameters were extracted from the voice signals and used for classification. The dataset was split into a training (65%) and test (35%) set, which equated to 38/20 for the normals and 23/13 for the abnormals.

E. The ANN classification technique

The same 22 parameters were used for the GP classification and the same 65/35% split for the training and test data sets. In this case, the parameters were input to 3 layer feed-forward ANN with a sigmoidal activation function in the hidden layer. Two different training algorithms were used; gradient descent with momentum backpropagation (TRAINGDM), and resilient backpropagation (TRAINRP). The results were not found to be dependent on the actual number of hidden nodes.

3. RESULTS AND DISCUSSION

A. Classifications using the full parameter set.

The results obtained when the 22 short-term and long-term parameters were used by the GP and the ANN are given in Table 3.

	Normal (Lx0,Lx1)	Abnormal (Lx5,Lx6)
GP	99.6±2.4%	97.2±2.9%
ANN	90.2±2.1%	87.5±3.9%

Table 3. Classification accuracies using the GP and ANN

The classifications for the ANN were slightly lower than those obtained using the "leave one out" cross validation strategy which is generally regarded as one of the most accurate methods and by leaving out a single patient's voice sample we can ensure to avoid inter versus intra speaker effects [6]. However, the GP was clearly found to give the more accurate classifications.

B. Classifications using the impact parameter set.

One of the advantages of using the GP is that it provides the impact factor of each parameter on the classification. Table 4 shows how each parameter contributed in the generated program. The Table shows the frequency percentage of the best thirty generated programs containing the referenced input; the average effect of removing all instances of that input, and the maximum impact of that input. In these cases, the greater the value, the more impact removal of that input had.

Parameter	Frequency	Average Impact	Maximum impact
VS	1.00	13.69	17.78
MF ₀	0.67	7.41	10.50
J ₀	0.77	4.45	9.78
N ₀	0.23	1.13	2.20
M ₀	0.17	0.32	0.45
P ₀	0.27	0.27	0.27
RHE	0.17	0	0
SD ₀	0.10	0	0
P ₁	0.10	0	0
SD ₃	0.10	0	0
P ₃	0.10	0	0
M ₁	0.07	0	0
SD ₁	0.07	0	0
P ₄	0.07	0	0
FHNNE	0.07	0	0
SD ₂	0.03	0	0
P ₂	0.03	0	0
M ₄	0.03	0	0
M ₂	0	0	0
M ₃	0	0	0
SD ₄	0	0	0
F ₀	0	0	0

Table 4. Contribution of each parameter

It may be seen from the Table that only 6 of the 22 parameters were found to have a significant impact on the classification. These parameters were N₀, M₀, P₀, MF₀, J₀, and VS.

Both the GP and the ANN were re-trained and tested using just these 6 parameters, and the results are shown in Table 5.

	Normal (Lx0,Lx1)	Abnormal (Lx5,Lx6)
GP	99.2±3.1%	96.4±3.7%
ANN	88.6±2.7%	81.5±4.2%

Table 5. Classification accuracies using GP and ANN

V. CONCLUSIONS.

A preliminary study has been made involving the use of GP to classify recovered (normal) voices and abnormal voices in acoustic signals taken from patients recovering from cancer of the larynx. Initially, a collection of 22 short-term and long-term parameters were extracted from the signal and used as input to the GP, and also an ANN. The GP provided much more accurate classifications than the ANN.

Examination of the impact factors for the voice parameters suggests that there are only 6 significant factors. The results obtained from both the GP and the ANN using just these parameters were only slightly poorer than for the full parameter set, again with the GP providing the more accurate classifications.

One of the advantages of the ANN is the ability to produce multiple outputs, enabling classifications to be made corresponding to the 7-point scale for voice quality used by SALTS. Work is now taking place to extend the GP approach to multiple classifications.

REFERENCES

- [1] Gray, H., Maxwell, R., Martinez-Perez, I., Arus, C. and Cerdan, S. "Genetic programming for classification of brain tumours from nuclear magnetic resonance biopsy spectra, in Genetic Programming", 1st International Conference on Genetic Programming, GP-96, Stanford, US, 1996.
- [2] Nordin, P., Keller, R., and Francone, F. "Genetic Programming: an introduction on the automatic evolution of computer programs and its applications." Wolfgang Banzhaf Publishers, Inc. 2002.
- [3] Ngan, P., M. Wong, M., Leung, K. and Cheng, J. "Using grammar based genetic programming for data mining of medical knowledge, in Genetic Programming" 3rd International Conference on Genetic Programming, GP-98, Madison, US, 1998.
- [4] Somorjai, R., Nikulin, A., Pizzi, N., Jackson, D., Scarth, G., Dolenko, B., Gordon, H., Russell, P., Lean, C., Delbridge, L., Mountford, C. and Smith, I. "Computerized consensus diagnosis - A classification strategy for the robust analysis of MR spectral. Application to H-1 spectra of thyroid neoplasma", *Magn. Reson. Med.* **33**, 257-263, 1995.
- [5] Ritchings RT, McGillion M, Moore CJ "Pathological voice quality assessment using artificial neural networks." *Medical Engineering and Physics* 24 (2002), pp561-564, PII S1350-4533(02)00064-4.

- [6] Godino-Llorente, JI, Ritchings, RT, Berry C “The Effects of Inter and Intra Speaker Variability on Pathological Voice Quality Assessment” *3rd International Workshop on Models and Analysis of Vocal Emissions for Biomedical Applications*, Firenze, Italy 2003
- [7] Berry, C and Ritchings, RT. “A comparative study of intelligent voice quality assessment using impedance and acoustic signals.” *4th International Workshop on Models and Analysis of Vocal Emissions for Biomedical Applications*, Firenze, Italy 2005.
- [8] Fourcin, A.J., Abberton E., Miller, D, Howell D. Laryngograph : “Speech pattern element tools for therapy, training and assessment.” *European Journal of Disorders of Communication* 30(2), 1996, pp.101-115
- [9] Rabiner, L. and Juang, B.H. Fundamentals of speech recognition. New Jersey Prentice Hall, 1993.
- [10] Moore C.J., Manickam K., Slavin N. “Voicing recovery in males following radiotherapy for larynx cancer.” *4th International Workshop on Models and Analysis of Vocal Emissions for Biomedical Applications*, Firenze, Italy 2005.

Voice recovering / enhancement

A METHOD FOR CHANGING SPEECH QUALITY AND ITS APPLICATION TO PATHOLOGICAL VOICES

Hisao Kuwabara

Teikyo University of Science & Technology, Uenohara, Kitatsuru-gun, Yamanashi 409-01, Japan
Tel: (0554)63-4411, Fax: (0554)63-4431, E-mail: kuwabara@ntu.ac.jp

Abstract: Speech quality is an interesting and very important aspect not only from linguistic and/or phonetic viewpoint but also from the viewpoint of speech technology. This study has been conducted from the latter point of view. A method has been developed based on the analysis-synthesis technique which enables to control voice quality by independently manipulating the voice source and the vocal tract resonant characteristics. Through this method, it is possible to investigate the amount of contribution of individual acoustic parameters to a certain voice quality including voice individuality. Formant frequencies and their bandwidths are used as the acoustic parameters to characterize the vocal tract configuration and the pitch frequency as the voice source. These acoustic parameters extracted from a natural speech are modified or changed to some extent and then a is synthesized making use of the modified acoustic parameters. Speech intelligibility and voice individuality are found to be controlled by this method. An application to a pathological voice has also been made to control the voice quality. It has been found that the method is capable of improving the so-called “roughness” or “hoarseness” of the pathological voice to a certain extent.

I. INTRODUCTION

Using the analysis-synthesis system we have developed [1], voice quality of natural speech has been controlled by changing formant trajectories that are supposed to have a close relation with such voice qualities as intelligibility, clearness, articulateness, and so on. Correlation analysis between psychological and acoustic distances reveals that the formant trajectory has the largest correlation with the voice quality of announcer's speech sounds, followed by pitch frequency [2]. This result suggests that the quality of speech sound of non-professional speakers may possibly be improved by altering the dynamics of formant trajectory patterns.

Based on the experimental evidence mentioned above, an experiment has been performed to change and improve the quality of natural speech making use of the analysis-synthesis system.

Formant trajectories are extracted from voiced portions by LPC method and the dynamics of these trajectories are altered depending on the formant pattern itself. The

method for altering the formant pattern is the same as that we have proposed earlier for the normalization of coarticulated vowels in continuous speech. [3]. This method is applied to the formant and pitch trajectories extracted from a natural speech, and the quality-controlled speech sounds are synthesized using the analysis-synthesis system to present to listeners for perceptual judgments.

II. ANALYSIS-SYNTHESIS SYSTEM

Fig. 1 illustrates the block diagram of the analysis-synthesis system. Low-pass filtered input speech is digitized in 12 bits at a rate of 15 kHz. A short time LPC analysis based on the autocorrelation method is performed to obtain LPC coefficients and the residual signals. Formant frequencies and their bandwidths are estimated by solving a polynomial equation. A modification of the spectral envelope is equivalent to a manipulation of the coefficients that would result in a frequency response of the filter equal to the modified envelope. These acoustic parameters (pitch periods, LPC coefficients, formant frequencies, bandwidths, residual signals) are stored for later synthesis. This analysis-synthesis system is capable of analyzing input speech either pitch synchronously or non-synchronously dependent on the type of input speech and the aim of speech analysis or synthesis. When we analyze a pathological speech, as described in a later section, which is difficult or impossible to define pitch periods from the input speech, analysis is generally performed with a fixed frame length.

III. METHOD OF FORMANT TRAJECTORY MANIPULATION

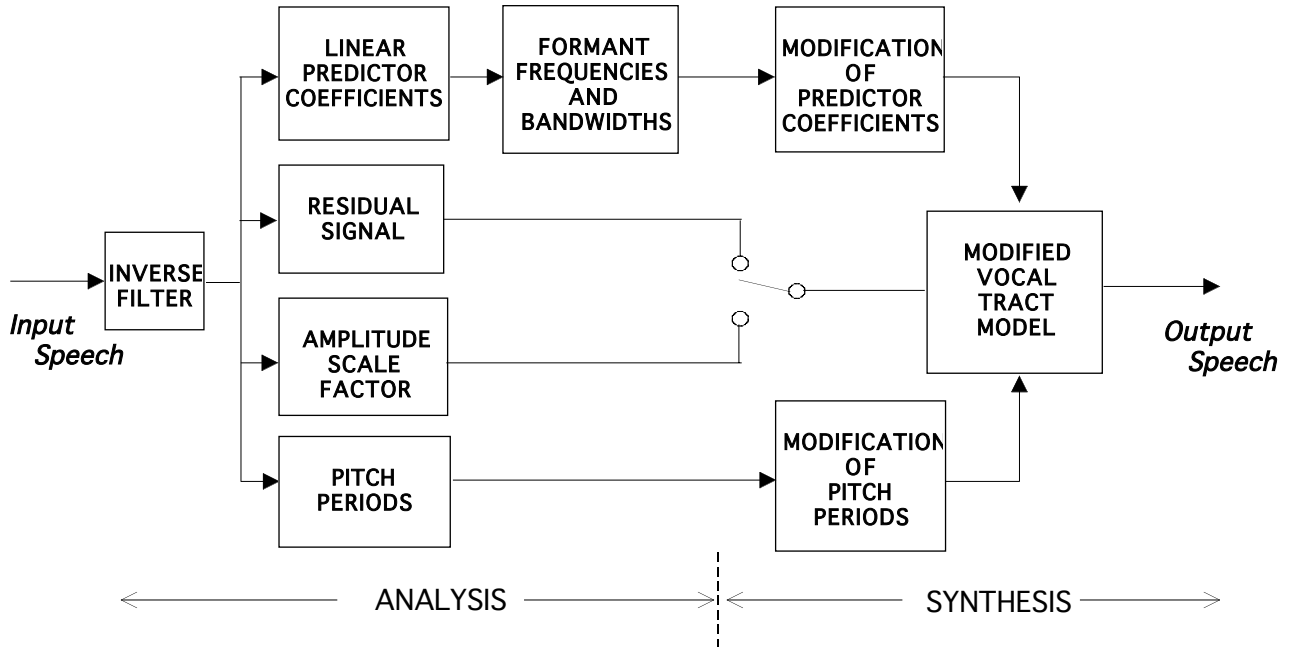
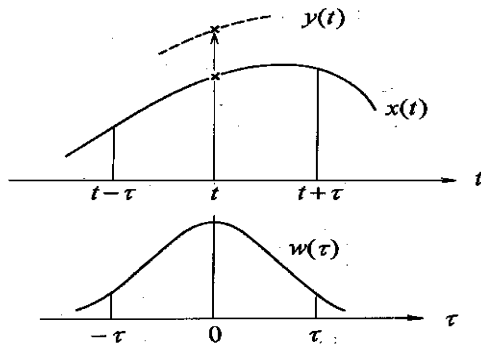


Fig. 1 Block diagram of analysis-synthesis system for voice conversion.

The method of formant modification has already been reported in an article [4]. The outline of the method is the following. For each pitch period, formant frequencies and their bandwidths are calculated first by solving the polynomial equation. Then, some modification is made on the original formant frequencies and/or bandwidths and accordingly on the predictor coefficients. A synthesis filter (vocal tract resonance filter) is formed using the



$$y(t) = x(t) + \int w(\tau) \cdot \{x(t) - x(t-\tau)\} d\tau$$

$$w(\tau) = 7.3 \cdot \exp\left\{-\frac{\tau^2}{2 \cdot (0.52)^2}\right\}$$

Fig. 2 Graphic illustration for using time-varying dynamic pattern of acoustic feature.

modified coefficient. The residual signal has also been used as the input to this filter.

After extracting formant trajectories using the method proposed by Kasuya [5], modification of them has been conducted in such a way that the preceding and

succeeding acoustic features contribute to the present value with the same weight if the time differences from the present are equal, and that the amount of contribution is proportional to the difference from the present acoustic feature [3]. This process is illustrated in Fig. 2. Suppose $x(t)$ be the time-varying pattern of a formant frequency, the new value $y(t)$ is defined as the sum of the original value $x(t)$ and the additional term of contribution by contextual information. The contribution is assumed to be a weighted sum of differences between values at the present time t and at different time $t \pm \tau$. Thus, $y(t)$ is given by,

$$y(t) = x(t) + \int_{-T}^T w(\tau) \{x(t) - x(t+\tau)\} \cdot d\tau \quad (1)$$

where $w(\tau)$ is the weighting function which is given as

$$w(\tau) = \alpha \cdot \exp(-\tau^2 / 2\sigma^2). \quad (2)$$

The time interval $(-T, T)$ from which the contextual information should be taken into account is theoretically infinite. But actually it must take a finite number and is not determined theoretically but is decided empirically or experimentally. In this study, $T=150ms$ and $\sigma=52ms$ have been experimentally determined. Given $\alpha > 0$, the dynamics of the original formant trajectory is emphasized, while for $\alpha < 0$, it becomes de-emphasized.

Equation (1) is applied to each of the three formant trajectories without vowel/consonant distinctions except for voiceless consonant. The time interval in equation (1) during which the weighted sum is calculated is 300 ms,

a 150 ms forward and backward each. This is the result for $\alpha = 7.3$ which, in our previous study, represents a proper value for the purpose of normalizing coarticulation effects of vowels in continuous speech. It is noticed from the figure that the new formant trajectories are emphasized their up-and-down dynamic movements as compared to those of the raw formants.

As far as we have tested, this method of incorporating contextual information is capable of not only normalizing the coarticulation effect of vowels in continuous speech but also has some advantage for vowel recognition using the formant frequencies with conventional Euclidean distance from the reference vowel. The method is also capable of improving the intelligibility of some lazily spoken continuous speech.

IV. METHOD OF PITCH MANIPULATION

Pitch frequency manipulation is quite simple as described in Fig.3. At the pitch synchronous analysis stage, the residue signal obtained for each pitch period has exactly the same data length as the pitch period. If we give the residue signal as an input to the vocal tract model, exactly the same waveform as the original speech

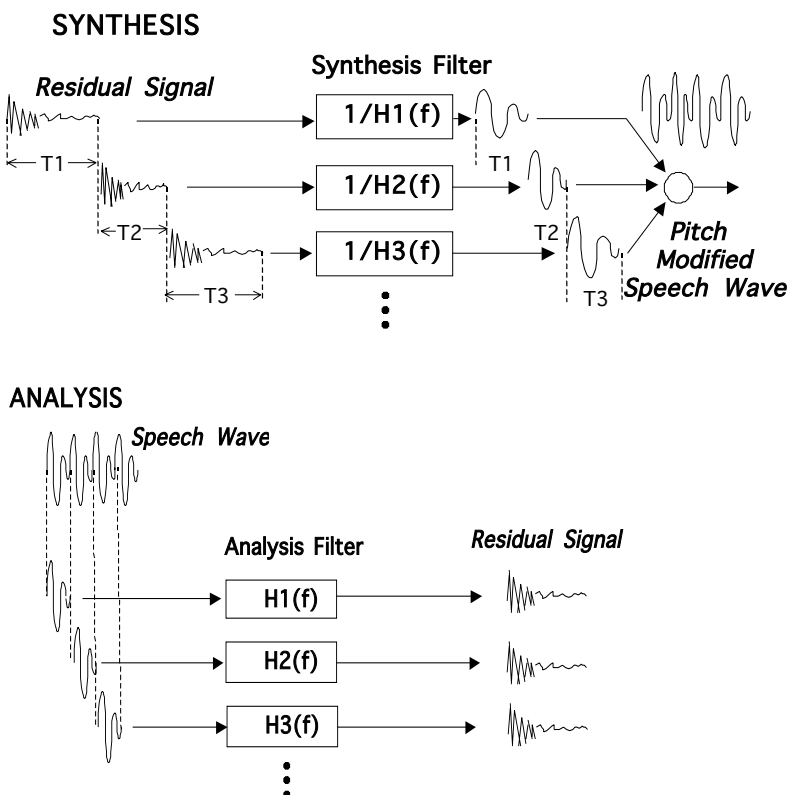


Fig.3 A method of manipulating fundamental frequency.

will be obtained. Thus, pitch frequency change can basically be given by controlling the length of the residual signal.

To raise pitch frequency, some data at the last part of the residue are eliminated and to lower the frequency, zero

signals are added to the last part of the residue.

Of course there are some discrepancies on the frequency domain between the pitch-modified speech and the original speech. However, there is no serious voice change in terms of perceptual voice quality when the pitch frequency change is less than 50% from the original.

V. ENHANCEMENT OF PATHOLOGICAL SPEECH

An attempt has been made to improve the quality of a pathological speech using the analysis-synthesis system we have developed. The pathological speech used in this experiment is a voice uttered by a patient who has a disease in his vocal cord. Because of malfunction of the vocal cord vibration, the resultant speech wave lacks clear periodicity and its voice quality is "hoarse". The experiment has been designed to create the fundamental frequencies into the pathological speech waves in order to improve the quality as close to a normal speech as possible.

Fig. 4 represents the block diagram to improve the quality of pathological speech. It requires two kinds of input speech: a pathological speech to be improved and a

normal speech utterance of the same sentence from another speaker. From the pathological speech inputted, voiced portions are at first detected and the spectral envelopes are extracted through LPC analysis. Next, the normal speech is analyzed by the same method and the pitch frequencies are detected to combine with the spectral information extracted from the pathological speech. If the normal speech of the same content can not immediately be available, artificial pulse trains could be used as the voice source.

In the analysis stage, after making voiced/voiceless distinction, the voiceless portions (voiceless consonants and devocalized vowels) are thoroughly kept in memory and the LPC analysis is performed for the voiced portions to obtain the LPC coefficients that carry spectral information and the residual signals from which pitch periods can be estimated. For the pathological speech, the frame length (analysis window) is set at 20 ms and the frame shift is a half of the window length.

In the feature extraction stage, the residual signals for the pathological speech are discarded after obtaining spectral information. Contrary to this, only the pitch frequency contour is needed from the normal speech.

For the normal speech, however, a process of time alignment has been undertaken before feeding to analysis in Fig.4. This process is shown in Fig.5. The voiced parts of the normal speech are analyzed pitch synchronously and the length for each part

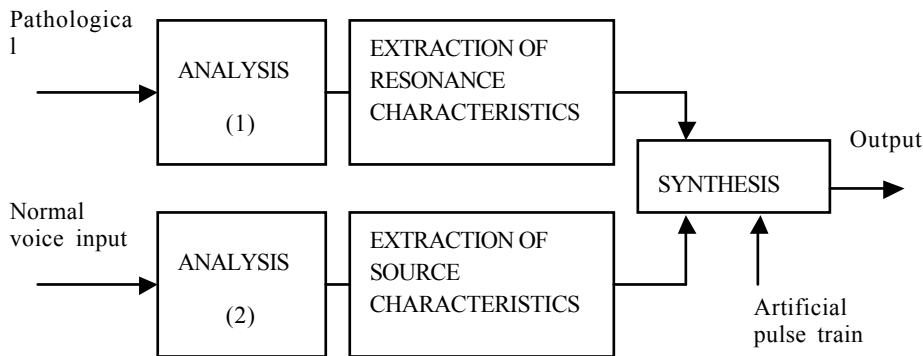


Fig. 4 Block diagram of speech analysis for improving pathological voice.

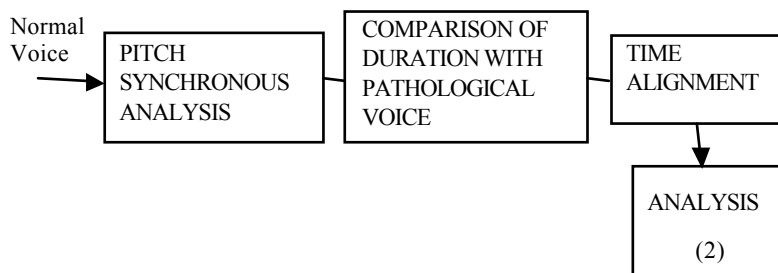


Fig. 5 Time alignment process with a normal speech voice.

is compared with the corresponding part for the pathological speech in order to make the length equal to that of the pathological speech with accuracy of less than one pitch period. This has been done simply by eliminating or inserting additional pitch periods.

The normal speech, after being time-aligned, is LPC analyzed again and the pitch frequencies are extracted for every voiced portion. The pitch frequencies or the residual signals are fed into the synthesis filter as the voice source. The synthesis filter is made from the predictor coefficients obtained from the pathological speech. The resultant output speech has, therefore, the same spectral characteristics as the pathological speech and the same source characteristics as the normal speech. As far as we have tested, the quality of the synthesized speech has been found to be far better than the original speech, though it is not as good as the normal speech.

VI. CONCLUSIONS

Improvement of voice quality has been achieved using an analysis-synthesis system capable of modifying pitch, formant frequencies, and formant bandwidths. According to the results of analysis for professional announcers' speech sounds, it is obvious that speech intelligibility closely relates to the dynamics of formant and pitch patterns. It has been found to be possible to improve the speech intelligibility without changing voice individuality by emphasizing the movement of time-varying pitch patterns. Another application of this

analysis-synthesis system has also been made to enhance a pathological speech which has little periodicity and "hoarse" in voice quality. By adding fundamental frequency component taken from a normal speaker, the voice quality of the pathological speech has been improved to a great extent.

REFERENCES

- [1] H. Kuwabara, (1984) "A pitch synchronous analysis/synthesis system to independently modify formant frequencies and bandwidths for voiced speech," SPEECH COMMUNICATION, Vol.3, pp.211-220
- [2] H. Kuwabara, and K. Ohgushi, (1984) "Acoustic characteristics of professional announcers' speech sounds," ACUSTICA, Vol.55, pp.233-240
- [3] H. Kuwabara, (1985) "An approach to normalization of coarticulation effects for vowels in connected speech," J. Acoust. Soc. Am., Vol.77, pp.686-694
- [4] H. Kuwabara, and K. Ohgushi, (1987) "Contributions of vocal tract resonant frequencies and bandwidths to the personal perception of speech," ACUSTICA, Vol.63, pp.120-128
- [5] H. Kasuya, (1983) "An algorithm to choose formant frequencies obtained by linear prediction analysis method," Trans. IECE Japan, Vol.J66-A, pp.1144-1145

METHODS FOR FORMANT EXTRACTION IN SPEECH OF PATIENTS AFTER TOTAL LARYNGECTOMY

R. Pietruch¹, M. Michalska², W. Konopka², A. Grzanka^{1,3}

¹Institute of Electronic Systems, Warsaw University of Technology, Warsaw, Poland

²Department of Otolaryngology, Medical University of Lodz, Lodz, Poland

³Department of Prevention of Environmental Hazards, Medical Academy of Warsaw, Poland

Abstract: The paper shows the methods for imaging power spectral density of speech and extracting formant frequencies from continuous voice. The methods will be used to improve the patients' rehabilitation after the total laryngectomy surgery. The adaptive algorithms and transversal filters were implemented to estimate the transfer function of human vocal tract model. The estimation methods were based on statistical, Auto-Regressive model of speech production. The pilot study on formant frequencies, especially F1 and F2 formants, and their linear separation for each vowel has been presented. The method for recognition pathological voice has been proposed.

Key words: Speech signal spectrum analysis, adaptive filters, formant tracking and total laryngectomy

I. INTRODUCTION

Laryngectomy is a partial or complete surgical removal of the larynx, usually performed as a treatment for laryngeal cancer. After the loss of vocal cords patients are not able to vocalize their speech. It is difficult for them to generate phonation, which would be understandable and communicative. Their voice is hoarse, weak, and strained. The main goal of phoniatric rehabilitation is to teach patients how to articulate understandable speech. During the therapy subjects are learning how to force pharyngo-esophageal segment to induce resonance and articulate alternative voice. Esophagus should become a vicarious source and substitute vocal cords. A certain percentage of laryngectomees never acquires an alaryngeal voice and is unable to use an electronic larynx. They usually communicate by silently articulated words with some ejectives from intra-oral pressure. This voice called silent mouthing is not a truly oesophageal voice.

To improve and simplify the medical analysis the computer program has been written. It visualizes power spectral density (PSD) of speech. The algorithm presented in this paper has been implemented to estimate PSD and to track formants from continuous speech in real time. The estimation of vocal tract model parameters and formants extraction was used for comparing natural voice with oesophageal and silent mouthing speech.

II. METHODOLOGY

A. Linear prediction and adaptive filters

The algorithm proposed in this paper attempts formant extraction from voice signals. The tracking formant algorithms have been proposed e.g. in papers [1], [2]. In presented applications the Auto-Regressive (AR) statistical process models speech dynamics. It was assumed that human speech is a linear transformation of white noise. AR process was used instead of Auto-Regressive Moving Average (ARMA) model. Thus, the voice spectrum analysis was simplified and nasal tract transmittance influence was eliminated. The digital Infinite Impulse Response (IIR) filter equivalent to natural vocal tract transmittance [3] models the AR process. The filter transmittance H estimated for n -th sample, depends on signal frequency f , it is a function

of complex number $z = e^{2\pi j \frac{f}{f_s}}$, where f_s is a sampling frequency. According to [4, 5], the amplitude of H is given by equation (1):

$$\hat{A}(n, f) = \left| \hat{H}(n, f) \right| = \left| \frac{\hat{Q}(n)}{1 - \sum_{k=1}^p \hat{h}_k(n) z^{-k}} \right| \quad (1)$$

H transmittance can be presented in time units, according to equation $n = tf_s$. Variable $Q(n)$ is a temporary power of prediction error, which is analogical to the power of signal generated with larynx or noise produced by air turbulences [6].

The linear prediction has been applied to estimate the inversed transversal filter parameters. Linear prediction coefficients (LPC) are the AR parameters h_k . The transversal filter was used instead of lattice filter because of simpler numerical complexity. However the PARCOR reflection coefficients can be computed from the LPC [7].

B. Recording Procedures

Fifty Polish-speaking patients who had undergone the total laryngectomy and twenty subjects from control group were recorded with the use of a digital camera, Panasonic NV-DS65EGE. The recordings were made in the sound-treated booth in order to minimize the background noises. An electret-condenser microphone was connected to the camera and supplied with the R6, 1.5V battery. A potentiometer between microphone and camera input was used to adapt the signal power. The microphone was positioned on a clip mounted around a neck. The distance between mouth and microphone was about 15cm. The linguistic material was presented on cards. Sentences were read twice.

The audio-video material was recorded on MiniDV tape. The Pinnacle Studio video card was used to transfer the recordings to computer for acoustic analyses. The data was stored on MPEG format files. The audio signals were digitized with 44,1 kHz sample rate. The Signal-to-Noise ratio (SNR) of recorded tracks was about 45dB, according to calculations on MatLab 6.0 application. The SNR was calculated as the proportion of the power of silent and speech signals based on 1000 selected samples. The actual range of speech signal power is about 60dB [8].

A computer program was written to visualize spectral density and track the formants of human speech. It processes the audio data from WAVE and MPEG multimedia files. For WAVE format files audio signals were decimated down to 8 kHz sample frequency using CoolEdit Pro 2.0 software. For the vowels analysis based on two first formants the 8kHz sample frequency was used because these formants appear in the 4kHz range.

C. Spectrum estimation and tracking formants

The spectrum of speech signal is calculated from the vocal tract filter coefficients. The number of estimating filter parameters h_k , can be changed in the program according to the sampling frequency f_s and the nature of voice. For vowel analysis from signals sampled with $f_s = 8\text{kHz}$ the number of LPC was set to $k = 8$. According to the literature [3, 8], up to four formants should be placed in the 0-4kHz-frequency range. To check if formants are not blended the number of filter coefficients was increased to $k = 16$. It was checked then if one formant didn't split into two. This method had significant results especially for Polish vowels /o/ and /u/ where F1 and F2 formants are very closed.

Calculation of the filter estimated LPC parameters h_k in n -th sample is based on Recursive algorithm based on Least-Squares error minimization (RLS). Haykin listed detailed steps of algorithm in [9]. The constants in algorithm were matched experimentally by authors and set as: $\alpha = 0.05$, $\lambda = 0.985$.

By experimental research it is proven that RLS algorithm is characterized by a fast rate of convergence. According to the literature [9] the mathematical formulation and therefore the implementation of RLS is relatively simple and efficient in computation. In [9] Haykin shows a numerical instability problem considered in finite precision arithmetic. Applied method cures the divergence of standard RLS algorithm.

According to experiments, listed algorithm is suitable for a real time implementation on the personal computer for sound data sampled with up to 44kHz frequency.

The amplitude of speech spectrum has an exponentially falling character, about -12dB per octave [3]. To equalize the overall energy distribution the speech is pre-emphasized using a high-pass FIR filter with parameter vector $h = [1 \ -0.9735]$.

According to Christensen method [10] the local minimums of second derivative of power spectrum $A(m,n)$ were searched for the formants extraction. This method can separate some blended formants. It was assumed in algorithm that the second derivate must be negative.

III. RESULTS

A. Tracking formants results.

The time-frequency spectrograms are presented in Figures 2, 3 and 4. The level of gray is proportional to the amplitude. Local minimums were colored black for better vision.

The comparison of pathological (Fig.2, 3) and natural voice (Fig.1) shows the huge differences in the articulation of speech. Shorter articulation of vowels, and higher noise level can be seen for esophageal voice (Fig.2). The pauses are longer. However the formants of esophageal voice match (with little variation) the natural speech spectrum (Fig.1).

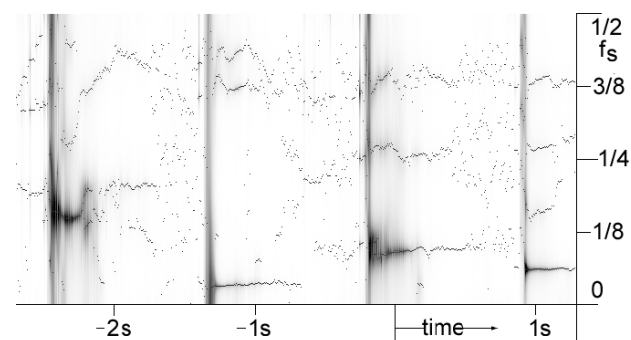


Fig.1 Spectrogram of natural voice (Polish vowels /a/, /i/, /e/ /y/), X axis: time, Y axis: f/f_s , $f_s = 8\text{kHz}$.

For silent mouthing (Fig.3) the differences between each vowel formants are insignificant. Thus, it is hard

to recognize each vowel from the spectrum. Presence of noise is more evident than in the alaryngeal group.

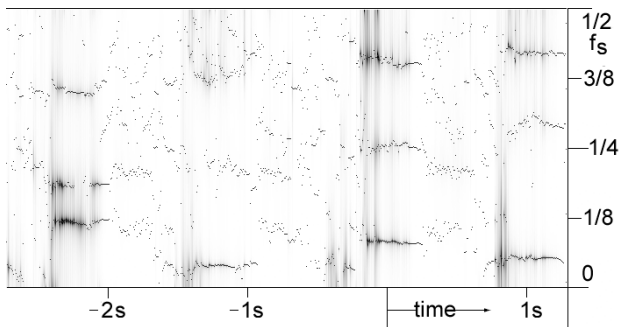


Fig.2 Spectrogram of esophageal speech (Polish vowels /a/, /i/, /e/, /y/), X axis: time, Y axis: f/f_s , $f_s=8\text{kHz}$.

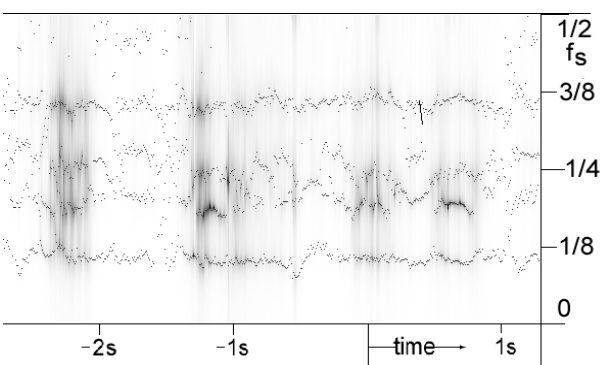


Fig.3 Spectrogram of silent mouthing voice (Polish vowels /a/, /i/, /e/, /y/), X axis: time, Y axis: f/f_s , $f_s=8\text{kHz}$.

It is evident that there are higher frequencies of first formant for silent mouthing vowels articulation (Fig. 3). In this speech no fundamental frequency excitation sources are involved in speech production. Although the vocal tract parameters are similar, the transfer function is different because of other source of air turbulences [3]. Moreover, the speech is distorted and the spectrum covered by the air turbulences noise from tracheotomy tube and its spectrum with regular resonances. Thus, the spectrum is distorted and the speech less intelligible.

B. Vowels classification.

It is well known that vowels are identified mostly through their formant frequencies [9] and therefore a major part of the perceptual information contained in voiced speech is encoded in these formant frequencies [7]. This paper is concerned with the differences between the formant frequencies of normal and pathological voice.

Mean values and deviations of the first and second formants of the vowels produced by normal, esophageal and silent mouthing voices have been presented

in Figures 4, 5 and 6. The measurements were performed for 3 subjects of each group.

The universal vowel production characteristics were obtained for alaryngeal and normal speech. The acoustic characteristics presented in Fig. 4 and 5, match the theoretical frequencies of Polish vowels formants from [3]. It can be seen, that for the normal speech the vowels subspaces in F1 and F2 formants dimensions can be linearly separated (Fig. 4). The relative positions of formant frequencies were maintained for alaryngeal voice (Fig. 5).

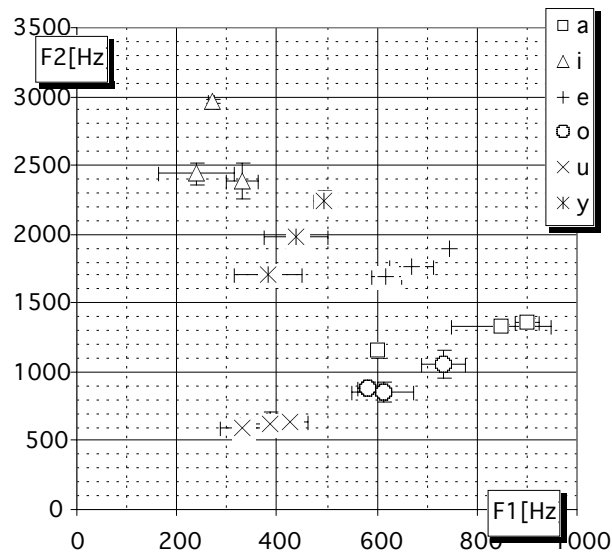


Fig. 4. Vowels in normal speech (Polish) in the F1 and F2 formants dimensions

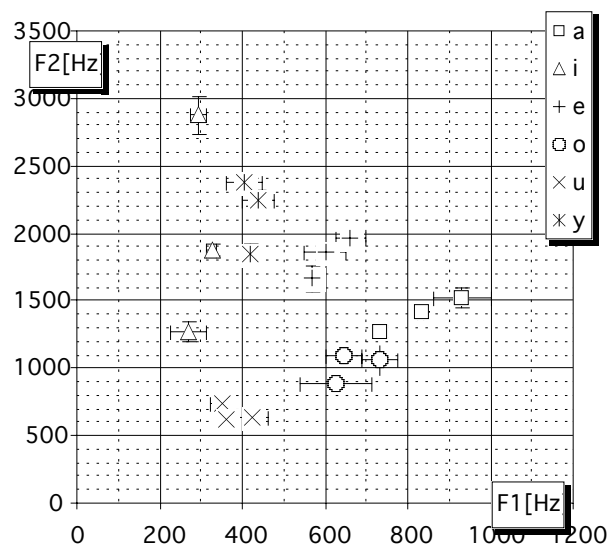


Fig. 5. Vowels in esophageal speech (Polish) in the F1 and F2 formants dimensions

The Fig. 6 shows how the pathology affects the speech spectrum. For the patients, who haven't learned the esophageal voice, it is impossible to recognize vowels by two first formants. Moreover, it has been observed that the formants of vowels in the silent mouthing are more dispersed, unclear and less stable than in alaryngeal voice. Significant deviations of temporal formant frequencies are seen on Fig. 6.

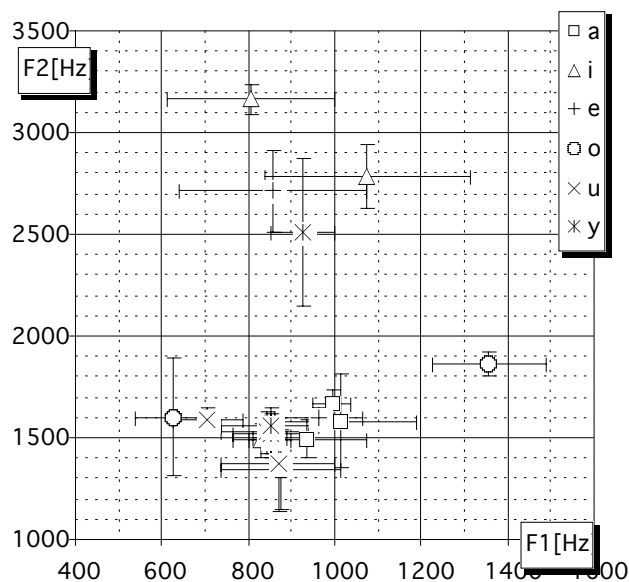


Fig 6. Vowels in silent mouthing speech (Polish) in the F1 and F2 formants dimensions

The figures with objective data prove how important the rehabilitation and learning an esophageal voice is. The pronunciation of vowels causes the biggest problems to laryngectomees. Vowels should be articulated with the use of low fundamental frequency. Patients should then learn how to use the source of phonation alternative to laryngeal voice, to acquire useful intelligible voice production.

IV. DISCUSSION

Initial tests' results show the field for the future work on improving pathological speech with the computer methods. A linear or nonlinear separation methods, e.g. neural networks or SVM can be used for vowel recognition. However, we are not able to recognize silent mouthing speech based on two first formants; therefore we use other parameters, e.g. lips and jaw expression from image analysis.

V. CONCLUSION

It has been presented that formant frequencies equivalent to vocal tract coefficients are very sensitive to pathology of speech organs. This indicates that formants are objective descriptors for evaluation of rehabilitation after the laryngeal surgery and speech intelligibility. Our approach is developed for efficient and accurate tracking formants from the smooth AR spectrum. Eliminating noise and fundamental frequency with its harmonics due to the use of adaptive algorithm allows extracting formants in a simple way. The computer program on formant extraction can be used for objective analysis of vicarious voice of laryngectomees.

REFERENCES

- [1] B. Chen and P.C. Loizou, "Formant Frequency Estimation in Noise" in *IEEE Int. Conf. Acoustics, Speech, and Signal Processing*, vol. I, Montreal, 2004, pp.581-584.
- [2] L. J. Lee, H. Attias, L. Deng and A. Acero, "A structured speech model with continuous hidden dynamics and prediction-residual training for tracking vocal tract resonances" in *Proceedings of the 2004 IEEE International Conference on Acoustics, Speech, and Signal Processing*, Montreal, 2004.
- [3] R. Tadeusiewicz, *Sygnał mowy*, 1st ed., Warsaw: Wydawnictwa Komunikacji i Łączności, 1988, pp.158-186.
- [4] R. Goldberg and L. Riek, Chapter 3, 4 in *A Practical Handbook of Speech Coders*, Boca Raton: CRC Press, 2000.
- [5] T. Zielinski, *Od teorii do cyfrowego przetwarzania sygnałów*, Krakow: Wydział EAIiE AGH, 2002.
- [6] L. Rutkowski, *Filtry adaptacyjne i adaptacyjne przetwarzanie sygnałów: teoria i zastosowania*, Warsaw: Wydawnictwa Naukowo Techniczne, 1994, pp.49-85
- [7] S. Saito, *Speech Science and Technology*, Tokyo: Ohmsha, 1992, pp. 63-94.
- [8] Z. Zyszkowski, *Podstawy elektroakustyki*, 3rd ed., Warsaw: Wydawnictwa Naukowo Techniczne, 1984, pp.218-277
- [9] S. Haykin, *Adaptive filter theory*, Englewood Cliffs: Prentice Hall, 1991, pp. 477-485.
- [10] R. Christensen, W. Strong and P. Palmer "A comparison of three methods of extracting resonance information from predictor-coefficient coded speech" in *IEEE Trans. Acoust., Speech, and Sig. Proc. ASSP-24(1)*, 1976, pp. 8-14.

OPTIMISED GSVD FOR DYSPHONIC VOICE QUALITY ENHANCEMENT

Claudia Manfredi, Cloe Marino, Fabrizio Dori, Ernesto Iadanza

Department of Electronics and Telecommunications
Università degli Studi di Firenze, Via S.Marta 3, 50139 Firenze, Italy
manfredi@det.unifi.it

Abstract: This paper concerns the problem of enhancing voice quality for people suffering from dysphonia, caused by airflow turbulence in the vocal tract, for irregular vocal folds vibration.

A generalized subspace approach is proposed for enhancement of speech corrupted by additive noise, regardless of whether it is white or not. The clean signal is estimated by nulling the signal components in the noise subspace and retaining the components in the signal subspace. Two approaches are compared, taking into account both signal and noise, or signal only, eigenvalues. An optimised adaptive comb filter is applied first, to reduce noise between harmonics. Objective voice quality measures demonstrate improvements in voice quality when tested with sustained vowels or words corrupted with “hoarseness noise”. The intention is to provide users (disabled people, as well as clinicians) with a device allowing intelligible and effortless speech for dysphonics, and useful information concerning possible functional recovering. This will be of use to people in social situations where they interact with non-familiar communication partners, such as at work, and in everyday life.

Keywords: hoarseness, voice denoising, GSVD, comb filtering, voice quality, pitch, noise, formants.

I. INTRODUCTION

Signal subspace methods are used frequently for denoising in speech processing, mainly with speech communication [1], [2]. Until now, few results are available concerning their application for voice quality enhancement in the biomedical field [3]. In this paper, the objective of noise reduction is to improve noisy signals due to irregular vocal folds vibration. This problem is of great concern, for rehabilitation and from the assistive technology point of view. Commonly, surgical and/or pharmacological treatments allow restoring voice quality, with patient’s recovering to an acceptable or even excellent level. However, sometimes patients can only partly recover, with heavy implications on their quality of life.

The idea behind subspace methods is to project the noisy signal onto two subspaces: the signal subspace (since the signal dominates this subspace), and the noise subspace. The noise subspace contains signals from the noise

process only, hence an estimate of the clean signal can be made by removing or nulling the components of the signal in the noise subspace and retaining only the components of the signal in the signal subspace. The decomposition of the space into two subspaces can be done using either the singular value decomposition (SVD) [4], [5] or the Quotient SVD (QSVD) or GSVD [1],[6],[11]. Though computationally expensive, GSVD was found robust and effective in reducing noise due to turbulences in the vocal tract, which is typically coloured. GSVD is implemented here with two choices for separating the signal and the noise subspaces, to compare performance. Specifically, the first choice is based on classical GSVD, where both the signal and the noise subspace eigenvalues are used for filtering [6]. The second one corresponds to retaining the signal subspace eigenvalues only [1].

An adaptive comb filter is applied first, as it was shown to significantly reduce noise between the harmonics in the spectrum. The comb filter is optimised, in the sense that it is applied on windows whose length varies according to varying pitch.

Real data coming from dysphonic subjects are successfully denoised with the proposed approaches.

II. MATERIALS AND METHODS

Firstly, optimised adaptive comb filtering is performed on data windows of varying length, obtained with a new two-step robust adaptive pitch estimation technique [7]. The essence of comb filtering is to build a filter that passes the harmonics of the noisy speech signal y , while rejecting noise frequency components between the harmonics [8],[9]. Ideally, spacing between each “tooth” in the comb filter should correspond to $F_0(1/T_0)$ in Hz, which is often highly unstable in pathological voices. The proposed comb filter, based on an adaptive two-step pitch estimator, is capable to adapt to fast pitch variations and successfully reduces noise as evaluated by an adaptive implementation of the Normalised Noise Energy technique (ANNE) [7], thus being suited as a pre-filtering step. The filter that has been used in this paper has a Hamming window shape, which is obtained from the following equation (with $K=3$):

$$a(i) = \frac{0.54 + 0.46 \cos(2\pi i / 2K + 1)}{\sum_{i=-K}^K 0.54 + 0.46 \cos(2\pi i / 2K + 1)} \quad (1)$$

This step is followed by Generalised Singular Value Decomposition (GSVD) of signal and noise matrices, whose entries are suitably organised, as shown in eq. (4). GSVD-based voice denoising aims at diminishing the uncorrelated and added noise from the voice signal, whether it is white or not. The noisy signal y at time instant t , y_t , can be expressed as:

$$y_t = d_t + n_t \quad (2)$$

Where d =clean signal, n =(coloured) noise. The goal is to estimate d from y . The noisy signal is segmented into frames y_i , $i=1, 2, \dots$, of varying length M_i , obtained according to the previously cited robust adaptive pitch estimation procedure. The GSVD amounts to finding a non-singular matrix X and two orthogonal matrices U , V of compatible dimensions, which simultaneously transform both the Hankel noisy speech matrix H_y and the noise matrix H_n into nonnegative diagonal form matrices C and S such as:

$$\begin{aligned} U^T H_y X &= C = \text{diag}(c_1, \dots, c_k), c_1 \geq c_2 \geq \dots \geq c_k \\ V^T H_n X &= S = \text{diag}(s_1, \dots, s_k), s_k \geq s_{k-1} \geq \dots \geq s_1 \\ C^T C + S^T S &= I_k \end{aligned} \quad (3)$$

Where $L+K=M+1$, $K < L$. The H_y matrix has the form:

$$H_y = \begin{bmatrix} y_0 & y_1 & \dots & y_{K-1} \\ y_1 & y_2 & \dots & y_K \\ \vdots & \vdots & \dots & \vdots \\ y_{L-1} & y_L & \dots & y_{M-1} \end{bmatrix} \quad (4)$$

Similarly for H_n .

The values $c_1/s_1 \geq c_2/s_2 \geq \dots \geq c_k/s_k$ are referred to as the generalised singular values of H_y and H_n . Notice that one can choose to work with Toeplitz matrices instead of Hankel matrices. There are no fundamental differences between the two approaches.

It was shown [1], [2], [6], [11] that the filtered signal can be obtained either from the matrix:

$$H_y^p = U \begin{bmatrix} C_p S_p^{-1} & 0 \\ 0 & 0 \end{bmatrix} X^{-1} \quad (5)$$

or from the matrix:

$$H_y^p = U \begin{bmatrix} C_p & 0 \\ 0 & 0 \end{bmatrix} X^{-1} \quad (6)$$

where U and X are as in eq. (3) and $C_p = \text{diag}(c_1, \dots, c_p)$, $S_p = \text{diag}(s_1, \dots, s_p)$, are sub-matrices of C and S respectively and p is the signal subspace dimension. Eq. (5) corresponds to classical GSVD, where both the signal and the noise subspace eigenvalues are used for filtering, and will be referred to as GSVD in what follows. Eq. (6) corresponds to retaining the signal subspace eigenvalues only, and will be referred to as OSV (Only Signal Values). Two problems were encountered with GSVD, i.e. the choice of the noise covariance matrix and that of the signal subspace dimension p . Commonly, in speech communication settings, the noise covariance matrix is computed using noise samples collected during speech-absent frames. To deal with the problem under study, different choices were tested. Among them, one takes

into account the signal noisy component as obtained from a preliminary SVD decomposition of the signal under study: the noise subspace is reconstructed and used to fill matrix H_n . While giving almost good results, this choice was disregarded, due to both the larger computational load and to better results obtained with the following approach: on each signal frame of varying length, an AutoRegressive (AR) model is identified, and the model residuals are evaluated. The residual variance is then used to construct the diagonal matrix S of eq. (3).

The second problem is the optimal choice of the number p of retained singular values for denoised signal reconstruction. Classical order selection criteria were applied to GSVD, such as AIC, MDL [9], as well as a new criterion named DME [10], but best results were obtained with $p=2$. It will be named as GSVD_{fix} in what follows. As for OSV, p was chosen such as [1]:

$$c_p > s_p \text{ and } c_{p+1} < s_{p+1} \quad (7)$$

This was in fact the choice that gave the best results.

Finally, three objective indexes are defined, closely related to the signal characteristics. A frequency threshold value $f_{th}=4\text{kHz}$ is defined, based on the usual range for voiced sounds (first four formants) in adults, as well as on experimental results obtained from threshold tuning in a dataset of voiced and unvoiced sounds. The subscript “non-filt” refers to the original signal, while “filt” refers to the denoised signal:

$$\text{PSD}_{\text{low}} = 10 \log_{10} \frac{\text{PSD}_{\text{non-filt}}(f \leq f_{th})}{\text{PSD}_{\text{filt}}(f \leq f_{th})} \quad (8)$$

measures the ratio of the PSDs evaluated on the “harmonic range”;

$$\text{PSD}_{\text{high}} = 10 \log_{10} \frac{\text{PSD}_{\text{non-filt}}(f \geq f_{th})}{\text{PSD}_{\text{filt}}(f \geq f_{th})} \quad (9)$$

is the ratio of the PSDs, evaluated on the “noise range”. A

$$\text{QER} = 10 \log_{10} \frac{\sum_{n=1}^M y^2(n)}{\sum_{n=1}^M (y(n) - y_{\text{filt}}(n))^2} \quad (10)$$

good denoising procedure should give PSD_{low} values near to zero (no loss of harmonic power), but high PSD_{high} values (loss of power due to noise).

Finally, a measure of the denoising effectiveness (quality enhancement ratio, QER) is defined as:

QER is thus the ratio between the signal energy and that of the removed noise. $\text{QER} > 0$ corresponds to good denoising [10].

III. RESULTS

A set of about 20 voice signals (word /aiuole/) coming from adult male patients were analysed with the proposed approach. All patients underwent surgical removal of T1A glottis cancer, by means of laser or lancet technique. Perceptual evaluation with GIRBAS scale showed good recovering, however, residual hoarseness was found in

Special session on
Physical and mechanical models and devices

MODELLING OF INFLUENCE OF VELOPHARYNGEAL INSUFFICIENCY ON PHONATION OF VOWEL /A/

Vampola T.¹, Horáček J.², Veselý J.², J.Vokřál³

¹Dept. of Mechanics, Faculty of Mechanical Engineering, Czech Technical University in Prague, Czech Republic

²Institute of Thermomechanics, Academy of Sciences of the Czech Republic, Prague, Czech Republic

³Phoniatic Laboratory, 1st Faculty of Medicine, Charles University Prague, Czech Republic

Abstract: The effects of velopharyngeal insufficiency (VFI) or clefting on acoustic frequency-modal characteristics of human supraglottal spaces are investigated. Finite element (FE) modelling is supported by experimental investigation using a physical model of the vocal and nasal tract fabricated by the rapid prototyping technique from the FE model. The FE model was developed from magnetic resonance images (MRI) of the subject during phonation. Finally the influence of the VFI on phonation of the vowel /a/ is numerically simulated in time domain and supported by clinical investigation.

Keywords: biomechanics of voice, acoustics, cleft

I. FE MODEL AND MATHEMATICAL FORMULATION

The FE model of a male vocal tract for the Czech vowel /a/ was created by transferring the data directly from MRI images and adding afterward the nasal tract manually [1]. A connection of the nasal and oral cavities was considered in the back area of the soft palate modelling the velopharyngeal insufficiency. The FE model is presented in Fig. 1. A degree of the velopharyngeal insufficiency was modelled by varies sizes of the area joining the nasal and oral cavities.



Fig. 1 FE model of the supraglottal spaces for vowel /a/ with the nasal cavity joint by cleft model.

The wave equation for the acoustic pressure can be written as:

$$\nabla^2 p = \frac{1}{c_0^2} \frac{\partial^2 p}{\partial t^2}, \quad (1)$$

where c_0 is the speed of sound. Equations of motion for the acoustic system after discretization can be written as

$$\mathbf{M}\ddot{\mathbf{P}} + \mathbf{B}\dot{\mathbf{P}} + \mathbf{K}\mathbf{P} = \mathbf{F} \quad (2)$$

where \mathbf{M} , \mathbf{B} , \mathbf{K} are the global mass, damping and stiffness matrices, \mathbf{P} is the vector of nodal acoustic pressures and \mathbf{F} is the effective “fluid load”.

The acoustic modal and transient analysis were realised by the system ANSYS considering $c_0 = 343 \text{ ms}^{-1}$ and the air density $\rho_0 = 1.2 \text{ kgm}^{-3}$. Zero acoustic pressure ($p=0$) was assumed at the lips and nostrils. Other boundary walls of the acoustic spaces were considered acoustically absorptive. The acoustic damping was modelled by the boundary admittance coefficient ($\mu = 0.005$).

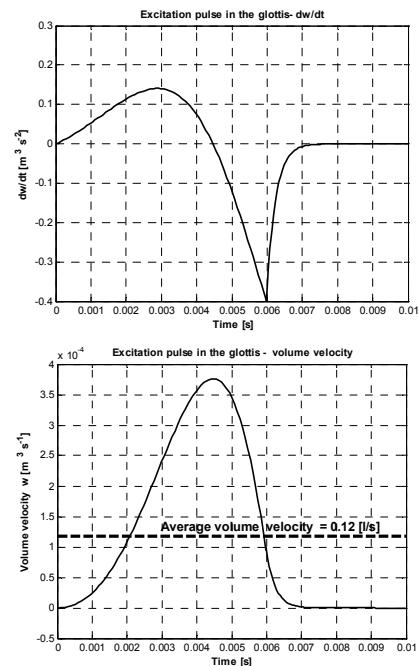


Fig. 2 Excitation L-F pulse used in transient analysis for modeling the phonation in time domain and its integral.

The supraglottal spaces were excited at the position of the vocal folds by pulses given by the derivative of the airflow volume velocity in accordance with the Liljencrants-Fant model [2]:

$$\begin{aligned} \frac{d}{dt}(w(t)) &= E_0 e^{\alpha t} \sin(\omega t), \quad 0 < t < t_e, \\ \frac{d}{dt}(w(t)) &= -\frac{E_e}{\varepsilon t_a} (e^{-\varepsilon(t-t_e)} - e^{-\varepsilon(t_c-t_e)}), \quad t_e \leq t \leq t_c \end{aligned} \quad (3)$$

The parameters of the excitation pulses were adjusted according to the prescribed mean volume flow rate in the glottis (0.12 l/s) and the fundamental (pitch) frequency ($F_0=100$ Hz) - see Fig. 2.

II. PHYSICAL MODEL AND MEASUREMENT SET-UP

The model for experimental analyses was created from the FE model by the CAD program Unigraphics utilizing the triangular mesh that describes the inner surface of the supraglottal spaces. After adding some constructional elements the 3D computer model was the input for the Rapid Prototyping technology. The model made of thermoplast ABS was fabricated by the Fused Deposition Modelling technology on the machine FDM 1650-STRATASYS with the accuracy ± 0.1 mm.

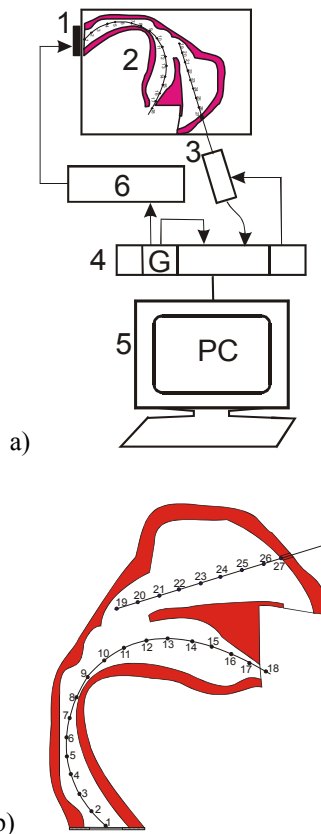


Fig. 3 - a) measurement set up: 1- miniature loudspeaker, 2 - the model, 3 - B&K microphone probe 4182, 4 and 5 - B&K front-end and PC with SW B&K PULSE, 6 - power amplifier LDS PA25E; b) schema of the physical model with 27 measurement points inside the supraglottal spaces.

The model construction enabled to change the magnitudes of the area A (cleft size) connecting the nasal cavities with the vocal tract ($A=0, 42, 132$ and 252 mm²). The model and the measurement set-up are schematically shown in Fig. 3. Random excitation was used in experimental modal analysis.

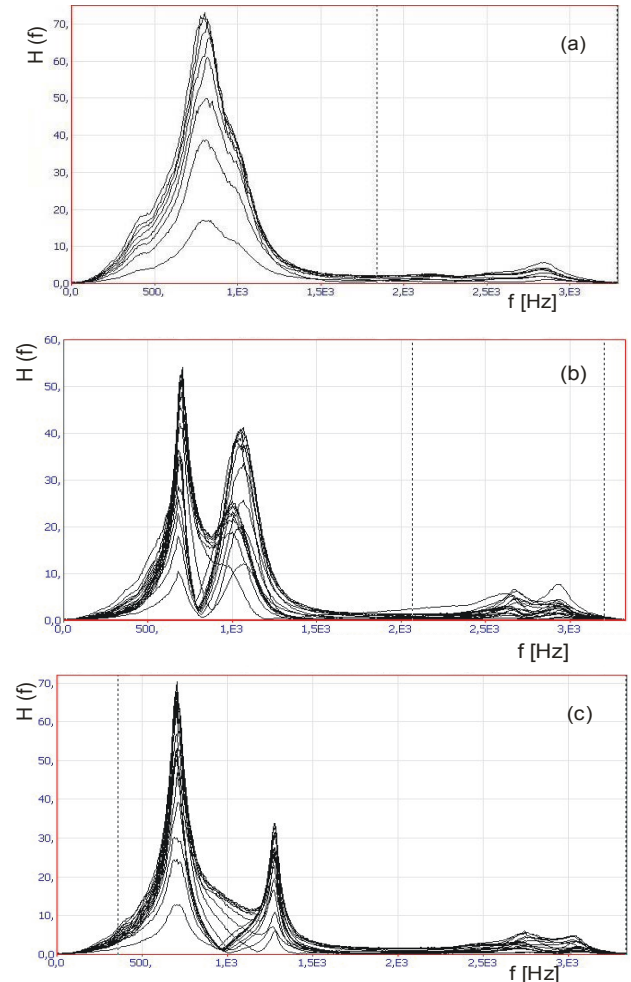


Fig. 4 Measured resonance curves for cleft areas: a) $A=0$, b) $A=42$, c) $A=132$ mm².

III. RESULTS OF THE ACOUSTIC MODAL ANALYSIS

The resonance curves measured inside the model (in the points marked in Fig. 3b) are shown in Fig. 4. The results of the computational and experimental modal analysis are summarized in Fig. 5, where the calculated and measured natural frequencies are compared for fourth magnitudes of the area A . In the case of velopharyngeal insufficiency ($A>0$) new nasopharyngeal (oro-nasal) natural frequencies appeared between the formants F2 and F3. Measured modes of vibration for the formants F1-F3 and the nasopharyngeal frequency f_{naso} are shown in Fig. 6 for $A=132$ mm² and the corresponding calculated mode shapes are presented in Figs. 7 and 8. The first

calculated oro-nasal acoustic mode shape with the predominant vibrations in the horizontal direction (see Fig. 8a) was not excited in the experiments.

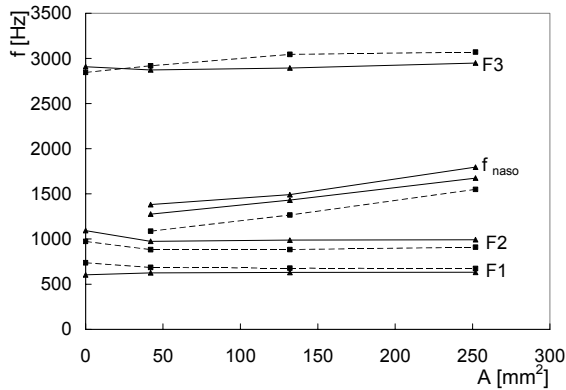


Fig. 5 Calculated (—) and measured (-----) formant (F_1 - F_3) and nasopharyngeal frequencies for the vowel /a/ for increasing area A of the cleft.

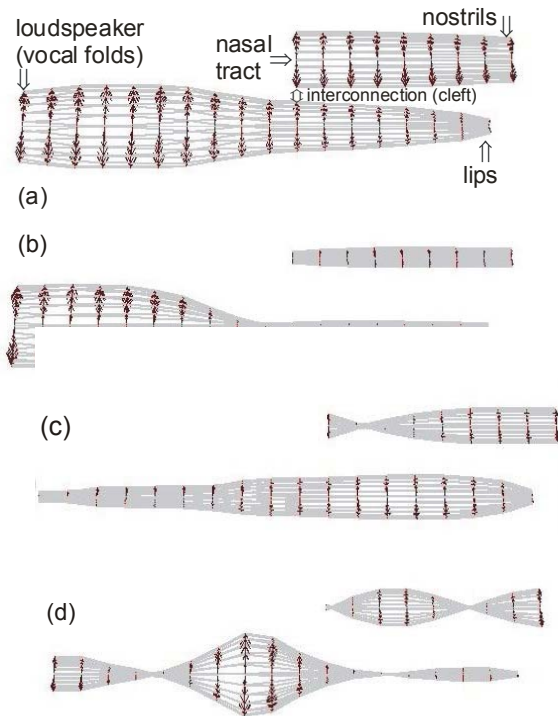


Fig. 6 Measured acoustic mode shapes of vibration for the cleft size $A=132$ mm². The double amplitudes of the pressure are shown in 27 measurement points along the vocal and nasal tracts - a) $F_1= 679$ Hz, b) $F_2= 884$ Hz, c) $f_{\text{naso}}= 1266$ Hz, d) $F_3= 3042$ Hz.

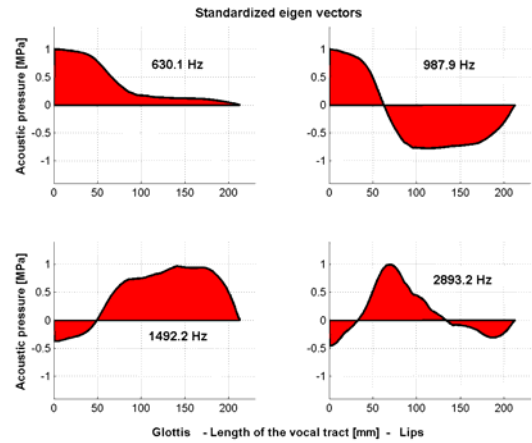


Fig. 7 Computed acoustic mode shapes of vibration for the cleft size $A=132$ mm².

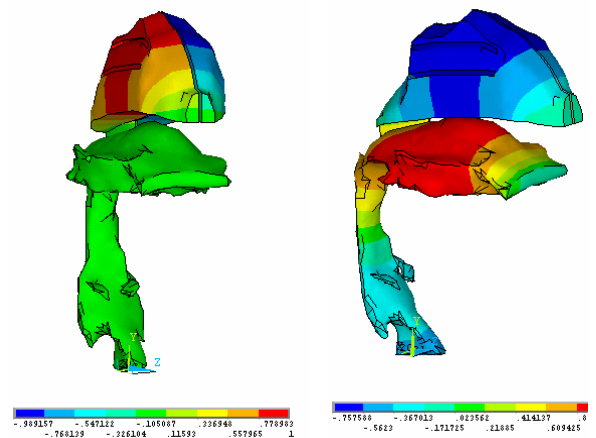


Fig. 8 Computed acoustic oro-nasal modes of vibration for the cleft size $A=132$ mm² ($f_{\text{naso}}= 1432$ Hz and 1492 Hz).

IV. NUMERICAL SIMULATION OF PHONATION

The behavior of the FE model was tested by a broadband frequency pulse. The power spectral density of this pulse is presented in the Fig. 9.

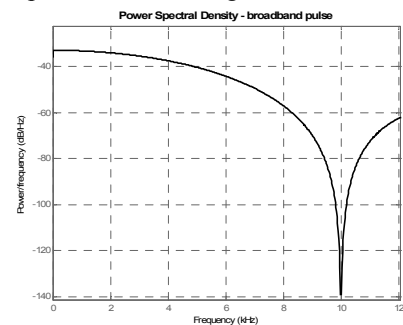


Fig. 9 Power spectral density of the broadband frequency pulse for testing the FE model by the transient analysis.

The results of transient analysis in the frequency domain are presented in Fig. 10 for the broadband frequency pulse and in the Fig. 11 for L-F pulse model.

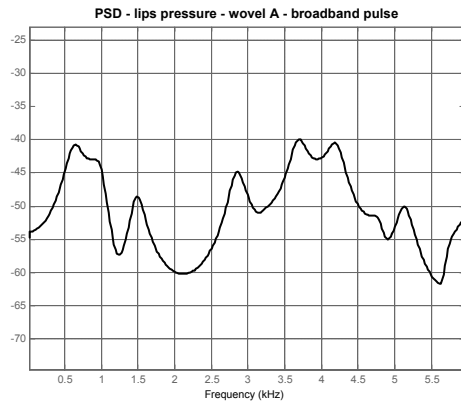


Fig. 10 Power spectral density of the pressure near the lips for Czech vowel /a/ for broadband frequency pulse and the cleft size $A=132\text{mm}^2$.

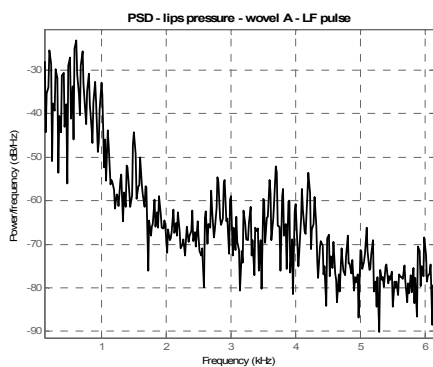


Fig. 11 Power spectral density of the pressure near the lips for vowel /a/ for L-F pulse ($A=132\text{mm}^2$).

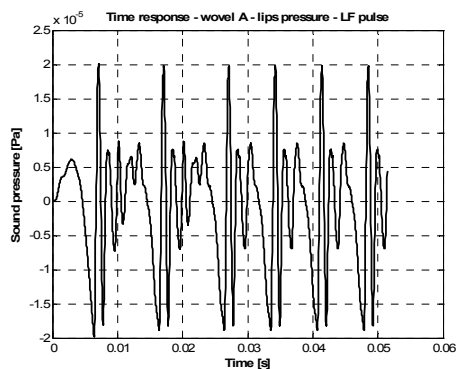


Fig. 12 Acoustic pressure near the lips for LF pulse.

The formant frequencies $F1 \approx 630$ Hz, $F2 \approx 987$ Hz and $F3 \approx 2893$ Hz can be found in the frequency response functions in Fig. 11. The formant frequencies are in good agreement with the data known for Czech vowels. Another resonant frequencies $f_{\text{nasal}} \approx 1432, 1492$ Hz appears in Fig. 5 and 11 due to the velopharyngeal insufficiency.

V. CLINICAL INVESTIGATION

The theoretical results were compared with the results of the acoustic voice analysis. Eight adults with mild velopharyngeal insufficiency phonated vowel /a/ and pronounced the interconnection /ama/. The nasal and oral signals were picked up by microphones of the head part of Nasometer 6200-3 (Kay Elemetrics Corp.) and analysed by Multi-Speech (Kay El. Corp.) programme. The new resonant region (formant) was found between formants F2 and F3. Its position was located between 1800 Hz to 2050 Hz, the relative intensity of harmonics in this region was between -7 dB to $+3$ dB with regard the formant F3. The example of the acoustic analysis is shown in Fig. 13.

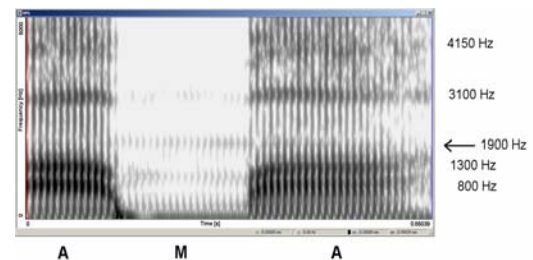


Fig. 13 Acoustic analysis of the pronounced interconnection /ama/.

VI. CONCLUSIONS

The time response functions for the pressure near the lips were obtained by the transient analysis of the FE models of the vocal tract for the model excited by a broadband frequency pulse and L-F pulse. The formant frequencies F1 – F3 evaluated from the resonances of the calculated frequency response functions are in good agreement with the experimental data. The existence of calculated oronasal formant was verified by the measurements on physical model as well as on subjects suffered by the velopharyngeal insufficiency.

ACKNOWLEDGEMENT

This research is supported by the Grant Agency of the Czech Republic by the project No 106/04/1025 "Modeling of vibroacoustic systems focusing on human vocal tract".

REFERENCES

- [1] Dedouch, K.; Horáček, J.; Vampola, T.; Kršek, P.; Švec, JG, 2001. Mathematical modelling of male vocal tract. In: *Proc. MAVÉBA*, Sept.13-15, 2001, Firenze, pp. 6-8
- [2] Fant, G.; Liljencrants, J.; Lin, Q., 1985. A Four Parameter Model of Glottal Flow. In *STL-QPSR 4*, KTH, Stockholm, Sweden, pp.1-13.
- [3] Vohradník, M., 2001. *Communication disorders by velopharyngeal insufficiency*. Prague - Dolní Brezany: Scriptorium, 2001, pp.134-145 (in Czech).

Two-Mass Models of the Bird Syrinx

Riccardo Zaccarelli*, Coen Elemans†, W. Tecumseh Fitch‡, Hanspeter Herzel*

July 20, 2005

Abstract

Self-sustained vibrations within the syrinx of birds are simulated using symmetric two-mass models. The first system that will be presented here is a rescaled version of the well-known model of human vocal fold vibrations. Moreover, a novel model of the syrinx of a ring dove is introduced. We show that the intensity of harmonics depends strongly on the geometry of the vibrating tissue and the driving pressure. This leads to a discussion how birds can control the strength of overtones.

1 Introduction

Two-mass models of vocal folds vibrations have been used successfully to describe the normal voice [1, 2], vocal fold paralysies [3, 4, 5, 6], phonation onset [7], voice instabilities at high pressures [8] or source-tract coupling [9, 10]. Goller and Larsen [11] and Elemans et al. [12] have shown that sound generation in many birds is induced also by an interaction between air flow and biomechanical vibrations of labia or thickened membranes. Consequently, biomechanical models can be exploited to study the sound generation in the birds syrinx [13, 14, 15].

In this paper we adapt the well-known simplified two-mass model to the dimensions of a syrinx in order to study the onset of sound generation and control of higher harmonics (overtones). In a first model version we simply rescale the two-mass to the size of a songbird syrinx. Then we derive a somewhat more realistic model describing the syrinx of

a ring dove. We find that both models exhibit self-sustained oscillations at realistic parameter values. In the classical two-mass model collision occurs at higher pressures leading to strong harmonics. Contrarily, in the model of the dove syrinx collision is avoided leading to more pure tones. Finally, we relate these observations to the widely discussed topic how birds control the intensity of their harmonics [16, 17, 18, 19].

2 Methods and Results

The models discussed in this paper are sketched in Figure 1 and Figure 2 with the parameters listed in the corresponding tables. The first model strongly resembles the widely used simplified two-mass model of vocal folds vibrations [5, 7, 8].

In this model the masses represent the vibrating labia of songbirds according to the findings of Goller and Larsen [11]. The second model is adapted to the syrinx of a ring dove [12]. Here upper and lower masses are joined by plates leading to a much smoother shape of the vibrating tissue. The equations of motions of both models read as follows:

$$\dot{x}_1 = v_1 \quad (1)$$

$$\dot{v}_1 = \frac{1}{m_1} \left(F_1 - r_1 v_1 - k_1 x_1 + I_1 + \right. \\ \left. - k_c (x_1 - x_2) \right) \quad (2)$$

$$\dot{x}_2 = v_2 \quad (3)$$

$$\dot{v}_2 = \frac{1}{m_2} \left(F_2 - r_2 v_2 - k_2 x_2 + I_2 \right. \\ \left. - k_c (x_2 - x_1) \right) \quad (4)$$

The pressure forces F_i are derived from the Bernoulli equation and the jet assumption (see [5] for details). The collision forces I_i are chosen as in

*Humboldt University Institute for Theoretical Biology (ITB) Invalidenstr. 43, D-10115 Berlin, Germany

†Experimental Zoology Group, Wageningen University P.O. Box 338, 6700 AH Wageningen, The Netherlands

‡School of Psychology, University of St. Andrews, St. Andrews, Fife, KY16 9AJ, Scotland

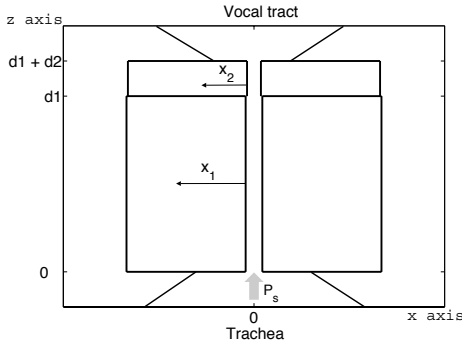


Figure 1: The rescaled two-mass model of the songbird's syrinx.

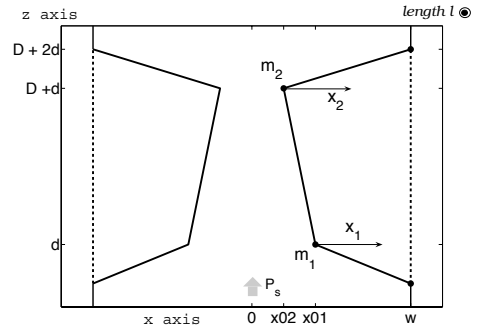


Figure 2: The model of the ring dove syrinx: the point masses are joined by three mass-less plates.

symbol	description	value
l	length of the glottis	0.3 cm
a_{01}	lower rest area	0.0021 cm ²
a_{02}	upper rest area	0.00175 cm ²
d_1	1 st mass thickness	0.1 cm
d_2	2 nd mass thickness	0.02 cm
m_1	1 st mass	0.0015 g
m_2	2 nd mass	0.0003 g
k_1	1 st mass stiffness	0.08 g/ms ²
k_2	2 nd mass stiffness	0.008 g/ms ²
r	damping constant ($r_1 = r_2$)	0.002 g/ms
k_c	coupling constant	0.0025 g/ms ²

Table 1: Parameters of the rescaled two-mass model shown in Fig. 1

earlier studies [1, 5, 8].

Figure 3 shows the onset of self-sustained oscillations for increasing pressure P_s and varying stiffness k_1 . It turns out that the onset pressure of the rescaled model can be below 0.004 (4 cm H₂O) for appropriate parameters. The points A and B refer to nearly sinusoidal oscillations near the onset and to oscillations with strong overtones (compare Fig. 4).

In Figure 5 simulations of the second model are shown for high driving pressure ($P_s = 0.05$). Even at such a high pressure the areas remain positive, i.e. the masses do not collide. Consequently, the spectrum in Figure 4 has almost no harmonics. We get easily oscillation for slightly negative initial rest areas, i.e. if the syrinx is closed in the rest position. Probably negative rest areas are necessary to com-

symbol	description	value
W	width of the trachea	0.3 cm
l	length of the trachea	0.3 cm
w	membrane's width	0.15 cm
d	1 st mass height	0.05 cm
$d + D$	2 nd mass height	0.25 cm
m	masses ($m_1 = m_2$)	0.005 g
k	stiffness	0.1 g/ms ²
r	damping constant	0.01 g/ms
k_c	coupling constant	0.0025 g/ms ²

Table 2: Parameters of the model of the ring dove syrinx (see Fig. 2)

pensate the amount of pressure acting on the first plates on the left and right membranes (see Figure 2). These simulations illustrate that the configuration of the syrinx and the driving pressure can easily control the intensity of harmonics ranging from almost pure tones to quite pronounced overtones.

3 Discussion

It has been shown above that rescaled biomechanical models originally developed to describe vocal fold vibrations can be adapted to model the birds syrinx. Both sound producing organs are excited by the same principle: in the opening phase a high pressure drives the vibrating structure apart and during closure the pressure is reduced due to the Bernoulli force. The fundamental frequency is governed by the mass and stiffness of the vibrating tissue. A slightly convergent rest position leads to

the onset of self-sustained oscillations at realistic pressures (see Figure 1).

Around our default parameters given in Table 1 we found no voice instabilities. Our simulations represent symmetric vibrations. Interestingly, the same model equations can be used to model a single vibrating structure (a “hemi-syrinx”). In this case only the sound intensity is reduced but onset pressure or intensity of harmonics are identical.

The amount of harmonics in our simulations was quite variable. In all model version almost pure tones are found near the onset of vibrations (i.e. near the Hopf bifurcation line shown in Figure 3). In the rescaled two-mass model sketched in Figure 1 strong harmonics appear at higher pressures due to collision.

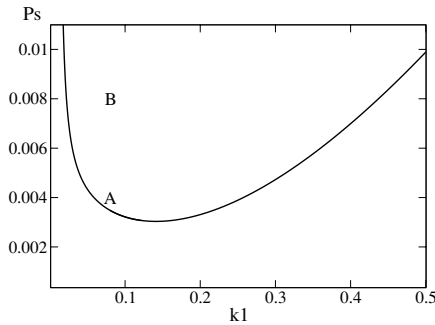


Figure 3: Variation of the onset pressure depending on the stiffness: at points A and B, i.e. close and relatively far from the Hopf bifurcation, we evaluated the power spectrum of the flow derivative (see Figure 4).

In our model of the ring dove syrinx no collision occurs at default parameters even for very high pressures. Consequently, harmonics are fairly weak. These simulations reveal that the intensities of overtones depend strongly on the configuration of the syrinx and thus muscles can easily control the amount of harmonics.

There is a long debate about the control of harmonics in bird songs [16, 17, 18, 19, 20]. Often bird songs sound like a whistle and not much energy is found at overtones [18]. However, in some spectrograms very pronounced overtones are visible

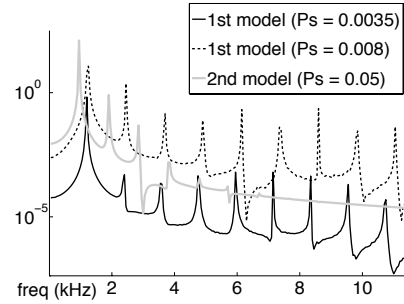


Figure 4: Power spectra at two different regimes corresponding to the letters A (solid line) and B (dashed one) in Fig. 3. Close to the Hopf bifurcation point (A) ($P_s \simeq 0.0034$) we observe less intense harmonics. The thick grey line refers to the ring dove model.

[11]. In order to imitate human speech [17] or other sounds, birds need a fine control of their overtones. These ongoing discussions can be enlightened by simulations of appropriate models. In a recent paper, Riede et al. illustrated how varying tracheal configurations can suppress the second harmonic in pigeons [16].

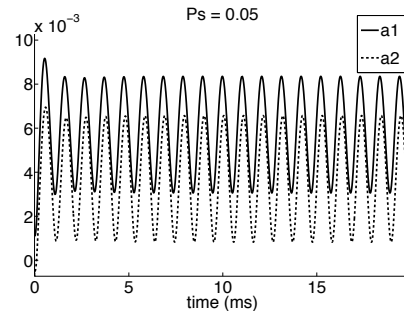


Figure 5: Tracheal area variation during oscillation of the ring dove syrinx model: even with a huge pressure the areas are always greater than zero.

In this paper we have shown that the geometry and the rest position of the syrinx can influence the harmonic spectra drastically. For a small upper mass and a rectangular geometry, collisions leading to strong harmonics can be avoided only near the phonation onset. At higher pressures counteracting forces would be required to diminish collisions. The

avoidance of strong collisions in song birds might be achieved by the medium tympaniform membrane (MTM) attached to the vibrating labia [21]. Such a possible function of the MTM will be discussed in more details in a forthcoming study.

In our ring dove model the smoother configuration and equal upper and lower masses counteract collisions even at high pressures. This is presumably due to a stronger effect of the subsyngial pressure acting on both masses.

Recent studies of ring dove vocalizations reveal [22] that there are more harmonics during inspiratory phonation even at low intensities. This implies that asymmetries between outflow and inflow of the air have to be taken into account. This will be treated in a more sophisticated model. Our simulations are a first step towards more realistic modeling of the syrinx. In subsequent studies we will incorporate the MTM and the dynamic control of the associated muscles.

4 Acknowledgment

We acknowledge support from the Deutsche Forschungsgemeinschaft (grant He 2168/7).

References

- [1] K. Ishizaka, J. L. Flanagan: "Synthesis of Voiced Sounds From a Two-Mass Model of the Vocal Cords", *Bell. Syst. Tech. J.*, 51, 1233-1268 (1972)
- [2] X. Pelorson, A. Hirschberg, R. R. Van Hassel, A. P. J. Wijnands, Y. Auregan: "Theoretical and experimental study of quasisteady-flow separation within the glottis during phonation. Application to a modified two-mass model", *J. Acoust. Soc. Am.*, 96, 3416-3431 (1994)
- [3] N. Isshiki, M. Tanabe, M. Sawada: "Arytenoid adduction for unilateral vocal cord paralysis", *Arch. Otolaryngol.*, 104, 555-558 (1978)
- [4] M. E. Smith, G. S. Berke, B. R. Gerratt, J. Kreiman: "Laryngeal paralyses: Theoretical considerations and effects on laryngeal vibration" *J. Speech. Hear. Res.*, 35, 545-554 (1992)
- [5] I. Steinecke, H. Herzel: "Bifurcations in an asymmetric vocal-fold model", *J. Acoust. Soc. Am.*, 97, 1874-1884 (1995)
- [6] P. Mergell, H. Herzel, I. R. Titze "Irregular Vocal Fold Vibration - High-Speed Observation and Modeling" *J. Acoust. Soc. Am.*, 108, 2996-3002 (2000)
- [7] P. Mergell, H. Herzel, T. Wittenberg, M. Tigges, U. Eysholdt: "Phonation onset: vocal fold modeling and high-speed glottography". *J. Acoust. Soc. Am.*, 104, 464-470 (1998)
- [8] J. J. Jiang, Y. Zhang, J. Stern: "Modeling of chaotic vibrations in symmetric vocal folds" *J. Acoust. Soc. Am.*, 110, 2120-2128 (2001)
- [9] P. Mergell, H. Herzel: "Modelling biphonation - The role of the vocal tract", *Speech Communication*, 22, 141-154 (1997)
- [10] H. Hatzikirou, W. T. Fitch, H. Herzel: "Voice instabilities due to Source-Tract Interactions", *Acustica*, in press.
- [11] F. Goller, O. N. Larsen: "A new mechanism of sound generation in songbirds", *Proc. Natl. Acad. Sci. USA*, 94, 14787-14791 (1997)
- [12] C. P. H. Elemans, L. Y. Spierts, U. K. Mueller, J. L. van Leeuwen, F. Goller: "Superfast muscles control dove's trill", *Nature*, 431, 146-146 (2004)
- [13] M. S. Fee, B. Shraiman, B. Pesaran, P. P. Mitra: "The role of nonlinear dynamics of the syrinx in the vocalization of a songbird", *Nature*, 395, 67-71 (1998)
- [14] N. H. Fletcher: "Bird Song: A quantitative acoustic model", *J. Theor. Biol.*, 135, 455-481 (1998)
- [15] R. Laje, G. B. Mindlin: "Diversity within a birdsong", *Phys. Rev. Lett.*, 89, 288102 (2002)
- [16] T. Riede, G. J. L. Beckers, W. Blevins, R. A. Suthers: "Inflation of the esophagus and vocal tract filtering in ring doves", *Journal of Experimental Biology*, 207, 4025-4036 (2004)
- [17] D. H. Klatt, R. A. Stefanski: "How does a mynah bird imitate human speech?", *J. Acoust. Soc. Am.*, 55, 822-832 (1974)
- [18] S. Nowicki, P. Marler, A. Maynard, S. Peters "Is the tonal quality of birdsongs learned?", *Ethology*, 90, 225-235 (1992)
- [19] G. J. L. Beckers, R. A. Suthers, C. ten Cate: "Pure-tone birdsong by resonance filtering of harmonic overtones", *Proc. Natl. Acad. Sci. USA*, 100, 7372-7376 (2003)
- [20] G. J. L. Beckers, B. S. Nelson, R. A. Suthers, "Vocal-Tract Filtering by Lingual Articulation in a Parrot", *Current Biology*, 14, 1592-1597 (2004)
- [21] M. S. Fee: "Measurement of the linear and nonlinear mechanical properties of the oscine syrinx: Implications for function", *J. Comp. Physiol. A.*, 188, 829-839 (2002)
- [22] C. P. H. Elemans: "Mechanical properties of syringeal muscles in Ring doves (*Streptopelia risoria*)", PhD thesis, Experimental Zoology Group, Wageningen University, 92-107 (2004)

A PHYSICAL MODEL FOR ARTICULATORY SPEECH SYNTHESIS. THEORETICAL AND NUMERICAL PRINCIPLES

N. Ruty¹, J. Cisonni¹, X. Pelorson¹, P. Perrier¹, P. Badin¹, A. Van Hirtum¹

¹Institut de la Communication Parlée, UMR5009-CNRS, Institut National Polytechnique de Grenoble, France

I. INTRODUCTION

The objective of this study is to develop a simple physical model able to produce articulatory synthesis of continuous vowel transitions. The proposed model considers simplified physical approximations for the glottal source, acoustical propagation in the vocal tract and lip radiation. The articulatory quality of the synthesized results is interpreted in terms of the simplifications applied in each model element.

II. THEORETICAL DESCRIPTION

A. Source models

Two types of glottal flow sources are considered. Both were chosen because they are well-known and representative for two different modeling approaches.

The first one is the Liljencrants-Fant (LF) model described in [1]. This analytical ad-hoc model is easily controllable because only four wave shape parameters are needed. Fig. 1 shows a typical period of glottal flow derivative synthesized by this model during a period t_0 , corresponding to a fundamental frequency $F_0 = 1/t_0$. The derivative of the flow is described by these two equations:

$$E(t) = E_0 e^{\alpha t} \sin(\pi t / t_p) \quad \text{if} \quad t < t_e \quad (1)$$

$$E(t) = E(t_e) \frac{e^{\varepsilon(t-t_e)} - e^{\varepsilon(t_0-t_e)}}{1 - e^{\varepsilon(t_0-t_e)}} \quad \text{if} \quad t_e < t < t_0 \quad (2)$$

where t_0 , t_e , t_a and E_0 are the control parameters of the model, $\varepsilon = 1/t_a$ and α are calculated using the method described in [2], as a function of t_0 , t_e , t_a and t_p . Such a parametric description of the glottal flow is very popular due to its simplicity and its computational efficiency. Although it involves almost no physics it will be used in the following as a reference.

As a more physical alternative, we propose the use of the symmetrical two mass model [3] schematically depicted in Fig. 2. The two mass model is capable to simulate flow-induced vibrations of the vocal folds when coupled to an airflow model [4]. This model is controlled by a set of mechanical parameters: the masses (m), stiffness (K , K_c) and damping (r). The applied parameter values determine the mechanical response, i.e. the

resonance frequencies and the quality factors [5]. The applied flow model accounts for an unsteady flow separation point (using Liljencrants 'ad-hoc' criterion) allowing to predict the pressure distribution within the glottis. The influence of viscous losses and inertia of air on the main flow is also considered. This way, the pressure forces exerted by the flow on the vocal folds walls can be estimated from the calculated pressure distribution. The mechanical differential equations are numerically solved in order to estimate the vocal folds displacement and the glottal flow velocity. An example of the source signal (derivative of the volume flow) obtained with this model is depicted in Fig. 3.

B. Acoustical propagation

Acoustical wave propagation inside the vocal tract is described in the time domain [6]. First the geometry of the vocal tract is concatenated into a finite number of tubes of area A_i , where (i) is the index of the tube in the flow direction. In each tube (i) the pressure distribution at a location x along the vocal tract axis can be written as:

$$p_i(x, t) = [p_i^+(t - x/c) + p_i^-(t + x/c)] \quad (3)$$

with p_i pressure, x position, p_i^+ and p_i^- respectively the travelling and regressive pressure waves in tube (i).

Assuming continuity at the junction between the tubes (i) and ($i+1$), one obtains:

$$\frac{1}{A_i} (p_i^+(t - l_i/c) - p_i^-(t + l_i/c)) = \frac{1}{A_{i+1}} (p_{i+1}^+(t) - p_{i+1}^-(t)) \quad (4)$$

$$p_i^+(t - l_i/c) + p_i^-(t + l_i/c) = p_{i+1}^+(t) + p_{i+1}^-(t)$$

where l_i is the length of the tube (i), A_{i+1} the area, and p_{i+1} is the pressure in the tube ($i+1$).

The travelling and regressive component of the pressure in the tube ($i+1$) are given by:

$$p_{i+1}^+(t) = \beta_i p_i^+(t - l_i/c) + r_i p_{i+1}^-(t) \quad (5)$$

$$p_i^-(t + l_i/c) = -r_i p_i^+(t - l_i/c) + \phi_i p_{i+1}^-(t)$$

where $r_i = \frac{A_{i+1} - A_i}{A_{i+1} + A_i}$ is the reflection coefficient at the junction (i), $\beta_i = 1 - r_i$ and $\phi_i = 1 + r_i$ are the propagation coefficients.

In first approximation, the reflection coefficient at the glottis is considered to be $r_0 = 1$. The reflection coefficient at the lips is discussed in the following subsection.

C. Reflection coefficient at the lips

The acoustical behavior of the lips is approximated by the radiation from a piston set in an infinite rigid baffle. This radiation impedance is calculated using the analytic formula described in [7]:

$$Z_r = \pi a^2 \rho c (1 - J_1(2ka)/(ka) + S_1(2ka)) \quad (6)$$

where a is the radius of the equivalent piston (i.e. the lips aperture), ρ the air density, c the sound velocity, $k = 2\pi f/c$, f is the frequency, J_1 is the first kind Bessel [7] function of order 1, and S_1 the Struve function of order 1.

This analytic form is used for calculations, only the Bessel and Struve functions are approximated. Given Z_r , the normalized reflection coefficient is calculated as following:

$$R = \frac{1 - Z_r / (\pi a^2 \rho c)}{1 + Z_r / (\pi a^2 \rho c)} \quad (7)$$

D. Glottis/vocal tract coupling

Using the LF model for the glottal source, the source signal is simply injected at the entrance of the vocal tract, i.e. the tube with index $i = 0$. Next, the propagation is calculated for each time step.

The use of the two mass vocal fold model allows to account for the interaction between the source and the vocal tract. Indeed, the acoustical pressure past the glottis ($i=0$) is constantly varying with time due to the multiple reflections. These variations modify the pressure drop between the entrance and the outlet of the glottis. Since the pressure distribution within the glottis depends on the total pressure drop across the glottis, the forces and thus the vocal fold movements can be affected by the acoustical pressure fluctuations.

III. FROM THEORETICAL DOMAIN TO NUMERICAL DOMAIN

A. Vocal Tract and articulatory synthesis

The concatenation of the vocal tract into elementary tubes imposes, for calculation efficiency, a sample frequency $F_e = c/L_x$; where $L_x = L/N$ is the length of a vocal tract tube retrieved as the ratio between the total vocal tract length L and the number of tubes N . Thus, a modification of the vocal tract shape (a variation of

length) implies a variation of the sample frequency. In order to keep a sound signal sampled at a constant frequency and considering a continuous vocal tract variation, the generated signal is resampled following the method proposed in [8]. Firstly, the numeric signal $x(n)$ is converted in an analogical signal. Then, this continuous signal is sampled at a fixed frequency. The resampled signal $y(m)$ is defined by:

$$y(m) = x(mT_s) = \sum_{n=N1}^{N2} x(n) \cdot \frac{\sin(\pi \cdot \frac{mT_s - nT_e}{T_e})}{\pi \cdot \frac{mT_s - nT_e}{T_e}} \cdot W(mT_s - nT_e) \quad (8)$$

Where m is the new sample index, T_s and T_e correspond to the periods associated with respectively F_s and F_e as $T_s = 1/F_s$, $T_e = 1/F_e$, and W is the applied time (Hamming) window, with $N1$ et $N2$ its limits.

This way, the continuous variation between two vowels can be computed.

B. Reflection function: from theory to filter design

We want to design a filter with a frequency response as close as possible to the reflection coefficient. As observed in [9], numerical treatment and more precisely inverse FFT of the reflection coefficient is likely to cause disturbances, due to sampling and windowing effects. Therefore some of the approximations can be erroneous. The applied digitisation of the vocal tract yields a sampling frequency of around 80000Hz. The exact value depends on the vocal tract length corresponding to the vowels we want to synthesize. The reflection coefficient at the lips is calculated for frequencies ranging between 0 and 40000Hz, for a total of 2^{15} values. Then the inverse FFT of this signal is computed. From this reflection function, the first thirty coefficients are kept as filter coefficients.

IV. RESULTS AND DISCUSSION

A. Validity of the approximated transfer function

The validity of the mentioned hypothesis concerning vocal tract propagation and lip radiation needs to be tested. Therefore the theoretical transfer function of the acoustical model is computed following the method described in [10]. The comparison with the FFT of the impulse response described in III.B is presented in Fig. 4 for a sampling frequency of 80000Hz, and for two extreme equivalent piston radii (0.001m and 0.02m). From this figure it can be seen that the mean error concerning the reflection coefficient is less than 10% at the most. Note that the commonly used low frequency

approximation: $Z_r = \pi a^2 \rho c \left[\frac{1}{2} (ka)^2 + i \frac{8ka}{3\pi} \right]$ [11] can

lead to strong departures even at moderate frequencies (of order of 4 kHz). In figure 5 a comparison between the computed transfer function a 32 sections approximation of the vowel [i] and the theoretical prediction is shown. A very good agreement can be observed.

B. Variation of vocal tract length

Fig. 6 shows the spectrogram of the transfert function of a uniform vocal tract. The length of the vocal tract is continuously varying from 10cm up to 17cm by steps of 1mm. The method to simulate this lengthening is detailed in subsection III.A. As expected, the spectrogram exhibits no discontinuities and hence the method seems appropriate to simulate vowel transitions.

C. Some examples of synthesis

As a typical example, Fig. 7 and Fig. 8 present the results of a synthesised vowel [a]. This vowel is chosen as an example because it is an extreme part of the vocalic triangle Fig. 7 shows a time simulation of 1s and Fig.8 shows the frequency representation. The example shown is obtained with the LF source model, the acoustics is simulated as explained previously and using a resample frequency of 16kHz.. Further simulations using the two mass model for the source lead to an increase in perceptual quality since this approach accounts for vocal tract/source interaction and hence results in high quality articulatory synthesis.

V. CONCLUSION

The current study presents a simplified physical model for articulatory synthesis of continuous vowel transitions. The relevance of a high frequency radiation description has been shown. Further, the numerical implementation – including variable sampling frequency- has been developed and validated. Typical synthetic examples – including vowel transition- will be played during the conference [12].

REFERENCES

- [1] G. Fant, J. Liljencrants, Q. Lin, "A four-parameter model of glottal flow," *STL-QPSR*, vol. 4, pp. 001-013, 1985.
- [2] R. Veldhuis, "A computationally efficient alternative for the Liljencrants-Fant model and its perceptual evaluation," *J. Acoust. Soc. Am.* 103 (1), pp 566-71. 1998
- [3] N. J. C. Lous, G. C. J. Hofmans, R. N. J. Veldhuis, A. Hirschberg, "A Symmetrical Two-Mass Vocal-Fold Model Coupled to Vocal Tract and Trachea, with

Application to Prosthesis Design". *Acta Acustica United with Acustica*. Vol. 84 (6). pp 1135-50. 1998.

- [4] X. Pelorson, A. Hirschberg, Van Hassel, R.R. A.P.J. Wijnands, Y. Auregan, "Theoretical and experimental study of quasisteady-flow separation within the glottis during the phonation, Application to a modified two-mass model," *J. Acoust. Soc. Am.* 96 (6). pp 3416-31. 1996
- [5] I. Lopez, A. Van Hirtum, M.H. Schellekens, N.M. Driessen, A. Hirschberg, X. Pelorson, "Buzzing lips and vocal folds: the effect of acoustical feedback", in *Flow Induced Vibrations*; de Lanfre & Axisa, Paris, France. 2004
- [6] D. O'Shaughnessy, *Human and machine*, Speech Communication, Addison-Wesley Publishing Company. 1997, pp 41-127.
- [7] P.M. Morse, K. Uno Ingard, *Theoretical acoustics*, Mc Graw-Hil Book Company vol. New York. 1968, pp.383-388.
- [8] H.Y. WU, P. Badin, Y.M. Cheng, B. Guérin, "Simulation du conduit vocal: réalisation de la variation continue de longueur dans un modèle de Kelly-Lochbaum," *Bulletin du Laboratoire de la Communication Parlée*, vol. 1, pp. 01-27, 1987.
- [9] J.D. Polack, X. Meynial, J. Kergomard, C. Cosnard, M. Bruneau, "Reflection function of a plane sound wave in a cylindrical tube," *Revue. Phys. Appl.*, vol. 22, pp. 331-337, 1987.
- [10] X. Pelorson, R. Laboissière, S. El Masri, "Vocal tract acoustics at high frequencies," *Proc. 4ème Congrès Français d'Acoustique*, vol. 1, pp. 401-404, 1997.
- [11] G. Fant, *The acoustic theory of speech production*. Mouton, The Hague, 1960.
- [12] <http://www.icp.inpg.fr/~rutu>

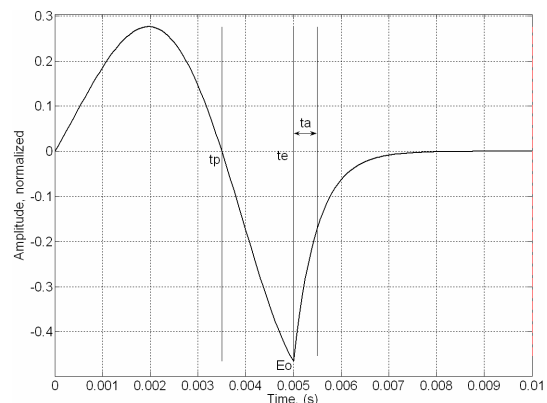


Figure 1: Derivative of the glottal airflow, generated with the LF model

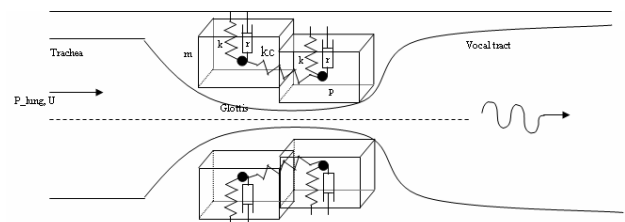


Figure 2 : two mass model of vocal folds, P_{lung} is the subglottal pressure, U the volume airflow, m the masses, k and kc the stiffness of the spring, and r the damping.

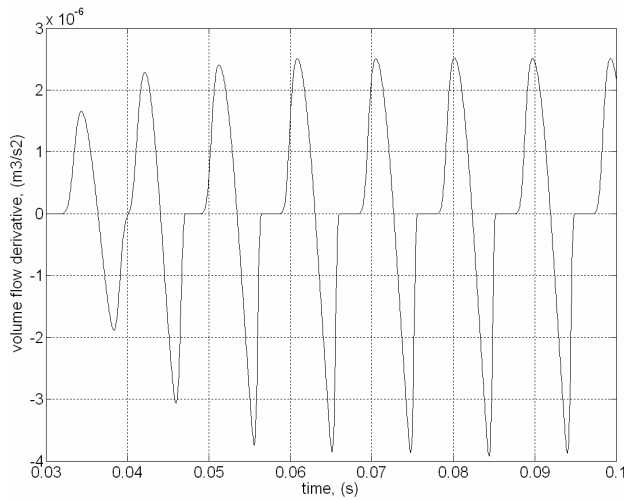


Figure 3: glottal volume flow derivative, generated with the 2 mass model for a subglottal pressure increasing from 0 to 600 Pa.

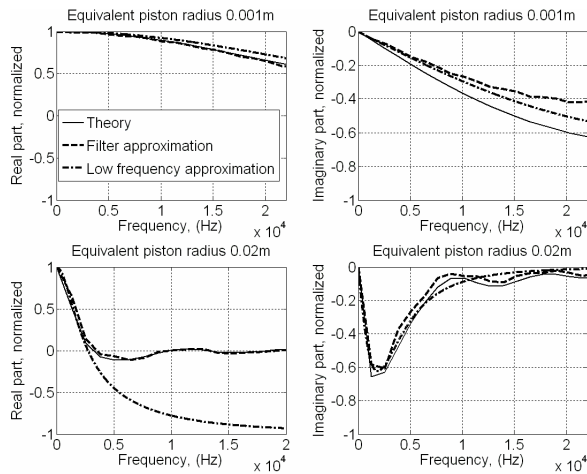


Figure 4: comparison of the theoretical reflection function and its filter approximation, 30 coefficients for the FIR filter, for a sample frequency of 80kHz. Two extreme values of the equivalent piston radius are considered (0.001m and 0.02m).

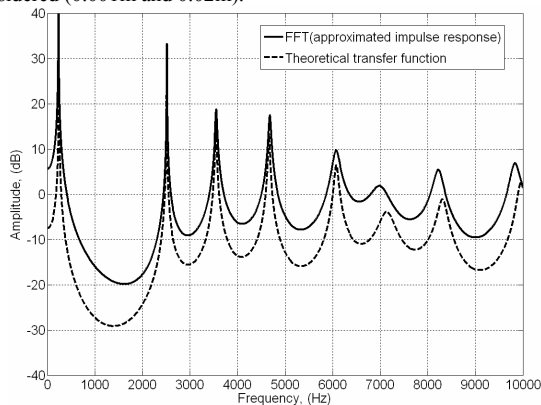


Figure 5: comparison of the theoretical transfer function and the inverse FFT of the impulse response, for the vowel [i], resampled at 44kHz.

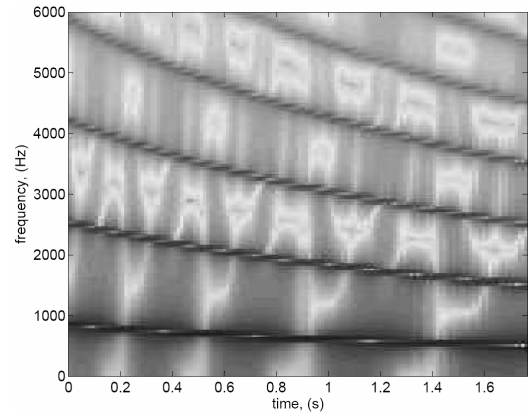


Figure 6: Spectrogram for a continuous variation of the tube length, from 0.1m to 0.17m, reference of sampling frequency $F_s=20000$ Hz, tube section dimension $0.04*0.03m^2$.

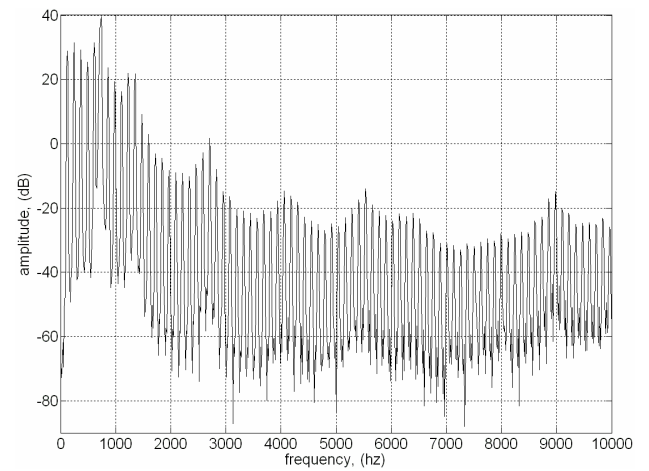


Figure 7: Frequency representation of the synthesized voiced sound [a]. Resample frequency 44kHz, duration 1s, fundamental frequency 123Hz.

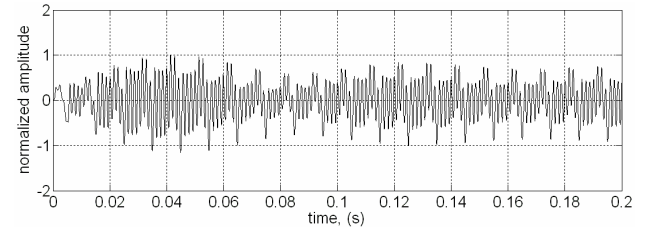


Figure 8: Time representation of the synthesized voiced sound [a]. Resample frequency 44kHz, duration 1s, fundamental frequency 123Hz.

PHYSIOLOGICAL CONTROL OF LOW-DIMENSIONAL GLOTTAL MODELS WITH APPLICATIONS TO VOICE SOURCE PARAMETER MATCHING

Federico Avanzini¹, Simone Maratea¹, Carlo Drioli²

¹ Department of Information Engineering, University of Padova, Padova, Italy

² Institute of Phonetics and Dialectology, ISTC-CNR, Padova, Italy

A set of rules is proposed for controlling a 2-mass glottal model through activation levels of laryngeal muscles. The rules convert muscle activities into physical quantities such as fold adduction, mass, thickness, depth, stiffness. A codebook is constructed between muscular activations and a set of relevant voice source parameters, and its applications to voice source parameter matching are explored.

I. INTRODUCTION

Features of the voice source signal (i.e., the glottal flow) are known to be relevant for characterizing voice quality and speaker identity. Parametric models of the voice source fit the glottal signal with piecewise analytical functions, using a small number of parameters. As an example, the Liljencrants and Fant (LF) model [8] characterizes one cycle of the flow derivative using as few as four parameters (see section II and Fig. 1). Physical models of the glottal system describe the vocal fold with two [10] or more [14] coupled mechanical oscillators, driven by the intraglottal pressure. Physical models capture the basic non-linear mechanisms that initiate self-sustained oscillations, and can simulate subtle features (e.g. interaction with the vocal tract); however the large number of parameters typically involved makes it hard to employ these models for voice source matching purposes needed in many applications, ranging from rule-based speech synthesis [13] to analysis and assessment of voice quality, including the detection and classification of voice pathologies [6].

We have addressed the issue of identification of physically-based models in previous studies [3], [7] using a hybrid approach in which the vocal fold is treated as a linear oscillator, while a non-linear block that accounts for interaction with glottal pressure is modeled as a regressor-based mapping: given a target glottal flow signal, weights for the regressors can be estimated in order to fit the target.

In this study we explore a different approach, in which the dimension of the control space of a 2-mass model (see Fig. 2) is drastically reduced by applying a

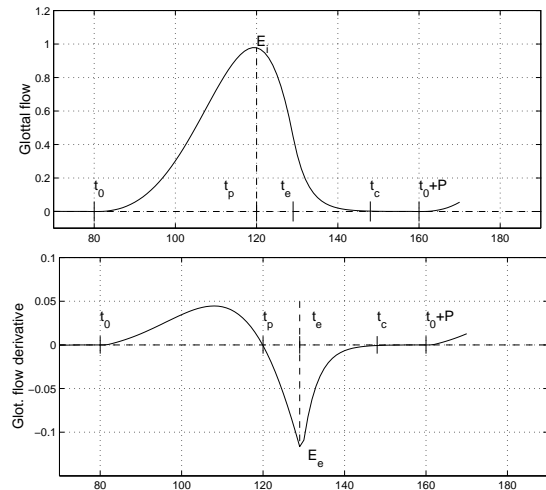


Fig. 1. Glottal flow and derivative: time of glottal opening t_o ; time and value t_p, E_i of flow maximum; time and value t_e, E_e of flow derivative minimum; time of glottal closure t_c ; glottal period P .

set of rules that map three muscular activation parameters to the low-level physical parameters of the model. The rules are developed after Titze and Story [18] and are described in section III.

Having a physiologically-motivated, low-dimensional control space, we construct in section IV a codebook between the muscle activation parameters and a set of relevant voice source parameters, and we explore its potentials in fitting target flow waveforms.

II. VOICE SOURCE PARAMETERS

Some cues of the glottal waveform have been recognized to be particularly relevant for the study of the perceptual influence of the voice source characteristics, and for comparing different voice qualities. Referring to Fig. 1, typical [8], [1] voice source quantification parameters extracted from the flow and the differentiated flow are: $T_o = t_p - t_o$ (opening phase duration), $T_{pp} = t_e - t_p$ (positive to negative peak interval duration), $T_{ret} = t_c - t_e$ (return phase duration), $T_c = t_o + P - t_c$ (closed phase duration), $T_{open} = T_o + T_{pp} + T_{ret}$ (open phase duration). Derived parameters are the *speed*

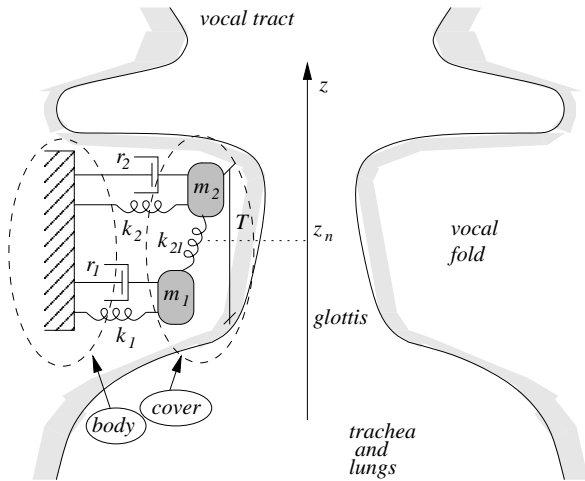


Fig. 2. The 2-mass model used in this work.

quotient $SQ = T_o/(T_{pp} + T_{ret})$, the open quotient $OQ = T_{open}/T$, the opening quotient $OingQ = T_o/T$, the closing quotient $CingQ = (T_{pp} + T_{ret})/T$, the return quotient $RQ = T_{ret}/T$, the peak-to-peak quotient $PPQ = T_{pp}/T$, and the amplitude quotient $AQ = E_i/E_e$. The spectral tilt of the voice source can be quantified by parameters such as the harmonic richness factor $HRF = (\sum_{i=2}^N H_i)/H_1$, where H_i denotes the amplitude of the i th harmonic partial.

A wide range of glottal configurations allows a speaker to choose over different phonation modalities: geometric and mechanical fold properties determine the frequency and mode of vibration; vocal fold adduction (i.e., relative distance) has an important role in determining the closed phase duration and the abruptness of closure, and affects the perceived phonation quality. As opposed to "normal" voice quality, *breathy*, *pressed*, *creaky*, are terms commonly found in the literature to denote special phonation types. In breathy voice the glottal closure is incomplete, the voicing is inefficient and air leaks between folds throughout the vibration cycle. A distinctive characteristic of breathy voice is hence an audible friction noise. On the opposite side, pressed voice occurs when vocal folds are pressed together and the glottal cycle is characterized by an abrupt closure, a reduced open phase duration, and a small vibration amplitude. Creaky voice is characterized in a somewhat similar way, additionally the tight compression of the folds may occasionally produce irregular vibrations, perceived as a crackling quality.

The analysis and matching of inverse filtered voice samples from subjects with varying voice quality, age, and sex, permitted to gain understanding of the relations between the voice source characteristics and the perceived voice quality [11], [4], [5], [12], [15], [1].

TABLE I

RULES FOR PHYSIOLOGICAL CONTROL OF THE 2-MASS MODEL.

Fold elongation	$\epsilon = G(Ra_{CT} - a_{TA}) - Ha_{LC}$
Fold length	$L = L_0(1 + \epsilon)$
Cover depth	$D_c = \frac{D_{muc} + 0.5D_{lig}}{1 + 0.2\epsilon}$
Fold thickness	$T = \frac{T_0}{1 + 0.8\epsilon}$
Nodal point position	$z_n = (1 + a_{TA})T/3$
Adduction	$\xi_0 = 0.25L_0(1 - 2a_{LC})$

III. A PHYSIOLOGICALLY CONTROLLED 2-MASS MODEL

In this section we search a link between laryngeal muscle activation and mechanical properties of the low-dimensional 2-mass model depicted in Fig. 2 and based on the Ishizaka-Flanagan model [10]. Low-level parameters (modal frequencies, effective mass in vibration, stiffness, fold thickness, fold length, rest position) are not independently controlled by the vocalist: in order to understand the oscillatory characteristics in a physiologically motivated control space, a set of rules has to be found that transforms muscle activations to geometrical and viscoelastic parameters of the model.

We follow the analysis by Titze and Story [18] who, based on experimentations and cadaveric examinations, developed a set of rules for controlling parameters of their 3-mass vocal fold model [14]. Specifically, the model is controlled by the (normalized) activation levels of three muscles: cricothyroid (a_{CT}), thyroarytenoid (a_{TA}) and lateral cricoarytenoid (a_{LC}).

The 3-mass model developed in [14] uses two masses to describe the cover tissue and a third, larger mass to describe the body. In this work we adapt Titze and Story's rules set to the 2-mass model by ignoring any references to this third mass. Therefore we select the rule subset given in table I. Here D_{mus} , D_{muc} , and D_{lig} are the anatomical resting depths for thyroarytenoid muscle, mucosa, vocal ligament, respectively; T_0 and L_0 are the resting thickness and length, respectively. The factors G (gain of elongation), R (torque ratio), and H (adductory strain factor) are empirical constants (for this study we let $G = 0.2$, $R = 3.0$, $H = 0.2$ in accordance with [18]). Values for D_{mus} , D_{muc} , D_{lig} are chosen after [14]. The low-level parameters $k_1, k_2, k_{12}, m_1, m_2$ of the 2-mass model are then derived from the geometrical parameters D_c, T, L, z_n , together with the tissue density ρ , the cover shear modulus μ_c , and the cover fiber stress σ_c [18].

We have developed a MATLAB/Octave¹ implementation of the 2-mass model, completed by the physi-

¹Open source software, a high-level language for numerical computations mostly compatible with MATLAB (www.octave.org).

ological link between laryngeal muscle activation and mechanical properties of the model, with the activations a_{TA} , a_{LC} and a_{CT} varying in the range $[0, 1]$.

IV. NUMERICAL SIMULATIONS

The 2-mass model with physiological control was used to run a set of simulations for the exploration of the control space (a_{TA} , a_{LC} , a_{CT}). All the simulations used a sampling rate $F_s = 22.05$ kHz. The subglottal pressure p_s was held fixed at the value 0.8 kPa. The anatomical resting depths of layers of vocal folds tissue were chosen in accordance with Titze and Story [14].

A. Phonation regions

A first set of simulations was performed in order to determine the phonation region in the control space. Simulations were run using two configurations. First an ideally open glottis (i.e., with zero supraglottal pressure) was considered. Second, a vocal tract load was taken into account by coupling the 2-mass glottis model with a cylindrical vocal tract model.

The phonation region was searched for each of the two configurations. Following Titze *et al.* [18], at each point (a_{TA} , a_{LC} , a_{CT}) the existence of self-sustained stable phonation was determined by applying a zero-crossing multiple-detector to the last 50 ms of the simulated glottal area signal. In this way we arbitrarily not consider “always-open glottis” phonation.

For both configurations, phonation regions are comparable with results by Titze and Story [18] on the 3-mass model. In particular, a_{CT} has little influence on the shape of the self-sustained phonatory region. For the open-glottis configuration, it simply acts as a switch that restricts phonation in the range $a_{CT} \in [0, 0.7]$, while for the cylindrical vocal tract configuration phonation occurs in the entire range $a_{CT} \in [0, 1]$.

The 2-D phonation region in the a_{LC} - a_{TA} plane (with a_{CT} fixed) is wedge-shaped. For the open-glottis configuration, the region is contained in the rectangle $a_{TA} \in [0, 0.9]$ and $a_{LC} \in [0.35, 0.5]$, while for the cylindrical vocal tract configuration the bounding rectangle is given by $a_{TA} \in [0, 1]$ and $a_{LC} \in [0.2, 0.5]$. Thus, following expectations the phonation region is larger when a vocal tract load is coupled to the glottis. Given the similarity between these results and those reported in [18], we consider our selected rules a valid link between laryngeal muscle activation and mechanical properties of the 2-mass model.

B. A physiological-to-acoustic codebook

Having determined the phonation regions in the control space, we analyze the properties of the voice source signal in such regions. We chose a set of relevant acoustic parameters, namely

TABLE II
PHYSIOLOGICAL-TO-ACOUSTIC CODEBOOK: RANGES FOR THE
RELEVANT VOICE SOURCE PARAMETERS.

	F_0	SQ	OQ	$OingQ$	$CingQ$	RQ
Open-glottis configuration						
Mean value	251	1.36	0.63	0.36	0.26	0.02
Min. value	217	0.90	0.51	0.29	0.19	0
Max. value	367	2.01	0.94	0.52	0.43	0.13
Cyl. vocal tract configuration						
Mean value	253	1.66	0.80	0.49	0.30	0.02
Min. value	179	1.13	0.35	0.23	0.12	0
Max. value	816	2.79	0.90	0.59	0.41	

$F_0, SQ, OQ, OingQ, CingQ, RQ$ (see section II for definitions) and developed a MATLAB/Octave script for automatic analysis and extraction of these parameters from the glottal flow signal. Using this tool, the signals produced by every triple a_{TA}, a_{LC}, a_{CT} in the phonation region were analyzed, resulting in a physiological-to-acoustic codebook of the form

$$(a_{TA}, a_{LC}, a_{CT}) \mapsto (F_0, SQ, OQ, OingQ, CingQ, RQ).$$

Table II provides indications about the ranges of the voice source parameters within the codebook. From this, a few remarks can be made.

First, F_0 values appear to be high, considering that a set of parameters typical for males has been used. This suggests that the choice of physical parameters made in section III (specifically, keeping the same values used in [18] for the vocal fold cover tissue, while discarding any description of the vocal fold body) is not optimal.

Second, values for the return quotient RQ are extremely low. This reflects a general limitation of low-dimensional physical models of the glottis, in which glottal closure always occurs abruptly and results in poor modeling of the closing phase.

The codebook has been tested in order to verify its potentials in fitting target flow waveforms. Target signals were constructed by superimposing a noisy component to synthetic glottal flow waveforms obtained from the LF model [8]. The fitting procedure works as follows:

1. The set $F_0, SQ, OQ, OingQ, CingQ, RQ$ of voice source parameters is extracted from the target signal.
2. A triple a_{TA}, a_{LC}, a_{CT} is determined in such a way that it minimizes the distance between its image in the codebook and the target voice source parameter vector.
3. A fitting signal is resynthesized with the 2-mass model controlled by the selected triple a_{TA}, a_{LC}, a_{CT} .

Figure 3 shows an example of the results. The opening, closing, and flow maximum points (t_o, t_c, t_e) are accurately matched. On the other hand the opening and

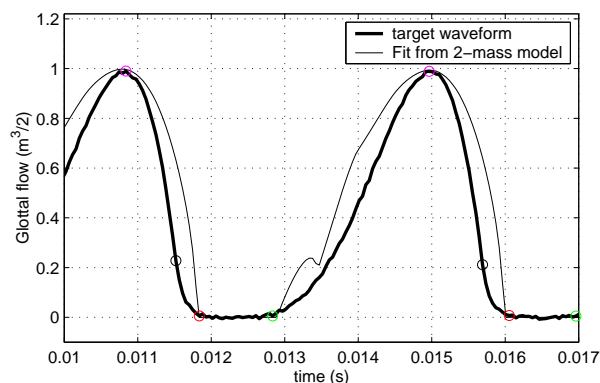


Fig. 3. Results from the fitting procedure. The target waveform is constructed by superimposing a noisy component to synthetic glottal flow waveforms obtained from the LF model.

especially the closing phases are poorly matched. As already mentioned, this is an intrinsic limitation of the 2-mass model. As a consequence the time and value of the negative peak of the flow derivative are mismatched.

V. DISCUSSION

The results presented in this work are still very preliminary. Among the points that need further discussion and refinements, the following can be mentioned.

The codebook described in section IV does not include the subglottal pressure p_s among the varying physiological parameters. The parameter p_s is known to have a major influence on relevant voice source parameters, in particular the phonation fundamental frequency is known to increase almost linearly with p_s [16]. For this reason the physiological control space should be expanded to include p_s .

A second limitation of the results comes from the characteristics of the vocal tract load: neither the open glottis nor the cylindrical vocal tract configurations provide a realistic simulation of the load, while it is known that the load characteristics also influence relevant voice source parameters (e.g., the glottal flow skewness). Better simulations of voice source/vocal tract interaction can be realized, see e.g. [17].

Finally, as already mentioned, the 2-mass model provides a poor description of the glottal flow near closure. While accurate finite-element models are able to provide qualitative behaviors in agreement with observations of glottal closure during normal voice production [9], such behaviors are not easily simulated with a low-dimensional model.

Nonetheless, the preliminary results suggests that the proposed approach can be successfully used for voice source parameters matching applications. The following points can be mentioned.

First, the muscle activation control space allow exploration of a wide region of the voice source parameter space. Second, with respect to our previous works [3], [7], this approach leads to more robust resynthesis, since no regressor-based black-box element is used and consequently stability is guaranteed by construction. Finally, the same approach can be extended to lower dimensional glottal models (e.g., [2]), in order to construct an efficient analysis/synthesis tool.

REFERENCES

- [1] P. Alku and E. Vilkman. A comparison of glottal voice quantification parameters in breathy, normal and pressed phonation of female and male speakers. *Folia Phoniatr. Logop.*, 48(5):240–254, Sep. 1996.
- [2] F. Avanzini, P. Alku, and M. Karjalainen. One-delayed-mass model for efficient synthesis of glottal flow. In *Proc. Eurospeech Conf.*, pages 51–54, Aalborg, Sep. 2001.
- [3] F. Avanzini, C. Drioli, and P. Alku. Synthesis of the Voice Source Using a physically informed model of the glottis. In *Proc. Int. Symp. Mus. Acoust. (ISMA'01)*, pages 31–34, Perugia, Sep. 2001.
- [4] D. Childers and C. Lee. Vocal quality factors: analysis, synthesis, and perception. *J. Acoust. Soc. Am.*, 90(5):2394–2410, November 1991.
- [5] D. G. Childers and C. Ahn. Modeling the glottal volume-velocity waveform for three voice types. *J. Acoust. Soc. Am.*, 97(1):505–519, Jan. 1995.
- [6] M. Döllinger, U. Hoppe, F. Hettlich, J. Lohscheller, S. Schuberth, and U. Eysholdt. Vibration parameter extraction from endoscopic image series of the vocal folds. *IEEE Trans. Biomedical Engineering*, 49(8):773–781, Aug. 2002.
- [7] C. Drioli and F. Avanzini. Hybrid parametric physiological glottal modelling with application to voice quality assessment. *Medical Engineering & Physics*, 24(7–8):453–460, Sep. 2002.
- [8] G. Fant, J. Liljencrants, and Q. Guang Lin. A four-parameter model of glottal flow. *STL-QPSR*, 26(4):1–13, 1985.
- [9] H. E. Gunter. A mechanical model of vocal-fold collision with high spatial and temporal resolution. *J. Acoust. Soc. Am.*, 113(2):994–1000, Feb. 2003.
- [10] K. Ishizaka and J. L. Flanagan. Synthesis of voiced sounds from a two-mass model of the vocal cords. *Bell Syst. Tech. J.*, 51:1233–1268, 1972.
- [11] P. J. Price. Male and female voice source characteristics: inverse filtering results. *Speech Commun.*, 8(2):261–277, February 1989.
- [12] E. L. Riegelsberger and A. K. Krishnamurthy. Glottal source estimation: Methods of applying the LF-model to inverse filtering. In *Proc. IEEE Int. Conf. Acoust. Speech and Signal Process. (ICASSP'93)*, pages 542–545, Minneapolis, 1993.
- [13] M. Sondhi. Articulatory modeling: a possible role in concatenative text-to-speech synthesis. In *Proc. 2002 IEEE Workshop on Speech Synthesis*, pages 73–78, S. Monica (CA), Sep. 2002.
- [14] B. Story and I. Titze. Voice simulation with a body cover model of vocal folds. *J. Acoust. Soc. Am.*, 97:1249–1260, 1995.
- [15] H. Strik. Automatic parametrization of differentiated glottal flow: Comparing methods by means of synthetic flow pulses. *J. Acoust. Soc. Am.*, 103(5):2659–2669, May 1998.
- [16] I. R. Titze. On the relation between subglottal pressure and fundamental frequency in phonation. *J. Acoust. Soc. Am.*, 85(2):901–906, Feb. 1989.
- [17] I. R. Titze and B. H. Story. Acoustic interactions of the voice source with the lower vocal tract. *J. Acoust. Soc. Am.*, 101(4):2234–2243, Apr. 1996.
- [18] I. R. Titze and B. H. Story. Rules for controlling low-dimensional vocal fold models with muscle activation. *J. Acoust. Soc. Am.*, 112(3):1064–1077, Sep. 2002.

USING BIOMECHANICAL PARAMETER ESTIMATES IN VOICE PATHOLOGY DETECTION

P. Gómez, C. Lázaro, R. Fernández, A. Nieto, J. I. Godino, R. Martínez, F. Díaz, A. Álvarez, K. Murphy, V. Nieto, V. Rodellar, F. J. Fernández-Camacho

GIAPSI, Facultad de Informática, Universidad Politécnica de Madrid
Campus de Montegancedo, s/n, 28660, Boadilla del Monte, Madrid, Spain

It has been shown in previous work that biomechanical parameters related to the cord body dynamics can be indirectly estimated from the power spectral density of the mucosal wave correlate [4]. In the present study the use of these measurements to estimate the presence of parameter unbalance will be shown. The role of these parameters together with the classical distortion ones in relation to pathology detection and classification will be explored. Results using normophonic as well as pathologic voice will be presented and discussed.

I. INTRODUCTION

Classically, Voice Processing focused onto detecting pathological voice by means of distortion parameter estimation directly from the voice trace [7][2], albeit the detection process being masked by the vocal tract and other supra-structures of the vocal apparatus. More advanced methods remove the influence of the vocal tract, to obtain an indirect estimation of the glottal source [1]. The first and second derivatives of the glottal source are correlates of the glottal aperture and the relative speed between cord centers of mass [3][5]. The glottal aperture correlate can be seen as being composed of two main parts: a slow-varying average movement, which is referred to as “the average acoustic waveform” [8], and a fast-varying waveform, resulting from the mucosal wave traveling on the body-cover structure [10][11]. The dynamics of the body would be reflected in the average glottal aperture, whereas the dynamics of the cover would be retained by the mucosal wave correlate (see Figure 1).

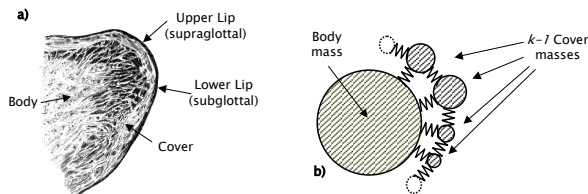


Figure 1. a) Cross-section of the left vocal cord showing the body and cover structures (taken from [9]). b) k -mass model of the body and cover.

It may be expected that the power spectral density (psd) of the average acoustic wave would be determined by

the dynamics of the cord center of masses, whereas the power spectral density of the mucosal wave correlate would be mostly influenced by the cover dynamics. Moving one step ahead, separating both signals would become an important target for estimating vocal fold biomechanics. In a previous work [4] it was shown that estimates of the cord mass and stiffness could be obtained from the power spectral density of the average acoustic waveform. Through this paper the methodology for parameter unbalance estimation will be presented. Experiments using pathologic and normophonic samples will also be given.

II. CORD BODY BIOMECHANICAL ESTIMATES

Glottal source reconstruction by inverse filtering, as used in the present study, is due to Alku [1]. Relevant details on its recursive implementation by paired lattices are to be found in [5]. By removing the vocal tract influence a given voice trace can be processed to render the relative speed between cords, the glottal aperture and the glottal source as shown in Figure 2.

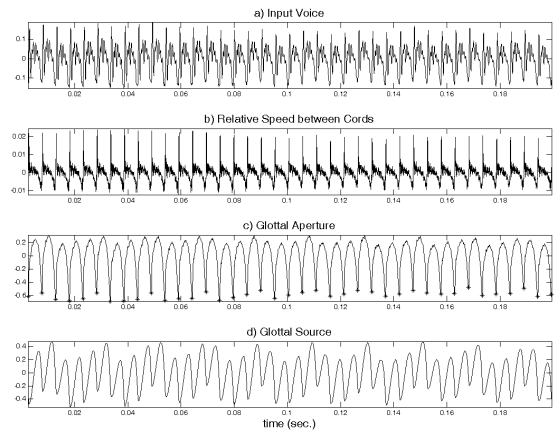


Figure 2. Glottal source estimation. a) input voice (sample 00B), b) second and c) first derivatives of the glottal source, d) glottal source (unlevelled).

Detecting the cord body mass, stiffness and damping is based on the inversion of the integro-differential equation of the one-mass cord model

$$f_{xl} = v_{lb} R_{lb} + M_{lb} \frac{dv_{xl}}{dt} + \frac{1}{C_{lb}} \int_{-\infty}^t v_{lb} dt \quad (1)$$

where the biomechanical parameters involved are the lumped masses M_{lb} , the elastic parameters C_{lb} and the losses R_{lb} . The equivalent model is shown in Figure 4.

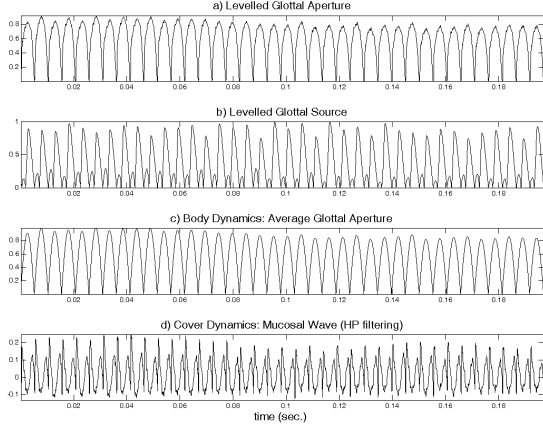


Figure 3. Estimation of the mucosal wave correlate: a) Levelled first derivative of the glottal source, b) Levelled glottal source, c) average acoustic waveform, d) mucosal wave correlate

The estimation of the body biomechanical parameters is related to the inversion of this model, associating the force f_{xl} on the body with the velocity of the cord centre of masses v_{lb} in the frequency domain.

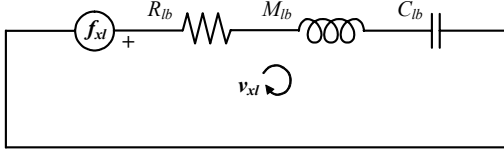


Figure 4. Electromechanical equivalent of a cord body

The relationship between velocity and force in the frequency domain is expressed as the cord body admittance. It will be assumed that the power spectral density of the levelled glottal aperture (1st derivative of the glottal source) is related to the square modulus of the body admittance $Y_{bl}(s)$ as

$$T_{mb}(\omega) = |Y_{bl}|^2 = \left| \frac{V_{lb}(\omega)}{F_{xl}(\omega)} \right|^2 = \left[\left(\omega M_{lb} - (\omega C_{lb})^{-1} \right)^2 + R_{lb}^2 \right]^{-1} \quad (2)$$

which shows a maximum value at

$$T_1 = T_{mb}(\omega = \omega_r) = \frac{G_b}{R_{lb}^2} \quad (3)$$

$$\omega_r = \sqrt{\frac{1}{M_{lb}C_{lb}}} \quad (4)$$

where G_b is a factor of scale between the average acoustic waveform power spectral density and the square modulus of the cord body admittance. The value of the third harmonic will be given by

$$T_3 = T_{mb}(\omega = 3\omega_r) = \frac{1}{\left(\frac{8}{3}\right)^2 \omega_r^2 M_{lb}^2 + R_{lb}^2} \quad (5)$$

From this expression the following estimate for the body mass may be obtained

$$M_{lb} = \frac{3}{8\omega_r} \left[\frac{T_1 - T_3}{T_1 T_3} \right]^{\frac{1}{2}} = \frac{3}{8\omega_r} \sqrt{r_{13}} \quad (6)$$

$$r_{13} = \frac{T_1 - T_3}{T_1 T_3} \quad (7)$$

The value of C_{lb} could be derived from (4). The curve fitting after estimating the biomechanical parameters for a real trace (sample 00B) is shown in Figure 5.

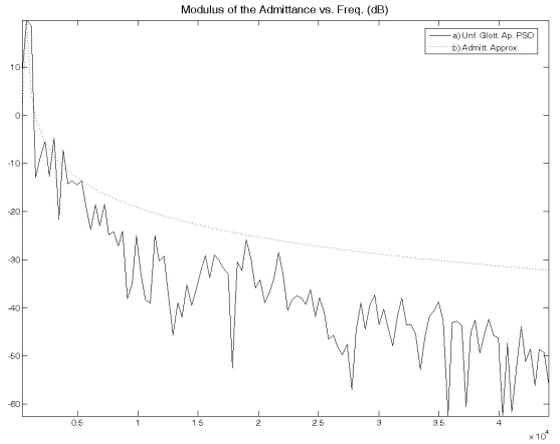


Figure 5. Parametric fitting of a specific average acoustic waveform for sample 00B (full line) against the admittance approximation (dot line)

III. PARAMETER UNBALANCE

A slight unbalance between waveform cycles may be observed in Figure 3.a) and c). Even cycles appear to be larger than odd ones. As estimations of mass, stiffness and damping will be available on a cycle frame basis, the unbalance of these parameters (**BMU** – Body Mass Unbalance, **BLU** – Body Losses Unbalance and **BSU** – Body Stiffness Unbalance) may be defined as

$$\begin{aligned} m_{uk} &= (\hat{M}_{bk} - \hat{M}_{bk-1}) / (\hat{M}_{bk} + \hat{M}_{bk-1}) \\ r_{uk} &= (\hat{R}_{bk} - \hat{R}_{bk-1}) / (\hat{R}_{bk} + \hat{R}_{bk-1}) \\ c_{uk} &= (\hat{C}_{bk} - \hat{C}_{bk-1}) / (\hat{C}_{bk} + \hat{C}_{bk-1}) \end{aligned} \quad (8)$$

where $1 \leq k \leq K$ is the *cycle window* index and \hat{M}_{bk} , \hat{R}_{bk} , and \hat{C}_{bk} are the *k-th cycle* estimates of mass, losses and compliance on a given voice sample. Other parameters of interest are the deviations of the average values of mass, losses and compliance for the *j-th* sample \bar{M}_{bj} , \bar{R}_{bj} , and \bar{C}_{bj} relative to average estimates from a normophonic set of speakers (inter-speaker) as

$$\begin{aligned}
m_{dj} &= (\overline{M}_{bj} - \overline{M}_{bs}) / \overline{M}_{bs} \\
r_{dj} &= (\overline{R}_{bj} - \overline{R}_{bs}) / \overline{R}_{bs} \\
c_{dj} &= (\overline{C}_{bj} - \overline{C}_{bs}) / \overline{C}_{bs}
\end{aligned} \quad (9)$$

these parameters are known as **BMD** (Body Mass Deviation), **BLD** (Body Losses Deviation) and **BSD** (Body Stiffness Deviation).

IV. RESULTS AND DISCUSSION

The key tool in the classification into pathologic and normophonic samples used in this research is Principal Component Analysis (PCA), conceived as the optimal solution to find the minimum order of a linear combination of random variables x_j showing the same variance as the original set, where the components of x_j correspond to different observations (samples) of a given input parameter (j -th parameter). A variant of Principal Component Analysis known as *multivariate measurements analysis* (see [6], pp. 429-30) has been used with the distortion parameters given in Table 1.

Table 1. List of parameters produced from voice

Coeff.	Description
x_1	pitch
x_2	jitter
x_{3-5}	shimmer-related
x_{6-7}	glottal closure-related
x_{8-10}	HNR-related
x_{11-14}	mucosal wave psd in energy bins
x_{15-23}	mucosal wave psd singular point values
x_{24-32}	mucosal wave psd singular point positions
x_{33-34}	mucosal wave psd singularity profiles
x_{35-37}	biomechanical parameter deviations (8)
x_{38-40}	biomechanical parameter unbalance (9)

This methodology has been applied to 20 normophonic and 20 pathologic samples (4 samples with polyps, 6 samples with bilateral nodules, 5 samples with Reinke's Edema, and 5 samples with reflux inflammation) as listed in Table 2. Sample conditions are

N – Normophonic

BP – Bilateral Polyp

LVCP – Left Vocal Cord Polyp

BRE – Bilateral Reinke's Edema

BN – Bilateral Noduli

LR – Larynx Reflux

RE – Reinke's Edema

RVCP – Right Vocal Cord Polyp

These samples were processed to extract the set of 40 parameters listed in Table 1, of which two subsets were defined for classification: $S_1 = \{x_{2-39}\}$, including most of the parameters available, and $S_2 = \{x_2, x_3, x_8, x_{35-39}\}$ including *jitter*, *shimmer*, *HNR*, deviations (*BMD*, *BLD* and *BSD*), and unbalances (*BMU* and *BLU*). The results of the clustering process are shown in Figure 6 as biplots against the two first principal components from PCA analysis. It may be seen that the clustering process assigned most of normophonic samples to one cluster

(with the exception of *00B* and *024*) both for S_1 as well as for S_2 . The results using S_2 are given in Table 3.

Table 2. Values of x_{35-39} for the samples studied

Trace	Condit.	BMD	BLD	BSD	BMU	BLU
001	N	-0.632	-0.136	-0.540	0.027	0.039
003	N	-0.154	-0.145	-0.137	0.079	0.056
005	N	-0.039	-0.299	-0.213	0.078	0.044
007	N	-0.492	-0.461	-0.573	0.036	0.046
00A	N	-0.542	-0.207	-0.567	0.065	0.064
00B	N?	1.320	0.642	1.250	0.149	0.191
00E	N	-0.054	0.012	-0.128	0.159	0.098
010	N	-0.408	0.164	-0.491	0.115	0.103
018	N	-0.031	-0.205	-0.167	0.078	0.076
01C	N	-0.557	-0.315	-0.581	0.058	0.052
024	N?	0.631	1.330	1.200	0.120	0.124
029	N	0.101	-0.111	0.416	0.057	0.048
02C	N	-0.329	-0.253	-0.079	0.035	0.040
02D	N	-0.227	-0.193	0.022	0.116	0.053
032	N	-0.507	-0.019	-0.367	0.038	0.071
035	N	0.424	-0.302	-0.021	0.099	0.065
043	N	0.219	0.156	0.466	0.059	0.030
047	N	-0.497	1.070	-0.180	0.076	0.052
049	N	-0.157	0.160	0.029	0.113	0.079
04A	N	-0.005	1.770	0.073	0.098	0.075
065	BP	0.240	7.490	3.220	0.835	0.712
069	LVCP	0.560	3.490	2.460	0.408	0.318
06A	BRE	0.142	2.860	1.760	0.300	0.331
06B	BN	0.427	3.860	2.150	0.339	0.326
06D	BN	0.573	3.540	2.160	0.338	0.339
071	BRE	0.417	3.210	1.870	0.306	0.348
077	LR	2.000	3.170	3.660	0.460	0.320
079	RE	0.658	2.860	2.170	0.396	0.333
07E	BN	0.843	2.990	2.340	0.328	0.303
07F	LR	0.420	2.850	1.950	0.332	0.309
083	LR	0.253	2.880	1.900	0.391	0.333
092	BRE	0.216	2.750	1.720	0.469	0.353
098	RE	0.187	2.830	1.720	0.360	0.339
09E	BN	1.400	11.700	5.510	0.637	0.518
09F	LR	0.062	2.920	1.660	0.309	0.334
0A0	RVCP	0.156	3.020	1.720	0.333	0.338
0A9	LVCP	0.012	3.600	1.660	0.293	0.311
0AA	LR	-0.091	2.970	1.600	0.268	0.315
0B4	BN	0.154	4.280	1.870	0.305	0.338
0CA	BN	-0.057	3.040	1.630	0.310	0.361

Table 3. Clustering results for S_2

Cluster	Samples
c_{21} (o)	001, 003, 005, 007, 00A, 00E, 010, 018, 01C, 029, 02C, 02D, 032, 035, 043, 047, 049, 04A
c_{22} (o)	00B, 024, 065, 069, 06A, 06B, 06D, 071, 077, 079, 07E, 07F, 083, 092, 098, 09E, 09F, 0A0, 0A9, 0AA, 0B4, 0CA

To further clarify the analysis a 3D plot of the results vs the three most relevant input parameters in S_2 as established by PCA is presented in Figure 7. The most relevant parameter according to this combination seems to be **BSD** (x_{37}). The larger x_{37} , the stiffer the cord and the less normophonic the production. The second most relevant parameter seems to be **jitter** (x_2). The third most relevant parameter is **BLD** (x_{36}) associated to the profile of the spectral profile peak (Q factor).

THE EFFECT OF THE FLOW MASK ON PHONATION

R. Orr and B. Cranen

Department of Language and Speech, Radboud University Nijmegen, The Netherlands

This study is an investigation of the effect of the presence of the flow mask on voicing behaviour. Microphone and flow recordings were inverse filtered and compared to examine the possible effects of the flow mask. Closing quotient (CIQ), open quotient (OQ) and the amplitude difference between the first and second harmonics (H1-H2) were the parameters used to characterise the inverse filtered signals. The presence of the flow mask used for the recording of oral flow had an effect on these parameters, which is interpreted as being indicative of a more tense or more efficient voicing behaviour in the presence of the mask.

I. INTRODUCTION

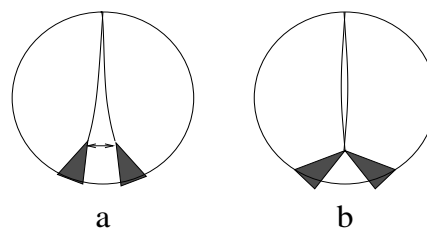
One source of objective characteristics of phonation is the inverse filtered oral flow or sound pressure wave, e.g. [1,2,3]. The former is registered with a flow mask [1] and the latter with a pressure sensitive microphone at a short distance from the mouth. Similar parameters can be extracted from both, with the exception of DC flow, which cannot be extracted from microphone recordings.

Each type of voice recording has its own advantages and drawbacks. Microphone recordings are non-intrusive, may produce more natural voicing, and are more practical for field-work, but do not easily provide a measure of DC flow. Flow recordings do provide DC flow, but the experimental setup is more complicated, and the flow mask may affect voicing behaviour. Obvious practical advantages make the microphone the instrument of choice for speech recordings in voice research. Furthermore, the information gained from the DC flow measure is not fully understood.

DC flow has been investigated by numerous researchers, e.g. [4,5,6], and is used in some measures of breathiness and vocal efficiency [4,6]. However, the precise relationship of DC flow to voice quality is unclear. Large values of DC flow indicate insufficient glottal closure extending into the membranous part of the vocal folds during maximum glottal closure, while small values [6] may indicate glottal opening in the cartilaginous part of the vocal folds during maximum closure. In [7], it is suggested that there may be two types of incomplete glottal closure, each of which has different implications for the shape of the glottal waveform.

A glottal chink in both the membraneous and cartilaginous parts of the vocal folds (diag. a in Fig. 1), may indicate more gradual glottal opening/closing, leading to a more sinusoidal waveform. When the glottal chink is found in only the cartilaginous parts of the vocal folds, the glottal waveform may show abrupt changes in flow, despite presence of DC flow (diag. b in Fig. 1). Thus, DC flow may not be an

Fig. 1. Two ways to model glottal leakage: a) a linked leak



created by abduction and b) a parallel chink in the cartilaginous portion of the glottis. Taken from [7].

accurate means of determining voice efficiency. It is even suggested [6] that small amounts of DC may be due to vertical phasing as a result of a mucosal wave, in voices where there is complete closure.

As long as the relationship between DC and the glottal waveform remains unclear and even contradictory, there is no reason to prefer flow recordings over microphone recordings for voice analysis, and it may be preferable to focus on the parameters which do indicate a consistent relationship, although this depends on assumptions made about the relationship between flow and microphone recordings.

Theoretically, parameters extracted from either type of recording should represent the same information [8]. In earlier work [9], flow derivative and sound pressure were compared for a group of 70 subjects. The recordings were made in a loosely controlled situation, where subjects were asked to phonate as naturally as possible. The recordings were inverse filtered, and source parameters were extracted from each voicing condition for each subject. Since the subjects produced the two recordings within a relatively short period of time of about five minutes, large between-session variance was not expected. Perceptual tests were not carried out, as the mask distorts the acoustical signal so that perceptual comparisons are not possible.

The results of a microphone/flow comparison were not similar. When the data for each subject were analysed, the flow and microphone parameter values did not correlate. Moreover, analyses of variance indicated that there were statistically significant differences between flow and microphone results. A number of possible reasons were suggested for this. Normal within-subject variation may be large enough [4] that direct comparisons of separate utterances for the same speaker cannot be made in a loosely controlled experimental setup. Subjects were sometimes perceived to be uncomfortable with the mask, and this may have introduced physical tension in the voicing apparatus in general. The acoustic distortion produced by the mask may also have an effect on the data. Auditory feedback for the subject wearing the mask is muffled, and this could also lead to some change

in voicing strategy in phonation production in the presence of the mask.

While it is very difficult to make direct comparisons on different utterances, such large differences between flow and microphone data were not expected. A more thorough understanding of the comparability of flow and microphone signals is important, as research on the voice source in the speech community comes from both flow and microphone data, and both are used to characterise aspects of voice quality for many purposes. The aim of this study then was to compare, under more controlled circumstances, phonation produced with and without a flow mask. A single subject experiment was designed to give maximal control over the possible confounding factors suggested from the results of the previous work and we present here the data that was collected from such a setup.

II. METHODOLOGY

Subject: The subject was a female phonetician with experience in producing experimental speech, and who was familiar with the aims of the experiment. A single subject was chosen for this analysis for three reasons.

Firstly, laryngeal settings for normal voice production can differ considerably from subject to subject. Distinctive individual differences within a subject group may make the comparison and interpretation of mean scores spurious for this particular investigation.

Secondly, a speaker with some experience and understanding of the production of different voice qualities was required. In order to get an impression of whether the inverse filtering produced realistic parameter values for both flow and microphone utterances, the subject was required to produce three different voice qualities for which relative values are already established in other published research. If the relative values produced for the different voice qualities concur with those of other research, this would help to confirm that the signal processing procedure was robust.

Thirdly, it was necessary to control phonation in order to limit within-speaker variability as much as possible. The production of voice tokens which are as similar as possible requires insight and control which naïve subject groups may not have. We therefore wanted a speaker who was properly trained in the area of voice production.

Although the results of a single subject experiment cannot be generalised to the population as a whole, if a single trained speaker does not produce comparable voicing behaviour for mask and no-mask conditions, then we would reason that an untrained speaker is even less likely to do so.

Phonation Task: The utterance /paepaepaepae/ was produced by the subject, at a rate of about 1.5 syllables per second, using *modal* voice, and also using assumed *breathy* and *creaky* voice. For each voice quality, 20 repetitions of the utterance were recorded first with a pressure sensitive microphone and then with a Rothenberg mask. In total, 40

utterances in each voice quality were recorded. A voice therapist was present during all recordings to ensure that the required voice qualities were actually produced. Fundamental frequency was kept constant at around 173 Hz, using a tuning fork for reference at the beginning of each sequence of utterances.

Measurements: Microphone recordings were made with a Bruel and Kjaer (B&K) microphone (4133) at approximately 10cm from the mouth and a B&K amplifier 2619.

Oral flow was measured with a circumferentially vented pneumotachograph mask (Glottal Enterprises) with a heated double screen wire mesh, in combination with a Glottal Enterprises amplifier (MS-100A2). Before and after the flow recordings, the flow sensors were calibrated in order to get absolute flow measures and to ensure the consistency of the measurements.

The signals were recorded synchronously on an analogue 14-channel FM-recorder (TEAC XR510). The recordings were made at a tape speed of 19.05 cm/s allowing a flat frequency response up to 5kHz. The microphone signals were recorded on 3 different channels with low, medium and high input gains. In this way, at least one version of each signal would have an acceptable SNR. Flow signals were similarly recorded at two different levels on two different channels.

Signal Processing: All signals were synchronously digitised at a 10kHz sampling rate.

The microphone signal, which prior to digitisation had already been filtered by means of an analogue high-pass filter (cut-off frequency 22.4Hz) in the B&K amplifier, was treated with a second digital high-pass filter to eliminate any remaining low frequency distortions, using a linear phase filter and with a cut-off frequency of approximately 20 Hz and a flat frequency response above 70Hz. It was then phase-corrected to compensate for phase distortion introduced by the analogue high-pass filter of the microphone amplifier. This signal was automatically inverse filtered by means of pitch synchronous inverse filtering using covariance LPC on the closed glottis interval (CGI). The start of the CGI was determined from the peak in the EGG derivative. The inverse filtered signal was then low-pass filtered at 1500Hz, again using a linear phase filter.

The calibrated flow signal was inverse filtered in the same way as the microphone signal and low-pass filtered with a linear phase filter with a cut-off frequency of 1500Hz.

Characterisation of the acoustic voice source: OQ and CIQ were extracted from each glottal cycle over the stable stationary parts of the vowel in order to compare results from the most reliably inverse filtered speech samples. A modal value was determined for each utterance. Fig. 2 shows the moments on the source wave which were used to calculate OQ and CIQ. The spectral parameter H1-H2 was calculated from the sections at the start of the final vowel. These

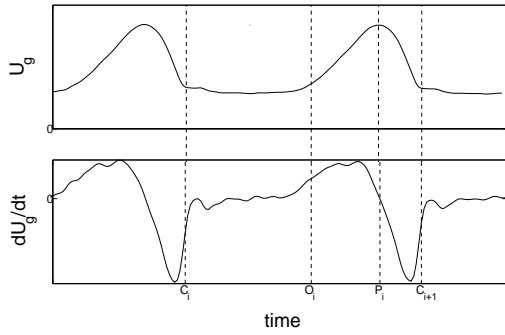


Fig.2 Moments on the glottal flow waveform (upper window) and flow derivative (lower window) from which the time-related parameters OQ and CIQ were derived. OQ is derived as $(C_{i+1} - O_i)/(C_{i+1} - C_i)$ and CIQ is derived as $(C_{i+1} - P_i)/(C_{i+1} - C_i)$

selections were divided into equal length sections of 1024 samples. The first harmonic peaks in the spectrum were detected, and their frequencies and amplitudes were recorded. H1-H2 represents the difference in amplitude (dB) between f_0 and the component with double that frequency. The values used in the comparison were average values from the 1024 sample sections. As a mean value was used, we decided not to include the dying out part of the last vowel, where vocal effort would be reduced such that the laryngeal musculature would relax and produce a less efficient voice. This approach was tested on data from earlier work [9], and the spread of values per glottal cycle was smaller, giving more representative values for the utterance.

III. ANALYSIS

Fig. 3 shows scatterplots of the data separated for flow/microphone recordings (mask/no-mask conditions). The visual data indicates that the mask has some effect on the source parameters. A statistical power calculation could not be made for the estimation of an appropriate significance level, as there is insufficient normative data for estimating a perceptually relevant difference in our parameters. We chose to look at *effect size* η_p^2 , when $p \leq 0.01$. It was expected that, as the subject concentrated on maintaining a stable voice quality, much of the variance would be attributable to the experimental conditions, and the effect of the mask, if present, should be clear. A real effect of the flow mask was considered present if, for an analysis of variance¹ (ANOVA), there was a medium effect size η_p^2 , ($0.15 > \eta_p^2 > 0.06$) [10] for values of $p \leq 0.01$. Significant results are shown in bold in Table 1.

¹ Type II ANOVA, calculated according to the principle of marginality, testing each term after all others, ignoring the term's higher order relatives [11, 12]

V. RESULTS AND DISCUSSION

Relative parameter values mostly concur with other research. *Breathy* voice has larger OQ , smaller CIQ and larger H1-H2 values than *modal* voice. *Creaky* voice shows a greater range of values than *modal* voice and has larger CIQ and smaller H1-H2 values. *Modal* and *creaky* OQ were centred around similar values, but were more spread for *creaky* voice. *Modal* values are close to what has been observed for *pressed* voice. The voice therapist who was present at the recordings confirmed this perceptually. It is reasonable to expect that if the known differences are properly represented, then the unknown effect of the mask will also be properly represented.

Table 1. ANOVA results: effects of the mask factor, with means and standard deviations (sd)

	F ($df=1$)	mean(sd) mask	mean(sd) no-mask	p	η_p^2
<i>breathy</i>					
H1-H2	0.00	-16.60(3.0)	-16.59(5.57)	0.96	0.00
CIQ	39.69	0.36(0.02)	0.41(0.03)	0.00	0.42
OQ	98.60	0.73(0.03)	0.81(0.02)	0.00	0.71
<i>modal</i>					
H1-H2	43.26	-0.87(0.8)	-2.94(1.12)	0.00	0.54
CIQ	23.73	0.21(0.02)	0.24(0.03)	0.00	0.36
OQ	1.53	0.51(0.03)	0.53(0.01)	0.22	0.03
<i>creaky</i>					
H1-H2	1.72	-0.85(2.43)	-2.11(4.2)	0.20	0.04
CIQ	114.36	0.16(0.01)	0.21(0.02)	0.00	0.68
OQ	39.61	0.43(0.03)	0.57(0.11)	0.00	0.44

As can be inferred from Table 1, values for the three chosen parameters were lower for *mask* condition than for *no-mask* condition. *Mask* values were less spread than *no-mask* values. Of the nine combinations of voice quality and source parameter, only two (H1-H2 for *creaky* and *breathy* voice) showed mask values that did not conform to the overall result. Another combination, OQ for *modal* voice, followed the general trend of values, but did not represent a significant result according to the set criteria. Although an effect was not demonstrable for these three combinations of dependent variable and *mask* factor, the effect is systematically present for the other six combinations. This is supported by the large effect size for these combinations.

The generally lower H1-H2, CIQ and OQ values could indicate more deliberate and tense vocal behaviour. Auditory feedback of muffled speech produced with the mask is a likely cause of this effect. Muffled auditory feedback may influence the speaker to put more effort into accurately producing the intended voice quality. The smaller spread of

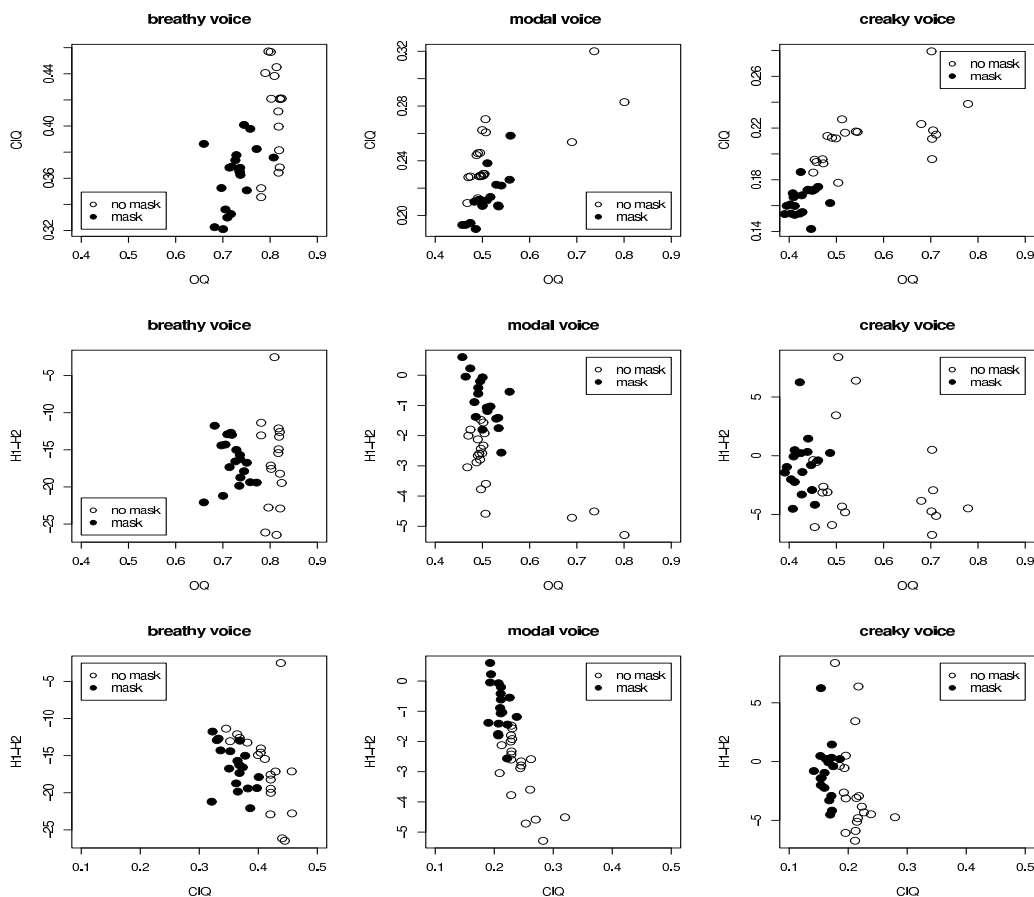


Fig. 3 Scatterplots of the three voice qualities, modal, breathy and creaky, showing the mask and no-mask conditions for three combinations of the parameters OQ, CIQ and HI-H2. Note that the y-axes are different for each plot.

mask values may reflect extra focussing on the phonation task. It is interesting to note that the mask seems to reduce parameter variability on a subconscious level, but that the speaker was not able to consciously limit variability.

V. CONCLUSION

There was a systematic difference between source parameters extracted from flow and microphone speech. Flow mask recordings produced lower parameter values than microphone recordings. This may indicate increased vocal tension, more deliberate vocal behaviour caused by muffled auditory feedback, or a combination of both. This effect should be noted in future comparisons of flow and microphone data

REFERENCES

- [1] M. Rothenberg, "A new inverse-filtering technique for deriving the glottal flow waveform during voicing", *J. Ac. Soc. Am.*, vol. **56**(6), pp. 1632-1645, 1993.
- [2] P. Alku, "Glottal wave analysis with pitch synchronous iterative adaptive inverse filtering", *Speech Comm.* **11**(2-3), 109-118, 1992.
- [3] A. Ní Chasaide & C. Gobl, "Voice Source Variation" in *Handbook of Phonetic Sciences*, J. Laver & W. Hardcastle, Eds. Blackwell, 1995, pp. 427-462.
- [4] E. Holmberg, *Aerodynamic Measurements of Normal Voice*, Stockholm University, Sweden, 1993.
- [5] J. Iwarsson, *Breathing and Phonation*, Stockholm, Sweden, 2001.
- [6] S. Hertegård, *Vocal Fold Vibrations as Studied with Flow Inverse Filtering*, Stockholm, Sweden, 1994.
- [7] B. Cranen & J. Schroeter, "Modelling a leaky glottis", *J. Phonetics*, **20**, pp. 165-177, 1995.
- [8] J. L. Flanagan, *Speech Analysis, Synthesis and Perception*, Springer, Berlin, 1972.
- [9] R. Orr, B. Cranen & F. de Jong, "An investigation of the parameters derived from the inverse filtering of flow and microphone signals", in *Voice Quality: Functions, Analysis and Synthesis (VOQUAL '03)*, C. d'Alessandro & K. R. Scherer, Eds. Geneva, Switzerland, 2003, pp. 35-40.
- [10] J. Cohen, *Statistical Power Analysis for the Behavioural Sciences*, Lawrence Erlbaum Assoc. Hillsdale, NJ, 1988.
- [11] J. Fox, *Applied Regression, Linear Models, and Related Methods*, Sage, 1997
- [12] T. Rietveld & R. van Hout, *Statistical Techniques for the Study of Language and Language Behaviour*, Mouton de Gruyter, 1993.

A non-invasive device to measure mechanical interaction between tongue, palate and teeth during speech production

Christophe Jeannin^{1,5}, Pascal Perrier¹, Yohan Payan², André Dittmar³, Brigitte Grosgeat^{4,5}

¹Institut de la Communication Parlée, INPG, Grenoble, France

²TIMC, Grenoble, France

³Laboratoire des microsystèmes et microcapteurs biomédicaux, INSA, Lyon, France

⁴Laboratoire d'Etude des Interfaces et des biofilms en Odontologie, Lyon, France

⁵Hospices Civils de Lyon, Service d'odontologie, Lyon, France

Christophe.Jeannin@icp.inpg.fr, perrier@icp.inpg.fr

Abstract

This paper describes an original experimental procedure to measure the mechanical interaction between the tongue and teeth and palate during speech production. It consists in using edentulous people as subjects and to insert pressure sensors in the structure of their complete dental prosthesis. Hence, there is no perturbation of the vocal tract cavity due to the sensors themselves. Several duplicates are used with transducers situated at different locations of the complete denture according to palatography's results, in order to carefully analyze the production of specific sounds such as stop consonants.. It is also possible to measure the contact pressure at different locations on the palate for the same sound.

Index Terms—speech production, tongue/palate interaction, complete denture, pressure transducer

I. INTRODUCTION

Speech motor control has been often compared with the control of other skilled human movements such as pointing or grasping [1]. This approach was very helpful and permitted the elaboration of important hypotheses that were the basis of major speech production theories. However, a peculiarity of speech movement has been often overseen, namely the fact that speech articulators, and especially the tongue, are not moving in a free space. Indeed, the vocal tract is a very narrow space, and tongue is most of the time in mechanical interaction with external structures, such as the palate or/and the teeth. Hamlet & Stone [2] and Fuchs et al. [3] have found a number of evidences supporting the hypothesis that these external structures would be integrated in speech motor control strategies, and would, consequently, significantly contribute to the control of speech movement accuracy.

Now, two questions can be raised:

- (1) What is the quantitative nature of the interaction between tongue and external structures? In other words, are these structures only geometrical limits of the space in which tongue is allowed to move, or are they mechanical objects that are actually used to position and shape the tongue?
- (2) What are the changes in speech motor control strategies induced by dramatic modifications of these external structures, as it is the case for instance for edentulous people?

Quantitative measurements of the intensity of the force exerted by the tongue on the teeth provide an interesting basis to address these issues. In addition, this technique provides interesting information about the order of magnitude of the intensity of muscular forces involved in the generation of tongue movements during speech production.

In this aim, a number of experimental set-ups have been developed in the past to measure tongue pressure against the palate in various experimental conditions [4]. The limits of these techniques, beside the inherent complexity of their calibration, lie in the fact that they actually induce slight perturbations of the speech production, because they modify the geometry of the vocal tract. Honda et al. [5] have shown that speakers can compensate quite easily and quite quickly for brutal changes in the thickness of an inflated palate, in that sense that they could adapt tongue positions in reference to the variable palatal shapes. However, it is not clear whether the intensity of the palate/tongue interaction was or not affected by these brutal changes.

In this paper, we will present a new experimental procedure that aims

- (1) at measuring the interaction between tongue, teeth and palate without perturbing the production of speech, and
- (2) at studying how speech motor control strategies evolve for edentulous people, from the moment where an artificial denture is put back in the mouth. Finally, preliminary results of a pilot study will be presented.

II. EXPERIMENTAL DEVICE AND METHODS

The basic principle and the originality of the method presented in this paper is to use edentulous people as subjects, and to insert pressure sensors in their complete dental prosthesis, in such a way that the geometry of the vocal tract remains exactly the same as when their normal dental prosthesis is in place.

A. Experimental device

General description

The complete denture, in which the pressure sensor is included, is placed inside the mouth. A sheath goes from the premolar area to the connector placed outside the mouth, via the labial commissure. Then, a wire goes from the connector to the amplifier, from the connector to a data sampling board and then to the computer.

A microphone is also connected to an amplifier to record the acoustic speech signal simultaneously with the pressure exerted by the tongue against the palate and/or the teeth. This amplifier is in turn linked to the data sampling board.

Description of the complete dental prosthesis

The dental prosthesis is made of resin and consists of complete artificial denture and of an artificial palate. Artificial teeth are similar in shape and size to natural teeth. The artificial palate must be at least 3mm thick to avoid breakage. Hence, both the pressure sensor and the wires connecting it with the connector outside of the mouth can be easily inserted in the prosthesis, without creating any additional change of the oral cavity (fig. 1).

For each edentulous patient, the dental prosthesis that is designed for obvious medical purposes is accurately duplicated thanks to a specific prosthesis design technique. Several duplicates are thus realized, in order to have different possible positions for the pressure sensor. Thus, the sensor can be inserted in the prostheses before the experiment with the patient, and no time is wasted during the experiment itself, when the tongue/palate/teeth interaction is measured at different locations.

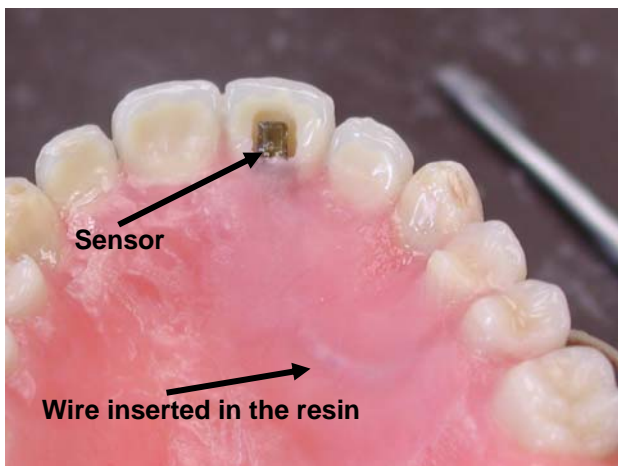


Figure 1: Complete dental prosthesis with a sensor inserted in a front incisor. The wire connecting the sensor to the external connector can be seen on the right hand side of the picture, at the level of the first premolar. It goes then to the sensor inside the structure of the palate.

Pressure sensor description

The sensor is made of a strain gauge sensor which is composed of thirteen layers (fig. 2). Each layer plays an important role in measuring capabilities of the transducer.

The intraoral area is a very difficult environment mainly because of three factors:

- Permanent moisture due to saliva

- Variable temperature
- Mechanical constrains

Therefore, the sensor must be electrically insulated and water proof. Moreover, it must be sturdy in order to go through several experiments.

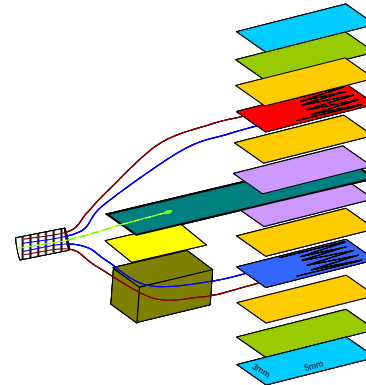


Figure 2: The 13 layers of the pressure sensor

The middle layer is made of a steel cantilever beam which is 10/100 mm thick. It supports on each side an active strain gauge. The gauges (Vishay, ref EA06 062 AQ 350) are placed in a half Wheatstone bridge configuration.. This strain gauge has been chosen because of its stability in temperature.

Gauges are bonded on a metallic support with M-Bond 200 adhesive (Vishay measurement group). Wires of 0,1mm diameter are soldered with tin on the gauge. The area of solder is 1mm² small and there are 4 points, 2 by side.

The two next layers are made of protective coating. M-Coat A (Vishay measurement group).

In any case, during the construction, the thickness of all the liquid components such as protective coating or bonding must be very small, in order to preserve the mechanical properties of the sensor. Consequently just one application of each component by layer can be done.

Figure 3 shows a detailed picture of such a sensor.



Figure 3: The pressure sensor connected to its wire.

Associated instrumentation tools:

Before sampling the signal goes through an amplifier (2100 series by Vishay Measurement) featuring a digital control display and different settings possibilities with 2100 maximal gain range and a bandwidth of 5kHz (at 0,5dB, and 15 kHz at -3 dB). It can hold up to two transducers.

To record the acoustic signal, a microphone is placed near the patient. It is linked with an amplifier and then with the data sampling board (DT 9800 series by Data translation) that is connected directly to the host computer via a USB port. This board can accept up to 16 analog inputs that can be simultaneously sampled at different rates (from 50 Hz to 20 000 Hz). For these experiments, 2 or 3 inputs are used: one for the acoustic signal and one or two for the tongue pressure.

B. Methods

Pressure sensor calibration

Since the transducers are handmade, some differences can exist between them. Therefore, they have to be calibrated individually to convert electric signals into mechanical units such as strength or pressure.

The soft body characteristics of the tongue suggests that pressure should be more appropriate. Indeed, due to the tongue deformation in contact with a solid structure, the contact area is always large and can't be reduced to a specific point. However, the transformation of the sensor displacement into mechanical pressure is not obvious, because of the visco-elastic properties of the tongue. Indeed, in case of contact with external structures, the shape of the tongue varies over time and this variation is strongly dependent of the visco-elastic properties of the tongue. Hence, establishing a good approximation of the relation between the strain exerted on the sensor and the contact pressure is not a simple task. In this aim, we designed and tested 2 different devices to calibrate the sensors:

- The first device uses weights to convert electrical signals into strength.

This is the fastest and easiest way to calibrate the transducer. Small lead beads hanging out of the middle of the edge of the steel cantilever beam were used. Since the weight of the lead is known, the electric signal can be converted into mechanical strength. This allows an evaluation of the intensity of the mechanical interaction, as well as a comparison of them under different experimental conditions. However, it is not a good approach to quantitatively assess their absolute values of the pressure at contact location.

- The second device called "dried water column" converts electric signals into pressure.

The weight of a water column is applied on the whole surface of the sensor. A latex membrane which is not tensed (to avoid signal due of it) is attached to the end of the column and is in contact with the sensor. The electric signal is compared to the level of water. This is a nice way to account for the soft body characteristics of the tongue, and to give an idea of the pressure at contact location. However, it does not model the true viscoelastic characteristics of the tongue. Consequently, the conversion from sensor displacement to contact pressure does not strictly apply to the contact between tongue and teeth and palate.

In both cases, the calibration of the sensors has to be done very carefully and to be explained in order to know what kind of information can be extracted from the data.

Palatography

In order to know with enough accuracy where the sensors should be inserted to measure tongue-palate/teeth interaction during speech production, the exact locations of the main contact regions have to be determined. [6]. This is why, during a preliminary session, palatographic recordings are carried out, with the prosthesis in the mouth



Figure 4: Tongue contacts regions on the prosthesis obtained with palatography for /t/ (left) and /d/ (right), and for a female subject in a pilot experiment.

With complete dental prostheses, electropalatography (EPG) can not be used because of obvious incompatibility reasons between the prosthesis and the EPG device [7]. Therefore, pink powder (occlusion spray red "okklufine premium™") is applied on the teeth and on the artificial palate. When tongue is in contact with one of these structures, the powder is removed from the area of contact. Thus, when the subject is asked to pronounce a specific phoneme in isolation, the edges of the contact areas can be determined for this phoneme. These edges are highlighted with a black pen before removing the powder. This technique is not as accurate as

EPG, but accurate enough to determine where to set the sensor when tongue and palate/teeth interaction is investigated for this phoneme.

Figure 4 shows an example of the results thus obtained during the production of the alveolar stops /t/ and /d/, for a female subject in a pilot experiment.

Data acquisition

As exemplified above, for each subject, each prosthesis is dedicated to the measurement of tongue – palate/teeth interactions in a vocal tract region that is strongly related to the production of a specific phoneme. Sounds are repeated several times by the subjects both in isolation and within short carrier sentences such as, for the alveolar stop /t/, “toto a tête sa tête”.

For each sound, according to the palatography results, the transducers are placed in the specified area.

III. RESULTS

Figure 5 shows an example of results obtained for /d/ in a pilot study carried out with an 80 years old female subject. The sensor was inserted in the most front contact area measured with palatography (see fig. 4, right panel). It can be seen that the acoustic release of the stops is well-synchronized with the abrupt decrease of tongue pressure in the palate. The vertical axis represents the intensity of force exerted by the tongue on the steel cantilever.

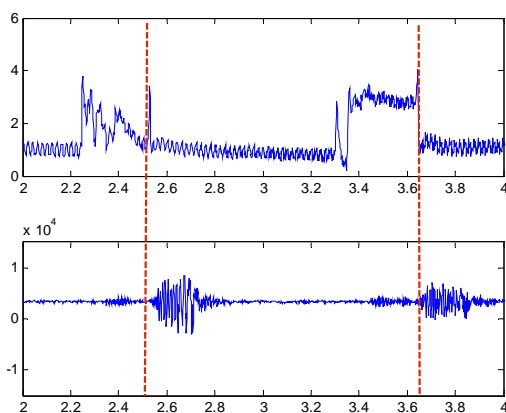


Figure 5: Acoustic speech signal (low panel) and tongue force in the alveolar region (upper panel) during two repetitions of [de]

Obviously, the pressure patterns depict a noticeable variability. The origin of this variability has to be clarified, to know whether it is related to the experimental device or whether it reveals the intrinsic intra-speaker variability of speech production. The maximal order of magnitude of the force is around 0.003N which is in agreement with other kind of data published in the literature.

IV. CONCLUSION

An original device for the measurement of the mechanical interaction between tongue and teeth and/or palate was presented. It adapted to a specific kind of subjects, namely edentulous patients. Using the complete dental prosthesis to insert force sensors, the device permits the measurement of contact pressure without introducing any additional perturbation than the prosthesis itself.

This experimental setup will permit to study speech production either by patients who have been wearing their prosthesis for years and have completed the adaptation process to it, or by patients that just received the prosthesis, in order to study how they adapt to its new denture..

REFERENCES

- [1] Flanagan J.R., Ostry D.J. & Feldman A.G. (1990). Control of human jaw and multi-joint arm movements. In G.E. Hammond (Ed.), *Cerebral control of speech and limb movements* (pp. 29-58). Amsterdam, The Netherlands: Elsevier Science Publishers B.V. (North-Holland).
- [2] Hamlet, S.L. and Stone, M. (1978). Compensatory alveolar consonant production induced by wearing a dental prosthesis. *Journal of Phonetics*, 6, 227-248.
- [3] Fuchs, S., Perrier, P., Geng, C. & Mooshammer, C. (2005). What role does the palate play in speech motor control? Insights from tongue kinematics for German alveolar obstruents. In J. Harrington & M. Tabain (eds). *Speech Production: Models, Phonetic Processes, and Techniques*. Psychology Press: Sydney, Australia (In Press)
- [4] Wakumoto, M., Masaki, S., Honda, K. & Ohue, T. (1998). A pressure sensitive palatography : Application of new pressure sensitive sheet for measuring tongue-palatal contact pressure. *Proceedings of the 5th Int. Conf. on Spoken Language Processing, Vol. 7*, 3151 – 3154.
- [5] Honda, M., Fujino, A. & Kaburagi, T. (2002). Compensatory responses of articulations to unexpected perturbation of the palate shape. *Journal of Phonetics*, 30 (3), 281-302.
- [6] Kelly S., Mai A., Manley G. and McLean C. - *Electropalatography and the linguagraph system*. Medical engineering & physics, 2000; vol 22, issue 1: pp. 47-58
- [7] Searl JP. - *Comparison of transducers and intraoral placement options for measuring lingua-palatal contact pressure during speech*. *J Speech Lang Hear Res.* 2003 Dec;46(6):pp.1444-56.

Poster session

ASSESSMENT OF GLOTTAL INVERSE FILTERING BY USING AEROELASTIC MODELLING OF PHONATION AND FE MODELLING OF VOCAL TRACT

P. Alku¹, J. Horáček², M. Airas¹, A-M. Laukkanen³

¹Lab. of Acoustics and Audio Signal Processing, Helsinki University of Technology, Finland

²Institute of Thermomechanics, Academy of Sciences of the Czech Republic, Prague, Czech Republic

³Dept. of Speech Communication and Voice Research, University of Tampere, Finland

Performance of glottal inverse filtering (IF) is evaluated in this paper by using speech material produced with computational modelling of voice production represented by an aeroelastic model of vocal folds and a Finite Element (FE) model of the vocal tract. An inverse filtering algorithm was used in order to estimate the glottal flow from the speech pressure signal generated by the model. Comparison between the estimated glottal flow and the original flow generated by computational modelling shows that the IF method is able to yield an accurate estimate for the glottal flow.

I. INTRODUCTION

Inverse filtering (IF) is a non-invasive method to estimate the source of voiced speech, the glottal volume velocity waveform. In this technique, a model for the vocal tract transfer function is first computed. The effect of the vocal tract is then cancelled from the produced speech waveform by filtering this through the inverse of the model. As an input to IF, it is possible to use either the oral flow recorded in the mouth with a flow mask (e.g. [1]) or the pressure waveform captured by a microphone in free field outside the mouth (e.g. [2]).

Performance of an inverse filtering method is practically impossible to assess with natural speech. This comes from the fact that it is not possible to analyse how closely the estimated glottal flow given by an inverse filtering algorithm corresponds to the true glottal flow because the latter can not be measured. It is, however, possible to assess inverse filtering by using synthetic speech that has been created using a known, artificial waveform of the glottal excitation. This kind of evaluation, however, is not truly objective, because speech synthesis and inverse filtering analysis are typically based on similar models of the human voice production apparatus (e.g. the source filter model [3]).

In the current study, we combine *physical modelling* of voice production in order to synthesize speech with a

known, realistic glottal flow waveform. By using the pressure signals given by the physical models as an input to an inverse filtering method, it is then possible to analyze how closely the obtained estimate of the voice source matches the original glottal flow.

The paper first describes in section II the methodology used both in physical modelling (sections IIA and IIB) and in inverse filtering (section IIC). The results obtained for a sustained male vowel are described in section III and the paper is finished with short conclusions in section IV.

II. METHODOLOGY

A. Aeroelastic model of the vocal folds

Recently an aeroelastic model was developed by Horáček et al. [4, 5] that allows numerical simulation of self-oscillations of the vocal folds. The incompressible 1-D fluid flow theory is used in the model for expressing the unsteady aerodynamic forces and the Hertz model is used for the impact forces. The parameters of the model, i.e., the mass, stiffness and damping matrices are approximately related to the geometry, size and material density of real vocal folds as well as to a prescribed fundamental frequency (F0) and damping. In this contribution, the output of the numerical simulation, i.e., the intraglottal airflow rate is used to excite an FE model of human vocal tract representing the vowel /a/.

Symmetric oscillations are assumed and hence the vibration of only one vocal fold is modelled. Vocal fold oscillations are simulated by a vibrating element of length L with mass m and moment of inertia I with two-degrees-of-freedom supported by an elastic foundation in the wall of a channel conveying air (Fig. 1). The motion of an equivalent three mass system on two springs can be described by the following equation:

$$\overline{\mathbf{M}}\ddot{\mathbf{V}} + \overline{\mathbf{B}}\dot{\mathbf{V}} + \overline{\mathbf{K}}\mathbf{V} + \mathbf{F} = \mathbf{0}, \quad (1)$$

where $\overline{\mathbf{M}}$, $\overline{\mathbf{B}}$, $\overline{\mathbf{K}}$ are the structural mass, damping and stiffness matrices, respectively, and ${}^T\mathbf{V}=[V_1(t), V_2(t)]$ is the

vector for rotation and translation of the vibrating element. The vector for nonlinear aerodynamic and collision forces can be expressed as

$$\begin{aligned} {}^T\mathbf{F} &= [F_1(t), F_2(t)], \\ F_{1,2} &= \rho \sum_{i,j=0}^2 \sum_{k,l=0}^2 {}^{1,2}K_{i,j,k,l} [V_1^{(i)}(t)]^k [V_2^{(j)}(t)]^l \end{aligned} \quad (2)$$

where the superscripts of V_1 and V_2 denote the order of time derivatives and $K_{i,j,k,l}$ are constant coefficients. For the numerical simulations Eq. 1 was transformed into a system of four 1st order ordinary differential equations and 4th order Runge-Kutta method was used for the calculations.

The following parabolic function is used to approximate the geometry of the vocal folds:

$$a(x) = 1.858 - 159.86 x^2 \quad (3)$$

The airflow velocity U_0 at the inlet ($x=0$) to the glottal region is simply related to the mean glottal volume velocity according to $Q = U_0 2H_0 h$ and to the static subglottal pressure according to:

$$P_{\text{sub}} = 1/2 \rho U_0^2 \left\{ H_0 / [H_0 - a(L)] \right\}^2 \quad (4)$$

During the vocal folds collision, the static subglottal pressure is constant that equals the pressure in the lungs (P_{lungs}). H_0 and h denote the height and width of the channel, respectively. Using tissue density $\rho_h = 1020 \text{ kg/m}^3$, thickness $L = 6.8 \text{ mm}$ and length of the vocal fold $h = 10 \text{ mm}$, eccentricity (e), total mass (m) and moment of inertia (J) were calculated. As the value of air density we used $\rho = 1.2 \text{ kg/m}^3$. A tuning procedure was used to adjust the stiffness of the elastic foundation of the vibrating element and the damping coefficients in order to approximate the fundamental frequency F_0 by setting the natural frequencies $f_1 = F_0$, $f_2 = F_0 + 5 \text{ Hz}$ and 3dB half-power bandwidths $\Delta f_{1,2}$ of both resonances. The optimum distance between the two supporting springs was adjusted to $l = 0.344L$, for which the real values of the stiffness coefficients c_1 , c_2 can be calculated for the prescribed frequencies f_1, f_2 . In the example studied in this paper, the following values were used for the input data: prephonatory glottal half-width $g = 0.2 \text{ mm}$, $F_0 \cong 100 \text{ Hz}$, $\Delta f_1 = 23 \text{ Hz}$, $\Delta f_2 = 29 \text{ Hz}$, $U_0 = 1.6 \text{ m/s}$, $Q = 0.18 \text{ l/s}$, $P_{\text{lungs}} = 380 \text{ Pa}$ and the Hertz coefficient for the vocal folds collisions $k_H = 730 \text{ Nm}^{-2/3}$. The following main output data resulted from the simulation: open quotient $OQ = 0.72$, skewing (speed) quotient $QS = 1.56$, closing quotient $CQ = 0.28$, fundamental frequency $F_0 = 1/T = 100.77 \text{ Hz}$

calculated from the period T of the self-oscillations, maximum glottis opening $GO = 1.27 \text{ mm}$, maximum impact stress $IS = 1328 \text{ Pa}$ and supraglottal pressure $SPL = 124 \text{ dB}$.

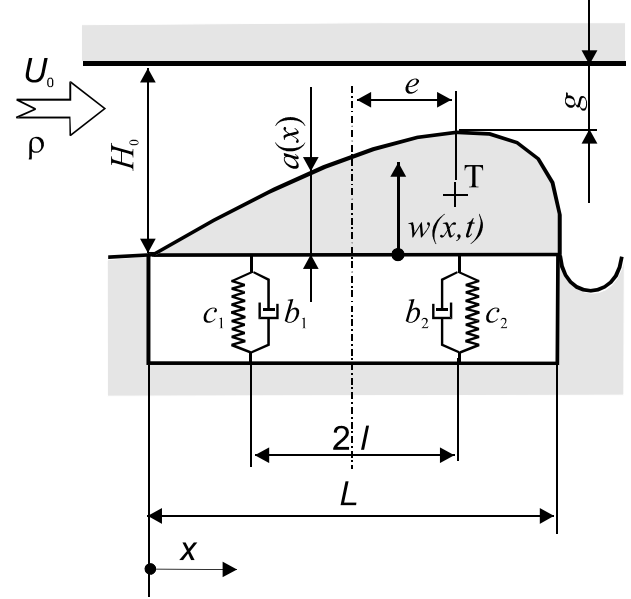


Figure 1. Two-degrees of freedom model of the vocal fold.

B. FE model of the vocal tract

FE modelling was used in numerical simulation of the vocal tract filtering by using the Czech vowel /a/ produced by a male speaker. The model was designed based on MRI data described in [6]. The vocal tract geometry was obtained from a native Czech speaker during phonation. The MRI of the vocal tract for the mid-sagittal cross-section and the designed FE model are shown in Fig. 2. The vocal tract was modelled by the ANSYS FE code using acoustics finite elements FLUID 30 with speed of sound $c_0 = 343 \text{ m/s}$ and $\rho = 1.2 \text{ kg/m}^3$.

The acoustic pressure p is described by the equation:

$$\nabla^2 p = \frac{1}{c_0^2} \frac{\partial^2 p}{\partial t^2} \quad (5)$$

and in FE formulation it can be written in the matrix form in the global co-ordinate system as

$$\mathbf{M} \ddot{\mathbf{P}} + \mathbf{B} \dot{\mathbf{P}} + \mathbf{K} \mathbf{P} = \mathbf{f}(t) \quad (6)$$

where \mathbf{M} , \mathbf{B} , \mathbf{K} are the mass, acoustic boundary damping and stiffness matrices, respectively; \mathbf{P} and \mathbf{f} are the vectors of nodal acoustic pressures and excitation forces, respectively. The transient analysis with the Newmark integration method was used for numerical simulation of

the acoustic signal near the lips whereas the excitation was applied at the position of the vocal folds. The effect of outgoing acoustic energy was modelled by an absorption boundary condition at the lips, where a boundary admittance was prescribed in correspondence to the 3dB half-power bandwidth known for formant (acoustic resonant) frequencies. The excitation signal was the intraglottal airflow volume velocity $Q(t)$ resulting from the aeroelastic model of the vocal folds.

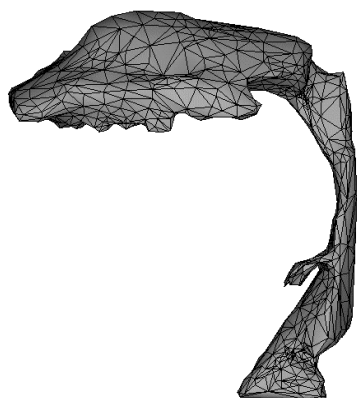
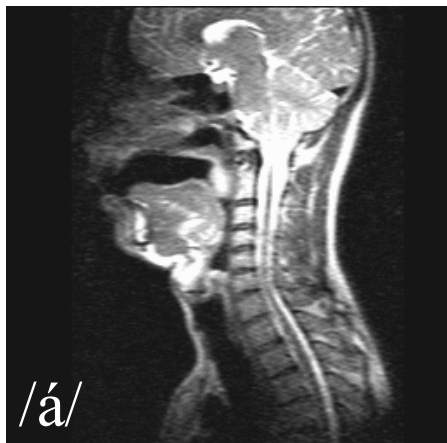


Figure 2. MRI of the male subject during phonation (upper) and FE model of the vocal tract for the Czech vowel /a/ (lower).

C. Inverse filtering

The inverse filtering method used is based on our previous experiments in developing automatic methods to estimate the glottal flow from the speech pressure waveforms with the Iterative Adaptive Inverse Filtering (IAIF) method [7]. The current method, the flow diagram of which is shown in Fig. 3, is a slightly modified version from our previous ones. Parametric spectral models that are used in various blocks of the flow diagram are computed with the Discrete All-pole Modeling (DAP) method [8] instead of the conventional linear predictive analysis. This makes it possible to obtain estimates of the formant frequencies that are less biased by the harmonic

structure of the speech spectrum. The detailed description of the IAIF-method can be found in [9].

The IAIF method has limitations. It is based on straightforward linear modelling of speech production without taking into account, for example, the interaction between the glottal source and the vocal tract. Moreover, the digital model of the vocal tract is a pure all-pole filter, which is not accurate for nasals. Despite these inherent limitations, the proposed technique provides a promising method to estimate the glottal flow especially given the fact that the method can be implemented (if desired) in a completely automatic manner with a reasonable computational cost.

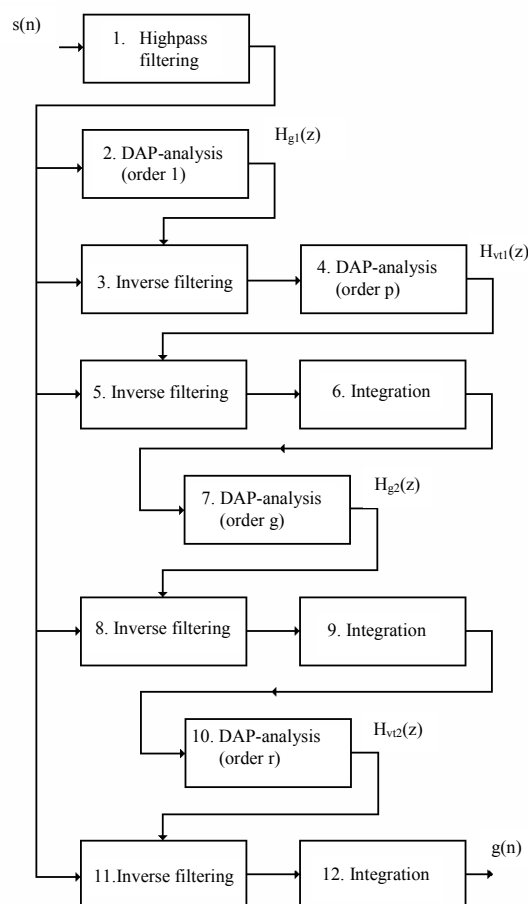


Figure 3. Block diagram of the IAIF method

III. RESULTS

The vowel sound produced by the physical modelling was inverse filtered with the IAIF method by using the following parameters (see Fig. 3): $p = r = 12$, $g = 4$. The sampling frequency was 10 kHz. The length of the analysis window was 50 ms. The lip radiation effect

(blocks no 6, 9 and 12 in Fig 3) was cancelled by a first order all-pole filter with its pole at $z = 0.96$.

The glottal flow estimate computed by the IAIF method is shown together with the original flow generated by physical modelling in Fig. 4. Both of the two time-domain waveforms were parameterised using the Normalized Amplitude Quotient (NAQ) [10]. The value of the NAQ parameter equalled 0.2085 and 0.2038 for the original and estimated flow, respectively. Hence, in terms of the NAQ parameter, the difference between the estimated glottal flow and the original one was approximately 2 %.

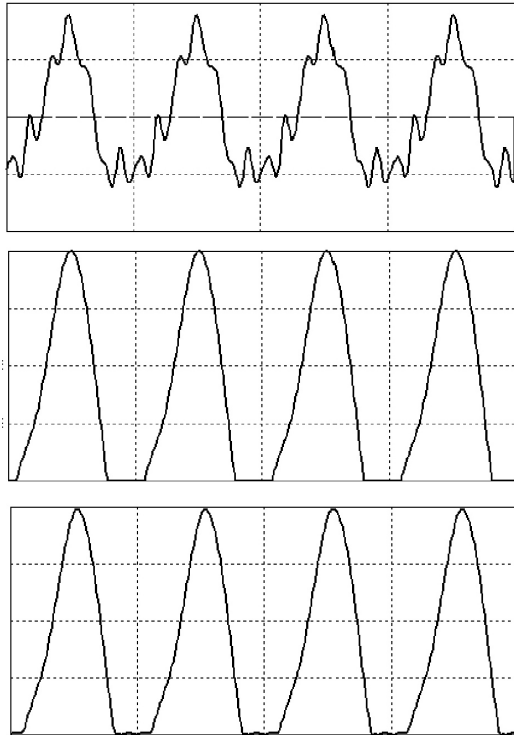


Figure 4. Speech pressure signal (top) and glottal flow (middle) generated by physical modelling. Estimated glottal flow (bottom) given by inverse filtering. All signals are in the time-domain, length of panel 40 ms.

IV. CONCLUSIONS

Evaluation of inverse filtering methods is problematic because direct measurements of the glottal flow are difficult, if not impossible. In addition, using synthetic speech as test material does not make a fully objective evaluation possible, because voice synthesis and inverse filtering are typically based on the same voice production models.

The present study aimed to avoid these fundamental limitations by using a vowel produced with physical modelling in evaluation of inverse filtering. The results were encouraging in showing that the difference between

the original flow generated by physical modelling and estimated one was small.

The experiments of the present study were based on single vowel sound. In order to better understand the limitations of inverse filtering, the characteristics of the test material should be expanded. In particular, the range of F0 values used in the evaluation should be expanded to cover the pitch range of female speech.

ACKNOWLEDGEMENTS

This study was supported by the Academy of Finland (projects 200859 and 205962) and by the Grant Agency of the Academy of Sciences of the Czech Republic, project No IAA20766401 *Mathematical modelling of human vocal folds oscillations*.

REFERENCES

- [1] M. Rothenberg, "A new inverse-filtering technique for deriving the glottal airflow waveform during voicing," *J. Acoust. Soc. Amer.*, vol. 53, pp. 1632-1645, 1973.
- [2] D.Y Wong, J.D. Markel, and A.H. Gray, Jr., "Least squares glottal inverse filtering from the acoustic speech waveform," *IEEE Trans. on Acoust., Speech, and Signal Proc.*, vol. 27, pp. 350-355, 1979.
- [3] G. Fant, *The Acoustics Theory of Speech Production*, the Hague: Mouton, 1960.
- [4] J. Horáček, P. Šidlof, and J.G. Švec, "Numerical modelling of leakage-flow-induced vibrations of human vocal folds with Hertz impact forces," In: 3rd International Workshop MAVIBA 2003, pp. 143-146.
- [5] J. Horáček, P. Šidlof, and J.G. Švec, "Numerical simulation of self-oscillations of human vocal folds with Hertz model of impact forces," In: Langre E, Axisa F, eds. *Flow-Induced Vibration*. Ecole Polytechnique, Paris, pp. 143-148.
- [6] K. Dedouch, J. Horáček, J.G. Švec, P. Kršek, R. Havlík, and J. Vokřál, "Acoustic analysis of a male vocal tract for Czech vowels," In: Proc. Phoniatic Days of Eva Sedláčková, 11-13 Sept. 2003, Brno, pp 60-63.
- [7] P. Alku, "Glottal wave analysis with pitch synchronous iterative adaptive inverse filtering," *Speech Comm.*, vol. 11, pp. 109-118, 1992.
- [8] A. El-Jaroudi and J. Makhoul, "Discrete all-pole modeling," *IEEE Trans. Signal Proc.*, vol. 39, pp. 411-423, 1991.
- [9] P. Alku, B. Story, and M. Airas, "Evaluation of an inverse filtering technique using physical modeling of voice production," in CD Proc. of Int. Conf. on Spoken Lang. Proc. 2004.
- [10] P. Alku, T. Bäckström, and E. Vilkman, "Normalized amplitude quotient for parameterization of the glottal flow," *J. Acoust. Soc. Amer.*, vol. 112, pp. 701-710, 2002.

COUGH ANALYSIS AND CLASSIFICATION BY LABELLING SOUND IN SWINE RESPIRATORY DISEASE

M. Guarino¹, A. Costa¹, S. Patelli¹, M. Silva², D. Berckmans²

¹Department of Veterinary and Technological Sciences for Food safety, Faculty of Veterinary Medicine, via Celoria, 10, 20133 Milan, Italy

²Laboratory for Agricultural Buildings Research Katholieke Universiteit Leuven, Kasteelpark Arenberg 303001 Leuven, Belgium

I. INTRODUCTION

Coughing is one of the most frequent presenting symptoms of many diseases affecting the airways and the lungs of both humans and animals. In piggeries, the continuous on-line monitoring of cough sound can be used to build an intelligent alarm system for the early detection of diseases [1,2,3]. In a first study, with experiments under laboratory conditions, algorithms have been developed to detect cough sounds and to classify the animals whether they were ill or not. In this study, the algorithm was tested in field conditions.

Sound analysis is an interesting method to monitor health status since it needs no physical contact with the animals. Moreover the used microphone in these tests is a very cheap type.

When a pig is infected with a respiration disease, the respiration system is changing, causing the characteristics of the air going through the air pipe to produce a different sound. When it is possible to monitor and analyze the sound of a cough signal, an on-line disease monitor can be developed.

A main application is early detection of disease to reduce the use of antibiotics. In previous studies, an accurate algorithm is presented to detect citric acid induced coughing originating from healthy individual piglets. An intelligent free field recognizer is proposed to distinguish between coughing, evoked in absence or presence of a respiratory infection.

Health care management is a critical and demanding issue in current livestock production. Discarding the economic cost related to large scale diseases, early detection of diseases is important considering public health care issues like reducing antibiotics residuals. Also for reasons of animal welfare and monitoring and tracing of the food production chain, online disease monitoring is important. Therefore currently great effort is spent to the development and application of sensors and sensing techniques for diagnosis in the agricultural sector [4]. With respect to objective and automated detection of respiratory diseases in livestock, it has been shown that artificial intelligence is successfully applicable to obtain automated cough recognition from free field cough recognition.

In the work of Van Hirtum and Berckmans [6] an accurate algorithm is presented to detect citric acid induced coughing originating from healthy individual piglets under laboratory test conditions. In their work an intelligent free field recognizer is proposed to distinguish between coughing evoked in absence or presence of a respiratory infection. A drawback of the developed algorithm is that it is time consuming to run, what can cause problems when applying it in practice. Furthermore, the results are obtained on a database which is registered on individual subjects housed in a laboratory test-installation consisting of a laboratory inhalation-chamber. The test-installation, described by Van Hirtum and Berckmans [6] and Urbain et al. [7], allows to control environmental housing conditions, medical follow-up and to reduce environmental noises. So cough sounds are registered in optimal environmental sound conditions. Therefore the performance of the developed algorithms to recognize cough in field conditions needs to be assessed in order to validate the usage of sound analysis in livestock health management.

To this purpose, in a previous study [8], coughs were registered in field conditions keeping one microphone near the animal.

In that study, limiting the spectral frequency to the range from 2 kHz to 14 kHz allowed to eliminate low-frequency noises from mechanical origin, while the cough sound exhibited an important energy-peak in this range.

The main objective of this study was to evaluate the accuracy of cough recognition algorithm on labeled coughs from all other sounds, recorded simultaneously with background noises using two microphones, one for noise and one for cough recording.

II. METHODOLOGY

Animals: 350 pigs (commercial crosses) were in the first period of the finishing phase, their mean weight at the beginning of the trial was around 75 kg and their mean age was 170 days. The fattening room was wide 14 x 21,10 m and was divided in 16 boxes with totally slatted floor.

The walls were made of concrete bricks and insulated (PVC thick sheet) and the roof is made of prefab plates of concrete. Roof inclination was 30 %.

A serological assay on blood sample to verify the presence of Pleuropneumonitis antibodies has been conducted on sick pigs to verify the source of coughing. After the slaughtering, Pleuropneumonitis was confirmed by the autopsy examine performed by the farm veterinarian.

Measurements: Pigs cough was recorded using a microphone linked to the PC sound card (Conexant, AC link audio16 bit).. This was done to record the cough sound in practical field conditions, without taking the acoustical characteristics of the stable into account. The recordings were made at a sample rate of 44100 Hz, with a resolution of 16bits. The coughs were sampled with a frequency of 22050Hz to gain calculation time.

The microphones were placed in the middle of the room, in the corridor, at 3 m and 18 m far from the entrance door. The data, collected in 5 days in a piggery, were labeled first by a veterinarian and then re-labeled in laboratory. The main objective of these tests was to evaluate the accuracy of cough recognition algorithm on labeled coughs from all other sounds. In the dataset there was a total of 396 different sounds.

Cough analysis: To visualize a sound the amplitude can be plotted in time. This representation method doesn't give any information about the frequency characteristics. In a spectrogram, the signal is analyzed using Fourier transformation in order to show how the frequencies change over time.

An example of an amplitude-time representation of a cough is given in figure 1.

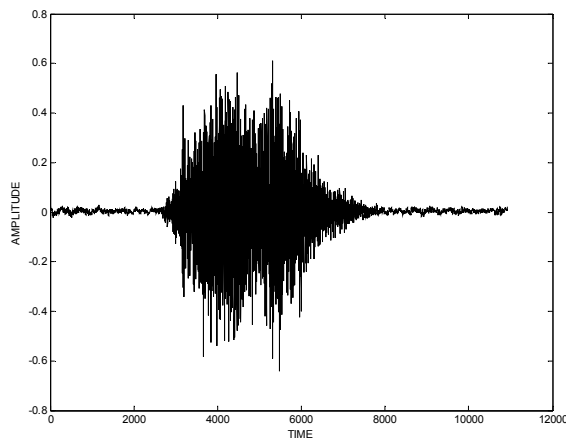


Figure 1. Amplitude variation in time (in samples) of a cough signal

The Spectrogram of the same signal is shown in figure 2.

The signal represented in figure 1 was a typical cough sound of a pig, the duration is only 0.7s.

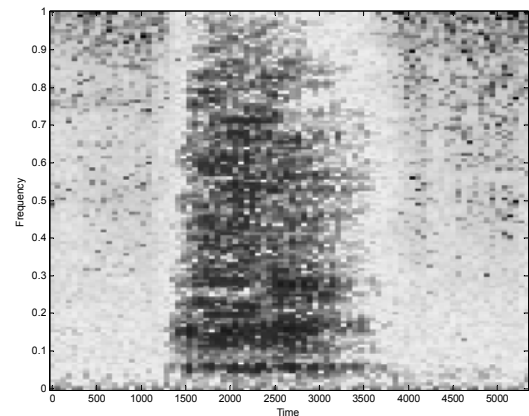


Figure 2. Spectrogram of the cough signal represented in figure 1.

Classification of the sounds:

In order to classify a sound, it has to be compared with a reference sound.

This is done using a method called “dynamic time warping”, already used successfully in a previous work (Van Hirtum et al., 2003), in which each sound is divided into frames of equal length and the features of each frame are stored in a feature vector. Thus, each sound is represented by a sequence of data feature vectors that form a sound template. The different duration of the cough sound results from non-uniform stretching and compression of the various portions in the cough sound. Consequently simple linear time alignment is not appropriate to compare two sounds of unequal duration. In order to compare two sound templates, the DTW algorithm uses one of them as a test pattern and the other one as a reference pattern. Taking frame by frame of the test sound template, DTW looks for the frame-path in the training template that results in the minimum distortion. For each test frame a set of specified frames in the training template is allowed for comparison.

Now, to test whether or not a certain sound is part of a specific class (cough, grunt, sneeze,...) the labeled sounds are divided into two groups: one test set and one training set.

Every sound in the test set is compared with all the sounds in the training set. If, at least, half of the sounds in the training set classifies the tested sound as a cough, the tested sound is marked as *cough*. If, on the other hand, more than half of the sounds in the training set classify the tested sound as non-cough, the sound is assumed *not cough*.

In order to have a good idea of the performance of the algorithm that was used to recognize the sounds, a method is required that shows how many sounds were classified in the correct way. This involves the number of coughs that were classified as coughs out of the total set

of cough sounds as well as the number of other sounds (grunts, screams, sneeze) that were classified as non-coughs out of the total set of non-cough sounds. So the performance of correct cough classification (P_{CC}) can be written as:

$$P_{CC} = \text{Nr. of correct cough classifications} / \text{Nr. of total cough sounds}$$

In the same way, the performance of the algorithm to classify other sounds as non-coughs (performance of correct non-cough classification, P_{NCC}) can be written as:

$$P_{NCC} = \text{Nr. of correct non-cough classifications} / \text{Nr. of total non-cough classifications.}$$

The total performance (TP) can then be written as:

$$TP = (P_{CC} + P_{NCC}) / 2$$

To have a representative performance of the algorithm, the test set and the training set are defined as followed: The test set consists of 10% of the total amount of sounds to be classified. The training set consists of 90% of the cough sounds. With this 10 % of the test set, 10 % of the ‘other’ sounds are mixed, to have a representative snap check. A permutation is applied 10 times, until all cough sound have been in the test class. The number of miscalculations is counted in order to have an estimate of the performance of the algorithm.

III. RESULTS

An overview of recorded sounds is given in table 1.

Although the average performance of the algorithm for cough sounds is about 72,6 % (see Figure 3), while the performance for other sounds, including sneezes, grunts, sounds of doors being opened and screams, is about 61.7% (see Table 2), this is a first step in a fully automated cough recognition system for the monitoring of swine epidemics.

Sound files:	
coughs	186
grunts	67
screams	62
doors, noise..	40
sneezes	41
Total	396

Table 1: an overview of the data on which the cough recognition algorithm is tested.

It is possible to see the variation in cough recording accuracy depending on the day of observation, due probably to different environmental conditions.

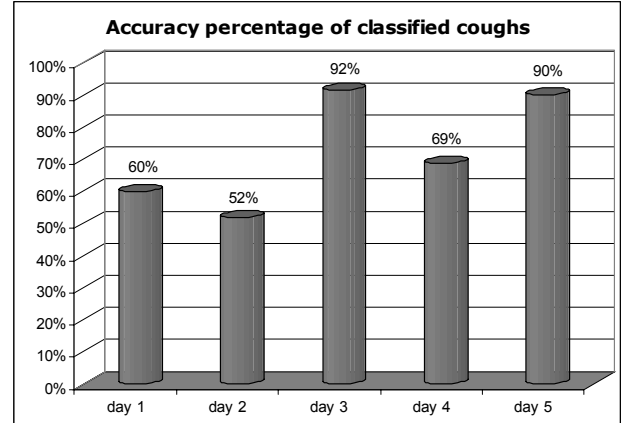


Figure 3. Average performance of the algorithm for cough sound recognition.

Days	Sounds correctly classified / Total sounds	Correct classification %
Day 1	29/60	48,33%
Day 2	19/42	45,24%
Day 3	21/40	52,50%
Day 4	104/157	66,24%
Day 5	174/239	72,80%
TOTAL	347/538	61,77%

Table 2. Average performance of the algorithm for sounds recognition.

The sounds of pig cough and noise background recorded of good quality are presented in figure and bad quality tracks in Figure 4 and 5 respectively.

IV. DISCUSSION

It is expected that better results will be obtained with different electronics.

Although the algorithm is tested off-line in this study, a fully automated recognition system involves an on-line application of the algorithm. A possible method of doing so is by, simultaneously as the sound information is acquired, letting a window of a certain sample length slide across this incoming sound. By detecting energy within this time frame, the algorithm could decide whether or not the signal in the frame is of interest for further processing. A method for classifying the different sounds may be a similar approach as the one that was followed in this study. Though, a drawback of this system is that the training set of the sounds should encounter as much as variability in order to have a good classification performance.

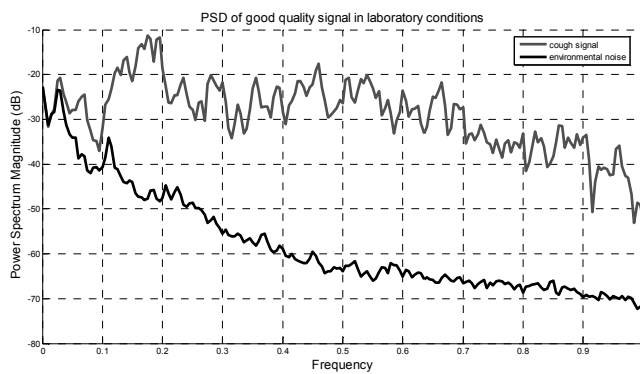


Figure 4: PSD of a signal acquired from a good quality recording. The black line represents the cough signal,, the grey line represents the noise in that signal.

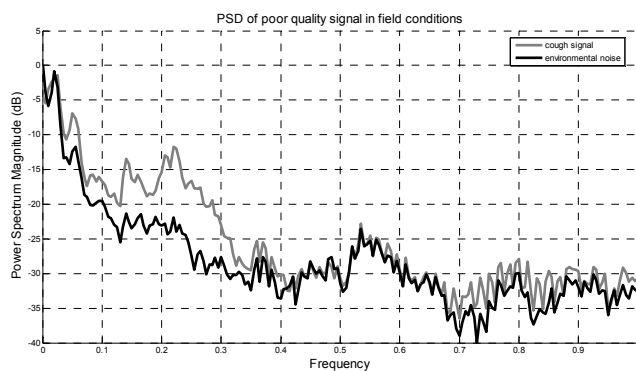


Figure 5: PSD of a signal acquired from a bad quality recording. The black line represents the cough signal, the grey line represents the noise in that signal.

V. CONCLUSION

In the future other methods for classification should be examined. For example, using sound models that serve as a “template” of a certain sound.

These models can be “mapped” onto the specific sound and by adjusting the model parameters, it might be possible to search for the best model of a certain sound. One might conclude that online model based sound analysis has a high potential for animal monitoring, but there is much to be done before such a fully automated on-line sound classification system can reach the daylight.

This research could lead, in future, to a real time automatic system of cough recognition in piggeries, that might be useful in preventing the spreading of respiratory diseases and lowering the excessive use of antibiotics in pig management. The algorithm presented here can be seen as a start to extrapolated existing techniques of voice

analysis towards less conventional “sounds” as coughs, grunts and pig screams. Although some research has been performed on cough analysis, the applications remain poor. By applying such experiments in field conditions, it might bring this approach of bio-acoustics as a possible disease monitoring system closer to reality. In this case the object is the swine, but this can easily be expanded to other species like cattle and poultry.

REFERENCES

- [1] A. V. Hirtum and D. Berckmans, "Objective recognition of cough-sound as biomarker for aerial pollutants," *International Journal of Indoor Air Quality and Health*, in press.
- [2] Hiew Y., Smith J., Earis J., Cheethma B. and Woodcock A., “Dsp algorithm for cough identification and counting”, *Proc. ICASSP '02*, Orlando, Florida, pp. 3888-3891, 2002
- [3] Aerts JM, Jans P, Halloy D, et al. Labeling of cough data from pigs for on-line disease monitoring by sound analysis. *Transactions of the ASAE* 48 (1): 351-354. Jan-Feb 2005
- [4] I. Tothill, "Biosensors developments and potential applications in the agricultural diagnosis sector," *Computers and Electronics in Agriculture*, vol. 30, pp. 205-218, 2001.
- [5] V. Hirtum, A. and Berckmans D., “Fuzzy approach for improved recognition of citric acid induced piglet coughing from continuous registration”, *J. Sound and Vibration*, vol. 266, pp. 667-686, 2003
- [6] V. Hirtum, A. and Berckmans D., “Intelligent free field cough sound recognition”, *Proc. ICONS '03*, Faro, Portugal, pp. 453-58, 2003
- [7] B. Urbain, J. Provoust, D. Beerens, O. Michel, B. Nicks, M. Ansay, and P. Gustin, "Chronic exposure of pigs to airborne dust and endotoxins in an environmental chamber," *Veterinary Research Communications*, vol. 27, pp. 569-578, 1996.
- [8] A. Van Hirtum, M. Guarino M., A. Costa., P. Jans., K. Ghesquire, D. Berckmans, P. Navarotto. 2003. Automatic detection of chronic pig coughing from continuous registration in field situations. *Proceedings of the 3rd International Workshop on Models and Analysis of Vocal Emissions for Biomedical Applications*. Florence 10-12 Dicembre 2003. pp. 251, 254.

WAVE-MORPHING IN THE FRAMEWORK OF A GLOTTAL PULSE MODEL

Julien Hanquinet¹, Francis Grenez¹, Jean Schoentgen^{1,2}

¹Department "Signals and Waves", Université Libre de Bruxelles, 50, Avenue F.-D. Roosevelt, 1050 Brussels, Belgium, jhanquin@ulb.ac.be

²National Fund for Scientific Research, Belgium

ABSTRACT

The presentation concerns a method of wave-morphing applied to a model of the phonatory excitation, the instantaneous frequency and the harmonic richness of which are controlled. This method is based on an interpolation between the Fourier coefficients of two template waveforms. The method enables morphing continuously from one waveshape to another. Possible applications are the simulation of diplophonia, biphonation and different phonation types.

I. INTRODUCTION

The presentation concerns a method of wave-morphing based on Fourier series. It enables continuously changing one waveform into another. This method is applied to a model of the phonatory excitation signal, which is the acoustic signal generated by the vibrating vocal folds and pulsatile glottal airflow.

Conventionally, glottis signals are modeled by means of a concatenation of curves that approximate the glottal pulse shape. The most popular model based on this technique is the Fant-Liljencrants model [1]. A sustained glottis signal is generated by repeating the basic pulse shape periodically.

We proposed here an alternative based on the Fourier signal representation, which offers a more flexible approach to phonatory excitation modeling. It enables controlling continuously the instantaneous frequency and harmonic richness of the synthetic phonatory excitation, as well as glottal pulse morphing. The morphing is carried out by interpolating the Fourier series coefficients between two different template glottal cycles.

II. MODEL OF THE PHONATORY EXCITATION

The model used to synthesize the phonatory excitation is based on Fourier coefficients. The Fourier coefficients are computed for a template cycle of the desired phonatory signal. The template cycle can be modeled or extracted from real speech. Here, we use the Fant-Liljencrants (LF) model [1] to synthesize the desired template. The LF parameters are chosen so that the condition of area balance is fulfilled, i.e. the cycle average is zero.

A discrete periodic signal y of cycle length N can be approximated by its Fourier series truncated at Nh harmonics .

$$y(n) \approx \frac{1}{2} a_0 + \sum_{k=1}^{Nh} a_k \cos(k \frac{2\pi}{N} n) + b_k \sin(k \frac{2\pi}{N} n). \quad (1)$$

In expression (1), coefficients a_k and b_k encode the shape of the cycles of signal y and parameter N represents the cycle length. By changing the value of N , one can create signals with the same shape as y , but with different cycle lengths. Note that the following condition must be respected.

$$Nh < \frac{N}{2}. \quad (2)$$

If N is assumed to be real, expression (1) can be written as follows.

$$y(n) = \frac{1}{2} a_0 + \sum_{k=1}^{Nh} a_k \cos(k\theta_n) + b_k \sin(k\theta_n), \quad (3)$$

where $\theta_n = \theta_{n-1} + 2\pi f \Delta$, f is the instantaneous frequency of signal $y(n)$ and Δ is the sampling step. Condition (2) becomes the following.

$$Nh < \frac{f_{\text{sampling}}}{2} \frac{1}{f}. \quad (4)$$

The generalization of N to real values, because of letting assume f any real positive value, introduces a quantization error of one sample at most in the cycle length. For many applications, this error is negligible when the sampling frequency is chosen sufficiently high.

Therefore, by means of a glottal cycle template, a signal with the same cycle shape, but the instantaneous frequency of which is controlled, can be synthesized by means of (3). Figure 1 shows an example of a phonatory excitation, for which the instantaneous frequency evolves continuously and linearly in time.

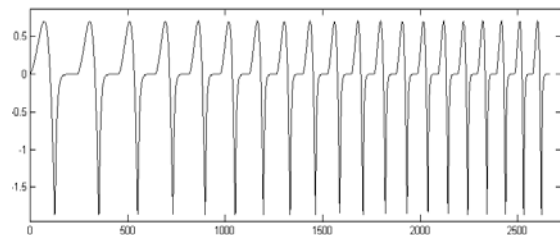


Figure 1 : Synthetic phonatory excitation, the instantaneous frequency of which evolves linearly from 75 to 200 Hz. The vertical axis is in arbitrary

units, and the horizontal axis is labeled in number of samples.

The harmonic richness of the synthetic signal can be controlled by modifying the Fourier coefficients as follows. This choice has been loosely inspired by [2].

$$\begin{aligned} a_k &\rightarrow a'_k = A^k a_k, \\ b_k &\rightarrow b'_k = A^k b_k, \end{aligned} \quad \text{with } 0 < A < 1. \quad (5)$$

One sees in expression (5) that the harmonics decrease, when the parameter A is less than one, the faster the higher their order.

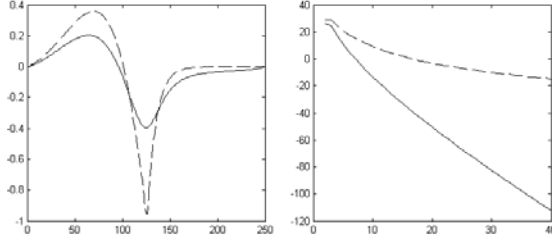


Figure 2 : The graph to the left shows two different cycles of the phonatory excitation. The dashed line is obtained with parameter A set to 1 and the solid line is obtained with parameter A set to 0.5. The vertical axis is in a.u. and the horizontal axis is labeled in samples. The graph to the right shows, dashed, the values in db of $|a_k + jb_k|$ and, solid, the values in db of $|a'_k + jb'_k|$ with A set to 0.5. The horizontal axis is labeled in the values of Fourier index k.

The control of the harmonic richness of the phonatory excitation may also be used to simulate onsets and offsets as illustrated in Fig.3.

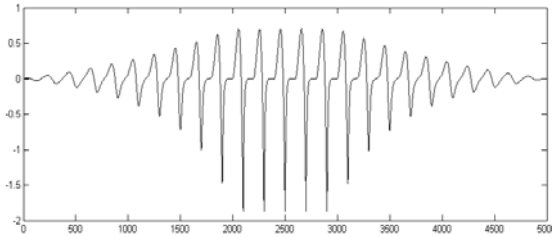


Figure 3 : Synthetic phonatory excitation where parameter A evolves linearly from 0 to 1 and from 1 to 0. The vertical axis is in a.u. and the horizontal axis is labeled in number of samples.

III. WAVE-MORPHING

Given two sets of Fourier coefficients X_1 and X_2 , in complex notation, computed for two different template cycles, intermediary shapes can be synthesized by interpolating the Fourier coefficients as follows (Figure 4).

$$X_k = X_{1k}^{1-Int} X_{2k}^{Int}, \quad (6)$$

where Int is an interpolation coefficient comprised between 0 and 1.

As a consequence, the Fourier phase and the logarithm of the Fourier magnitude are linearly interpolated. Therefore, coefficients a_k and b_k change as follows :

$$a_k = \frac{2}{N} |X_{1k}|^{(1-Int)} |X_{2k}|^{Int} \cos(\text{Arg}(X_{1k})(1-Int) + \text{Arg}(X_{2k})Int) \quad (7)$$

$$b_k = \frac{2}{N} |X_{1k}|^{(1-Int)} |X_{2k}|^{Int} \sin(\text{Arg}(X_{1k})(1-Int) + \text{Arg}(X_{2k})Int)$$

To avoid possible phase distortions in morphed signals, care should be exercised to respect the following condition.

$$|\arg(X_{1k}) - \arg(X_{2k})| < |\arg(X_{1k+1}) - \arg(X_{2k+1})| \quad (8)$$

To satisfy this condition, one computes the arguments of the two sets of complex Fourier coefficients X_1 , X_2 , and subtracts 2π from the argument of X_2 if condition (8) is not satisfied. The reason is that the phase of the morphed shape must be intermediary between the phases of the template cycles, which is possible provided that the arguments of coefficients X_1 and X_2 evolve quasi-monotonously.

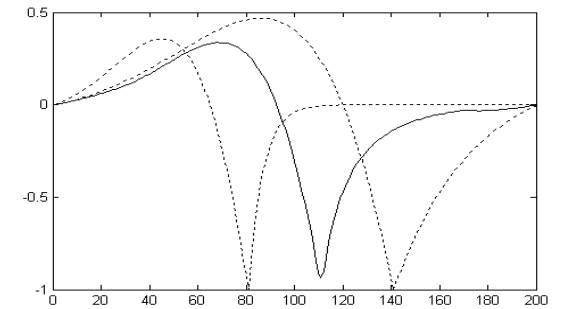
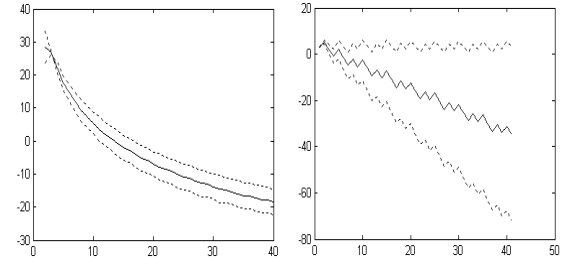


Figure 4 : Above, the graphs show the magnitude in db (to the left) and phase in radians (to the right) of the complex Fourier coefficients. Below, the dotted lines correspond to the template glottal cycles, and the solid line corresponds to the interpolated glottal cycle, with interpolation coefficient Int set to 0.5. Above, the horizontal axis is labeled in the values of Fourier index k. Below, the horizontal axis is labeled in number of samples.

IV. RESULTS

A. MORPHING

Figure 5 illustrates the phonatory excitation signal while morphing from one cycle template to another, e.g. illustrating the transition from one phonation

type to another. The interpolation coefficient evolves, between samples 600 and 3600, linearly from zero to one.

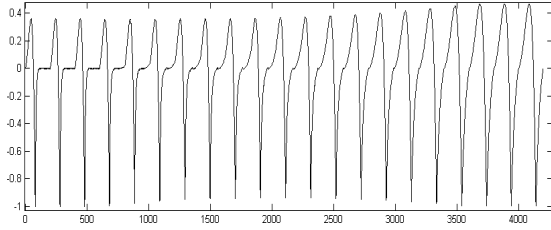


Figure 5 : Morphed synthetic phonatory excitation. The vertical axis is in a.u. and the horizontal axis is labeled in number of samples.

B. DIPLOPHONIA

Diplophonia refers to periodic phonatory excitation signals whose mathematical periods comprise several unequal glottal cycles. A repetitive sequence of different glottal cycle shapes can be simulated by modulating the interpolation coefficient, i.e. by continuously interpolating the Fourier coefficient between two sets of template coefficients X_1 , X_2 , computed from two different reference glottal cycles. Similarly, a modulation of the instantaneous frequency may simulate a repetitive sequence of glottal cycles of unequal lengths. The temporal evolution of the interpolation coefficient as well as phase may then be written as follows.

$$Int_n = \frac{1}{2}(1 + \sin(\theta_n / Q)) \quad (9)$$

$$\theta_{n+1} = \theta_n + 2\pi\Delta(f_0 + f_1 \sin(\theta_n / Q)) \quad (10)$$

The instantaneous frequency oscillates between $f_0 - f_1$ and $f_0 + f_1$. Parameter Q fixes the number of different glottal cycles within the mathematical period of the phonatory excitation. In practice, parameter Q is a small integer.

Figure 6 shows an example of diplophonia obtained by modulating the interpolation coefficient as well as the phase according to expressions (9) and (10), with Q set to two.

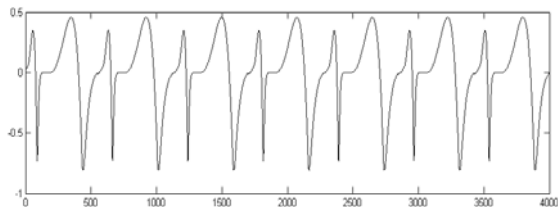


Figure 6 : Synthetic phonatory excitation demonstrating diplophonia. The vertical axis is in a.u. and the horizontal axis is labeled in number of samples.

C. BIPHONATION

Biphonation is also characterized by a sequence of glottal cycles of different shapes and lengths. But in this case, two glottal cycles are never identical. Biphonation reflects the presence in the spectrum of the signal of at least two harmonic series, the fundamental frequency of which form an irrational ratio. Biphonation is therefore characterized by discrete spectra with irrational ratios between the frequencies of some of the partials. Biphonation is also simulated by means of expression (9) and (10), with parameter Q equal to an irrational number.

Figure 7 shows an example of biphonation obtained with Q set to the constant e (2.71).

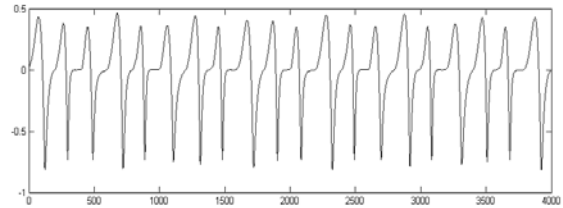


Figure 7 : Synthetic phonatory excitation demonstrating biphonation. The vertical axis is in a.u. and the horizontal axis is labeled in number of samples.

Note that diplophonia and biphonation can also be simulated by modulating phase (10) and parameter A instead of interpolation (9). This is because parameter A controls the harmonic richness and therefore the shape of the cycle. The control is less flexible however.

V. CONCLUSION

This presentation concerns a model of the phonatory excitation based on Fourier series. This model enables the control of the instantaneous glottal cycle length, instantaneous harmonic richness and glottal cycle shape via distinct parameters. This model also enables interpolating between two template cycle shapes. The shape of the cycles of the phonatory excitation may morph continuously from one shape to another. These possibilities are useful to simulate onsets and offsets, intonation, phonation type transients as well as diplophonia and biphonation.

REFERENCES

- [1] Fant G., Liljencrants J., Lin Q., "A four-parameter model of glottal flow", STL-QSPR, 4: 1-13, 1985.
- [2] Schoentgen, J., "Shaping function models of the phonatory excitation signal", J.Acoust. Soc. Am. 114(5): 2906-2912, 2003.

CHANGES OF VOCAL TRACT SHAPE AND AREA FUNCTION BY F0 SHIFT

T. Kitamura¹, P. Mokhtari¹, H. Takemoto¹

¹Department of Biophysical Imaging, ATR Human Information Science Laboratories, Kyoto, Japan

Abstract: Articulatory variation due to the production of vowels at five pitch frequency (F0) levels (110 Hz, 123 Hz, 130 Hz, 146 Hz, and 164 Hz) was analyzed by volumetric magnetic resonance imaging (MRI). Three Japanese male subjects produced sustained Japanese vowels /a/ and /i/. Observation of vocal tract area functions extracted from the MRI data revealed that F0 shift in vowel production affects not only the length of the vocal tract but also its shape. Analysis employing coefficient of variation for length-normalized area functions revealed that the shape of the vocal tract does not change proportionately by F0 shift and that each subject adopt different strategies for controlling F0 while maintaining the phonetic identity of the vowel.

I. INTRODUCTION

The larynx and the supra-laryngeal articulators are connected mechanically and interact with each other to produce speech sounds [1]. Vocal tract shape is thus affected by F0 change. Except for a few previous studies [2][3], however, effects of F0 shift on vocal tract shape have not been studied. In addition, differences of the effects among individuals and their acoustic manifestation have not been reported. The present study therefore aims to investigate possible effects of F0 shift on vocal tract shape and area function by examining individual variations of the interaction and their corresponding acoustic effects.

Effects on the shape of the vocal tract by changing F0 have been measured using several imaging systems. For instance, Hirai *et al.* [2] described differences in vocal tract shape during production of the Japanese vowel /a/ associated with 1.5-octave F0 falling by using magnetic resonance imaging (MRI). They also investigated mechanisms of F0 control in detail and proposed a physiological articulatory model with tongue-larynx coupling mechanism. Tom *et al.* [3] reported differences in vocal tract area function during production of the vowel /a/ under two registers, five F0 levels, and two loudness levels by using electron-beam computed tomography (EBCT).

However, those studies reported the results only for a single vowel of a single subject. Because each vowel has a different constriction location, effects on vocal tract shape may be different among vowels. Also, each speaker may adopt different strategies to control F0. In this study,

we thus investigated changes in articulation of a front and a back vowel at different F0 levels for three male subjects. Magnetic resonance images were acquired during producing the Japanese vowels /a/ and /i/ at five F0 levels, and analyzed for the effects on vocal tract shapes and area functions, as well as for the corresponding acoustic effects using a transmission line model.

II. MRI DATA ACQUISITION

Magnetic resonance images of three Japanese male subjects were obtained during sustained production of Japanese vowels /a/ and /i/ with a Shimadzu-Marconi ECLIPSE 1.5T Power Drive 250 at the ATR Brain Activity Imaging Center. The subjects are denoted below as A, B, and C. The imaging sequence was a sagittal Fourier Acquired Steady State (FAST) series with 3.0-mm slice thickness, no slice gap, a 256 × 256 mm field of view (FOV), a 512 × 512 pixel image size, 18 slices, 90° flip angle (FA), 9-ms echo time (TE), and 4,900-ms repetition time (TR). The total acquisition time was approximately 15 sec. These parameters were selected to complete data acquisition in a single breath.

Each subject was positioned to lie supine on the platform of the MRI unit and put on non-magnetic intra-aural headphones. Harmonic complex tones whose fundamental frequency was 110, 123, 130, 146, or 164 Hz were presented through the headphones during scanning. The subjects were instructed to adjust their F0 to the fundamental frequency of the harmonic complex tone while maintaining steady phonation during scanning. Each subject's voice during the scan was recorded through an optical microphone (phone-or FOMRI). After the scan, each utterance was examined to confirm whether the subjects adjusted their F0 as instructed. Any MRI data outside a margin of F0 error of ± 5 Hz was excluded from further analysis. The data for the lowest F0, from subject B, were excluded on this basis.

III. METHOD

A. Morphological analysis

The effects of F0 on vowel articulation were analyzed with reference to the rigid structures. When the subjects' head position in the MR images was different across F0 levels, the MR images were aligned with reference to the

line connecting the anterior nasal spine and the posterior margin of the foramen magnum using an affine transformation. Following the alignment, outlines of the vocal tract, hyoid bone, and mandible were traced manually on the mid-sagittal plane to be superimposed together for each vowel.

B. Analysis of vocal tract area function

Cross-sectional areas along the mid-line of the vocal tract were extracted at 2.5-mm intervals from the MRI data set to obtain the area function. Intra-speaker variations of the vocal tract with respect to F0 were examined using the coefficient of variation as an index. Each vocal tract area function was resampled by cubic-spline interpolation in 44 equal-length sections [4], and the coefficient of variation for each section $cv(\mathbf{x})$ was obtained by

$$cv(\mathbf{x}) = \frac{s(\mathbf{x})}{\bar{A}(\mathbf{x})}, \quad (1)$$

$$\bar{A}(\mathbf{x}) = \frac{1}{N} \sum_f A(\mathbf{x}, f), \quad (2)$$

where $A(\mathbf{x}, f)$ is an interpolated vocal tract area functions for a given F0, \mathbf{x} is the index vector [1, 2, ..., 44], N is the number of F0 level, and $s(\mathbf{x})$ is the standard deviation of $A(\mathbf{x}, f)$.

C. Simulation using transmission line model

In order to estimate the acoustic effects of the changes in area function due to F0 shift, the first two formant frequencies were calculated by using a transmission line model. Calculations of the velocity-to-velocity transfer functions of the vocal tract were performed for the frequency region up to 4 kHz. The first (F1), second (F2), and third (F3) formant frequencies were then identified from the transfer functions using a peak-picking method.

IV. RESULTS AND DISCUSSIONS

A. Morphological analysis

Figure 1 shows all the tracings to depict the systematic change in the positions of the speech organs with F0 shift. The changes of the vocal tract shape on the mid-sagittal plane were considerably smaller than those in the previous studies [2][5]. The larynx tended to rise with F0 while the shape of the laryngeal cavity was almost constant for subjects A and B. In contrast, subject C did not exhibit obvious changes in larynx height, rather showing expanding laryngeal cavity with rising F0.

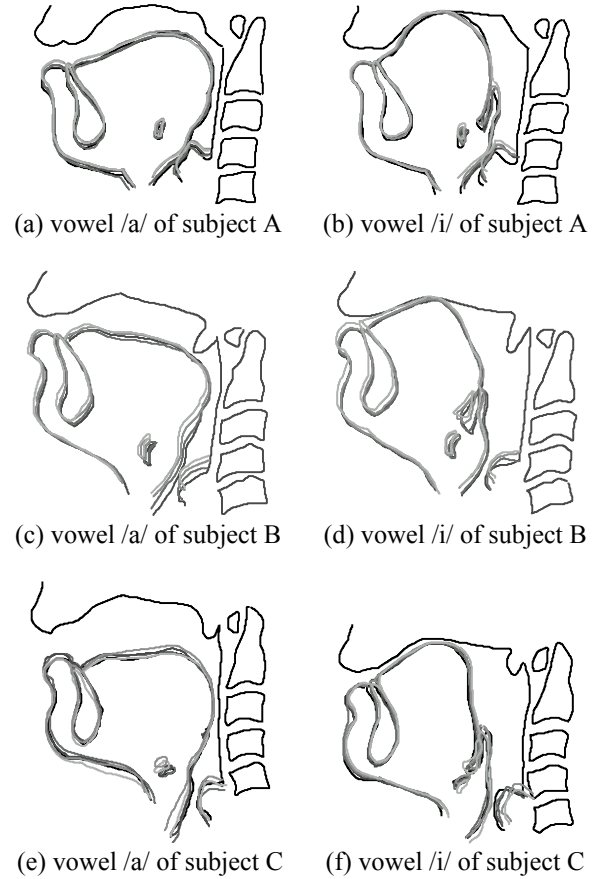


Figure 1: Superimposed mid-sagittal tracings for the Japanese vowels /a/ and /i/ obtained from three male Japanese subjects. F0 level corresponds to the degree of line saturation of the tracings: the black lines show outlines for the lowest F0 (110 Hz) and the lightest gray lines show those for the highest F0 (164 Hz). The anterior direction is to the left.

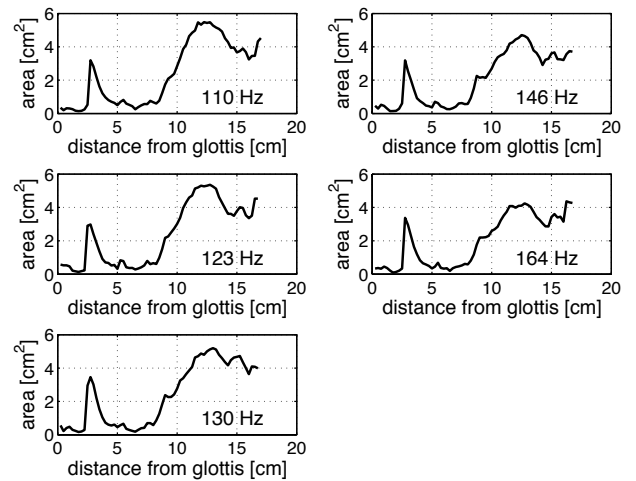


Figure 2: Vocal tract area functions at all F0 levels for the vowel /a/ of subject A.

Table 1: *Vocal tract length [cm] associated with variations in F0 and Pearson's correlation coefficient r between them.*

F0	Subject A		Subject B		Subject C	
	/a/	/i/	/a/	/i/	/a/	/i/
110 Hz	16.6	16.8	---	---	17.2	16.0
123 Hz	16.4	16.7	17.3	16.1	17.6	16.2
130 Hz	16.4	16.7	17.1	16.1	17.6	16.0
146 Hz	16.2	16.6	16.8	15.8	17.2	15.8
164 Hz	16.0	16.2	16.5	15.7	17.4	16.3
r	-0.99	-0.93	-1.00	-0.96	-0.04	0.26

B. Analysis of vocal tract area function

Figure 2 depicts vocal tract area functions for the vowel /a/ of subject A indicating that the F0 shift during vowel production affects not only the length of the vocal tract but also its shape. The areas of the oral cavity of the subject tended to decrease with rising F0 for the subject, although the changes of the vocal tract shape on the mid-sagittal plane were considerably small. This tendency was also found for the other subjects.

Figure 3 depicts the length-normalized mean area functions and their coefficients of variation (CVs) for each section. Non-uniform CV patterns demonstrate that the shape of the vocal tract does not vary proportionately with F0 shift, and sharp peaks of the CVs indicate large changes of the cross-sectional area at the sections among the data. The peak of the CV at the seventh section from the glottis for the vowels of subject A indicates that the junction between the lower pharyngeal and laryngeal cavities varies in location with F0 shift. The peak near the junction can also be found for the vowel /i/ of subject B. The peak of the CV at the 23rd section for the vowel /a/ of subject B indicates that the ratio of oral and the pharyngeal cavity lengths altered with F0 shift. Additionally, the sharp peak near the 42nd section for the vowel /i/ of all the subjects corresponds with movements of the lips with F0 shift.

The CVs at constricted sections are relatively smaller than those at non-constricted sections for the vowel /i/. Because vowel acoustics are relatively sensitive to changes in constriction area [7], this strategy contributes to preserving vowel features regardless of the F0 level.

In contrast to the local change of the shape of the vocal tract for subjects A and B, the lower pharyngeal and the laryngeal cavities (from the first section to the 15th section) of subject C varied widely with F0 changes. Thus, inter-speaker differences of the CV pattern indicate that the strategy to control F0 and vowel articulation varies from subject to subject.

Table 1 shows vocal tract length measured for each condition and Pearson's correlation coefficients with F0. These results indicate that there are strong negative correlations between vocal tract length and F0 for

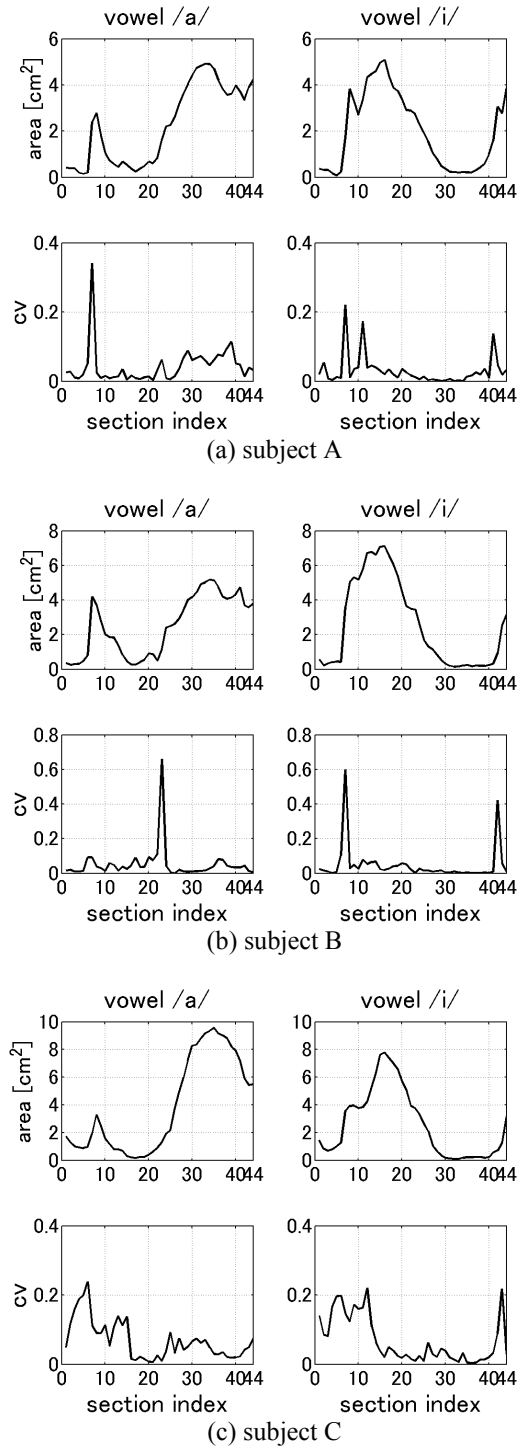


Figure 3: *Average and coefficient of variation (CV) of the length-normalized area function for three male subjects.*

subjects A and B, but not for subject C. The results are consistent with the observation that the larynx position rises with rising F0 for subjects A and B.

C. Simulation using transmission line model

Figures 4 and 5 depict the frequencies of the lower three formant (F1, F2, and F3) obtained from calculated transfer functions for the vowels /a/ and /i/ for the subjects. The frequencies do not increase uniformly with rising F0, indicating that the shape of the vocal tract does not change proportionately by F0 shift.

There is a positive correlation between F0 and F2 for the vowel /a/ of all the subjects ($r = 0.83$ for subject A, $r = 0.90$ for subject B, and $r = 0.56$ for subject C). The positive correlations are caused by the decrease of the area of the oral cavity with rising F0 for the vowel /a/ mentioned above. In contrast to the vowel /a/, there is no common positive or negative correlation between F0 and the formant frequencies for the vowel /i/.

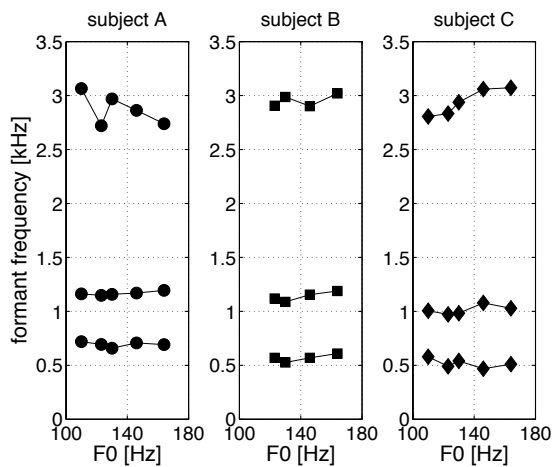


Figure 4: First (F1), the second (F2), and the third (F3) formants of velocity-to-velocity transfer functions for the vowel /a/ associated with variations in F0.

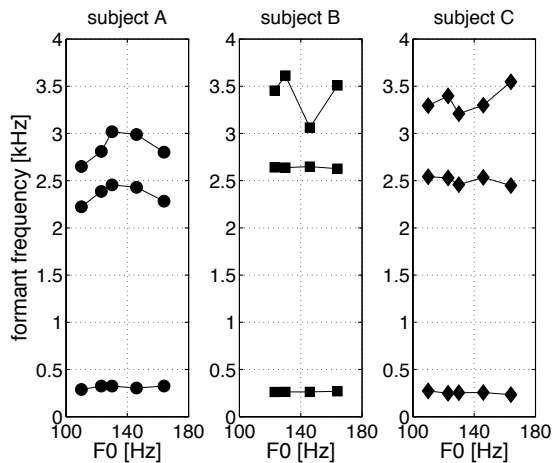


Figure 5: First (F1), the second (F2), and the third (F3) formants of velocity-to-velocity transfer functions for the vowel /i/ associated with variations in F0.

VI. CONCLUSIONS

Volumetric MRI was used to investigate changes in vocal tract configuration during vowel production with by F0 changes. The results for the Japanese vowels /a/ and /i/ of three male subjects demonstrated that F0 shift affects not only the length of the vocal tract but also the shape. The data also showed that the strategy for controlling F0 preserving vowel characteristics differs across individuals. The results of the analysis of intra-speaker variation of the vocal tract area functions indicated that the shape of the vocal tract changes non-uniformly with F0 and the regions of changes are different among vowel types and subjects. The results from the acoustical simulation indicated that the vowel /a/ tends to be neutralized with F0 rising while the vowel /i/ is kept constant over the F0 levels.

ACKNOWLEDGEMENTS

This research was supported in part by the Ministry of Internal Affairs and Communications on their Strategic Information and Communications R&D Programme and the National Institute of Information and Communications Technology.

REFERENCES

- [1] K. Honda, "Relationship between pitch control and vowel articulation," in Bless D. M. and Abbs J. H. (eds.) *Vocal Fold Physiology*, San Diego, College-Hill Press, 1983, pp. 286-297.
- [2] H. Hirai, J. Dang, and K. Honda, "A physiological model of speech organs incorporating tongue-larynx interaction," *J. Acoust. Soc. Jpn.*, vol. 51, pp. 918-928, 1995.
- [3] K. Tom, I. Titze, E. A. Hoffman, and B. H. Story, "Three-dimensional vocal tract imaging and formant structure: Varying vocal register, pitch, and loudness," *J. Acoust. Soc. Amer.*, vol. 109, pp. 742-747, 2001.
- [4] B. H. Story, and I. Titze, "Parameterization of vocal tract area functions by empirical orthogonal modes," *J. Phonetics*, vol. 26, pp. 223-260, 1998.
- [5] H. Hirai, K. Honda, I. Fujimoto, and Y. Shimada, "Analysis of magnetic resonance images on the physiological mechanisms of fundamental frequency control," *J. Acoust. Soc. Jpn.*, vol. 50, pp. 296-304, 1994.
- [6] K. Honda, "Formant frequency shift due to fundamental frequency change," IEICE Tech. Rep. SP86-122, 1986.
- [7] G. Fant, "Vocal-tract area and length perturbations," *STL-QPSR* vol. 4, pp. 1-14, 1975.

Comparison of LPC analysis and impedance vocal tract measurements

M. Kob, J. Stoffers, Ch. Neuschaefer-Rube

Chair of Phoniatrics and Pedaudiology, RWTH Aachen University – University Hospital Aachen

Pauwelsstr. 30, 52074 Aachen, Germany

1 Introduction

The acoustic measurement of the resonances in the space between vocal folds and lips, the vocal tract, allows a non-invasive, objective analysis of the spectral energy distribution for different articulatory cases. Whereas a conventional LPC analysis is successful only when applied to more or less stationary voice signals, an external excitation with subsequent measurement of the vocal tract impedance at the mouth can give reliable results when the voice signal is not stable or even missing.

This contribution addresses the problem how to compare results from impedance measurements with LPC measurements. For a set of normal speakers, both measurements have been performed simultaneously. Based upon the evaluation of the LPC curves, similar values for resonance frequency, amplitude and bandwidth were derived. In a study of 81 normal speakers the results from the evaluations are compared.

2 Method

The measurement set-up and the software used to evaluate the measurements allow a sequence of measurements consisting of three parts: the LPC analysis of the voice signal, the impedance measurement during phonation, and the impedance measurement without phonation. The concept for measurement of the vocal tract impedance at the mouth, VTMI, is described in detail in [2], and the procedure of clinical measurements is described in [4].

Measurements were performed in a group of 35 female and 46 male healthy speakers, using a simplified set-up without velocity sensor. One reason is the problem of clipping which can occur in the velocity sensor at high sound velocities. Comparisons between this set-up and the original 2-sensor set-up showed that results from both methods yield comparable results for the performed task.

A sample rate of 22050 Hz was chosen, and subsequent evaluations were limited to the frequency range 100..5000 Hz.

2.1 LPC measurement

The “linear predictive coding” method (LPC) is a well-established method to identify the formant structure of

a voice signal. The LPC curves are derived from a windowed part of the voice signal.

For the calculation of the LPC curves 28 coefficients were used to achieve a rather high pole density but not too many wrong identifications of formants. A Hamming window of 9525 samples was applied to the voice signal. The onset of the voice signal was automatically discarded.

2.2 Impedance measurement

All impedance measurements were performed using a linear swept sine from 250 Hz to 6000 Hz with a duration of 0.74 seconds. The signal-to-noise ratio was improved by application of a symmetric Hanning window of 15 ms length.

3 Evaluation and normalisation

3.1 Parameters

From the LPC curves the formant frequency, the formant bandwidth (3 dB decay), and the relative amplitude of the formants were calculated. The amplitude difference was calculated with respect to the highest formant in the frequency range 150..5000 Hz.

The resonances frequencies of the impedance curve were calculated from the minima of the impedance function $Z(f)$. Since no measures for the amplitude and bandwidth of the resonances could be directly derived from the impedance function, new measures had to be calculated: the slope between a local minimum and maximum near a resonance was used, as well as the amplitude difference between these points. These values were normalised as well by division of the local amplitude difference by the difference between the absolute maximum and minimum in the frequency range of the evaluation.

3.2 Normal ranges

From each three LPC measurements of the six phonemes /a:/, /æ:/, /i:/, /o:/, /u:/, /l:/ the first four formants were evaluated with respect to mean values standard deviations of the formant frequencies, amplitudes and the bandwidths.

From the resonance and LPC curves the above parameter were automatically calculated and stored in an XML

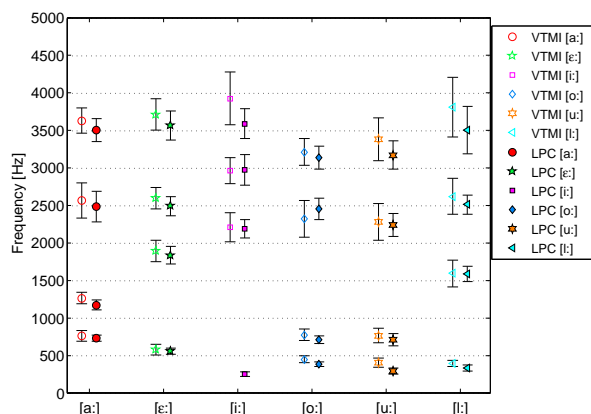


Figure 1: Male reference group: Comparison of formants and resonances from LPC and impedance analysis (automatic analysis, error bar corresponds to ± 1 standard deviation)

tree. Whereas the formant values of the LPC curves were easily calculated and simply copied to the tree, the resonance evaluation was more complicated. The number of detected resonance frequencies was much higher than the desired number of about four resonances between 100 and 5000 Hz. The reason is the presence of small variations in the impedance curve which can easily be misinterpreted as resonances. A selection of the four most probable resonances was achieved by weighting the resonance features according to scores for relative amplitude between maximum and minimum, slope between neighboured extrema, and the relative distance to the LPC formant frequency. For the four resonances with the highest scores the related bandwidth and frequencies were calculated.

In Figure 1 the frequencies of the formants (LPC) and resonances (VTMI) are plotted for the male normal group. The results indicate a high comparability of the results from the LPC and from the impedance analysis method, both with respect to the mean frequencies as well for the standard deviations. The missing first resonance for the vowel /i/ is caused by the weak excitation of the vocal tract with the swept sine below 250 Hz.

4 Case study

Pathological alterations of the vocal tract configuration can lead to a change in the resonance structure of the vocal tract [5]. Exemplarily for the results from an ongoing medical study we describe the application of the impedance method to the acoustic vocal tract characterisation of a 82 years old male patient (1.65 m, 55 kg), status after tonsillectomie.

Diagnosis: Expanded malignant tumour in the lower pharynx reaching down to the larynx on the left side (lower pharynx-larynx carcinoma, T4).

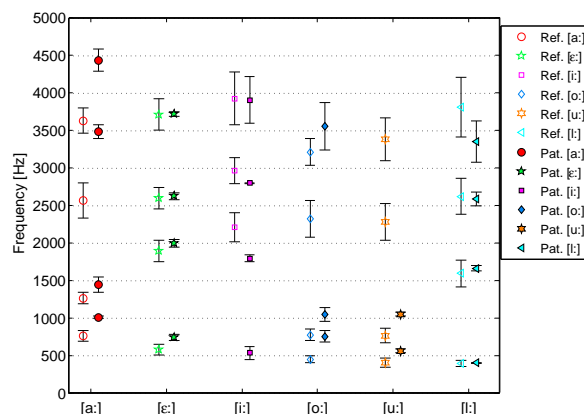


Figure 2: Comparison of vtmi measurement results of the reference group and a male patient with supraglottal tumour

CT and endoscopy results: We observe a tumorous process in the left lower part of the pharynx, beginning on the lingual bone level, extending into the larynx over a length of ca. 4.5 cm, crossing the median line ventrally. A partial corrosion of the thyroid cartilage by the tumour is seen. The endoscopy of the airways shows a big exulcering tumour, extending from the vocal cord level up over the ventricular folds side with infiltration of the laryngeal epiglottis area. Tongue basis, tongue directed epiglottis area and sinus piriformis visually clear of tumour.

Particular aspects for LPC and impedance measurements: The upper and lower jaw is toothless. A distinctive disphonia (strong „hoarseness“) is heard, the patient phonates with great effort and is not able to hold phonation for longer. The voice has a very high pitch. Figure 2 shows the results of the resonance frequency analysis of this patient compared to the standard values of the male reference group. It is evident that in several phonemes the resonances are shift to higher frequencies. For the phonemes /o/ and /u/, the third and fourth resonance are afflicted with high energy loss and have such low amplitude that they cannot be surely detected.

5 Discussion

Investigation of a reference group shows differences both in formant- and in resonance characteristics between male and female as well as between the two methods. The frequencies of LPC analysis and impedance measurements at the same subject are strongly correlated. Concerning the amplitude values, the impedance measurements shows a systematic lowering of the resonance amplitudes at frequencies below ca. 800 Hz. The deviation found in the patient's increase of the resonance values in the phonemes /a/ and /æ/ indicates an acoustical decrease of the length of the vocal tract by a tumour caused

narrowed supraglottal space. The absence of higher formants in /o/ and /u/ could be caused by a higher sound-absorption of the altered tissue. A systematic examination of further patients with similar diseases is planned and should give additional clues in view of a correlation of physiological and acoustical properties of the vocal tract.

References

- [1] M. Kob, Ch. Neuschaefer-Rube (2001): A method for measurement of the vocal tract mouth impedance. Conference CD-ROM, 2nd Int. Workshop on Models and Analysis of Vocal Emissions for Biomedical Applications – MAVeBA, file "papers/26.pdf" 1-6.
- [2] M. Kob und Ch. Neuschaefer-Rube (2002): A method for measurement of the vocal tract impedance at the mouth. *Medical Engineering & Physics*, 24, 467-471.
- [3] M. Kob, Ch. Neuschaefer-Rube (2003): Acoustic analysis of overtone singing. *Proceedings 3rd Int. Workshop on Models and Analysis of Vocal Emissions for Biomedical Applications – MAVeBA*, 187-190.
- [4] M. Kob, J. Stoffers, M. Lievens, R. Katzer, Ch. Neuschaefer-Rube (2004): Application of impedance measurements for the diagnosis of articulatory dysfunction. *Proceedings CFA/DAGA 2004*, 1145.
- [5] S. Koppetsch und K. Dahlmeier (2003): Funktionelle Störungen der Artikulation bei intra-oralen Tumoren – eine prä- und postoperative Langzeitstudie. *Sprache–Stimme–Gehör*, 155-160.

SOURCE VOICE CHARACTERISTICS OF THE ARTIFICIAL VOCAL FOLDS

V. Misun

Department of solids of bodies, mechatronics and biomechanics. Brno University of Technology,
Brno, Czech Republic

Abstract: Specialised literature presents a number of models describing the function of the vocal folds. In most of those models an emphasis is placed on the effect of Bernoulli's air underpressure during the air passage through the glottis. The author defines a principle of the vocal folds function with a working version name „principle of the compressed air bubble“. The paper deals with the experimental analysis of these artificial vocal folds and, first of all, with the properties and characteristics of the source voices generated by them. The main forces acting on the vocal folds during phonation are as follows : subglottal air pressure, elastic and inertia forces of the vocal folds structure.

I. INTRODUCTION

There have been several modified versions of the vocal folds function described in literature – [1], [2]. Most of them are based on the principle of the myoelasto-dynamic theory. They share a common predominant view whose central idea is that of an expressive effect of what is called Bernoulli's underpressure (negative pressure) produced within the space of the glottis at an increased speed of the airflow which passes between the vocal folds in motion.

Due to the numerous weak points found in the principles as defined by different authors in the literature there has been another principle defined and developed, preliminary called „compressed air bubbles“, in short „bubbles“ - [3]. The paper deals with the experimental analysis of these artificial vocal folds and, first of all, with the properties of the source voices generated by them [6].

II. DEFINITION OF THE „COMPRESSED AIR BUBBLES“ PRINCIPLE

The transport of the compressed air bubbles (air column, small air volume) through the glottis from the subglottal to the supraglottal space are the fundamental idea of this principle. The air bubbles with the higher subglottal pressure should be shifted as soon as possible to the upper part of the glottis. After the glottis opening the bubbles expand from the higher subglottal air pressure so that the acoustic pressure amplitude to be

source voice generated has the highest value in this case. This condition is very important for a higher intensity of voice generation.

According to this principle of the vocal folds function, the main forces acting on the vocal folds during phonation are as follows :

- the subglottal air overpressure acts on the relatively large inner subglottal surface, producing a considerable higher force opening the vocal folds,
- resilient forces of the vocal folds muscles which act against the opening of the vocal folds,
- forces of inertia of the vocal folds structure.

The forces of inertia of the air bubbles cannot play a significant role with regard to the low value of air density, a small size of the moved bubbles and also to small changes of the airflow speed.

The driving phenomenon for the vocal folds during phonation is the compressed air in the subglottal space, which always reaches a higher resulting air pressure value here than within the supraglottal space, and is the function of the glottis opening g . So that the basic characteristics of the vocal folds motion and the model function is the relation of the resulting subglottal air pressure and the opening between the vocal folds in the form defined by relation $p_{RSg}(g)$ – [6].

III. EXPERIMENTAL ANALYSIS OF THE ARTIFICIAL VOCAL FOLDS

Based on the compressed air bubble principle there have been artificial vocal folds developed for speaking aloud [4], [5]. Their design allows for changing the fundamental frequency of the source voice to match the male or female voice.

In order to test and verify the above defined principle of the bubbles there were some experiments carried out. Fig.1 represents a diagram of experimental analysis of a specific type of artificial vocal folds (geometry, arrangement, frequency tuning). The substitute vocal folds are placed inside the vocal folds box in the way dividing its space into two areas : the subglottal area – 1, the supraglottal area – 2. Into the subglottal area 1 is taken compressed air from the pressure vessel. In each area, a required acoustic pressure is measured with an appropriate microphone M1, M2 .

IV. MEASUREMENT RESULTS

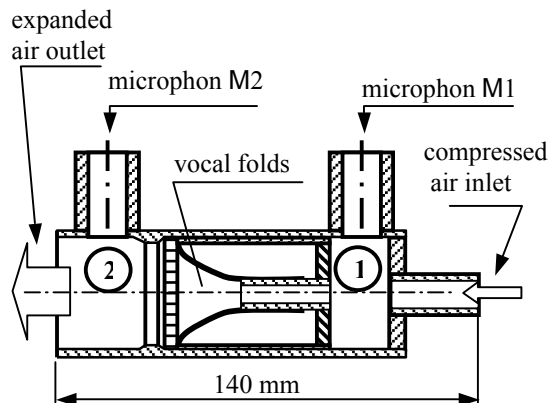


Fig.1 Diagram of the vocal folds location in the vocal folds box

The general measurement set is shown in Fig.2. In addition, a static mean value of the subglottal air pressure p_{SGS} is measured in the subglottal area, using a water column height, h . By setting of its mean value, the intensity of the source voice during phonation may be simulated by means of artificial vocal folds.

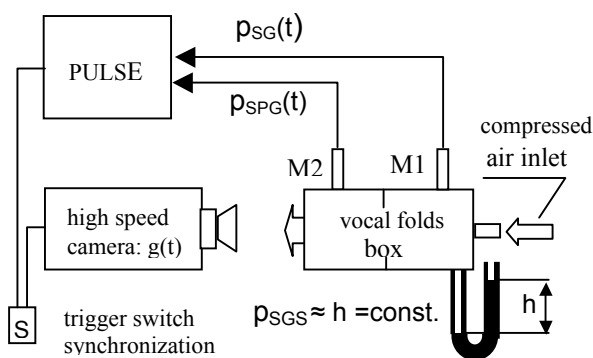


Fig.2 Measurement set of the vocal folds experimental analysis

The following variables were recorded during the phonation measurement - Fig.2 :

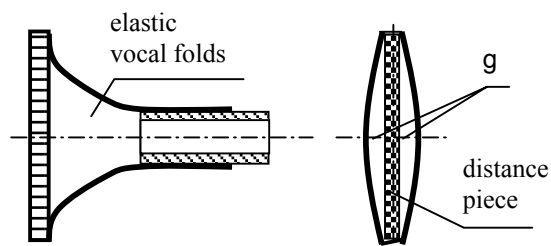
- water column height, h , characterizing the set mean value of the subglottal air pressure, p_{SGS}
- microphone M1 recorded variable air pressure in the subglottal space (measured by PULSE), $p_{SG}(t)$
- microphone M2 recorded acoustic pressure in the supraglottal space (measured by PULSE), $p_{SPG}(t)$
- the course of the opening $g(t)$ between the two vocal folds during their phonation (recorded by a high-speed Olympus camera).

The synchronization of all variables to be measured was ensured by means of trigger switch, S.

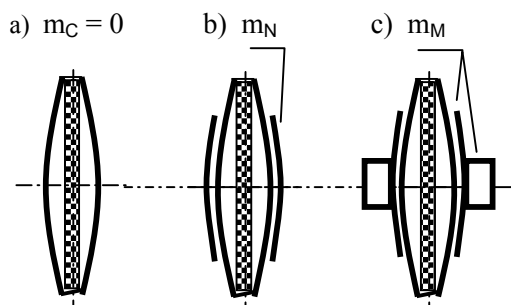
The characteristics of the artificial vocal folds vary, of course, depending on the type of the vocal folds measured. The individual types are distinguished by capital letters : C – basic type, M, N. They differ in geometry and in their additional masses, m_j ($j = C, M, N$) which in turn also changes their fundamental frequency tuning F_{0j} .

The parameters of the individual vocal folds type :

- type C – basic type: $m_C=0$, $F_{0C}=240$ Hz
- type M : m_M , $F_{0M}=132$ Hz
- type N : m_N , $F_{0N}=144$ Hz.



A. Scheme of the vocal folds



B. Additional masses of vocal folds

Fig.3 Types of the artificial vocal folds measured

Fig.4 represents the course of variable subglottal air pressure $p_{SG}(t)$ of a type C vocal folds, measured at a water column height of $h = 119$ mm, which corresponds to value $p_{SGS} = 1120$ Pa.

Fig.5 represents the spectrum of supraglottal acoustic pressure $p_{SPG}(t)$ behind the vocal folds. This acoustic pressure presented is the source voice generated by the type C vocal folds. The spectrum contains significant discrete components, which are harmonic components to the fundamental phonation frequency ($F_0 = 240$ Hz) of the vocal folds. All those harmonic components together form the „source voice“ of a given artificial vocal fold type.

Through the analysis of the high-speed camera recordings we shall obtain the course of the openings between the vocal folds as a time function - $g(t)$. Fig.6 represents the evaluation of the course of opening $g(t)$ based on the high-speed camera recordings.

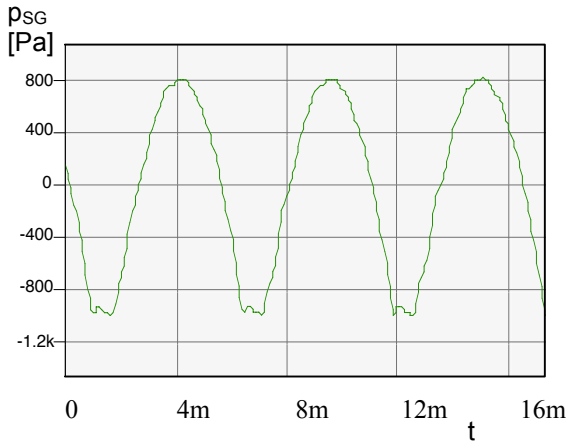


Fig.4 Variable subglottal air pressure course $p_{SG}(t)$

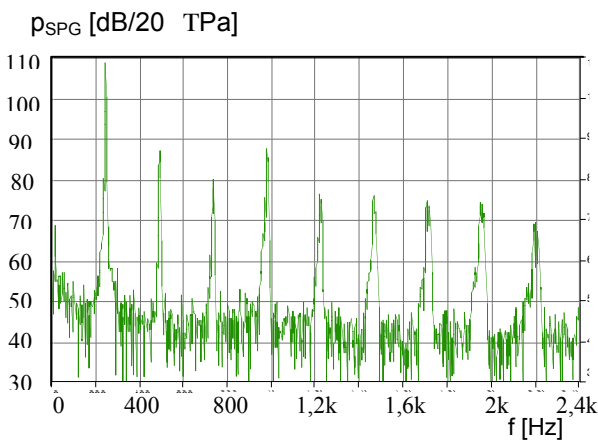


Fig.5 Spectrum of the artificial vocal folds source voice

It also specifies a volume of air $V_{SG}(t)$ passing through the specific value during phonation. A total volume of air passing through the vocal folds (volume of the bubble) during one period can then be obtained by means of integrating the course of $V_{SG}(t)$ in time.

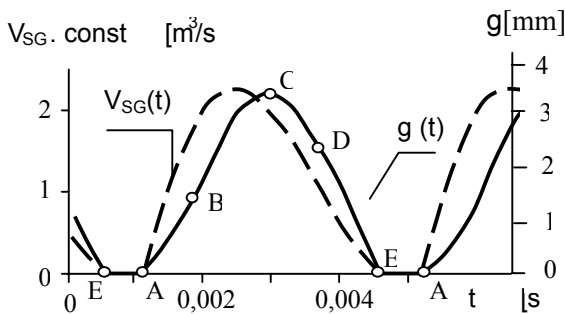


Fig.6 Course of the glottis opening $g(t)$ and of the air passing volume of $V_{SG}(t)$.

Based on the known courses $p_{SG}(t)$ – PULSE and $g(t)$ – camera, a $p_{SG}(g)$ relation needs to be established,

whereby we shall obtain a hysteresis loop characterizing the vocal folds motion. In Fig.7 this relation is shown for a type C vocal folds along with the mean value of $h = 119$ mm and it means $p_{SGS} = 1120$ Pa subglottal air pressure to be given.

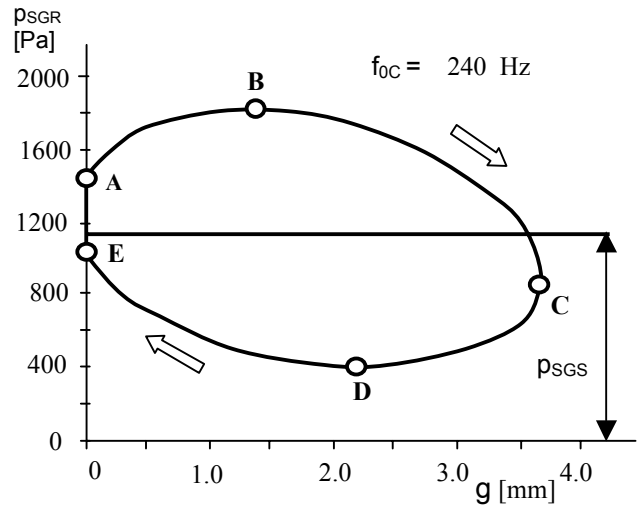


Fig.7 Course of $p_{SGR}(g)$ for p_{SGS} value

V. DISCUSION

The phonation period starts at point E with the increase of the air subglottal pressure continuing up to point A, with the vocal folds closed during this phase. At point A the vocal folds start opening and due to the increased subglottal air pressure begin to move away from each other. At the point where the elastic forces of the vocal folds prevail over the air pressure forces, the vocal folds start to come closer again at point C.

During part of ABCDE cycle the vocal folds are open. The vocal folds opening occurs at a higher air pressure $p_{SGR}(t)$ while their closing happens at lower values. As a result we obtained a loop whose area characterizes the energy supplied to the vocal folds by the changing air subglottal pressure which causes the vocal folds motion and consequently the acoustic supraglottal pressure origin. So that the phonation and generation of the source voice is created in this case.

The high-speed camera can also evaluate the flow of air through the vocal folds. To make the air visible a cigarette smoke was used. The recording in Fig.8 shows that the air passing through the artificial vocal folds is in the shape of sets of independent small volumes – air bubbles.

The following conclusions result from the analysis of the experimental data and the relations evaluated :

- the flow of air through the vocal folds may be defined by means of the passing compressed air bubbles (small air volumes) from the subglottal to

the supraglottal areas,

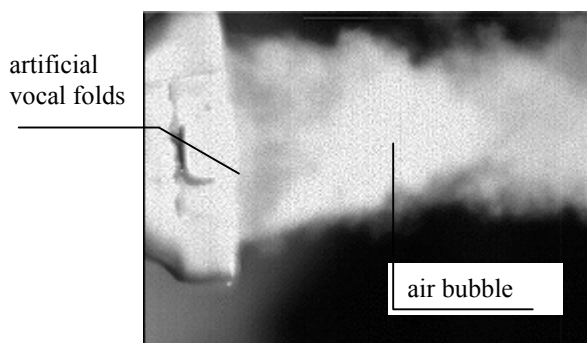


Fig.8 The bubbles expanding in the supraglottal space

- these bubbles expand in the supraglottal space beginning whereby generating acoustic waves, whose fundamental frequency and corresponding harmonic components define the source voice of the vocal folds,
- relation $p_{RSG}(g)$ is characterized by a loop of oval shape, which is abruptly ended during the contact of the vocal folds, i.e. at a $g=0$ value; during that time the subglottal pressure significantly increases as needed,
- as the value of mean subglottal pressure $p_{SGS,i}$ increases, the area of the loops is enlarging, i.e. the relevant subglottal pressures are growing (primarily the upper branches) and also the values of maximum opening of the vocal folds g_{max} are rising,
- this fact defines and explains the change to the intensity of the source voice; it is only through this parameter $p_{SGS,i}$ that the change of voice intensity may be achieved,
- the presence of bubbles (periodic action) is a necessary conditions for generating a sufficient number of harmonic components to excite formants of individual vowels,
- fundamental frequency of the vocal folds vibrations is given by their mass-elastic structural properties only,
- main forces acting on the vocal folds during phonation are as follows : subglottal air pressure, elastic forces of the vocal folds structure, and forces of inertia of the vocal folds system.

VI. CONCLUSION

The experimental analysis of the artificial vocal folds verifies the fact that the vocal folds function is based on the sequential flow of the compressed air bubbles through the phonating vocal folds – when

generating a loud voice. As a result of closing of the vocal folds the subglottal air pressure increases promptly, so that its value is high enough after the vocal folds opening. After expansion of such bubble in the supraglottal space there are acoustic waves generated with several harmonic components and with varied, however falling amplitudes. The correctness of the function of the artificial vocal folds is documented by the experimental verification of the spectra of several artificial vocal folds types.

The intensity of the generated source voice is determined solely by the mean value of the subglottal pressure whose value is set consciously by an individual by the lung activity. Humans also consciously set the height of their fundamental voice tones. Those represent the only two parameters that humans are able to define by will when speaking aloud.

Acknowledgements: The paper has been written within the framework of the solution of the grant projects GA CR No. 106/98/K019 named “Mathematical and Physical Modelling of Vibro-Acoustic Systems in Voice and Hearing Biomechanics Concentrated on Development of Compensatory Aids and Prostheses”.

REFERENCES

- [1] Pickett J.M., „The Acoustics of Speech Communication – Fundamentals, Speech Perception Theory, and Technology”, *Allyn and Bacon*, USA, 1999
- [2] Titze I. R., “Principles of Voice Production”, *Prentice Hall*, Englewood Cliffs, New Jersey, USA, 1994
- [3] Misun, V., “New Principle of the Vocal Folds Function”. *Proc. Inter. Confer. Advances in Quantitative Laryngology and Speech Research*. Hamburg, Germany, 2003, pp. 8.
- [4] Misun V., “External excitation of the vocal tract through the sinus nasal”, *Proc. wc2003 – World Congress on Medical Physics and Biomedical Engineering*, Sydney, Australia, 2003, pp. 4
- [5] Misun, V., “External excitation of the vocal tract after laryngectomy”, *MAVEBA*, Firenze, Italy, 2003, pp. 27-30.
- [6] Misun V., Prikryl K., „The source voice generation on the basis of the compressed air bubble principle”, *ICVPB- 2004*, Marseille, 2004, pp.6.
- [7] Misun V., “Device for stimulating the voice organ”. Patent No WO 2005/011532, *World Intellectual Patent Organisation*, Geneva, Switzerland, 10.2.2005.
- [8] Misun V., “Modelling of the vocal folds function”, *Proc. of 2nd European Medical and Biological Engineering Conference (EMBE’02)*, Vienna, Austria, 2002, pp. 242-243.

AUTOMATIC CLASSIFICATION OF VOICE DISORDERS IN COURSE OF NEURODEGENERATIVE DISEASE

T. Orzechowski¹, A. Izworski¹, I. Gatkowska², M. Rudzińska³

¹Department of Automatics, AGH University of Science and Technology, Krakow, Poland

²Computer Linguistic, Jagiellonian University, Krakow, Poland

³Collegium Medicum, Jagiellonian University, Krakow, Poland

I. INTRODUCTION

The study presented in this publication is the first from the planned complex, interdisciplinary studies. The examination was carried out on patients of CM-UJ clinic in Krakow who suffered from neurodegenerative disease with the damage of the extrapyramidal system with dysarthria-type changes in speech. Control examinations of healthy persons have also been carried out. The elements whose realization was tested had been chosen based on the linguistic knowledge in the scope of phonetics as well as on experience resulting from long-term practice as a speech pathologist. The linguistic material was selected in such a way as to pinpoint voice changes characteristic for patients with dysarthria. During the examination, phrases based on Polish idioms were also recorded for further analyses.

II. VOICE PHYSIOLOGY

Voice and speech production requires close cooperation of numerous organs which from the phoniatric point of view may be divided into organs:

- producing expiration air stream necessary for phonation (lungs, bronchi, trachea),
- amplifying the initial tone (larynx),
- forming tone quality and forming speech sounds (root of the tongue, throat, nasal cavity, oral cavity).

III. VOICE PATHOLOGY

Apart from typical changes caused by neurodegenerative disease (e.g. shivering of the body, limbs, muscle stiffness) changes in the voice may also be observed. The research shown in work (Intensive voice treatment LSVT® 2001) indicate the serious problem of speech pathology occurrence with as much as 75% of patients. Thus it may be concluded that voice constitutes one of the more crucial components of neurological diagnosis.

Patients suffering from neurodegenerative diseases (and such patients were examined by the authors) show dysarthria-type speech alternations. Dysarthria is a group phonation and articulation disorder which result from

damage to the movement control systems of the central or peripheral nervous system also responsible for the speech apparatus. The disorders occur although the speech plan is preserved [3]. Other definitions characterize dysarthria as handicapped production of articulated speech sounds resulting from disturbances to nervous mechanisms of voice production, modulation, intensity, timbre and resonance [2]. Nowadays dysarthria is described as a group of motor speech impairment result from a disruption of muscular control due to lesions of either the central or peripheral, or both, nervous systems. Communication Independence for the Neurologically Impaired CINI – 1994).

Due to the dominating symptom of disorder [3] 6 types of dysarthria have been specified. In our study, patients suffered from hypokinetic and hyperkinetic types. Parkinson disease and Parkinson syndrome (damage to the extrapyramidal system; speech impairment related to slowness) are accompanied by hypokinetic dysarthria-type changes in speech. Its most important characteristics in relation to isolated sounds are: distortions, loudness limitations. Distorted articulation is caused by quick and limited tongue and lips movements, sounds reduced down to slurring. Impairment in the speech process consist in sudden pauses in phonation. The voice is monotonous, quiet, weak and vanishing. The other type of dysarthria occurring in neurodegenerative diseases of the extrapyramidal system is hyperkinetic dysarthria. Phonation is distorted, sudden pauses in speech may occur. Moreover, incorrect articulation occurs as well as irregular breaks in articulation, sound elongation, repetition of sounds caused by abnormal muscular tension. Hypernasality may also occur, and the loss of air caused by throat and palate impairment result in the shortening of phrases. There are variations of speech loudness, the voice is trembling, tense and stifled, weak, with breaks.

IV. CHARACTERIZATION AND CLASSIFICATION OF SOUNDS USED IN THE EXAMINATION

During the examination both consonants and vowels were used. Patients were asked to pronounce the sounds in isolation.

The vowel group consisted of [a], [e] and [i]. This particular choice was related to the difference in the elevation of the tongue as well as to the gap between the lips.

	Division related to the degree of tongue elevation	Division related to the degree of mouth opening
[i]	high	ajar
[e]	medium-high	half ajar
[a]	low	open

Tab.1. Division of vowels.

The closer the tongue to the hard or soft palate, the smaller the degree of the oral gap, the lower the tongue, the bigger the gap. The position of the tongue in relation to the horizontal axis of the oral tract constitutes the basis for the division of vowels into more or less front or back. In our examination we used front vowels. High front vowel [i] is characterized by the very close position of the middle part of the tongue moving up the oral cavity towards the hard palate. In the case of the low front vowel [a], both the hump on the low-situated tongue as well as the spot on the hard palate, towards which the tongue rises, are situated a bit more to the back.

The consonant group consisted of [s], [x], [p], [k] and [g]. This category of sounds may also be divided into groups and subgroups, based on various articulation criteria. One of them is the manner of articulation, limiting to a different degree the flow of air through the voice channel, up to a complete lack of flow.

[s] and [x] sounds are examples of fricatives. They are consonants in the articulation of which particular parts of the speech organ move closer together creating a narrow gap. Airflow which has proper mass and speed passes through the gap and is disturbed. This gap may be formed in various places of the vocal tract under the larynx. The [s] consonant belongs to front-tongue dental speech sounds, whereas [x] belongs to back-tongue palatal speech sounds.

Sounds [p], [k] and [g] are plosives. The first phase of their duration consists in a solid obstruction built up somewhere within the oral tract, initially completely blocking the airstream coming up from the larynx. This blockage is then usually released abruptly, so that the air that was compressed behind the obstacle can escape with a kind of explosive movement, producing a 'cracking' or 'popping' sound.

The [p] consonant is a bilabial, whereas [k] and [g] are back-tongue palatal consonants.

5. EXAMINATION METHOD

The examined group consisted of 18 patients between the ages of 20 and 80 and a comparative group of healthy persons with similar age range. Patients suffered from hypokinetic and hyperkinetic types of movement

disorders. The voice of the examined patients was recorded with high-quality digital equipment in a soundproof room in order to eliminate any undesirable factors which could negatively affect the results. First, particular sounds were isolated from the recorded voice and then they were processed (filtration and spectrum analysis). Spectrum analysis contains numerous details, thus parameterization was necessary for automatic classification.

Firstly, the features of the spectrums of diagnostically essential sounds were verified.

V.1. Changes in sounds realization

Voice signals consist of several waves with different frequencies and amplitudes. The inner ear of humans decomposes the incoming acoustical waves into separate frequencies. Thus, it is appropriate to transform the PCM data into the frequency domain before analyzing it further. This can be achieved using Fourier Transformations.

Using the linear Fourier transform, a continuous signal can be transformed between its time domain representation, denoted by $h(t)$, and the frequency domain representation $H(f)$.

$$H(f) = \int_{-\infty}^{\infty} h(t) e^{-j2\pi ft} dx \quad (1)$$

The audio signal is sampled at a fixed sampling rate, so the function is not continuous $h(t)$ but discrete $x(k)$.

Consider a series $x(k)$ with N samples of the form x_0, x_1, \dots, x_{N-1}

$$X(n) = \frac{1}{N} \sum_{k=0}^{N-1} x(k) e^{-jk2\pi n/N} \text{ for } n = 0..N-1 \quad (2)$$

If N is a power of 2, the Fourier transform can be calculated very efficiently. It is known as *Fast Fourier Transformation* (FFT), and implemented in most of languages of technical computing (e.g. MATLAB®).

The power spectrum matrix $P(n; t)$, where n is the index for the frequency and t for the time frame:

$$P(n, t) = \left| X_t(n) \right|^2 \frac{1}{N} \quad (3)$$

The index n ranges from 1 to $N=2+1$.

It is convenient to use the Bark Frequency Scale instead of Hz. The name has been chosen in memory of Barkhausen, a scientist who introduced the phon to describe loudness levels for which critical-bands play an important role. The Bark scale ranges from 1 to 24 Barks, corresponding to the first 24 critical bands of hearing [Hz].

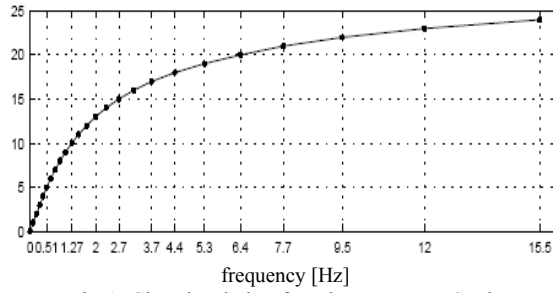


Fig.1. Charakteristic of Bark Frequency Scale

A critical-band value is calculated by summing up the values of the power spectrum within the respective $f_{low}(i)$ and $f_{high}(i)$ frequency limits of the i critical-band.

$$CB = \sum_{n \in I(i)} P(n, t) \quad (4)$$

$$I(i) = \{n : f_{low}(i) < f(n) \leq f_{high}(i)\}$$

where i, t, n are indexes, CB is a matrix containing the power within the i -th criticalband at a specific time interval t .

With the patients, changes in sounds articulation are visible (precisely, transition into another sound during realization). It is both audible and detectable through spectrum comparison. These changes were particularly observable for the following consonants, for which the occurring change has also been indicated:

- [k] \rightarrow [a] / [k] \rightarrow [y]
- [g] \rightarrow [y] / [g] \rightarrow [e]
- [s] \rightarrow [y]
- [h] \rightarrow [a]

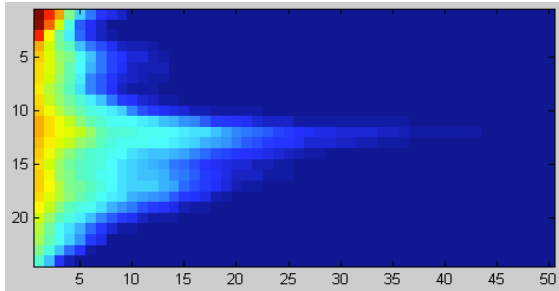


Fig.2a. Voice signal [k] without changes

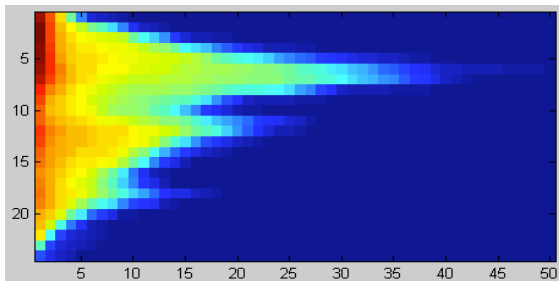


Fig.2b. Voice signal [k] with changes [k] \rightarrow [a]

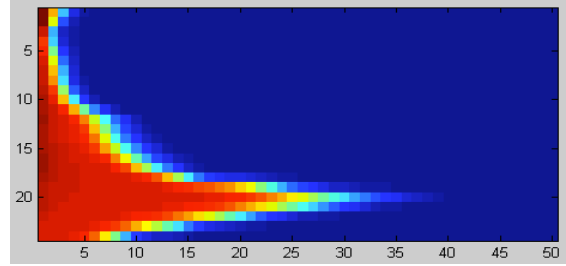


Fig.3a. Voice signal [s] without changes

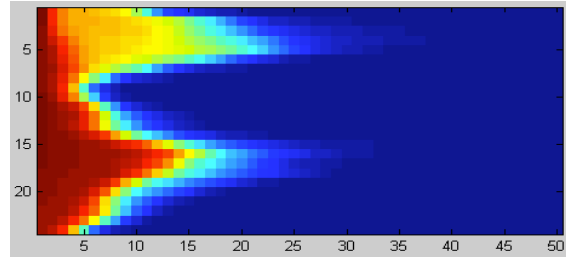


Fig.3b. Voice signal [s] with changes [s] \rightarrow [y]

Each piece of voice is represented by CB matrix. Firstly, the information represented each group of people was combined using median method. The median proved to be the simplest approach with a comparable quality to other more complex methods. Classification was done using simple distance comparison between CB matrixes. This distance can be used as another voice characterization parameter.

Ther result of this distortion is caused by the weakening of the elasticity of the larynx muscles, that is why a consonant is followed by a vowel, which does not require as much tension.

V.2. Intensity of sounds pronounced many times in isolation

The patients were asked to repeat the same plosive four or more times. The request was based on the knowledge that during the realization of a sequence of the same sounds, sound sequence distortions could be expected and slurring could occur. By analysing the duration and intensity of consecutive sounds, it was noticed with most of the patients that the intensity of the last sounds was respectively lower than the intensity of the first sound. This is due to muscle stiffness, characteristic for Parkinson disease. These symptoms were not observed with most of the members of the control group.

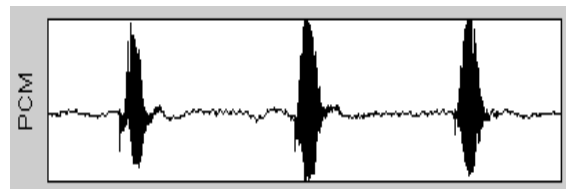


Fig.4a. Last 3 sounds of the healthy person, [p]

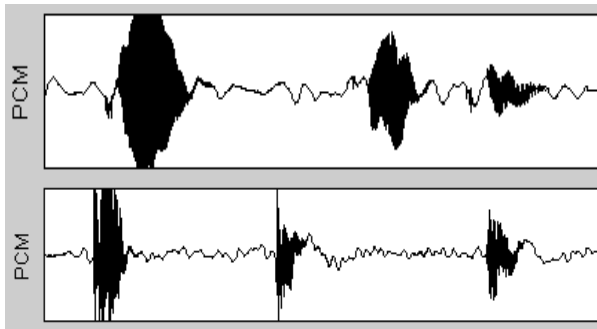


Fig.4b. Last 3 sounds of patients with neurodegenerative diseases.

V.3. Continuous sound analysis

The patients were asked to pronounce the tested sounds [a], [e], [i], [s] or [x] on one breath. The sound emitted for a long period of time allowed for spectral analysis aiming at observing the transition of frequency changes related to pathological trembling. The values received were compared with the values obtained in the control group. With some patients, a slight difference in the voice spectrum in the range between 4-8 [Hz] was observed. This range is characteristic for Parkinson disease tremor. However, at this stage of the study, the results are not reliable enough and require further work, in order for this element to be another voice characterization parameter.

With many patients, distinct and varying breaks in phonation were observed. With healthy persons, gradual quietening took occurred, whereas the patients ended the emission abruptly.

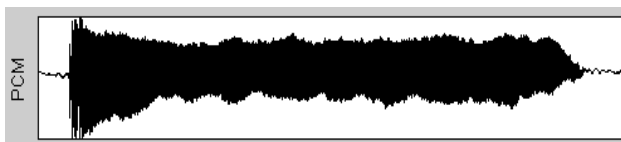


Fig.5a. PCM of healthy person, continuous [a]

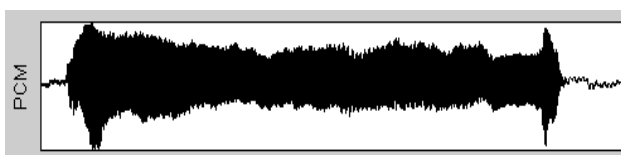


Fig.5b. PCM of person with neurodegenerative diseases.

The authors analyse differences within the range of realization of vowels at different heights.

6. CONCLUSION

The results presented here constitute the beginning of tests concentrated on automatic voice classification. The authors referred both to the question of duration parameterization as well as voice spectrum parameterization. The main goal set for the future studies

is such defining of descriptors, which together with particular search algorithms will enable proper interpretation of a patient's voice changes. The proposition of recording, processing and analysis of speech as a digital signal is also presented.

Further analysis of the isolated sounds is planned, compared in realization between the patients and healthy persons, taking sex, age and phrase analysis into consideration. With patients the dynamics of disease progression is also registered.

Moreover, some linguistic material on the level of phrases was recorded and a technical analysis is being prepared. In this study, the prosodic elements of speech – rhythm, pace, intonation, accent and melody will be analysed. The elements mentioned above are available in subjective diagnostic (defining the type of dysarthria). The authors wish to examine the characterization of changes in speech unavailable in subjective examination as well as to create a complex model of automatic classification. In order to achieve this, the newest methods of signal recording, processing and analysis will be implemented.

BIBLIOGRAPHY

- [1] P. Duus: *Neurologisch-Topische Diagnostik*, Stuttgart, 1983.
- [2] D. F. Johns: *Clinical management of neurogenic communicative disorders*, Boston, College Hill, 1985
- [3] F. Darley, A. Aronson, J. Bron: Cluster of deviant speech dimension in the dysarthrias, *Journal of Speech and Hearing Research*, 12, pp. 462-496, 1969
- [4] L. Ramig, S. Sapir, S. Countryman: Intensive voice treatment (LSVT®) for patients with Parkinson's disease: a 2 year follow up., *J Neurol Neurosurg Psychiatry*, 7, 1, pp.439 – 498, 2001
- [5] H. Wróbel: *Gramatyka współczesnego języka polskiego - Fonetyka i fonologia*, Kraków, PAN, 1995 (in Polish).
- [6] A. Prusiewicz: *Foniatryka kliniczna*, PZWL, Warszawa, 1992 (in Polish).
- [7] A. Izvorski, R. Tadeusiewicz: Artificial Intelligence Methods in Diagnostics of the Pathological Speech Signals, in: *Speech and Language Technology*, vol. 6, PPA, Poznań, pp. 183 – 197, 2002
- [8] E. Pampalk: *Islands of Music, Analysis, Organization, and Visualization of Music Archives*, Technischen Universität Wien, 2001.
- [9] A. Ralston: *A first course in numerical analysis*, New York, 1965.
- [10] T. Körner: *Fourier Analysis*, England, Cambridge University Press, 1988.
- [11] D. C. Hanselman, B. L. Littlefield: *Mastering MATLAB 7*, 2004

NEWBORN'S CRY FROM RISK AND NORMAL PREGNANCIES

Mirjana Sovilj, Tatjana Adamovic, Misko Subotic, Nikoleta Stevovic

Institute for Experimental Phonetics and Speech Pathology, Belgrade, Serbia and Montenegro

Abstract. Previous researches of the prelingual period indicated that primal cry and the first cry represent the inception of verbal communication.

The aim of this work was to study qualitative characteristics of crying of newborns from risk pregnancies and newborns from regular pregnancies in the function of prediction of verbal communication development.

The research was carried out on the sample of N=10 babies divided into two groups, aged 15 days. E group (N=5) comprised newborns from risk pregnancies, and C group (N=5) comprised newborns from normal pregnancies. Crying in the examined sample was digitally recorded and spectrographically analyzed.

The research results point to the possibility that certain acoustic characteristics of crying can be used in the prediction of verbal communication development and that the researches in this area should be intensified and continued.

Key words: newborn's cry, verbal communication, prelingual period, spectrographic analysis

1. INTRODUCTION

Newborn's cry, as an elementary particle of the development of verbal communication, was the topic of numerous scientific researches aimed not only at broadening the knowledge of controlling the process of crying production and brain organization itself, but only at examining the possibilities of crying as a diagnostic-differential instrument.

The first baby's cry, as stated by Kostic (1991), appears as a spontaneous physiological reaction that does not depend on its communication with the social environment [2]. The same author thinks that, during the first two months of life, a newborn reacts to hunger, discomfort and pain by crying. Physiological needs of a child's organism are the means of sound expressed through crying and thus they lie in the basis of communication between a child and his parents (Kostic, 1980) [3].

Researches of Sovilj and Djokovic (1993) support the fact that the development of speech communication is commenced by the first cry. Proceeding from the standpoint that the first cry contains all acoustic elements of the speech acoustic structure: formant

forms, noise forms and combined formant-noise forms of acoustic structure, which are normally present in speech (Kostic, Stosic 1963) [4], Sovilj and Djokovic analyzed the first cry-(ing) from birth until the end of the first month, reaching the results that indicate the existence of phases in the development of cry-(ing), from the first cry to crying (30 days), which are significant not only for the monitoring of the development of hearing, and future speech and language, but also for the development of methodological procedure for early detection of speech and hearing impairment and speech habilitation of hearing impaired children, which is carried out from the first month, in the prelingual phase [6].

Sovilj (1995) [7] also emphasizes that the first day after birth global control connection between hearing and voice is established. On the basis of spectrographic analyses, Truby and Lind (1965) established three important types of crying: basic phonation cry, turbulent, dysphonic cry, and strongly expressed hyperphonation cry [9].

The most complete model for the production of these types of cries was developed by Golub (1980), separating crying production into subglottal, glottal and supraglottal production zone connecting muscle activity with each type of crying [1].

Proceeding from the assumption that crying of hearing impaired children differs from crying of their normally hearing peers, due to the lack of auditory feedback, Moller and Schonweiler (1997) reached the results that coincided indicating that crying of normally hearing babies differs from crying of those with profound hearing impairment. Main statistically significant differences were found in the distribution of energy in different frequency ranges, duration of crying, and some melodic parameters [5].

In this paper, which is a pilot research, crying was studied through the analysis of ranging of the movement of the basic laryngeal voice in newborns' crying as the carrier of the quantitative monitors of speech (QMS): intensity, frequency and duration. QMS are the carriers of suprasegment speech structure and their variation forms the matrix. In the later period of speech-language development, sounds, syllables, words and sentences, followed by the development of accents of words, accents of melodies and melody sentence are built into this matrix. Previous researches at the Institute

for Experimental Phonetics and Speech Pathology (Sovilj, 2002) as well as the results of foreign researchers, indicated that suprasegment structure of mother tongue develops as early as in the fetal period [8]. This fact points even more to the necessity and significance of researching the cry as a nucleus of verbal communication and finding ways of its use in early detection and diagnostics, i.e. early prediction of hearing, speech and language development.

2. AIM

The aim of this research was to study qualitative characteristics of crying of newborns from risk pregnancies and newborns from regular pregnancies in the function of prediction of verbal communication development.

3. METHODOLOGY

For the needs of spectrographic analysis of a newborn's cry, crying before nursing was digitally recorded in home conditions, on the 30th day after birth, because of the clear stabilization of the acoustic field of crying when a child has physiological needs, compared to the inception of vocalization, when a child is in homeostasis. The research was carried out on the sample of N=10 newborn babies, 15 days of age, divided into two groups. The experimental group (E) comprised N=5 newborns from risk pregnancies, and the control group (C) comprised N=5 newborns from normal pregnancies. Newborns from E group were born from the pregnancies with the risk of a miscarriage from 6-7 month. All newborns were born normally in the 9th month.

During the recording, we used the directed microphone that was positioned near newborn's mouth on the defined distance of 10 cm. The recording lasted for about 3 minutes, which was a sufficient time period for obtaining the repeated stable characteristics of crying. Digitalized recordings were transferred into COOL program, from which the trained researcher, by means of auditory control and visual control of the recording, selected the signal (cry) that occurred most frequently, and transferred it to PRATT program for spectrographic signal analysis. The recorded cry was digitalized by the speed of choice 22050 Hz, 16-bit resolution, and it was recorded on one channel (mono). Spectrographic analysis obtained: minimal, maximal and mean values and their standard deviations of duration (Du), intensity (I) and frequency (FFo) of basic laryngeal tone.

Besides crying, for the psychophysiological assessment of newborns we provided the data on body size at birth (body weight – BW and body length - BL).

The obtained data were statistically processed by the application of T-test significance of the differences between the examined groups.

4. RESULTS AND DISCUSSION

In order to obtain more reliable and objective indices of crying characteristic in the monitored groups, we proceeded from the fact that newborn's voice in the monitored period (15 days) is not connected with the control of the movement of speech organs meant for speech production, but solely with its general physiological state and needs.

In that sense, newborn's body was observed from the aspect of the complete resonatory and energy space, whose influence on the voice (crying) can be represented by longitudinal mass (LM), which represents the relation of BW and BL given in the formula

$$LM = \frac{BW}{BL}$$

Having on mind that constitution plays an important role in voice impostation, we normalized intensity and frequency values on crying duration and newborn's longitudinal mass.

Normalized IFo and FFo values were calculated according to the following mathematical formulas:

$$CIFo = \frac{x \text{ IFo}}{DU \cdot LM}$$

(average crying intensity)
(coefficient of crying intensity)

$$CIFo = \frac{x \text{ FFo}}{DU \cdot LM}$$

(average crying frequency)
(coefficient of crying intensity)

Intensity

Table 1 Crying intensity in E and C group

Statistical parameters				
	dB-min	dB-max	dB-average	dB-SD
Experimental group				
X	73.37	83.12	79.79	1.97
SD	4.87	3.90	5.45	0.95
Control group				
X	78.83	88.22	83.94	2.20
SD	7.26	2.03	5.39	1.60

Results of the movement of the laryngeal tone intensity in newborns' crying (Table 1) indicate that mean value of Fo intensity in C group is 83.94 dB, and 79.79 dB in E group, which indicates that newborns' crying from normal pregnancies (C group) is 5% more intense.

Average value of Fo minimal intensity in C group is (78.83 dB: 73,37 dB) 7% higher than in E group, whereas average value of maximal intensity of Fo crying in C group (88,22 dB: 83,12 dB) is 6.8% higher than in E group.

Frequency

Table 2 Frequency of Fo crying in E and C group

Statistical parameters	Average Fo frequency			
	Hz min	Hz max	Hz average	Hz SD
Experimental group				
X	245.26	500.99	369.17	71.18
SD	93.59	31.53	58.70	39.01
Control group				
X	223.50	498.08	361.80	75.69
SD	79.80	44.01	72.20	24.79

Table 2 presents the results of laryngeal voice frequency in newborns' crying. Mean value of FFO crying in C group is 361.80 Hz, and in E group it is 369.17 Hz, i.e. laryngeal voice of newborns' crying from risk pregnancies is 2% higher compared to newborns from regular pregnancies.

Average minimal value of frequency in C group is (223.50Hz : 245.26Hz) about 9% lower compared to E group.

Average value of maximal frequency in C group (498.08 Hz: 500.99 Hz), is about 0.6% lower compared to E group.

Duration

Table 3 Crying duration in E and C group

Statistical parameters	DU in group	
	E group	C group
X	1.08	1.70
SD	0.26	0.73

Results of laryngeal voice duration in newborns' crying (Table 5) in the examined sample, indicate that average duration of crying in C group is 1.7 sec, and in E group it is 1.08 sec. i.e. that crying of newborns from normal pregnancies is 36.5% longer.

The analysis of average BW values (Table 4) indicated that newborns from C group had 19% higher BW compared to E group, but the differences between the groups are not statistically significant.

Table 4 Body weight in E and C group

Statistical parameters	BW	
	E group	C group
X	2790	3440
SD	803	305

Table 5 Body length in E and C group

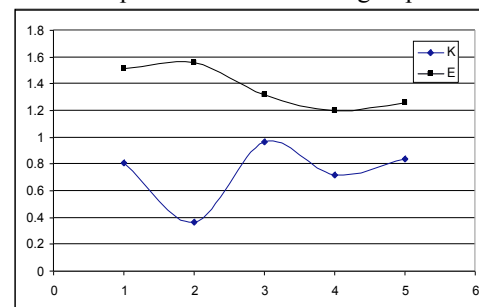
Statistical parameters	BL	
	E group	C group
X	48.00	51.40
SD	5.15	2.97

Results of the average value of BL (Table 5) indicate that newborns from C group had about 7% greater BL compared to E group.

Table 6 C-IFo E and C group

T-Test	C-FFo C and E group	
	C group	E group
X	3.375906279	6.508190577
df	4	
Tab. test	-5.574036129	
p(T<=t)	0.002538411	
critical	2.131846486	

Graph 1 C IFo in E and C group



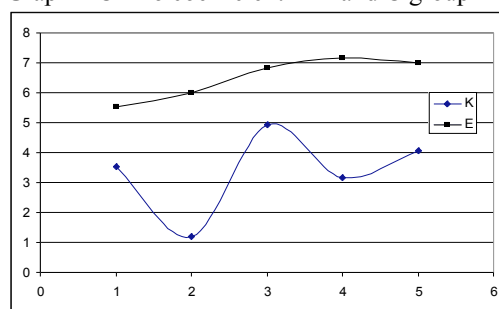
Data in Table 6 and Graph 1 indicate that C-IFo average value in E group is 1.373, and in C group 0.741. Comparing mean C-IFo values in E and C group, we obtained statistically highly significant difference on the level $p = 0.007$, which indicates that this coefficient can be a reliable parameter for assessment of newborns' crying characteristics and further researches, on a larger sample, will enable their use not only for the early detection of difficulties in speech and language development, but also for the assessment of the general psychophysiological development.

Results in Table 7 and Graph 2 indicate that average value C-FFo in E group is 6,508, and in C group 3,375. Comparing mean values of C-FFo E and C group, we obtained statistically highly significant difference on the level $p = 0,002$, which indicates that this coefficient can be a reliable parametre in the assessment of newborns' crying characteristics, and further researches will enable their use not only for the early detection of difficulties in speech and language development, but also for the assessment of the general psychophysiological status of a newborn child.

Table 7 C-FFo in E and C group

T test C- Ifo E and C group		
	C group	E group
X	0.7417	1.3733
df	4	
Tab. -test	-4.1408	
p (T<=t)	0.0071	
critical	2.1318	

Graph 2 C-FFo coefficient in E and C group



On a more precise level, C-Ifo and C-FFo indicated the presence of regularities in the connection of three parametres: intensity of crying frequency, duration, and newborn's longitudinal mass i.e. their interdependence, as the expression of psychophysiological state of a child, which classifies them as rather precise measures for the prediction of speech development and psychophysiological status.

CONCLUSION

The results obtained in our research, when comparing the values of QMS parametres in newborns' crying on the 15th day after birth from E and C group, indicate the following:

- C-Ifo and C-FFo represent valid parametres for the assessment of newborn's crying characteristics

- when the characteristics and tendencies of the characteristics of laryngeal voice in newborns' crying are perceived globally, it is noted that crying of newborns from normal pregnancies (C group) has the tendency of: larger intensity, lower tone and longer duration compared to crying of newborns from risk pregnancies, whose crying, according to the movement of QMS, can be characterized as crying of the shorter expiratory fork, hypotonic and hypertensive.

- the obtained tendencies of crying characteristics indicate that newborn's crying can be relevant parametre for the prediction of not only speech and language development, but also of the psychophysiological status of a newborn child.

Further researches, on a larger sample, will enable defining of limit values of coefficients for population of newborns from normal and risk pregnancies.

This research was financed by the Ministry of Science and Environment Protection of the republic of Serbia, within the project of basic researches, N^o 1784.

LITERATURE

- [1] Golub H. L. (1980): A physioacoustic model of the infant cry and its use for medical diagnosis and prognosis, Thesis, Massachusetts Institute of Technology, Boston.
- [2] Kostic Dj. (1991): Cooing and Babbling, Notes and discussion, No 2, IEPSP, Belgrade.
- [3] Kostic Dj. (1980): Speech and the Hearing Impaired Children, Indian Statistical Institute, Calcutta.
- [4] Kostic Dj., Stosic M. (1963): Acoustic Structure of a Newborn's Cry, IEPSP, Belgrade.
- [5] Moller S., Schonweiler R. (1997): Analysis of Infant Cries for the Early Detection of Hearing Impairment, in: Proc. 5th European Conf. on Speech Communication and Technology (Eurospeech '97), Europ. Speech Com. Ass. ESCA, GR-Rhodes.
- [6] Sovilj M., Djokovic S. (1993): Development of Newborn's Cry(-ing) from Birth Until the end of the First Month, Defectological theory and practice, Belgrade.
- [7] Sovilj M. (1995): The Development of New-born Infant's Cry(-ing) from Birth Until the End of the First Month, European Decade of the Brain, Amsterdam, 1995.
- [8] Sovilj M. (2002): Children's Speech – Quantitative Monitors of Speech, *Zaduzbina Andrejevic*, Belgrade.
- [9] Truby, H. M., Lind, L. (1965): Newborn Infant Cry, Almqvist & Wiksells, Uppsala.

COMPLEXITY ANALYSIS OF NORMAL AND DEAF INFANT CRY ACOUSTIC WAVES

Kathiresan Manickam, Haizhou Li,

Institute of Infocomm Research (I²R), 21 Heng Mui Keng Terrace, Singapore 119613

Abstract: This work describes the complexity found in the normal and the deaf crying acoustic waves. Using approximate entropy, in a single figure, the complexity of the auto-covariance of the signal is computed. Thus, using this complexity value, we are able to discriminate the normal and the deaf infants crying domains with ($P < 0.01$).

Keywords: Infant Cry, Complexity, deaf infant

1. INTRODUCTION

The infant crying waves, seemingly chaotic, carry useful and nevertheless essential information to establish its culture. Such entity vividly clarifies an infant's physiological anatomy and psychological condition. Physiological quantities from the laryngeal configuration, i.e. the length of the vocal tract, in return exemplify the resonance and formant effects. Psychologically, the infant's mental stamina correlates with the origins of a cry type. Modes of cries are unequivocally classified as normal, pathological, pain, hunger, etc. Hitherto, cry from a "normal" and "deaf" infant has been notably studied in literature [1]. Curiosity may result in the selection of the deaf population as the target group. Deaf infants cry exhibit contrasting acoustical characteristics compared to their rivals, the healthy infant population. Following investigation, it became apparent that the caseload for the deaf population is ever increasing in most institutions. It also came to light that both deaf and healthy infants commonly share attributes like pain or hunger cry. But, the hearing impaired infants acquired anatomical deficiency. Despite this setback, paediatricians have expressed that infant's cry is reciprocal to adult's speech.

Modes of infant's cry can be qualitatively characterised with commonly employed acoustics cues. Accordingly, normal crying features constitute of raising-falling pitch pattern, ascending-descending melody and high intensity seen from the spectrum [2-3]. Pathological infant crying correlate well with some normal infant's acoustics features. Spectral intensity will be lower than normal, rapid pitch shifts, generally glottal plosives, weak phonations and silences during the crying. Parameters, incorporating the pitch and formant descriptions, have been well utilised in the infant cry analysis up till now. Clement et al have substantiated that variations in the pitch

between hearing impaired and normal groups become meaningful from 8.5 months onwards [1]. In reality, this time gap is a result of lack of auditory feedback on the speech. Thus, evidence proves that a deaf group tends to voice louder since they want to hear themselves.

Pitch, a famously captured feature, aids in distinguishing cry types, as well as for a diagnostic tool, etc. La Gasse states, "The cry has enormous potential diagnostic". His quotation suggests that extremely high pitched cry indicates the pathological status of the infant which needs urgent medical attention [4]. A typical example is when infants exposed to drugs tend to have high pitch with variation at lower amplitude. The consequent effect of these drugs is the instability of the neural control of the vocal tract. Consequently, the vocal tract configuration determines the structure of the formant. Nevertheless, estimating the exact formant frequencies is complex [5]. A Fort et al has incorporated a parametric model using poles and zeros method to estimate fundamental frequency and formants from an infant cry, the conventional method involving the glottal pressure and tract configurations.

Regardless of these scientific features, experts in this field are able to distinguish the modes of cries. Garcia has mentioned that parents are specialists who were able to differentiate modes of cry solely using their instincts and comparing different types of cries [2-3]. However, uncertainty in the therapeutic service has brought irrefutable questions. A professional has quoted, "A deaf infant's characteristic varies from one another based on three factors: degree of loss; type and period of rehabilitation and the age of pathology identification". Consequently, concrete answers are unavailable scientifically (energy, pitch, duration, etc) regarding cry prosodic information which has forced us to lead this research in order to create an expert system to verify the cry status. The expert system should be able to analyse and classify modes of cry signals and probably, being realistic, at a later stage, diagnostic applications. Because the cry signals are noisy and evidences are showing their chaotic features, currently, analysing such signals itself has become problematic.

Deaf infants revealed more variations in their phonation using false vocal cords producing falsetto

waveforms [1]. Emergence of these irregular signals is the source for this paper. Since cry is an early form of adult speech, it is acceptable to use the conventional speech processing techniques to quantify these complex signals [6]. In this paper, our aim is to analyse if there is any complexity difference between the deaf and normal infant crying populations. Thus this initial step might help us in the diagnostic process.

II. CRY WAVE COMPLEXITY

Fig 1 below shows an example waveform of deaf and normal infant. Cry breaks and amplitude variations are often seen in the deaf infants. This propagates us to our initial comment regarding irregularity, chaos and complexity. Quantifying non-linear biological signals, due to their complex structure, require a reliable approach. Since we are aware of variability statistics like median, mean, standard deviation etc, it is observed that such methods are insufficient to quantify an erratic waveform. A suitable candidate, using regularity statistics, approximate entropy (ApEn), might rescue us from this problem [7]. One of our initial studies discriminates the phonation voice quality changes seen in healthy and radiotherapy larynx cancer patients using approximate entropy [8-9]. A segment from the waveform will be used as reference to identify a similar segment across the entire data.

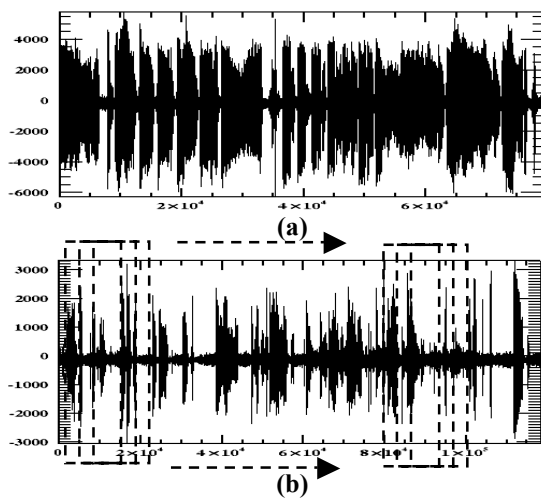


Figure 1
Infant Cry Waveform

(a): Normal Infant Cry Waveform

(b): Deaf Infant Cry Waveform

Abscissa: Time **Ordinate:** Amplitude

Because of the temporal sliding window across the desired signal of analysis, Fig 1 (dashed line); approximate entropy has a possible potential for characterising the complexity of a similar pattern. The complexity itself is expressed in a single featured Fig that branched to either a large value

(that means more complicated pattern) or a small value (with more determinable pattern). The single parameter is so robust that the detailed medical characteristics can be displayed in a simplistic scientific means. Investigating time domain signals requires suitable normalisation in order to compare across all individual infants.

Auto-covariance function of a frame, 1024 points, might ease this criterion. By doing this, white and other non-structured noises will result in low lags. Non-cry or cry breaks may produce low lag which is often seen in the deaf more than the normal infant as in Fig 1. However, alternating burst of cries and non-cries for the deaf groups will result in high complexity estimate. Low or zero lags will produce nil or low complexity. Fig 2 shows examples of auto-covariance signals for both disciplines (normal and deaf). More determinable features are normally observed from the healthy infant with a low complexity (0.148) as in Fig 2. A portion of the auto-covariance function is a classic example of the low complexity healthy infant's crying since it retains a sinusoidal waveform. Fig 3, demonstrates a typical example of deaf cry which earns a higher complexity estimate (0.719). The undeterminable irregular auto-covariance waveform is the cause for high computation.

III. COMPLEXITY ANALYSIS

The present corpus is a collection of infant crying samples, from early born up to 7 months. A total of 31 normal and 103 deaf infant cries were analysed in this research. Cry signals were recorded and sampled at 8 KHz. The data files were stored, visualised and analysed using software written in scientific language IDL from Research Systems. The recorded signal is divided into frames of 1024 data points each. To normalise the data frames, each frame was performed with auto-covariance function. Complexity value is calculated for each auto-covariance frame based on $N=1024$, $m=3$ and $r=0.2*\sigma$. Each frame produces a complexity value and these complexities do not always conform to a normal distribution. Subsequently, the median from the collection of the complexities was calculated and used for further analysis.

Fig 4 shows the distribution of the median complexity for an individual infant. The ratio of a normal infant below 0.6 and above 0.6 is nearly 5:1. A reversed scenario is echoed in the deaf population. The ratio of a deaf infant with below 0.6 to above 0.6 is nearly 1:4.

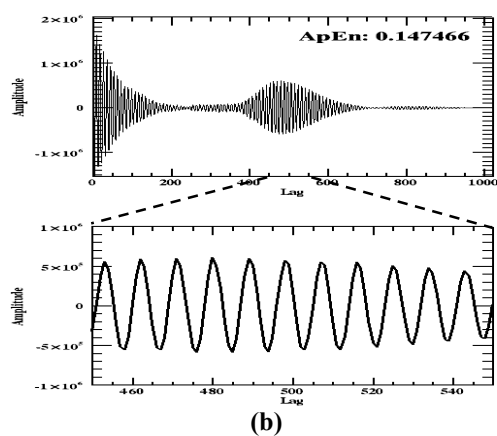
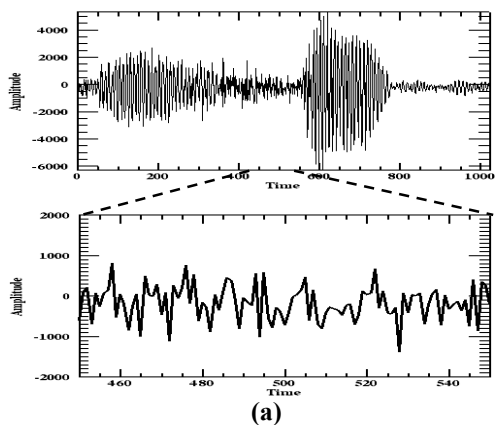


Figure 2
Normal Infant Cry Waveform

(a): Cry Waveform
(b): Auto-Covariance Cry Waveform
Top: Entire Frame Signal
Bottom: Portion of Frame Signal
Abscissa (a): Time **Abscissa (b):** Lag **Ordinate:** Amplitude

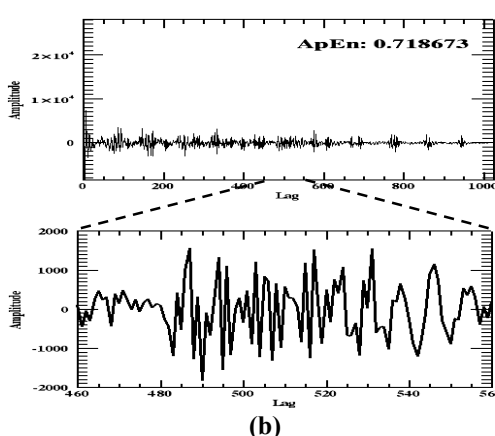
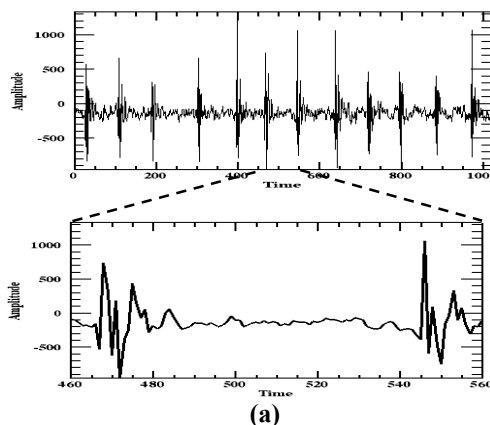


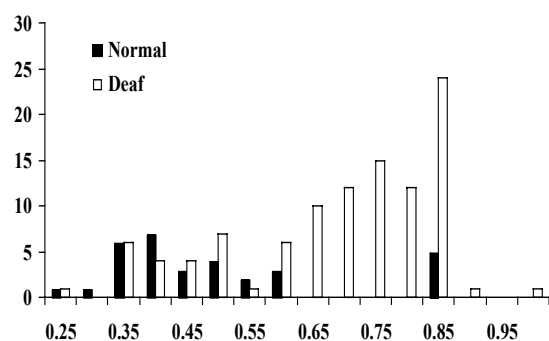
Figure 3
Deaf Infant Cry Waveform

(a): Cry Waveform
(b): Auto-Covariance Cry Waveform
Top: Entire Frame Signal
Bottom: Portion of Frame Signal
Abscissa (a): Time **Abscissa (b):** Lag **Ordinate:** Amplitude

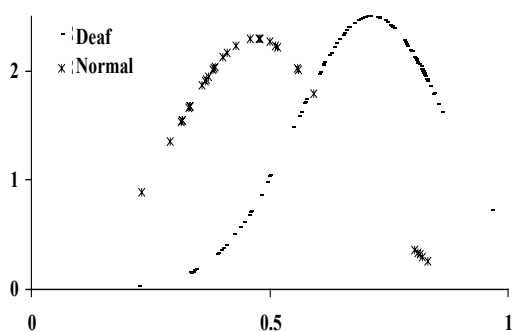
The distribution clearly shows a distinct separation between the deaf and normal infant population. Assuming that these two populations (deaf and normal) are independent, Wilcoxon Rank Sum Test showed that these two populations were indeed significantly different with ($P < 0.01$). Deafness is the most common of all forms of permanent damage following meningitis. Early detection and therapy might reduce the effect or severity following such disease.

IV. CONCLUSION

Despite successfully discriminating the normal and deaf infant crying modes using complexity analysis (approximate entropy), further research has to be carried out in order to reduce the over-lapping portion between the two domains. Nevertheless, this initial study on the infant cry wave analysis is encouraging but more features need to be incorporated like pitch, formant, and energy to enhance the findings.



(a)



(b)

Figure 4

(a): Histogram of Normal & Deaf Infant Cry Complexity

Abscissa: Median Complexity

Ordinate: Frequency of the Complexity

(b): Probability Density Function of Normal & Deaf Infant Cry Complexity

Abscissa: Median Complexity

Ordinate: Probability Density

REFERENCES

- [1] Clement, Chris J. / Koopmans-van Beinum, Florian J. / Pols, Louis C. W. (1996): "Acoustical characteristics of sound production of deaf and normally hearing infants", *ICSLP*, 1549-1552.
- [2] Jose Orozco Garcia and Carlos A Reyes Garcia, (2003) "Acoustic Features Analysis for Recognition of Normal and Hipoacusic Infant Cry Based on Neural Networks" Lecture Notes in Computer Science, 2687:615 – 622, ISSN: 0302-9743
- [3] Jose Orozco Garcia and Carlos A Reyes Garcia, (2003) "A Study on the Recognition of Patterns of Infant Cry for the Identification of Deafness in Just Born Babies with Neural Networks." 8th Iberoamerican Congress on Pattern Recognition, CIARP 2003, Havana, Cuba, 342-349, ISBN 3-540-20590.
- [4] Medical News Today: Babies cry linked to their neurological and medical status, 16 May 2005. www.medicalnewstoday.com
- [5] K Wermke, W Mende, C Manfredi, P Brusciaglioni, (2002) "Developmental aspects of infant's cry melody and formants", *Medical Engineering Physics* 24:501-514.
- [6] Qiabing Xie, Rabab K Ward and Charles A Laszlo, (1996) "Automatic Assessment of Infants' Levels-of-Distress from the Cry Signals", *IEEE Trans Speech and Audio Processing* 4:4:253-265.
- [7] Pincus S M, (2001), "Assessing Serial Irregularity and its Implications for Health", *Ann NY Acad Sci*, 954:245-267.
- [8] Moore C J, Manickam K, Willard T, Jones S, Slevin N, Shalet S, (2004) 'Spectral Pattern Complexity Analysis and the Quantification of Voice Normality in Healthy & Radiotherapy Patient Groups', *Medicine Engineering Physics*, 2004,26(4), 291:301
- [9] Manickam K, Moore C J, Willard T and Slevin N, 'Quantifying Aberrant Phonation Using Approximate Entropy in Electro- Laryngography' (*Journal of Speech Communications-In press Corrected Proof*)

most of them. By applying the proposed adaptive comb filter, followed by GSVD or OSV, voice quality results enhanced in most cases. The following figures are relative to one case (lancet operated). Each plot shows F_0 , noise and formants tracking, as obtained by means of the cited robust, adaptive, high-resolution tool, along with F_0 and noise mean values.

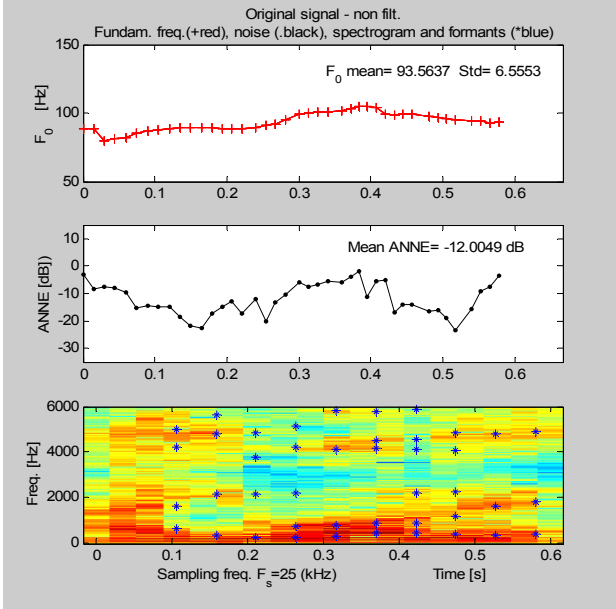


Figure 1 – Non-filtered signal: F_0 , noise and formant tracking (superimposed on the spectrogram). High noise level is found, also in the high-frequency region.

Specifically, fig.1 is relative to the non-filtered signal: F_0 is almost stable, but the harmonics noise level is high (around -12 dB). The spectrogram shows strong noise also in the high-frequency region.

Fig.2 concerns comb-filtered signal. It shows still stable F_0 , but harmonics noise is now lowered (from -12dB to about -18 dB). In the spectrogram, lower noise energy is shown also in the high-frequency spectral region.

Fig.3 refers to the signal filtered with comb and $GSVD_{fix}$. Harmonics noise is slightly raised (from -18 dB to about -14 dB), but the spectrogram evidences very low noise in the high frequency region.

Finally, fig.4 shows the results obtained for the signal filtered with comb and OSV with signal subspace as from eq.(7). Harmonics noise is lower than with GSVD (around -16.5 dB) and the spectrogram results comparable to the GSVD one. In all the figures (1)-(4) formant tracking is also reported, showing that the harmonics structure of the original signal is preserved with filtering.

The last fig.5 compares the values of PSD_{low} , PSD_{high} and QER for the applied denoising techniques, specifically comb, comb+ $GSVD_{fix}$, comb+OSV, relative to the non-filtered signal. Best results are obtained with comb+ $GSVD_{fix}$. As shown in the figure, comb alone performs only a slight enhancement, while

comb+ $GSVD_{fix}$ gives the best results with respect to other methods, with $PSD_{low} \cong 0dB$, $PSD_{high} \gg 0$, and $QER < 0$. Notice that previous results obtained with SVD_{fix} gave: Mean $F_0=97.8Hz$ with $std=28.6Hz$, mean ANNE=-11.1dB $PSD_{low}=-2.1$ dB, $PSD_{high}=16.5$ dB, $QER=3.1$ dB [3]. With comb + SVD, we obtained: Mean $F_0= 92.6$ with $std= 7.3$, mean ANNE=-16.5dB, $PSD_{low}=-1.8dB$, $PSD_{high}=17.2dB$, $QER=4.3$ dB.

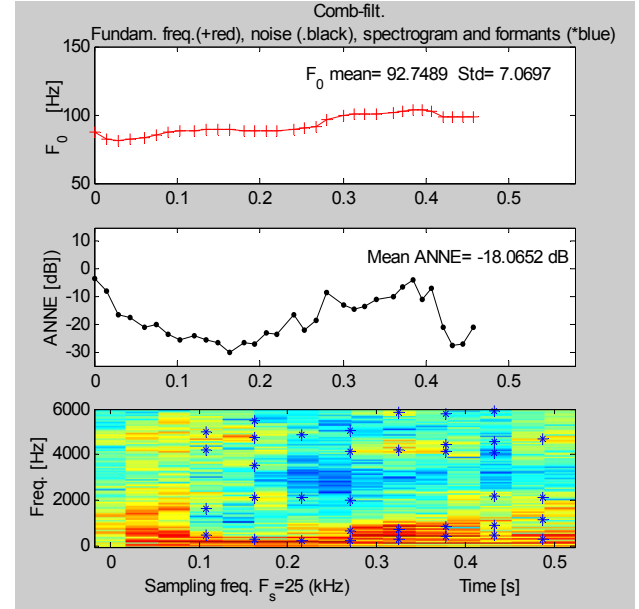


Figure 2 – Comb-filtered signal: F_0 , noise and formant tracking (superimposed on the spectrogram). Harmonics noise is lowered (from -12dB to about -18 dB).

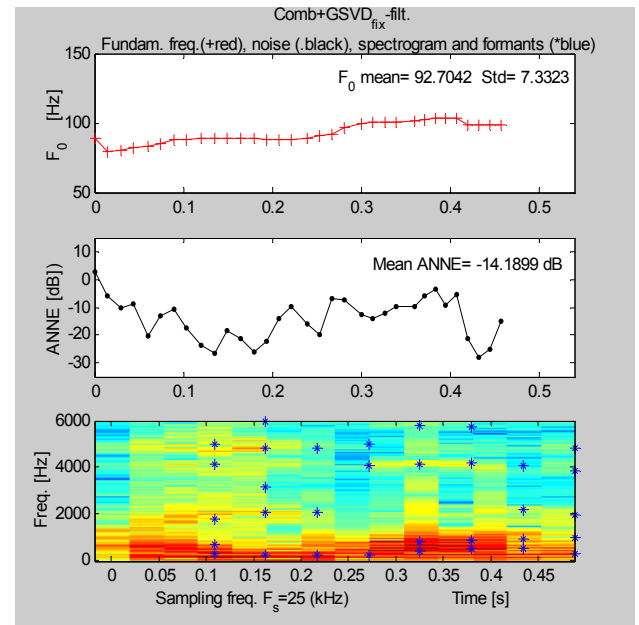


Figure 3 – Signal filtered with comb and $GSVD_{fix}$. F_0 , noise and formant tracking (superimposed on the spectrogram). The spectrogram evidences lowered noise in the high frequency region.

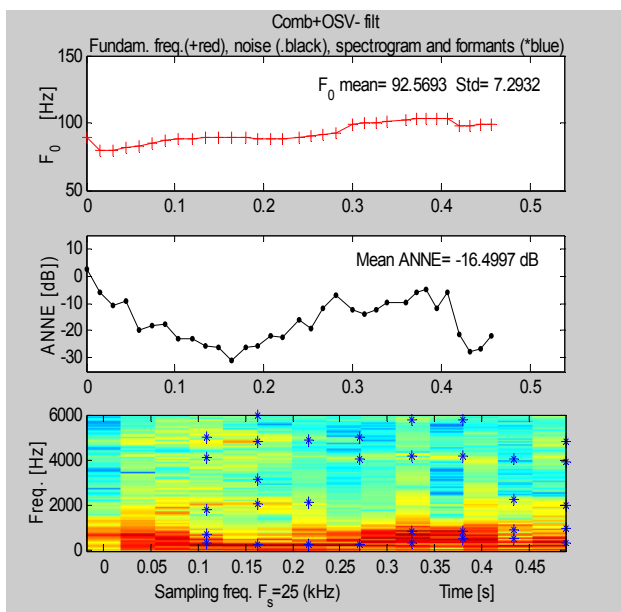


Figure 4 - Signal filtered with comb and OSV with signal subspace as from eq.(7): F_0 , noise and formant tracking (superimposed on the spectrogram). Spectrogram comparable to fig.3.

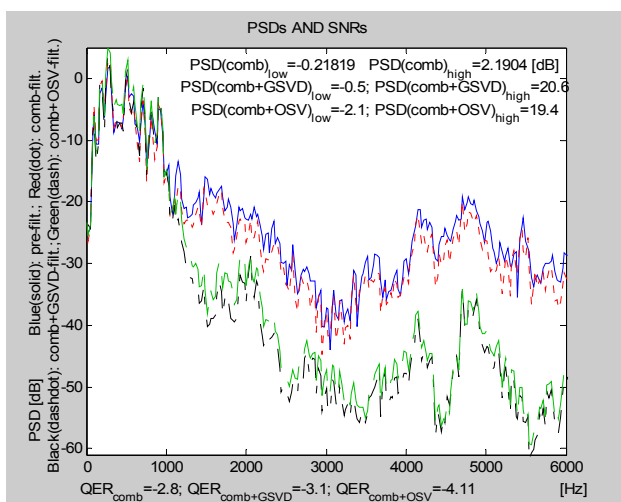


Figure 5 – Comparison among PSD and QER values obtained from eqs. (8)-(10) for comb, comb+GSVD_{fix}, comb+OSV, related to the non-filtered signal. Best results are obtained with comb+GSVD_{fix}.

This means that with SVD alone F_0 becomes more unstable and harmonics noise is increased. By pre-filtering with adaptive comb, results become comparable to comb+GSVD_{fix} and comb+OSV, although a little bit worse. Similar results were obtained over all the dysphonic voices data set.

IV. FINAL REMARKS

A hoarse voice denoising procedure is proposed, based on an optimised comb filtering and low-order GSVD decomposition of voice data matrices. An automatic tool

is provided, for robust pitch, noise and formant tracking. The whole procedure was found effective in increasing the quality of voice, as measured by few but effective objective indexes, while preserving the harmonic structure of the original signal. A perceptual comparison of results with GIRBAS scale will be available in the next future.

This tool could be of help both for clinicians, in order to follow patient's rehabilitation, after surgery or drug treatment, and for dysphonic subjects, for testing and enhancing their fluent speech quality by means of a simple and cheap mobile device. As a drawback, GSVD has a significant computational load, and for time being it is only used as an off-line algorithm. Recursive updating of GSVD, instead of re-computing it on each data window, would be desirable for real-time voice signal processing and is a topic of current research.

REFERENCES

- [1] Jensen S., Hansen P., Hansen S., Sorensen J., "Reduction of broad-band noise in speech by truncated QSVD", *IEEE Trans. on SAP*, vol.3, p.439-448, 1995.
- [2] Asano F, Hayamizu S, Yamada T, Nakamura S. Speech enhancement based on the subspace method. *IEEE Trans. Speech Audio Proc.* P.497-507, 2000.
- [3] Manfredi C., D'Aniello M., Brusciaglioni P., "A simple subspace approach for speech denoising", *Log. Phon. Vocol.*, vol.26, p.179-192, 2001.
- [4] Ephraim Y, Van Trees H L. "A signal subspace approach for speech enhancement". *IEEE Trans.Speech Audio Proc.*,1995; n.3, p.251-266.
- [5] Rao B D., Arun K S. "Model based processing of signals: a state space approach". *Proc. IEEE* n.80, p.283-309, 1992.
- [6] Ju G., Lee L., "Speech enhancement based on Generalised Singular Value Decomposition approach", *Proc.ICSLP 2002*, p.1801-1804, 2002.
- [7] Manfredi C. Adaptive noise energy estimation in pathological speech signals. *IEEE Trans. Biomed. Eng.* 2000; 47: 1538-1542.
- [8] Lim J.S., Oppenheim A.V., Braida L.D., "Evaluation of an adaptive comb filtering method for enhancing speech degraded by white noise addition", *IEEE Trans. Acoust.,Speech,Signal Proc.*, n.4, p.354-358, 1978.
- [9] Deller J R, Proakis J G, Hansen J H L. *Discrete-time Processing of Speech Signals*. New York: Maxwell McMillan, 1993.
- [10] Manfredi C., Peretti G., "A new insight into post-surgical objective voice quality evaluation. Application to thyroplastic medialisation", *IEEE Trans. Biom.Eng.*, 2005 (to appear).
- [11] Hu Y., Loizou P.C., "A generalised subspace approach for enhancing speech corrupted by coloured noise", *IEEE Trans. Speech Audio Proc.*, vol.11, p.334-341, 2003.

Special session on
Methods for voice measurements

CLINICAL VOICE MEASUREMENT USING EGG/LX SIGNALS 4TH INTERNATIONAL MAVEBA WORKSHOP

Adrian Fourcin^{1 2}

¹Department of Phonetics & Linguistics, University College London, UK, fourcin@btinternet.com

²Laryngograph Ltd. www.laryngograph.com

Abstract

Nearly fifty years ago, Philippe Fabre[1] initiated a method for the non-invasive electrical measurement of vocal fold vibration that is now known generically as “electro-glottography” — egg. The name has arisen from the initial misinterpretation of the waveform, but the technique itself has now come into widespread daily use in the voice clinic, although for vocal fold contact rather than glottal opening measurements. The present extremely brief discussion is concerned with three particular aspects of the ways in which the approach can be usefully linked to basic aspects of voice perception and production — the psychophonic use of the data in the measurement of sustained vowels and connected speech production; the use of these criteria in “pitch” based quantitative assessments; and the application of the technique in vocal fold closed phase duration appraisal. Particular attention is given to pathological voice analysis.

I. INTRODUCTION

The use of non-invasive electrical sensing, during fluent speech production, of vocal fold contact has especial research and clinical advantage in the definition of:

- contact closure epoch
- instantaneous period & intra period irregularity
- peak acoustic excitation
- closure duration value and variability
- precision stroboscopic trigger instants.

The approach also makes it feasible to link objective measurement to pitch perceptual processing.

II. METHODOLOGY

Using pitch perception to guide voice measurement

For most practical purposes the really important aspects of voice are those that can be heard, and the dominant dimension in hearing voice is pitch. This simple concept leads to the possibility of using some simple quantitative criteria to detect and quantify the differences between “good” and “bad” voices.

Classically, pure tones provide a basic reference for both the definition and perceptual investigation of pitch. Subjective psychophysical data have been stably established over many years. Maximum discriminability is reached between 1 kHz, C6, near the top of the soprano register, and 2kHz with an average best just noticeable difference, jnd, of about 0.7% at 200Hz and 0.4% or 4 Hz in the region of 1kHz with individual jnd sensitivities going down to 0.1% [2]. Auditory pitch detection for the frequency ranges of the speaking and singing voice appear to employ mechanisms which operate on the basis of temporal processing [2]. This level of pitch discrimination implies an average ability to detect temporal differences between successive periods of about 4 μ s, and for some individuals, 1 μ s. This temporal signal processing ability for pitch perception is

paralleled in auditory lateralisation where interaural time differences of about 2 μ s to 10 μ s are detectable.

For steady complex tones and vowels in the fundamental frequency range of conversational speech, the pitch discrimination jnds are even smaller than those obtained with pure tones. Wier and Moore [2], within the range 200 to 600 Hz, reported jnd values from about 0.15% to 0.3%. For vowel-like sounds with simple changing fundamental frequency contours, however, the ability to perceive differences in fundamental frequency is drastically reduced and the jnd may be 8% at about 100 Hz. This increase in, and magnitude of, jnd has also been found for whole word utterances with simple intonation contours, the jnd here never being less than 6%. When more complex contours are used, the differences needed to achieve reliable detection may be as great as 20%. The subjective results for these stimulus types are not as well established as for sustained sounds and there is a dependence on the duration of the tone. There is, however, a good working consensus between a large number of reported observations [t'Hart, 2]. These established observations give clear implications in respect of the accuracy criteria which should be aimed at for the analysis of the separate categories of sustained sounds and connected speech.

A basic set of tools for accurate voice pitch measurement

Tool 1

Most methods of voice pitch analysis depend on the use of the acoustic signal of speech sampled at low rates which do not correspond to the requirements imposed by the pitch dL performance of the ear. The essential need which has to be met is best defined by an example taken from the singing voice. At a voice frequency of 1000Hz in the soprano range the human ear can detect changes of

around 0.1% [2]. In order to do as well as this, but for only a single cycle, it is necessary to use a sampling frequency of 1MHz. This is what is done for the following measurements.

Tool 2

A second basic problem associated with conventional approaches to voice analysis comes from the inadequacy of pitch extraction algorithms based on the acoustic signal. A more reliable technique is to use the electrolyngographic [Lx, positive peak corresponding to maximum closure] output from the speaker's voice activity. This gives the basis for an accurate determination of each individual pitch period, Tx, that can be sampled at 1MHz to support measurements which, although very highly detailed for many purposes, are linked to the best that the ear can do and that provide for considerable flexibility in the choice of bin widths in analysis and graphical displays.

It is, of course, quite easy to deal with sustained sounds but the method must also be reasonably robust when applied to the rapidly changing waveform of running speech. An output for a practical system is shown below.

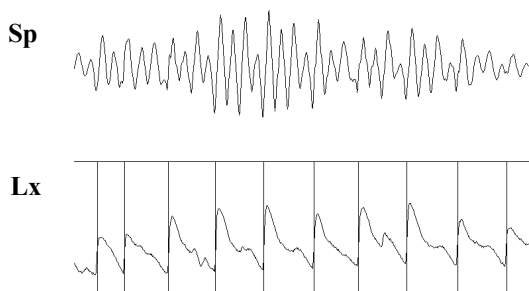


Figure 1 acoustic, Sp, and electrolyngograph, Lx, waveforms for a sample of pathological speech with automatically detected closure markers (55ms duration)

The figure shows the process of marker generation used for the definition of Tx for a pathological voice sample; the excerpt is from a sample of fluent speech. The speech acoustic waveform, Sp above, illustrates the difficulty of cycle definition if only acoustic data is available.

The use of period by period sampling gives a very clear view of the difficulties that may be encountered by a speaker with a voice disability and shows the remarkable precision of normal voice pitch control. This type of precision data analysis is also basic to the provision of measurements both for sustained sounds and for the analysis of running speech.

The current clinical techniques for the quantification of voice abnormality depend to an appreciable extent on the use of sustained sounds and the standard protocol uses the steady state in the centre of the sample. Period by

period analysis gives a clear indication of the onset and offset transients which this approach misses. The pathological speaker in general has difficulty in producing smooth voice onset and offset. This is clearly seen initially, where diplophonic breaks in the voice precede more steady production, and in the voice breaks at the end. As must be expected, perception leads production but it is striking and commonly observed, that the pathological voice does not have a jitter commensurate with the disability. This small difference results partly from the choice of the centre interval of a sound sustained at a comfortable pitch – and partly from the speaker's auditory monitoring ability for sustained sounds, and phonatory choice of a dominant mode.

III RESULTS & DISCUSSION

Connected speech and sustained vowels

For the majority of the population, speech communication is at the heart of our daily lives. Clinical voice measurement, however, is mostly directed towards the appraisal of the ability to produce a sustained vowel. Since there are quite substantial perceptual differences between our ability to hear pitch regularity in sustained vowel sounds as opposed to fluent speech, it would be of interest to make at least an initial appraisal of the ways in which perception and production may interact in the voice pitch structures of the two types of phonatory activity. There may additionally be an advantage in comparing pitch regularity inspired analyses based on the two types of spoken material simply with a view to contributing to filling the gap between clinical indices of severity of dysphonia based on vowel measurement and those using a perceptual evaluation of continuous speech. Most important of all, however, is both to make use of pitch criteria and to take account of the nature of pitched sounds. Regular repetition of an acoustic event and perceived pitch go hand in hand.

Analyses of ordinary running speech

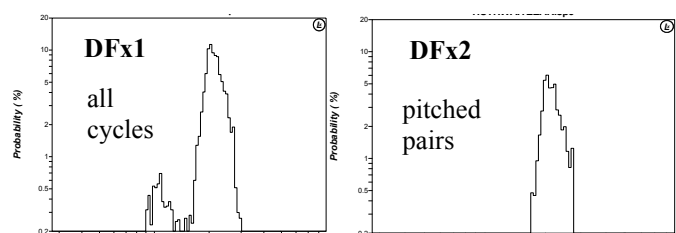


Figure 2 Vocal fold frequency, Fx, distributions for a 2m sample of pathological connected speech — speaker B

The two distributions in Fig 2 are very dissimilar. DFx1, on the left, shows the distribution of Fx values for every vocal fold period in the whole 2m. sample. DFx2 shows only those Fx values for which two successive periods

have been essentially the same. Two modes of vocal fold vibration are shown. The main at about 200 Hz is well defined. At about an octave below, the lower mode is more diffuse and is evidently associated with considerable period to period irregularity since the values of DFx1 and DFx2 are so different. Different pathologies give rise to different types of modal structural differences but for most cases the presence of voice pathology will be associated with marked discrepancies in magnitude and shape between these two forms of representation.

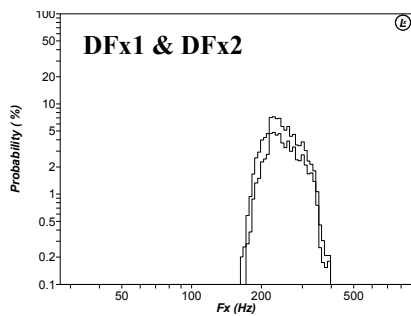


Figure 3 Overlaid Fx distributions for a normal sample (speaker A) AND for its “pitched” components

The use of accurate period by period information makes it easy to plot the occasions when two successive pitch periods have essentially the same value. For the normal voice this happens very often indeed. The pathological voice, however, is very easily identified by the ear as having period to period irregularity. This important feature is shown in the inner of the two distributions above in Figure 3. The two distributions together give an immediate insight into important aspects of voice quality – pitch height and range, modal structure, and regularity. These first and second order distributions are especially useful in general in pathological voice analysis.

Jitter and irregularity in connected speech

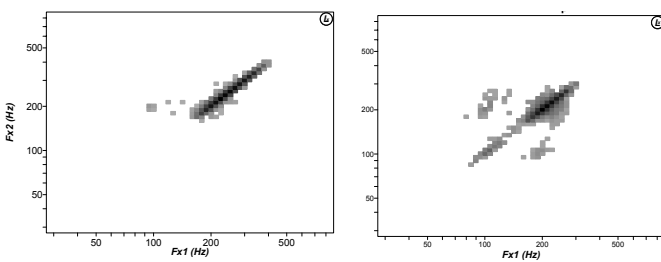


Figure 4 Vocal fold period crossplots, Cfx speaker A on the left, B on the right

Jitter and intonation

The procedure basic to the ordinary application of the jitter criterion is applied only to sustained sounds and requires that the voiced sound being measured is held at as constant a pitch as possible by the speaker. The

essential concept, however, is directed at obtaining a quantitative assessment of pitch variability. The idea is just as applicable to ordinary connected speech so as to get an appraisal of the irregularity which may be inherent to the social use of a pathological voice.

An obvious first approach to the measurement of pitch irregularity in a sample of running speech is to determine the standard deviation of the spread of cycle to cycle differences in regard to periods or frequencies. A difficulty with this approach is that it will necessarily include ordinary intonational variations as part of the estimate of irregularity. The problem is perhaps best illustrated with reference to actual data. When vocal fold vibration is essentially regularly periodic the use of a period by period crossplot, as in Figure 4 A, gives a clearly defined diagonal line – since successive periods have almost the same values, apart from the variations arising from the intonational frequency related changes of connected speech. For the pathological voice, however, the shape of the crossplot is not so simply defined because successive vocal fold periods are very often markedly different and are not totally under the speaker’s cognitive control. This method of plotting the range of variability in period to period coherence is effectively similar to the application of the jitter criterion, used for sustained sounds, to the whole of a connected speech sample.

The interpretation of jitter in running speech, however, is not at all the same as that for sustained sounds. First, the pitch dLs are quite different in the two cases. The bin sizes needed for the adequate representation of significant changes in the present data involves 6% steps. The 0.1% resolution required for the analysis of sustained sounds is not appropriate. Second, the presence of intonational changes makes it necessary to ignore variations which are part of the normal patterning of vocal fold frequency change in running speech. Figure 4 A shows that there is indeed a centre continuous core of variation for the whole of the vocal fold frequency range and this is found for all normal speakers.

If the pitch difference limen value of 6% is applied to this data then it becomes possible to apply a theoretically founded criterion which makes it feasible in practice to separate the variability arising from intonation from that due to other causes. It is then only necessary to determine all the pitch deviations which are more than 6% away from the centre line in the graph showing Fx1 against Fx2 – where Fx1 is the frequency value of the first vocal fold cycle in any pair of cycles in the whole utterance and Fx2 is the frequency value of the immediately following cycle of the pair. Fx is used to denote the frequency value of a single vocal fold cycle,

the period of this cycle being measured from point of closure to point of closure.

Normal and pathological voice examples

The comparison of Figure 4A with 4B shows how the relatively small jitter differences sustained sounds from these speakers, of .3% & .8%, is related to quite marked structural changes in their samples of connected speech. In these particular instances, irregularity is 3.2% for the normal speaker and 14.7% for pathological speaker B. Both values were measured in the way described above as a percentage of the number of vocal fold periods, outside the centre core of intonation-dependent pitch change, relative to the total number of vocal fold periods in the whole spoken sample.

Loudness and Quality

Connected speech phonetogram

The standard phonetogram was designed to provide an overview of the dynamic range of a singer's voice and was based on the separate production of sustained sounds. The same principle can be applied to the analysis of the speaking voice to give first and second order "Dynamic Phonetogram" derived from the amplitude-frequency analyses of a complete sample of connected speech (also called Speech Range Profile).

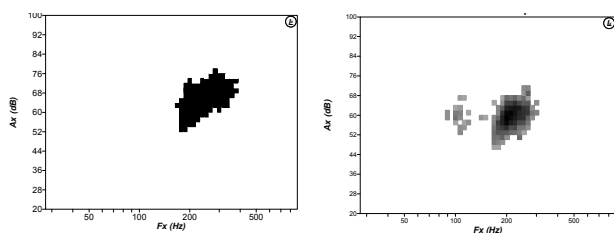


Figure 5 Second Order Dynamic Phonetograms derived from 2m. samples of connected speech:

normal speaker A, left; abnormal voice speaker, right

In both Figure 5A and B, only the second order distributions are shown. This has little effect on the presentation for speaker A; it does have a profound influence on the form and range of the data presentation for speaker B since the presence of a bimodal peak in loudness is very evident in the first order distribution but not in the "pitch" related second order plot.

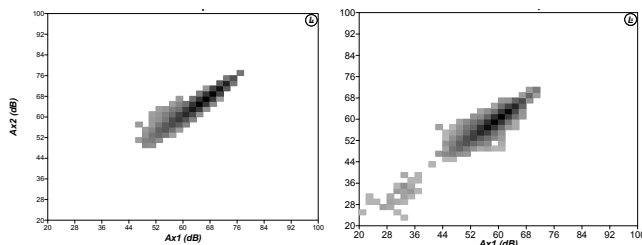


Figure 6 Period by period amplitude crossplots – CAx

A factor contributing to our perception of hoarseness comes from the irregularity of successive amplitude peaks in the cycle to cycle excitation of the vocal tract.

This is especially evident in connected speech and speaker A on the left, Fig. 6, has a smaller spread in these analyses than B. Using a similar measure of irregularity to that employed for CFx gives values respectively of 3.3% and 6.5%.

IV IN CONCLUSION

Voice quality, "closed" phase and pitch

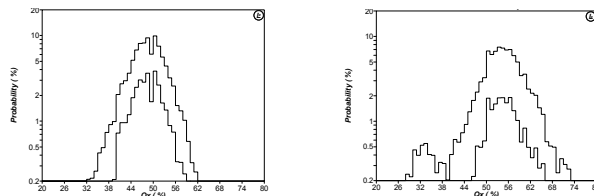


Figure 7 DQx 1&2 – distributions of first and second order "closed phase" as a function of vocal fold frequency, Fx

Voice quality is a complex attribute of voice but one important additional aspect comes from the regularity and duration of the closed phase from vocal fold cycle to cycle. First and second order plots can often give important information in regard to the physical nature of a pathological voice, in Fig 7 it is evident that speaker B has poor closed phase coherence, and range.

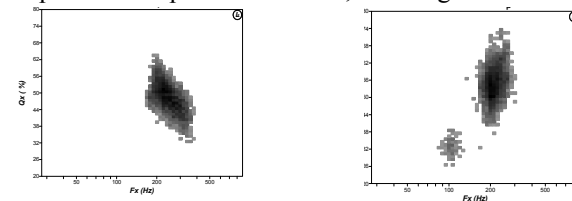


Figure 8 "Closed phase" ratio Qx as a function of vocal fold frequency – A left, B right

The pathological voice, B Fig 8, is substantially deviant and gives a range of Qx [the closed phase measure based on trans-glottal conductance] which is never found in the normal voice and relates to the irregularity as a function of pitch which can be clearly heard in her speaking voice. More generally, the Lx waveform can provide a sensitive basis for analysis that can be used effectively from the operatic voice to more extreme conditions [3].

I would like to acknowledge the great help received from Julian McGlashan FRCS and Dr Evelyn Abberton.

REFERENCES

[1] P.Fabre, "Un procédé électrique percutané d'inscription de l'accolement glottique au cours de la phonation Bull. Acad. Méd, 1957, pp.66-70
 [2] please see "Measuring Voice in the Clinic", www.laryngograph.com for reference list
 [3] A.Fourcin, "Precision Stroboscopy, Voice Quality and Electrolaryngography", in Ch 13 Voice Quality Measurement ed RD Kent & MJ Ball, 2000

FROM VOCAL QUALITY MEASUREMENT TO PERCEPTION

Rahul Shrivastav

rahul@csd.ufl.edu

Department of Communication Science & Disorders, University of Florida, Gainesville

Abstract: Quantification of vocal quality of a speech signal is essential in a number of applications. However, existing measures for this purpose are often characterized by poor sensitivity and specificity to perceptual judgments. These shortcomings may have arisen because (1) these measures are often validated against “noisy” perceptual data and (2) the non-linear and multidimensional relationships between the physical signal and perceptual judgments have often been ignored. This paper describes the psychometric principles underlying quantification of subjective judgments and the use of an auditory processing model as a signal processing front-end when measuring “breathy” voice quality. Preliminary data for quantification of “roughness” is also discussed.

INTRODUCTION

The speech signal is rich in information and conveys a large amount of information to a listener. For example, apart from the meaning contained in the utterance, the speech signal conveys such information as emotions, speaker identity, age and gender. A number of applications require accurate quantification of such perceptual attributes of a speech signal. In the clinical domain, one may need to quantify aspects such as speech intelligibility, voice quality, nasality, etc. These attributes are important because these are often affected by disease and are frequently the target of surgical, pharmacological or behavioral treatment. Precise quantification of these attributes can enhance the assessment and rehabilitation procedures by providing a baseline against which any change can be measured.

Various techniques to quantify these perceptual attributes have been developed over the years. Some of these require listeners to make a subjective decision using a particular rating scale (for example, the CAPE-V developed by the American Speech-Language and Hearing Association). Others use a variety of signal processing techniques to quantify certain aspects of the speech acoustic signal [1-4]. Unfortunately, all of these methods have been compromised by a variety of problems. The accuracy of subjective judgments has been measured by calculating the reliability and agreement within and across listeners. Reliability measures the degree to which one listener's ratings on a set of stimuli follow the same trends as that of another listener. Agreement, on the other hand is a measure of the probability that two listeners give the same stimulus

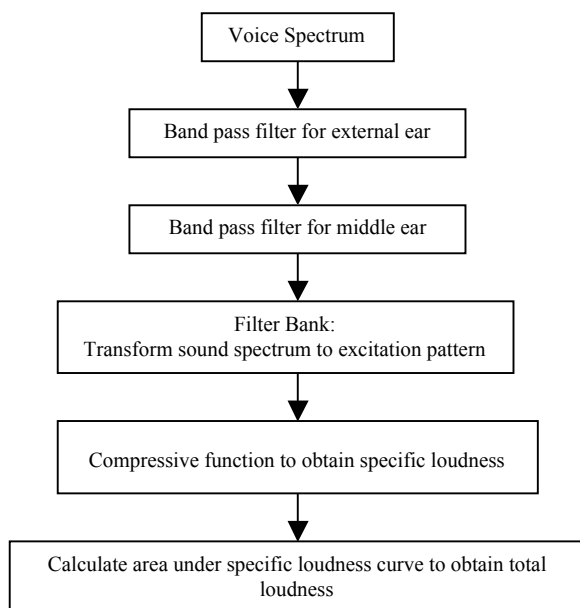
the same exact rating. Unfortunately, both reliability and agreement have been found to be poor for subjective ratings of voice quality [5-7]. Similarly, the accuracy of automated measures to quantify perception is measured by calculating the correlation between these measures and perceptual judgments of voice quality. Unfortunately, most automated measures have been observed to show poor to moderate correlation with perceptual data. Additionally, these measures often lack consistency and show poor sensitivity and specificity to the perceptual construct that they intend to quantify [8].

When attempting to quantify attributes such as voice quality, it is important to remember that these are inherently perceptual constructs. Attributes such as voice quality, nasality or “acceptability” of speech essentially reflect a listener's judgment about that particular construct. The speech signal itself does not possess *quality*; rather, it “evokes it in the listener” [8]. Therefore, any method to quantify such perceptual attributes must be validated against perceptual judgments made by listeners. These perceptual judgments serve as the gold standard for any other method to quantify perceptual attributes of speech. Unfortunately, perceptual judgments made by a listener are highly variable and are affected by a number of factors [9, 10]. While some of these factors are related to the stimulus characteristics, others are related to extraneous variables such as listener experience and training, instructions given to the listeners, nature of the scaling task and the experimental design. These extraneous variables introduce “noise” in the perceptual data, thereby, making it difficult to interpret the true perceptual magnitude of a given stimulus. However, these errors can be minimized through the use of appropriate experimental designs to obtain perceptual judgments [11]. These procedural modifications include multiple presentations of each stimulus to each listener, randomizing the order of stimulus presentation, modifying the instructions given to the listeners, etc.

Once a good estimate of the perceptual magnitude of an attribute has been obtained for several stimuli, these judgments may be used to develop a model that predicts listener judgments based on various stimulus characteristics. Such a model can be used to generate automated measures of vocal quality or other perceptual attributes of the speech signal. The development of such a model requires attention to the sensitivity of the human auditory system and the characteristics of the

acoustic-auditory transduction process. Previous research has shown that the relationship between a physical stimulus and its perceptual consequence is often non-linear. For example, the relationship between intensity and loudness may be described with a power law [12] and that between frequency and pitch is better described using non-linear scales such as the Bark, Mel or ERB-scales [13, 14]. In a similar manner, the perception of complex attributes such as voice quality may be best characterized by a non-linear function of specific stimulus characteristics. When the goal of measurement is to quantify perception, we need to (a) determine what aspects of the speech acoustic signal are perceptually relevant, and (b) determine the nature of the relationship between these stimulus characteristics and their perceptual consequences. One method to account for some of these non-linear processes is through the use of an auditory-processing model as a signal processing front-end. The general form of such a model is shown in Figure 1. The use of such front-ends has been shown to give better estimates of the perceptual judgments of voice quality [15, 16].

Figure 1: General form of an auditory processing model.



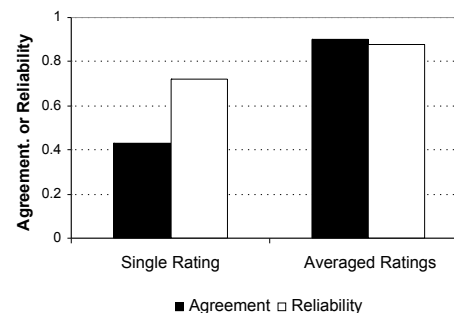
This paper describes a series of experiments to understand the perception of dysphonic voice quality. The first section describes the psychometric principles used to obtain a good estimate of the perceptual magnitude of dysphonic voice quality. In the second section, one particular auditory processing model and its utility in the quantification of “breathy” voice quality is described. And finally, preliminary data is presented on the perception of “rough” voice quality.

PSYCHOMETRIC THEORY TO QUANTIFY SUBJECTIVE JUDGMENTS OF VOICE QUALITY

A variety of techniques have been used for scaling perceptual magnitude of a physical stimulus [17]. It is necessary to differentiate two aspects in this process – sensory capability and response proclivity [18]. Sensory capability refers to the resolving power of the sensory mechanism; it defines the limits of the sensory system. On the other hand, response proclivity refers to the tendency of a listener to respond in a specific manner when encountering a specific stimulus. Since proclivity is affected by several factors, many unrelated to the stimulus itself, it is necessary to take appropriate steps to minimize “noise” in perceptual judgments.

For example, inter- and intra-rater reliability (measured as the correlation between ratings made within- or across-listeners) in perceptual ratings can be minimized by averaging multiple ratings of each stimulus by each listener [11]. Such precautions can avoid errors such as those arising due to “order-effects” and frequently seen with rating scales. If measurement of “agreement” (i.e. the probability that two raters would give the same stimulus exactly the same rating) is essential, the ratings from individual listeners should be normalized using standardized scores (z-scores) or other procedures. Figure 2 shows the improvement in reliability and agreement for perceptual ratings of breathiness when these procedures are used.

Figure 2: Improvement in reliability and agreement when multiple ratings of each stimulus from each listener are used. Each listener’s ratings were converted to corresponding z-scores.



Although these techniques help improve agreement and reliability of rating scale data, these measures may not necessarily indicate the true magnitude of the stimulus. Rather, rating scale measures may only provide the rank ordering of the stimuli tested in the experiment. Other techniques, such as magnitude estimation, magnitude production, matching or paired comparisons may be better suited to obtain an accurate estimate of perceptual “distance” between two stimuli.

AUDITORY PROCESSING MODEL AS A SIGNAL-PROCESSING FRONT END TO QUANTIFY “BREATHY” VOICE QUALITY
Breathiness in voices has been found to correlate with a number of acoustic measures, including aspiration noise,

frequency/intensity perturbation and spectral slope. However, the correlation between these measures and perceptual judgments of breathiness has been found to be inconsistent across different experiments.

Auditory processing models can allow us to estimate how acoustic signals may be represented in the auditory system. Several such models have been proposed [19-21]. One such model, proposed by Moore et al. (1997) was implemented for the study of breathy voice quality [15, 16]. This model simulates the outer and middle ear as band pass filters. The cochlear filtering is simulated with a filter-bank of asymmetric rounded-exponential filters. Finally, the neural excitation is modeled as a non-linear compressive function. The total neural excitation for a given sound provides an estimate of the loudness of that sound. The neural excitation within each “channel” is called the *specific* loudness.

This auditory processing model can also be used to simulate masking. Masking refers to the phenomenon where the loudness of a sound is reduced if it is presented along with a background noise. The loudness of a specific component, when it is presented simultaneously with an auditory masker is called the *partial* loudness.

The utility of this auditory processing model in predicting perceptual judgments of breathiness was tested in separate experiments [15, 16]. One experiment studied 13 voice stimuli, and compared the results to perceptual judgments obtained using a multidimensional scaling design. The other studied 27 stimuli and compared the results to perceptual judgments made on a 5-point rating scale. In both these experiments, the voice stimuli were first separated into a periodic component representing the complex wave produced by vocal fold vibration and an aperiodic component representing the aspiration noise. The auditory processing model was used to estimate the *partial loudness* of the complex wave, while treating the aspiration noise as an auditory masker. In both these experiments, the partial loudness of the complex wave was found to correlate highly with the perceptual judgments of breathiness. This measure accounted for greater variance in the perceptual ratings of breathiness than any other acoustic measure of breathiness. Figure 3 shows the relationship between partial loudness of the complex wave and perceptual judgments of breathiness.

The use of an auditory-processing model accounts for multiple factors that may affect breathiness – the overall intensity of the complex wave and aspiration noise, the spectral shape of these components as well as the non-linear interaction between the two. This, presumably, accounts for greater variance in the perceptual data than using conventional acoustic measures such as measures of noise or spectral slope. The change in partial loudness patterns for different voices is shown in Figure 4.

Figure 3: Linear regression predicting ratings of breathiness using partial loudness of the complex wave (and assuming that aspiration noise acts as an auditory masker).

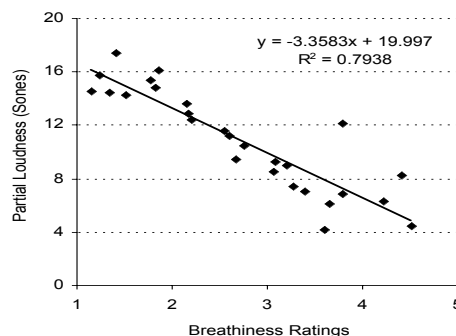
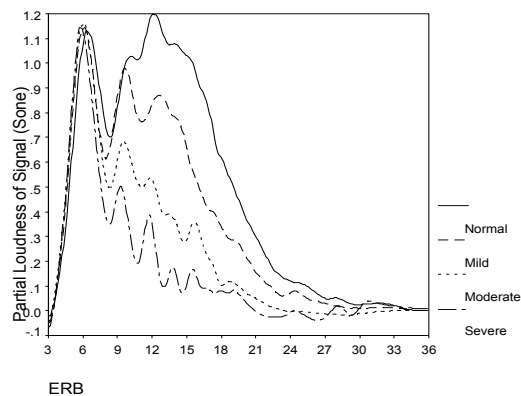


Figure 4: Partial loudness patterns for voices identified as normal, mild-, moderate- and severely- breathy.



ACOUSTIC CORRELATES FOR “ROUGHNESS” IN VOICES – PRELIMINARY DATA

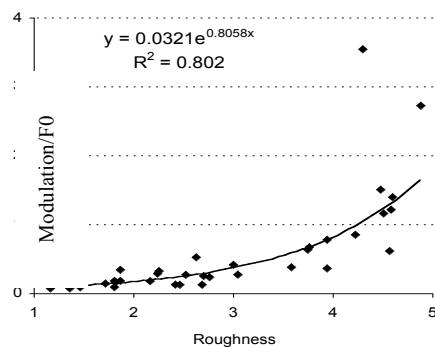
Many voices frequently observed in voice clinics are described as “rough.” A number of acoustic correlates for roughness have been proposed. These include, frequency/intensity perturbation, estimates of noise in the signal and the presence of subharmonics. However, as with breathy voices, these findings lack sensitivity and specificity.

From a psychoacoustic perspective, the perception of roughness is related to the amplitude and frequency modulation of a carrier wave. More specifically, the roughness of a sound is related to the amplitude modulation within a given critical-band [22]. The perception of roughness of a carrier wave is most sensitive to specific modulation frequencies.

A much simplified implementation of this model for roughness is obtained by: (1) determining the modulation frequencies in the vowel, (2) selecting a subset of these modulating frequencies, (3) calculating the “modulation amplitude” for these frequencies, and (4) determining the average modulation due to these frequencies.

The average modulation amplitude thus obtained was first normalized to the fundamental frequency of each stimulus, and was then used to predict perceptual judgments of roughness for 34 vowel samples. An exponential fit was found to account for 80.2% of the variance in the perceptual data. These data are shown in Figure 5. Measures such as shimmer, jitter and signal-to-noise ratio accounted for considerably less variance in the same perceptual data.

Figure 5: Perceptual ratings of roughness predicted by the normalized modulation amplitude of selected modulation frequencies.



CONCLUSIONS

Voice quality is essentially a perceptual construct. Any method to quantify perception must be validated against perceptual judgments. However, since perceptual judgments are highly variable, one needs to devise experiments that minimize response variability associated with non-stimulus factors. Additionally, methods to quantify perception are more likely to be successful if they simulate the mechanisms involved in the auditory-perceptual process. One way to achieve this is through the use of auditory-processing models as a signal-processing front end. The success of this approach is shown for quantification of “breathiness” and “roughness” in dysphonic voices.

ACKNOWLEDGEMENTS

Research funded by a grant from NIH/NIDCD (R21DC006690). Part of this work is being done in collaboration with David Eddins.

REFERENCES

1. Hillenbrand, J., R.A. Cleveland, and R.L. Erickson, *Acoustic correlates of breathy vocal quality*. Journal of Speech & Hearing Research, 1994. **37**(4): p. 769-78.
2. Deal, R.E. and F.W. Emanuel, *Some waveform and spectral features of vowel roughness*. Journal of Speech & Hearing Research, 1978. **21**(2): p. 250-64.
3. de Krom, G., *A cepstrum-based technique for determining a harmonics-to-noise ratio in speech signals*. Journal of Speech & Hearing Research, 1993. **36**(2): p. 254-66.

4. Milenkovic, P., *Least mean square measures of voice perturbation*. Journal of Speech & Hearing Research, 1987. **30**(4): p. 529-38.
5. Kreiman, J., et al., *Individual differences in voice quality perception*. Journal of Speech & Hearing Research, 1992. **35**(3): p. 512-20.
6. Kreiman, J., et al., *Perceptual evaluation of voice quality: review, tutorial, and a framework for future research*. Journal of Speech & Hearing Research, 1993. **36**(1): p. 21-40.
7. Rabinov, C.R., et al., *Comparing reliability of perceptual ratings of roughness and acoustic measure of jitter*. Journal of Speech & Hearing Research, 1995. **38**(1): p. 26-32.
8. Kreiman, J. and B. Gerratt, *Measuring voice quality*, in *Voice Quality Measurement*, R.D. Kent and M.J. Ball, Editors. 2000, Singular Publishing Group: San Diego. p. 73-101.
9. Poulton, E.C., *Bias in quantifying judgments*. 1989, Hove, U.K.: Lawrence Erlbaum Associates Ltd.
10. Thurstone, L.L., *The measurement of values*. 1959, Chicago: University of Chicago Press.
11. Shrivastav, R., C. Sapienza, and V. Nandur, *Application of Psychometric Theory to the Measurement of Voice Quality Using Rating Scales*. Journal of Speech, Language, & Hearing Research, In Press.
12. Stevens, S.S., *A scale for the measurement of a psychological magnitude: Loudness*. Psychological Review, 1936. **43**: p. 403-416.
13. Stevens, S.S., J. Volkman, and E.B. Newman, *A scale for the measurement of psychological magnitude: Pitch*. Journal of the Acoustical Society of America, 1937. **8**: p. 185-190.
14. Moore, B.C.J., *An Introduction to the Psychology of Hearing*. 4th ed. 1997, San Diego, CA: Academic Press.
15. Shrivastav, R., *The Use of an Auditory Model in Predicting Perceptual Ratings of Breathless Voice Quality*. Journal of Voice, 2003. **17**(4): p. 502-512.
16. Shrivastav, R. and C. Sapienza, *Objective Measures of Breathless Voice Quality Obtained Using an Auditory Model*. Journal of the Acoustical Society of America, 2003. **114**(4): p. 2217-2224.
17. Stevens, S.S., *Mathematics, Measurement and Psychophysics*, in *Handbook of Experimental Psychology*, S.S. Stevens, Editor. 1951, John Wiley & Sons, Inc.: New York.
18. Watson, C.S., *Psychophysics*, in *Handbook of General Psychology*, B.B. Wolman, Editor. 1973, Prentice Hall, Inc.: Englewood Cliffs, NJ.
19. Moore, B.C.J., B.R. Glasberg, and T. Baer, *A model for the prediction of thresholds, loudness and partial loudness*. Journal of Audio Engineering Society, 1997. **45**(4): p. 224-239.
20. Lopez-Poveda, E.A. and R. Meddis, *A human nonlinear cochlear filterbank*. J Acoust Soc Am, 2001. **110**(6): p. 3107-18.
21. Seneff, S., *Ajoint synchrony/mean-rate model of auditory speech processing*. Journal of Phonetics, 1988. **16**: p. 55-76.
22. Terhardt, E., *On the perception of periodic sound fluctuations (Roughness)*. Acustica, 1974. **30**: p. 201-213.

WHAT CAN BE SEEN IN VIDEOKYMOGRAPHIC IMAGES?

J. G. Svec^{1,2}, F. Sram², M.Fric², Q.Qiu¹, H. K. Schutte¹

¹ Groningen Voice Research Lab, Department of BioMedical Engineering, University Medical Center Groningen, University of Groningen, the Netherlands

² Center for Communication Disorders, Medical Healthcom, Ltd., Prague 8, the Czech Republic

Abstract: Kymographic imaging refers to a special way of displaying vibrations by putting together a great number of successive images of a vibrating object viewed through a thin slit. In medicine, the method has been found particularly well suited for imaging vibrations of the vocal folds, which are the ultimate source of human voice. Here we address the question on which vibratory characteristics of the vocal folds can be identified in high-speed videokymographic images and used in clinical practice when diagnosing origins of voice problems? The ultimate long-term goal of the research is to relate the displayed vibration characteristics to the tissue properties of the vocal folds and design strategies how undesirable tissue properties can be altered through conservative or surgical treatment.

ACKNOWLEDGMENTS:

The research has been supported in the Netherlands by the STW project G5973 and in the Czech Republic by the EUREKA E!2614 project.

OBJECTIVE VOCAL FOLD VIBRATION ASSESSMENT FROM VIDEOKYMOGRAPHIC IMAGES

S. Bianchi, L. Bocchi, C. Manfredi, G. Cantarella*, N. Migali*

Department of Electronics and Telecommunications, Università degli Studi di Firenze
Via S. Marta 3, 50139 Firenze, Italy

* Otolaryngology Department, University of Milan, Ospedale Maggiore IRCCS, Via F. Sforza 35, 20122 Milano, Italy

Abstract - Vocal folds oscillation crucially influences all the basic qualities of voice, such as pitch and loudness, as well as the spectrum. Stroboscopy provides the standard view of the larynx. Videokymography is a new diagnostic tool developed to overcome specific limitations of stroboscopy in severely dysphonic patients with an aperiodic signal. It registers the movements of the vocal folds with a high time resolution on a line perpendicular to the glottis.

The main focus of this paper is on measuring and tracking quantitative parameters for objective vocal fold function assessment from videokymographic (VKG) examinations of subjects with normal and pathological laryngeal function. Active contour search is realised, by properly adjusted snake algorithm. Examples are reported, showing the robustness and reliability of the proposed technique.

I. INTRODUCTION

Vibration of the vocal-folds is a highly relevant aspect of voice production, both in normal and in pathological voices. The periodicity, or lack of periodicity, critically determines the quality of voice. It is typically described in terms of jitter and/or shimmer, period to-period correlation, or by spectral characteristics. Another method for acquisition of physiological data is direct visual inspection of the vocal folds vibration by means of stroboscopy. An admitted limitation of the stroboscopic image is that vocal fold vibration must be relatively periodic to visualize a slow motion representation of the phonatory cycle. In fact, aperiodicities associated with some voice qualities make stroboscopy inappropriate, since any disturbance of the vibration distorts the resulting stroboscopic image.

The kymographic concept introduced by [1], [2] seems to be an optimal solution, since each vibratory cycle is documented in terms of a sequence of several images, which can be acquired directly from a single-line camera [1] or by extraction from high-speed image sequences [3],[4]. Videokymography allows isolation of specific portions of the glottic image (taken at up to 7812 images per second) to be analyzed for closure. Such kymographic images give a good view of the

movements of the vocal folds, periodic or nonperiodic, but only for part of the image, i.e., the single line. This study aims at offering an automatic quantitative method to obtain vibration properties of human vocal folds via videokymography, by developing a digital image processing algorithm optimized for the analysis of videokymography (VKG) recordings, such as intensity adjustment, noise removal and glottis identification. The presented method extends previous work [5] and combines an active contour model with a parameter extraction algorithm that can accurately track the vibrational wave in videokymograms and automatically quantify its properties in terms of few parameters, useful for clinicians. Tracking parameters, other than simply measuring their mean value and std, is in fact considered of utmost importance by clinicians, as irregular patterns can be found at their instant of occurrence during phonation and put into relation with images and acoustic signal analysis. Specifically, the amplitude and period ratios between right and left vocal fold, as well as the ratio between opening and closing phase are considered [6]. When required, more parameters could be added, on analogy to [7]. Examples are given concerning pathological subjects, that show the robustness of the contour detection algorithm.

II. MATERIALS AND METHODS

Videokymography (VKG) is based on a special camera, which can operate in two different modes: standard and high-speed. In the standard mode, the camera provides standard images displaying the whole vocal folds at standard video frame rate (30/25 frames/s, with 720x486/768x576 pixels of resolution). In the high-speed mode, the video camera delivers images from only a single line selected from the whole image, at the speed of approximately 7875/7812.5 line-images/s and 720x1/768x1 pixels resolution. The resulting high-speed image, called "videokymogram", displays the vibratory pattern of the selected part of the vocal folds. Kymographic recording is divided into video frames, i.e. segments of approx. 15/18 ms duration. Images are not in colour, and continuous high-intensity light is desirable.

The vibratory pattern displayed in kymographic images is dependent on the measuring position. There are two factors which influence the resulting image:

- 1- position along the glottal axis
- 2- angle with respect to the glottal axis.

In normal cases, the position in the middle of the vocal folds is usually considered to provide the representative vibratory pattern of the whole vocal folds. In case of vocal fold lesions, however, the vibration characteristics generally differ along the glottal axis.

The angle of the measuring line is, as a standard, adjusted to be perpendicular to the glottal axis. When using VKG, the measuring position is adjusted prior to the examination.

Usually, there is only limited time available for the examination. Therefore, phonation at comfortable pitch and loudness is mostly targeted for kymographic imaging.

Despite its usefulness, in our knowledge, until now no quantitative analysis of VKG images is commercially available, and only few work has been made towards its fulfillment [6], [7]. At present, physicians perform only qualitative evaluation of VKG parameters, basically by visual inspection of subsequent frames, or by manual measures from printed images. Such analysis prevents from reliable comparison among wide sets of data, and hence from finding and defining standard reference values for classification and assessment of treatment effectiveness. Based on such requirements, this work aims at providing first results that would allow filling this gap.

Parameter extraction is obtained here by means of two subsequent stages: image analysis, for vocal folds contours detection, followed by signal analysis, for parameter evaluation from data sets representing vocal folds edges. Specifically, and with reference to Fig.2, the parameters to be measured and tracked are:

- R_{amp} , the ratio between the right and left vocal fold amplitudes, related to possible asymmetries between the two folds;
- R_{per} , the ratio between the right and the left vibratory periods, inversely related to possible frequency variations due to pathology;
- R_{oc} , the ratio between opening and closing phase (Open and Closed, respectively), basically related to glottal insufficiency.

For healthy voices, such parameters should be equal or close to one, and almost constant during all phonatory cycles. Any asymmetry due to pathology can thus be quantified by evaluating and tracking the above-mentioned parameters.

A First stage: Edge detection

The correct detection of the vocal folds contour is carried out in a two-step process, the first one aiming at finding an initial contour to which active snakes are applied in the second step.

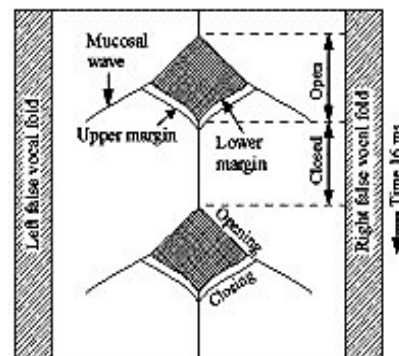


Figure 2: Main parameters for objective videokymographic image analysis (from [1]).

A.1 First step: initial contour

The following routine, that handles some basic settings, is executed before the snake. It normalises grey levels, initialises contour, takes notice of black lines, to be disregarded by the algorithm, thus finding the significant rows in the image. Then, it sets to 0 the level of the image outside the right and left edges, defined by the user. This allows avoiding noisy fluctuations of the grey levels not overlapped with the vocal folds. The routine scans the significant rows and, for each of them, determines the largest interval of pixels with a grey level lower than a pre-specified threshold. A first contour is thus obtained, by storing the interval coordinates for each line in two separate arrays.

A.2 Second step: snake active contour

Snakes are planar deformable contours that are useful in several image analysis tasks. They are often used to approximate the locations and shapes of object boundaries on the basis of the reasonable assumption that boundaries are piecewise continuous or smooth [8]. Representing the position of a *snake* parametrically by $v(s)=(x(s),y(s))$ with s in $[0,1]$, its energy can be written as:

$$E_{snake} = \int E_{int} [v(s)] ds + \int E_{ext} [v(s)] ds \quad (1)$$

where E_{int} represents the internal energy of the snake due to bending and it is associated with *a priori* constraints, E_{ext} is an external potential energy which depends on the image and accounts for *a posteriori* information. The final shape of the contour corresponds to the minimum of this energy.

In the original technique [9] the internal energy is defined as:

$$E_{int} [v(s)] = \frac{1}{2} \left[a(s) \left(\frac{\partial v(s)}{\partial s} \right)^2 + b(s) \left(\frac{\partial^2 v(s)}{\partial s^2} \right)^2 \right]. \quad (2)$$

This energy is composed of a first order term controlled by $a(s)$ (*tension* of the contour) and a second order term controlled by $b(s)$ (*rigidity* of the contour).

The external energy couples the snake to the image. It is defined as a scalar potential function whose local minima coincide with intensity extremes, edges, and other image features of interest:

$$E_{\text{ext}}[v(s)] = -c(\nabla G_s * I(x,y))^2 \quad (3)$$

where $I(x,y)$ is the image intensity, G_s is a Gaussian of standard deviation s , ∇ is the gradient operator and c a weight associated with image energies [8], [9], [10].

As concerns the energy minimization, the original model employs the variational calculus to iteratively minimize the energy. There may be a number of problems associated with this approach such as algorithm initialization, existence of local minima, and selection of model parameters. Among existing methods, the greedy algorithm [10] exhibits a low computational cost, provided the initial position of the snake is relatively close to the desired contour. In our application, the technique described in step 1 provides a fairly good approximation of the real contour, therefore allowing us to utilize the active contour and the snake algorithm to perform a fine tuning of the contour on the image. Each vocal fold has been modelled as an independent snake, having its extreme point constrained to belong to the first and the last scan line of the image, respectively. Notice that, differently from [7], the snake is applied on the whole contour and not on sequential rows. This makes the search particularly efficient and robust.

B Second stage: parameter extraction and tracking

In this stage, data consist of (time, edge value) pairs, for each fold, obtained as described in the previous steps. As already said, three clinically relevant parameters are extracted from data.

R_{amp} = ratio between the average amplitude of the left vocal fold and that of the right vocal fold. The amplitude is defined as the distance between each point and a fictitious closed-fold point, chosen to be halfway between the minimum values of the folds.

R_{per} = ratio between the right vocal fold period and the left vocal fold period. The period is defined as the mean value among all periods in the frame. Each period is obtained by evaluating the distance between consecutive maximum edge values, determined relatively to the closed-fold point axis.

R_{oc} = ratio between the opening and closing phase of the folds, determined searching consistent, non noise-generated interruptions of the time coordinate.

Following [7] as well as future clinicians suggestions, more parameters could be easily added and extracted.

III. EXPERIMENTAL RESULTS

Algorithms were applied to a set of VKG recordings (Kay Elemetrics VKG Camera, Model 8900®), ORL

Dept., Ospedale Maggiore, Milano, Italy, belonging to both normal and pathological patients. Specifically, 11 patients (6 male, 5 female, age 24-81, mean 52 years) were analysed, affected by: leucoplachia, granuloma, polyp, dysphonia, and possibile vocal fold paralysis. The work was carried out under C++ development environment.

Each image has been processed and visually inspected to qualitatively assess the contour identification. Both the results of the first step (before the application of the snake algorithm), and of the second one, as optimized through the active contour, are considered. Notice that the first step works reasonably well in about 80% of the test cases, although there is a considerable amount of noise which reduces the reliability of the measured parameters. In the remaining 20% of cases, the images present few dark zones, which cause the detection of artefacts appearing as anomalous contours. The application of the active contour method, however, greatly reduces the presence of both noise and artefacts, achieving an accurate contour detection.

Fig.3 shows the results obtained with the first step (Fig.3a) and the second step (Fig.3b) for one patient: male, 75 years old, affected by leucoplachia on the left vocal fold. The figure is relative to a single VKG frame out of about 450, for about 2min. total duration of the whole visit, which comprises laryngoscopic, VKG and simultaneous audio recording of sustained /a/. Notice that the first step gives almost irregular initial contours, while the second one smoothes the lines and successfully removes outliers.

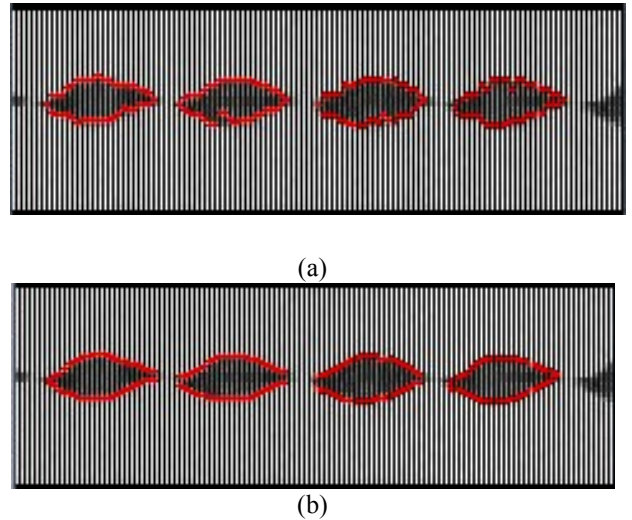


Figure 3 – Edge contour detection. (a) first step: preliminary contour; (b) second step: final contour.

Fig.4 shows the tracking of the three parameters R_{oc} , R_{amp} , R_{per} on a set of about 90 subsequent frames. Notice that, due to the length of the exam, the emission slightly changed with time, ranging from /a/ to /ae/ and /ao/ (F_0 varied in the range 140Hz-230Hz).

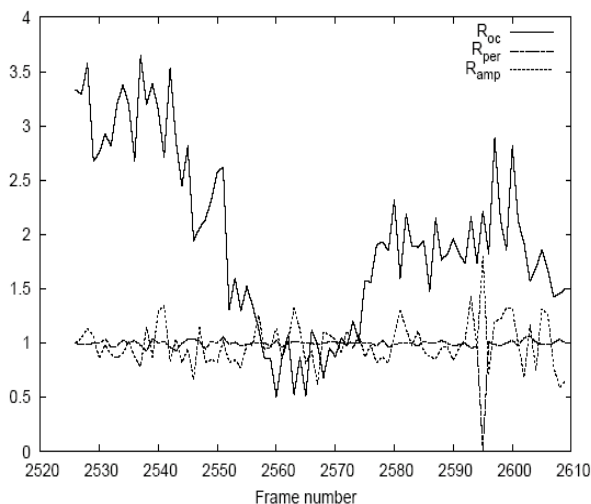


Figure 4 - R_{oc} , R_{amp} , R_{per} tracking along 90 VKG frames

This fact, in conjunction with pathology, and the difficulty of the operator to keep the endoscope fixed on the same line through the whole analysis, caused possible changes in the VKG parameters, as pointed out in fig.4 as far as R_{oc} is concerned, which shows a mean value $R_{oc-mean}=1.96$, with 0.8 std. Instead, R_{amp} and R_{per} are quite stable: $R_{amp-mean}=0.99$, $std=0.2$, $R_{per-mean}=1$, $std=0.02$, according to the pathology under study, that does not causes strong irregularities in the vocal folds oscillation.

Similar results were obtained with the other recordings. Both visual inspection of contours and objective parameters tracking have provided clinicians with useful details and information, also in cases not clearly distinguishable with stroboscopy alone.

IV. FINAL REMARKS

Kymographic imaging provides valuable information on the dynamic behaviour of the laryngeal tissues that is not so clearly distinct in the classical stroboscopic viewing, especially in case of early or non-specific lesions, irregular closure patterns, vocal fold weakness, paralysis, that may also allow for the differentiation of weakness due to overuse, aging, paresis, or early stages of neurological conditions. The information can be used in basic research, vocal fold modelling, as well as in clinical practice, as, for instance, in evaluating the results achieved by phonosurgery.

Hence, the need for automatic evaluation and tracking of objective parameters, extracted from VKG images, is of great concern. This paper aims at providing a basic set of such parameters, by means of active contour techniques for edge detection. Specific adjustments were made in a first step, in order to deal with high varying and noisy images as those under study.

Current research focuses on refinements of the proposed technique, as well as on the estimation of a wider set of parameters. A user-friendly interface is also under

construction, with the aim of making the analysis fully automatic and allowing easily storing and retrieving patient's data.

V. REFERENCES

- [1] Svec, J.G., and Schutte, H.K. (1996), Videokymography: High-Speed Line Scanning of Vocal Fold Vibration," *J. Voice* 10, 201-205.
- [2] Schutte, H.K., Švec, J.G. and Šram, F., 1997. Videokymography: Research and Clinical Issues. *Log. Phon. Vocol.*, 22(4): 152-156.
- [3] Tigges, M., Mergell, P., Herzel, H., Wittenberg, T., and Eysholdt, U. (1997), Observation and modelling glottal biphonation," *Acustica/Acta acustica* 83, 707-714.
- [4] Larsson, H., Hertegard, S., Lindestad, P.-A., and Hammarberg, B. (2000). "Vocal Fold Vibrations: High-Speed Imaging, Kymography and Acoustic Analysis," *Laryngoscope* 110, 2117-2122.
- [5] C. Manfredi, L. Bocchi, G. Peretti, "First results on quantitative analysis of videokymographic images", *MEDICON04 Conf.*, 1-5 Aug. 2004, Ischia Island, Italy.
- [6] G. Peretti, C. Piazza, M. Giudice, C. Balzanelli, C. Mensi, M. Rossini (2001): "Videokymography", *Acta Phon. Lat.*, 24, pp.71-77.
- [7] Q. Qiu, H.K. Schutte, L. Gu, Q. Yu (2003), "An Automatic Method to Quantify the Vibration Properties of Human Vocal Folds via Videokymography", *Folia Phoniatrica et Logopaedica*, 55:128-136.
- [8] Cheung, K.-W., Yeung, D.-Y., And Chin, R. T. (2002): 'On deformable models for visual pattern recognition'. *Pattern Recognition*, 35, pp.1507-1526.
- [9] M. Kass, A. Witkin, D. Terzopoulos, (1988): 'Snakes: Active contour models'. *Int. J. Computer Vision*, 1, pp. 321-331.
- [10] McInerney, T. and Terzopoulos, D. (1996): 'Deformable models in medical image analysis: a survey'. *Medical Image Analysis*, 1, pp.91-108.
- [11] J.G.Svec, F.Sram (2002): "Kymographic imaging of the vocal folds oscillations", *Proc. ICSLP-2002*, Sept. 16-20, 2002, Denver, CO, USA, vol.2, pp.957-960.

DYNAMIC DIGITAL IMAGE CORRELATION OF A DYNAMIC PHYSICAL MODEL OF THE VOCAL FOLDS

S. Mantha, L. Mongeau, T. Siegmund

School of Mechanical Engineering, Purdue University, IN, U.S.A.

Abstract: An experimental study of the vibratory deformation of the human vocal folds was conducted. Experiments were performed using model vocal folds made of soft silicone rubber, and an air supply system. The model self-oscillated at fundamental frequencies and flow rates typical of the human folds. Time-averaged mass flow rates and transglottal pressures were measured along with the sound pressure upstream of the orifice. The deformation of the vocal fold was measured using a high-speed three-dimensional digital correlation system. The imaging set-up is composed of a high-speed digital camera and a prism beam splitter allowing two images to be obtained from different viewpoints in every image frame. Commercially available digital image correlation software was used to analyze the images, and to calculate the strain fields at the vocal fold superior surface. Results were obtained for vocal folds made of isotropic material and two different vocal fold lengths. The deformed shape of the model vocal folds, strains on the superior surface, and the time-varying vocal fold wall displacement were obtained.

Keywords: Digital image correlation (DIC), high-speed video, strain fields, collision

I. INTRODUCTION

Many techniques are available for the visualization of laryngeal pathology. Methods based on inverse filtering of radiated voice sound pressure signals, for example, or electroglottography provide useful information about the mean flow rate and waveform of the glottal source. Optical techniques for the study of vocal fold vibrations have become readily available following the widespread use of high-speed digital photography. Among these optical methods, videoendoscopy, stroboscopy and high-speed photography have shown to provide a good visual impression of the vocal fold dynamics [1]. In addition kymographic image sequences allow for a convenient visualization of vibration patterns [2]. These widely known methods, however, provide little quantitative insight into the fundamental deformation processes taking place in the tissue during self-oscillation of the vocal folds. To obtain quantitative measures of deformation, a micro-suture technique was applied to study mucosal wave propagation [3].

This method is invasive and allows for measurement of only a few discrete image points. Another non-invasive method, laser triangulation, was used but this approach is again limited to only local measurement points [4].

In the present paper, the application of a digital image correlation (DIC) technique to the study of vocal fold dynamics and deformation is described. This method allows for noninvasive synchronous measurements of the entire displacement field of the deformed vocal folds. The capabilities of the technique were investigated using a physical model of the vocal fold system [5]. The results so far are encouraging, and suggest that the procedure can be successfully used provided a suitable speckle pattern can be applied onto the surface of the deformable body.

II. THE VOCAL FOLD MODEL

The physical models of the vocal folds were built for a generic vocal shape [5, 6] following procedures described in [7]. The material used to cast the model folds was a silicone rubber, Ecoflex, manufactured by [8]. The vocal folds were made of one single isotropic material. The material was characterized by a hardness value of $H_{ooo}=31$ on an OOO durometer scale. Uniaxial tensile tests were conducted. The tangent modulus at $\varepsilon=0$ was determined to be $E=5$ Kpa. The magnitude of the elastic modulus is thus approximately within the lower range of the longitudinal elastic properties of the human vocal fold cover [9].

III. EXPERIMENTAL SET-UP

The experimental set-up used in the investigation is depicted in Figure 1. The main components included an air-supply system connected to an air duct assembly. The model larynx was assembled in a rigid frame with zero glottal opening. The frame containing the model larynx was placed at the upstream exit of the air duct. The experimental set-up was connected to a mass flow meter, a pressure transducer and a HP DAC system. Images of the superior surface of the model larynx were obtained by the use of a high-speed digital camera, Memrecam fx K3, NAC Image Technology, [10], at a frame rate of 3000 frames per second.

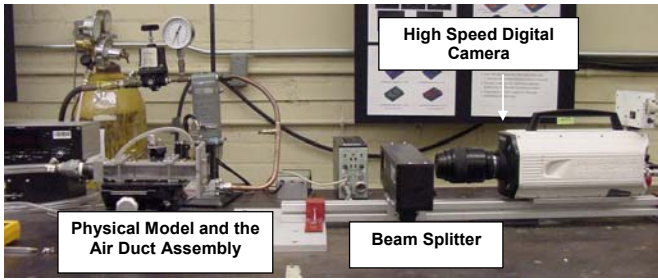


Figure 1: Experimental set-up.

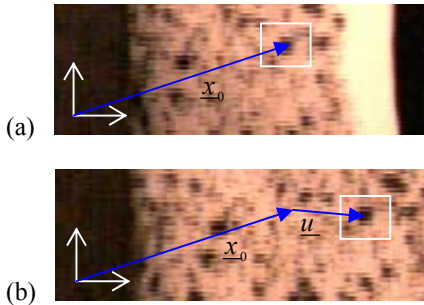


Figure 2: Tracking a point on the superior vocal fold surface from (a) a reference to (b) a deformed state through gray value patterns in subsets.

A 3D-DIC system was employed. The analysis consists of two steps: (a) a stereo correlation technique to determine in plane displacements (u, v) [11] and (b) stereo triangulation [12] to obtain the out-of-plane deformation (w) . For the determination of the in-plane displacements through a DIC analysis, images of the object under consideration at two different stages of deformation were compared; see Fig. 2(a) for the image of the reference state and Fig. 2(b) for the image of the deformed state. The stereo correlation analysis requires that any point in the undeformed stage of the object, \underline{x}_0 is matched with the corresponding point in the deformed stage, $\underline{x} = \underline{x}_0 + \underline{u}$. In DIC, such a correlation is obtained by searching for matching gray scale patterns in corresponding images. So-called “subsets”, i.e. parts of digital images, are traced via their gray value distribution from the undeformed reference image to the deformed image, as shown Fig. 2. The uniqueness of the matching lies on the creation of a non-repetitive speckle pattern on the object’s surface. To obtain the speckle pattern, first a white pigment was mixed into the silicone rubber material during model preparation. Subsequently, black enamel paint was used to obtain the speckle pattern on the superior surface of the pseudo vocal folds. The application of the speckle pattern to the pseudo vocal folds is non-invasive and did not add any significant mass to the system.

For the stereo triangulation, two images of the object at each stage of deformation are required in order to obtain the out-of-plane displacement information. This was accomplished by obtaining two images of the object simultaneously in one single CCD frame at each time instant through the placement of a beam splitter in the optical axis

between the camera and the model larynx, Fig. 3. With this set-up two images of the model larynx are obtained at offset image positions and are recorded on a common digital image frame. These images provide a “left” and “right” view of the model larynx. Thus, the deformed shape of the vocal folds can be obtained by triangulation.

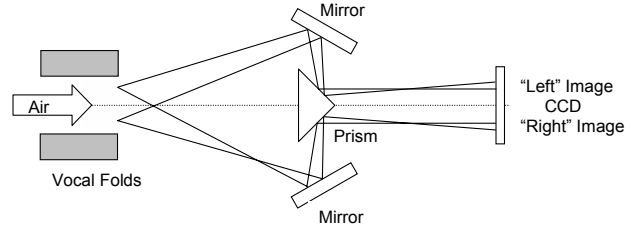


Figure 3: Image set-up with beam splitter. (Figure not to scale)

The digital image correlation analysis was performed using the program VIC-3D [13]. In the specific version of the program employed here, the image correlation was accomplished using an iterative spatial domain-correlation algorithm [14]. Calibration for focal length, image center and lens distortion was performed using a calibration target.

IV. RESULTS

Experiments were conducted on two larynx models with lengths $L = 17$ mm and 22 mm, respectively. First, for each model, the airflow rate was increased stepwise until self-oscillation was detected. Table 1 summarizes the phonation onset data. Phonation frequencies and onset pressures were within the range of physiological values. Six measurements were undertaken at higher mass flow rates, beyond the phonation threshold. The phonation frequency changed slightly as the mass flow rate was increased, Fig. 4(a). A maximum in the measured phonation frequency was reached for a flow rate of 550 cc/s. As discussed in the following, this behavior is associated with the onset of the occurrence of vocal fold closure and collision. Collision occurred at a vocal fold length dependent critical mass flow rate. For both models a linear relationship between pressure and mass flow rate was obtained, Fig. 4(b).

Kymographic images, shown in Figure 5, were obtained for $L=22$ mm at flow rates of 406 and 690 cm^3/s . These images clearly demonstrate the difference between the vibration processes at low and high flow rates. At low flow rates, no closing or collision of the vocal folds was observed. At larger flow rates, significant closure and collision takes place. Low and high flow rate regimes are distinguished based on the flow rate – frequency response such that a drop in frequency was observed for flow rates beyond the onset of closure/collision.

	$L=17$ mm	$L=22$ mm
Onset pressure	0.73 Kpa	0.87 Kpa
Mass flow rate	165 cm^3/s	406 cm^3/s
Phonation frequency	92.9 Hz	88.75Hz

Table 1: Phonation onset data of model larynx.

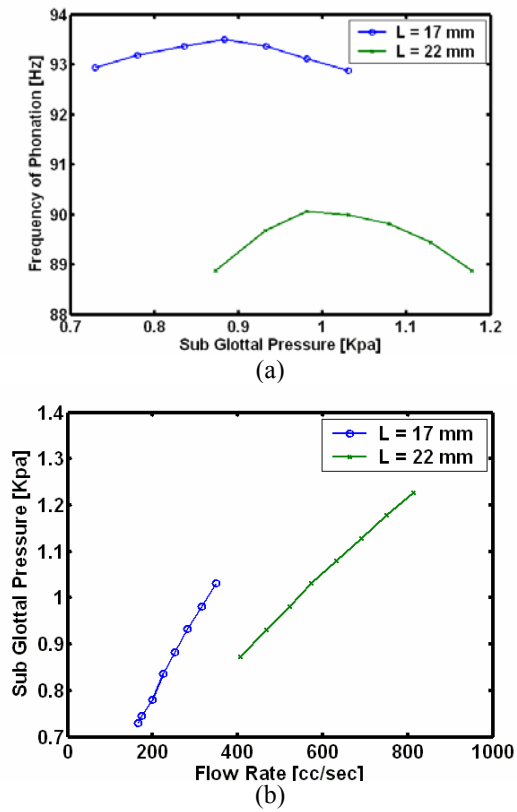


Figure 4: (a) Phonation frequency vs. Subglottal Pressure; (b) Subglottal pressure vs. mass flow rate for the model with $L=17$ mm and 22 mm

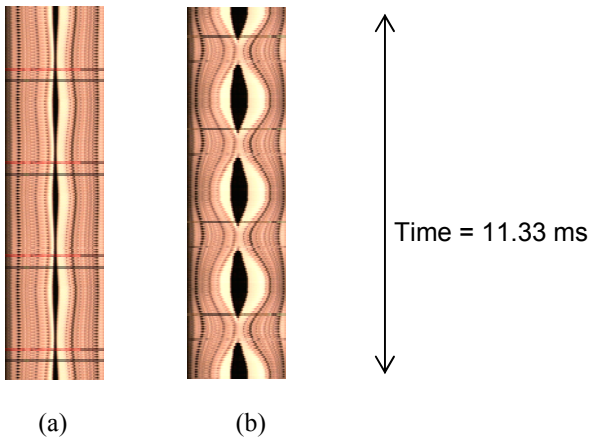


Figure 5: Sequence of five kymographic images (produced from a single kymographic image) for (a) flow rate of 406 cm³/s (the phonation threshold), and (b) flow rate of 690 cm³/s. The Kymographic image location indicated by a line in Figs. 6(a) and (c). $L=22$ mm.

Figure 6 shows typical digital image analysis results. Superior views of the model larynx are shown for a flow rate of 690 cm³/s at maximum glottal opening, Fig. 6(a), and during the stage of glottal closure, Fig. 6(c). Figures 6(b) and (d)

shows the distribution of the transverse strain component, ϵ_{xx} , obtained from DIC on the superior surface for the images in Fig. 6(a) and (c), respectively. The strain contours are shown on the deformed superior surface. In the position of maximum opening the vocal folds are deformed by a combination of a bulging-type deformation and the opening motion. The maximum value of the out-of-plane displacement was determined to be $w_{\max} = 3.5$ mm. This value is larger than that reported in humans, e.g. in [4] $w_{\max} = 1.5$ mm was reported. At the point of maximum glottal opening, the transverse strain, ϵ_{xx} , is less than zero at the mid-section of the superior surface. During the closing process vocal fold contact occurs, Fig. 6(c). Closure of the glottal opening is not complete and two distinct open areas are visible during the closing stage. These open areas are located at the anterior and posterior ends of the model larynx; see Fig. 6(c). Such incomplete closure has been observed in actual glottal measurements [15] and 3D finite element simulations [16]. Even during the closing stage the model larynx retains some of the bulging deformation. A local minimum of the out-of-plane displacement is seen at the midsection of the superior surface, $w = 1.65$ mm, while the two locations of maximum out-of-plane displacement, $w = 1.81$ mm, coincide with the locations of partial opening. During closure the characteristics of the strain fields changes significantly. At the midsection of the vocal folds the strain, ϵ_{xx} , is positive (tensile stress) and significant in amplitude, $\epsilon_{xx} \approx 0.1$.

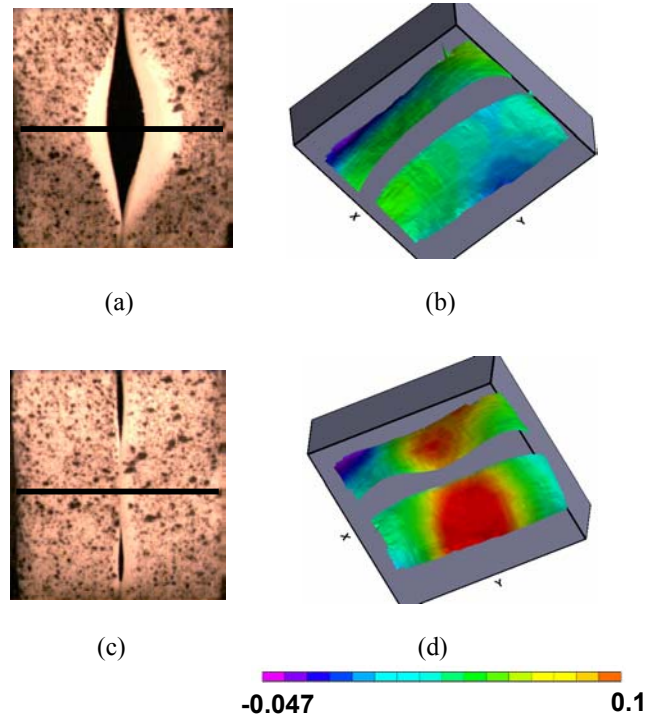


Figure 6: The model larynx ($L = 22$ mm, flow rate of 690 cm³/s) (a) Image at maximum open position; and (b) contour of ϵ_{xx} ; (c) image for closed state; and (d) contour of ϵ_{xx} .

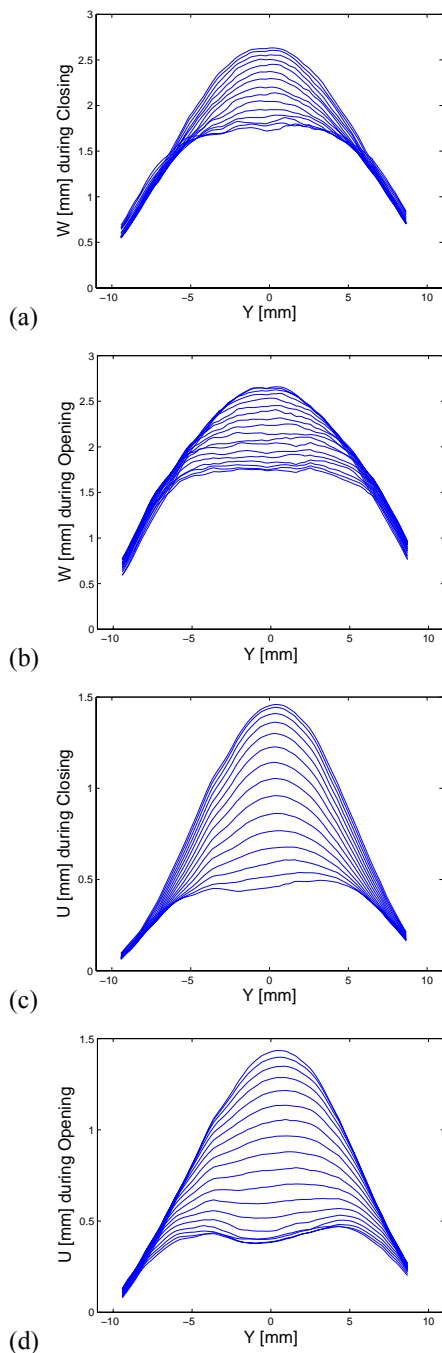


Figure 7: Out-of plane (a, b) and in-plane (c,d) displacements along the medial surface. $L=22\text{mm}$

The DIC method was also used to extract details of the time history of the wall displacement. Figure 7 shows the out-of-plane (w) and in-plane (u) displacements obtained for points along a line parallel to the medial surface at a position 1.5 mm from the centerline of the undeformed larynx for a flow rate of $406\text{ cm}^3/\text{s}$. Fig. 7(a) and (b) show that the model larynx remains in a bulged state due to the mean static pressure in all stages, $w_{\max}=2.63\text{ mm}$ and $w_{\min}=1.72\text{ mm}$. The main out-of-

plane vibratory displacements occur in the center of the vocal fold over a span of around $L/2$ with the outer parts of the folds almost fixed during oscillation. The range of the out-of-plane displacement was found to be $\Delta w = 0.91\text{ mm}$. Figs. 7(c) and (d) illustrate the process of glottal opening. The model larynx remains in an open state due to the mean static pressure in all stages, $u_{\max}=1.45\text{ mm}$ and $u_{\min}=0.40\text{ mm}$. The main vibratory displacement occurs again in the center section of the vocal fold over a length of $3L/4$. The range of the in-plane displacement was $\Delta u = 1.10\text{ mm}$.

V. CONCLUSION

The application of a three-dimensional DIC method for the non-contact and non-invasive measurements of displacement and strain fields in self-oscillating vocal folds has been described. The method was implemented and applied in the laboratory to measurements of the superior vocal fold surface of a rubber physical model. It provided time-resolved, full field measurements of several parameters of interest in phonation studies, including the out-of-plane displacements (the so-called mucosal wave height), the glottal opening displacement, as well as the strain fields corresponding to these displacements. The study demonstrates the linear dependence of subglottal pressure over mass flow rate and also the effectiveness of DIC method in estimating the strain fields. Furthermore, it was found that while the out-of-plane displacements exceed those of the in-plane displacements, the vibration amplitudes of these two degrees of freedom are similar. Stress will be obtained from measured mechanical properties of the solid in future studies. The outlook for applications in clinical studies is promising.

ACKNOWLEDGMENTS

This work was supported by grant R01 DC005788 from the National Institute for Deafness and other Communication Disorders (NIH-NIDCD).

REFERENCES

- [1] Tigges, M., et al., Proc. SPIE Vol. 2927 (1996) 209-216.
- [2] Švec, J. G., et al., J. Acoust. Soc. Am. 108 (2000) pp. 1397.
- [3] Berry, D.A., et al., J. Acoust. Soc. Am. 110(2001) pp. 2539.
- [4] Manneberg, G., et al., Opt. Eng. 40 (2001) 2041-2044.
- [5] Thomson, S. L., Ph.D. Thesis, Purdue University, 2004
- [6] Scherer, R.C., et al., J. Acoust. Soc. Am. 109 (2001) pp.1616.
- [7] Thomson, S. L., et al. MAVÉBA 2003.
- [8] Smooth-On, Inc.
- [9] Zhang, K., et al., J. Acoust. Soc. Am. (2005) submitted.
- [10] NAC Image Technology, Inc.
- [11] Chu, C.T., et al., Exp. Mech. 25 (1985) pp. 232.
- [12] Helm, J.D., Opt. Eng. 36 (1997) pp. 2361.
- [13] Correlated Solutions, Inc.
- [14] Sutton P., et al., Image Vision Comp. 4 (1986) pp. 143.
- [15] Holzrichter, J.F., et al. J. Acoust. Soc. Am. 117 (2005) pp. 1373.
- [16] de Oliveira Rosa, M., et al. J. Acoust. Soc. Am. 114 (2003) pp. 2893.

FAST FFT-BASED MOTION COMPENSATION FOR LARYNGEAL HIGH-SPEED VIDEOENDOSCOPY

Szymon Ciecwiwa¹, Dimitar D. Deliyski², Tomasz P. Zielinski¹

¹ Department of Instrumentation and Measurement, AGH University of Science and Technology, Cracow, Poland

² Department of Communication Sciences and Disorders, University of South Carolina, Columbia, South Carolina, USA

Abstract: Six methods for endoscopic motion compensation for laryngeal high-speed videoendoscopy (HSV) are compared. Two of them are based on tracking the maximum of the cross-correlation function of two images; two are based on minimization of the L_2 -norm and L_2 -like distance between two images; and the other two make use of the peak present in the cross-power FFT-based spectrum of two images. All six methods are applied to compensate the motion, at the sub-pixel level, of the endoscopic lens relative to the vocal folds in HSV recordings. The new motion compensation methods based on FFT cross-power spectrum demonstrated remarkable computational speed and acceptable accuracy. While accuracy was best for the L_2 -minimization techniques, they were slower and had a limited motion-tracking range.

I. INTRODUCTION

Sub-pixel compensation of endoscopic (camera lens) motion in high-speed videoendoscopy (HSV) is an imperative preprocessing operation making further automatic evaluation of vocal fold movement possible [1]. Endoscopic motion affects the time alignment of the HSV image pixels, which makes it difficult to track the dynamic characteristics of the laryngeal anatomic structures (Fig.1). Successful applications of HSV motion compensation (MC) techniques have been recently reported in [1], where the MC method was based on minimizing the L_2 -distortion of the smooth time differential of HSV using convolution. The results demonstrated that sub-pixel endoscopic MC is a valid, reliable, and accurate technique with immediate possibility of implementation in laryngeal HSV and that the MC technique can be further optimized for speed and performance. No other studies specifically addressing MC of HSV have been published.

This study proposed, implemented and tested several techniques, optimized for speed, as an alternative to [1]. Of particular interest is a new, and very fast, FFT-based method [2-6], which allows the estimation of the spatial shift of two similar images. The different versions of this method are compared in [7].

The problem of endoscopic MC for HSV is complex due to the dynamics of the vocal folds during phonation (Fig.1). Laryngeal HSV is essentially different from any other medical image because it registers the motion of an organ that moves very fast (70-400 Hz), affecting practically all connected tissues and creating motion

across the whole image. The motion of the connected tissues contains a fast component, comparable in speed with the vocal folds, but also slower components, some of which are comparable with the speed of the endoscopic motion (less than 15 Hz). No clear spatial outlier can show the motion relative to the camera lens located on the tip of the endoscope. Fortunately, the endoscopic motion and the changes in the glottis during phonation have different dynamics. This dynamic difference is used to build the missing outlier by computing the time differentials of the HSV image sequence pixel by pixel [1].

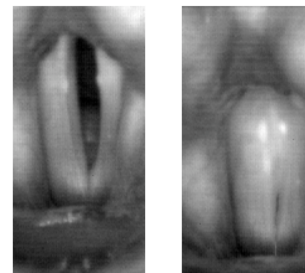


Fig. 1. Open and closed phase of the vocal folds in two different x-y positions.

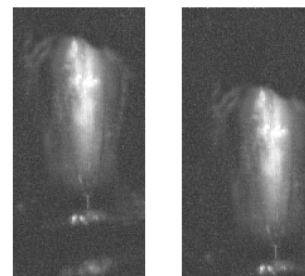


Fig. 2. Smoothed time-differential images of vocal folds in two different x-y positions.

In order to dynamically separate the fast vocal fold movements from the slow camera lens motion it is necessary to smooth the HSV. Smoothing of the time differential of the HSV image (Fig.2) has been found to be very effective when building the missing spatial outlier for endoscopic motion tracking [1]. Larger smoothing enhances MC when low-pitch or irregular vocal fold vibrations are present, however it might limit the responsiveness of the MC techniques to fast endoscopic motion.

II. METHODOLOGY

A. Motion Compensation Methods

Given that $f_1(x, y)$ and $f_2(x, y)$ are two continuous functions, in this case two images, where the second function is a shifted in space version of the first one: $f_2(x, y) = f_1(x-x_0, y-y_0)$, we can find the displacement $\{x_0, y_0\}$ making use of one of the following methods.

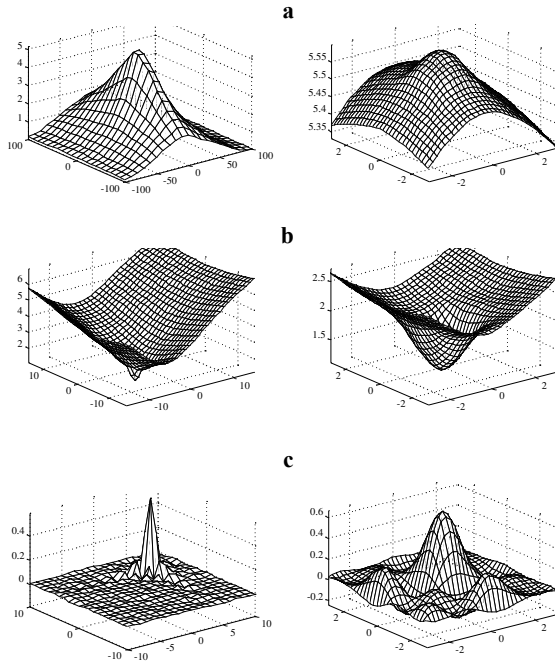


Fig. 3. Detection matrices (similarity measures) for different methods used for HSV motion detection: **left** – higher searching range; **right** – lower searching range after interpolation ($dx = a$, $dy = b$); **a**) maximum of correlation similarity; **b**) minimum of L_2 -like similarity; **c**) peak for cross-power spectrum similarity.

Correlation function methods. The classic method for $\{x_0, y_0\}$ detection relies on the properties of the convolution (cross-correlation) function of $f_1(x, y)$ and $f_2(x, y)$, which is defined as follows:

$$D_C(a, b) = \int_{-\infty}^{\infty} \int_{-\infty}^{\infty} f_1(x, y) f_2(x+a, y+b) dx dy \quad (1)$$

The function $D_C(a, b)$ reaches its maximum for $a = x_0$ and $b = y_0$. However, the maximum is flat (as shown in Fig.3a) and computation is time consuming. We can observe that $f_2(x, y)$ is shifted back by x and y dimensions by a and b , to fit the original image $f_1(x, y)$. This method can be realized by computing the convolution function of two images, which is slow. Speed optimization can be achieved by defining equation (1a) $D_{\Delta\Delta}(a, b) = D_C(a, b)$ for a limited range of a and b [1]. Such approach is appropriate when estimating small shifts within 5 pixels.

L_2 -norm and L_2 -difference minimization methods. The spatial shifts can be determined simply by minimizing

the difference between two images while artificially shifting one of them and computing a similarity measure of their difference, such as:

$$D_{|\Delta|^2}(a, b) = \int_{-\infty}^{\infty} \int_{-\infty}^{\infty} |f_1(x, y) - f_2(x+a, y+b)|^2 dx dy \quad (2)$$

$$D_{|\Delta|}(a, b) = \int_{-\infty}^{\infty} \int_{-\infty}^{\infty} |f_1(x, y) - f_2(x+a, y+b)| dx dy \quad (3)$$

where (2) represents the L_2 -norm measure of the image difference, while (3) is a L_2 -like measure known as the average magnitude difference function (AMDF). The minima of such functions are flat as it is shown in Fig.3b.

FFT-based cross-power spectrum method. It is known that Fourier spectra of images $f_1(x, y)$ and $f_2(x, y)$ are related as:

$$F_2(\omega_x, \omega_y) = F_1(\omega_x, \omega_y) \cdot e^{j(\omega_x \cdot x_0 + \omega_y \cdot y_0)} \quad (4)$$

where $F_1(\omega_x, \omega_y)$ and $F_2(\omega_x, \omega_y)$ denote Fourier transforms of both images. Since it can be shown that:

$$G_{12}(\omega_x, \omega_y) = \frac{F_2(\omega_x, \omega_y) \cdot F_1^*(\omega_x, \omega_y)}{|F_2(\omega_x, \omega_y) \cdot F_1^*(\omega_x, \omega_y)|} = e^{j(\omega_x \cdot x_0 + \omega_y \cdot y_0)} \quad (5)$$

the inverse Fourier transform of $G_{12}(\omega_x, \omega_y)$ results in:

$$g_{12}(x, y) = \text{Fourier}^{-1} [G_{12}(\omega_x, \omega_y)] \quad (6)$$

characterized by a sharp Dirac delta function centered at (x_0, y_0) (Fig.3c-left). This property is very useful for motion detection. In the discrete case above, the property still holds, and direct and inverse fast Fourier transform algorithms can be applied. Thus, the Dirac impulse takes a form of a 2D sinc function, the interpolation of which is presented in Fig.3c-right.

$$\Phi(x, y) = \frac{\sin[\pi(x+x_0)]}{\pi(x+x_0)} \cdot \frac{\sin[\pi(y+y_0)]}{\pi(y+y_0)} \quad (7)$$

The project described herein studied a variety of sub-pixel adaptations based on this method. Only the most successful two of these are presented.

Sub-pixel extensions. Similarity matrices $D_C(a, b)$ (1), $D_{\Delta\Delta}(a, b)$ (1a), $D_{|\Delta|^2}(a, b)$ (2), $D_{|\Delta|}(a, b)$ (3), and $\Phi(x, y)$ (7) can be easily interpolated as it is shown in Fig.3-right for sub-ranges $(-a_{\max}, a_{\max})$ and $(-b_{\max}, b_{\max})$ around the extrema. Adaptive strategies for changing the values of a and b can be applied.

Such strategy is to replace the interpolation of the 2D sinc Dirac impulse (7) (Fig.3c-left) with more effective techniques, as presented below.

For discrete images (4) can be presented as follows:

$$F_2(r, c) = F_1(r, c) \cdot e^{j2\pi(r \cdot \Delta r / N_r + c \cdot \Delta c / N_c)} \quad (8)$$

where r and c denote row and column index, respectively, and N_r and N_c designate number of rows and columns. Phases of these spectra are related by:

$$\Phi[F_2(r,c)] = \Phi[F_1(r,c)] + 2\pi \left[r \cdot \frac{\Delta r}{N_r} + c \cdot \frac{\Delta c}{N_c} \right]$$

or equivalently:

$$\Phi[r,c] = \Phi[F_2(r,c)] - \Phi[F_1(r,c)] = [\alpha \cdot r + \beta \cdot c],$$

where:

$$\alpha = 2\pi\Delta r / N_r, \quad \beta = 2\pi\Delta c / N_c$$

(9)

As shown, $\Phi[r, c]$ is a 2D discrete function describing a plane in 3D space (i.e. points $\Phi(r_i, c_i)$ lay on a plane). After estimation of α and β coefficients' values on this plane, we can calculate the shift between images from (9). The computation of α and β is reduced to a simple least square problem easily solvable when the values of the function $\Phi[r, c]$ are known for at least two points

$$\begin{bmatrix} r_1 & c_1 \\ r_2 & c_2 \\ \vdots & \vdots \\ r_K & c_K \end{bmatrix} \begin{bmatrix} \alpha \\ \beta \end{bmatrix} = \begin{bmatrix} \Phi(r_1, c_1) \\ \Phi(r_2, c_2) \\ \vdots \\ \Phi(r_K, c_K) \end{bmatrix} \quad (10)$$

$$\mathbf{Ax} = \mathbf{b}$$

that can be solved in a least square (LS) sense:

$$\mathbf{x} = (\mathbf{A}^T \mathbf{A})^{-1} \mathbf{A}^T \mathbf{b} = \text{pinv}(\mathbf{A}) \cdot \mathbf{b} \quad (11)$$

In Matlab language (11) is equivalent to $\mathbf{x} = \mathbf{A} \backslash \mathbf{b}$.

B. Experimental Design

Initial Testing of Basic Methods: The first step toward developing a robust MC algorithm was to test the accuracy and speed performance of the basic functions for detection of spatial shifts described in the previous section. The performance of the following basic functions was compared on artificially shifted by x and y images at different shift directions and magnitudes: *Convolution* $D_C(a, b)$ (1), *Correlation* $D_{\Delta\Delta}(a, b)$ (1a), *L2-norm* $D_{|\Delta|^2}(a, b)$ (2), *AMDF* $D_{|\Delta|}(a, b)$ (3), *FFT CP* $\Phi(x, y)$ (7), and *FFT LS* which is *FFT CP* with an LS extension replacing the interpolation. Three parameters were reported: average execution time (in ms); mean absolute error ϵ_M (in pixels by x and y); and absolute range of error ϵ_R (in pixels by x and y). These measurements do not warrant accuracy of the whole MC implementation.

MC Algorithm: The MC algorithm implemented in these experiments was the same algorithm used in [1] with the

basic functions replacing the *Convolution* function. It consists of the following main steps: (i) Establishing dynamic vocal fold outliers for MC by computing pixel by pixel the time differentials of the HSV image sequence; (ii) Eliminating the high-frequency components of the vibrating vocal folds via smoothing; (iii) Suppressing the effect of the boundary discontinuities of the image frames (only necessary for *Convolution*); (iv) Detecting the displacement between adjacent frames by using one of the six methods; (v) Computing the displacement vectors (motion trajectories); (vi) Subtracting the motion trajectories from the spatial coordinates of the original HSV image using two-dimensional spline interpolation.

Performance on Simulated Motion: To assess the accuracy in extreme conditions, the MC method was tested on simulated data with known motion trajectories. These data are identical to and described in more detail in [1]. Although the proposed methods are expected to work better for lower motion frequencies, these data allow for a thorough testing in extreme conditions, in which all frequencies of the covered range 0.1 to 15 Hz are equally represented. The data consisted of 2-second long (4000 frames) HSV movies with exactly known motion trajectories. Motion varied from 0 to 8 pixels by x and y in nine different magnitudes. Two types of motion curves, a random and a cyclic, were added to two real HSV recordings, one of a male and one of a female speaker, totaling 34 HSV recordings with simulated motion. The data were analyzed by each modified technique. The following parameters were reported: average speed of computation S_C (in seconds per one second of HSV data); mean absolute error ϵ_M and absolute range of error ϵ_R (in pixels) as defined in [1]. Assessing the MC method on data with simulated motion was important to show whether the detected trajectories really correspond to motion and to assess the accuracy of the method in extreme motion conditions with known characteristics.

Performance on Real Motion: Testing the MC methods on real HSV data is important to account for factors unaccounted for in simulated motion such as nonuniform illumination, quality of the image, scaling, camera artifacts, and differences in glottal shapes, which are likely to affect the reliability of MC. The error is computed by iterating the MC process since the estimated motion trajectory at the second iteration is the residual motion not compensated for during the first iteration.

III. RESULTS AND DISCUSSION

Basic Methods: The results obtained from testing the basic MC methods are presented in Table 1. The FFT-based techniques were found to be several times faster relative to the correlation and L_2 -based techniques. L_2 -

norm and *FFT LS* were found to be the most accurate. Additional observations include: noise was not found to be destructive for tracking shifts, and all methods except for *FFT CP* were more sensitive to horizontal movement, since vocal folds are vertical.

Table 1: Comparison of accuracy and speed of the newly implemented basic methods for motion compensation.

MC method	Time [ms]	\mathbf{e}_M [pixels]		\mathbf{e}_R [pixels]	
		by x	by y	by x	by y
<i>Convolution</i>	2700	0.07	0.07	0.16	0.12
<i>Correlation</i>	380	0.14	0.09	0.51	0.15
<i>L₂-norm</i>	460	0.09	0.07	0.24	0.13
<i>AMDF</i>	460	0.20	0.17	0.27	0.21
<i>FFT CP</i>	140	0.23	0.22	0.52	0.57
<i>FFT LS</i>	60	0.08	0.07	0.40	0.22

Data with Simulated Motion: The results from testing the MC algorithms on simulated motion are shown in Table 2. They generally agree with the results from testing the basic methods. All MC methods demonstrated satisfactory sub-pixel accuracy and all alternative techniques were significantly faster relative to *Convolution*.

Table 2: Accuracy (average with range in parentheses) and speed of computation results from testing six MC algorithms on 34 HSV samples with simulated motion.

MC method	S_C [s/s]	\mathbf{e}_M [pixels]	\mathbf{e}_R [pixels]
<i>Convolution</i>	513.306	0.168 (0.000-0.331)	0.380 (0.000-0.931)
<i>Correlation</i>	33.556	0.064 (0.000-0.181)	0.221 (0.000-0.664)
<i>L₂-norm</i>	35.259	0.064 (0.000-0.181)	0.221 (0.000-0.664)
<i>AMDF</i>	34.430	0.069 (0.000-0.188)	0.229 (0.000-0.677)
<i>FFT CP</i>	14.039	0.091 (0.000-0.351)	0.538 (0.000-2.904)
<i>FFT LS</i>	7.644	0.272 (0.002-0.577)	0.606 (0.003-2.241)

Correlation, *L₂-norm* and *AMDF* had almost identical performance and best accuracy of all methods. Their mean absolute error was 0.065 pixels and their speed of computation was 15 times higher relative to *Convolution*. The serious disadvantage of these three methods is their limited range of shift tracking, which limits their implementation for certain types of HSV material. They would have difficulties with recordings including phonatory breaks, vocal offsets and onsets, or intermittent obstructions in the view of the vibrating vocal folds, making it difficult to recover when visible vibration resumes. *Convolution*, *FFT CP* and *FFT LS* do not have this limitation.

The fastest methods were *FFT LS* and *FFT CP* outperforming *Convolution* 67 and 37 times, respectively. The accuracy of these two methods was lower but still acceptable at the sub-pixel level. The increased error was mainly due to the extreme frequency testing conditions to which the methods were subjected. Considering the exceptional robustness of the *FFT LS* method, further investigation is necessary to understand and eliminate the sources of errors in order to build a practical tool for motion compensation, which is highly necessary.

Data with Real Motion: A limited testing on real clinical HSV recordings (14 samples) was performed. Results were consistent with the data from Table 2. Speed ratios and accuracy data were found to be in the same proportions. On the 2nd iteration the residual errors were found to be smaller relative to the data with simulated motion. As expected, *Correlation*, *L₂-norm* and *AMDF* could not track over shifts including voice offsets, onsets and breaks, while *Convolution*, *FFT CP* and *FFT LS* could. No instances of data degradation were reported up to the 4th iteration for *Convolution*, *FFT CP* and *FFT LS*.

IV. CONCLUSION

The fast FFT-based approach has been applied successfully for the endoscopic motion compensation in HSV recordings of vocal folds. Results demonstrated that application of the FFT-based cross-power spectrum approach is highly beneficial: the method is 67 times faster than the convolution-based approach and offers acceptable sub-pixel accuracy. Further improvement of accuracy is possible and testing on a large dataset of real HSV recordings is recommended.

REFERENCES

- [1] D. Deliyski: "Endoscope Motion Compensation for Laryngeal High-Speed Videoendoscopy," *Journal of Voice*, vol. 19, no. 3, pp. 485-496, 2005.
- [2] H. Shekarforoush, M. Berthod, J. Zerubia: "Subpixel Image Registration by Estimating the Polyphase Decomposition of the Cross Power Spectrum," *Int. Conf. on Computer Vision and Pattern Recognition*, 1996.
- [3] H. Foroosh, J. Zerubia, M. Berthod: "Extension of phase correlation to sub-pixel registration," *IEEE Trans. on Image Processing*, vol. 11, no.3, pp. 188-200, 2002.
- [4] H. Stone, M. Orchard, E.-C. Chang, S. Martucci: "A fast direct Fourier-based algorithm for subpixel registration of images," *IEEE Trans. on Geo. and Remote Sensing*, vol. 39, no. 10, pp.2235-2243, Oct. 2001.
- [5] Y. Keller, A. Averbuch: "A projection-based extension of the phase correlation method," submitted to the *IEEE Transactions on Signal Processing*, 2005.
- [6] H. Tuo, L. Zhang, Y. Liu: "An FFT-based registration methods for images from different bands," *Int. Conf. on Information Technology & Applications iCITA'05*, Sidney 2005
- [7] V. Argyriou, T. Vlachos: "Using gradient correlation for sub-pixel motion estimation of video sequences," *IEEE Int. Conference on Acoustics, Speech and Signal Processing ICASSP-2004*, Montreal 2004.

VERTICAL MOTION DURING MODAL AND PRESSED PHONATION: MAGNITUDE AND SYMMETRY

Heather S. Shaw, Dimitar D. Deliyski

Department of Communication Sciences and Disorders, University of South Carolina, Columbia, South Carolina, USA

Abstract: Vertical motion of the vocal folds during phonation is a possible diagnostically significant feature. However, it is difficult to judge vertical motion through the typical two-dimensional stroboscopic display. Through high-speed videoendoscopy (HSV), the dynamics of vocal fold vibration are easier to appreciate; however, the traditional HSV is also two-dimensional. Recently, a method to display a three-dimensional (3D) image of vocal fold vibration was published. This method, as well as stroboscopy and HSV, was utilized to study vertical motion magnitude and symmetry during modal and pressed phonations in normophonic speakers. Vertical motion judgments were rated as at least 16% more possible from the HSV-derived playbacks than from stroboscopy. The assessments from the 3D playback were different than those from the two-dimensional HSV playback for magnitude, however a similar trend was realized. The findings demonstrate consistently greater magnitudes of vertical motion during pressed phonations. Asymmetry of vertical motion was appreciated in both modal and pressed phonations. The results of this study concur with the concept of increased vertical motion during pressed phonation and recommend further investigations of the typicality of this important feature of vocal fold vibration in various modes and registers of normal and pathologically influenced phonation.

I. INTRODUCTION

Visualizing vocal fold vibratory behavior is widely accepted as an integral part of a complete voice evaluation. This vibratory behavior is known to move in three dimensions: laterally, longitudinally, and vertically. The lateral movement of vocal fold vibration is the most widely discussed and utilized in clinical voice evaluations as an indication of vocal fold stiffness. The longitudinal motion of vocal fold vibration has begun to be investigated and used as part of the clinical visualization protocol. However, the normal limits of variation in longitudinal motion remain unclear. The third dimension of vocal fold vibration, vertical motion is not a common feature rated during the stroboscopic evaluation. While furthering our knowledge of lateral and longitudinal vocal fold vibratory deviations and their prevalence in various disorders is an important task, this paper narrows its scope to investigating the vertical motion of vocal fold vibration.

Vertical motion of vocal fold vibration has been suggested to have an increased magnitude during pressed or heavy phonations [1]. Hirano has related pressed phonation to be a result of the contraction of the thyroarytenoid muscle and relaxation of the vocal ligament [2]. This relation of the physiological components has been furthered to provide the concept that the relaxed vocal ligament may lead to an increase in pliable tissue, which may then be prone to move vertically during pressed phonation [1]. Conversely, less vertical motion may be appreciated during modal and, especially, falsetto phonations due to increased tension in the vocal ligament.

An increase in vertical motion during pressed phonation is a suggested contributing factor in the vocal fold pathologies of nodules and varices [1,3,4]. Pressed phonation is often realized in persons with voice disorders characterized by strain and muscle tension dysphonia. Given the relation between these common features of functional voice disorders and pressed phonation, it is natural to continue the investigation of vertical motion by studying the vibratory patterns during differing modes of phonation.

An in-depth paper on the presence and hypothetical detrimental impact of vertical motion in vocal fold vibration was accomplished [1]. The increase of vertical motion in pressed versus falsetto phonation was demonstrated, as was the intra-cycle variability of vertical motion during pressed phonation. These findings for vertical motion rely on visualization techniques, such as HSV, that provide true intra-cycle information.

Studies of the medial surface of the vocal folds in excised larynges using HSV have allowed for the observation of the vertical motion of vocal fold vibration from a view not achievable clinically [5,6]. Within such investigations, the presence of lateral, longitudinal, and vertical components of vocal fold vibration have been documented and relatively quantified. The variation of subglottal and supraglottal pressure as well as vocal fold tension has been noted to impact these components of vocal fold vibration in excised larynges.

While vertical motion appears to be a fundamental feature of vocal fold vibration, the difficulty of rating a three-dimensional behavior with intra-cycle variations from stroboscopy, a two-dimensional representation without intra-cycle information, remains. Recently, a comprehensive set of representations and image

processing techniques to extract significant vocal fold features from HSV images was introduced [7]. Of particular interest to this paper is the vertical motion display, which allows for the observation of vertical motion from a three-dimensional (3D) playback. This technique capitalizes on the fact that the pixel intensity of the image is a quadratic function of the distance between the vocal folds, and the light source and camera lens. Thus, allowing pixel intensity to provide information regarding vertical motion. The specific implementation of the 3D display was presented at the Voice Foundation Symposium in June 2005.

The purpose of this study is to provide a preliminary investigation of the vertical motion inherent in vocal fold vibration. The research questions to achieve this goal were:

1. Can vertical motion be assessed through a three-dimensional display?
2. What is the variation in vertical motion and vertical level of approximation for normophonic speakers?
3. Does the amount of vertical motion vary with mode of phonation?

II. METHODOLOGY

Participants: Fifty-two vocally normal participants ranging in age from 18-65 years old were recruited from Columbia, SC and Charlotte, NC. Twenty-four male and twenty-eight female participants were divided among three age ranges, 18-33, 34-49, and 50-65. The data collection, storage, and use were in accordance with human subjects regulations. The data for this study was recorded at Presbyterian Hospital's Voice Center in Charlotte, NC. The speech-language pathologists involved with data collection were specifically trained in voice and followed a specified protocol. During the process of accepting participation in the study through the informed consent form, the participants completed a short medical and voice history, as well as a modified voice quality self-assessment. Speech-language pathologists utilized the history, self-assessment, and perceptual judgment to determine vocal normality.

Instrumentation and Procedures: Stroboscopy and HSV were utilized during data collection. Data collection from new methods and those routinely used in the clinic allowed for a comparison between assessment methods. Data collection occurred in quiet rooms typically employed for the assessment of voice patients in the hospital clinic.

Endoscopy and Stroboscopy: Standard clinical procedures were utilized for endoscopy and stroboscopy. The locating of the vocal folds and the initial phonation were conducted with continuous halogen light. Stroboscopy was used to capture phonation at habitual

pitch and loudness allowing both intensity and frequency to be controlled for during each sample. A Kay Elemetrics Rhino-Laryngeal Stroboscopic system Model 9100B coupled to a 70-degree rigid endoscope was used. A laryngeal contact microphone was utilized to track vocal fold vibratory frequency.

High-Speed Videoendoscopy: Kay Elemetrics High-Speed Video System Model 9700 equipped with a camera that captured 2,000 frames per second with 120 x 256 pixel resolution was utilized. A 70-degree rigid endoscope (Kay Elemetrics Model 9106), the same as that used in the above described procedures, and a 300 W constant Xenon light source (Kay Elemetrics Model 7152) were coupled with the system. The recording of HSV was synchronized with the acoustic recording, captured via a head-mount condenser microphone, to allow for comparisons between physiological and acoustic events. Participants were instructed to phonate the vowel /i/ at habitual pitch and during pressed phonation. To achieve pressed phonation, participants were asked to phonate "as if lifting a heavy box". The speech-language pathologists also provided models of pressed phonation.

The HSV images were processed for motion compensation [8] and removal of reflection spots resulting in the HSV playback. Subsequently, the 3D playback movie, a multi-colored image relating to the extent of vertical motion of the vocal folds, was produced, as seen below in Fig. 1.

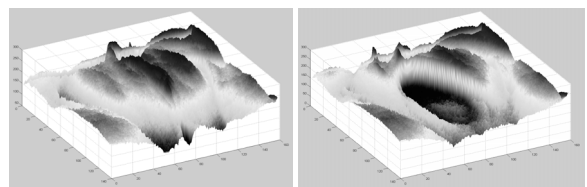


Fig. 1. Three-dimensional graphic representations of a closed and open phase within a single glottal cycle.

Visual Perceptual Judgments: Visual perceptual parameters were developed to assess vertical motion from the three playbacks, stroboscopy, HSV playback, and the 3D playback. Two voice scientists perceptually evaluated the dynamic visual images obtained from the fifty-two participants. The recordings of habitual phonation from the three playbacks amounted to 156 images that were judged by each perceptual rater. From HSV and 3D playbacks, 104 pressed phonation recordings were also rated. Twenty percent of the recordings were randomly introduced into the data set to obtain intra-rater reliability. Therefore, both perceptual raters judged 312 images for the features of vertical motion and vertical level of approximation. The entire data set was randomized prior to perceptual ratings.

Vertical motion was assessed for *presence* or *absence*, *magnitude*, and for left-to-right vocal fold *symmetry* of

magnitude through stroboscopy, HSV playback, and 3D playback. *Magnitude* of vertical motion was rated, separately for the left and right vocal folds, on a six-point scale, with 0=absent, 1=severely decreased, 2=moderately decreased, 3=typical, 4=moderately increased, and 5=severely increased. *Presence* of vertical motion was understood if the magnitude was assigned a rate of 1-5. Vertical motion *symmetry* was calculated by the differences in magnitude ratings. If the ratings of the left versus right vertical motion magnitude differed, then the vertical motion magnitude was considered asymmetrical. Additionally, *vertical level of approximation* and *ability to judge* vertical motion from the images were rated categorically, as present or absent and able to judge or not able to judge, respectively.

Statistical Analysis: Measures from the visual-perceptual judgment of the stroboscopic, HSV, and 3D playbacks were compared. The instances and percentage of typical and atypical ratings were calculated. Correlation and paired t-tests were employed to determine intra-rater and inter-rater reliability. A correlation of above 0.70 and/or an alpha level above 0.20 on a paired t-test was considered to demonstrate a substantial reliability. An alpha level above 0.20 was utilized to determine the lack of statistically significant variation between and within the perceptual raters.

III. RESULTS

Presence of vertical motion was noted bilaterally in stroboscopy, HSV, and 3D playbacks for all instances of modal and pressed phonations. No cases of unilateral or absent vertical motion were rated from the recordings of vocal fold vibration from normophonic speakers. No differences between stroboscopy, HSV, or the 3D playbacks was realized.

The *magnitude* of vertical motion was rated as typical during modal phonation for 60, 49, and 54% of playbacks for stroboscopy, HSV, and 3D playbacks, respectively. For pressed phonation, magnitude of vertical motion was less likely to be rated as typical, 34 and 42% of cases for HSV and 3D playbacks. Reduced vertical motion was realized in 15, 13, and 25% of modal phonations as visualized through stroboscopy, HSV, and the 3D playbacks. While during pressed phonations, vertical motion was appreciated to be reduced in only 10 and 14% of HSV and 3D playbacks. Increased vertical motion was apparent in 25, 38, and 21% of visualizations of modal phonation as displayed by stroboscopy, HSV, and 3D playbacks. Pressed phonations visualized through HSV and 3D playbacks were rated as having increased vertical motion in 56 and 44% of cases.

Asymmetry of vertical motion magnitude was noted in 22, 27, and 12% of modal phonations visualized through stroboscopy, HSV, and 3D playbacks. For pressed phonation, 22 and 14% of recordings were perceived as

revealing asymmetrical magnitudes of vertical motion when viewed by HSV and 3D playbacks.

Vertical level of approximation was rated as unequal in 14.5, 11, and 14% of modal phonations as viewed by stroboscopic, HSV, and 3D playbacks. Similarly, for pressed phonations 11 and 14% of cases rated from HSV and 3D playbacks had perceivably unequal vertical levels of approximation.

The *ability to judge* vertical motion was calculated from each of the three playbacks. The raters reported not being able to judge vertical motion for 19% of stroboscopic files, 3% of 3D playback files, and 1% of HSV playback files. Files rated as not able to be judged were excluded from presence, magnitude, symmetry, and vertical level results.

Intra-rater reliability, as assessed by correlation and t-tests, was moderate to high for HSV playback and stroboscopy over both pressed and modal phonation, ranging from 0.52 to 0.94. For correlations below 0.70, the t-test had a p-value above 0.30 with the exception of symmetry rated from stroboscopy by judge 2. Correlation and t-tests revealed lower intra-rater reliability for judgments of magnitude from the 3D playback. Inter-rater reliability as assessed through percent agreement within one scalar level ranged from 87 to 100%, with a mean of 96.5%.

IV. DISCUSSION

Presence of vertical motion was apparent throughout all evaluations of normophonic speakers. Presence was equally likely during modal and pressed phonations. Additionally, the three types of displays viewed were equally sensitive and specific to the presence of vertical motion. Given the consistency of vertical motion presence in normophonic speakers, it would be interesting to ascertain whether persons with voice disorders, especially those resulting from or resulting in decreased vocal fold mucosa pliability, demonstrate a similar consistency.

Magnitude of vertical motion was rated as typical for 58% of the images across all displays for modal phonation, and for 57% of the images rated from the two HSV-derived playbacks. These centralized ratings give credence to the ability to judge the vibratory feature of magnitude of vertical motion for normophonic speakers and the ability to utilize the ratings for preliminary estimates of the typicality of magnitude variations. The majority of participants exhibited increased magnitude of vertical motion during pressed phonations. However, normophonic speakers also demonstrated typical or decreased vertical motion during pressed phonation. Typical or decreased vertical motion may have been the result of achieving the vocal quality of pressed phonation by manipulating the laryngeal mechanism differently. Since increased medial compression of the vocal folds

from the contraction of the thyroarytenoid muscles would lead to an increased amount of pliable tissue, with the inclusion of the vocal ligament available to move vertically, it may be hypothesized that decreased medial compression with increased respiratory volume was utilized.

While *symmetry* of vertical motion magnitude has not been specifically discussed in the literature, a number of articles have discussed lateral and longitudinal asymmetries. Given the possible significance of vertical motion, assessing asymmetry allows for a more comprehensive view of vibratory behavior. The results indicate that an average of 19% of normophonic speakers exhibited asymmetry of vertical motion. The cause of variation in ratings from the 3D playback, versus the stroboscopic and HSV playback should be further explored. It is likely that the added dimension, allowing for increased accuracy when judging vertical motion, and the novelty of the 3D playback are the causes of the differences.

Vertical level of approximation was found to be unequal for at least 11% of normophonic speakers in modal and pressed phonations. A difference of 3.5% was noted between the playbacks. Vertical level was perceived as unequal more often from the 3D playback than for the HSV playback. This may be related to the additional information available from the 3D playback and the subsequent ability of the raters to use the information when making judgments of vertical level. The prevalence of unequal vertical level in normophonic speakers was unexpected.

The relatively large amount of recordings rated as not *able to be judged* from the stroboscopic as compared to the other playbacks is indicative of the difficulty of rating this vibratory feature through stroboscopic playbacks. This difference in ability to judge vertical motion is likely due to the fact that stroboscopy does not provide true intra-cycle information. This difficulty is highlighted by the clinical lack of reporting and utilization of vocal fold vertical motion as an indicator of laryngeal function. The widely used visual-perceptual vocal fold rating protocols include vertical level of approximation, but not vertical motion. Perhaps clinically important information is being disregarded.

V. CONCLUSION

The increased magnitude of the vertical motion of vocal fold vibration during pressed phonation for normophonic speakers strengthens the hypothesis of the detrimental impact of this type of phonation on the vocal fold tissue. There is undoubtedly additional information regarding vocal fold vibration available through the study of vertical motion. It is important to understand the typicality and variation of vertical motion for normophonic speakers as well as persons with laryngeal

pathology through the clinical perspective of videoendoscopy, as well as to further investigate vertical motion using excised larynges.

Given the results of presence, magnitude, and asymmetry of vertical motion of vocal fold vibration, the clinical significance of these findings is compelling. An additional feature of vocal fold vibration that provides insight into the pliability of the vocal fold mucosa would be valuable. The finding of unequal vertical level of approximation in normophonic speakers questions the typicality of variation in vertical level. Further research to ascertain the normal limits of vertical level differences should be undertaken. Additionally, further investigation of the influence of mode and register of phonation on vertical motion should be conducted. Studying the effect of manipulating subglottal pressure during these productions in vivo will increase our knowledge of the mechanisms driving vertical motion during phonation. Since observing vertical motion is reliant on the ability to visualize intra-cycle information, it is likely that technological advancements leading to the ability to capture vocal fold vibration at higher frame rates would be beneficial. Refinement of the 3D playback to eliminate the artifacts of light reflection is also necessary.

REFERENCES

- [1] A. Sonninen, and A. Laukkanen, "Hypothesis of whiplike motion as a possible traumatizing mechanism in vocal fold vibration," *Folia Phoniatica et Logopaedica*, vol. 55, 189-198, 2003.
- [2] M. Hirano, "Vocal mechanisms in singing: Laryngological and phoniatic aspects," *Journal of Voice*, vol. 2, 51-69, 1998.
- [3] I. Hochman, R.E. Hillman, R.T. Sataloff, S.M. Zeitels, "Ectasias and varices of the vocal fold: Clearing the striking zone," *Annals of Otolaryngology, Rhinology, and Laryngology*, vol. 108, 10-16, 1999.
- [4] P. Grey, "Microlaryngostroboscopy and 'singers nodes'," *Journal of the Otolaryngological Society of Aust*, vol. 3, 525-527, 1973.
- [5] D.A. Berry, D.W. Montequin, and N. Tayama, "High-speed digital imaging of the medial surface of the vocal folds," *Journal of the Acoustical Society of America*, vol. 110 (5), 2539-2547, 2001.
- [6] I.R. Titze, J.J. Jiang, and T.Y. Hsiao, "Measurement of mucosal wave-propagation and vertical phase differences in vocal folds vibration," *Annals of Otolaryngology Rhinology and Laryngology*, vol. 102(1), 58-63, 1993.
- [7] D.D. Deliyski, and P.P. Petrushev, "Methods for Objective Assessment of High-Speed Videoendoscopy," *Proceedings: 6th International Conference: Advances in Quantitative Laryngology, Voice and Speech Research AQL-2003, Hamburg, Germany*, 28, 1-16, 2003.
- [8] D.D. Deliyski, "Endoscope motion compensation for Laryngeal High-Speed Videoendoscopy," *Journal of Voice*, vol. 19(3), 485-496, 2005.

MUCOSAL WAVE MAGNITUDE: PRESENCE, EXTENT, AND SYMMETRY IN NORMOPHONIC SPEAKERS

Heather S. Shaw, Dimitar D. Deliyski

Department of Communication Sciences and Disorders, University of South Carolina, Columbia, South Carolina, USA

Abstract: Visualization of the vocal fold structure and function is imperative for accurate diagnoses and optimal treatment for persons with voice disorders. With the advent of commercial High-Speed Videendoscopy (HSV) systems, an increased amount of variation has been appreciated in the diagnostically relevant features of mucosal wave presence, magnitude, and symmetry. This study presents findings from the assessment of mucosal wave from stroboscopy, HSV playback, mucosal wave playback, and mucosal wave kymography playback. The results from this study demonstrate the prevalence of features of 'atypical' mucosal wave during modal productions of /i/ by normophonic persons. Utilizing modal and pressed phonations, an increased understanding of the effect of medial compression and increased subglottal pressure on mucosal wave was realized.

I. INTRODUCTION

One diagnostically significant feature of vocal fold vibration is the mucosal wave. The mucosal wave is the propagation of the epithelium and superficial layer of the lamina propria from the inferior to the superior surface of the vocal folds during phonation. A typical mucosal wave, as viewed through stroboscopy, should travel one-half of the width of the superior surface of the vocal fold during modal phonation [1]. The mucosal wave of vocal fold vibration is an accepted indicator of tension and pliability of the vocal fold tissue. The mucosal wave is usually reduced during high pitch phonations due to the excessive tension on the tissues. A reduced mucosal wave during modal phonation signifies stiffness, which may result from a lesion, edema, or scar. Conversely, a larger than normal mucosal wave signifies flaccidity of the laryngeal musculature underlying the vocal fold tissue, possibly indicating paresis or muscle atrophy due to aging. Thus, the importance of assessing mucosal wave during functional evaluations and for medical diagnoses is evident. For example, mucosal wave has been the sole feature of vocal fold vibration that could provide visual information upon which cysts and polyps could be differentiated [2].

The characteristics of normal mucosal waves have been investigated via stroboscopy. Multiple research articles have included mucosal wave as a dependent variable to answer various questions regarding normal and pathological vocal fold movement. Two main areas of research have investigated the impact of vocal fold

elongation, such as that seen in high frequency productions, and the impact of variations in subglottal pressure on mucosal wave magnitude and velocity.

Of interest is a conclusion regarding the typicality of lateral phase of mucosal wave symmetry in normophonic speakers in [3]. The results of reviewing fifty-seven videostroboscopic laryngeal examinations indicated that asymmetry was appreciated in 10.5% of normophonic participants during modal and falsetto phonations and in 36.5% of participants during falsetto phonations only. The conclusion was that the degree of magnitude and not merely presence of asymmetry should be considered the diagnostically significant feature. This conclusion leads to the necessity of further investigation of the symmetry and magnitude of mucosal waves.

The findings of a prevalent 'normal' amount of asymmetry may lead to an increase in over-diagnoses of laryngeal pathology, unless the typicality of variation is understood. Additionally, there is a possibility that symmetrical mucosal waves with supposed atypical magnitude may be present in persons with and without laryngeal pathologies. This finding would modify the conclusions from [3,4]. Given the prevalence of asymmetry seen in stroboscopic images and the increased amount of laryngeal dynamics visible through HSV, it is intuitive that an even larger population of normophonic speakers would have apparent variations in mucosal wave as viewed through HSV in comparison to stroboscopy.

Preliminary studies of the horizontal and vertical displacements, velocity, and vertical phase of the mucosal wave have been accomplished utilizing excised canine larynges [5,6,7]. The results are commensurate with the findings from in vivo human stroboscopic studies of mucosal wave. No further investigations of the typicality of variation in mucosal magnitude or symmetry have been published.

The purpose of this research was to investigate the normality of variation of mucosal wave presence, magnitude, and symmetry and to compare modal and pressed phonation across these features. The specific research questions were:

1. What is the variation in mucosal wave magnitude for normophonic speakers?
2. What degree of mucosal wave magnitude asymmetry can be appreciated in normophonic speakers?
3. How do the features of mucosal wave compare across modal and pressed phonations?

II. METHODOLOGY

Participants: Fifty-two vocally normal participants ranging in age from 18-65 years old were recruited from Columbia, SC and Charlotte, NC. Twenty-four male and twenty-eight female participants were divided among three age ranges from 18-33, 34-49, and 50-65. The data collection, storage, and use were in accordance with human subjects regulations. The data for this study was recorded at Presbyterian Hospital's specialized voice center in Charlotte, NC. The speech-language pathologists involved with data collection were specifically trained in voice. During the process of accepting participation in the study through the informed consent form, the participants completed a short medical and voice history, as well as a modified voice quality self-assessment. Speech-language pathologists utilized the history, self-assessment, and perceptual judgment to determine vocal normality.

Instrumentation and Procedures: Data collected for this study included: information from case history reports, stroboscopy, and high-speed videoendoscopy (HSV). Data collection from methods routinely used in the clinic and those that are new, allowed for a comparison between assessment methods. Data collection occurred in quiet rooms typically employed for assessment of voice clients in the hospital clinic.

Endoscopy and Stroboscopy: Standard clinical procedures were utilized for endoscopy and stroboscopy. The locating of the vocal folds and the initial phonation were conducted with continuous light. The stroboscopic light was used to capture phonation at three different pitch levels, habitual, low, and high, held at a near-constant intensity. The participants were asked to phonate at their habitual loudness while varying their pitch over samples. This allowed both intensity and frequency to be controlled for during each sample. A Kay Elemetrics Rhino-Laryngeal Stroboscopic System Model 9100B coupled to a 70-degree rigid endoscope was used. A laryngeal contact microphone was utilized to track vocal fold vibratory frequency.

High-Speed Videoendoscopy: Kay Elemetrics High-Speed Video System Model 9700 equipped with a camera that captures at 2000 frames per second (fps) with 120 x 256 pixel resolution was utilized. High-speed cameras require an intense light source for visualization of the vocal folds to be realized. A 70-degree rigid endoscope (Kay Elemetrics Model 9106), the same as that used in stroboscopy and a 300 W constant Xenon light sources (Kay Elemetrics Model 7152) were coupled with the system. The recording of HSV was synchronized with the acoustic recording, captured via a head-mount condenser microphone, to allow for comparisons between physical and acoustic events. Participants were instructed to phonate /i/ at habitual pitch and during pressed

phonation. To achieve pressed phonation, participants were asked to phonate "as if lifting a heavy box". Additionally, auditory examples of pressed phonation were provided.

Image Processing: Image processing included: motion compensation [8] and removal of reflection spots. These pre-processing techniques allowed for valid and accurate results from the kymographic playbacks. The compensation techniques were necessary to secure that anatomical structures subjected to kymography are time-aligned. It has been noted that if endoscope motion is unaccounted for it may affect the validity of the data [9]. The image processing techniques allowed for the evaluation of mucosal wave from the visual image.

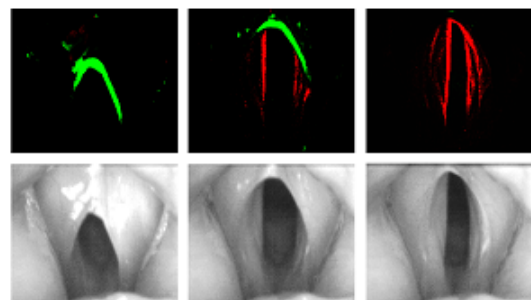


Fig. 1. Frames of Mucosal Wave (MW) playback (top) at different phases of the intra-glottal cycle and the corresponding HSV frames (bottom). The opening phase velocity on the MW images is encoded in shades of green, and the closing phase velocity is displayed in red.

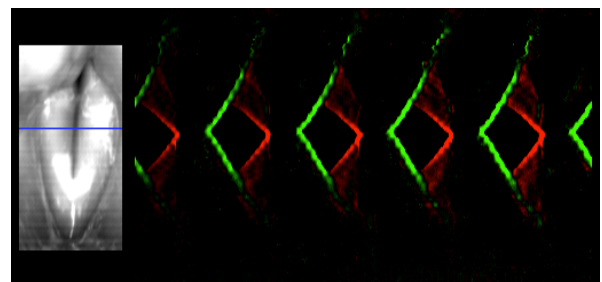


Fig. 2. Mucosal Wave Kymography (MKG) of consecutive glottal cycles during sustained phonation. The mucosal wave extent appears as a double edge during the closing phase.

Images were obtained using both stroboscopy and HSV. From stroboscopy, one image, the stroboscopy playback was rated. Stroboscopy provides a view of mucosal wave without true cycle-to-cycle information. From HSV, three playbacks were rated: the high-speed videoendoscopy playback, the mucosal wave (MW) playback, and the mucosal wave kymography (MKG) playback. HSV playback was defined as the typical

playback of the recording after motion compensation. The HSV playback provided a view of mucosal wave, which allowed for the visualization of true cycle-to-cycle information. Playback of the image with the mucosal wave highlighted in green for opening phase and red for closing phase was defined as MW playback (Fig. 1). The MW playback utilized velocity, encoded as intensity, to highlight the medial edges of the vocal folds and possibly provide easier magnitude ratings. The image from the mucosal wave playback presented as a movie from posterior to anterior was termed MKG playback. The MKG playback provides a view in which mucosal wave propagation and magnitude variations in the time domain may be more easily judged (Fig. 2).

Visual Perceptual Judgments: The motion images obtained from the fifty-two participants were visually evaluated and rated for specific features of the mucosal wave by two voice specialist. Images from fifty-two participants in four different views for two modes of phonation amounted to 394 images that were rated. In addition, 20% of the images were randomly repeated to obtain intra-rater reliability. Therefore, a total of 473 images were judged for features of mucosal wave.

Mucosal wave magnitude was rated, separately for the left and right vocal folds, on a six-point scale, with 0=absent, 1=severely decreased, 2=moderately decreased, 3=typical, 4=moderately increased, and 5=severely increased. Presence of mucosal wave was understood if the magnitude was assigned a rate of 1-5. Mucosal wave asymmetry was calculated by the differences in magnitude ratings. If the ratings of the left versus right mucosal wave magnitude differed, then the mucosal wave magnitude was considered asymmetrical. Mild asymmetry was characterized by a rating difference of one-point, moderate asymmetry by a difference of two-points, severe asymmetry by a difference of three-points, and profound asymmetry by a difference of four or more points.

III. RESULTS

The results for bilateral presence of mucosal wave, mucosal wave magnitude of the right and left vocal folds, and symmetry of mucosal wave magnitude are displayed in Tables 1-3, respectively.

	Strobe	HSV	MW	MKG
Habitual	79	72	66	65
Pressed		79	88	71

Table 1. Mean percent of recordings rated as having present mucosal wave bilaterally.

	Rating	Strobe	HSV	MW	MKG
Right	Typical	24	14	14.5	13
	Decreased	61	49	58	55
	Increased	5	4	2	2
Left	Typical	32	15	17	10.5
	Decreased	60	39	58	50
	Increased	5	5	3	2

Table 2. Mean percent of habitual phonation recordings rated as having typical, decreased, or increased mucosal wave magnitude for the right and left vocal folds.

	Rating	HSV	MW	MKG
Right	Typical	14	16	15
	Decreased	40	58	53
	Increased	13	4	26
Left	Typical	20	25	16
	Decreased	45	58	50
	Increased	11	4	2

Table 3. Mean percent of pressed phonation recordings rated as having typical, decreased, or increased mucosal wave magnitude for the right and left vocal folds.

	Rating	Strobe	HSV	MW	MKG
Habitual	Asymmetrical	24	27	21	21
	(Mild)	(7)	(23)	(19)	(18)
Pressed	Asymmetrical		39	37	21
	(Mild)		(39)	(33)	(19)

Table 4. Mean percent of recordings rated as displaying any asymmetry of mucosal wave magnitude, and mean percent of recordings rated as displaying only mild asymmetry of mucosal wave magnitude.

Intra-rater reliability was judged high with a mean agreement of 94.8 and 93.8% for raters 1 and 2, respectively. Inter-rater reliability was similarly high with percent agreement within one scalar level of 82, 88, 91, and 73% for HSV, MW, MKG, and stroboscopy. Due to these results, the mean ratings were reported for presence, magnitude, and symmetry.

IV. DISCUSSION

Mucosal wave absence was noted for at least 22% of vocal fold vibration samples from normophonic speakers across all displays, as seen in Table 1. Whether the playback viewed was kymographic or not appeared to decrease the ratings of presence from habitual phonation samples by at least 8%. Ratings of pressed phonation demonstrated an increase in likelihood of allowing for the visualization of mucosal wave. The limitation of 2000 fps capturing of the HSV images can help to explain the absence of mucosal wave noted via HSV-derived playbacks. However, a similar absence of mucosal wave was noted via stroboscopy.

The narrow definition of mucosal wave used for this experiment was inclusive only of the differential between the lower and upper margins of the vocal fold. Since ratings of absent mucosal wave are not thought to be typical even with mild voice disorders, it is apparent that clinicians are utilizing additional visual features to rate mucosal wave. It is probable that clinicians are also utilizing the vertical motion of the surface propagation. Alternatively, it is possible that ratings of mucosal wave are confounded with ratings of glottal width or amplitude of vocal fold vibration.

Mucosal wave magnitude was overall reduced for ratings from HSV and HSV-derived playbacks, as seen in Table 2 and 3. It is likely that the norm for stroboscopy does not apply to HSV. The capture rate of the commercially available HSV camera, of 2000 fps was not sufficient to provide multiple samples within the closing phase of vibration for persons with F_0 above 200 Hz. This insufficient sampling may reduce the perception of mucosal waves as well as reduce their perceived magnitude. However, a significant number of recordings were rated as exhibiting decreased magnitude through stroboscopy.

Mucosal wave asymmetry of vocal fold vibration was realized in a more than one-fifth of the normophonic participants for habitual phonation, as seen in Table 4. Differences between pressed and habitual phonations were less evident during the MKG playback, than during HSV and MW playbacks. All of the asymmetries, from HSV-derived techniques, were rated as mild or moderate. That is, the vocal folds did not vary more than two points in magnitude. The magnitude of asymmetry may be a future guideline for assessment. The results of this study are consistent with previously reported results from stroboscopy [4] in that mucosal wave asymmetry was perceived in normophonic speakers. However, an increased percent of asymmetries were perceived in this study for all playbacks. The asymmetry of mucosal wave magnitude via the HSV playback was consistently increased in comparison to the other playbacks for both habitual and pressed phonations.

V. CONCLUSION

The results of this study reinforce the presence of asymmetrical mucosal waves in the vocal fold vibration of normophonic speakers. This asymmetry was noted in both pressed and modal productions. Additionally, 'atypical' findings were abundant for mucosal wave magnitude. These findings should be referred to when determining the abnormality of mucosal wave variations during clinical visualization procedures. The variation of ratings across the HSV-derived playbacks demonstrates the strength of utilizing different views providing a balance between specificity and sensitivity. Thus, the HSV-derived playbacks should be used as an ensemble to maximize the benefit of visualization. A major conclusion of this investigation is the finding that 2000 fps is insufficient to record the intra-cycle information necessary to assess features of mucosal wave.

REFERENCES

- [1] M. Hirano, and D. Bless, *Videostroboscopic examination of the larynx*. San Diego, CA: Singular Publishing Group, 1993.
- [2] J.A. Shohet, M.S. Courey, M.A. Scott, and R.H. Ossoff, "Value of videostroboscopic parameters in differentiating true vocal fold cysts from polyps," *Laryngoscope*, vol. 106(1), 19-26, 1996.
- [3] C.M. Haben, K. Kost, and G. Papagiannis, "Mucosal wave asymmetries in the clinical voice laboratory," *Journal of Otolaryngology*, vol. 31(5), 275-280, 2002.
- [4] C.M. Haben, K. Kost, and G. Papagiannis, "Lateral phase mucosal wave asymmetries in the clinical voice laboratory," *Journal of Voice*, vol.17 (1), 3-11, 2003.
- [5] D.A. Berry, D.W. Montequin, and N. Tayama, "High-speed digital imaging of the medial surface of the vocal folds," *Journal of the Acoustical Society of America*, vol. 110 (5), 2539-2547, 2001.
- [6] S.H. Sloan, G.S. Berke, B.R. Gerratt, J. Kreiman, and M. Ye, "Determination of vocal fold mucosal wave velocity in an in vivo canine model," *Laryngoscope*, vol. 103, 947-953, 1993.
- [7] I.R. Titze, J.J. Jiang, and T.Y. Hsiao, "Measurement of mucosal wave-propagation and vertical phase differences in vocal folds vibration," *Annals of Otology Rhinology and Laryngology*, vol. 102(1), 58-63, 1993.
- [8] D.D. Deliyski, "Endoscope motion compensation for Laryngeal High-Speed Videoendoscopy," *Journal of Voice*, vol. 19(3), 485-496, 2005.
- [9] D.D. Deliyski, and P.P. Petrushev, "Methods for Objective Assessment of High-Speed Videoendoscopy," *Proceedings: 6th International Conference: Advances in Quantitative Laryngology, Voice and Speech Research AQL-2003, Hamburg, Germany, 28, 1-16, 2003.*

MEASUREMENT OF CRICOTHYROID ARTICULATION USING HIGH-RESOLUTION MRI AND 3D PATTERN MATCHING

Sayoko Takano¹, Keisuke Kinoshita¹, and Kiyoshi Honda¹
¹ATR Human Information Science Laboratories, Kyoto, Japan

This study investigates the actions of the cricothyroid joint for F0 changes based on high-resolution MRI and 3D image analysis. The data from a male speaker's phonation at two fundamental frequencies were analyzed with a 3D pattern matching method to obtain displacement and angular changes of the thyroid and cricoid cartilages. Results show displacement of the two cartilages relative to each other in 3D. The largest difference between 110 Hz and 165 Hz was found to be 1.2 mm horizontally and 0.6 mm vertically with respect to the translation of the cricothyroid joint. This action is interpreted to be caused by the contraction of the cricothyroid muscle which draws the thyroid and cricoid cartilages together, and results in stretching of the vocal folds.

I. INTRODUCTION

It has been widely acknowledged that the cricothyroid joint offers a biomechanical basis for fundamental frequency (F0) control and that its action consists of two components, rotation and translation (gliding). While joint rotation has been believed to be an effective factor for stretching the vocal folds, the contribution of joint translation has been in question [1, 2]. This is because the measurement of the 3D actions of the cricothyroid joint during phonation is so difficult that it has never been examined.

Many researchers have investigated the actions of the cricothyroid joint both from laryngeal observation during phonation and examination of the mechanical mobility of excised cartilages. Using X-ray photography, Sonninen [3] reported that the cricothyroid joint translates anteroposteriorly by 3 mm for a three-octave change in F0. On the other hand, observations on laryngeal specimen reached two different conclusions. Mayet and Mundnich [4] and Maue [5] reported that the cricothyroid joint does not translate because the ligaments connecting the joint prevent it. On the other hand, Fink [1] noted that the cricothyroid joint does translate 1-2 mm by manually applying force on the excised larynx. Also, Vilkmán et al. [2], basing on their examination on joint mobility, showed that joint translation is greater when its rotation is less extreme.

Since the cricothyroid joint involves bilateral articulation

on both sides of the cricoid cartilage, its mobility can be three-dimensional and asymmetric. Therefore, observation of joint actions in vivo requires volume imaging techniques, such as magnetic resonance imaging (MRI). The use of MRI has been limited to morphological studies of the excised larynges [6] because its application to laryngeal observation in vivo faces two problems: insufficient image resolution due to the small size of the laryngeal structure and motion artifact due to respiratory and phonatory movements of the larynx. To solve these problems, the present authors attempted laryngeal MRI with a custom larynx coil for higher resolution and phonation-synchronized scan to minimize motion artifacts [7]. Preliminary experiments with these techniques showed that the cricothyroid joint exhibits both rotation and translation between two frequencies in half an octave range and further suggested that accurate measurement of joint actions requires 3D image analysis. This study therefore investigates actions of the cricoid and thyroid cartilages using a 3D pattern matching algorithm to describe six degrees of freedom of joint actions.

II. METHOD

MRI experiments were conducted to measure relative movement of the thyroid and cricoid cartilages during sustained phonation at two fundamental frequencies (F0).

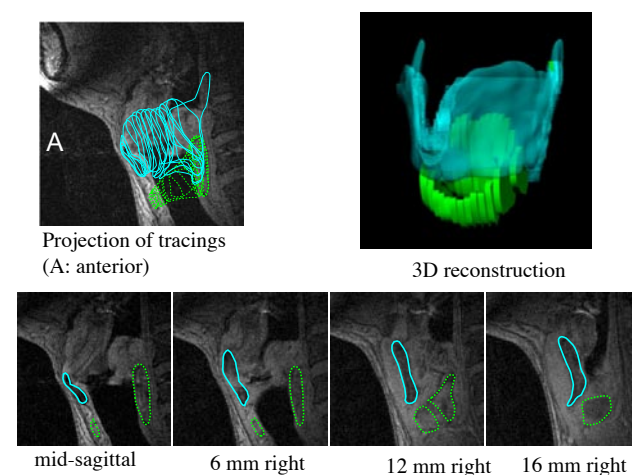


Fig. 1 Tracings and 3D reconstruction of the thyroid and the cricoid cartilages based on high-resolution MRI.

A custom larynx coil and phonation-synchronized MRI were combined to acquire laryngeal images with necessary resolution[7]. A 3D pattern matching program was developed to analyze the movement of the thyroid and cricoid cartilages in six degrees of freedom.

A. MRI acquisition

A Japanese male subject (54 y.o.) joined the MRI experiment using a clinical MRI scanner (Shimazu-Marconi, Magnex Eclipse 1.5T). The subject took a supine posture with fixed head position so as to measure the geometry in the absolute coordinate system. The task for the subject was to regularly repeat a sustained vowel production listening a guide tone. High-resolution MRI data were acquired for the vowel /a/ in two levels of F0: low F0 (110 Hz) and high F0 (165 Hz). The larynx coil, modified from a commercial surface coil, was placed over the neck at a natural head position [7]. The phonation-synchronized method was used to obtain static laryngeal images only during phonation by synchronizing MRI scan to each phonation [7].

The MRI scan settings were RF-FAST (TE=3.5 ms, TR=390 ms, and NEX=2), with 0.25×0.25 mm pixel size, 21 slices and 2 mm thick. In the images, cartilages were observed as darker regions than the surrounding tissue because they have been calcified. Fig. 1 shows a 3D model of the thyroid and cricoid cartilages.

B. 3D registration

A 3D registration method by pattern matching was

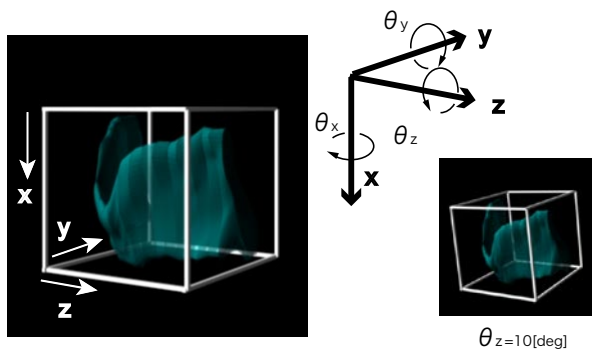


Fig. 2 Axis definition. Figure on the right illustrates the angular change around z-axis: θ_z ;

Table 1 Displacement and angular changes of the thyroid and cricoid cartilages estimated by 3D pattern matching.

	[mm]			[degree]		
	x	y	z	θ_x	θ_y	θ_z
thyroid	-6.0	-1.1	0.2	-0.7	2.2	-0.9
cricoid	-6.5	0.4	-0.4	-1.0	1.8	-7.9



Fig. 3 Region of interest (ROI) for 3D pattern matching.

developed to measure displacements and angular changes of the thyroid and cricoid cartilages from the data obtained at low and high F0. This analysis enables the estimation of the relative displacements of each cartilage from the “template” (low F0) to the “target” (high F0) in six degrees of freedom. The axes for the analysis were defined, as shown in Fig 2: x-axis: head/foot, y-axis: front/back, z-axis: right/left. The center for image displacement and angular changes was set to the centroid of the region of interest (ROI). To determine the action components of the cricothyroid joint, the data for the displacement and angular changes of each cartilage were converted into translation and rotation of the two cartilages at the cricothyroid joint.

As a “template” in 3D pattern matching, the dark region of the cartilages with the surrounding tissue was selected as ROI by manual tracing on the low F0 images (Fig. 3). Since the original data had nonisotropic voxels in the volume, each sagittal image was downsampled to have isotropic dimensions. Then the images were smoothed by a Gaussian filter (low-pass filter) to obtain a smooth correlation function over the search space.

The 3D registration of each cartilage was accomplished by finding the maximum correlation coefficient between the “template” and “target,” while applying image translation and rotation on the template’s ROI. This correlation method is often used for unclear or noisy data such as MRI. To avoid capturing a searched maximum in the local maximum, 30 random initial parameters were set to seek the global maximum. The output from this method was visually verified by comparing the template and matched target images in each slice. The maximum correlation coefficient between low and high F0 was 0.94 for the thyroid cartilage and 0.92 for the cricoid cartilage, respectively.

III. RESULTS AND DISCUSSION

The 3D reconstructed views of the thyroid and cricoid cartilages are shown in Fig. 4. As seen, the two cartilages are elevated from low to high F0, while the

Table 2 Translation of the cricothyroid joint from low to high F0.

	[mm]		
	x	y	z
left	0.5	-1.2	0.0
right	0.4	-0.5	0.0

cricoid cartilage rotates in the direction to stretch the vocal folds. The narrowing of the cricothyroid space from low to high F0 visually indicates joint rotation. Also, left/right asymmetry can be observed to be associated with the joint actions.

A. Displacement of each cartilage

Displacement of each cartilage obtained from the 3D pattern matching is shown in Table 1. The magnitude of these changes of both cartilages was the largest in the x-axis (sagittal plane) and smaller in the other axes. The thyroid and cricoid cartilages moved in the same direction in the x-axis, but not in the y- and z-axes.

Table 1 indicates that elevation of the cartilages from low to high F0 is most remarkable among the changes observed: vertical displacement (x-axis) of the thyroid cartilage was 6.0 mm and the cricoid cartilage was 6.5 mm. This means that vertical displacement of the cricoid cartilage is greater than the thyroid cartilage.

Horizontal displacement (y-axis) of the thyroid cartilage was 1.1 mm between low and high F0, while the cricoid cartilage was 0.4 mm. The horizontal displacement of the thyroid cartilage was larger than the

cricoid cartilage, which was in opposite directions of each other. These changes take place in the direction to stretch the vocal folds, agreeing with previous studies [3, 7]. In comparison to the data for low F0, lateral displacement of the thyroid cartilage in high F0 was 0.2 mm to the left and the cricoid cartilage was 0.4 mm to the right. These movements were also in the opposite direction of each other, which also contributed to changes in vocal fold length.

B. Angular change of each cartilage

Angular changes of each cartilage are also shown in Table 1. Between low and high F0, the angular change of the thyroid cartilage are -0.7, 2.2, and -0.9 degree in the x-, y-, and z-axis, respectively, while the angular change of the cricoid cartilage are -1.0, 1.8, and -7.9 degree in the x-, y-, and z- axes, respectively.

The angular change of the cricoid cartilages around the z-axis was found to be the greatest among the data, which was in the direction to stretch the vocal folds. The angular changes of the both cartilages are in the same direction, and the cricoid cartilage rotated more than the thyroid cartilage.

All these results suggest that movements of the thyroid and cricoid cartilages are three-dimensional and asymmetrical.

c. Actions of the cricothyroid joint

The values for displacement and angular changes of

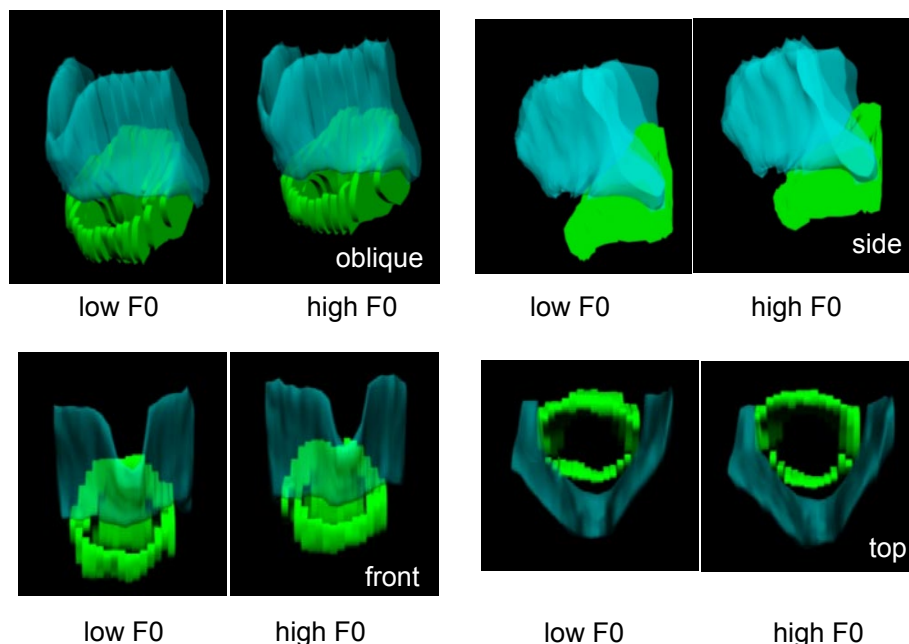


Fig. 4 3D reconstruction of the thyroid and cricoid cartilages with low and high F0.

Voice modelling and analysis

VOCALIZATION ANALYSIS TOOLS

H. J. Fell¹ and J. MacAuslan²

¹College of Computer and Information Science, Northeastern University, MA, USA

²Speech Technology and Applied Research, Bedford, MA USA

Abstract: We offer two tools for automated vocalization analysis. The Syllable tool uses the Stevens landmark theory to find landmarks in vocalizations digitized as "wav" files. The landmarks are grouped to identify syllable-like productions in these vocalizations and the results are summarized. The Vocalization-Age tool is intended for pre-speech vocalizations. It uses the landmark and syllable information to yield a vocalization age that has been shown to clinically distinguish typically-developing children from children who are at risk for later speech impairment.

I. INTRODUCTION

Many speech-related studies result in voluminous acoustic data and our projects are no exception. We have therefore developed two tools for automated vocalization analysis. One tool extracts and summarizes features from acoustic waveforms. The other tool computes a performance level of pre-speech productions. Beta-test versions of our software are now available for Matlab users.

Examples:

We have applied these tools to recordings collected in several studies.

- In the Early Vocalization Analysis (EVA) project [1], typically and atypically developing infants were recorded for 45 minutes at a time, for a total of more than 100 sessions.
- In a study of emotional stress in voice [2], we analyzed about 400 single-word, pre-existing audio recordings [SUSAS] of several subjects speaking many tokens in sometimes noisy environments.
- In the visiBabble project [3], 30 ten-minute in-home audio recordings of several children with severe speech delays were processed in real-time in a single-case-study design.
- In the UCARE project [4], 40 hours of pre-existing [5] video-taped sessions of children with physical or neurological impairments were analyzed with these tools.

Most of these recordings were made in less-than-ideal environments. Babies crawled on the floor and played with toys. Mothers, siblings, and graduate students were present and sometimes talked. The recordings also contain other environmental sounds such as air-conditioners or vacuum cleaners. Because our tools use knowledge-based speech-processing, they are robust to many of these contaminating sounds. For more subtle cases, e.g. a sib-

ling talking nearby, the researcher can specify recording sections to ignore.

II. THE SYLLABLE TOOL

The Syllable tool uses the Stevens landmark theory [6] to find acoustically abrupt events, consonantal *landmarks*, in vocalizations digitized as "wav" files. The tool also determines voicing intensity and fundamental frequency (F0) contours.

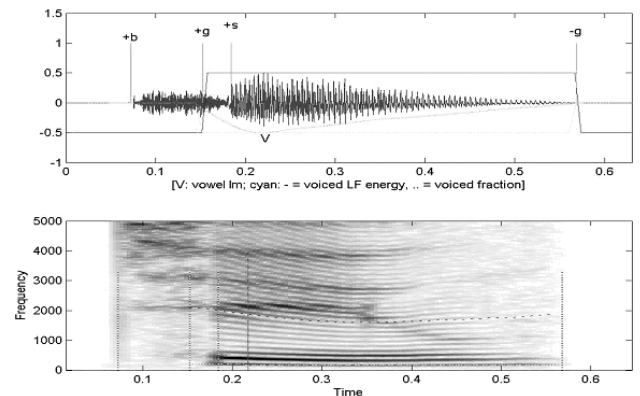


Figure 1: Syllable Analysis of "two" spoken by an adult female. The waveform (top) is shown with labeled landmarks (onset/offset of: b, bursts/frication; g, voicing; s, syllabicity) and strength of voicing; V denotes the nominal vocalic center of the syllable. The spectrogram (bottom) is shown with the F0 contour and its 10th harmonic (dashed line). Voice onset time VOT is measured by the interval between start of burst +b and onset of voicing +g.

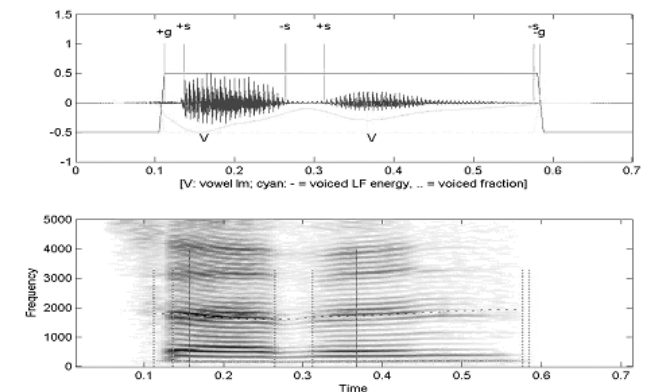


Figure 2: Syllable Analysis of "seven" spoken by an adult female. In the waveform (top), V denotes the nominal vocalic center of each syllable. Notice that voicing persists without a complete oral closure between the syllables. The second syllable is identified by a landmark-based rule, i.e., a syllable onset (+s) that is not closely preceded by a voicing onset (+g).

The landmarks are grouped to identify syllable-like productions in these vocalizations and the results are summarized.

III. THE VOCALIZATION AGE TOOL

The Vocalization Age (or *vocAge*) tool is specifically intended for pre-speech vocalizations. The digitized recording of a single session with a child is first analyzed by the syllable tool. The resulting information is then summarized and compared against data collected in ~100 sessions with six to 15 month-old, typically-developing infants. The tool thus derives a "vocalization age".

In an application of the *vocAge*, we found two specific screening rules [7] that clinically distinguish infants who may be at risk for later communication or other developmental problems from typically developing infants:

- An infant is (or is not) in the atypical group according as any session (respectively, no session) shows a "delay", i.e., difference between chronological and vocalization age, of at least 3.1 months.
- An infant is (is not) in the atypical group according as any (respectively, no) two consecutive sessions both show delays of at least 2.3 months.

IV. HOW THE TOOLS WORK

A. Landmarks

Landmark processing begins by analyzing the signal into several broad frequency bands (widths of 400-2000 Hz) selected to detect important speech features such as the second formant. Because of the different vocal-tract dimensions, the appropriate frequencies for the bands are different for adults and infants; however, the procedure itself does not vary. First, an energy waveform is constructed in each of the bands. Then the rate of rise (or fall) of the energy is computed, and peaks in the rate are detected. These peaks therefore represent times of abrupt spectral change in the bands. Simultaneous peaks in several bands identify consonantal landmarks.

B. Syllables and Utterances

The program identifies sequences of landmarks, e.g., +g-g or +s-g-b, as syllables based on the landmark order and inter-landmark timing. Among other constraints, syllables must contain a voiced segment of sufficient length. Figure 4 shows an example of this rule.

An utterance is a sequence of syllables in which gaps between syllables are no more than (nominally) 200 milliseconds long.

Both syllables and utterances may have properties of their own, such as a pitch template (rise/fall/rise) or a peak zero-crossing rate.

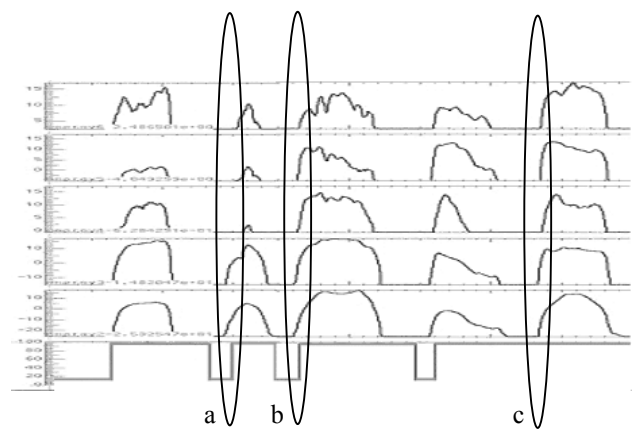


Figure 3: Initial spectral analysis of an infant utterance: voicing, i.e., presence of strong harmonic content, (bottom) and five frequency bands' energy waveforms. Landmarks are identified by large, abrupt energy increases or decreases that are simultaneous in several bands. (a) Too few bands show large, simultaneous changes in energy. (b) All bands show large, simultaneous energy increases immediately before the onset of voicing, identifying a +b (burst) landmark. (c) All bands show large, simultaneous energy increases during ongoing voicing, identifying a +s (syllabic) landmark.

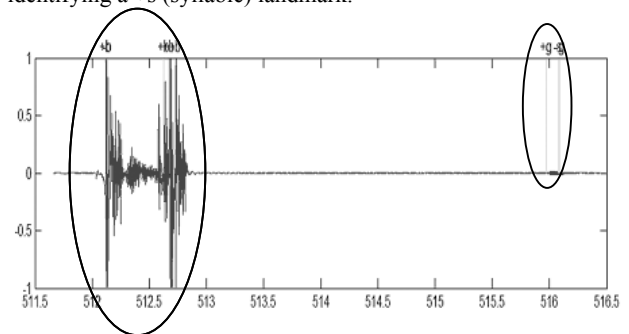


Figure 4: Ignored noise vs. recognized syllable. (Left segment) Noise marked by only +b and -b landmarks; (right segment) a faint babble marked by +g-s-g. Because any syllable must contain a voiced segment, the loud, noise segment is automatically ignored in subsequent processing. The babble, in contrast, has well defined voicing and sufficient duration and is hence retained.

C. Vocalization Age

There are many syllable and utterance measurements that the tool uses in forming the vocalization age:

- Number of syllables per utterance
- Number of occurrences and mean duration for each syllable type
- Number of syllables starting with a given onset landmark: +g, +s, etc.
- Number of syllables ending with a given offset landmark: -b, -g, etc.
- Number of syllables with n landmarks, $n = 2$ to 7.
- Standard deviations of related quantities, when they apply.

The Syllable tool can be set to extract and summarize exactly those measurements that are needed to compute the vocalization age.

V. USING THE TOOLS

We have applied these tools to recordings collected in several studies and we hope that other researchers will use the tools on their own data. Also, as we improve the feature collection capabilities of our tools, we, and perhaps others, will want to use them repeatedly on previously collected recordings. These tools can be run on all the recordings for a single "wav" file, a complete session, all the sessions of a subject, or an entire study with a single invocation. (See Figure 5.)

A. System Requirements

Currently, our software requires Matlab and the Matlab Signal Processing Toolbox. We run it under the Windows XP operating system.

B. Preparing Data

All sound files must be in "wav" format. Because much of our own data was collected using Entropic's ESPS-WAVES and saved in "sd" files, we also provide software to convert Entropic "sd" files to "wav" format. A user can run the Syllable and Vocalization Age tools on a single recording or on a directory tree containing recordings of (see Figures 5 and 6):

- a single session with a subject,
- all sessions of a subject,
- an entire study.

A simple text file may be included for any recording to indicate sections that should not be analyzed.

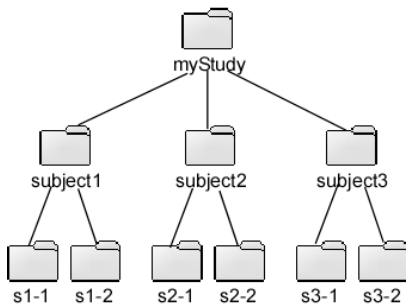


Figure 5: Arrangement of session data in a study. This figure represents a study with two sessions for each of three subjects.

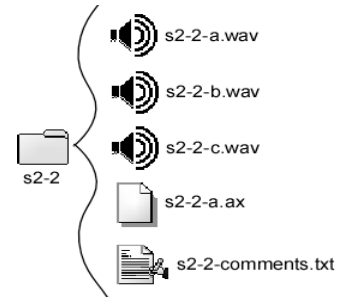


Figure 6: A session directory. This figure shows a folder containing three audio files from a single session, a text ("ax") file that marks segments to be ignored in one of the "wav" files, and a text file with the researcher's comments about the session.

C. Single-Subject Experiments

Single case study designs [8] are particularly suited to studies on a small heterogeneous group of subjects. For example, in our preliminary tests of visiBabble, a real-time visual-feedback system, we ran sessions in a variety of formats:

- 1) Baseline (recording, no graphic display);
- 2) Response (graphic display is always present, while recording);
- 3) A-B-A (display off-on-off).

Data was collected during all phases of all formats to allow a comparison of behavior during the baseline and feedback phases. The Syllable tool can analyze the landmarks and syllables for the A and B phases combined or separately.

D. Reports

A dialog box allows the user to select particular features to be summarized by the Syllable tool (see Figure 7). The tool will then generate, in the data directory, a tab-delimited report that can be easily copied into a spreadsheet for future analysis (see Table 1).

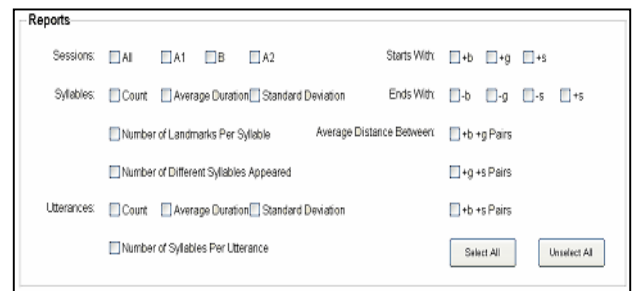


Figure 7: Dialog box for selecting report features.

VI. FURTHER DEVELOPMENT

We anticipate adding capabilities over the next two years while our visiBabble project is under development. We encourage other researchers to try a beta-test version and to suggest enhancements that would be useful to them.

ACKNOWLEDGEMENTS

The authors appreciate the encouragement and testing by Prof. Cynthia Cress, Univ. of Nebraska-Lincoln. We also thank Jun Gong for his programming contributions. This work was funded in part by National Institutes of Health STTR grant R42 DC005534.

Table 1: Summary of a Short Sample Session

The report summarizes the landmark, syllable, and utterance statistics of a sample, 30-second session. These statistics are among those used in the vocAge tool.

Total			
SyllableType	Count	Mean	StdDev
+g-g	3	704.000	532.626
+s-g	1	408.000	0.000
+g-g-b	3	96.000	36.368
+g+s-g	1	48.000	0.000
+b+g-g-b	1	344.000	0.000
+g+s-g-b	1	64.000	0.000
+g+s-s-g	1	160.000	0.000
+g+s+s	1	696.000	0.000
Total	12	343.333	382.559
2 lm/syl	4		
3 lm/syl	5		
4 lm/syl	3		
5 lm/syl	0		
6 lm/syl	0		
7 lm/syl	0		
Avg	2.917		
DiffSyl	8		
Utts	Count	AvDur	StDev
	8	531.000	486.982

Annotations:

- mean duration of +g-g syllables (points to StdDev of +g-g)
- mean duration of all syllables (points to Mean of Total)
- number of syllables with 2 landmarks (points to Count of 2 lm/syl)
- average number of landmarks/syllable (points to Avg)
- number of syllable types occurring (points to DiffSyl)
- total number of utterances (points to Count of Utts)

REFERENCES

- [1] H.J. Fell, J. MacAuslan, L.J. Ferrier, K. Chenausky, "Automatic Babble Recognition for Early Detection of Speech Related Disorders," *Journal of Behaviour and Information Technology*, 1999, **18**, no. 1, 56-63.
- [2] H.J. Fell, J. MacAuslan, "Automatic Detection of Stress in Speech," *Proceedings of MAVIBA 2003*, Florence, Italy, pp. 9-12.
- [3] H.J. Fell, J. MacAuslan, C. J. Cress, L. J. Ferrier, "Using Early Vocalization Analysis for visual feedback," *Proceedings of MAVIBA 2003*, Florence, Italy.
- [3] H.J. Fell, J. MacAuslan, C. Cress, L.J. Ferrier, "visiBabble for Reinforcement of Early Vocalization," *Proceedings of ASSETS 2004*, Atlanta, GA., pp. 161-168.
- [4] C.J. Cress, S. Unrein, A. Weber, S. Krings, H. Fell, J. MacAuslan, J. Gong, "Vocal Development Patterns in Children at Risk for Being Nonspeaking," submitted to *ASHA 2005*.
- [5] C.J. Cress, *Communicative and symbolic precursors of AAC*. Unpublished NIH CIDA Grant: University of Nebraska-Lincoln, 1995.
- [6] K.N. Stevens, S. Manuel, S. Shattuck-Hufnagel, and S. Liu, "Implementation of a model for lexical access based on features," *Proc. ICSLP (Int. Conf. on Speech & Language Processing)*, Banff, Alberta, **1**, 499-502, 1992.
- [7] H.J. Fell, J. MacAuslan, L.J. Ferrier, S.G. Worst, and K. Chenausky, "Vocalization Age as a Clinical Tool," *Proc. ICSLP (Int. Conf. on Speech & Language Processing)*, Denver, September 2002.
- [8] L.V. McReynolds, K.P. Kearns, *Single Subject Experimental Designs in Communication Disorders*, Baltimore: University Park Press, 1983.

NUMERICAL MODELLING OF EFFECT OF TONSILLECTOMY ON PRODUCTION OF CZECH VOWELS /A/ AND /I/

P. Švancara¹, J. Horáček²

¹Institute of Solid Mechanics, Mechatronics and Biomechanics, Brno University of Technology, Brno, Czech Republic

²Institute of Thermomechanics, Academy of Science of the Czech Republic, Prague, Czech Republic

Abstract: Aim of this study is to numerically examine the effect of tonsillectomy on production of Czech vowels /a/ and /i/. Similar experimental studies are not easily realisable on living subjects. The finite element (FE) models of the acoustic spaces corresponding to the human vocal tract for the Czech vowels /a/ and /i/ and acoustic space around the human head are used in numerical simulations of phonation. The acoustic resonant characteristics of the FE models are studied using modal and transient analyses (excitation by a short pulse). The production of vowels is simulated in time domain using transient analysis of FE model excited by Liljencrants-Fant's (LF) glottal signal model. Calculated results show that tonsillectomy causes significant frequency shifts down to lower frequencies for 2nd (down by ~40Hz) and 4th (down by ~120Hz) formants for the vowel /a/, and similar shifts for 2nd (down by ~100Hz) and 4th (down by ~50Hz) formants for the vowel /i/. The frequency shifts of formants after tonsillectomy significantly depends on position and size of the tonsils.

I. INTRODUCTION

The effects of tonsillectomy on the voice production were experimentally studied in several papers [1, 2]. Their main drawback is that the patients are not able to repeat the same manner of voice production during experiment before and after tonsillectomy. The results can be evaluated statistically only. Numerical modelling of this problem is not limited by these difficulties.

In the previous papers of the authors [3-5] acoustic characteristics of the human vocal tract of a healthy man and a man with velofaryngeal insufficiency were studied by FE modelling. Here, the FE models are used to examine the effect of tonsillectomy on production of Czech vowels /a/ and /i/. The FE models of the acoustic spaces of the vocal tract were created using magnetic resonance imaging technique. The FE mesh of a hollow sphere, representing an acoustic space around the human head, was added manually to the FE model of the vocal tract. The designed FE model is shown in Fig. 1. A single layer of infinite elements was matched onto the FE mesh of the outer surface of the sphere, for modelling the acoustic radiation into the infinite acoustic space. The infinite elements are based on an infinite geometry mapping, extending the elements to infinity, and on special shape functions.

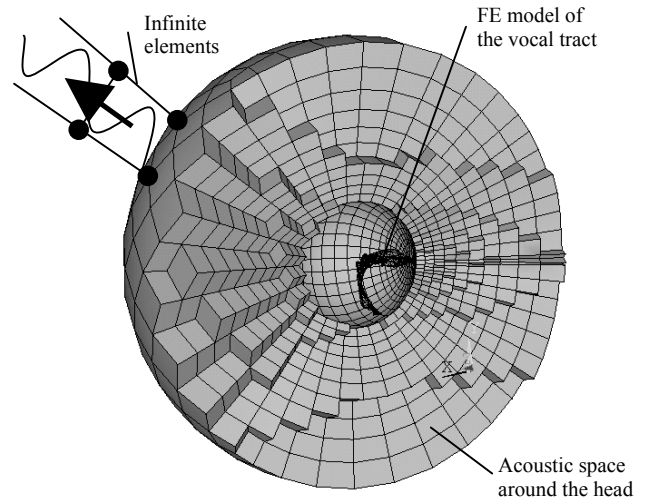


Fig. 1: FE model of the vocal tract for the vowel /a/ including an acoustic space around the human head.

The FE models were modified by adding acoustic spaces that arise in the vocal tract after tonsillectomy, see Fig. 2. Three basic FE models were created for each vowel, one for the vocal tract with tonsils, and two FE models for the vocal tract after tonsillectomy with added acoustic space 1.5 cm³ per one tonsil and with a reduced volume 0.7 cm³ per one tonsil considering a constriction of living tissue after operation.

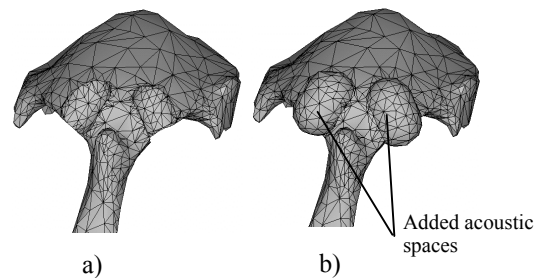


Fig 2: Detail of FE model of the vocal tract for the vowel /a/ a) vocal tract with tonsils b) vocal tract after tonsillectomy.

II. MATHEMATICAL FORMULATION

Wave equation for the acoustic pressure can be written as

$$\nabla^2 p = \frac{\partial^2 p}{c_0^2 \partial t^2}, \quad (1)$$

where c_0 is the speed of sound, with boundary conditions as follows

- on acoustically hard area $\partial p / \partial \mathbf{n} = 0$,
- on acoustically absorptive area a normal impedance $Z = p / v_n$ can be prescribed,

where \mathbf{n} is the normal to the boundary area and v_n is normal velocity.

Equations of motion after discretization can be written as

$$\mathbf{M} \mathbf{p}(t) + \mathbf{C} \dot{\mathbf{p}}(t) + \mathbf{K} \mathbf{p}(t) = \mathbf{f}(t), \quad (2)$$

where \mathbf{M} , \mathbf{C} , \mathbf{K} are mass, damping and stiffness matrices, \mathbf{p} is the vector of nodal acoustic pressures and \mathbf{f} is the vector of nodal acoustic forces. Newmark integration method was used for solution in time domain.

The acoustic transient and modal analysis were realized by the software code SYSNOISE 5.5 considering the speed of sound $c_0 = 353 \text{ ms}^{-1}$ and the air density $\rho_0 = 1.2 \text{ kgm}^{-3}$. Boundary walls of the vocal tract were considered acoustically absorptive with normal impedance $Z = 83 \text{ 666 kgm}^{-2}\text{s}^{-1}$ assuming for the soft tissue the Young modulus $E = 5 \text{ MPa}$ and density $\rho = 1400 \text{ kgm}^{-3}$ [6].

III. FREQUENCY MODAL AND RESONANT CHARACTERISTICS

Firstly the eigenfrequencies of the FE models of the vocal tract without the acoustic space around the head were studied using modal analysis, assuming zero acoustic pressure at the nodes belonging to the area of the lips and acoustically hard boundary walls. Calculated formant frequencies for both vowels and all three FE models are summarized in Table 1.

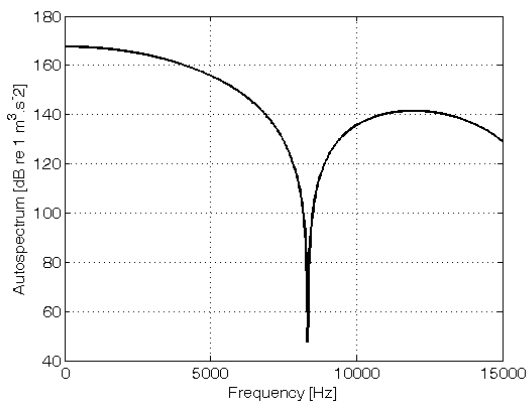


Fig. 3: Spectrum of the excitation pulse.

Then the resonant characteristics of the FE models with acoustic space around the head, infinite elements and absorption on the vocal tract walls were computed by transient analysis in time domain. The FE models were excited by a very short pulse of differential glottal flow (duration 0.25 ms) at the faces of FE elements in position

of the vocal folds. The spectra of the excitation pulse and the sound pressure calculated near the lips are shown in Figs. 3 and 4, respectively. The evaluated acoustic resonant frequencies were close to the formant frequencies obtained by the modal analysis.

Table 1: Calculated resonant frequencies.

Vowel /a/					
formant	With tonsil. [Hz]	After tonsill. [Hz]	Diff. [Hz]	After tonsill. reduced vol. [Hz]	Diff. [Hz]
F1	678	683	5	686	8
F2	1177	1137	-40	1150	-27
F3	2869	2875	6	2904	35
F4	4113	3992	-121	4038	-75
F5	4286	4308	22	4312	26
F6	4442	4494	52	4492	50
Vowel /i/					
formant	With tonsil. [Hz]	After tonsill. [Hz]	Diff. [Hz]	After tonsill. reduced vol. [Hz]	Diff. [Hz]
F1	258	248	-10	251	-7
F2	2374	2267	-107	2307	-67
F3	3188	3213	25	3198	10
F4	3809	3763	-46	3794	-15
F5	4778	4722	-56	4741	-37

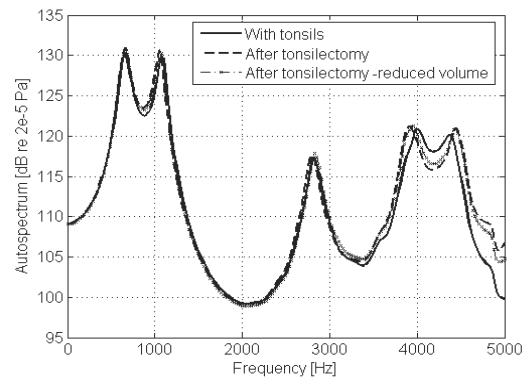


Fig. 4: Spectrum of the pressure response near the lips for the vowel /a/.

Results calculated by both methods for FE models with the tonsils are in good agreement with experimental data known for formants of the Czech vowels /a/ and /i/ [7, 8]. Tonsillectomy for the vowel /a/ caused the biggest decrease of formants F2 and F4 of about 40 Hz and 120 Hz, respectively. And for vowel /i/, the tonsillectomy caused the biggest frequency shift down of about 100 Hz for the formant F2, and about 50 Hz for the formants F4 and F5. For the model with consideration of constriction of tissue after operation the frequency shifts of the

formants are approximately two times smaller. We should note that the eigenfrequency F5 for the vowel /a/ is associated with a lateral acoustic mode shape of vibration in the horizontal direction.

As a next step a sensitivity of formants frequency shift on the position and size of tonsils were examined. Firstly, a penetration of the volumes of the tonsils and the vocal tract was changed, i.e., the portion of tonsil volume interference with the acoustic space of the vocal tract. Three cases of tonsil-vocal tract volume interference were considered: 1/2 (this case was used in previous calculations), 3/4 and 1/4. The results are summarized in Fig. 5.

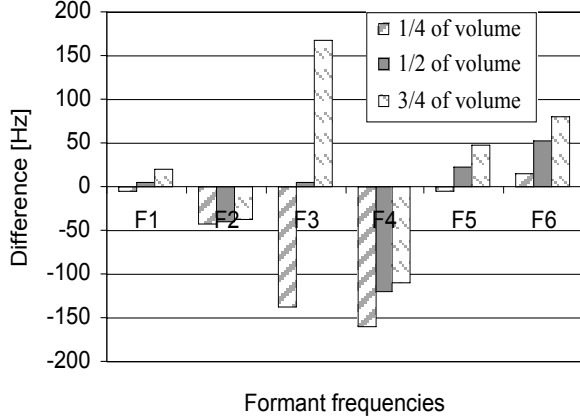


Fig. 5: Difference of formant frequencies before and after tonsillectomy for different positions of tonsils for the vowel /a/.

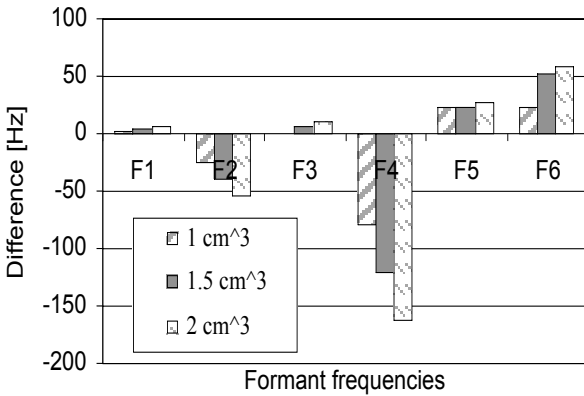


Fig. 6: Difference of formant frequencies before and after tonsillectomy for different size of tonsils for the vowel /a/.

Then for case of 1/2 of the tonsil-vocal tract volume interference, the volume of the tonsils was varied, and again three cases were analyzed for the tonsil volumes 1.5 cm³ (as in the previous calculations), 2 cm³ and 1 cm³ per one tonsil. The obtained differences in formant frequencies are shown in Fig. 6.

The results show that some formant frequencies are very sensitive to the change of position and size of the tonsils. For example, the difference in formant frequency F3 for the vowel /a/ changed from -137 Hz to +168 Hz with changing the portion of the tonsil volume interference with the acoustic space of the vocal tract.

The frequency changes of the most formants are more or less proportional to the size of the tonsils.

IV. NUMERICAL SIMULATION OF PRODUCTION OF VOWELS

The production of the vowels was simulated using transient analysis of FE model in time domain with excitation by Liljencrants-Fant's (LF) glottal signal model [9]. The LF model describes differentiated airflow in time domain. Each fundamental period of the glottal signal can be expressed as

$$\frac{dU_g(t)}{dt} = \begin{cases} E_0 e^{\alpha t} \sin \omega_g t & , 0 \leq t < t_e \\ -\frac{E_e}{\epsilon t_a} (e^{-\epsilon(t-t_e)} - e^{-\epsilon(t_c-t_e)}) & , t_e \leq t < t_c \end{cases} \quad (3)$$

where t is in the range $[0, t_c]$, t_c is equal to the fundamental period T_0 . The so-called waveshape parameters t_p , t_e , t_a , and E_e together with T_0 completely determine the shape of differential flow $dU_g(t)$. Figure 7 illustrates these waveshape parameters. Here, the following normalized parameters derived from the waveshape parameters were used:

- R_a the ratio of t_a to $t_c - t_e$,
- R_k the ratio of $t_e - t_p$ to t_p ,
- R_g the ratio of half fundamental period $T_0/2$ to t_p .

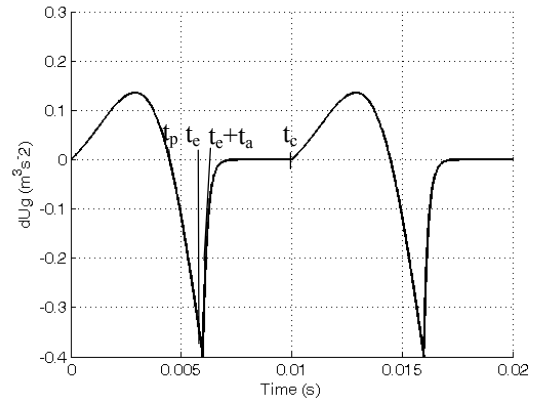


Fig. 7: Derivative glottal flow wave shape used for acoustic excitation of the vocal tract.

The parameters corresponding to a normal phonation were used ($R_a = 0.05$ ms, $R_k = 0.34$, $R_g = 1.12$, $E_e = 0.4$ m³s⁻²). The FE models were excited at the faces of FE elements in position of vocal folds by fifteen subsequent pulses of differential glottal flow with the period corresponding to the fundamental (pitch) frequency $F_0 = 100$ Hz. The numerical solution was realised by the transient analysis within the software SYSNOISE with the time step $\Delta t = 1.10 \cdot 10^{-5}$ s. The time responses – sound pressures and their spectra were calculated at distance 0.2 m in front of the lips (see the example in Fig. 8).

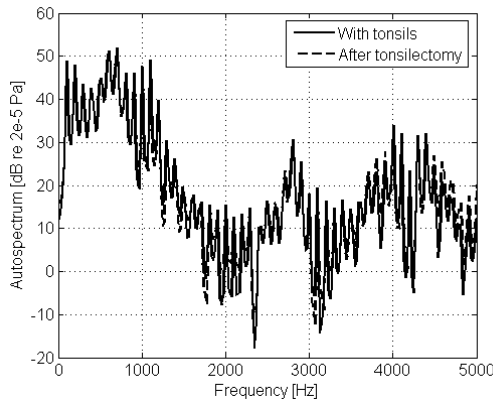


Fig. 8: Spectra of the calculated sound pressure at the distance 0.20 m in front of the lips for the vowel /a/ before and after tonsillectomy.

IV. DISCUSSION

Formant frequencies after tonsillectomy determined from the calculated spectra of the sound pressure near the lips show the same frequency shifts as results of the modal analysis. Solution in the time domain allows creating sound (audio) files for an acoustic checking of the quality of numerically produced vowels by listening. To achieve longer time duration of the sound files, the computed time sequences of sound pressure are repeated many times. Comparison of these sound files for the models with and without the tonsils shows a different colour of the phonated vowels. For the models with consideration of constriction of tissue after operation (reduced tonsil volume) the differences between the sounds before and after the tonsillectomy are not nearly audible.

V. CONCLUSION

Finite element (FE) models of the acoustic spaces corresponding to the human vocal tract for the Czech vowels /a/ and /i/ incorporating the acoustic spaces around the human head was created and the production of these vowels was simulated using the transient analysis in time domain with Liljencrants-Fant's (LF) glottal signal model. Designed FE models allow observing radiation of acoustic waves from the lips to the outer acoustic space. The time domain solution allows creating sound files for verification of the quality of numerically produced vowels by listening. This methodology can be used for an on-line subjective evaluation of the effects of tonsillectomy on the human voice production.

The formant frequencies evaluated from the calculated spectra of the acoustic pressure near the lips correspond well with the results of the performed acoustic modal analysis. The formants F2, F4 for the vowel /a/, and formants F2, F4 and F5 for the vowel /i/ are significantly lowered by the tonsillectomy. For the vowel /a/, the formant F2 was shifted down to the lower

frequencies by 40 Hz and the formant F4 by 121 Hz. For the vowel /i/, the formant F2 was decreased by 107 Hz and formants F4 and F5 were shifted down of about 50 Hz. However, the frequency changes of formants after the tonsillectomy significantly depend on position and size of the tonsils. For example, for the vowel /a/ the formant F3 was changed from -137 Hz to +168 Hz by changing a portion of the tonsil volume interference with the acoustic space of the vocal tract.

Consequently, it can be concluded that the effects of tonsillectomy on the voice production are very individual for each subject depending on a concrete anatomy of his vocal tract and position and size of the tonsils inside.

ACKNOWLEDGEMENTS

This research is supported by the Grant Agency of the Czech Republic by project No 106/04/1025 "Modelling of vibroacoustic systems focusing on human vocal tract".

REFERENCES

- [1] H. G. Ilk, O. Erogul, B. Satar, Y. Özkaptan, "Effects of Tonsillectomy on Speech Spectrum", *Journal of Voice*, Vol. 16, Issue 4, pp. 580-586, 2002.
- [2] H. Saida, H. Hirose, "Acoustic Changes in Voice after Tonsillectomy", *Acta Otolaryngol*, Vol. 523, pp. 239-241, 1996.
- [3] K. Dedouch, J. Horáček, T. Vampola, J. G. Švec, P. Kršek, R. Havlík, "Acoustic modal analysis of male vocal tract for Czech vowels", In *Interaction and Feedbacks '2002*, IT ASCR, Prague, pp. 13-20, 2002.
- [4] K. Dedouch, J. Horáček, T. Vampola, J. Vokřál, "Velofaryngeal insufficiency studied using finite element models of male vocal tract with experimental verification", In *3rd Int. Workshop MAVIBA*, Firenze, Italy, pp. 229-232, 2003.
- [5] P. Švancara, J. Horáček, L. Pešek, "Numerical Modelling of Production of Czech Vowel /a/ based on FE Model of the Vocal Tract", In: *Inter. Conference on Voice Physiology and Biomechanics*, Marseille, France, pp. 163-166, 2004.
- [6] A. Abé, K. Hayashi, M. Sato, *Data Book of Mechanical Properties of Living Cells, Tissues and Organs*, Tokyo: Springer-Verlag, 1996.
- [7] Z. Palková, *Phonetics and Phonology of the Czech Language*, Prague: Charles University Karolinum, 1994.
- [8] A. Novák, *Phoniatrics and pedaudiology. Voice disorders -principles of voice physiology, diagnostics, treatment, reeducation and rehabilitation*, Prague: Unitisk s.r.o., 1996.
- [9] G. Fant, J. Liljencrants, Q. Lin, "A Four Parameter Model of Glottal Flow", In *STL-QPSR 4*, Sweden, pp. 1-13, 1985.

GENERALIZED VARIOGRAM ANALYSIS OF VOCAL DYSPERIODICITIES IN CONNECTED SPEECH

A. Kacha¹, F. Grenez¹, J. Schoentgen^{1,2}

¹Department Signals and Waves, Faculty of Applied Sciences, Université Libre de Bruxelles, Brussels, Belgium

²National Fund for Scientific Research, Belgium
akacha@ulb.ac.be, fgrenez@ulb.ac.be, jschoent@ulb.ac.be

A generalized variogram is used to track vocal dysperiodicities in connected speech, which are summarized by means of a signal-to-dysperiodicity marker. To evaluate the variogram-based analysis, signal-to-dysperiodicity estimates are correlated with scores obtained by means of perceptual ratings of the degree of hoarseness, which are based on comparative judgments of pairs of speech samples. The corpora comprise four French sentences as well as vowels [a] produced by 22 male and female normophonic and dysphonic speakers.

I. INTRODUCTION

Many voice disorders cause voiced speech to deviate from perfect cyclicity. Dysperiodicities may be caused by additive noise owing to turbulence and modulation noise owing to external perturbations of the glottal excitation signal, as well as irregular dynamics of the vocal folds and involuntary transients between different dynamic regimes.

Techniques that have been proposed to estimate vocal dysperiodicities have been applied to sustained vowels, mainly. Indeed, many techniques lack robustness and accuracy when they are used to estimate vocal dysperiodicities in continuous speech or vowels including onsets and offsets spoken by severely hoarse speakers. The lack of robustness is a consequence of the assumptions of local stationarity and periodicity that are at the base of many speech analysis methods, and which are not valid in the case of speech produced by hoarse speakers. Up to date, there exists a comparatively small number of studies devoted to vocal dysperiodicities in continuous speech [2, 3].

In [4], we have proposed a generalized form of the variogram, as an alternative to the long-term prediction-based approach proposed in [5], to estimate speech signal dysperiodicities due to vocal disorders. The generalized variogram is derived from the conventional one. It enables tracking cycle length and cycle shape dysperiodicities and is unaffected by waveform changes that are segmental or suprasegmental in origin. In [4], synthetic vowels have been used to investigate the

performance of the generalized variogram while measuring dysperiodicities caused by jitter, shimmer and additive noise.

In the framework of this presentation, the variogram-based approach is evaluated by correlating signal-to-dysperiodicity estimates (SDR) with scores obtained by means of a perceptual rating of the degree of hoarseness, which is based on comparative judgments of pairs of speech samples.

II. METHODS

A. Corpora

Speech data comprise sustained vowels [a], including onsets and offsets, and four French sentences produced by 22 normophonic or dysphonic speakers (10 male and 12 female speakers). The corpus includes 20 adults (from 20 to 79 years), one boy aged 14 and one girl aged 10. Five speakers are normophonic, the other are dysphonic.

The sentences are the following: “Le garde a endigué l’abbé”, “Bob m’avait guidé vers les digues”, “Une poule a picoré ton cake” and “Ta tante a appâté une carpe”. Hereafter, they are referred to as S1, S2, S3 and S4, respectively. They have the same grammatical structure, the same number of syllables and roughly the same number of resonants and plosives. Sentences S1 and S2 are voiced by default, whereas S3 and S4 include voiced and unvoiced segments.

Speech signals have been recorded at a sampling frequency of 48 kHz. The recordings were made in an isolated booth by means of a digital audio tape recorder (Sony TCD D8) and a head-mounted microphone (AKG C41WL) at the laryngology department of a university hospital in Brussels, Belgium. The recordings have been transferred from the DAT recorder to computer hard disk via a digital-to-digital interface. Silent intervals before and after each recording have been removed.

B. Generalized Variogram

For a periodic signal $x(n)$ of period T_0 , one can write:

$$x(n) = x(n + kT_0), \quad k = \dots - 2, -1, 0, 1, 2, \dots \quad (1)$$

A measure of the departure from periodicity over an interval of length N is an indication of the amount of signal irregularity. For stationary signals, the dysperiodicity energy may be estimated via the minimum of the following expression. The expression between accolades is known as the variogram of the speech signal.

$$\hat{\gamma}(T) = \arg \min_T \left\{ \sum_{n=0}^{N-1} [x(n) - x(n+T)]^2 \right\}, \quad (2)$$

with $-T_{max} \leq T \leq -T_{min}$ and $T_{min} \leq T \leq T_{max}$.

Formally, the bracketed expression in (2) is equivalent to the difference between the contents of the current and a lagged analysis frame of length N . Index n positions speech samples within the analysis frame. When lag T is positive, the lagged frame is positioned to the right of the current frame, otherwise it is positioned to the left. Note that lag T is not requested to be equal to the glottal cycle length. Expression (2) is defined irrespective of whether the signal is voiced or unvoiced, regular or irregular.

Boundaries T_{min} and T_{max} are, in number of samples, the shortest and longest acceptable glottal cycle lengths. They are fixed to 2.5 ms and 20 ms, respectively (i.e. $50 \text{ Hz} \leq F_0 \leq 400 \text{ Hz}$).

The search for the minimum of (2) is performed to the left and right of the current window position, because comparing speech frames across phonetic boundaries is meaningless. In the case of cross-boundary comparisons, deviations from periodicity are due to differences in segment identity rather than dysperiodicity. The analysis frame length is fixed to 2.5 ms to include one cycle at most. Another reason, for choosing a short frame, is that cycle lengths are expected to evolve owing to intonation and segment-typical phonatory frequencies.

Speech signals are expected to be locally stationary at best. The signal amplitude evolves from one speech frame to the next owing to onsets and offsets, segment-typical intensity, as well as accentuation and loudness. Introducing a weighting coefficient to account for these slow changes in signal amplitude, definition (1) becomes:

$$x(n) = ax(n+T_0), \quad 0 \leq n \leq N-1. \quad (3)$$

Accordingly, the generalized empirical variogram may be written as follows.

$$\hat{\gamma}(T) = \arg \min_T \left\{ \sum_{n=0}^{N-1} [x(n) - ax(n+T)]^2 \right\}, \quad (4)$$

with $-T_{max} \leq T \leq -T_{min}$ and $T_{min} \leq T \leq T_{max}$.

Definition (4) is interpreted as the local energy of the signal dysperiodicities in a frame of length N . Weight a is constrained to be positive. It is defined to equalize the

signal energies in the current and shifted analysis windows:

$$a = \sqrt{\frac{E}{E_T}}, \quad (5)$$

expressions E and E_T are the signal energies of the current and lagged frames,

$$E = \sum_{n=0}^{N-1} x^2(n), \quad E_T = \sum_{n=0}^{N-1} x^2(n+T).$$

The analysis is carried out frame by frame. The analysis frame is shifted by 2.5 ms. Together with the choice of the analysis frame length, this guarantees that each signal fragment is included exactly once. The instantaneous value of the dysperiodicity is estimated as follows, with T_{opt} equal to the lag that minimizes generalized variogram (4) for the current frame position. Lag T_{opt} may be positive or negative.

$$e(n) = x(n) - ax(n+T_{opt}), \quad 0 \leq n \leq N-1 \quad (6)$$

C. Signal-to-Dysperiodicity Ratio

The marker that summarizes the amount of dysperiodicity within an utterance is defined as follows [7].

$$SDR = 10 \log \left[\frac{\sum_{n=0}^{L-1} \hat{x}^2(n)}{\sum_{n=0}^{L-1} e^2(n)} \right] \quad (7)$$

where L is the number of samples in the analysis interval and $\hat{x}(n) = x(n) - e(n)$ is an estimate of the clean signal.

The approximation of the optimal lag by an integer number of the sampling period introduces quantization noise, which has been reduced by over-sampling the signal by a factor of 8 and analysing the over-sampled signal.

D. Perceptual Ratings by Comparative Judgment of Speech Samples

The perceptual assessment exploits the ability of listeners to compare two stimuli in terms of grade, i.e., perceived overall degree of deviance of the voice. The aim is to hierarchize a set of recordings from the least to the most anomalous via comparative judgments of all possible sample pairs within the set. The procedure is the following.

1. The list of all possible different pairs of items is formed. An item is a recording belonging to a set of identical stimuli.

2. All scores are initialized to zero.
3. A randomly selected pair of speech recordings is presented to the listener, who is asked to point out the recording with the highest perceived hoarseness. The listener has also the option to label both recordings of a pair as equally hoarse.
4. The total score of the recording labeled as the most hoarse is increased by one. If both items of the pair are judged to be equally hoarse, the score of both recordings is increased by 0.5.
5. Steps 3 and 4 are repeated until all possible pairs that belong to a same session have been presented.
6. The samples are hierarchized on the base of their scores.

Sound samples have been presented via a digital-to-analog audio interface (Digidesign Mbox) and dynamic stereo headphones (Sony MDR-7506). Loudness has been fixed at a comfortable level by the listener. Listening sessions have been held in a quiet room. Each session has taken about one hour. At half-time, listeners have taken a rest of about five minutes.

The group of judges has been comprised of six naive listeners (one female, five males), i.e. listeners without training in speech therapy or laryngology. All reported normal hearing. Their ages ranged from 24 to 57. One listening session was devoted to a set of 22 stimuli. The total number of sessions has therefore been equal to 6 listeners x 5 stimuli = 30. The same experiment has been repeated by three listeners after a period of a day at least to gauge intra-judge reliability. The total number of retest sessions has therefore been equal to 3 x 5 = 15.

III. RESULTS

A. Scores of Perceived Hoarseness

Concordance between judges has been expressed by means of Pearson's product moment correlation (ρ_p) between listener scores. The scores of the four sentences have been arranged for a given judge into a single series by stacking the sentence scores. Correlation coefficients have been calculated by means of the score series of each listener. The values for sustained vowel [a] and sentences S1 to S4 are given below and above the diagonal of Table 1, respectively. While testing for the statistical significance of the Pearson product moment correlations, the method of Bonferroni has been used to account for multiple comparisons [6]. The number of independent measures involved in the test has been set equal to 22. The null hypothesis ($\rho_p = 0$) has been rejected for all table entries (one-tailed test, $\rho_{crit} = 0.56$, $p < 0.05$).

Table 1: Pearson's product moment correlation values between scores obtained via comparative judgments by six listeners for sustained vowel [a] (below the diagonal) and sentences S1 to S4 (above the diagonal).

	J1	J2	J3	J4	J5	J6
J1	—	0.91	0.83	0.86	0.76	0.86
J2	0.87	—	0.86	0.90	0.82	0.91
J3	0.90	0.87	—	0.83	0.74	0.84
J4	0.96	0.80	0.91	—	0.90	0.94
J5	0.84	0.69	0.80	0.89	—	0.92
J6	0.91	0.90	0.94	0.92	0.85	—

Intra-judge agreement has been examined by calculating Pearson's product moment correlation between the scores obtained during the test and retest sessions of three judges. For each judge, the scores of the four sentences have been stacked into a single series. The results are listed in Table 2. To account for multiple comparisons, Bonferroni's method has been used. The number of independent realizations involved in the test has been set equal to 22. The null hypothesis ($\rho_p = 0$) has been rejected for all table entries (one-tailed test, $\rho_{crit} = 0.46$, $p < 0.05$).

Table 2: Pearson's product moment correlation values between scores obtained via comparative judgments during test and retest sessions for three listeners.

	J1	J2	J3
[a]	0.96	0.98	0.90
S1 to S4	0.92	0.95	0.95

B. Measured Signal-to-Dysperiodicity Ratios

The SDR values of the speech signals corresponding to vowel [a] and four sentences have been computed for corpora comprising 22 speakers. The quartiles of the SDR values are given in Table 3. Fig. 1(a) shows as an example phonetic segments [lœ] of French sentence S1 that has been assigned a median hoarseness score of 20 and a SDR value of 8.9 dB. Fig. 1(b) shows the corresponding sample-by-sample dysperiodicity (6).

C. Correlation Between Scores of Perceived Hoarseness and Measured Signal-to-Dysperiodicity Ratios

Pearson's product moment correlation values between SDR estimates and listener scores are given in Table 4 for sustained vowels [a] as well as sentences S1 to S4. Bonferroni's method has been applied to account for multiple comparisons (one-tailed test, $\rho_{crit} = 0.60$, $p < 0.05$). The number of independent realizations involved in the statistical test has been set equal to 22.

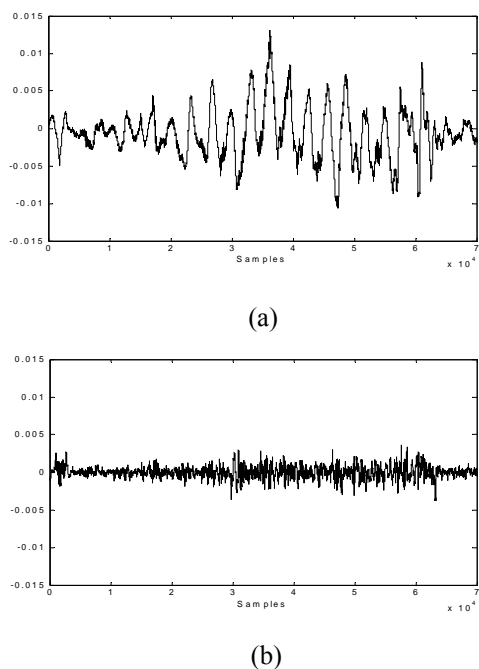


Fig. 1: Segments [læ] of sentence S1 spoken by a hoarse speaker (SDR = 8.9 dB) (a) and its sample-by-sample dysperiodicity (b).

Table 3: Quartiles of SDRs estimates in dB obtained via generalized variogram analyses of vowel [a] and sentences S1-S4 produced by 22 speakers.

	[a]	S1	S2	S3	S4
Min (dB)	5.61	8.3	7.1	8.6	7
Quartile 1 (dB)	18	15.7	17.2	16.4	13.9
Median (dB)	20	17.3	18	18	15.7
Quartile 3 (dB)	22.6	18.2	19.5	18.9	17.1
Max (dB)	26.3	20.6	22.6	22.4	19.4

Table 4: Pearson's product moment correlation between SDR values and hoarseness scores assigned by six judges for sustained vowel [a] and sentences S1 to S4. Median correlations are given in the last column.

	J1	J2	J3	J4	J5	J6	Med.
[a]	0.75	0.61	0.67	0.76	0.76	0.67	0.72
S1	0.74	0.71	0.79	0.66	0.53	0.65	0.69
S2	0.72	0.67	0.71	0.64	0.61	0.6	0.66
S3	0.66	0.66	0.73	0.62	0.55	0.59	0.64
S4	0.58	0.66	0.66	0.64	0.61	0.63	0.64

IV. DISCUSSION AND CONCLUSION

Experiments demonstrate the validity of perceptual rating of hoarseness based on comparative judgments of pairs of speech samples. Inter-listener and intra-listener agreement is well above statistical significance for both sustained vowel [a] and sentences S1 to S4 (Tables 1 and 2).

Correlation analyses show that the generalized variogram obtains SDR estimates that are statistically significantly correlated with the hoarseness scores assigned perceptually for vowel [a], as well as sentences S1 to S4. One sees in Table 4 that the highest correlation values are associated with sentences S1 and S2 as well as vowel [a], which are voiced throughout. Smallest correlations are observed for sentences S3 and S4 which include voiced and unvoiced segments. This observation agrees with the report of the listeners who designated sentences S3 and S4 as more difficult to assess than sentences S1 and S2. A possible explanation is that SDR values are determined by the vocalic segments in connected speech [5]. SDR values are therefore expected to correlate better with perceived hoarseness of all-voiced speech fragments, which are perceptually more prominent and more relevant to perceived hoarseness. The interquartile ranges of the correlation values between hoarseness scores and signal-to-dysperiodicity ratios are 0.66 – 0.76 for vowel [a] and 0.61 – 0.71 for sentences S1 to S4. These compare favourably with published values which are in the range 0.4 – 0.7 for typical phonatory features extracted from sustained vowels [a] [1].

REFERENCES

- [1] P. H. Dejonckere et al., "Differentiated perceptual evaluation of pathological voice quality: reliability and correlations with acoustic measurements," *Rev. Laryngol. Otol. Rhinol.*, vol. 117, pp. 219-224, 1996.
- [2] F. Klingholz, "Acoustic recognition of disorders: a comparative study of running speech versus sustained vowels," *J. Acoust. Soc. Am.*, vol. 7, pp. 2218-2224, 1990.
- [3] F. Parsa and D. G. Jamieson., "Acoustic discrimination of pathological voice: sustained vowels versus continuous speech," *J. Speech, Language, and Hearing Research*, vol. 44, pp. 327-339, 2001.
- [4] A. Kacha, F. Grenez and J. Schoentgen, "Dysphonic speech analysis using generalized variogram," *ICASSP*, pp. 917-920, Philadelphia, March 2005.
- [5] F. Bettens, F. Grenez and J. Schoentgen, "Estimation of vocal dysperiodicities in connected speech by means of distant-sample bi-directional linear predictive analysis," *J. Acoust. Soc. Am.*, vol. 117, pp. 328-337, 2005.
- [6] D. Moore and G. McCabe, *Introduction to the practice of statistics*, Freeman, New York, 1999.
- [7] Y. Qi, R. E. Hillman and C. Milstein, "The estimation of signal-to-noise ratio in continuous speech of disordered voices," *J. Acoust. Soc. Am.*, vol. 105, pp. 2532-2535, 1999.

MODELLING OF NON-STATIONARY PHONATION FOR CLASSIFICATION OF VOCAL FOLD VIBRATIONS

4TH INTERNATIONAL MAVEBA WORKSHOP

T. Wurzbacher, R. Schwarz, H. Toy, U. Eysholdt, J. Lohscheller

Department of Phoniatics and Pediatric Audiology, University Hospital Erlangen, Medical School, Erlangen, Germany

In contrast to the endoscopic examination of a stationary phonation, the examination of a non-stationary phonation screens a broader spectrum of vocal fold oscillations. For this reason, vocal fold vibrations are investigated and recorded with a high-speed camera system in eight normal and in eight pathological voices during a pitch raise. A quantitative analysis of the observed vocal fold dynamics in terms of symmetry and regularity is done with a time-dependent two-mass model of the vocal folds. The model's parameters are numerically optimized to emulate the observed non-stationary vocal fold vibrations. These parameters permit an objective interpretation of vocal fold oscillating asymmetries and allow a classification in normal and pathological cases. The practicability of the optimization algorithm is demonstrated with a set of 242 synthetically generated data sets. By applying the optimization procedure to the recordings of the 16 subjects a correct classification into groups of normal and pathological cases was achieved.

I. INTRODUCTION

Vocal fold examination in clinical routine is based on laryngeal endoscopic techniques. Conventionally, the examination condition for the assessment of vocal fold oscillation is a stationary sustained phonation, i.e. phonating a vowel at a constant pitch and intensity. Only fractions of the voice disorder that appear at this pitch and intensity level can be registered. This limits the diagnosis of voice disorders. To overcome this drawback a non-stationary phonation is investigated that screens a broad phonation range. A "monotonous pitch raise" (MPR) paradigm is explored, where the proband is free to choose the starting and the end pitch of phonation [1].

High-speed glottography (HGG) is the state of the art real-time recording technique, which allows to observe the non-stationary vocal fold vibrations [2]. Objective medical diagnosis demands to extract parameters from the observed HGG vibrations that describe symmetry and regularity of vocal fold oscillations. These parameters enable a classification of vocal fold oscillation patterns. Quantitative parameters can be derived by adapting a biomechanical two-mass model (2MM) of vocal folds to the HGG vibration patterns. Recently, the adaptation of the vibration behavior of a 2MM succeeded in stationary

vibration patterns of normal voices and in cases of unilateral recurrent laryngeal nerve paralysis [3, 4]. However, the 2MM is restricted to the steady state section after the vocal onset i.e. on a stationary phonation. In order to model a pitch raise a time-dependent 2MM for the interpretation of MPR-based high-speed recordings is presented. The model's dynamic is adjusted with five time-dependent parameters, which are used to determine asymmetries in vocal fold vibrations. These parameters are numerically optimized in the sense that the vibration behavior of the 2MM is adapted to the HGG observed vocal fold vibrations. The performance of the proposed algorithm is tested with 242 predefined data sets and is applied to eight normal and to eight pathological cases.

II. METHODOLOGY

A. Examination Conditions

Eight young female subjects (average age of 20.3 years with standard deviation of 3.7 years) served as subjects for the endoscopic investigations. The subjects had a normal voice and exhibited no history or clinical signs for voice disorders. Eight further subjects (38.3 ± 13.4 years) suffered from different voice disorders as functional dysphonia (3), Reinke's Edema (1), unilateral vocal fold paralysis (3), and vocal fold polyp (1). All subjects were instructed to increase monotonically the pitch during the phonation of the vowel /a/ from a comfortable frequency up to an arbitrary higher one (MPR). No more instructions about pitch shift duration or frequency range were given.

For each subject a MPR-HGG sequence was recorded with a frame rate of 4.000 frames per second (High-Speed Endocam, Wolf corp., Knittlingen, Germany) [2].

The dynamics of the vocal folds are represented by the motions of the vocal fold edges. Their movements are extracted from the HGG sequences by image processing at the medial glottal third, as the oscillation amplitude of the vocal folds is largest in this region [5]. The time-varying deflections of two opposing vocal fold edge points from glottal midline are regarded as experimental trajectories $d_a^{\text{HGG}}(t)$ for the left ($a = l$) and right ($a = r$) side. In the following all characteristics that are marked by superscript HGG refer to the experimental trajectories.

B. Two-Mass Model, its Time-Dependent Extensions, and Symmetry Factors

To emulate experimental trajectories $d_a^{\text{HGG}}(t)$ a 2MM is chosen, since the model is able to represent the dominant modes of vocal fold vibrations [3], [6]. In the following a brief summary of the time-dependent extensions of the 2MM is depicted. Within the 2MM one vocal fold is represented by two coupled oscillators, which are set into vibrations by a subglottal air pressure $P_s(t)$. Incorporated nonlinearities are the driving Bernoulli force and the impact forces. These impact forces, which are represented by spring constants $c_{ia}(t)$, act as additional restoring forces when the model's masses get into contact. Indices used for the parameters indicate the lower ($i = 1$) and upper ($i=2$) plane of the model. The vibrating masses and spring tensions of the model are denoted by the parameters $m_{ia}(t)$ and $k_{ia}(t)$. The coupling between the lower and upper masses is represented by the spring constants $k_{ca}(t)$. The rest positions $x_{0,a}(t)$ of the upper and lower spring constants are assumed to be equal and the glottal length of the model is signed as $l(t)$. The model is described by a system of differential equations:

$$d/dt(\mathbf{x}) = \mathbf{A}(t) \mathbf{x} + \mathbf{b}(\mathbf{x},t) . \quad (1)$$

Matrix $\mathbf{A}(t)$ contains the aforementioned tissue properties while the non-linear parts are captured in vector $\mathbf{b}(\mathbf{x},t)$. The vector \mathbf{x} contains positions and velocities of the left, right, lower and upper masses (T transposed vector)

$$\mathbf{x}^T = [x_{1l} \ v_{1l} \ x_{2l} \ v_{2l} \ x_{1r} \ v_{1r} \ x_{2r} \ v_{2r}] . \quad (2)$$

In accordance with the vocal fold oscillations the model dynamic is described by the minimum opening formed by the vibrating masses. These 2MM oscillations are called theoretical trajectories $d_a(t)$. In equation (1) the more general form of Newton's second law

$$F_{ia} = m_{ia}(t) d/dt(v_{ia}(t)) + v_{ia}(t) d/dt(m_{ia}(t)) \quad (3)$$

has been accounted for. Hence, the time derivatives of masses $m_{ia}(t)$ are incorporated in the equations of motion. Equation (1) is numerically solved by a fourth order Runge-Kutta method with a step size h fixed to the frame rate of the HGG recordings $h=1/4000$.

The time-dependent parameters summarized in $\mathbf{A}(t)$ and $\mathbf{b}(\mathbf{x},t)$ influence the oscillation behavior of the model. The subglottal pressure $P_s(t)$ mainly affects the amplitude of the model's oscillation and to some minor extend the oscillation frequency [1]. $P_s(t)$ can be seen as a measure for the energy flowing into the system [3]. Furthermore, the masses $m_{ia}(t)$ and tensions $k_{ia}(t)$ predominantly influence the frequency as well as the amplitude of the oscillation [1]. In the model the parameters $m_{ia}(t)$, $k_{ia}(t)$,

..., are expressed in terms of Ishizaka's and Flanagan's [8] standard parameters $k_{0,ia}$, $m_{0,ia}$, ..., by introducing factors $Q_a(t)$, $R_a(t)$, and $U(t)$:

$$\begin{aligned} k_{ia}(t) &= k_{0,ia} Q_a(t), & k_{ca}(t) &= k_{0,ca}(t) Q_a(t), \\ m_{ia}(t) &= m_{0,ia}/Q_a(t), & c_{ia}(t) &= c_{0,ia}(t) Q_a(t), \\ x_{0,a}(t) &= x_{0,a} R_a(t), & P_s(t) &= P_{s0} U(t). \end{aligned} \quad (4)$$

As a measure of asymmetry between the oscillations of the left and right side of the model the ratios

$$Q(t) = Q_l(t) / Q_r(t) \quad \text{and} \quad R(t) = R_l(t) / R_r(t) \quad (5)$$

are introduced [7]. If $Q_l(t)$ and $Q_r(t)$, respectively $R_l(t)$ and $R_r(t)$ differ from each other the model's oscillation become asymmetric. Time-varying irregularities within non-stationary vocal fold vibrations are captured in time variations of the two symmetry factors. These irregularities can be described and visualized by a curve

$$C(t) := C(Q(t), R(t)) \quad (6)$$

in the $Q(t)$ — $R(t)$ plane. A curve $C(t)$ that represents symmetric and regular vibrations is close to the point of perfect symmetry (1,1), while a wide dithering of the curve indicates oscillating irregularities. Thus, from this curve $C(t)$ two characteristics can be derived that describe the degree of asymmetries in vocal fold vibrations:

- The distance d_g of the center of gravity of the curve $C(t)$ to the point (1,1) describes the mean degree of oscillation symmetry.
- The radius r_c of a circle that encloses 90 % of $C(t)$ is a measure of the oscillation stability over time.

A rating value R_v for vocal fold oscillation asymmetries is defined by the combination of both criteria:

$$R_v := d_v + r_c . \quad (7)$$

C. Parameter Optimization of Time-Dependent Two-Mass Model

In order to derive the curve $C(t)$ a parameter set of the 2MM $S(t) = [Q_l(t) \ Q_r(t) \ R_l(t) \ R_r(t) \ U(t)]$ has to be determined by an optimization procedure. Here, optimization means to find proper values of the parameter set $S(t)$ that adapts the model dynamics $d_a(t)$ to experimental trajectories $d_a^{\text{HGG}}(t)$. Due to the time-dependency of non-stationary vibrations, for each sampling point the parameter set $S(t)$ has to be optimized. The optimization of an entire non-stationary trajectory of about one second (number of samples $N = 4.000$) spans an optimization space of 20.000 parameters. The change of the parameters $S(t)$ is continuous over time.

In the following an algorithm is introduced that takes advantage of the continuous parameter variation and reduces the dimensionality of the solution space. A schematic overview of the algorithm is depicted in Fig. 1. The algorithm divides the trajectories $d_a^{\text{HGG}}(t)$ in K blocks. Each block κ represents one period of oscillation with $N\kappa$ samples. The time samples of the parameters and trajectories are indexed as $t_{n,\kappa}$, where κ represents the period and n the time sample within the period κ . The time constants of the parameter set $S(t)$ can be assumed to be beyond the period length. Thus, it is sufficient to optimize just the first $S(t_{0,\kappa})$ and the last $S(t_{N\kappa,\kappa})$ values of the parameter set of one period. The parameter values in between are obtained by linear interpolation. The continuity of the parameters of consecutive periods is ensured by an overlap of one sample, see Fig. 1.

The optimization of the parameter set $S(t)$ starts at period $\kappa=0$ of the experimental trajectories $d_a^{\text{HGG}}(t)$. Initial values for the parameters $Q_a(t_{n,0})$ with $n=\{0, N_0\}$ are derived by using a simple mass-spring oscillator equation [3]

$$Q_a(t_{0,0}) = Q_a(t_{N_0,0}) = 2\pi f_a (m_{0,1a} / k_{0,1a})^{1/2} \quad (8)$$

where f_a is the frequency of period $\kappa=0$. The factors $R_a(t)$ and $U(t)$ are set to one. Following initialization the parameter optimization is performed. Therefor, the error, also called objective function,

$$e_{\kappa} = 1/N\kappa \sum |d_a(t_{n,\kappa}) - d_a^{\text{HGG}}(t_{n,\kappa})|^2, \quad \kappa = 0, \dots, K-1 \quad (9)$$

between experimental and theoretical trajectories is minimized. Since the behavior of the 2MM is non-linear and the objective function is non-convex, a stochastic optimization procedure, ASA [8], is used to find the best fit. ASA adjusts the ten optimization parameters so that the objective function e_0 gets minimal.

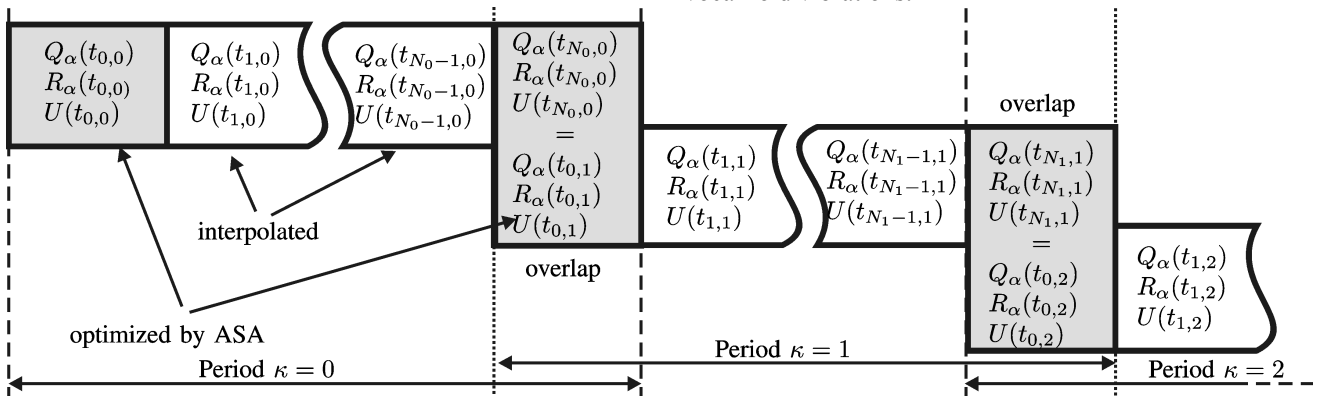


Fig. 1. Schematic overview of the period by period ASA (Adaptive Simulated Annealing [8]) optimization. The periods overlap by one sample. The number of samples in period κ is $N\kappa$. The parameters in gray-filled boxes are optimized, while the others are obtained by linear interpolation.

After the optimization of the first period $\kappa=0$ all the consecutive periods are processed. Due to the periods' overlap of one sample, the end state $S(t_{N\kappa-1,\kappa-1})$ of period $\kappa-1$ is identical to the start state $S(t_{0,\kappa})$ of period κ . Only one parameter set $S(t_{N\kappa,\kappa})$ at the last time index of the following periods is needed for optimization. Hence, the optimization periods has just five dimensions compared to the first period. Finally, a lowpass filter is applied to the elements of $S(t)$ to remove artifacts caused by the period by period processing.

D. Verification and Accuracy of the Optimization

In order to estimate the performance of the proposed optimization algorithm, 242 synthetically non-stationary trajectories with the 2MM where produced. For this, different predefined parameter sets $S^*(t)$ with varying slopes of pitch increase, subglottal pressure levels, and rest positions were generated. These sets were compared to the outcome of the ASA period by period optimization $S(t)$. The objective function is more sensitive to variations of $Q_a(t)$ than to variations of $R_a(t)$. Hence, the factors $Q_a(t)$ match very closely with a relative error of about 2.7%, whereas the factors $R_a(t)$ show a relative error of about 17.9%.

III. RESULTS

The optimization algorithm was applied to the experimental trajectories $d_a^{\text{HGG}}(t)$ of 16 subjects. For each subject the curve $C(t)$ (solid line) within the $Q(t)$ — $R(t)$ plane is depicted in Fig. 2. The curves $C(t)$ of the normal voices are located closer to the symmetry point (1,1) and they spread less across the plane than for the pathological cases. The resulting rating value R_v is shown for the normal and for the pathological cases in Fig. 3. The mean rating value of the normal voices is 0.25 and 0.51 for the pathological ones, respectively. Furthermore, the mean values of d_g and r_c are increased for the pathological vocal fold vibrations.

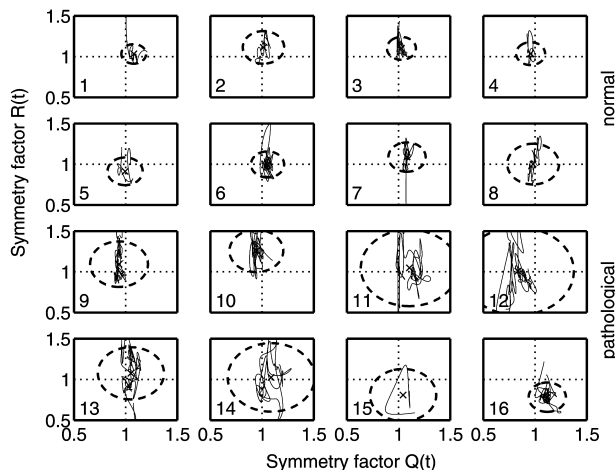


Fig. 2. Plots of the curve $C(t)$ for normal and pathological cases in the $Q(t)$ - $R(t)$ plane. Perfect symmetry is located at the point $(1,1)$. A circle is drawn around the center of gravity for each curve. The radius r_c is determined so that 90% of the curve $C(t)$ lies inside the circle. The subject number is printed in the lower left corner.

IV. DISCUSSION

The adaptation of a time-dependent 2MM to non-stationary vocal fold oscillations enables to derive a two dimensional parameter curve $C(t) = C(Q(t), R(t))$. From the curve $C(t)$ a rating R_v is calculated that quantifies different degrees of vocal fold asymmetries. Within this rating the mean degree of asymmetry is captured by the distance d_g of the point of gravity to the symmetry point $(1,1)$. The distance d_g can be regarded as counterpart of the asymmetries that are observable in stationary phonation. In contrast, the value r_c describes irregularities resulting from non-stationary vocal fold vibrations. In Fig. 3 a clear distinction between normal and pathological vocal fold vibrations is only possible by the combined evaluation of d_g and r_c . The rating value r_c — that can not be revealed in case of a stationary phonation — makes an important contribution to describe irregularities in non-stationary vocal fold vibrations. The rating R_v can be used as an objective measurement of voice quality in terms of vocal fold oscillation symmetries and regularities. It enables the classification of healthy and pathological voices in non-stationary phonation.

Further investigations will focus on the potential to classify even different kinds of voice disorders, the severity of dysphonia, and to quantify the outcome of voice therapy.

V. CONCLUSION

Dynamical changes of the vocal folds can be accessed by phonating a pitch increase during an endoscopic high-speed recording. Voice quality in terms of vocal folds' oscillation symmetry and regularity is expressed by a two

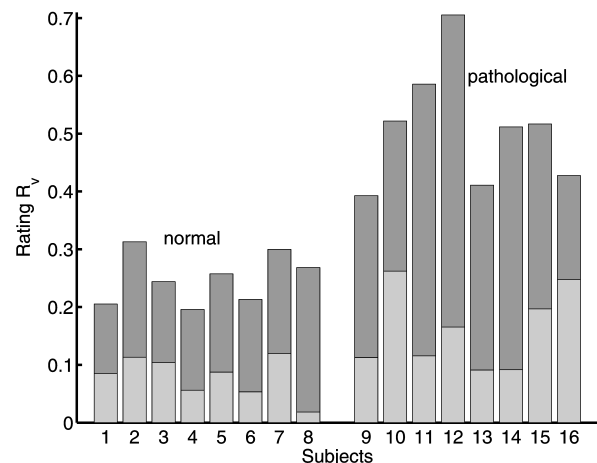


Fig. 3. Rating R_v of the normal and pathological subjects. Small values indicate a symmetrical and regular vibration. The rating is composed out of the distance d_g (light gray) from the center of gravity from the point $(1,1)$ and of the 90% radius r_c (dark gray), see Fig. 2.

dimensional parameter curve. This time-dependent curve gives quantitative information on the dynamical state changes of the vocal folds. A classification of vocal fold vibrations into a healthy and a pathological group is possible.

REFERENCES

- [1] U. Hoppe, F. Rosanowski, M. Döllinger, J. Lohscheller, U. Eysholdt, "Visualization of the laryngeal motorics during a glissando," *J. Voice*, vol. 17, pp. 370–376, 2003.
- [2] T. Wittenberg, M. Moser, M. Tigges, U. Eysholdt, "Recording, processing and analysis of digital high speed sequences in glottography," *Mach. Vision. Appl.*, vol. 8, pp. 399–404, 1995.
- [3] M. Döllinger, U. Hoppe, F. Hettlich, J. Lohscheller, S. Schuberth, U. Eysholdt, "Vibration parameter extraction from endoscopic image series of the vocal folds," *IEEE Trans. Biomed. Eng.*, vol. 49, pp. 773–781, 2002.
- [4] R. Schwarz, J. Lohscheller, T. Wurzbacher, U. Eysholdt, U. Hoppe, *Modeling vocal fold vibrations in case of unilateral vocal fold paralysis*, IASTED Biomed. Eng. Innsbruck, ACTA PRESS, Feb 2004.
- [5] U. Eysholdt, M. Tigges, T. Wittenberg, U. Pröschel, "Direct evaluation of high-speed recordings of vocal fold vibrations," *Folia Phoniatr. Logop.*, vol. 48, pp. 163–170, 1996.
- [6] K. Ishizaka, J. Flanagan, "Synthesis of voiced sounds from a two-mass model of the vocal coords," *Bell Syst. Techn. J.*, vol. 51, pp. 1233–1268, 1972.
- [7] P. Mergell, I. R. Titze, and H. Herzel, "Irregular vocal fold vibration - high speed observation and modeling," *J. Acoust. Soc. Am.*, vol. 108, pp. 2996–3002, 2000.
- [8] L. Ingber. Adaptive Simulated Annealing. [Online]. Available: <http://www.ingber.com/>

ANALYSIS OF SPANISH SYNTHESIZED SPEECH SIGNALS USING SPECTRAL AND BASIS PURSUIT REPRESENTATIONS

F. M. Martinez¹, J. C. Goddard, A². M. Martinez²

¹Biomedical Engineering, ²Computer and Systems, Department of Electric Engineering, Universidad Autonoma Metropolitana, Mexico City, Mexico

In speech, the sounds involved in an utterance are not produced independently of one another, but rather reflect the result of a complex process of sound concatenation. It is important to study these coarticulation effects in representations of speech signals since, for example, their cues can be helpful in the development of robust speech recognition systems. Representational tools, such as the spectrogram, are useful for visualizing spectral characteristics along the time axis; most of these tools are based on second-order statistics, and it is interesting to consider other methods which might be useful in studying the problem of coarticulation. In recent years, sparse signal representations using suitable dictionaries of functions seem to provide an attractive alternative. With this alternative in mind, the present paper applies spectral and basis pursuit techniques to spanish synthesized signals. The results on a reduced vocabulary show that some prosodic and coarticulatory cues can be obtained from the basis pursuit method compared to the spectral representation.

I. INTRODUCTION

In speech, it is well known that sounds are not produced in isolation, but influence and affect one other. This complex process of sound concatenation is called coarticulation. Coarticulation is related to the speed and the coordination of the movements of the vocal fold. For example, a vowel (V) produced between two nasal consonants (C), such an /m/, presents modifications in its spectral representation due to the effects of these adjacent consonants. In a CV segment with a stop consonant, the spectral representation shows the obstruction of the air flow and then the release of the accumulated air at the moment of the closing and opening of the vocal fold. Graphical representations of these acoustic events sometimes lack clarity when analyzing changes within the same speaker, so different types of analysis and representation methods could prove useful.

In the field of speech processing there are several methods of analysis and representation. The spectrogram is an efficient tool to visualize the spectral characteristics of the signal along the time axis; it is based on second-order statistics. Alternative representations might improve this one, for example, by showing 'hidden' elements hard to identify in the spectrograms. The information obtained by higher order statistics, for

example, might be useful since it may provide clues about new model configurations of speech signals that could be better than existing ones [1]. The most important problem with this kind of alternative signal analysis is a lack of understanding of their properties when applied to speech signals. Furthermore, the computational load is usually greater compared to the traditional second-order statistics based analysis [1], [2].

In a preliminary exploration of alternative techniques, this paper presents spectral and basis pursuit representations of speech signals using two different synthesized voices, spanish and mexican; spectrogram and basis pursuit algorithms were applied to the signals in order to study coarticulation effects.

The paper is organized as follows: in the next section the words selected, the effects to be analyzed and the speech representation methods are described. Results are presented and a discussion and conclusions are given.

II. METHODOLOGY

The data selected and the representation methods are described in this section.

A. Data

A set of two spanish words was selected. These words presented different combinations of spanish sounds, e.g. CV segments (stop-vowel or fricative vowel), CVV segments (liquid semivowel-diphthong) or CVC segments (liquid-vowel-fricative, stop-vowel-fricative, nasal-vowel, nasal).

For each word three different synthesized utterances were produced using mbrola [3]; tables 1 and 2 shows the acoustic characteristics of each utterance for the figures presented in this paper. The idea of studying synthesized utterances was because of the control available for specifying certain acoustic events precisely.

Table 1: Acoustic characteristics of the synthesized word 'areas'

phoneme name	duration (ms)	position of the pitch target (%)	pitch value (Hz)
a	108/108/108	30/30/30	130/130/130
r	50/50/50	- /50/ -	- / - / -
e	90/90/90	-/100/-	-/150/130
a	90/90/130	-/99/30	- / - / -

s | 110/110/110 | 99/99/99 | 80/80/80

Table 2: Acoustic characteristics of the synthesized word 'gatos'

phoneme name	duration (ms)	position of the pitch target (%)	pitch value (Hz)
g	50/50/50	- / - / -	- / - / -
a	120/90/90	- /90/90	- /100/150
t	85/85/85	- / - / -	- / - / -
o	90/35/35	90/60/60	100/123/350
s	110/110/110	- / - / -	- / - / -

For each utterance the spectrogram and the basis pursuit representations were obtained.

B. Spectrogram

The spectrogram algorithm splits the signal into overlapping segments and applies a window [4]. For each segment it computes the discrete-time Fourier transform for a given length (nfft) to produce an estimate of the short-term frequency contents. The matlab algorithm to compute the spectrograms was applied to the signals [5]. The spectrogram is computed from

$$\Gamma_y(\omega) = 2\pi \sum_{k=-\infty}^{\infty} |C_k|^2 \delta\left(\omega - k \frac{2\pi}{N}\right)$$

where $\Gamma_y(\omega)$ is the power density spectrum for a periodic signal $y(n)$, C_k the associated coefficients [6]

The set of parameters used is the following:

- sampling frequency = 16 KHz
- nfft = 256
- hamming window of nfft length
- no overlap between windows.

C. Basis Pursuit

In the last few years a number of papers have been devoted to the study of different ways of representing signals using dictionaries of suitable functions [7], [8]. A dictionary D is a collection of parameterized waveforms $(\phi_\gamma)_{\gamma \in \Gamma}$, and a representation of the signal s in terms of D is a decomposition of the form

$$s = \sum_{\gamma \in \Gamma} a_\gamma \phi_\gamma \quad (1)$$

Some commonly used dictionaries are the traditional Fourier sinusoids (frequency dictionaries), Dirac functions, Wavelets (time-scale dictionaries), Gabor functions (time-frequency dictionaries), or combinations of these. In this paper a wavelet symmlet was employed.

An important criterion for choosing a method consists in obtaining a sparse representation of the signal; Here,

this means that 'a few' of the coefficients a_γ in (1) are to be different from zero.

Chen et al [9] propose a method, called Basis Pursuit (BP), which is designed to produce such a sparse representation. A suitable representation is found by optimization with respect to the l_1 norm. More precisely if the signal s has length n and there are p waveforms in the dictionary, then the problem to solve is:

$$\min \|a\|_1 \text{ subject to } \Phi a = s \quad (2)$$

where a is a vector in \mathfrak{R}^n representing the coefficients and Φ is a $p \times n$ matrix giving the values of the p waveforms in the dictionary.

It can be shown that the problem can be converted to a standard linear program, with only positive coefficients, by making the substitution $a \leftarrow [u, v]$ and solving

$$\min l^T [u, v] \text{ subject to } [\Phi, -\Phi] [u, v] = s, \\ 0 \leq u, v \quad (3)$$

This formulation can be solved efficiently and exactly with interior point linear programming methods.

III. RESULTS

Figs 1 and 2 show the spectrogram and BP representations of the synthesized utterances of the word 'areas' produced by a spanish voice. Figs 3 and 4 show the spectrogram and BP representations of the synthesized utterances of the word 'gatos' produced by a mexican voice.

In each of the figures the segment to be analyzed is selected between the lines: the fricative-diphthong (CVV) segment for the word 'areas' and the vowel-stop-vowel (VCV) segment for the word 'gatos'.

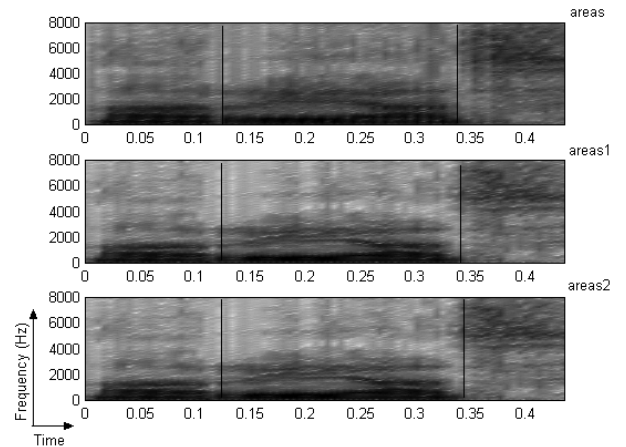


Fig.1 Spectrogram of the word "areas" (spanish synthesized voice)

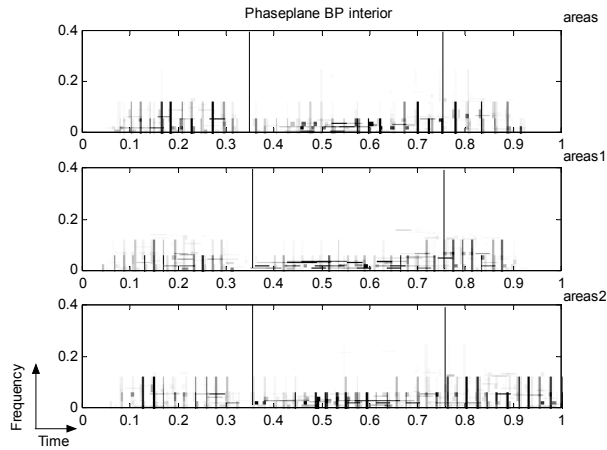


Fig.2 Phaseplane Basis Pursuit of the word “areas” (spanish synthesized voice)

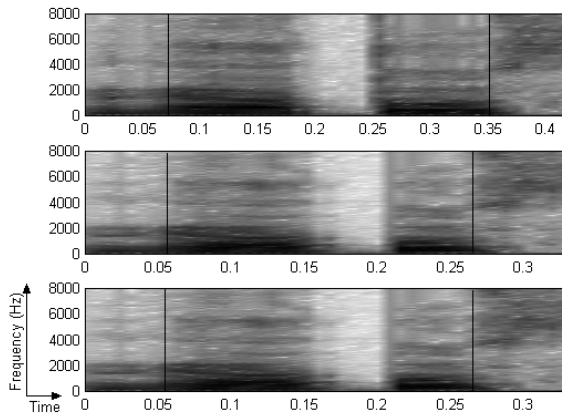


Fig.3 Spectrogram of the word “gatos” (mexican synthesized voice)

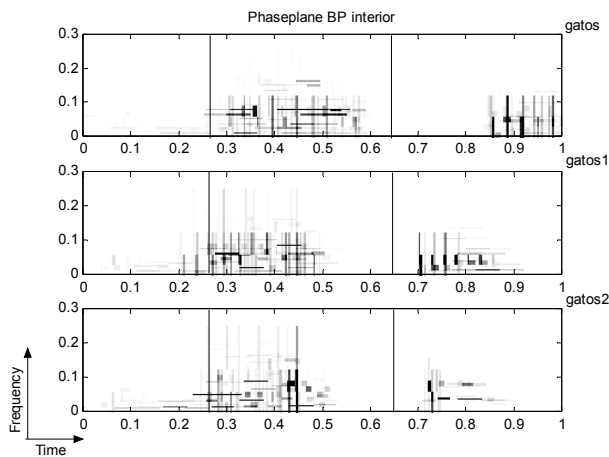


Fig.4 Phaseplane Basis Pursuit of the word “gatos” (mexican synthesized voice)

IV. DISCUSSION

The spectral representations show a very similar behavior for the three utterances in both examples. In the case of ‘areas’ (Fig 1) the CVV segment presents changes in energy and the effect of the diphthong (/ea/) can be seen in the vowel formants. In Fig 3, the spectral VCV segment remains without changes in the three utterances and the vowel configurations do not seem to be different.

The basis pursuit diagrams (Figs 2 & 4) show noticeable changes among the utterances for the same word. In Fig 2 the diphthong segment BP coefficients are presented in different arrays while in Fig 4, the VCV segment clusters its BP coefficients in different locations of time. It is important to notice that the number and energy level of the coefficients are also different for each utterance even for the same word.

One of the disadvantages that the basis pursuit interior point algorithm presents is the amount of processing time, since there are an important number of calculations involved. Table 3 presents the BP-Interior algorithm time durations (in seconds) for the example words.

Table 3: Time duration (secs) of BP-Interior Algorithm applied to the speech signals

Word	Spanish voice	mexican voice
Areas	539.8	302.47
Gatos	526.3	250.99

V. CONCLUSION

Spectral and basis pursuit representations were applied to synthesized speech signals in order to identify differences in coarticulatory effects among three utterances of the same word.

The study of basis pursuit applied to speech analysis shows possible advantages of the method over traditional approaches. These advantages present themselves in terms of the adequate localization of acoustic cues, obtained from a sparse representation. It is necessary to understand the effect of the dictionary on the acoustic cues for speech signals and to develop efficient methods to obtain the BP coefficients.

Further work in the development of atomic decompositions and higher order analysis tools will be addressed in the future.

REFERENCES

- [1] C. L. Nikias, A. P. Petropulu, *Higher-order Spectral Analysis*. Englewood Cliffs, NJ: Prentice Hall, 1993, pp. 1–5.
- [2] F. Martinez, H. Rufiner, J. Goddard and A. Martinez, “Analysis of Spanish Speech Signals using Higher Order Statistics”, IFMBE Proceedings of Third Latinamerican Congress on Biomedical Engineering, Joao Pessoa Brazil, 2004.
- [3] MBROLA Project, speech synthesis available in <http://tcts.fpms.ac.be/synthesis/mbrola.html>
- [4] Oppenheim, A.V., and R.W. Schaffer, *Discrete-Time Signal Processing*, Prentice-Hall, Englewood Cliffs, NJ, 1989, pp. 713-718
- [5] *Signal Processing Toolbox (4.0) User's Guide*, The Math Works, Natick, MA, 1998, pp. 0-363-0-367.
- [6] J. R. Deller, J.H. Hansen and J.G. Proakis, *Discrete-time Processing of Speech Signals*, IEEE Press, 2000.
- [7] S. Mallat, Z Zhang, “Matching Pursuit in a time-frequency Dictionary”, *IEEE Trans. Signal Processing*, vol. 41, pp. 3397-3415, 1993.
- [8] S. Mallat, Z Zhang, “Matching Pursuit in a time-frequency Dictionary”, *IEEE Trans. Signal Processing*, vol. 41, pp. 3397-3415, 1993.
- [9] S.S. Chen, D.L. Donoho and M. A. Saunders, “Atomic Decomposition by Basis Pursuit”, *SIAM Journal of Scientific Computing*, Vol.20, pp. 33-61, 1998.

Voiced excitation as entrained primary response of a reconstructed glottal master oscillator

F.R. Drepper

Forschungszentrum Jülich GmbH, D 52425 Jülich, Germany
f.drepper@fz-juelich.de

The transmission protocol of sustained voiced speech is hypothesized to be based on a fundamental drive process, which synchronizes the vocal tract excitation on the transmitter side and evokes the pitch perception on the receiver side. A band limited fundamental drive is extracted from a voice specific subband decomposition of a speech signal. When the near periodic drive is used as fundamental drive of a two-level drive-response model, a more or less aperiodic voiced excitation can be reconstructed as a more or less aperiodic trajectory on a low dimensional synchronization manifold described by speaker and phoneme specific coupling functions. In the case of vowels and nasals the excitation depends on a single phase of the fundamental drive. In the case of other sustained voiced consonants the excitation may include an additional coupling function, which depends on a delayed fundamental phase with a phoneme specific time delay. The delay may exceed the length of the analysis window. The resulting long range correlation cannot be analysed by methods assuming stationary excitation.

Keywords: voiced speech, fundamental drive, two-level drive-response model, generalized synchronization, delayed excitation

I. INTRODUCTION

The vocal tract excitation of voiced speech is generated by a pulsatile airflow, which is strongly coupled to the oscillatory dynamics of the vocal fold. The excitation is created immediately in the vicinity of the vocal fold and/or delayed in the vicinity of a secondary constriction of the vocal tract [1-3]. As has been pointed out by Titze [4], a mechanistic model of a dynamical system suitable to describe the self-sustained oscillations of the glottis cannot be restricted to state variables of the vocal fold alone.

Due to the strong nonlinearities of the coupled dynamics, non-pathological, standard register phonation dynamics is characterized by a stable synchronization of several oscillatory subsystems including the two vocal folds. The synchronization can furthermore be assumed to have the effect that some of these subsystems become topologically equivalent oscillators, whose states are one to one related by a non-singular invertible mapping (conjugation) [5]. Due to the pronounced mass density difference of about 1:1000 the coupling between the airflow and the glottal tissue is characterized by a dominant direction of interaction, such that the glottal oscillators can affirmatively be assumed to be a subset of those topologically equivalent oscillators. Therefore a glottal master oscillator can be defined, which enslaves (synchronizes) or drives the other oscillators including the higher frequency acoustic modes.

In the case of non-pathological voiced speech the observation of the air pressure signal or of the electro-glottogram reveals a unique frequency of phonation, the fundamental frequency. Time series of successive cycle lengths of oscillators, which are (implicitly) assumed to be equivalent to the glottal master oscillator show an aperiodicity with a wide range of relevant frequencies reaching from half of the pitch down to less than 0.1 Hz [6, 7]. Except at the high frequency end the deviation of the glottal cycle length from the long

term mean forms a non-stationary stochastic process. More or less distinct frequency bands or time scales have been described as: subharmonic bifurcation [8], jitter, microtremor and prosodic variation of the pitch [6, 7]. As a general feature, cycle length differences increase with the time scale (the relative differences ranging from less than 1 % up to more than 20%). In spite of the partially minor amplitudes of aperiodicity all or most of these frequency bands appear to be perceptually relevant. Some of them are known to play a major role for the non-symbolic information content of speech.

The relevant frequency range of the excitation of voiced speech extends at least one order of magnitude higher than the fundamental frequency. It is therefore common practice to introduce a time scale separation, which separates the high frequency acoustic phenomena of speech signals above the pitch from the subharmonic, subacoustic and prosodic ones below the pitch. A simple approach towards time scale separation starts with the assumption of a causal frequency gap, which separates the frequency range of the autonomous, lower frequency degrees of freedom from the dependent degrees of freedom (modes) in the acoustic frequency range.

In the main stream approach of speech analysis this has led to the more or less explicit assumption that the excitation is wide sense stationary in the analysis window, which is usually chosen as 20 ms [2, 3]. The latter assumption is closely related to the assumption that the excitation process can be described as a sum of a periodic process and filtered white noise with a time invariant, finite impulse response filter. In the case of voiced excitation there exists multiple evidence that this assumption is not fulfilled [9, 10]. In a first step of improvement the voiced excitation has been described as stochastic process in the basin of attraction of a low dimensional nonlinear dynamical system [9, 10]. The assumption of a low dimensional dynamical system, however, is in contradiction to the observed complexity of the glottal cycle lengths.

The present study introduces an analysis of (sustained) speech signals, which does not assume a periodic fundamental drive nor an aperiodic drive, which obeys a low dimensional dynamics. The assumption of a causal frequency gap is avoided by treating the more or less aperiodic voiced broadband excitation as an approximately deterministic response of a near periodic, non-stationary fundamental drive, which is extracted continuously from voiced sections of speech with uninterrupted phonation [11-12]. The extraction of the fundamental drive includes a confirmation that the drive can be interpreted as a topologically equivalent reconstruction of the glottal master oscillator which synchronizes the vocal tract excitation [11]. As an important property of non-pathological, standard register voiced speech the state of the fundamental drive is assumed to be described uniquely by a fundamental phase, which is related to pitch perception, and a fundamental amplitude which is related to loudness perception [11-12].

As result of a detailed study of the production of vowels (with a sufficiently open vocal tract to permit the manipulation of airflow velocity sensors) Teager and Teager [14] pointed out that the conversion of the potential energy of the compressed air in the subglottal

airduct to convective, acoustic and thermal energy happens in a highly organized cascade. They observed that the astonishingly complex convective airflow pattern within the vocal tract (flow separations, vortex rings, swirly vortices along the cavity walls, ...) show a degree of periodicity in time, which is comparable to the one of the corresponding far field acoustic response. In the case of the sustained voiced consonants it is plausible to assume that at least a part of the convective flow pattern will show a similar periodicity in time. In the case of the voiced fricatives the vowel type periodicity is obviously restricted to the upstream side of the secondary constriction of the vocal tract and/or to the lower frequency bands. As an important feature of the highly organized energy cascade the irreversible conversion to acoustic and thermal energy occurs at different sites of the vocal tract and happens with distinctly different delays with respect to the primary convective pulse.

Assuming an average convection speed of less than 5 m/s [1, 15] the delay of the secondary excitation may exceed 20 ms. This is in contradiction to the mainstream assumption that the correlation of the excitation is restricted to the analysis windows. The continuous reconstruction of the glottal master oscillator for segments of uninterrupted phonation opens the possibility to describe the excitation as superposition of a direct and a delayed phase locked response with correct long range correlation. The excitation is reconstructed as part of a two-level drive-response model, which extends the validity range of the classical source-filter model and which is suited to bring additional light to the complex airflow pattern of voiced consonants, which are extremely difficult to analyse in vivo [14], in vitro [15] and in silico [15].

II. EXTRACTION OF THE FUNDAMENTAL DRIVE

The amplitude and phase of the fundamental drive are extracted from subband decompositions of the speech signal. The decompositions use 4th order complex gammatone bandpass filters with roughly approximate audiological bandwidths ΔF and with a subband independent analysis - synthesis delay as described in Hohmann [16].

The extraction of the fundamental phase ψ_t is based on an adaptation of the best filter frequencies F_j of the subband decomposition to the momentary frequency of the glottal master oscillator (and its higher harmonics). At the lower frequency end of the subband decomposition the best filter frequencies F_j are centred on the different harmonics of the analysis window specific estimate of the fundamental frequency. In the next higher frequency range the best filter frequencies are centred on pairs of neighbouring harmonics.

$$F_j = \begin{cases} \frac{j F_1}{\sqrt{j(j+1)}} \\ F_1 \end{cases} \quad \text{for} \quad \begin{cases} 1 \leq j \leq 6 \\ 6 < j \leq 11 \end{cases} \quad (1a)$$

$$\Delta F_j = \begin{cases} F_1 \\ 2 F_1 \end{cases} \quad \text{for} \quad \begin{cases} 1 \leq j \leq 6 \\ 6 < j \leq 11 \end{cases} \quad (1b)$$

It is further assumed that voiced sections of speech are produced with at least two subbands, which are not distorted by vocal tract resonances or additional constrictions of the airflow. In the case of subbands with separated harmonics, $1 \leq j \leq 6$, the absence of a distortion is detected by nearly linear relations between the unwrapped phases of the respective subband states. For sufficiently adapted centre filter frequencies such subbands show an (n:m) phase locking. The corresponding phase relations can be interpreted to result from (n:1) and (m:1) phase relations to the fundamental drive. The latter ones are used to reconstruct the phase velocity of the fundamental drive. In the case of a subband with paired harmonics, $6 < j \leq 11$, the phase relation to the fundamental drive is obtained by

determining the Hilbert phase of the modulation amplitude of the respective subband.

The phase velocity of the fundamental drive is used to improve the centre filter frequencies. For voiced sections of speech the iterative improvement leads to a fast converging fundamental phase velocity $\dot{\psi}_t$ with a high time and frequency resolution. Based on a, so far, arbitrary initial phase, successive estimates of $\dot{\psi}_t$ lead to a reconstruction of the fundamental phase ψ_t , which is uniquely defined for uninterrupted segments of voiced phonation.

The fundamental amplitude A_t is assumed to be related to loudness perception [17] by a power law. The exponent $1/\nu$ is chosen such that the fundamental amplitude represents a linear homogenous function of the time averaged amplitudes $\bar{A}_{j,t}$ of a synthesis suited set of subbands,

$$A_t = \left(\sum_{j=1}^N (g_j \bar{A}_{j,t})^\nu \right)^{1/\nu} \quad \text{with} \quad \sum_{j=1}^N g_j^\nu = 1. \quad (2)$$

The weights g_j are proportional to inverse hearing thresholds. In the range up to 3 kHz they can be roughly approximated by the power law $g_j \approx h_j^\mu$, where h_j represents the (integer) centre harmonic number, which approximates the ratio F_j/F_1 . The present study uses $\nu = 0.3$ [18] and $\mu = 1$ [3]. The synthesis suited set of subbands is generated by replacing the over complete subband set $6 < j \leq 11$ by a set $6 < j \leq N$, which is spaced equidistantly on the logarithmic frequency scale with 4 filters per octave,

$$F_j = 5 \cdot 2^{(j-5)/4} F_1 \quad \Delta F_j = 2^{(j-5)/4} F_1 \quad (3)$$

The feasibility of the extraction of the fundamental drive as well as the validity of its interpretation as a reconstruction of a glottal master oscillator of voiced excitation is demonstrated with the help of simultaneous recordings of a speech signal and an electro-glottogram, which have been obtained from the [pitch analysis database of Keele University](#) [19]. The upper panel of figure 1 shows the analysis window for a segment of the speech signal, which was taken from the /w/ in the first occurrence of the word "wind" spoken by the first male speaker. The lower panel shows the reconstruction of the fundamental phase (given in wrapped up form), based on the set of separable subbands with the harmonic numbers 2, 3 and 5. The near perfectly linear phase locking of these subbands, which is used for the reconstruction of the drive, is demonstrated in figure 2. The subband phases Φ_j are given in a partially unwrapped form, depending on the respective centre harmonic number h_j . The enlarged

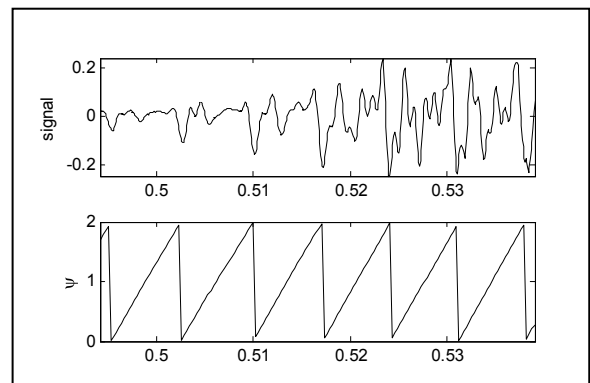


Figure 1, upper panel: 45 ms of a speech signal, which was taken from the /w/ in the word "wind" representing part of a publicly accessible pitch analysis data base [19]. The lower panel shows the reconstruction of the fundamental phase ψ in units of π . The time scale (in units of seconds) corresponds to the original one.

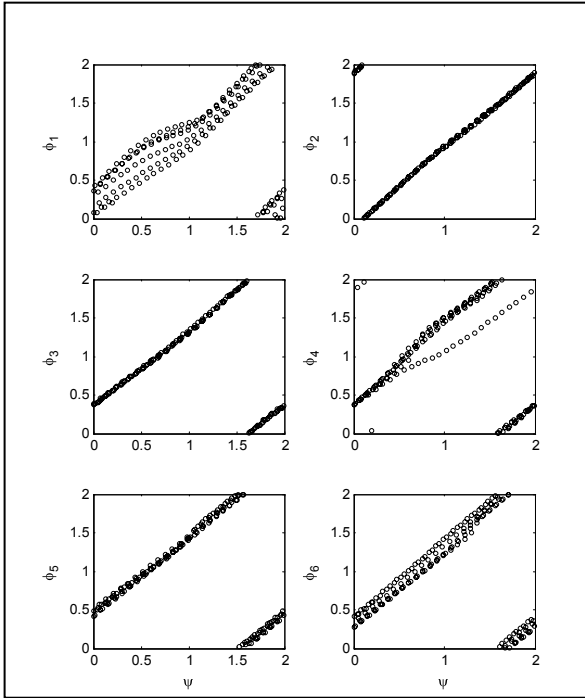


Figure 2: Relation of subband phases Φ_j , ($j=1,2,\dots,6$), obtained from the speech signal of figure 1, to the fundamental phase ψ . The subbands 2, 3 and 5 are characterized by near perfectly linear phase relations, whereas the other subbands are found to be unsuited for the reconstruction of the fundamental phase.

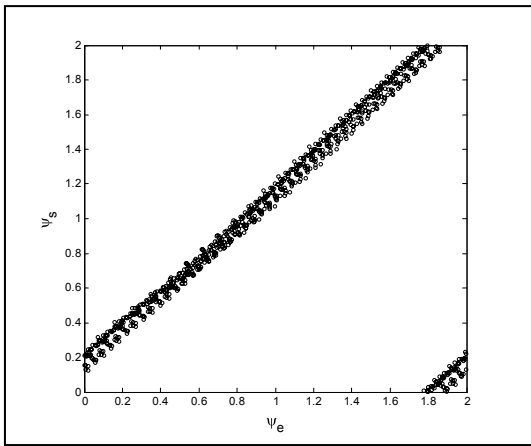


Figure 3: Relation between the wrapped up fundamental phase ψ_s , obtained from the speech signal, and the fundamental phase ψ_e , obtained from the electro-glottogram.

range of the subband phases is normalized by the same centre harmonic number. Alternatively the fundamental phase can also be obtained from a subband decomposition of the electro-glottogram. The exchangeability of the two phases is demonstrated in figure 3, which shows the relation between the two fundamental phases for the speech segment, which covers the “win” part of the word “wind”, uttered by the first female speaker. The phase shift between the two phases did not change significantly during the 160 ms being covered.

In spite of the arbitrariness of the initial fundamental phase, the reconstruction of the glottal master oscillator can be used as fundamental drive of a two level drive – response model, which is suited to describe voiced speech as secondary response. The additional subsystem describes the excitation of the vocal tract as primary response of the fundamental drive and the classical secondary response sub-

system describes the more or less resonant “signal forming” on the way through the vocal tract as action of a linear autoregressive filter. The subband decomposition (1) and (3) being used for the reconstruction of the fundamental drive can also be used with advantage to achieve a numerically robust reconstruction of the excitation.

III. ENTRAINMENT OF THE PRIMARY RESPONSE

Due to the slow velocity of the glottal tissue (compared to the velocity of sound) the excitation $E_{j,t}$ of a voiced subband with index $1 \leq j \leq N$ can be assumed to be restricted (enslaved or entrained) to a generalized synchronization manifold (surface) in the combined state space of drive and response [20-22]. In the simplest case the time dependence of subband excitation $E_{j,t}$ can thus be replaced by a dependence on the simultaneous state of the fundamental drive. More generally, the dependence of the state of the primary response on the state of the fundamental drive may degenerate to a multi-valued mapping, which can, however, be expressed by a unique function of the unwrapped fundamental phase ψ_t [11-12],

$$E_{j,t} = A_t G_{j,p}(\psi_t) = A_t \sum_{k \in S_{j,p}} c_{j,k} \exp(ik \frac{\psi_t}{p}). \quad (4)$$

As part of the improved time scale separation the generalized synchronization manifold is assumed to be the product of the slowly variable fundamental amplitude A_t and the potentially fast varying complex coupling function $G_{j,p}(\psi_t)$, the real part of which describes the subband excitation. In its general form, $G_{j,p}(\psi_t)$ represents a $2\pi p$ periodic function of the unwrapped fundamental phase ψ_t with an integer period number $p \geq 1$ and can thus be well approximated by the finite Fourier series in equation (4). Voiced excitations are characterized by values of p , which are distinctly smaller than the number of fundamental cycles within the analysis window. The case $p=1$ corresponds to the normal voice type characterized by a unique mapping [20], whereas $p=2$ is suited to describe the period doubling voice type [4]. The unwrapped fundamental phase can be assumed to be approximately proportional to time. When $2\pi p$ exceeds the length of the analysis window, equation (4) is therefore suited to describe a fully general excitation, including the unvoiced case.

The excitation parameters $c_{j,k}$ cannot be determined independently from the parameters, which characterize the vocal tract resonances. In the standard approach the parameter estimation is performed hierarchically, by making the higher level assumption that the excitation has a nearly white (or tilted) spectrum. To achieve a comparable numerical robustness, the parameter estimation is done separately for the different frequency bands. The band limitation can be used to reduce the number of resonances (poles of the autoregressive filter), which are relevant for the respective subband. The complex subband $\{X_{j,t}\}$ can thus be described by the following nonlinear conditional stochastic process with a two-level drive – response model as deterministic part (skeleton) [11-12],

$$X_{j,t+\Delta} = b_j X_{j,t} + A_t G_{j,p}(\psi_t) + A_t \sigma_j \xi_{j,t}, \quad (5)$$

where Δ denotes the subband specific prediction step length, b_j the complex subband specific resonator parameter, $\xi_{j,t}$ a $(0,1)$ Gaussian complex white noise process and σ_j the time independent part of the standard deviation. As an important computational advantage the estimation of the complex excitation and resonator parameters $c_{j,k}$ and b_j can be reduced to multiple linear regression. The summation index set $S_{j,p}$ of equation (4) is chosen in accordance to the respective bandpass filter. The decomposition into subbands is used to estimate equation (5) with a subband specific integer time step

length Δ . The aggregated coupling function, which results from the sum of all subband specific coupling functions, can be compared to the excitation of the (single level) broadband source - filter model.

Vowels and nasals are characterized by the fact that the time points of the glottal closure can be detected as a unique pulse (or as a unique outstanding slope). Since there is no syllable without a vowel kernel, such kernels can be used to resolve the arbitrariness of the initial fundamental phase.

In the case of voiced speech segments, which contain other sustainable voiced consonants, the continuous reconstruction of the fundamental phase can be used advantageously to extend equation (5) by a second excitation term $A_{i-\tau} G_{j,p}(\psi_{i-\tau})$ with a coupling function, which depends on a delayed fundamental phase. According to Teager and Teager [14] the delay τ can be interpreted as result of the comparatively slow subsonic convective transport of kinetic energy to the site of the phoneme specific secondary constriction of the vocal tract, where the conversion to acoustic energy takes place.

IV. DETERMINISTIC APERIODICITY AMPLIFICATION OF VOICED CONSONANTS

As a striking result, the assumption of generalized synchronization of the primary response does not only hold in the case of vowels but also in the case of many sustained voiced consonants. In the case of the voiced approximant /l/ the aggregated coupling function shows several steep slopes which indicate a sensitive dependence on the phase of the fundamental drive (figure 4). The sensitive dependence can be interpreted as effect of the superposition of the response of the direct excitation and the one of the delayed excitation resulting from an intermittently turbulent airflow. The interference between the two responses may lead to a sensitive dependence on the recent history of the fundamental phase. First results show that the deterministic aperiodicity amplification is a widespread feature of voiced speech. Its occurrence shows a marked dependence on the speaker and on the fundamental phase.

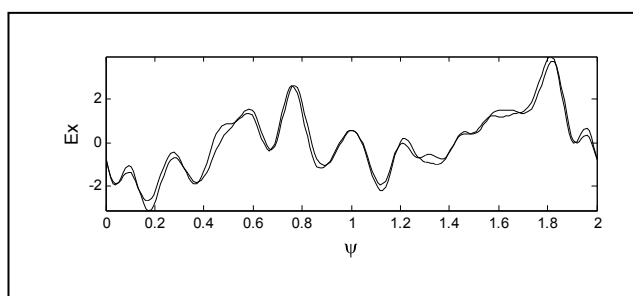


Figure 4: Aggregated fundamental phase dependent coupling function reconstructed with period $p = 2$ for the voiced approximant /l/ of the word “along” uttered by the first male speaker. The two curves correspond to the odd and even periods. The disagreement of the two curves shows a marked dependence on the fundamental phase.

The continuous reconstruction of the fundamental phase for speech segments with uninterrupted phonation opens the possibility to complement the analysis of the spectral properties of the speech signal by a run time analysis. The run time differences may refer either to a travel time difference of the primary acoustic pulse or to a build up time of the turbulence at the secondary constriction of the vocal tract. The coupling functions with periodicity $p = 2$ are suited to describe a voice type, which cannot be classified uniquely by using cycle lengths differences (figure 4). It is hypothesized that the fundamental phase dependent coupling functions are suited to serve as additional cue for phoneme recognition and as fingerprint for speaker identification.

V. CONCLUSION

The transmission protocol of voiced human speech is based on the production and analysis of complex airflow pattern in the vocal tract of the transmitter. The present study demonstrates that the analysis on the receiver side can be focussed on the mode locking of the pulsed airflow by replacing the time dependence of the excitation of the classical source - filter model by a fundamental phase dependence, which can be described by a low dimensional generalized synchronization manifold (surface or coupling function). The evolution of speech has lead to many voiced phonemes and syllables which can be distinguished by properties of one dimensional coupling functions and of a closely related two-level drive - response model. To make the coupling functions visible with increased precision, a voice specific subband decomposition of the speech signal has been proposed, which is suited to extract a precise fundamental phase. The extraction relies on the fact that non-pathological voiced speech leaves at least two subbands undistorted by vocal tract resonance or secondary constriction.

The author would like to thank V. Hohmann, B. Kollmeier, J. Nix, Oldenburg, M. Kob, C. Neuschaefer-Rube, Aachen, G. Langner, Darmstadt, N. Stollenwerk, Porto, P. Grassberger, M. Schiek and P. Tass, Jülich for helpful discussions.

References

- [1] Fant G. *Acoustic theory of speech production*, Mouton, 'S-Gravenhage (1960)
- [2] Vary P., U. Heute, W. Hess, *Digitale Sprachsignalverarbeitung*, B.G. Teubner Verlag, Stuttgart (1998)
- [3] Schroeder M.R., *Computer Speech*, Springer (1999)
- [4] Titze I.R., *Acta Acustica* **90**, 641-648 (2004)
- [5] Kantz H., T. Schreiber, *Nonlinear time series analysis*, Cambridge Univ. Press (1997)
- [6] Winholtz W.S. and L.O. Ramig, *J.Speech Hear. Res.* **35**, 562-573 (1992)
- [7] Schoentgen J. and R. de Guchteneere, *Speech Communication*, **21**, pp. 255-272 (1997)
- [8] Herzel H., D. Berry, I.R. Titze and I. Steinecke, „Nonlinear dynamics of the voice“, *Chaos* **5**, 30-34 (1995)
- [9] Kubin G., “Nonlinear processing of speech” in *Speech Coding and Synthesis* (W. B. Kleijn and K. K. Paliwal, eds.), pp. 557-610, Amsterdam: Elsevier (1995)
- [10] Moakes P.A. and S.W. Beet, “Analysis of non-linear speech dynamics” in *ICSLP 94*, Yokohama, pp. 1039-1042 (1994)
- [11] Drepper F.R. in C. Manfredi (editor), *MAVEBA 2003*, Firenze University Press (2004)
- [12] Drepper F.R., *Fortschritte der Akustik-DAGA '05*, a, b (2005)
- [14] Teager H.M. and S.M. Teager, “Evidence for nonlinear sound production in the vocal tract,” in *Proc NATO ASI on Speech Production and Speech Modelling*, pp. 241-261 (1990)
- [15] Zhao, W., Zhang, C., Frankel, S.H., and Mongeau, L., *J. Acoust. Soc. Am.*, Vol. 112, No. 5, pp. 2134-2154, 2002
- [16] Hohmann V., *Acta Acustica* **10**, 433-442 (2002)
- [17] Moore B.C.J., *An introduction to the psychology of hearing*, Academic Press (1989)
- [18] Sottek R., *Modelle zur Signalverarbeitung im menschlichen Gehör*, Verlag M. Wehle, Witterschlick/Bonn (1993)
- [19] ftp.cs.keele.ac.uk/pub/pitch
- [20] Afraimovich V.S., N.N. Verichev, M.I. Rabinovich, *Radiophys. Quantum Electron.* **29**, 795 ff (1986)
- [21] Rulkov N.F., M.M. Sushchik, L.S. Tsimring, H.D.I. Abarbanel, *Phys. Rev. E* **51**, 980-994 (1995)
- [22] Rulkov et al., *Phys. Rev. E* **64**, 016217 (2001)

SPEECH ANALYSIS USING HIGUCHI FRACTAL DIMENSION

Jari Turunen, Tarmo Lipping & Juha T. Tantt

Tampere University of Technology, Pori

P.O.Box 300, Pohjoisranta 11, FIN-28101 Pori

{jari.turunen, tarmo.lipping, juha.tantt}@pori.tut.fi

Speech analysis for identification and recognition purposes is a demanding task, especially to find recognition parameters for some consonants. In this paper, we show the initial analysis results of speech corpus, sampled with two sampling rates, 22050 and 8000 Hz, using Higuchi fractal dimension. The study shows that it might be possible to use fractal dimension value for classification of for example plosives /k/, /p/ and /t/. However, the analysis seems to be very sensitive to the sampling frequency in speech analysis.

I. INTRODUCTION

Linear speech analysis and models has served successfully the speech processing areas for decades. However, there has also been an interest to research and evaluate nonlinear methods in order to find better way to model speech, especially for speech recognition purposes.

Several studies have found evidences for nonlinear behavior in speech. Different nonlinear techniques have been tested with time series over several decades in order to improve modeling and estimation when compared to linear methods. For example, the logarithmic a-law/ μ -law compression in Pulse Code Modulation (PCM) coding has worked successfully over the years. However, the precise "practical" nonlinearity form for vocal tract model is not known and the search for good alternatives for the describing the human vocal tract with linear methods is currently going on. The Hammerstein model, Volterra series and Wiener filters have been tested experimentally as well as the chaotic time series modeling with very good results. However, the disadvantages are, when compared to the linear models, the more complex parameter computations and in some cases, the stability preservation. Also, different types of neural networks have been tested for several purposes in speech processing. Neural network is easy to design, train and test but there still remains a fear that the unique and documented experiment is unrepeatable even with the same data [1-17].

The nonlinear signal processing field is enormous, in that sense that the number of different functions, equations and/or systems that can be used for speech modeling and analysis is practically infinite.

The chaotic models have worked successfully for vowels and nasals [4, 5] and Teager energy operator [18

,19] has been used to indicate several features of speech, for example speech resonances and modulations.

In this paper we study the effect of Higuchi Fractal dimension for different phonemes.

II. METHODS AND DATA

Higuchi fractal dimension [20] is a method developed for estimating the amount of self-similarity of the data. Higuchi [20] used his method for magnetic field data and in [21, 23-25] Higuchi's method was used for electroencephalography data.

Method described in [20], defines the discrete time series:

$$X[1], X[2], \dots, X[n]$$

to be constructed to a new time series:

$$X_k^m; X[m], X[m+k], X[m+2k], \dots, X\left(m + \left\lceil \frac{N-m}{k} \right\rceil k\right), \\ m = 1, 2, \dots, k$$

where m is the initial time and k is the interval time, N is the total number of samples. For example if $k=3$ and $N=100$, three time series are obtained as follows:

$$X_3^1; X(1), X(4), X(7), \dots, X(100)$$

$$X_3^2; X(2), X(5), X(8), \dots, X(98)$$

$$X_3^3; X(3), X(6), X(9), \dots, X(99)$$

The length of the curve, defined in [20] is:

$$L_m(k) = \frac{\left\{ \left[\sum_{i=1}^{\left\lceil \frac{N-m}{k} \right\rceil} |X(m+ik) - X(m+(i-1)k)| \right] \frac{N-1}{\left\lceil \frac{N-m}{k} \right\rceil k} \right\}}{k}$$

$L_m(k)$ represents normalized sum of "segment length". Each "segment length" represents the absolute value of difference between magnitude values of pair of points distant k samples, starting from m^{th} sample. The length of the curve $L(k)$ is mean of k values $L_m(k)$, for $m=1, 2, \dots, k$. The fractal dimension D is the least square estimate of the slope of the curve evaluated on $1..k_{\max}$ values on $L(k)$. If the curve is plotted on doubly logarithmic scales, for $1..k_{\max}$ in $\ln(1/k)$ and $L(k)$ in

$\ln(L(k))$, the data should fall on a straight line with a slope (-D). It should be noted that Higuchi fractal dimension is not related with chaotic attractor dimension.

For example, the Higuchi value of white noise, with maximum amplitudes [-1,1] with $k_{max} = 10$, is 1, and straight line with slope is zero.

The algorithm and evaluation was performed using Matlab environment. In our preliminary experiments, several k_{max} values were tested. If the k_{max} values was increased beyond 25 the Higuchi fractal dimension values tend to get closer to one as the k_{max} increases. Similarly, if the k_{max} value was decreased below 8, the Higuchi values tend to progress towards zero. The k_{max} value 10 gave best results in our experiments.

Table 1. Phonemes and their corresponding example words.

phon.	word	phon.	word	phon	word
/p/	pin	/tS/	chin	/i/	see
/b/	bay	/dZ/	jam	/a/	father
/t/	toy	/m/	me	/O/	sort
/d/	die	/n/	not	/Î/	bird
/k/	key	/N/	sing	/u/	too
/g/	get	/l/	light	/ei/	day
/f/	five	/r/	ring	/ai/	fly
/v/	van	/w/	win	/Oi/	boy
/T/	thick	/j/	yes	/ou/	go
/D/	then	/l/	sit	/au/	cow
/s/	see	/e/	get	/i«/	ear
/z/	zinc	/Q/	cat	/u«/	tour
/S/	ship	/Ã/	hut	/e«/	air
/Z/	measure	/A/	hot	/q/	[silence]
/h/	he	/U/	put	/«/	banana

Table 2. Number of different phonemes in each phoneme category.

phon.	#	phon.	#	phon	#
/p/	83	/tS/	89	/i/	154
/b/	61	/dZ/	52	/a/	96
/t/	191	/m/	72	/O/	162
/d/	66	/n/	236	/Î/	92
/k/	140	/N/	48	/u/	145
/g/	60	/l/	61	/ei/	156
/f/	211	/r/	152	/ai/	216
/v/	107	/w/	106	/Oi/	96
/T/	138	/j/	48	/ou/	151
/D/	61	/l/	153	/au/	95
/s/	205	/e/	173	/i«/	44
/z/	115	/Q/	72	/u«/	37
/S/	80	/Ã/	130	/e«/	68
/Z/	38	/A/	72	/q/	3
/h/	48	/U/	48	/«/	30

The OTAGO speech corpus [22] was used in the tests. The phonemes were manually checked and identified. The data, which was used in experiments, is presented in Table 1 and Table 2. The sampling frequency was 22050 Hz and total number of samples was 4661.

The phoneme lengths varied from minimum of 143 samples in /b/ to 10949 samples in /a/ sampled with 22050 Hz frequency. The /q/ is a silence “phoneme” recorded by the microphone (background noise). We performed two tests with Higuchi analysis: the first one with 22050 sampling frequency and the second one with 8000 Hz sampling frequency. The lower sampling frequency was obtained by resampling the data from the original data by using Matlab “resample” command.

III. RESULTS

The results are shown in Figures 1-6. The Figures 1-3 show the fractal dimension values for phonemes sampled at 22050 Hz and Figures 4-6 show the fractal dimension values for 8000 Hz data.

In the figures, the boxes show the lower quartile, median and the upper quartile of all sampled phoneme values. The lines show the deviation for the rest of phoneme data and outliers are presented with ‘+’ sign.

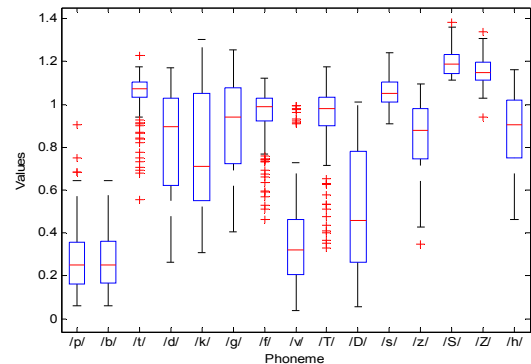


Figure 1. The fractal dimension values for phonemes /p/ to /h/ sampled at 22050 Hz frequency

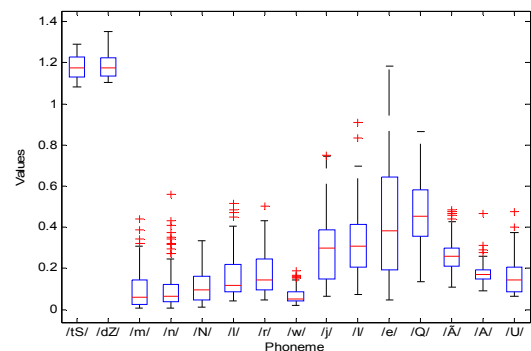


Figure 2. The fractal dimension values for phonemes /tS/ to /U/ sampled at 22050 Hz frequency

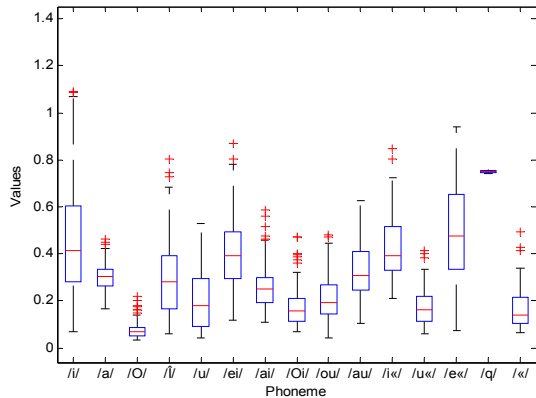


Figure 3. The fractal dimension values for phonemes /i/ to /k/ sampled at 22050 Hz frequency

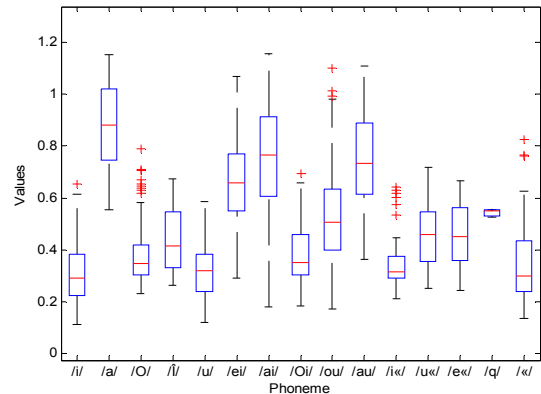


Figure 6. The fractal dimension values for phonemes /i/ to /k/ sampled at 8000 Hz frequency

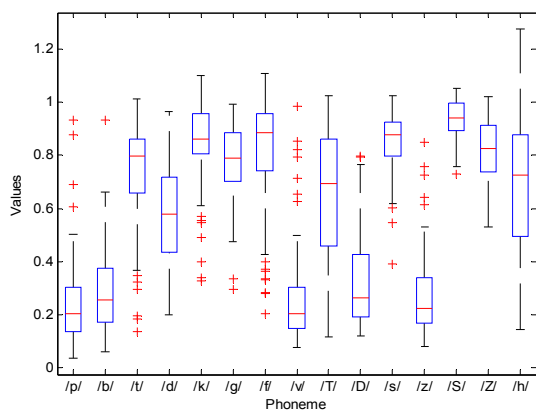


Figure 4. The fractal dimension values for phonemes /p/ to /h/ sampled at 8000 Hz frequency

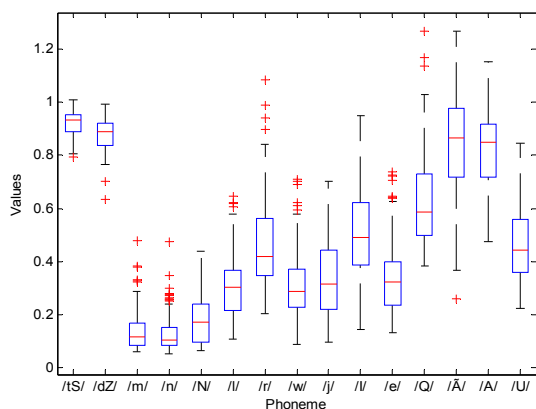


Figure 5. The fractal dimension values for phonemes /tS/ to /U/ sampled at 8000 Hz frequency

IV. DISCUSSION

When looking the Figures 1-3 with $F_s=22050$ Hz, the Higuchi Fractal dimension reveals interesting things from the phonemes. For example plosives /p/, /t/ and /k/ has been very difficult to separate from each other by using other methods, but it seems that they are possible to separate by using Higuchi fractal dimension. The quartile bars and the whole data deviation in plosive /k/ does not separate from /t/ as well as the /p/, although the median is different by visual inspection. In addition, the grouping of the fricatives can be seen from the figures 1-2. The fricatives /s/, /z/, /f/, /Ts/, /Tz/ and /q/ (that means background noise) are concentrated near one (from 0.8 to 1.2). This may also be interpreted that the Higuchi fractal dimension is very sensitive to background noise.

The nasals /n/ and /m/, semivowels /v/ and /w/ and all vowels have median values below 0.5. The Higuchi values of vowels, interestingly, seem to correlate with the vowel production mechanism somehow, in the sense of tongue position in the mouth. For example, lower fundamental frequency vowel /U/ has smaller Higuchi value when compared to higher fundamental frequency vowel /i/.

All seems to separate nicely with 22050 Hz recordings but unfortunately speech is usually sampled and transferred with much lower, 8000 Hz sampling frequency. The interesting phenomena do not appear in same depth anymore in lower sampling frequency. When looking the figures 4-6 the phonemes do not show similar behavior as they did in figures 1-3. The plosives /t/ and /p/ do separate in figure 4, but the quartile bars are much closer (and slightly overlapping) to each other than in figure 1. The values of phoneme /k/ are higher than in previous analysis. The fricatives /s/, /z/, /f/, /Ts/, /Tz/ and /q/ show overall dropping in median values especially in

the case of /z/. Also phonemes seem to have overall increase in the median values. The Higuchi values for vowels have higher values than in 22050 Hz sampling frequency, but in the case of vowel /i/, the fractal dimension values are dropped.

When thinking the Higuchi fractal dimension value computation, the differences between two sampling frequency results seems to follow the filtering properties. The Higuchi fractal dimension measures the amount of self-similarity by searching the difference between adjacent samples. The downsampling will smooth the fine structure of the signal.

The selection of k_{\max} parameter is also very important for the analysis. In our case the both sampling frequencies 22050 and 8000 Hz the $k_{\max}=10$ seems to be good for speech analysis purposes. Several k_{\max} values were tested, well beyond 50, because in vowels the fundamental cycle repetition is approximately 50-140 samples in 8000 Hz sampling frequency. k_{\max} values beyond 50 provided fractal dimension values that are all approaching one rather than providing better separation between consonants and vowels. With lower sampling frequencies some critical information may be lost, which may be useful for recognition purposes with this method.

Higuchi fractal dimension is useful tool, and the algorithm is very simple and easy to compute providing single number for example analysis and recognition purposes.

REFERENCES

- [1] Kubin G., "Nonlinear Processing of Speech", Speech Coding and Synthesis, Elsevier Science, Amsterdam, 1995.
- [2] Townshend B., "Nonlinear prediction of speech", IEEE ICASSP: 425-428, 1991.
- [3] Langi A., Soemintaputra K. & Kinsner W., "Multifractal Processing of Speech Signals", IEEE ICICS: 527-531, 1997.
- [4] Banbrook M., McLaughlin S. & Mann I., "Speech Characterisation and Synthesis by Nonlinear Methods", IEEE Trans. Speech and Audio Proc, 7 (1): 1-17, 1999
- [5] Miyano T., Nagami A., Tokuda I., Kazuyuki A., "Detecting nonlinear determinism in voiced sounds of Japanese vowel /a/", in *Int. Journal of Bifurcation and Chaos*, 10 (8), 1973-1979, 2000.
- [6] Thyssen J., Nielsen H. & Hansen S., "Non-linear short term prediction in speech coding", IEEE ICASSP, (1): 185-188, 1994.
- [7] Kumar A. & Gersho A., "LD-CELP Speech Coding with Nonlinear Prediction", IEEE Signal Processing Letters, 4 (4), 89-91, 1997.
- [8] Ma N. & Wei G., "Speech Coding with Nonlinear Local Prediction Model", IEEE ICASSP: 1101-1104, 1998.
- [9] Birgmeier M., Bernhard H. & Kubin G., "Nonlinear Long-Term Prediction of Speech Signals", IEEE ICASSP: 1283-1286, 1997.
- [10] Kubin G., "Synthesis and Coding of Continuous Speech with The Nonlinear Oscillator Model", IEEE ICASSP: 267-270, 1996.
- [11] Ohmura H. & Tanaka K., "Speech Synthesis Using a Nonlinear energy Damping Model for The Vocal Folds Vibration Effect", IEEE ICSLP, (2): Acoustic Analysis, #11, 1996.
- [12] Abarbanel H., "Chaotic Signals and Physical Systems", IEEE ICASSP, (4): 113-116, 1992.
- [13] Singer A., Wornell G. & Oppenheim A., "Codebook Prediction: A Nonlinear Signal Modeling Paradigm", IEEE ICASSP (5), 325-328, 1992.
- [14] Diaz-de-Maria F. & Figueiras-Vidal A., "Radial Basis Functions for Nonlinear Prediction of speech in Analysis-by-Synthesis Coders", IEEE ICASSP: 788-791, 1995.
- [15] Hennebert J., Hasler M. & Dedieu H., "Neural networks in speech recognition", Proc. 6th Microcomputer School, Prague, 1994.
- [16] Fackrell J., "Bispectral Analysis of Speech Signals", doctoral dissertation, University of Edinburgh, 1996.
- [17] Turunen J., Tantt J., & Loula P., "Hammerstein model for speech coding", in *Eurasip JASP* (12), 1238-1249, 2003.
- [18] Teager H., "Some Observations on Oral Air Flow During Phonation", in *IEEE Transactions on ASSP*: 28, 599-601, 1980.
- [19] Teager H., & Teager S., "Evidence of Nonlinear Production Mechanisms on Vocal Tract" in *NATO adv. Study Inst. On Speech Production and Speech Modelling*, Kluwer, Bonas France, 1990.
- [20] Higuchi T., "Approach to an irregular time series on the basis of the fractal theory", in *Physica D*, 31, 277-283, 1988.
- [21] Accardo A., Affinito M., Carrozzini M. & Bouquet F., "Use of fractal dimension for the analysis of electroencephalographic time series", in *Biological Cybernetics*, 77 (5), 339-350, 1997.
- [22] OTAGO speech corpus, available URL: <http://translator.kedri.info/datasets/corpus/otago>.
- [23] T. Lipping, E. Olejarczyk and M. Parts. Fractal dimension analysis of the effects of photic and microwave stimulation on the brain function. Proceedings of the World Congress on Biomedical Engineering and Medical Physics, Sydney, Australia, 24-29.08.2003 (on CD ROM).
- [24] T. Lipping, E. Olejarczyk and M. Parts. Analysis of photo-stimulation and microwave stimulation effects on EEG signal using Higuchi's fractal dimension method. In *Optical Methods, Sensors, Image Processing, and Visualization in Medicine*, A. Nowakowski and B. B. Kosmowski eds., Proc. SPIE, vol. 5505 (SPIE, Bellingham, WA, 2004), pp. 174-178.
- [25] A. Anier, T. Lipping, S. Melto, S. Hovilehto. Higuchi fractal dimension and spectral entropy as measures of depth of sedation in intensive care unit. Proc of the 26th IEEE EMBS Annual International Conference, San Francisco, USA, September 1-5, 2004, pp. 526-529.

**Special session on
Neurological dysfunctions**

EFFECT OF PARKINSON'S DISEASE ON VOCAL TREMOR

L. Cnockaert^{1*}, J. Schoentgen^{1†}, P. Auzou²³, C. Ozsancak³⁴ and F. Grenez¹

¹ Université Libre de Bruxelles, Department Waves and Signals, Brussels, Belgium

² Service d'explorations fonctionnelles neurologiques, Groupe HOPALE, Berk sur Mer, France

³ EA 2683, CHRU Lille, France

⁴ Service de Neurologie, Centre Hospitalier de Boulogne sur Mer, France

lcnockae@ulb.ac.be

Vocal tremor is encountered in different neurological diseases and could be used for their characterisation. In this paper, vocal tremor features have been extracted for speakers with Parkinson's disease and control speakers. It is shown that Parkinson's disease has significant effects on vocal tremor features. For speakers with Parkinson's disease, the average vocal frequency is higher and the vocal tremor frequency is higher. This can be explained by higher vocal tremor components in the frequency band 8 – 12Hz.

I. INTRODUCTION

The objective of this paper is to report data about the vocal tremor features of parkinsonian and control speakers, as well as an improvement to the vocal tremor analysis presented in [1].

Vocal tremor is a narrow-band low-frequency perturbation of the vocal frequency. It is characterised by its average amplitude and average frequency. The amplitude of the perturbation is about a few percent of the average vocal frequency. The tremor frequency range is subject to discussion. A definition including most of the frequency ranges is given by Titze who defines the vocal tremor as the 1-15Hz modulation of the vocal frequency [2]. The origins of vocal tremor are reported to be neurologic or due to an interaction between neurological and biomechanical properties of the vocal folds [2]. Influence of blood flow, heartbeat and breath are also reported [3]. The lower frequency limit should be chosen in accordance with the effects that should be taken in account.

In this paper, the estimation of vocal tremor features has been obtained by means of an improvement of the analysis developed in [1]. The vocal frequency trace is first calculated. The vocal frequency estimates are obtained for each time sample by means of the instantaneous frequency calculated in an automatically selected frequency-band of a wavelet transform of the speech signal. Using this method, no windowing of the signal is necessary and instantaneous

F_0 variations can be tracked. A second wavelet transform has been introduced, in order to improve the precision and robustness of the method. This is necessary to track correctly fast F_0 variations and to handle speech signals from a clinical environment, where older and dysphonic speakers are encountered. Instantaneous values of the vocal tremor features are then obtained by means of a wavelet transform of the vocal frequency trace.

In this paper, the vocal tremor features have been extracted for parkinsonian and control speakers and statistical results about the differences between both groups are presented.

II. VOCAL FREQUENCY ESTIMATION

The instantaneous frequency $IF(t)$ of a band-pass signal $s(t)$ is usually defined by means of its Hilbert transform $H[s(t)]$ and its associated analytical signal $s_a(t)$ [4].

$$s_a(t) = s(t) + jH[s(t)] \quad (1)$$

$$\Phi(t) = \arg[s_a(t)] \quad (2)$$

$$IF(t) = \frac{d\Phi(t)}{dt} \quad (3)$$

The IF can also be defined by means of a continuous wavelet transform $CWT(\lambda, t)$ using an analytical wavelet $\psi_a(t)$ [5]. The continuous wavelet transform of a signal $x(t)$ is defined as

$$CWT(\lambda, t) = \int_{-\infty}^{+\infty} x(u) \frac{1}{\sqrt{\lambda}} \psi^* \left(\frac{u-t}{\lambda} \right) du, \quad (4)$$

where $\psi(t)$ is an analytical mother wavelet and $CWT(\lambda, t)$ is the wavelet transform coefficient for a scale factor λ , at time t . The amplitude and phase of the complex CWT coefficients thus obtained are the envelope and instantaneous phase of the spectral components of the signal in the frequency-band centred on the central frequency f_c of the wavelet [6]. The time-derivative of the phase of the complex CWT coefficients is therefore an estimate of the instantaneous frequency (IF) of the signal in that frequency-band. The evolution of the IF in different frequency-bands of the signal can thus be studied by means of the CWT coefficients.

*The first author is a fellow with the FRIA (Belgium).

†The second author is a Senior Research Associate with the Fonds National de la Recherche Scientifique (Belgium).

Here, the complex Morlet wavelet is used (Fig. 1) [7]:

$$\psi_{\omega_c}(t) = C e^{-i\omega_c t} \left[e^{-\frac{t^2}{2\sigma_t^2}} - \sqrt{2} e^{-\frac{\omega_c^2 \sigma_t^2}{4}} e^{-\frac{t^2}{\sigma_t^2}} \right]. \quad (5)$$

The scale λ of the wavelet is determined by the central

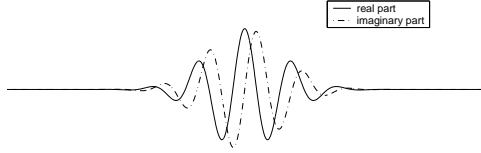


Fig. 1. Complex Morlet wavelet for $\omega_c \sigma_t = 5$.

frequency $f_c = \frac{\omega_c}{2\pi}$, which is the frequency of oscillation of the wavelet. The parameter σ_t fixes its decay. The product $\omega_c \sigma_t$ must be constant for a wavelet family. C normalizes the energy. The effective duration of the wavelet can be defined as $2\sigma_t$.

A F_0 estimate can be given by the IF based on the phase of the CWT coefficients whose amplitudes are at a maximum in the interval from 50 Hz to 500 Hz [1].

To minimize the smoothing of the IF on the wavelet effective duration, this effective duration $2\sigma_t$ should be as small as possible for each wavelet central frequency f_c and the wavelet parameter $\omega_c \sigma_t$ should therefore also be small. On the other hand, when $\omega_c \sigma_t$ decreases, the spectral bandwidth of the wavelets increases and it becomes more difficult to localize the CWT amplitude peak around the vocal frequency.

To obtain a high sensitivity to the F_0 variations and have a robust method, two wavelet transforms are thus combined. At first, a wavelet transform with a fine frequency resolution is computed to identify the maximum in the CWT and secondly a wavelet with a fine time resolution is used to estimate the IF.

The procedure is as follows:

- 1) A first wavelet transform is computed, with a high $\omega_c \sigma_t$ parameter, for the reliability, where the wavelet central frequency \hat{f}_c corresponding to the maximal amplitude of the CWT is obtained. The wavelet parameter $\omega_c \sigma_t$ is chosen equal to 5.
- 2) A second wavelet transform is computed, with a low $\omega_c \sigma_t$ parameter, for the sensitivity to high frequency perturbation, where the F_0 value is estimated by the IF corresponding to the wavelet central frequency \hat{f}_c obtained at the first step. The wavelet parameter $\omega_c \sigma_t$ is chosen equal to 2.5. This second wavelet transform must be computed only for the wavelet central frequencies associated with the maximum in the first step.
- 3) Finally, a filtering is necessary to eliminate the residual oscillations, which appear at a frequency equal to the vocal frequency.

III. TREMOR FEATURE ESTIMATION

To analyse the F_0 features, another CWT is performed on the F_0 trace extracted in the first stage in order to determine the tremor frequency and tremor amplitude.

A. Tremor amplitude

In the literature, the tremor amplitude is defined as the maximal or the standard deviation of the F_0 trace, normalized by the average F_0 [8]. A definition of the tremor amplitude is used, based on the wavelet transform coefficients [1]:

$$TA(t) = \frac{\sqrt{\sum_{f_c > f_{min}} CWT^2(2\pi f_c, t)}}{\bar{F}_0} \quad (6)$$

where \bar{F}_0 is the average F_0 .

B. Tremor frequency

The perturbation of the vocal frequency usually presents more than one frequency component. To take all the frequency components into account, the tremor frequency is obtained by the weighted sum of all instantaneous frequencies higher than f_{min} , for which the amplitude of the CWT energy is higher than a threshold. The weight is given by the corresponding wavelet transform energy. An instantaneous tremor frequency can thus be obtained [1]:

$$TF(t) = \frac{\sum_{f_c > f_{min}} [CWT^2(2\pi f_c, t) IF(2\pi f_c, t)]}{\sum_{f_c > f_{min}} [CWT^2(2\pi f_c, t)]} \quad (7)$$

where $IF(2\pi f_c, t)$ is the instantaneous tremor frequency based on the phase of the CWT coefficients in the f_c band.

C. Tremor energy distribution

Differences have been observed in the spectral energy distributions of the F_0 traces for control and parkinsonian speakers. To emphasize this difference, a ratio R of the spectral energy of the F_0 trace in the frequency-bands $(f_{min} - f_{mid})$ and $(f_{mid} - f_{max})$ has been calculated.

$$R = \sum_t \frac{\sum_{f_c=f_{min}}^{f_{mid}} CWT^2(2\pi f_c, t)}{\sum_{f_c=f_{mid}}^{f_{max}} CWT^2(2\pi f_c, t)} \quad (8)$$

IV. EXPERIMENTAL RESULTS

The proposed analysis has been carried out on a corpus of 28 parkinsonian and 28 control speakers (all male). The parkinsonian speakers have reported speech problems and are under treatment. The control speakers are healthy normophonic speakers in the same age-range. The speech signals are sustained vowel [a], sampled at 25kHz.

Fig. 2 and Fig. 3 show the vocal frequency, the CWT^2 coefficient, the tremor frequency and the tremor amplitude

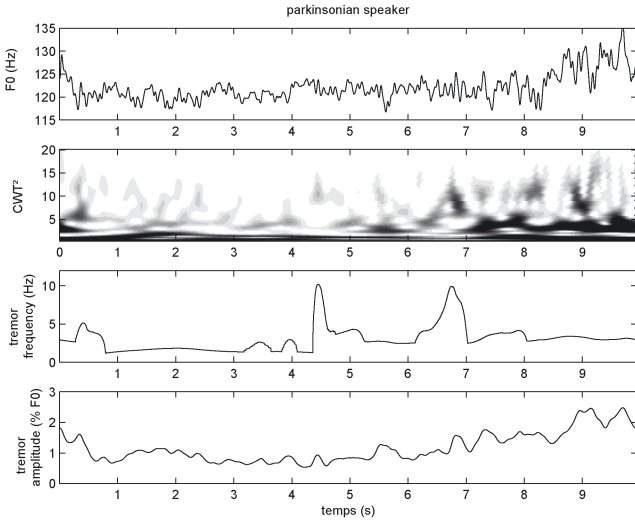


Fig. 2. Vocal frequency trace, CWT^2 coefficients (high amplitudes of the wavelet coefficients are represented in black, low amplitudes in white), tremor frequency and tremor amplitude for a parkinsonian speaker.

for a parkinsonian and a control speaker, whose average vocal frequency is around $120Hz$.

Fig. 4 shows the vocal tremor energy spectrum given by $E(f_c) = \sum_t CWT^2(2\pi f_c, t)$, for the same parkinsonian and control speakers as in Fig. 2 and Fig. 3.

The average values of the tremor features have been extracted, for 5-sec-long speech signal segments, taken at the beginning of the recordings, without the attack. The minimal and maximal frequencies, f_{min} and f_{max} have been chosen equal to $3Hz$ and $15Hz$. The optimal value of the middle frequency f_{mid} of the tremor energy ratio has been obtained by a systematic study of the comparison of the ratios for control and parkinsonian speakers, with f_{mid} in the frequency range $5Hz$ to $10Hz$. The optimal middle frequency is situated around $7Hz$. Fig. 5 shows the distribution of the average vocal frequency, average vocal tremor amplitude, average vocal tremor frequency and average vocal tremor energy ratio.

To emphasize differences between parkinsonian speakers and controls, a multivariate analysis of variance has been performed for all vocal tremor features, as well as a univariate analysis of variance for each vocal tremor feature. The MANOVA results are:

$$Pillai's Trace : F(4, 51) = .988, p < .001. \quad (9)$$

The results of the ANOVA are shown in Table I. The null hypothesis is that the means of both groups are equal.

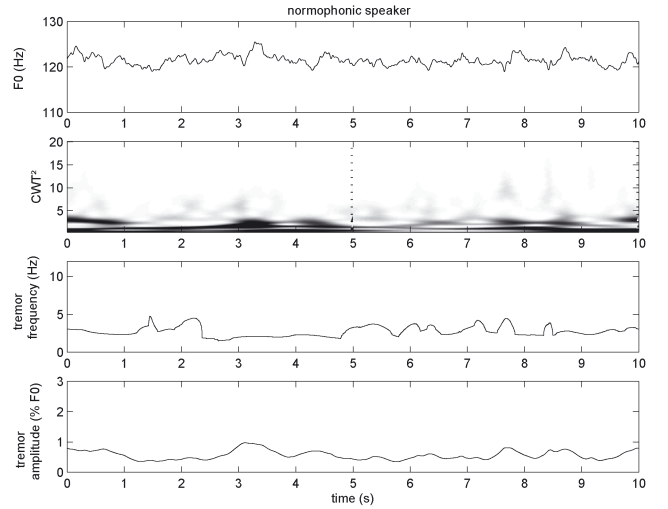


Fig. 3. Vocal frequency trace, CWT^2 coefficients (high amplitudes of the wavelet coefficients are represented in black, low amplitudes in white), tremor frequency and tremor amplitude for a control speaker.

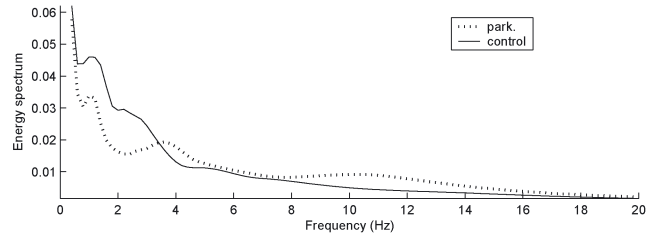


Fig. 4. Vocal tremor energy spectrum for a parkinsonian and a control speaker.

V. DISCUSSION

The lower frequency limit of the analyses has been set to $3Hz$. The reason is that not every vocal tremor source should be taken into account: influences of breath and blood flow, which occur around $0.5Hz$ and $1-2Hz$ respectively, are undesired and the lower frequency should be set higher. Indeed, we aim to isolate the direct effect of Parkinson's disease on vocal tremor. As this effect is expected at higher frequencies, a lower frequency limit of $3Hz$ is admissible.

A visual analysis of Fig. 2 and Fig. 3 shows that the vocal tremor features of the parkinsonian speaker are less stable and present rapid variations. This lack of short-time stability is the reason why average values of the tremor features will be compared. One can also observe, on the wavelet energy plane, that there seems to be more high frequency energy components for the parkinsonian speaker. This difference can also be seen in the energy spectrum on

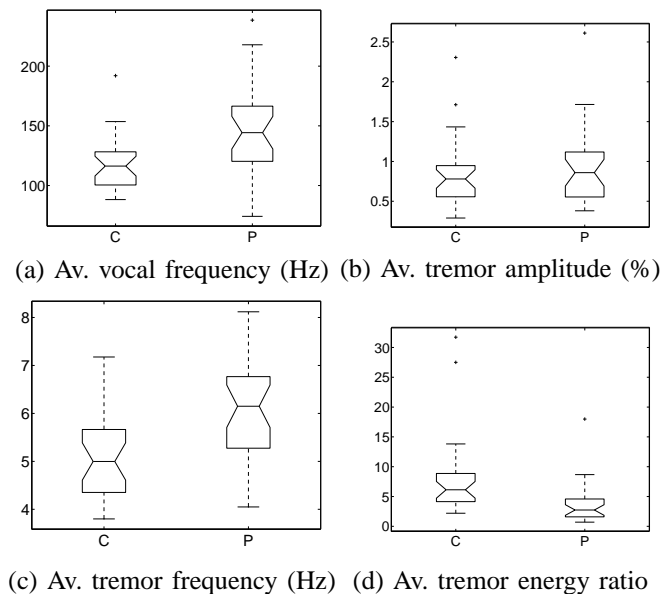


Fig. 5. Distributions of the average vocal frequency and of the average vocal tremor features, for a 5-sec-long speech segment (C: control, P: parkinsonian).

TABLE I. Effects of the health state on average vocal frequency, average vocal tremor amplitude, average vocal tremor frequency and average vocal tremor energy ratio ($3Hz - 7Hz / 7Hz - 15Hz$).

	F	p
Av. vocal frequency	11.874	.001
Av. VT amplitude	.718	.401
Av. VT frequency	16.277	.000
Av. VT energy ratio	9.575	.003

Fig. 4, where the spectrum of the control speaker decreases above $5Hz$ and where an energy peak is present around $10Hz$ for the parkinsonian speaker.

This is also confirmed by the statistical analyses: the multivariate analysis of variance of the vocal tremor features shows that there is a significant difference between the features of parkinsonian and control speakers. The univariate analyses of variance show that there are significant differences for the average vocal frequency, the average vocal tremor frequency and the average vocal tremor energy ratio ($3Hz - 7Hz / 7Hz - 15Hz$), taken on their own. The vocal tremor amplitude is not significantly different for parkinsonian and control speakers.

For parkinsonian speakers, the average vocal tremor frequency is significantly higher and the average vocal tremor energy ratio is significantly lower. These features are highly correlated, *Pearson Correlation* : $-.653, p <$

.001. Both show that higher frequency components are present in the spectrum of the vocal frequency for parkinsonian speakers than for control speakers.

VI. CONCLUSION

In this paper, we have improved an analysis method of vocal tremor and applied it to the extraction of the vocal tremor features for parkinsonian and control speakers. Statistical tests have shown a significant difference between both groups: parkinsonian speakers present a higher average vocal frequency and higher tremor frequency. Observation of the tremor energy spectrum has emphasized the presence of spectral peaks around $8 - 12Hz$, that could explain the higher tremor frequency. The average tremor amplitude is not significantly different between parkinsonian and control speakers.

VII. ACKNOWLEDGEMENTS

The authors would like to thank Mary Jan from the CHU Rouen, France for providing the corpus of parkinsonian and control speakers.

REFERENCES

- [1] L. Cnockaert, F. Grenez, and J. Schoentgen, "Fundamental frequency estimation and vocal tremor analysis by means of morlet wavelet transforms," *Proc. ICASSP, Philadelphia (USA)*, pp. 393–396, 2005.
- [2] I.R. Titze, "Definitions and nomenclature related to voice quality," in *Vocal Fold Physiology*, O. Fujimura and M. Hirano, Eds., pp. 335–342. San Diego, singular edition, 1995.
- [3] R.F. Orlikoff and R.J. Baken, "Fundamental frequency modulation of the human voice by the heartbeat: preliminary results and possible mechanisms," *J. Acoust. Soc. Am.*, vol. 85, pp. 888–893, 1989.
- [4] B. Boashash, "Estimation and interpreting the instantaneous frequency of a signal - part i : Fundamentals," *Proceedings of the IEEE*, vol. 80, no. 4, pp. 520 – 539, 1992.
- [5] T. Le-Tien, "Some issues of wavelet functions for instantaneous frequency extraction in speech signals," *Proc. IEEE Tencon 1997*, pp. 31–34, 1997.
- [6] St. Mallat, *A Wavelet Tour of Signal Processing*, San Diego: Academic Press, 2nd edition, 1999.
- [7] D.B. Percival and A.T. Walden, *Wavelet methods for time series analysis*, Cambridge University Press, 2000.
- [8] J. Schoentgen, "Modulation frequency and modulation level owing to vocal microtremor," *J. Acoust. Soc. Am.*, vol. 112, no. 2, pp. 690 –700, 2002.

EVALUATION OF SPEAKER NORMALIZATION FOR SUICIDALITY ASSESSMENT

Khazaimatol S. Subari², D. Mitchell Wilkes², Stephen E. Silverman³, Marilyn K. Silverman³,
and Richard G. Shiavi¹

¹ Department of Biomedical Engineering, Vanderbilt University, Nashville, Tennessee, USA

² Department of Electrical and Computer Engineering, Vanderbilt University, Nashville, Tennessee, USA

³ Department of Psychiatry, Yale University School of Medicine, New Haven, Connecticut, USA

Abstract: When reviewing his clinical experience in treating suicidal patients, one of the authors observed that successful predictions of suicidality were often based on the patient's voice independent of content. Using the Gaussian mixture model to represent the mel-cepstral features of voiced speech, speech of suicidal persons can be distinguish from that of depressed and control persons. The question then becomes can warping of the frequency axis improve the classification. The results show that warping of the frequency axis using the third format or Gaussian mixture model technique produces the best classification results.

Keywords: Speech, suicide, mel-cepstrum, frequency warping, classification

I. INTRODUCTION

Identification of individuals at imminent suicidal risk requires gathering and weighing a variety of information and data from numerous sources by experienced clinicians [1]. Our own studies are showing that near-term suicidality is associated with changes in speech production and articulation that differ from non-suicidal persons [2],[3]. One of the challenges that immediately arose is what speaker normalization method best improves speaker categorization? While studies on normalization mostly concentrate on reducing error rates in word or speaker recognition systems, none have been conducted on emotionally disturbed patients. Vocal tract length normalization (VTLN) is an acoustic normalization aiming at decreasing speech variability due to differing vocal tract lengths among speakers. VTLN performs a transformation in the frequency domain known as frequency warping in order for the formants of all the speakers to be located at the same frequency in the spectrum [4]. There are two main methods; formant-based normalization, and maximum-likelihood-based normalization. The former determines the warping factor directly based on the location of the formant frequencies. The latter, generates a model and designates the warping factor that maximizes the likelihood of the test data given the statistical model. Eide et al. [5] and Zhan et al. [6]

also proposed that a nonlinear warping may be more effective than linear warping.

The model of VTLN is crucial for the implementation of the normalization method correctly. For the formant-based normalization, the models will be based on the median of the formants of the training speakers, while for the maximum-likelihood based normalization; Gaussian Mixture Models (GMM) will model the form of the standard speaker. Gender dependant and gender independent models of VTLN and the effects of linear and nonlinear warping are also investigated.

II. DATABASE FORMULATION

Analyses were performed on sets of audio recordings for 15 males and 15 females. Each set contained 5 near-term suicidal patients, 5 depressed patients, and 5 non-depressed control subjects collected from existing databases. All the patients used in this research were white Caucasians between the ages of 25 and 65. Because of the inability to record psychiatric speech in controlled settings, all of the speech samples were recorded during real-life situations. A high-risk, near-term suicidal patient was defined as one who has committed suicide or attempted suicide and failed within minutes to weeks from the time of their voice recordings. The audio recordings of the depressed and control groups were extracted from the database of an ongoing study in the Vanderbilt University Department of Psychiatry. The selected non-depressed control subjects met the following criteria: 1) a Hamilton rating scale (17 item version) for a depression score of 7 or less [7]; 2) a Beck depression score of 7 or less [8]. The depressed patients met the following criteria: 1) major depressive disorder as defined by the research diagnostic criteria [9]; 2) a Beck depression score of 20 or greater; 3) a Hamilton rating scale for depression score 14 or greater.

All of the selected audio recordings were digitized using a sixteen-bit analog to digital converter. The sampling rate was 10 KHz, with an anti-aliasing filter (i.e., 5KHz low-pass) precisely matched to the sampling rate. The digitized speech waveforms were then imported into a MicroSound Editor where silence pauses exceeding 0.5 seconds were removed to obtain a record of continuous

speech. Thirty seconds of continuous speech from each subject were stored for analyses.

III. METHODS

A. General Procedures

For all audio recordings, the formants were estimated by taking the roots of the autocorrelation LPC function of each voiced sample segment of the waveform. Subsequently, the speech was divided into overlapping segments of 30 ms per segment sample. The sample segments went through a voiced/unvoiced classification process and the unvoiced segments were discarded.

Three different normalization procedures were compared: normalization based on median of the third formant; normalization based on the first three formants; and normalization based on the Gaussian Mixture model (GMM). The features used for classification were the cepstral coefficients. A GMM was used to model the features and each was trained using the *hold-out* procedure [10]. The Maximum Likelihood (ML) classifier was used to classify each pattern in pair-wise comparisons and assess the effectiveness of the normalizations.

B. Mel-Cepstral Feature Extraction

The mel-cepstral features were extracted using the following procedure:

1. Each signal is divided into segments of 30 ms of voiced speech,
2. The logarithm of the discrete Fourier transform (DFT) of each segment is computed,
3. Each log-spectrum is filtered with 16 triangular filters whose center frequencies are based on the mel-scale,
4. The frequency scale is normalized to account for variations in vocal tract length,
5. The inverse DFT is calculated to obtain the cepstral coefficients,
6. The first four coefficients are retained as features [10].

C. Normalization based on median of F_3

In order for a segment to be included in the warping factor estimation, the following criteria had to be met:

1. The probability that the segment is voiced is ($p_v > 0.8$),
2. $F_1 > 400$ Hz
3. $2000 \text{ Hz} < F_3 < 3000$ Hz

For the sequence of T_i segments that meet these requirements for a speaker i , the median of the third formant is calculated and stored. This process was repeated for all 30 speakers. The normalization factor α_i , for a given speaker i , would be the median of his/her third formant over the median of the third

formant of the remaining speakers. This is represented by the following equation:

$$\alpha_i = \frac{\text{median}\left(\left\{\left[F_3\right]_i\right\}_{t=1}^{T_i}\right)}{\text{median}\left(\left\{\left\{\left[F_3\right]_i\right\}_{t=1}^{T_i}\right\}_{i=1}^{30}\right)} \quad (1)$$

where the numerator is a representation of the speaker i 's vocal tract length and the denominator is a representation of the baseline vocal tract length.

D. Normalization based on median of F_1, F_2, F_3

The median of the first three formant frequencies for each speaker was recorded. The warping function ω_i , for a given speaker i , was subsequently computed by calculating the slope of a plot with the median of the formant frequencies F_1, F_2 and F_3 of speaker i , on the abscissa, over the average of the median of each formant of all remaining speakers in the training set on the ordinate. These formants are represented by the following equations:

for new speaker i ,

$$\left[F_n\right]_i = \text{median}\left(\left\{F_n\right\}_{t=1}^{T_i}\right) \quad (2)$$

for the standard speaker:

$$F_n = \text{median}\left(\left\{\left[F_n\right]_i\right\}_{i=1}^{30}\right) \quad (3)$$

For $n = 1, 2, 3$, where T_i is the number of sample segments for speaker i , and F_n are the formant frequencies. The best-fit line is set to intercept at zero, and the calculated slope represents the warping factor for that given speaker. This process is repeated for all 30 recordings in the database.

E. Normalization based on one GMM model for all warping factors

The acoustic vectors used to train and test the model are the Mel-cepstral coefficients of speech as described in A1. The procedure used to determine the best warping factor is a multi-step procedure developed by Welling et al. [11].

1. For each class, one Gaussian probability density function is trained on all unnormalized features for that class.
2. Using the class conditional density functions determined in step 1, the warping factor that maximizes the maximum likelihood function for each subject is chosen as the first estimate of the subject's α_i . Warping factors ranging from 0.80 to 1.12 with an increment of 0.02 were used [12].

- Using the warping factors in step 2 a four component GMM was developed for each class. Using the GMM, step 2 was repeated to determine the best warping factor for each subject.

F. Gender Dependant and Independent Normalization

Two sets of warping factors were calculated for each subject. One set was gender-dependant and constructed from two subsets of 15 females and 15 male speakers considered separately. The gender-independent set was determined by combining the male and female data into one data base.

G. Nonlinear Warping

For nonlinear warping the warping equation is

$$f' = f\alpha^{3f/8000} \quad (4)$$

IV. RESULTS AND DISCUSSION

Table 1 presents the sample statistics of the warping factors derived from the three techniques. Female speakers are shown to have lower warping factors when compared to the male speakers in the gender-independent computations.

Table 1. Average, Ave, and standard deviation, Std, of warping factors for male, m, and female, f, subjects for the three methods and gender independence and dependence.

	Independent			Dependant		
	GMM	F3	1-3 F2,	GMM	F3	1-3 F2,
Ave-f	1.04	1.00	0.99	1.06	1.01	1.00
Std-f	0.02	0.04	0.06	0.02	0.05	0.07
Ave-m	1.05	1.02	1.02	1.04	1.00	1.00
Std-m	0.02	0.04	0.05	0.02	0.05	0.05

These results are somewhat inconsistent with that of the researches who proposed this technique [13]. Females, due to their shorter vocal tracts are expected to present higher warping factors (greater than 1.00). This is slightly true for the gender dependent factors. However, there is no clear distinction between the warping factors of males and females in both gender dependant and gender independent computation of the warping factor. Both genders exhibit warping factors around the 1.00 value.

Table 2 tabulates the classification performance results using the baseline system with no VTLN, the various speaker normalization techniques grouped under gender dependant and gender independent models, and implementation of these techniques through linear or nonlinear warping functions, whenever possible. The first row reports the classification rate observed when testing with unwarped feature vectors.

Table 2: Results of Classification rates. Highest in each main category is highlighted

Warping Factor Derivation	Warping Function	% Correct Classification		
		Control-Depressed	Control-Suicidal	Depressed-Suicidal
Baseline (No VTLN)		85	80	75
GENDER INDEPENDENT				
1. GMM	Linear	80	85	80
	Non-linear	85	85	85
2. F ₃	Linear	85	80	80
	Non-linear	80	85	85
3. Slope F ₁ , F ₂ , F ₃	Linear	85	75	85
Average F ₃ + F ₄ [24]	Linear	75	80	80
Gender Dependant				
1. GMM	Linear	80	85	75
	Non-linear	80	80	80
2. F ₃	Linear	80	85	80
	Non-linear	80	85	85
3. Slope F ₁ , F ₂ , F ₃	Linear	90	80	85

Implementation of the various normalization techniques yielded encouraging results. The ML classifier yielded a classification as high as 90% between control and depressed patients and 85% between depressed and suicidal subjects. Surprisingly, for our baseline investigation, the results obtained were relatively higher than some obtained with normalization. In a comparison between gender independent and gender dependant normalizations, gender independent normalizations showed superior classification performance. Except for the formant-based technique via the use of the first three formant frequencies, all classification rates using gender independent models are consistently high (up to 85%) for all three diagnostic classes. The Maximum-likelihood technique with nonlinear warping seems to be the best, yielding 85% in all cases. Although warping with the third format is slightly less effective but its simplicity makes the arguement for its use on a large scale. In a comparison between linear and nonlinear frequency warping, nonlinear frequency warping showed an overall superior classification performance for all diagnostic classes.

REFERENCES

- [1] W. J. Fremouw, M. Perczel, and T. E. Ellis, *Suicide Risk: Assessment and Response Guidelines*. New York: Pergamon Press, 1990.
- [2] D. J. France, R. G. Shiavi, S. E. Silverman, and W. D.M., "Acoustical properties of speech as indicators of depression and suicidal risk," *IEEE transactions on Biomedical Engineering*, vol. 47, pp. 829-837, 2000.
- [3] A. Ozdas, R. Shiavi, D. Wilkes, M. Silverman, and S. Silverman, "Analysis of fundamental frequency for near term suicidal risk assessment," presented at Conference on Systems, Man, and Cybernetics, Nashville, TN, 2000.
- [4] P. Dognin, A. El-Jaroudi, and J. Billa, "Parameter Optimization for Vocal Tract Length Normalization," presented at ICASSP, Istanbul, 2000.
- [5] E. Eide and H. Gish, "A parametric Approach to Vocal Tract Length Normalization," presented at ICASSP, Atlanta, GA, 1996.
- [6] P. Zhan and M. Westphal, "Speaker Normalization Based on Frequency Warping," presented at ICASSP, Munich, Germany, 1997.
- [7] M. Hamilton, " A rating scale for depression," *J Neurol Neurosurg Psychiatry*, vol. 23, pp. 56-62, 1960.
- [8] A. T. Beck, C. Ward, M. Mendelson, J. Mock, and J. Erbough, "An inventory for measuring depression," *Arch Gen Psychiatry*, vol. 4, pp. 561-571, 1961.
- [9] R. Spitzer, J. Endicott, and E. Robins, "Research diagnostic criteria: rationale and reliability," *Archives Geneneral Psychology*, vol. 35, pp. 773-782, 1978.
- [10] A. Ozdas, R. G. Shiavi, D. M. Wilkes, M. K. Silverman, and S. E. Silverman, "Analysis of Vocal Tract Characteristics for Near-term Suicidal Risk Assessment," *Methods of Information in Medicine*, vol. 43, pp. 36-38, 2004.
- [11] L. Welling, S. Kanthak, and H. Ney, "Improved Methods for Vocal Tract Normalization," presented at ICASSP, Phoenix, AZ, 1999.
- [12] L. Lee and R. C. Rose, "A Frequency Warping Approach to Speaker Normalization." , Vol. 6, No. 1, pp. 49-60, Jan. 1998., *IEEE Transactions on Speech and Audio Processing*, vol. 6, pp. 49-60, 1998.
- [13] E. B. Gouvea and R. M. Stern, "Speaker Normalization through Formant-based Warping of the Frequency Scale," presented at Eurospeech, Rhodes, Greece, 1997.

Infant cry – Singing voice

INTERACTION PATTERNS BETWEEN MELODIES AND RESONANCE FREQUENCIES IN INFANTS' PRE-SPEECH UTTERANCES

Kathleen Wermke¹, Werner Mende², Anne Kempf¹, Claudia Manfredi³, Piero Brusciaglioni⁴, Angelika Stellzig-Eisenhauer¹

¹Center for Pre-Speech Development & Developmental Disorders, Department of Orthodontics, Julius-Maximilians-University Wuerzburg, Germany; ²Berlin-Brandenburg Academy of Science, Berlin, Germany; ³Dept. of Electronics and Telecommunications, Faculty of Engineering, University of Firenze, Italy; ⁴Dept. of Physics, Faculty of Mathematics, Physics and Nat. Sci., University of Firenze, Italy

INTRODUCTION

Melody, the time function of the fundamental frequency is a key quantity for characterizing infants' utterances during the first months of life. However, additional quantities, describing the voluntary control of the vocal tract become increasingly important during pre-speech development. From a physiological point of view laryngeal phonation and vocal tract based articulation are anatomically different and independently controlled systems. For speech acquisition these two systems have to interact systematically. For instance, melody movements increasingly influence resonance frequencies of the vocal tract and vice versa.

A prominent phenomenon of a melody - resonance frequency interaction is the increasing occurrence of periods of close parallel synchronous movements of melodies and lower resonance frequencies. We call such movements 'tuning periods' when a resonance frequency moves inside a close neighborhood, a 'vicinity tube', of one of the lower harmonics and when this situation lasts for at least 20 ms. Vicinity is given by our analysis bandwidth. Tuning develops either by movements of resonance frequencies to track the melody, or conversely, by movements of the melody to approach certain resonances, or by both processes taking place simultaneously. Here, the term 'tuning' is used in a purely descriptive sense, without considering the mechanisms that are producing this phenomenon as well as without considering what is cause or effect. It is not yet clear, how much mechanical couplings inside the vocal system contribute, and how much intentional neuro-physiological control contribute to the production of longer tuning periods.

Another prominent feature of melody-resonance interaction is resonance frequency transition. Here, transition is defined as coherent and smooth movements of a resonance frequency from the vicinity of one harmonic to the vicinity of another harmonic. The duration of a transition depends on several factors, e.g., neuro-physiological maturity and integrity of the underlying control systems, achieved training level, type of utterance or syllable-structure.

Such well-formed and smooth transitions and the above-mentioned coherent tuning periods represent probably the predispositions for fast couplings (and de-couplings) of phonation and articulation and for acquiring the necessary flexibility for producing fast sequences of phonological structures in later fluent speech. At about babbling age, phonation and articulation are acting completely in concert. The production of babble - syllables is characterized by fast formant transitions which lay already within the time range of fluent speech (e.g. Oller 2000).

METHODS

Data Acquisition. Spontaneous cry utterances were recorded from the 8th week until the 25th week of life in home environment by trained persons using SONY-DAT-recorders (TCD-D100, 48 KHz/16 bit, mono) and SONY-microphones (ECM-MS957).

Data Analysis. We selected for analysis a set of 800 voiced utterances with a high signal-to-noise ratio out of our cry database. Beside broad- and narrow-band spectrograms high resolution melody computations were made using a CSL-Speech Lab 4400/ MDVP (KAY Elemetrics) in combination with a post-processing and interactive removal of outliers and macro-pitch errors. Our basic resolution in time was down to one pitch period and the frequency resolution was about 3 Hz at 500 Hz. An additional low-pass (Gaussian~40 Hz) filtering of the melody was applied to reduce the short-time variability of the melody. Resonance frequency estimation was performed by means of the LPC analysis tool of the CSL (adaptive coefficient estimation, frame length 10-20 ms, frame step 5 ms). If necessary, an interactive frame by frame check was done with different frame lengths and polynomial degrees in order to exclude critical cases with overlapping resonances. Our standard analysis bandwidth (10 ms frame ÷ 100 Hz) in resonance frequency estimation corresponds to a theoretical relative error band of $\pm 20\%$ at 500 Hz or $\pm 0.2 / \#$ for the resonance in the vicinity of the #-th harmonic. However, in analyzing pre-speech data with mean fundamental frequencies not higher than 350 Hz and in case of a smooth sequence of consecutive resonance points (from LPC-frames) we got a much lower uncertainty than formally given by the frame-window related analysis bandwidth. For statistical evaluations of the transition times and tuning durations the analysis was confined to signals with fundamental frequencies under 450 Hz in order to avoid uncertainties of the LPC coding algorithms for higher F0. Recordings with overlapping broad resonances were checked using the bandwidth graphics provided by the CSL-speech Lab and resonances which could not be separated were excluded from further analysis. Here, the focus was set to the two lowest resonance tracks in the frequency range up to 4000 Hz (R1, R2).

For a quantitative characterization of melody-resonance interactions we measured and evaluated two quantities, tuning times and transition times. Tuning time was defined as the duration of a parallel synchronous movement of a resonance within the vicinity tube of a harmonic that lasts longer than 20 ms. Transition time between two tuning phases was defined as the residence time of a resonance in the intermediate space between the two vicinity tubes.

DIAGRAMS

The displayed time-frequency diagrams contain the melody and its harmonics on a linear frequency scale. The diagrams are designed in order to visualize the interaction of resonance tracks with the harmonics of the melody. The maximum intensity of a resonance frequency is drawn as a point in the diagram. Consecutive points yield frame by frame the resonance track synchronous to the melody.

In the diagrams a resonance frequency point with a distance ≤ 100 Hz from the nearest harmonic at a given time point is marked red. The (red-coloring) vicinity tube around each harmonic coincides precisely with our analysis bandwidth. Only periods of more than four successive red points (>20 ms) are considered as tuning periods. Resonance points in the intermediate space deviating more than 100 Hz from both

adjacent harmonics were marked by blue points. So, transitions consist of a relatively smooth sequence of blue points meeting at both ends the tuning periods at two different harmonics.

Note that in the black and white printed version red and blue points appear grey and black in the diagrams.

SUBJECTS

Subjects were eight infants, six healthy infants and two infants suffering from a cleft-lip-palate (CLP-infants). All infants were term-born German infants.

The six healthy infants were participants of the German Language Development Study (www.glad-study.de), established at the Children's Hospital Lindenhof / Charité, Berlin. These infants were without neurological or developmental disorders. Within the GLaD-study, regular medical and developmental check-ups were carried out. The status of language acquisition at 24 months was assessed by standardized tests for German children. Children below the critical values in both tests at two years, were regarded as SLI-at-risk infants (N=2) in the present investigation. Children above the critical values in both tests form the normal language development group (N=4). Specific language impairment (SLI) is defined as an impairment of oral language despite of having normal intelligence, and adequate learning environment, and despite of having physical or emotional or hearing problems (Bishop & Edmundson 1987). Hence, four of the six healthy infants had a normal language outcome, whereas two of them were retarded at two years (SLI-at-risk infants).

The two CLP-infants, suffering from a unilateral cleft-lip-palate were treated at the Department of Orthodontics of the University Würzburg. CLP-infants exhibit different resonance conditions mainly caused by an open oro-nasal space and a velum dysfunction. The CLP-infants had no other malformations and no neurological disorders.

RESULTS

The interactive tracking method of resonance frequencies and the analysis of their interaction with the melody using a special visualization concept allowed an assessment of the stepwise development of articulatory activity in very young infants. Two characteristic patterns of interaction of melody and resonance could be detected and investigated, namely tuning and transition phenomena.

Developmental changes exhibiting an increasing perfection of tuning between melody and the two lowest resonance frequencies were found. Moreover, increasingly faster resonance transitions were observed.

Averaging over the observation period, the mean duration of transitions between tuning phases for the four healthy infants with normal language development was 61.5 ms (range 20 – 148 ms). Compared to these infants, the two infants exhibiting an at-risk state for SLI at 24 months showed significantly longer mean transition times (mean 75 ms; range 35 – 470 ms). Distributions of observed transition times and developmental changes will be shown at the conference. In contrast to SLI-at-risk infants, the two CLP-infants produced resonance frequency transitions as fast as the normal infants, but only when carrying a special palatal plate, which separates the oral space from nasal space.

From our observation period, representative examples are presented for typical interaction patterns between melodies having low resonance frequencies.

As a representative example of early melody-resonance-interaction, in Figure 1 a mitigated cry of a healthy infant about 9 weeks old is displayed. The cry has a relatively simple melody in form of a single rising-falling arc and shows

already longer periods of tuning with stable and coherent tracks of R1 and R2 following the melody. This seems to be a first trace of intentional 'playing' with the resonances. At this early age, a coupling between melody and resonances occurred regularly in healthy infants. But, the resonances R1 and R2 often still show a swing in behavior at the beginning of an utterance. This is interpreted as a sign for a yet immature control capacity for phonatory - articulatory couplings.

The example in Figure 1 demonstrates also a behavior observed in many other utterances, a tendency to correct larger deviations from a preceding tuning not in the direction to the instantaneously nearest harmonic, but to force a restoration toward the former tuning situation. This points to an underlying neuro-physiological re-directional control process instead to mechanical forces. R1 and R2 seem to stabilize each other, which is particularly effective in cases where the resonances have octave distance (Fig. 1).

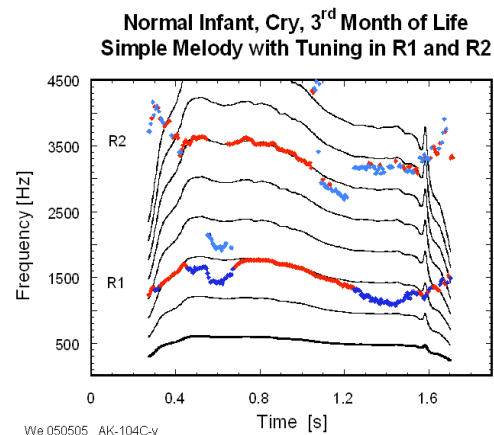


Fig. 1: This cry contains relatively long periods of tuning with stable and coherent tracks of R1 and R2 following the melody. A kind of 'playing' with the resonances possibly released by nearby laying strong harmonics is observable. At this age, many utterances still show a tendency to correct stronger deviations from the tuning condition not by moving resonances in direction to the nearest harmonic but to force a back-movement to the former tuning situation.

In Figure 2, a more developed interaction feature in form of coherent and well-formed resonance transitions of R1 and/or R2 is displayed.

Figure 3 demonstrates that resonance transitions occur not only between consecutive harmonics, but also over two harmonics. The observed strong and parallel movements of R1 and R2 as well the aptitude to climb two harmonics upwards or downwards straightforwardly in only one step are interpreted as an advanced transition feature.

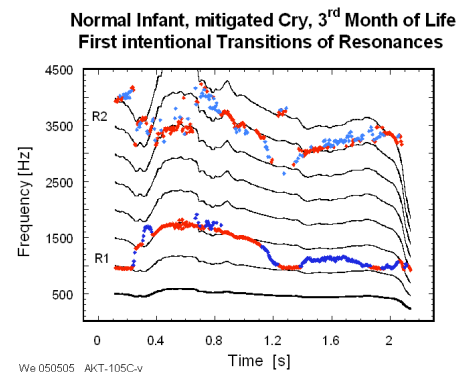
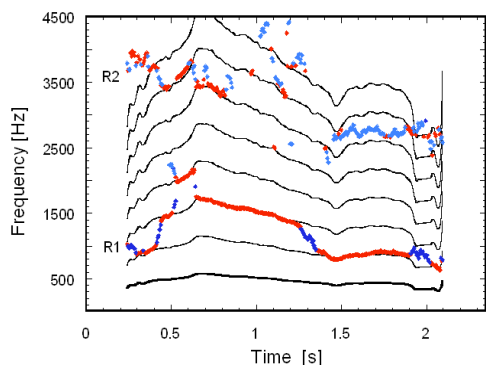


Fig. 2: An important feature of articulatory development: In R1 and R2 a transition from one harmonic to another (3rd – 2nd and 7th – 6th) occurs at the same time. R2-transitions exhibit higher fluctuations and are less stable. After a long tuning period of about 600 ms a relatively soft, but coherent R1-transition downward follows. After a short tuning period at the 2nd harmonic the cry ends with a free running R1.

A subsequent stage of pre-speech development is shown in Figure 4. In this babbling utterance complex interactions in form of fast transitions and accurate tunings occur and produce fast changes of the resonances with short residence times on certain harmonics. The interaction processes in R2 proceed essentially parallel to R1, but often with somewhat lower stability and coherency.

**Normal Infant, mitigated Cry, 3rd Month of Life
Tuning and Advanced Transitions of Resonance R1**

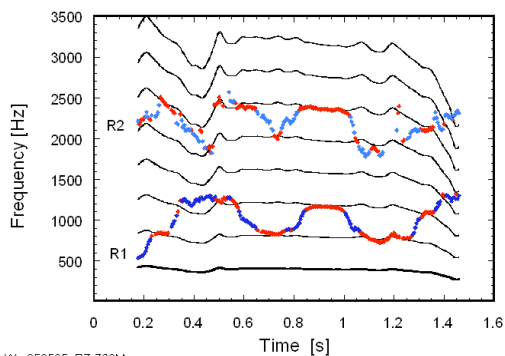


We 050505 AK-106M-v

Fig. 3: A two-step R1-transition upwards is followed by a one-step transition downwards. After a longer perfect tuning a further downward R1-transition occurs. The melody consists of two arcs with the frequency maximum of the first arc occurring about 80 ms later than the R1-resonance maximum.

The two investigated SLI-at-risk infants exhibited a kind of poverty of melody complexity and a sparseness of resonances in their pre-speech utterances. Particularly, R1-transitions were prolonged and unstable. Compared to the healthy infants with normal language development, the SLI-at-risk infants had a significantly longer mean transition time of 75 ms (range 35 – 470 ms). Here a typical example for such a more instable and longer lasting transition is displayed (Fig. 5).

**Normal Infant, early Babbling, 4th Month of Life
Short, stable Tuning and complex Transitions in R1 and R2**

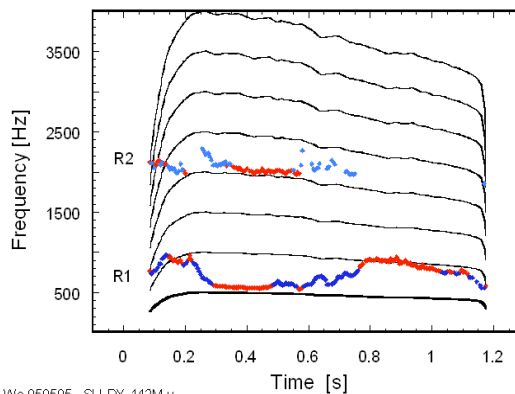


We 050505 BZ-728M-v

Fig. 4: In syllable-like utterances fast transitions in R1 and R2 alternate with tuning intervals.

In Figure 6 an example is displayed for demonstrating the observation that CLP-infants carrying a palatal plate are capable of exhibiting transition processes comparable to those found in healthy infants with normal language development. However, it was found that CLP-infants more often show instable R2 or higher resonances.

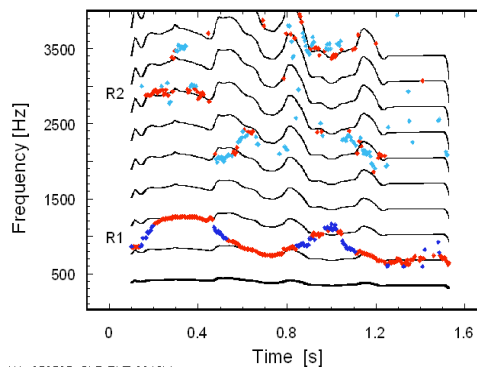
**SLI-at-risk Infant, mitigated Cry, 3rd Month of Life
Prolonged Transition in R1 and decaying R2**



We 050505 SLI-DY-142M-y

Fig. 5: In SLI-at-risk infants prolonged and unstable transitions of R1 and R2 were regularly observed. Here, the second R1-transition is considerably prolonged and unstable, even in this relatively simple transition from the first to the second harmonic. The development of R2 is also disturbed.

**Cleft Lip Palate Infant, 4th Month of Life
Normal R1, Strongly disturbed Resonance R2**



We 050505 CLP-BXT 8812M-v

Fig. 6: This mitigated cry consists of a vibrato-like melody modulation while the lowest resonance frequency (R1) moves two times up and down, like in non-cleft infants at this age. The movement of R1 is adjusted to the melody by transitions from the second to the third harmonic of the melody while exhibiting strong tuning phases at both harmonics.

DISCUSSION

The present investigation confirmed and complemented earlier results concerning a systematic training and a first establishment of articulation activity during infants' crying at a very early age (Wermke et al. 2002, 2005). The establishment of tuning between melody and resonance frequencies and a mastering of fast transitions seems to require a training period before being at disposal for intentional use in vocal production. At about the fourth month of life, a rapid expansion of the infant's pre-speech repertoire occurs. Utterances contain more vowel-like elements and near-syllables. So, it was anticipated that voluntary articulatory activity has to be trained step by step well before this age. The presented results strongly supported this hypothesis.

Here, characteristic interaction phenomena, namely transitions of resonance frequencies between harmonics of the melody could be identified for the first time in infants younger than four months. The mastering of such advanced transitions is an essential prerequisite for performing fast and accurate shifts between vowel formants in speech. Based on our experience,

we interpret the systematicity in the production of advanced transitions as a training phase enabling the brain to establish a prospective time organization in vocal sound production necessary for fluent speech: Vocal tract articulators often have to be pre-adjusted to anticipated, but nevertheless in parallel threads planned melody movements. The observed time organization, where resonance movements often lead the course of the melody, points to higher cerebral control mechanisms underlying sound production already in young infants (see Fig. 3 for the 80 ms time lead of resonances).

It is hypothesized that the observed interaction patterns are not produced by chance. Particularly, the investigated transitions of lower resonance frequencies share many features with later formant transitions necessary for vowel articulation in speech-like babbling and word production. The observed developmental changes suggest that the fast resonance transitions are necessary presuppositions for the extremely short transitions between the phonological units in later speech. The identification of such transitions as well as the demonstration of increasingly stronger tunings between phonation and articulation supports the idea of learning and training of language-related features during infants' crying and points to a continuous developmental path from crying to word production. This hypothesis is also supported by the finding, that fast switches between tuning and resonance transition are generally learnt in healthy infants with normal language outcome within a short time span. In contrast to them, infants being at risk for developing SLI exhibit the displayed training phases over a much longer time span; sometimes they need even several months. Moreover, the longer mean resonance transition times observed in SLI-at-risk infants point to a relation of these early articulatory activities to later language performance. Concerning processing auditory information in the brain, a disturbed time organization is reported for SLI-at-risk infants and is interpreted as an important component in developing a Specific Language Impairment (e.g. Tallal 1989, Jusczyk 1997, Weber et al. 2004). The present findings suggest the idea that also in controlling vocal production a disturbed time organization may characterize SLI-at-risk infants.

In CLP-infants, the finding that a palatal plate seems to enable the infants to produce transition phenomena comparable to those in healthy non-cleft infants is very important for treatment strategies to minimize later speech and language impairments caused by the malformation. Both infants received a special palatal plate during the first days after birth and the plates were only removed by the parents to clean them after feeding. For a next investigation to be conducted, it is hypothesized that CLP-infants who were not supplied with a palatal plate will exhibit more deviations in the observed melody-resonance-interaction patterns.

However, in face of the high variability between infants, the cases studied here were not yet sufficient to and further work is necessary to confirm the formulated hypotheses and to generalize the presented results..

CONCLUSION

The present paper provided time functions (tracks) of the resonance frequencies and investigated the interaction between these tracks and harmonics of the melody. This approach allowed to investigate pre-articulatory activity at a very early age and to observe early developmental processes directed toward speech and language acquisition. An increasing unfolding of tuning between melody and lower resonance frequencies as well as resonance frequency transitions were found in utterances of 2- to 3-months-old infants. This vocal behavior was interpreted as an early articulatory activity in infant's crying. In a broader perspective, it is seen as a

language-related behavior, preparing formant tuning and focalization in later speech. Far reaching medical applications are seen for infants with disturbances of the time organization of vocal production and for CLP-infants. .

References

1. Oller, D. K. The Emergence of the Speech Capacity. Lawrence Erlbaum Associates, Mahwah, NJ, 2000.
2. Wermke, K., Mende W., Manfredi C., Brusciaglioni, P. Developmental aspects of infants' cry melody and formants. *Med. Eng. Phys.* 2002;24: 501-514
3. Wermke K., Mende W., Manfredi C., Brusciaglioni, P. & Stellzig-Eisenhauer A. Tuning phenomena of melodies and resonance frequencies (formants) in infants' pre-speech utterances. *Poster presented at the 149th Meeting of the ASA*, Vancouver 16-20 May 2005
4. Bishop D.V.M., Edmundson A. Specific language impairment as a maturational lag: Evidence from longitudinal data on language and motor development. *Dev Med Child Neurol.* 1987;29:442-459
5. Tallal P., Ross R., Curtiss S. Familial aggregation in specific language impairment. *J Speech Hear Disord.* 1989;54:167-173
6. Jusczyk P. (ed.). The discovery of spoken language. Bradford, Cambridge, MA, 1997
7. Weber Ch., Hahne A., Friedrich M., Friederici A.D. Discrimination of word stress in early infant perception: Electrophysiological evidence. *Cog Brain Res.* 2004;18:149-161

Acknowledgement

We thank Peter Wermke for his engaged work in all aspects of data analysis. The data characterizing the developmental state of the six healthy subjects were kindly provided by Volker Hesse, head of the pediatric clinic of the Krankenhaus Lichtenberg, teaching hospital of the Charité, Berlin. The status of language outcome of these six infants were kindly made available by Zvi Penner and Petra Schulz, principal investigators of the research group „language production and comprehension“ at the Charité – University Medical Center Berlin, Department of Audiology and Phoniatrics, headed by Prof. Dr. M. Gross.

The study was supported in part by the Deutsche Forschungsgemeinschaft (German Research Foundation, DFG) (WE-1724/4-1) as part of the Research Group 381 - Frühkindliche Sprachentwicklung und spezifische Sprachentwicklungsstörungen. Further support was provided by the Gruter Institute of Law and Behavioral Research Portola Valley, USA.

AERODYNAMICAL MODEL OF HUMAN NEWBORN LARYNX: AN APPROACH OF THE FIRST CRY

R Nicollas¹, J Giordano², L Francius², J Vicente², Y Burtschell², M Medale², B Nazarian³,
M Roth³, M Ouaknine¹, A Giovanni¹

¹ Laboratoire d'Audiophonologie clinique et expérimentale. Université de la Méditerranée. CHU Timone, 264 Rue Saint Pierre. 13385 Marseille cedex 05. France

² Laboratoire de l'IUSTI, UMR 6595 CNRS-Université de Provence. Technopôle de Chateau-Gombert, 5 Rue Enrico Fermi 13453 Marseille cedex 13. France

³ IRM fonctionnelle. IFR sciences du cerveau. CHU Timone, 264 Rue Saint Pierre. 13385 Marseille cedex 05. France

Abstract: First cry has been much studied especially from an acoustical point of view. However, the mechanisms of sound production are unclear. Thus, following studies we previously performed, we extend in this present work our simulations to a more realistic geometry obtained by MRI images of a fetal larynx. This work confirms the major role of vortices and may be that of the supraglottis and the fluid flow interactions.

Introduction: Vocal folds of newborns are histologically different from children and adults. Reinke's space is not clearly individualized. As shown by Titze, this structure is absolutely needed for vocal fold vibration [1]. The hypothesis for vocal production in newborn is that the air column generates itself the acoustic waves from which the voice appears. Some other possible vibrators within the mammalian production system include the vocal tract [2].

Anatomical measurements were performed and a preliminary virtual model was designed to modelize turbulences with vocal folds in phonatory position [3]. Despite acoustic waves were not detected through this simplified geometry, those results however suggested that newborn phonation is a vortex effect coupled with a vibration of supraglottic structures.



Fig. 1: Saggital view of a MRI acquisition of a human fetal larynx. Those data were used for computing a realistic geometrical model exported to Fluent®

Material and methods: Therefore, in the present study, we have undertaken a much more realistic geometrical model based on 3D MRI images (fig. 1) of a fetal human laryngotracheal tract. These frames allowed us to build a 3D numerical model using 18 horizontal slices with 50 points on each perimeter. It was exported to Gambit® in order to build up the mesh (fig. 2) to be computed with Fluent®. Moreover, based on this 3D geometry, a 2D axisymmetric model was also built to be used with Fluent® and CARBUR. The later is a

research code developed in our laboratory and is dedicated to the study of compressible fluid flows [4]. This code is based on the discretization of the Navier-Stokes equations by a finite volume method. A second order scheme, for both space and time, with a Van Leer slope limiter has been used to solve the set of compressible Navier-Stokes and energy equations.

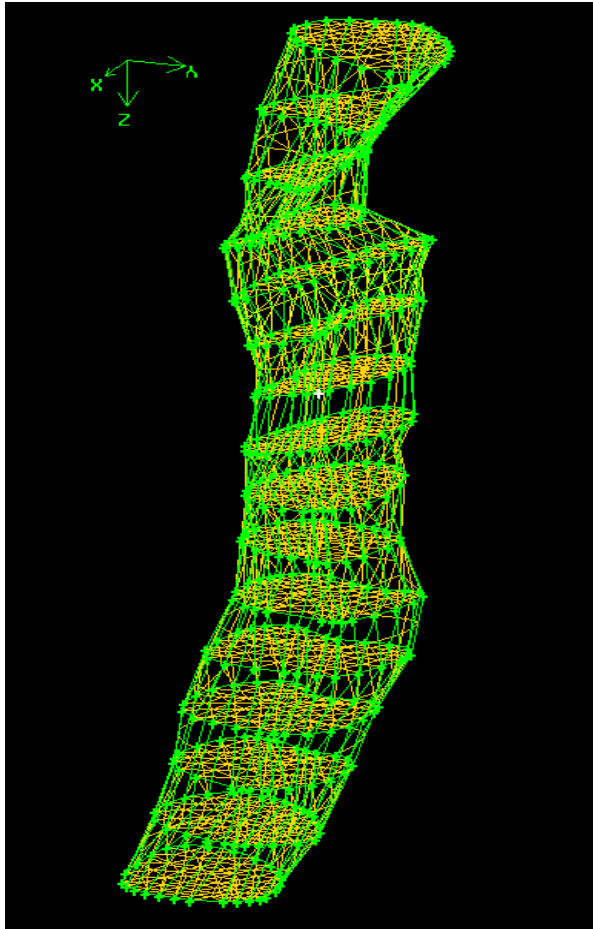


Fig. 2: Example of mesh obtained after exporting MRI slices to Gambit®.

Results: The fluid flow computations performed with Fluent® consider the flow as fully compressible and unsteady for the duration of the cry. The fluid flow is driven by a pressure drop of 6000 Pa, imposed between the inlet and the outlet of the computational domain. Furthermore, a no-slip boundary condition is imposed on the laryngotracheal wall. Several probe points have been considered in the computational domain in order to extract fluid flow

characteristics such as acoustical waves, dynamical vortices, etc.

In this first step, the ability of a rigid wall configuration to produce acoustic waves is studied as well as the amplification by the supraglottic structures. In order to validate numerical results obtained on the realistic model, calculations were also performed with both CARBUR and Fluent® on a simplified geometry.

Thus, on the simplified geometry, we found highly unsteady flow with vortex generation upon the vocal folds. The main source of vortices is the Kelvin-Helmholtz's instability which appears on the shear layer. Fig. 3 shows a Schlieren of the fluid flow obtained with CARBUR where typical vortices structure are displayed. Moreover, the time evolution shows that subglottic pressure waves increase vortices shedding.

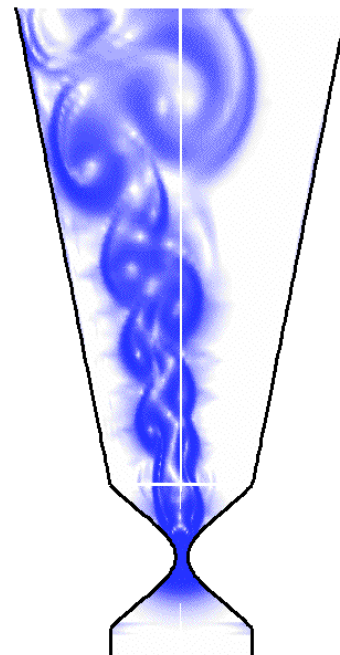


Fig. 3: Vortex structure induced by the instability behind the sharp channel expansion over the vocal folds.

We confirm with this realistic model the presence of vortices structures we observed in our previous study with a simplified geometric shape. Fig. 4, where are plotted streamlines coloured by velocity magnitude, shows the acceleration of the fluid flow in the glottic area and the

creation of vortices. One can note a boundary detachment just upon the posterior part of the glottis, where two counter rotative vortices are generated.

Whatever the code and the geometrical model, the maximum velocity just upon the glottis is about 110 m/s.

Computations are actually in process to determine the implication of these vortices in sound generation.

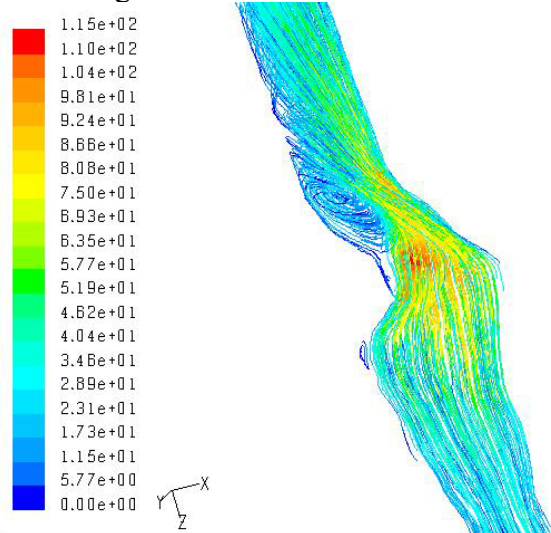


Fig. 4: Streamlines coloured by the velocity magnitude on the 3D realistic model.

In a second step of our study, fluid-structure interaction will be considered using a dedicated research code we have developed [4]. This code is based on the coupling of CARBUR and MARCUS. The later, another research code developed in our laboratory, deals with the dynamics of deformable structures [4]. The space discretization is carried by a finite element method, whereas, the temporal time discretization is achieved with the Newmark's algorithm. The numerical coupling between the fluid flow and the structural dynamics models is performed through boundary conditions. The fluid flow imposes a pressure distribution on the structure boundary, which in return imposes a new geometry to the fluid domain [4].

Conclusion and perspectives: Sound production by the neonatal larynx is a multifactorial problem, which needs the

understanding of multiphysic phenomena such as the vortex sound generation, the coupling between the aerodynamic and the supraglottic structures. Our numerical simulations have pointed out the vortex generation upon the glottis and an amplification of the vortex shedding by the pressure waves. We also observed a high degree of instability of the outflow, which let us suppose that fluid-structure interaction phenomena may occur. The next step will be to calculate the sound radiation due to source terms previously identified [5].

Keywords: newborn, phonation, vocal folds, aerodynamic, modelization, fluid-structure interaction.

References

1. **Titze IR, Talkin DT:** A theoretical study of the effects of various laryngeal configurations of the acoustics of phonation. *J Acoust Soc Am* 1979 ; 66 : 60-74.
2. **Fitch WT, Neubauer J, Herzel H:** Calls out of chaos: the adaptive significance of nonlinear phenomena in mammalian vocal production. *Animal behav* 2002 ; 63 : 404-418.
3. **Nicollas R¹, Ouaknine M¹, Giovanni A¹, Berger J², To JP², Dumoulin D², Triglia JM¹:** Physiology of vocal production in the newborn. MAVIBA Firenze Dec 2003
4. **Giordano J, Jourdan G, Burtschell Y, Medale M, Zeitoun DE, Houas L:** Shock wave impacts on deforming panel, an application of fluid-structure interaction. *Shock Waves* Feb 2005, DOI (10.1007/s00193-005-0246-9).
5. **Gloerfelt X, Bailly C., Juvé D:** Direct computation of the noise radiated by a subsonic cavity flow and application of integral method. *Journal of sound and Vibration* 2003 ; 266 : 119-146.

HIGH-PITCHED VOICE SIMULATION USING A TWO-DIMENSIONAL VOCAL FOLD MODEL

Seiji Adachi[†] and Jason Yu[‡]

ATR Human Information Science Laboratories, Keihanna Science City, Kyoto 619-0288 Japan[†]
School of Engineering Science, Simon Fraser University, 8888 University Dr. Burnaby, BC V5A 1S6 Canada[‡]

Voiced sounds were simulated with a computer model of the vocal fold composed of a single mass vibrating both parallel and perpendicular to the airflow. The major improvement of the present model over the two-mass model is that it has a wider continuous frequency range where self-excitation is possible both below and above the first formant frequency of the vocal tract. The two-dimensional model can therefore successfully be applied to the sound synthesis of a high-pitched soprano singing, where the fundamental frequency sometimes exceeds the first formant frequency.

I. INTRODUCTION

An acoustic tube generally yields an inductive load in the frequency below a resonance peak, while the load turns out to be capacitive in the frequency above the peak. In speech, the fundamental frequency (F0) is usually lower than the first formant frequency (F1) of the vocal tract. Therefore, the vocal folds always vibrate with an inductive load.

In high-pitched soprano singing, however, F0 enters the range of F1 in normal speech. The soprano singer then raises F1 as F0 approaches F1 by increasing the jaw opening.[1] As a result, F1 is always tuned close to F0. A more recent measurement of the vocal tract resonance[2, 3] confirms this effect in the middle range of soprano singing. It also shows that F1 cannot be raised above a certain point (roughly 1 kHz), and the order of F0 and F1 is reversed in the high range. These observations imply that the vocal folds should vibrate in the vicinity of the frequency region near F1 where the acoustic load can be both inductive and capacitive.

In speech synthesis by simulating all the processes in the voice production, the two-mass model of the vocal fold vibration[4] has been widely used. It was shown that this model can simulate self-sustained oscillation with a capacitive acoustic load of the vocal tract. As shown in Section IV, however, self-sustained oscillation can not be obtained in a large frequency range just above F1. This means that musical tones in this range can not be synthesized. The voice range simulated by the two-mass model, therefore, becomes narrower.

This paper proposes a model of vocal fold vibration that can successfully simulate self-excited oscillation in a wide frequency range on both sides of F1 with no discontinuity of vibration. The model approximates the vocal folds as a pair of single masses that can vibrate both parallel and perpendicular to the airflow. The high-pitched singing voice is simulated as well as the normal speech voice in this paper. In addition, the mechanism for self-excitation both in the capacitive and inductive acoustic loads is discussed.

II. TWO-DIMENSIONAL MODEL OF VOCAL FOLDS

The proposed model was originally developed to simulate the vibration of a brass player's lips.[5] The model is a combination of two earlier models: the swinging-door model and the transverse model.[6] The former employs a valve (lips or vocal folds) that operates by the pressure difference between the upstream and downstream regions. The latter employs a valve that operates by the Bernoulli pressure generated by a flow passing through the valve aperture.

The complete description of the model including the equation of motion can be found in [7]. The pair of modeled vocal folds are schematically represented by parallelograms with two sets of a spring and a damper as shown in Fig. 1 (a). The left and right vocal folds are assumed to vibrate symmetrically. The vocal fold simultaneously executes both swinging and elastic motions. The former is driven by the trans-glottal pressure difference, and the latter is driven by the Bernoulli pressure generated at the glottis. The swinging motion implies that the motions parallel and perpendicular to the airflow are not independent but coupled with each other. This differentiates the current model from other two-dimensional models, such as those proposed by Liljencrants[8] and Flanagan and Ishizaka[9]. During one cycle of oscillation depicted in Fig. 1 (b), the tip of the vocal fold makes an elliptic trajectory, while the glottis retains a rectangular shape.

Forces acting on the vocal fold are illustrated in Fig. 1 (c). These are Bernoulli force $\vec{f}_B(t)$ in the glottis, force due to the pressure difference $\vec{f}_{\Delta p}(t)$, contact force $\vec{f}_C(t)$, and restoring force $\vec{f}_R(t)$ from both springs. Figure 1 (c) also shows the lateral dimension (width) w and the length

[†]sadachi@atr.jp

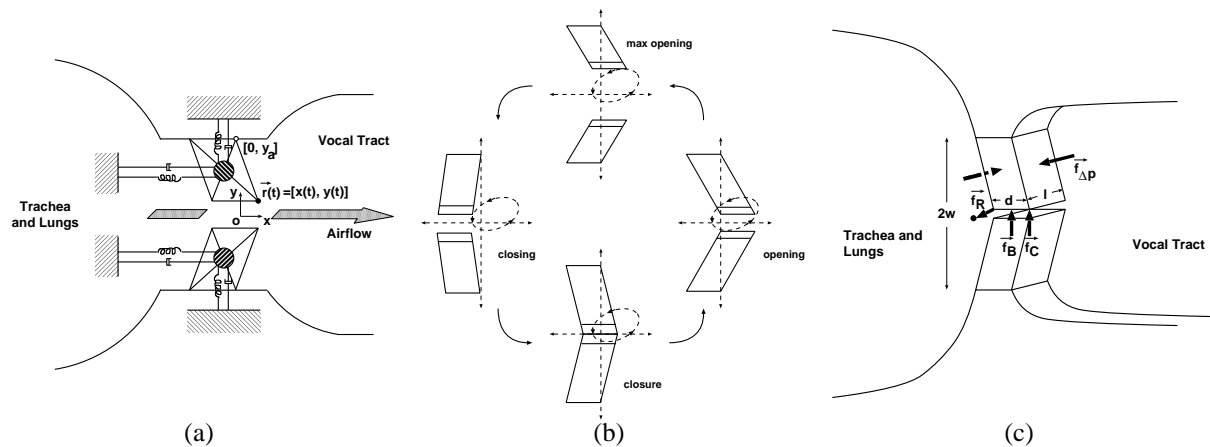


Figure 1: The two-dimensional model of vocal fold vibration: (a) Schematic diagram of the model. (b) Motion of the vocal folds allowed in this model. Four different phases in a single cycle of oscillation are shown. (c) Forces acting on the vocal fold and the dimensions of the vocal fold.

l and thickness d of the vocal fold. To simulate vocal fold vibration, we have to know the external forces $\vec{f}_B(t)$ and $\vec{f}_{\Delta p}(t)$, both acting on the vocal folds. These forces are determined by the acoustic response of the vocal tract and fluid dynamics.

Synthesized sound can be obtained by solving the equation of motion for the vocal fold vibration, a modeled equation for the air flowing through the glottis and the input impedance of the vocal tract that can be determined from the shape of the vocal tract by the transmission line method. The parameters that can control the system of the voice production are the rest position of the vocal fold (x_0, y_0) , subglottal pressure p_0 and the resonance frequency of the vocal fold f_r .

III. VOWEL SIMULATION

As a typical sound generated by the two-dimensional vocal fold model, simulation result of vowel /e/ is shown in Fig. 2. The control parameters are set to $x_0 = 0.2$ mm, $y_0 = -0.02$ mm, $p_0 = 800$ Pa and $f_r = 120$ Hz.

The trajectory of the vocal fold has a smooth oval shape, and the oscillation is in the counter-clockwise direction for the upper mass. This result is in accord with common observations of vocal fold vibration.[10] The glottal area waveform has a symmetric shape in the opening and closing phases with the duty ratio of 0.68. The simulated glottal flow is a more symmetric shape than that assumed by the Rosenberg model[11]. This may be due to the inclusion of the flow generated by the mechanical motion of the vocal folds. The simulated pressure waveforms both at the entrance and at the exit of the vocal tract resemble those by the two-mass model.

The five Japanese vowels /i/, /e/, /a/, /o/ and /u/ are sim-

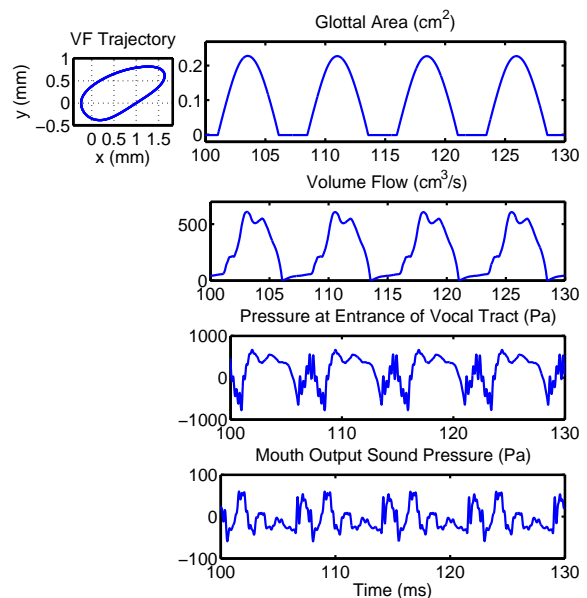


Figure 2: Simulation results for vowel /e/ showing trajectory of the vocal fold, glottal area, volume flow, pressure at entrance of vocal tract, and output pressure.

ulated with the vocal tract shapes obtained from a Japanese male speaker. The sound spectra of the simulated vowels are shown in Fig. 3. F_0 's of the simulated sounds are 126.3, 133.7, 134.1, 130.8 and 127.7 Hz for vowels /i/, /e/, /a/, /o/ and /u/, respectively. Each simulated vowel has the typical first and second formant frequencies. A simple listening test also confirms that the simulated vowels have the same quality as those synthesized with the two-mass model.

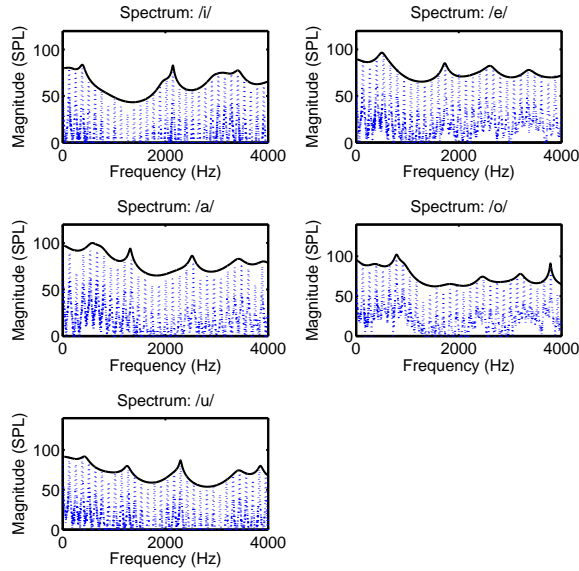


Figure 3: Simulated sound spectra for vowels /i/, /e/, /a/, /o/ and /u/. The solid lines show the spectrum envelopes estimated by LPC analysis.

IV. HIGH-PITCHED VOICE SIMULATION

The response of the two-dimensional and two-mass models with a capacitive acoustical load was investigated by driving the oscillation frequency to values between the first resonance frequency (F_1) and the first anti-resonance frequency (F_1').

A. Straight tube load

The two vocal fold models were attached to a cylinder of 17 cm length and 5 cm² cross-sectional area. Calculated F_1 and F_1' are 516 and 977 Hz, respectively, the capacitive region lies between F_1 and F_1' . The models were then driven at the range of the vocal fold resonance frequency f_r , and the sound frequency was measured. When increasing the f_r , the subglottal pressure p_0 should also be increased to obtain self-excitation. The other parameters x_0 and y_0 are set to 0.2 and -0.05 mm, respectively, in this experiment. The relationship between sound frequency and f_r for the two-dimensional model is plotted with a solid line in Fig. 4 (a). The relationship for the two-mass model is shown in Fig. 4 (b). In these figures, p_0 change is also plotted with dash-dot lines.

When the sound frequency increases beyond F_1 , the acoustic load changes from the inductive to capacitive behavior. The sound frequency of the two-dimensional model increases smoothly with f_r . Self-excitation is possible in the capacitive region continuously nearly up to F_1' . On the other hand, the two-mass model has a jump in frequency at

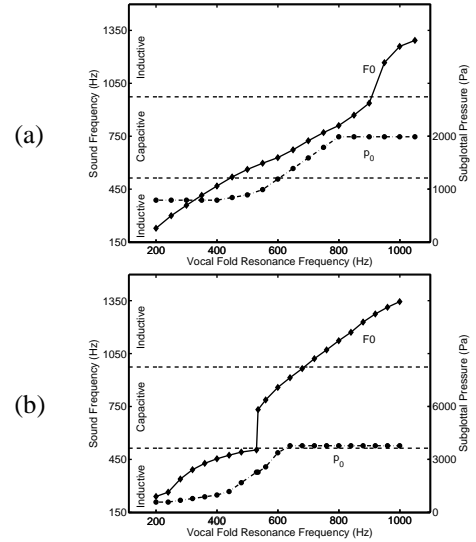


Figure 4: Straight-tube simulation. (a) Two-dimensional model. (b) Two-mass model.

F_1 . The jump covers about the lower half of the capacitive region. Therefore, no self-excitation can be generated between 506 and 735 Hz. Hence, the two-dimensional model is capable of producing a wider continuous range of frequencies for self-excitation than the two-mass model.

B. Vocal tract load

The same experiment was performed with an acoustical load of an actual vocal tract of a female speaker pronouncing vowel /a/. F_1 and F_1' of this vocal tract are calculated to be 874 and 1014 Hz, respectively. The result of the two-dimensional model is shown in Fig. 5 (a). The result of the two-mass models is shown in Fig. 5 (b).

We can observe similarities with the previous experiment. The two-dimensional model is capable of continuing self-excitation beyond F_1 . The sound frequency increases smoothly over F_1 and falls into the capacitive region. On the other hand, the two-mass model again has a jump in the frequency when it reaches F_1 . In this case, however, the frequency jump is between 842 and 1106 Hz, and no self-excited oscillation can be generated in the entire capacitive region.

V. DISCUSSIONS

The circular motion of the vocal fold is schematically illustrated in the left panel of Fig. 6. This section clarifies that this motion makes possible the self-sustained oscillation both with an inductive and capacitive vocal tract load.

The glottis is maximally opened at phase 2 and completely closed near phase 4. Therefore, a glottal area wave-

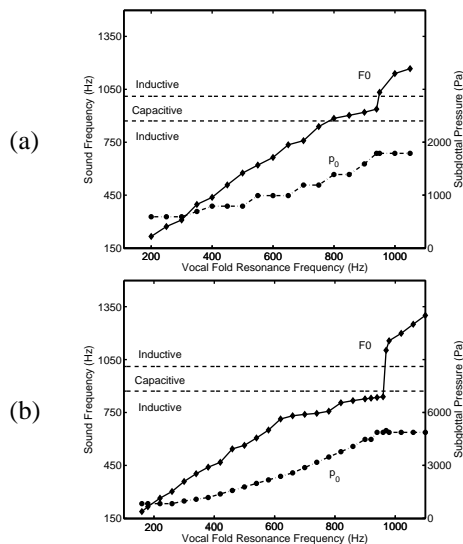


Figure 5: /a/ vowel simulation. (a) Two-dimensional model. (b) Two-mass model.

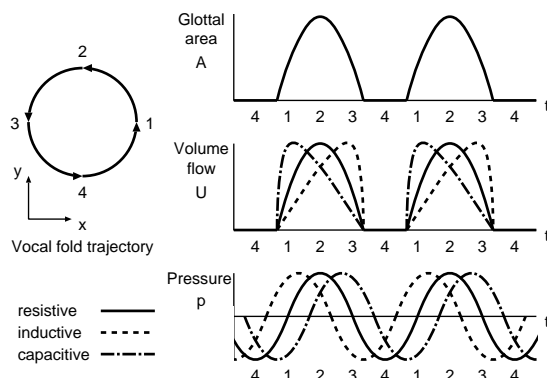


Figure 6: Schematic vocal fold trajectory and waveforms of glottal area, volume flow and pressure at the vocal tract entrance. Solid lines are for the case where the acoustic load is resistive ($F_0 \approx F_1$), dashed lines are for the inductive load ($F_0 < F_1$) and dash-dot lines are for the capacitive load ($F_0 > F_1$).

form $A(t)$ shown in the upper-right panel is generated. When F_0 is well below F_1 , the vocal tract acoustic load is inductive. In this case, according to [12], the volume flow $U(t)$ has a waveform with the slower rise and the abrupt fall as indicated by the dashed line in the middle-right panel. Because the phase of pressure $p(t)$ at the vocal tract entrance leads $U(t)$ up to 90 degree, $p(t)$ has a waveform as plotted by the dashed line in the lower-right panel. We then find that the glottal pressure, which is not very far from $p(t)$, pushes the vocal fold at phase 1 and sucks it at phase 3. Because the direction of the pressure is the same as that of the velocity of the vocal fold, the pressure becomes a driving force. This is the same mechanism for the one-mass

vocal fold model to maintain self-sustained oscillation.

When F_0 is close to F_1 , the vocal tract acoustic load becomes large and resistive. In this case, volume flow and pressure waveforms become symmetrical as indicated by the solid line. In this case, the glottal pressure does not drive the oscillation. Instead, $p(t)$ pushes the vocal fold upstream at phase 2 and downstream at phase 4 and becomes a driving force. This mechanism works even if the acoustic load becomes capacitive when F_0 exceeds F_1 . The waveforms of volume flow and pressure are depicted in the dash-dot line. Pressure $p(t)$ takes its maximum between phase 2 and 3 and its minimum between phase 4 and 1. This causes a force in the direction of the vocal fold velocity.

Acknowledgment: This research was conducted as part of ‘Research on Human Communication’ with funding from the National Institute of Information and Communications Technology.

REFERENCES

- [1] J. Sundberg, *The science of the singing voice* (Northern Illinois Univ. Press., DeKalb, 1987) pp. 124–129.
- [2] E. Joliveau, J. Smith and J. Wolfe, “Tuning of vocal tract resonance by sopranos,” *Nature* **427** 116 (2004).
- [3] E. Joliveau, J. Smith and J. Wolfe, “Vocal tract resonances in singing: The soprano voice,” *J. Acoust. Soc. Am.* **116** 2434–2439 (2004).
- [4] K. Ishizaka and J.L. Flanagan, “Synthesis of voiced sounds from a two-mass model of the vocal cords,” *Bell Syst. Tech. J.* **51**(6), 1233–1268 (1972).
- [5] S. Adachi and M. Sato, “Trumpet sound simulation using a two-dimensional lip vibration model,” *J. Acoust. Soc. Am.* **99** 1200–1209 (1996).
- [6] S. Adachi and M. Sato, “Time-domain simulation of sound production in the brass instrument,” *J. Acoust. Soc. Am.* **97** 3850–3861 (1995).
- [7] S. Adachi and J. Yu, “Two-dimensional model of vocal fold vibration for sound synthesis of voice and soprano singing,” *J. Acoust. Soc. Am.* **117** 3213–3224 (2005).
- [8] J. Liljencrants, “A translating and rotating mass model of the vocal folds,” *STL Quarterly Progress and Status Report*, 1, Speech Transmission Laboratory (Royal Institute of Technology (KTH), Stockholm, Sweden), 1–18 (1991).
- [9] J.L. Flanagan and K. Ishizaka, “Computer model to characterize the air volume displaced by the vibrating vocal cords,” *J. Acoust. Soc. Am.* **63** 1559–1565 (1978).
- [10] T. Baer, “Observation of vocal fold vibration: Measurement of excised larynges,” in *Vocal folds physiology*, edited by K.N. Stevens and M. Hirano (University of Tokyo Press, Tokyo 1981), pp. 119–133.
- [11] A.E. Rosenberg, “Effect of glottal pulse shape on the quality of natural vowels,” *J. Acoust. Soc. Am.* **49**, 583–590 (1971).
- [12] M. Rothenberg, “Acoustic interaction between the glottal source and the vocal tract,” in *Vocal folds physiology*, edited by K.N. Stevens and M. Hirano (University of Tokyo Press, Tokyo 1981), pp. 305–323.

EFFECT OF VOCAL LOUDNESS VARIATION ON THE VOICE SOURCE

J. Sundberg

Abstract: The physiological correlate of perceived vocal loudness is the overpressure of air under the glottis, or the subglottal pressure P_{sub} . Variation of vocal loudness, i.e., of P_{sub} has strong effects on the waveform of the transglottal airflow, also called the voice source. As the voice source is the primary sound itself, which after filtering by the vocal tract resonator is radiated through the lip opening, variation of P_{sub} has strong effects on the voice timbre. The waveform of the voice source, called the flow glottogram, can be obtained by inverse filtering, which implies that the vocal sound is filtered by the inverted frequency curve of the vocal tract. A flow glottogram is characterized by triangular air pulses, occurring when the vocal folds open the glottis and allows an airstream to pass. These air pulses are interleaved by episodes of zero airflow occurring when the vocal folds close the glottis, arresting the air stream. Important flow glottogram characteristics are (1) the relative duration of the closed phase, or Q_{closed} , (2) the peak amplitude of the flow pulse and (3) the maximum flow declination rate corresponding to the steepness of the trailing end of the flow pulse. These voice source characteristics show a reasonably simple relationship to acoustic properties of vocal sounds. The peak-to-peak amplitude of the flow pulse is strongly correlated with the amplitude of the lowest spectrum partial, the fundamental.

The maximum flow declination rate determines the sound level and Q_{closed} is strongly correlated with the dominance of the fundamental in the spectrum.

When P_{sub} is increased from very low to low, Q_{closed} increases markedly, but an increase from a high to a very high P_{sub} does not affect Q_{closed} appreciably. An increase of P_{sub} also leads to an increase of maximum flow declination rate and generally also of the peak-to-peak amplitude. Another consequence of an increased P_{sub} is that the higher partials in the spectrum gain more in sound level than the lower partials. Thus, a 10 dB increase of the overall sound level of a vowel is typically accompanied by a 15 dB increase of the partials near 300 Hz. This means that the slope of the spectrum, and hence also of a long-term-average spectrum varies with. All these effects of P_{sub} variation on the voice source imply that comparisons of acoustic spectrum characteristics of a voice, e.g., before and after treatment, must be made for the same degree of vocal loudness. If this condition is not met, the effect of the loudness difference between the recordings compared must be compensated for.

ASSESSING VIBRATO QUALITY OF SINGING STUDENTS

N. Amir, O. Amir, O. Michaeli

Department of Communication Disorders, Sackler School of Medicine, Tel Aviv University, Tel-Aviv, Israel

Many studies have been carried out on vibrato in the singing voice, though usually on singing of professional singers. In the present study we examine vibrato quality in sustained notes as sung by students, rather than professionals, in an attempt to find objective measures for assessing vibrato quality in singing students. A set of 78 notes was assessed subjectively by 5 experienced musicians. A set of acoustic measures was then extracted, and analyzed statistically to obtain two indicators: presence or absence of vibrato, and in the case of presence – an indication of vibrato quality. Discrimination between presence and absence of vibrato was 82% correct; the predictor of vibrato quality achieved a significant correlation coefficient of 0.7395 with the subjective judgments.

I. INTRODUCTION

Vibrato in the singing voice has been the subject of several previous studies. Recent studies have focused on quantitative analysis of vibrato parameters, examining the rate of pitch modulation, changes in this rate, and depth of pitch variation [1,2].

Some of these studies have tried to find correlations between acoustical parameters and perception of vibrato quality. These were conducted on the vibrato of accomplished singers. From their conclusions, it seems that perceptual evaluation of vibrato quality in these cases is strongly influenced by individual musical taste, since these singers usually have very good control over their vibrato parameters.

A previous study we carried on the effect of vocal warm-up on singer's voices [3], on the other hand, left us with the impression that amongst students of singing, quality of vibrato varies to a very large extent. This motivated us to examine whether some acoustic measures could be found, that would correlate well with perceptual judgments made by singing teachers. Eventually, this could lead to a form of visual feedback that would aid these students in assessing their vibrato quality.

In the present study we used the same recordings that were used in the warm-up study [3], and submitted them for judgment of vibrato quality to 5 singing teachers. We then carried out a detailed acoustic analysis of the pitch over the closing two seconds of each recording, using various quantitative measures extracted from the raw pitch contour. Statistical analyses were then applied to

find the acoustic measures which correlated best with the subjective assessment of vibrato quality.

II. METHODOLOGY

Participants: Twenty young female singers participated in this study. All participants had professional classical voice training for a mean period of 5.4 years (SD = 2.9). Sixteen singers were conservatory students, and the remaining four were graduates of a music academy. Overall mean age was 18.62 years (SD = 3.2), mean weight was 61.5 kg. (SD = 13.4) and mean height was 164.9 cm. (SD = 6.1). All singers were healthy, with no remarkable medical history.

Recording procedures: Participants were recorded individually in a quiet room while sustaining the vowel /a/ in three different pitches: 20, 50 and 80% of their vocal range. Each reference tone was presented by a piano in a random order, and the singer was asked to sustain the produced vowels (target tones) as accurately as possible for 3-5 seconds. The singers were not specifically instructed to produce vibrato in their sung tones. All vocal productions were recorded through a microphone (ACO Pacific, Inc.) situated approximately 15 cm from the subject's mouth, using a Sony-TCD D7 digital recorder (Sony, Tokyo, Japan). Sampling rate for the recording was set for 48 kHz (16 bits per sample). Vocal productions of duration less than 2 seconds were also excluded from the analysis, leaving 78 recordings that were analyzed in all.

Subjective Evaluation: The 78 recordings that were chosen for this study were presented, in a random order, to five judges for evaluation. Of the judges, three were singers and two were musicians with extensive experience in accompanying singers. Mean age of the judges was 23 years (SD = 2.12).

Each judge was, independently, presented with a simple computerized questionnaire. For each recording, the judges were, first, required to decide whether it contained vibrato or no. If a recording was judged to contain vibrato, the judge was asked to rate its quality on a 4-point scale, where 1 represents "poor", 2 "fair", 3 "good", and 4 "very good". The judges were allowed to listen to each recording only once, yet they could advance through the recordings at their own pace. Recordings that were judged by four or more listeners as containing

vibrato were considered, for the purpose of this study, as containing vibrato.

Acoustic Analysis: Vibrato is defined as a periodic variation in fundamental frequency. It is most often found to be closely sinusoidal, with a frequency in the range of 5 to 7 Hertz (see, for example, Prame's papers, [1,2]). We implemented a Pitch Detection Algorithm (PDA) in Matlab, based on the autocorrelation method. Although the original recorded productions varied in length between 5 seconds and 1.5 seconds, only the last two seconds of each recording were analyzed. Pitch detection was performed over successive 20 ms windows, with overlap of 10 ms, with a worst-case frequency resolution of 0.12 Hz. For the windowing scheme described, this resulted in 200 pitch points for each file.

Most previous studies performed relatively basic analyses on the raw data, usually measuring vibrato rate and extent. Evidently, when studying the vibrato of professional singers, the vibrato is steady enough for these to be the dominant factors in determining its quality. In contrast, in the present study, we found these features to be insufficient, and in some cases even inapplicable. In fact, the wide range in pitch contours produced by the students examined here, required the use of more generalize measures that would be able to detect whether vibrato exists at all, and assess its quality if it is present.

In order to do so, we implemented the methods used in detecting pitch itself. Since pitch is defined as periodic oscillation in the voice signal, periodic oscillation of the pitch can be measured with the same methods. We therefore applied two further analyses to the pitch contour: autocorrelation (after removal of DC) and the Fourier transform. Several illustrative examples are provided in Figures. 1-3. Figure 1 demonstrates a pitch curve, which was rated by the listeners, as not containing vibrato, Figure 2 demonstrates an unsteady vibrato, which was rated by the listeners at 1.4, and Figure 3 demonstrates an example of a steady vibrato, rated at 2.75. Each figure includes (from top to bottom): (a) the pitch contour, after average has been removed; (b) the autocorrelation of the pitch contour; (c) the Fourier transform of the pitch contour.

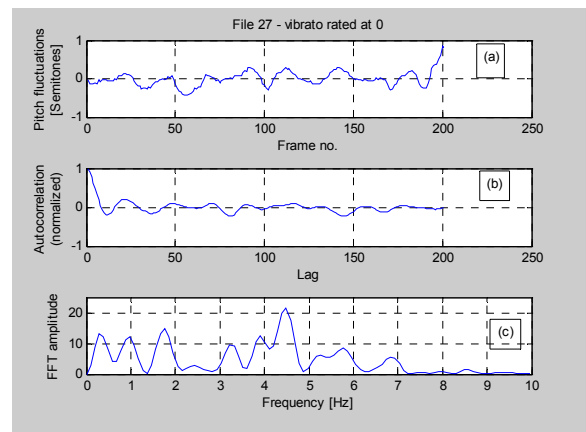


Fig. 1 – An example of a production with no vibrato

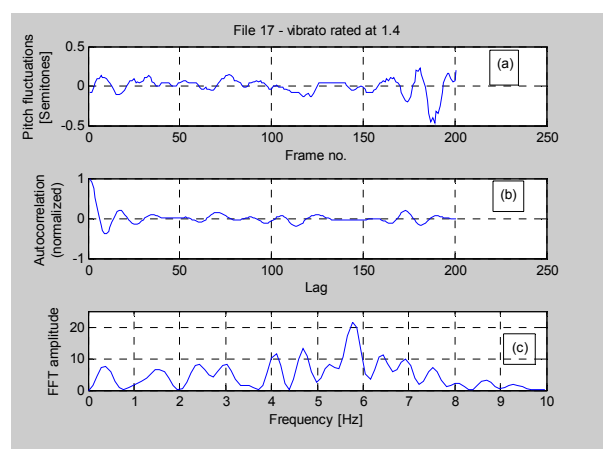


Fig. 2 – An example of a production with poor vibrato

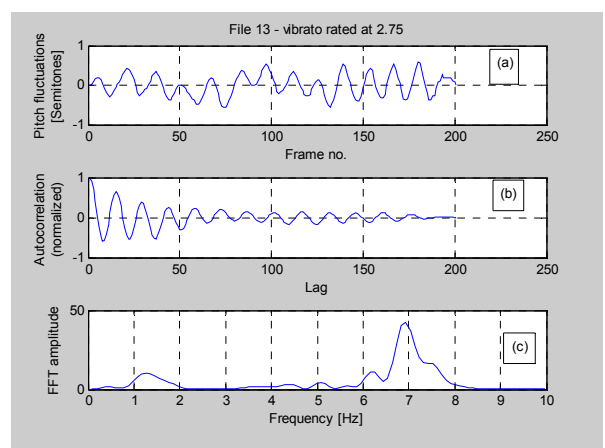


Fig. 3 – An example of a production with good vibrato

From this raw data, a series of several potential measures were then calculated:

1. Energy between 4.5 and 7.5 Hz as compared to energy between 1 and 10 Hz.
2. Energy between 5 and 7 Hz as compared to energy between 1 and 10 Hz.
3. Index and height of the first peak in the autocorrelation of the pitch contour.
4. Index and height of the first trough in the autocorrelation.
5. Variance of the pitch contour.
6. Mean and standard deviation of a curve representing local extent of vibrato
7. Several additional measures of peak height and width in the FFT of the pitch contour

III. RESULTS

The analysis was carried out in two stages: the first to determine a measure for presence/absence of vibrato, and the second to find a measure that correlates with the perceptual judgment of vibrato.

A. Presence of vibrato

Logistic analysis was applied to the raw measures presented in the previous section, in order to find a predictor that would be in optimal agreement with the perceptual judgments. The results obtained by this predictor are summarized in table 1.

Table 1 – Classification results for vibrato existence

		Predicted		Total
		No	Yes	
Actual	No	20	8	28
	Yes	6	44	50
	Total	26	52	78

Table 1 shows an overall recognition rate of 82%. False positives are more prevalent (28%) than false negatives (12%).

B. Rating of vibrato

The acoustic measures were analyzed statistically in order to find a predictor that would correlate well with the judges' average rating of those recordings judged to contain vibrato. Eventually, it was found that a linear regression analysis applied to four measures gave a predictor that has a statistically significant correlation of 0.7395 with the judge's subjective ratings. These four measures were:

1. Height of the first autocorrelation peak

2. Absolute height of highest peak above 2 Hz in the FFT of the pitch contour
3. Width of the highest peak in the FFT
4. The number of spectral peaks above a third the height of the highest peak

C. Agreement between judges

Agreement among judges' ratings of vibrato quality was assessed using Kendall's coefficient of concordance, and yielded a value of 0.619 ($p < 0.001$). This analysis was based on the productions which were identified as demonstrating vibrato.

IV. DISCUSSION

The present results show that relatively good agreement can be obtained between subjective and automated assessment of vibrato quality of singing students. Obviously, the agreement between the subjective and objective measures is bounded by the inter-judges subjective agreement variability.

The methods utilized here, on singing students can be expected to demonstrate a ceiling affect, when applied to recordings of professional singers – this will be examined, in the future, in further detail.

V. CONCLUSION

Acoustic measures of vibrato, which were conceived specifically for identification and evaluation of vibrato among singing students were shown, here, to provide a relatively reliable predictor of vibrato presence and quality as evaluated by listeners.

REFERENCES

- [1] E. Prame, "Measurements of the vibrato rate of ten singers," *J. Acoust. Soc. Am.*, vol. 96(4), pp. 1979-1984, 1994.
- [2] E. Prame, "Vibrato extent and intonation in professional Western lyric singing," *J. Acoust. Soc. Am.*, vol. 102(1), pp. 616-621, 1994.
- [3] O. Amir, N. Amir, O. Michaeli, "Evaluating the influence of warm-up on singing voice quality using acoustic measures," *In press, Journal of Voice*.

ACKNOWLEDGMENTS

The authors would like to thank Ms. Esther Shabtai for her advice and assistance in the statistical analysis of the data.

Non-human sounds

VOCAL PRODUCTION MECHANISMS IN RUFFED LEMURS: A PROSIMIAN MODEL FOR THE BASIS OF PRIMATE PHONATION

M. Gamba, C. Giacomia

Department of Animal and Human Biology, Università degli Studi di Torino, Torino, Italy.

Abstract: The island of Madagascar is one of the planet's foremost biodiversity hotspots and it is threatened with large-scale destruction by unsustainable human activities. The ruffed lemur, like all other lemurs, is endemic to Madagascar and inhabits the eastern rainforests of the island. A captive breeding project for this species has been underway since the Sixties and lead to a relatively great population of captive ruffed lemurs. Part of this population was recorded for the purpose of this study and phonetic analysis of the ruffed lemur calls is presented in this paper. As reported from studies on human and non-human primate vocal communication, ruffed lemurs show acoustic cues on actual (or even exaggerated) vocalizer body size when emitting inter-group and agonistic vocalizations. The vocal repertoire of *Varecia* sp. also features submissive, affiliative and pre-copulation calls, showing different formant patterns that contradict the use of the uniform, or flared, tube system as a valid model of non-human primate phonation.

I. INTRODUCTION

Like other primates, including humans, lemurs are conspicuously vocal and are capable of modifying both the shape of the airway and the oscillation of the vocal fold [11]. Previous studies have shown lemurs of Madagascar produce a wide range of vocalizations, comprising alarm calls, several contact calls, mating calls and screams [12][11]. The thesis that speech differs from non-human primates vocal communication because of the lack of a continual articulation, often caused an under evaluation of non-human primates phonatory processes. Thus the fact that non-human primates can produce rapid changes in the vocal tract shape and length has been rarely investigated. Recent evidences emerging from studies of various primate species demonstrate that formants are meaningful acoustic features of non-human primate calls [16][17][3] and that rapid changes in vocal tract shape and length are not uniquely human as they can be assessed from the dynamic pattern of certain acoustic parameters [15]. First (F1) and second (F2) formants of non-human primates calls can distinguish, when plotted, different vocal types, as it happens for human vowels. This is particularly interesting, although it has been never investigated, in lemurs. If it is true that non-human primates share, to a certain degree, with humans the ability to act voluntary changes in vocal tract shape during vocalisation, by articulation of the tongue, the mandible and the larynx, lemurs could represent a simplified model, as lip protrusion is absent. This paper

provides the first phonetic analysis of a wide range of calls by ruffed lemurs, previously classified on the basis of on-screen subjective recognition. We will show ruffed lemur calls can be described as discrete categories and how the variation in the first two formants may characterise vocal type differences.

II. METHODOLOGY

Study animals were captive ruffed lemurs kept in several institutions across Europe and United States. We recorded natural occurring vocalization emitted by *Varecia variegata variegata* at Parco Natura Viva (Bussolengo-Vr, Italy), Mulhouse Zoo (France), Rheine Der Naturzoo and Koln Zoo (Germany), Apenheul (Apeldoorn, The Netherlands), St. Louis Zoo (USA), Twycross Zoo, Drusillas Park (Alfrinston) and Banham Zoo (UK).

The vocal repertoire of the black and white ruffed lemur is the most studied among lemurs. Previous works [12] [8] have recognised 16 vocal types, 8 of which we considered in this study because of their vowel like acoustic structure and because emitted by adult males. Pereira and colleagues [12] offered a detailed qualitative description of both behavioural and vocal repertoire of the black and white ruffed lemur. Additional works [11][8] provided important elements that are summarised in the following brief descriptions. According to Pereira and colleagues [12], we could consider these vocalizations as part of 3 broad categories: Loud (High Amplitude) Call (HA), Moderate Amplitude Calls (MA) and Low Amplitude Calls (LA).

Roar Shriek Chorus [Roar (HA, abbr. R), Shriek (HA, abbr. S)] - The chorus is a structurally complex and variable group call, including simultaneous contributions by all the adults in the group. This composite vocalization lasts from 5 to 30 seconds [12] and features two types of emission. One is a wide-band noisy sound called "roar" and the other is a frequency modulated narrow-band component called "shriek". Both these emissions are characterized by great amplitude. The roar shriek choruses resemble the inter-group spacing calls of other primates (e.g. *Alouatta* sp., [19]). In captivity, these call were frequently evoked by sudden extra-group noises, therefore the fall of metallic boxes, birds' calls, loud voices has been recorded as eliciting the chorus.

Bray (MA, abbr. B) - This vocalization is mainly emitted by males and is more frequent in the breeding season than in the rest of the year. Black and white ruffed lemurs in captive semi-free ranging groups emitted brays only in the reproductive season [12].

Wail (MA, abbr. W) - This call denotes urgency for re-aggregation [12]. This vocalization is present only at the end of the roar shriek chorus. Wail is particularly rich in harmonic overtones and can appear as a tonal or noisy-tonal vocalization.

Abrupt Roar (HA, abbreviated AB) - This roaring vocalization shows a rapid series of 2-5 roar-like sounds. It was recorded mainly from adult males and often follows a sudden disturbance or the presence of large birds particularly in the breeding season [12] [7]. Observations by Simons (in [12]) and Petter (in [13]) showed that abrupt roars could be exchanged during inter-group communication.

Appeasement call (MA, abbr. AP) - The appeasement call (the “whine” in [12], assertion/courtship call in [11]) is a vocalization exclusively emitted by males during the breeding season. Males are emitting this call when approaching the female to mate. This call is usually characterized by a clear tonal structure with harmonics over a noisy variable pattern.

Chatter (MA, abbr. C) - The chatter is a high-pitched vocalization comprising a rapid series of brief narrow units. According to Pereira and colleagues [12], this call is directed towards dominants. The call varies in duration and in number of units according to the severity of the agonistic encounter. This call can be referred to a general voiced bared-teeth display (common in many other primate species, e.g. *Pan* sp., [20]) both because of its acoustic structure and phonation mechanism and its contextual use. During the emission of the chatter there is a strong horizontal and vertical retraction of the lips, so that the teeth are maximally exposed.

Mew (LA, abbr. M) - This vocalization is a tonal emission and usually shows a moderate to absent frequency modulation. A slow rise in pitch is often present in adults. The mew can vary in duration but it lasts on average 0.8 s [7]. All group members were seen emitting mews in relaxed context but this emission plays a key role in the mother-offspring communication since the early stages after birth [8].

Recordings were made on TDK DA-RXG tapes using a Sony TCD-D100 Digital Audio Tape recorder and a Sennheiser ME66 directional microphone with K3U power module. The sample available for acoustic analysis consisted of 8750 sounds. For the purpose of conducting this research, we have chosen 80 high-quality vocalizations, 10 per vocal type.

Acoustic analyses were performed in Praat 4.3.04, a toolkit to do phonetic analysis by computer [1]. Praat use was combined with Akustyk 1.7.6, which is a comprehensive vowel analysis software package by B. Plichta (Michigan State University). To characterize source we measured several features of the fundamental frequency (F0), by using the F0 contour extraction in Praat. The F0 contour and formant pattern fitting were both inferred during a step by step monitored process, where operator could interrupt the analysis and modify the analysis parameters. A Praat script was used to automate file opening and editing as well as file saving of

the measurements. Typical preset values were changed according to acoustic properties of the different vocal types, for example 650-1100 Hz was the pitch analysis range in Chatter, while 180-440 Hz was the range used for Mews. To characterize vocal tract (filter), we measured first 2-5 formants, depending on the number of formants detectable from the spectrogram, using Linear Predictive Coding (LPC). Formant presets were modified as well per type. Extensive on-screen examination of all the vocal types was necessary to determine intra- and inter-individual variation. Formant analysis in this study is the result of an application of the Burg’s method [2], with superimposition over the signal spectrogram. A number of autocorrelation-based LPC spectra was overlaid independently derived FFT spectra of the same vocalization to ensure the goodness of the LPC analysis. Typical maximum formant was 12000 Hz and number of formants 3-7. Window length was 0.05 s and dynamic range 22.0 Hz.

III. RESULTS

Articulatory manoeuvres characterize abrupt roars, appeasement calls, brays, chatters, shrieks, roars and wails. Mews, even presenting a different acoustic structure, are emitted with mouth closed and in absence of detectable articulation. For each vocalization we selected a stable portion and calculated mean values of F1 and F2 using LPC coefficients in Praat. Mean values and standard deviations are shown in Table 1. ANOVA, applied over data from the acoustic analysis, showed a significant difference among the first formants [F1 (N = 80, $R^2 = 0,931$, $p < 0.001$); F2 (N = 80, $R^2 = 0,925$, $p < 0,001$)] measured in the considered vocal types. According to Tukey’s HSD test for post-hoc comparisons, F1 and F2 values of this sample differed significantly between vocal types. Matrixes of pair wise comparison probabilities are shown in Tables 2 and 3.

Following previous studies [9] [18], we assumed that a prosimian vocal tract could be simplified as a uniform tube with cylindrical section and a certain length. Applying the formula published by Lieberman and Blumstein [10], we calculated formant values from different vocal tract lengths. The black line in Figure 1 indicates predicted values of F1 and F2 in case of a uniform tube model. If *Varecia*’s vocal tract could be modelled as a uniform tube, we should expect all of the vocal types situated along the black line (Fig. 1).

Table 1. Mean values and Standard Deviations for each vocal type.

Vocal Type	F1 (Hz)		F2 (Hz)	
	Mean	Std.Dev.	Mean	Std.Dev.
R	850	124	2010	343
B	1019	91	2085	164
W	1141	83	2694	299
AB	1206	130	3327	377
S	1492	217	5183	301

AP	2452	191	5110	300
C	2807	143	5118	524
M	3472	631	5855	845

Table 2. Matrix of pair wise comparison probabilities for the first formant (F1). Significant results for $p < 0.05$.

	R	B	W	AB	S	AP	C	M
R	1,000							
B	0,000	1,000						
W	0,523	0,000	1,000					
AB	0,000	0,063	0,000	1,000				
S	0,000	0,000	0,000	0,000	1,000			
AP	0,062	0,000	0,578	0,000	0,000	1,000		
C	0,164	0,000	0,003	0,000	0,000	0,000	1,000	
M	0,694	0,000	0,671	0,000	0,000	0,151	0,069	1,000

Table 3. Matrix of pair wise comparison probabilities for the second formant (F2). Significant results for $p < 0.05$.

	R	B	W	AB	S	AP	C	M
R	1,000							
B	0,000	1,000						
W	0,000	0,000	1,000					
AB	0,000	1,000	0,000	1,000				
S	0,000	0,007	0,000	0,008	1,000			
AP	0,000	0,000	1,000	0,000	0,000	1,000		
C	0,000	1,000	0,000	1,000	0,022	0,000	1,000	
M	0,039	0,000	0,053	0,000	0,000	0,018	0,000	1,000

Roar and Bray are reasonably fitting the line, and this also happens for Wails and Abrupt Roars. We estimated that these signals are resonating in vocal tracts that measure respectively $11,68 \pm 1,69$ cm, $10,59 \pm 0,92$ cm, $8,71 \pm 0,93$ cm, $7,57 \pm 0,75$ cm. The Shriek still partially overlay the uniform tube model predictive line, where a $5,46 \pm 0,27$ cm vocal tract length could be estimated. Appeasement calls and Chatters are both showing higher F1 values when compared to Shrieks, with Mews showing slightly increased F2 and a remarkable increase in F1. These four vocal types should be emitted from a vocal tract that is $4,35 \pm 0,28$ cm, $4,12 \pm 0,40$ cm, $3,50 \pm 0,49$ cm, $3,36 \pm 0,36$ cm. At least for 4 of the vocal types, the uniform tube model does not provide a satisfactory explanation for vocal tract resonance.

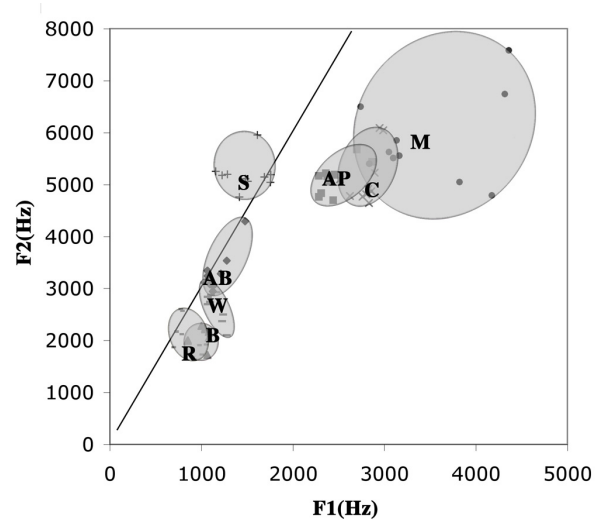


Figure 1. Formant chart of F1 and F2 in hertz-scale. An elliptically contoured distribution of the data is shown per vocal type.

IV. DISCUSSION

Vocalization emitted by ruffed lemurs may be properly characterised by the first formants, F1 and F2. The formant chart in Fig. 1 shows a clear separation of the uttering in 2 broad categories, Agonistic, long distance calls (Bray, Abrupt Roar, Roar and Wails) and Contact, intra-interaction calls (Mews, Chatter, Appeasement call). Shrieks show F1 values similar to the first group of calls but F2 resembles the intra-group ones. In these attempts to decode phonation mechanism across different vocal types in lemurs, we show evidence of the ability in these species to modify vocal tract length at least between different vocal types. As reported from studies in human and in non-human primates [4] [6] [14], there could be a functional value in providing information on actual (or even exaggerated) vocalizer body size through acoustic features of vocalization. This could be the case the *Varecia*'s vocal behavior in agonistic and inter-group contexts. On the other hand, it is extremely interesting to note appeasement calls, usually emitted by male before copulation, and chatter, denoting submission, share similar F1 and F2 values; this fact also occurs in Shrieks, with the all three showing F1 values between 5000 and 6000 Hz. For Shrieks it is plausible to have a vocal tract length around 5 cm, and the same is possible for Appeasement calls and Chatters.

The uniform tube vocal tract model seems to explain properly only part of the vocalisations emitted by ruffed lemurs. Recent studies about other non-human primates show that a 3-segment tube model with variable diameters is predicting better formant pattern in alarm calls [15]. The evident shift from the uniform tube model prediction showed by Mews suggests a different phonation mechanism. In fact this vocalization is always emitted with mouth closed.

V. CONCLUSION

The vocal repertoire of the ruffed lemurs shows these prosimians possess the ability to change the configuration of the vocal tract. Each vocal type is characterized by the values of formants F1 and F2 and vocalizations within a given type usually show similar formants. According to the model suggested in previous studies, we considered the primate vocal tract during vocalization as a uniform (or flared) tube and calculated F1 and F2 as the model would predict. Predicted formants were plotted against the one we measured. Agonistic long distance calls, showing longer vocal tract estimation, are situated along the line (Fig. 1). Other vocalization, whose contextual use is different, showed higher values in both formants. These calls show F1 values higher than predicted and do not fit the black line in Fig.1.

Prosimian primates diverged from the anthropoid branch (monkeys, apes, and humans) more than 60 million years ago and these results suggest that, even in lemurs, the flared tube model do not provide valid predictions when applied across the vocal repertoire.

This research was supported by the Università degli Studi di Torino and by grants to M.G. from the Parco Natura Viva – Centro Tutela Specie Minacciate.

REFERENCES

- [1] P. Boersma, "Praat, a system for doing phonetics by computer," *Glott International* 5:9/10, 341-345, 2001.
- [2] D.G. Childers, *Modern spectrum analysis*, IEEE Press, pp. 252-255, 1978.
- [3] W.T. Fitch, "Vocal tract length and formant frequency dispersion correlate with body size in rhesus macaques", *J. Acoust. Soc. Am.*, 102, pp. 1213-1222, 1997.
- [4] W.T. Fitch, "The phonetic potential of nonhuman vocal tracts: comparative cineradiographic observations of vocalizing animals," *Phonetica* 57, pp205-218, 2000.
- [5] W.T. Fitch, "The evolution of speech: A comparative review," *Trends Cogn. Sci.* 4, pp. 258-267, 2000.
- [6] W.T. Fitch, "Comparative Vocal Production and the Evolution of Speech: Reinterpreting the Descent of the Larynx," in A. Wray ed., *The Transition to Language*. Oxford, Oxford University Press, 2002.
- [7] M. Gamba, C. Trincherro, and C. Giacoma, "Development of vocalisations in *Varecia variegata variegata*," in D. Formenti, 13th Meeting of the Italian Primatological Society. *Folia Primatol* 71, pp. 288-298, 2000.
- [8] M. Gamba, C. Giacoma, and C. Avesani Zaborra, "Monitoring the vocal behaviour of ruffed lemurs in the nest-box," *Eaza News*, 43, pp. 28-29, 2003.
- [9] P. Lieberman, "Primate vocalization and human linguistic ability," *J. Acoust. Soc. Am.* 44, pp. 1574-1584, 1968.
- [10] P. Lieberman and S.E. Blumstein, *Speech physiology, speech perception, and acoustic phonetics*, Cambridge Studies in Speech Science and Communication. Cambridge: Cambridge University Press, 1988.
- [11] J.M. Macedonia and K.F. Stanger, "Phylogeny of the Lemuridae revisited: Evidence from communication signals," *Folia Primatol.* 63, pp. 1-43, 1994.
- [12] M.E. Pereira, M.L. Seeligson, and J.M. Macedonia, "The behavioral repertoire of the black-and-white ruffed lemur, *Varecia variegata variegata* (Primates: Lemuridae)", *Folia Primatol.* 51, pp. 1-32, 1988.
- [13] J.J. Petter and P. Charles-Dominique, "Vocal communication in prosimians," in *The Study of Prosimian Behavior*. eds. G.A. Doyle and R.D. Martin. Academic Press: New York, 1979.
- [14] D. Rendall, S. Kollias, C. Ney, and P. Lloyd "Pitch (F0) and formant profiles of human vowels and vowel-like baboon grunts: The role of vocalizer body size and voice-acoustic allometry," *J. Acoust. Soc. Am.* 117, 2, pp. 944-955, 2005.
- [15] T. Riede, E. Bronson, H. Hatzikirou and K. Zuberbuehler, "Vocal production mechanisms in a non-human primate: morphological data and a model," *Journ. Hum. Evol.* 48, pp. 85-96, 2005.
- [16] T. Riede and K. Zuberbuehler, "Pulse register phonation in Diana monkey alarm calls," *J. Acoust. Soc. Am.*, 113, pp. 2919-2926, 2003.
- [17] T. Riede and K. Zuberbuehler, "The relationship between acoustic structure and semantic information in Diana monkey alarm vocalization," *J. Acoust. Soc. Am.*, 114, pp. 1132, 2003.
- [18] C. Shipley, E.C. Carterette, and J.S. Buchwald, "The effect of articulation on the acoustical structure of feline vocalization," *J. Acoust. Soc. Am.*, 89, pp. 902-909, 1991.
- [19] R. Vercauteren Drubbel and J.P. Gautier, "On the occurrence of nocturnal and diurnal loud calls, differing in structure and duration, in Red Howlers of French Guiana," *Folia Primatol.* 60, pp. 195-209, 1993.
- [20] J.A.R.A.M. Van Hooff, "The facial displays of the catarrhine monkeys and apes" in *Primate Ethology*, D. Morris Ed., London, Widenfeld and Nicolson, 1967, pp 7-67.

LABELING OF COUGH DATA FROM PIGS FOR ON-LINE DISEASE MONITORING BY SOUND ANALYSIS

J.-M. Aerts¹, P. Jans¹, D. Halloy², P. Gustin², D. Berckmans¹

¹Laboratory of Agricultural Building Research, Department of Agro-Engineering and Economics, Katholieke Universiteit Leuven, Belgium;

²Department of Pharmacology, Pharmacotherapy and Toxicology, Universite de Liege, Belgium.

Abstract. More objective and automated detection of respiratory diseases in pig houses should be possible by on-line sound analysis of cough monitoring. To develop automatic algorithms for pig cough recognition, experiments and well-labeled cough data are needed. The objectives of this article are: (1) to give a short overview of the attained results in cough recognition, and (2) to define a methodology to label the cough data in a pig house. Human observers labeled coughs by audiovisual observation in a laboratory test installation with ten pigs during periods ranging from two days to two weeks. Simultaneously, sound registration was done with audio equipment. The sound registrations were listened to by another observer to compare the number of coughs in the registration with the number labeled during the experiment. It was found that there were underestimations of up to 94% in the number of coughs. The underestimation in the number of coughs could be reduced to 10% when the observer used an additional labeling sound signal on the scene each time coughing was observed. In addition, differences were found between two independent observers scoring pig's coughs in an audiovisual manner on the scene. For future research, we suggest an investigation of how an observer using software labeling could improve the labeling results.

I. INTRODUCTION

is not only crucial for the animals' health and welfare [6,7], but also for the consumer because early detection of animal diseases can reduce residuals of antibiotics in meat products [8]. Therefore, great effort is spent to the development and application of sensors and sensing techniques for diagnosis in livestock farming [9]. Sound production by animals is a candidate bio-signal that can be measured easily at a distance and without causing additional stress. Research has been reported on sound analysis applied to animal sounds in general [10,11,12,13,14,15] and to farm animals in particular [16,17,18,19]. Sounds produced by pigs have been analyzed in relation with communication [20,21,22,23] stress [24,25], welfare [10,17], pain [26,27], and health

[19]. Because respiratory diseases cause important economic losses in pig production [19], several researchers in recent years have focused on cough detection algorithms. Examples can be found in the work of [28,18,13]. A common characteristic of the developed algorithms is that they are trained based on data sets (training data sets) in order to classify the measured sounds (e.g., with neural networks). As a consequence, the failure or success of the development of an algorithm depends highly on the quality of the training data set. In order to quantify the success rate of such algorithms, the data sets (training as well as validation) are labeled. This means that the recorded files are listened to by a human and every sound is marked and described. However, the person who labels the sound files in the laboratory is not necessarily the same person who attends the experiments on the scene (observer). In some cases, e.g., measurements at night, an observer is not even present during the experiments. Because listening to sounds in general and cough sound files in particular is prone to subjectivity and human error, questions have arisen about the accuracy of the classical labeling procedure. In the reported research, the objective was to analyze the accuracy of the labeling of cough sounds in pig and to improve the labeling procedure for cough sounds.

II. METHODOLOGY

Animals and Housing

Throughout the experiments, the same group of ten piglets (Belgian Landrace) was used. They weighed about 9 kg at the start of the experiment. The pigs were housed in a 2 × 5 m pen with a partially slotted floor that was situated in the test facilities of the Faculty of Veterinary Medicine, Université de Liège (Belgium). Room air temperature was 20°C ±2°C. The ventilation rate was 8 m³ h⁻¹ per pig. A light scheme of 16 h of light and 8 h of darkness was applied. Light intensity was 60 lx during the light period. During the experiments, the piglets were fed a commercial feed, and water was freely available.

Digital Sound Recording

The sounds were recorded by using a standard multimedia microphone (U.S. Blaster, 20 Hz to 20 kHz frequency response), connected to a sound card (Sound

Blaster, 16 bit). The microphone was positioned 0.3 m above the pen. The sound files were recorded as .wav files (plain sound file) with a frequency of 22.050 Hz. In the laboratory, the sound files were listened to by Cool Edit Pro (version 1.2a).

Experiments

In total, four experiments were carried out. During the first three experiments (Exp1, Exp2, and Exp3), the pigs' coughs were scored during one hour a day (0830 h to 0930 h) in the test installation by an observer. The experiments lasted 22, 19, and 17 days for Exp1, Exp2, and Exp3, respectively (see table 1). During the recording time, an observer was present in the test facility in order to score (count) the coughs. The recorded sound files were then scored by a second person in the laboratory by looking at the shape of the signal (in the time domain) on a computer screen and by listening to the sound file by headphone at the same time (i.e., audiovisual scoring).

In the fourth experiment (Exp4), the listening time was extended to five 1 h periods a day (0830 h to 0930 h, 1330 h to 1430 h, 1830 h to 1930 h, 2330 h to 0030 h, and 0430 h to 0530 h), during five non-consecutive days (see table 1). Each time a cough was observed, the observer produced a typical sound, called a "ping," to label the sound as a cough. The "ping" was made by hitting a glass bottle with a metal stick. The hypothesis was that this typical sound could be easily recognized by the person scoring the sounds afterwards in the laboratory.

The first day of Exp4 was carried out with two observers in the test installation. They could both see and hear the piglets, but they could not see each other. For this part of the experiment, no labeling sound ("ping") was used.

Statistics Used

Statistical significance between mean values of coughs counted was tested using a two-sample t-test. Since the observations on the two populations of interest were collected in pairs, a paired t-test was used [29]. In order to test the hypothesis on the equality of the mean numbers of coughs counted on the scene and in the laboratory (see table 1), the data from Exp1, Exp2, and Exp3 were used. The data from Exp4 were not used for this analysis since the observations were made in a different way (labeling sound). For testing the hypothesis on the equality of the mean numbers of coughs counted by observer 1 and observer 2 during the first 24 h of Exp4 (see table 2), the data of the five observation periods were used.

III. RESULTS AND DISCUSSION

Table 1 gives an overview of the counted coughs in the four experiments. In this research, we used a total of 83 h of audiovisual observations of the pigs' coughs.

Table 1. Scoring of the cough sounds by observer present in

Experiment	Listening Protocol	Duration (days)	Number of Coughs Counted by Audiovisual Scoring:		Under-estimation (%)
			On the Scene	In the Lab	
Exp1	1 h/day	22	47	18	62
Exp2	1 h/day	19	97	6	94
Exp3	1 h/day	17	43	17	61
Exp4	5 h/day ^[a]	5	265	239	10

^[a] During Exp4, a labeling sound ("ping") was used.

the test installation compared with audiovisual scoring afterwards in the laboratory on the recorded audio file.

From table 1, we see clearly that it is not possible to make a well-labeled reference data set just by audiovisual scoring of the recorded files in the laboratory because underestimations of up to 94% occur. It could be demonstrated that the average number of coughs counted by audiovisual scoring in the laboratory was significantly different from the number of coughs counted by the observer in the test installation ($P < 0.2$). This implies that reliable labeling demands at least one observer in the pig house, which is a time-consuming and mentally exhausting job. When the coughs are marked by a well-recognizable sound ("ping") in the audio file (Exp4), an underestimation of about 10% between the different scoring methods was observed. This deviation could be the result of an over- (or under-) estimation of the number of coughs in a series (bout). When, in practice, a bout of coughing occurs, the observer could only make his labeling sound at the end of the series.

Another possible problem, which cannot be put easily into figures, is the conditioning aspect of the labeling sound. Since the pigs could hear the labeling sound themselves, it is possible that, by hearing the labeling sound each time they cough, the pigs get used to it and after a while begin to cough voluntarily to hear the labeling sound. Studies with humans have shown that voluntary cough sounds have different features from "normal" cough sounds [14]. Indications for this conditioning effect might be found in the fact that the average counted number of coughs per hour of observation in Exp4 (with labeling sound) was on average 10, whereas the average counted number of coughs (on the scene) per hour for Exp1, Exp2, and Exp3 (without labeling sound) ranged between 2 and 5. However, for a more in-depth analysis of the possible conditioning effects of labeling sounds, more experiments should be performed. Although the use of a typical labeling sound reduced the underestimation to 10%, this is not the way a reliable reference data set of cough sounds can be achieved.

When looking at table 2, we see that there is a difference (but not statistically significant) between the two observers counting the coughs of the same animals at the same time. This gives rise to the thought that there is no real completely objective way to label pigs' cough sounds in practice. We could approach a more objective labeling by mixed subjective observations, but then we would need a number of observers in the pig house, which leads to other problems (e.g., increased costs).

Table 2. Number of cough sounds counted of the same animals at the same time by two different observers in the pig house during the first 24 h of Exp4.

No. of Observations	Time of the Observation	Number of Coughs Counted by:	
		Observer 1	Observer 2
1	0830 h - 0930 h	8	10
2	1330 h - 1430 h	13	12
3	1830 h - 1930 h	7	8
4	2330 h - 0030 h	0	0
5	0430 h - 0530 h	12	7

An alternative to the auditory labeling of cough sounds is software labeling. While recording the sounds in a pig house on a portable computer, we can run an extra program. Whenever a cough sound is heard, a key on the portable computer is pressed, and the program keeps record of the relative time in the recorded audio file. This way, we could get around the problem that pigs might cough to hear the label sound, and we can label each cough, even when coughs come in a series.

In general, it is not easy to reliably distinguish between different animal vocalizations (classification). In order to solve this problem, several authors used signal analysis techniques in combination with classification procedures to identify individual vocalizations in a more objective way [21,25,27]. They used classification techniques based on training data sets. Most of the time, individual sounds are labeled by ethologists listening to the recorded data in the laboratory (e.g., [16,17]). Due to (mechanical) background noises, it is not always easy to reliably label individual sounds [16]. As described in the reported research, labeling individual cough sounds of pigs can be performed most reliably by at least one observer on the scene in the pig house. However, in most cases described in the literature, labeling was performed on recorded sound data, and no indication is given of the accuracy of the labeling procedure compared with labeling results of observers during the experiment. Accuracy of the labeling procedure is sometimes expressed as the correlation between the scores of two independent persons listening to the recorded sound data. Weary and Fraser [17] used this method for labeling the calls of piglets at weaning and found a correlation between two independent scorers of 0.98. In our experiments, the correlation between the scores of two independent observers in the pig house was 0.85.

All together, we can state that labeling individual sounds in an audio file, to use as a reference set in algorithm

training, is a difficult task and must be done very carefully.

IV. CONCLUSION

With the rising interest in animal vocalizations as a valuable biological response variable, there is a growing need for good labeling methods. Cough recognition algorithms cannot satisfy in-field situations when they are not developed, or trained, by a stable, reliable reference set.

Audiovisual observation on a recorded pig sound file is clearly insufficient for accurate labeling of cough sounds. Up to 94% underestimation of the number of cough sounds was scored in an audiovisual way on the computer. Audiovisual observation of the animal on the scene, together with a typical labeling sound, reduced the underestimation to 10%. Since the labeling sound can possibly stimulate the pigs to cough (due to conditioning), this method is probably not suited for generating high-quality data sets (for training and validation). Therefore, we suggest performing additional research to test alternative labeling methods. One of the possible alternatives is to put at least one audiovisual observer in the pig house with a portable computer. While recording the sound file, another program could keep track of the elapsed time. When a cough sound is heard, the observer could press a key on the portable computer. As a result, we could get a sound file and a relative time for all cough sounds during the period of observation, without influencing the animals with labeling sounds.

There were also differences between two independent observers who labeled pigs' cough sounds in an audiovisual way on the scene in the pig house.

V. REFERENCES

- [1] Gates, R. S., L. W. Turner, H. Chi, and J. L. Usry. 1995. Automated weighing of group-housed, growing-finishing swine. *Trans. ASAE* 38(5): 1479-1486.
- [2] Korthals, R. L., R. A. Eigenberg, G. L. Hahn, and J. A. Nienaber. 1995. Measurements and spectral analysis of tympanic temperature regulation in swine. *Trans. ASAE* 38(3): 905-909.
- [3] Aarnink, A. J. A., and M. J. M. Wagemans. 1997. Ammonia volatilization and dust concentration as affected by ventilation systems in houses for fattening pigs. *Trans. ASAE* 40(4): 1161-1170.
- [4] Wang, X., Y. Zhang, L. Y. Zhao, and G. L. Riskowski. 2000. Effect of ventilation rate on dust spatial distribution in a mechanically ventilated airspace. *Trans. ASAE* 43(6): 1877-1884.

- [5] Wathes, C. M., J. B. Jones, H. H. Kristensen, E. K. M. Jones, and A. J. F. Webster. 2002. Aversion of pigs and domestic fowl to atmospheric ammonia. *Trans. ASAE* 45(5): 1605-1610.
- [6] Predicala, B. Z., R. G. Maghirang, S. B. Jerez, J. E. Urban, and R. D. Goodband. 2001. Dust and bioaerosol concentrations in two swine-finishing buildings in Kansas. *Trans. ASAE* 44(5): 1291-1298.
- [7] Van Hirtum, A., and D. Berckmans. 2004. Objective cough-sound recognition as a biomarker for aerial factors. *Trans. ASAE* 47(1): 351-356.
- [8] Mottier, P., V. Parisod, E. Gremaud, P. A. Guy, and R. H. Stadler. 2003. Determination of the antibiotic chloramphenicol in meat and seafood products by liquid chromatography-electrospray ionization tandem mass spectrometry. *J. Chromatogr. A* 994(1-2): 75-84.
- [9] Tothill, I. 2001. Biosensors developments and potential applications in the agricultural diagnosis sector. *Comput. Electron. Agric.* 30: 205-218.
- [10] Weary, D. M., and D. Fraser. 1995. Signaling need: Costly signals and animal welfare assessment. *Appl. Animal Behav. Sci.* 44(2-4): 159-169.
- [11] Hayward, T. J. 1996. Classification by multiple-resolution statistical analysis with application to automated recognition of marine mammal sounds. *J. Acoust. Soc. America* 101(3): 1516-1526.
- [12] Murray, S. O., E. Mercado, and H. L. Roitblat. 1998. Characterizing the graded structure of false killer whale (*Pseudorca crassidens*) vocalizations. *J. Acoust. Soc. America* 104(3): 1679-1688.
- [13] Van Hirtum, A., and D. Berckmans. 2002a. Assessing the sound of cough towards vocality. *Med. Eng. and Phys.* 24(7-8): 535-540.
- [14] Van Hirtum, A., and D. Berckmans D. 2002b. Automated recognition of spontaneous versus voluntary cough. *Med. Eng. and Phys.* 24(7-8): 541-545.
- [15] Madsen, P. T., D. A. Carder, W. W. L. Au, P. E. Nachtigall, B. Møhl, and S. H. Ridgway. 2003. Sound production in neonate sperm whales. *J. Acoust. Soc. America* 113(6): 2988-2991.
- [16] Weary, D. M., and D. Fraser. 1997. Vocal response of piglets to weaning: Effect of piglet age. *Appl. Animal Behav. Sci.* 54(2-3): 153-160.
- [17] Ikeda, Y., G. Jahns, W. Kowalczyk, and K. Walter K. 2000. Acoustic analysis to recognize individuals and animal conditions. CIGR Paper No. P8207. Bonn, Germany: CIGR.
- [18] Chedad, A., D. Moshou, J.-M. Aerts, A. Van Hirtum, H. Ramon, and D. Berckmans. 2001. Recognition system for pig cough based on probabilistic neural networks. *J. Agric. Eng. Res.* 79(4): 449-457.
- [19] Van Hirtum, A., and D. Berckmans. 2003. Fuzzy approach for improved recognition of citric acid induced piglet coughing from continuous registration. *J. Sound Vib.* 266(3): 667-686.
- [20] Weary, D. M., G. L. Lawson, and B. K. Thompson. 1996. Sows show stronger responses to isolation calls of piglets associated with greater levels of piglets need. *Animal Behav.* 52(6): 1247-1253.
- [21] Weary, D. M., M. C. Appleby, and D. Fraser. 1999. Responses of piglets to early separation from the sow. *Appl. Animal Behav. Sci.* 63(4): 289-300.
- [22] Appleby, M. C., D. M. Weary, A. A. Taylor, and G. Illmann. 1999. Vocal communication in pigs: Who are nursing piglets screaming at? *Ethology* 105(10): 881-892.
- [23] Marchant, J. N., X. Whittaker, and D. M. Broom. 2001. Vocalisations of the adult female domestic pig during a standard human approach test and their relationships with behavioural and heart rate measures. *Appl. Animal Behav. Sci.* 72(1): 23-39.
- [24] Schrader, L., and D. Todt. 1998. Vocal quality is correlated with levels of stress hormones in domestic pigs. *Ethology* 104(10): 859-876.
- [25] Schön, P.-C., B. Puppe, and G. Manteuffel. 2000. Classification of stress calls of the domestic pig (*Sus scrofa*) using LPC-analysis and a self-organizing neuronal network. *Arch. Tierz.* 43: 177-183.
- [26] Weary, D. M., L. A. Braithwaite, and D. Fraser. 1998. Vocal response to pain in piglets. *Appl. Animal Behav. Sci.* 56(2-4): 161-172.
- [27] Taylor, A. A., and D. M. Weary. 2000. Vocal responses of piglets to castration: Identifying procedural sources of pain. *Appl. Animal Behav. Sci.* 70(1): 17-26.
- [28] Van Hirtum, A., J.-M. Aerts, D. Berckmans, B. Moreaux, and P. Gustin. 1999. On-line cough recognizer system. *J. Acoust. Soc. America* 106(4:2): 2191-2191.
- [29] Wonnacott, T. H., and R. J. Wonnacott. 1977. *Introductory Statistics*. New York, N.Y.: John Wiley and Sons.

AUTHOR INDEX

- Adachi S., 195
Adamovic T., 101
Aerts J.-M., 211
Aguilera-Navarro S., 11, 15
Airas M., 73
Alku P., 73
Alvarez A., 59
Amir N., 201
Amir O., 201
Auzou P., 177
Avanzini F., 55
Badin P., 51
Berckmans D., 77, 211
Berry C., 3, 23
Bianchi S., 121
Bocchi L., 121
Bruscaglioni P., 187
Burtschell Y., 191
Cantarella G., 121
Cieciwa S., 129
Cisonni J., 51
Cnockaert L., 177
Costa A., 77
Cranen B., 63
Deliyski D.D., 129, 133, 137
Diaz F., 59
Dittmar A., 67
Dori F., 37
Drepper F.R., 167
Drioli C., 55
Elemans C., 47
Eysholdt U., 159
Fell H.J., 147
Fernandez R., 59
Fernandez-Camacho F.J., 59
Fitch W.T., 47
Fourcin A., 111
Francius L., 191
Fric M., 119
Gamba M., 207
Gatkowska I., 97
Giacoma C., 207
Giordano J., 191
Giovanni A., 191
Goddard J.C., 163
Godino J.I., 59
Godino-Llorente J.I., 11, 15
Gomez P., 59
Gomez-Vilda P., 11, 15
Grenez F., 81, 155, 177
Grosogoeat B., 67
Grzanka A., 33
Guarino M., 77
Gustin P., 211
Halloy D., 211
Hanquinet J., 81
Herzel H., 47
Honda K.H., 141
Horacek J., 43, 73, 151
Iadanza E., 37
Izworski A., 97
Jans P., 211
Jeannin Ch., 67
Kacha A., 155
Kempf A., 187
Kinoshita K.K., 141
Kitamura T., 85
Kob M., 89
Konopka W., 33
Kuwabara H., 29
Laukkanen A.M., 73
Làzaro C., 59
Li H., 105
Lipping T., 171
Lohscheller J., 159
MacAuslan J., 147
Manfredi C., 37, 121, 187
Manickam K., 7, 105
Mantha S., 125
Maratea S., 55
Marino C., 37
Martinez A.M., 163
Martinez F.M., 163
Martinez R., 59
Medale M., 191
Mende W., 187
Michaeli O., 201
Michalska M., 33
Migali N., 121
Misun V., 93
Mokhtari P., 85
Mongeau L., 125

- Moore C. J., 7
Murphy K., 59
Nazarian B., 191
Neuschaefer-Rube Ch., 89
Nicollas R., 191
Nieto A., 59
Nieto V., 59
Orr R., 63
Orzechowski T., 97
Osma-Ruiz V., 11, 15
Ouaknine M., 191
Ozsancak C., 177
Patelli S., 77
Payan Y., 67
Pelorson X., 51
Perrier P., 51, 67
Pietruch R., 33
Qiu Q., 119
Ritchings T., 3, 23
Rodellar V., 59
Roth M., 191
Rudzinska M., 97
Ruty N., 51
Sáenz-Lechón N., 11, 15
Schoentgen J., 19, 81, 155, 177
Schutte H.K., 119
Schwarz R., 159
Shaw H.S., 133, 137
Sheta W., 23
Shiavi R., 181
Shrivastav R., 115
Siegmond T., 125
Silva M., 77
Silverman M.K., 181
Silverman S.E., 181
Slevin N., 7
Sovilj M., 101
Sram F., 119
Stellzig-Eisenhauer A., 187
Stevovic N., 101
Stoffers J., 89
Subari K.S., 181
Subotic M., 101
Sundberg J., 199
Svancara P., 151
Svec J.G., 119
Takano S.T., 141
Takemoto H., 85
Tanttu J.T., 171
Toy H., 159
Turunen J.J., 171
Vampola T., 43
Van Hirtum A., 51
Vesely J., 43
Vicente J., 191
Vokral J., 43
Wermke K., 187
Wilkes D.M., 181
Wurzbacher T., 159
Yu J., 195
Zaccarelli R., 47
Zielinski T., 129

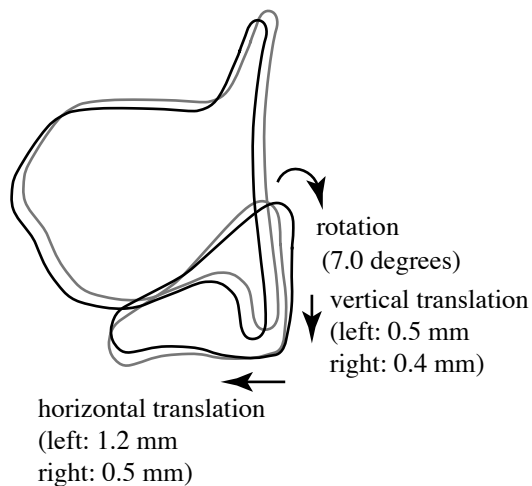


Fig 5. Actions of the cricothyroid joint between low and high F0.

the thyroid and cricoid cartilages were converted into the translation of the cricothyroid joint, as shown in Table 2.

The translation of the left cricothyroid joint are 0.5, -1.2, and 0.0 mm in the x-, y-, and z-axes, respectively. In the same way, the translations of the right cricothyroid joint are 0.4, -0.5, and 0.0 mm in the x-, y-, and z-axis, respectively.

The anteroposterior translation (y-axis) of the cricothyroid joint was found to be the largest (-1.2 mm), the vertical translation (x-axis) of the cricothyroid joint was found to be of some extent (0.5 mm), and the lateral translation (z-axis) of the cricothyroid joint was found to be zero (0.0 mm). These results apparently show that both translation and rotation of the cricothyroid joint contribute to stretch the vocal folds, as shown in Fig. 5. These results agree with previous studies [1,2,3, and 7], not [4,5].

Translation of the cricothyroid joint is caused by forward movement of the thyroid cartilage. This joint action has left/right asymmetry, and horizontal translation was larger than vertical translation. Although the contribution of the vertical translation to F0 control is still unclear, this action is presumably caused by the constriction of the cricothyroid muscle to approximate the thyroid and cricoid cartilage for stretching the vocal folds.

IV. CONCLUSION

The action of the cricothyroid joint was observed by estimating the displacement and angular changes of the laryngeal cartilages using high-resolution MRI and a 3D

pattern matching method.

- (1) The movement of the thyroid and cricoid cartilages had left/right asymmetry, suggesting six degrees of freedom in the motion of thyroid and cricoid cartilages.
- (2) The angular change of the thyroid cartilage was in the same direction as the cricoid cartilage, but left-right and front/back displacement was inconsistent between the thyroid and cricoid cartilages.
- (3) The anteroposterior translation of the cricothyroid joint was 1.2 mm, and vertical translation was 0.5 mm in the vertical direction.

ACKNOWLEDGEMENTS

We would like to give special thanks to the members of the ATR Brain Activity Imaging Center. This research was supported in part by the National Institute of Information and Communications Technology. This work was also supported in part by a Grant-in-Aid for Scientific Research No. 16791035, Japan Society for the Promotion of Science.

REFERENCES

- [1] Fink, R. B., and Demarest, R. J. (1978). *Laryngeal Biomechanics*. Harvard University Press.
- [2] Vilkmann, E. A., Pitkanen, R., and Suominen, H. (1987). Observation on the structure and the biomechanics of the cricothyroid articulation. *Acta Oto-laryngol*, 103, pp. 117-126.
- [3] Sonninen, A. (1956). The role of the external laryngeal muscles in length-adjustment of the vocal cords in singing. *Acta Oto-laryngol*, 130, pp. 9-97.
- [4] Mayet, A. and Mundnich, K. (1958). Beitrag zur anatomie und zur funktion des M. cricothyroidus und der cricothyreoidgelenke, *Acta Anat.* 33, pp. 273-288.
- [5] Maue, W. M. (1971). Cartilages and Ligaments of the Adult human larynx, *Arch. Otolaryngol*, 94, pp. 432-439.
- [6] Selbie, W. S., Gewalt, S. L., and Ludlow, C. (2002). Developing an anatomical model of the human laryngeal cartilages from magnetic resonance imaging. *J. Acoust. Soc. Am*, 112(3), pp. 1077-1090.
- [7] Takano, S., Honda, K., Masaki, S., Shimada, Y., and Fujimoto, I. (2003). Translation and rotation of the cricothyroid joint revealed by phonation-synchronized high-resolution MRI. *Proc. EuroSpeech*. Geneva, pp. 2397-2400.
- [8] Masaki, S., Tiede, M., and Honda, K. (1999). MRI-based speech production study using a synchronized sampling method, *J. Acoust. Soc. Jpn. (E)*. 20(5), pp. 375-379.